

**Hydrothermal Alteration and Exploration Vectors at the Island Gold Deposit,  
Michipicoten Greenstone Belt, Wawa, Ontario**

by

Tyler Justin Ciufo

A thesis

presented to the University of Waterloo

in fulfillment of the

thesis requirement for the degree of

Master of Science

in

Earth Sciences

Waterloo, Ontario, Canada, 2019

© Tyler Justin Ciufo 2019

### **Author's Declaration**

I hereby declare that I am the sole author of this thesis. This is a true copy of the thesis, including any required final revisions, as accepted by my examiners.

I understand that my thesis may be made electronically available to the public.

A handwritten signature in purple ink, reading "Tyler Ciufu". The signature is written in a cursive style with a large initial 'T' and 'C'.

Tyler Justin Ciufu



## Abstract

The Island Gold deposit is a high-grade orogenic gold deposit located in the Goudreau Lake Deformation Zone (GLDZ), within the Michipicoten greenstone belt. This belt is situated within the larger Wawa-Abitibi terrane which is an area of significant gold endowment in the Superior Province. This underground mine is operated by Alamos Gold Inc. (formerly operated by Richmond Mines Inc.). At the end of 2016, the Island Gold Mine had estimated indicated and measured resources of 478,800 tonnes at 5.94 g/t Au (91,400 oz) as well as inferred resources estimated at 3,041,800 tonnes at 10.18 g/t Au (995,700 oz). Simultaneously, proven and probable mineral reserves were estimated at 2,551,000 tonnes at 9.17 g/t Au (752,200 oz). This thesis integrates petrology, geochemistry, electron probe microanalysis, U-Pb zircon geochronology, and multiple sulphur isotopic study to characterize the nature and timing of alteration associated with the auriferous zones at this deposit.

The protoliths of pre-gold mineralization lithologies identified at the Island Gold deposit, listed from oldest to youngest, include dacitic volcanic rocks, iron formation, gabbro, and tonalite–trondhjemite.  $V_{GD}$  extensional and  $V_1$ - $V_2$  shear-related quartz ( $\pm$  carbonate) veins, that often contain visible gold, post-date and alter these lithologies. Protoliths of post-mineralization gold lithologies include quartz diorite, gabbro/low-K lamprophyre (spessartite), and silica-poor diorite–monzodiorite. Late  $V_3$  extensional quartz-carbonate veins result in local, inconsistent alteration and remobilization of certain elements. Later tourmaline ribbons invade pre-existing structures. Lastly, diabase–quartz diabase dykes sharply cut all lithologies and vein types. Greenschist facies metamorphism has variably affected all lithologies, resulting in metamorphic minerals that mainly include actinolite, carbonates (mainly calcite), chlorite (ripidolite), chloritoid, epidote, hematite, plagioclase, quartz, and white mica.

Archean U-Pb LA-ICP-MS ages of  $2735 \pm 8$  Ma and  $2738 \pm 9$  Ma obtained from zircons in altered and least-altered dacitic samples are consistent with previous geochronological studies. Analysis of uniform cathodoluminescent zircons and rims in the altered sample yielded anomalous Proterozoic ages ranging from *c.* 975 to 1499 Ma, which are attributed to unidentified alteration event(s) that post-date auriferous quartz veining.

Alteration related to auriferous quartz veining at this deposit results in the significant and consistent enrichment of Au,  $K_2O$ , Rb, S, and Te as well as typically the depletion of  $Na_2O$  in alteration envelopes hosted by dacite, gabbro, and the tonalite–trondhjemite. Alteration minerals associated with  $V_1$ - $V_2$  auriferous quartz veining include biotite, Ca-Mg-Fe carbonates, chlorite (ripidolite), plagioclase, quartz, sulphides (pyrite  $\pm$  pyrrhotite  $\pm$  chalcopyrite), and white mica (muscovite  $\pm$  phengite). The alteration associated with  $V_1$ - $V_2$  veining remains relatively consistent with varying distance parallel to the GLDZ and elevation.

Aside from auriferous alteration resulting in  $Na_2O$  depletion, alteration-derived biotite, and insignificant proportions of alteration-derived potassium feldspar at the Island Gold deposit, the gold-related alteration at orogenic gold deposits east of the Kapuskasing Structural Zone is similar to the alteration identified at the Island Gold deposit. This overall consistency of the alteration between these deposits and the Island Gold deposit supports a common genetic process for these orogenic gold deposits.

Multiple sulphur isotope study of sulphide minerals from auriferous quartz veins and associated ore zones dominantly suggests a mantle/igneous parentage. The auriferous fluid that produced these veins was likely derived from the mantle, exsolved from a cooling crustal intrusive body, or the dehydration of igneous rocks due to metamorphism.

## Acknowledgements

As I write this section, I have come to realize and sincerely appreciate the considerable number of people that were involved with this project. I thank all of those involved because without their contributions, this thesis would not have been possible. Above all, this thesis has taught me that teamwork is needed to achieve any goal.

Co-supervisors Dr. Chris Yakymchuk and Dr. Shoufa Lin (University of Waterloo) provided guidance, managed project funding, helped with the interpretation of data, and proofread this thesis. I was fortunate to have them both as thesis supervisors. Regardless of their busy schedules, they always made time to answer my questions and were open to discussion. Dr. Chris Yakymchuk also assisted with LA-ICP-MS analyses and completed the reduction of the raw LA-ICP-MS data. Dr. Jean Richardson, Dr. Brian Kendall (University of Waterloo), and Dr. Patrick Mercier-Langevin (Natural Resources Canada), proofread this thesis and provided guidance and recommendations. I learned so much as a result of everyone's input and thank them for their guidance, patience, and hard-work.

I want to thank Katia Jellicoe, Ivan Edgeworth, Adrian Rehm, Carson Kinney (past and present students at the University of Waterloo), and the Geology team and other staff at the Island Gold mine for their support including their assistance with work in the field, at the mine, and/or in the lab. Without their help, ideas, and expertise, this thesis would not have come to fruition. I hope that this thesis provides answers to some of the questions that were brought forward over the course of this project.

Valérie Bécu (Natural Resources Canada) created purchase orders and managed the shipment of samples to Activation Laboratories Ltd. and Vancouver Petrographics Ltd. She also managed the funding allocated by Natural Resources Canada/the Geological Survey of Canada for analyses. In addition, she provided the STPL geochemical reference materials as well as compiled and provided the results of previous analyses of these reference materials. Kathleen Lauzière (Natural Resources Canada) managed the Targeted Geoscience Initiative Program and compiled sample information and whole-rock geochemistry data for the open file report and database. I want to express my gratitude to Valérie and Kathleen for their advice as well as invaluable efforts which ensured that this project ran smoothly.

Sulphur isotopic laboratory analyses were conducted by Dr. Nanping Wu and Dr. James Farquhar at the University of Maryland Stable Isotope Laboratory. They also read preliminary portions of this thesis pertaining to sulphur isotopes and provided suggestions and guidance regarding the interpretation of this data. Additional sulphur isotopic analyses were conducted by Rick Heemskerk and staff at the University of Waterloo-Environmental Isotope Laboratory. SEM-MLA laboratory work was conducted by Dr. David Grant, Dylan Goudie, and Memorial University staff at the CREAT Network's Micro Analysis Facility SEM/MLA Lab (at the Bruneau Centre). Electron microprobe laboratory analyses were conducted with the help of Marc Beauchamp at the Electron Microprobe Laboratory which is part of the Earth and Planetary Material Analysis Laboratory at Western University. Gold coating and cathodoluminescence imaging of zircons were conducted by Dr. Nina Heinig at the Waterloo Advanced Technology Laboratory. Dr. Shuhuan Li taught me how to operate the SEM-EDS at the Environmental Particle Analysis Laboratory (University of Waterloo) and allowed me to use it for analysis of samples for this thesis. Whole-rock geochemical laboratory analyses were conducted by staff at Activation Laboratories Ltd. (Actlabs) in Ancaster, Ontario. Thin sections were created by staff

at Vancouver Petrographics Ltd. in Langley, British Columbia. I wish to express my sincere gratitude to all those involved with the work and support summarized in this paragraph.

Thanks to those that provided funding for this thesis including Alamos Gold Inc., Richmond Mines Inc. (acquired by Alamos Gold Inc. in 2017), the Geological Survey of Canada/Natural Resources Canada (Targeted Geoscience Initiative), the Natural Sciences and Engineering Research Council, and the University of Waterloo. A variety of other support, such as accommodations and meals, were also provided by Alamos Gold Inc./Richmont Mines Inc. and associated staff while conducting field work.

Lastly, I want to thank Sonja Mazurak-Ciufo, Holden Ciufo, David Ciufo, and Christine Henstridge for their assistance with grammatical proofreading and their unwavering support. Without them I would not have found my passion for geology, and for that, I am eternally grateful. I must add that I am thoroughly impressed by their ability to patiently sit through my frequent, and typically unprompted, informational sessions about rocks.

## Table of Contents

Author's Declaration.....	ii
Abstract.....	iii
Acknowledgements.....	iv
Table of Contents.....	vi
List of Figures.....	x
List of Tables.....	xi
List of Abbreviations.....	xii
1.0 Introduction.....	1
1.1 Geological Setting.....	2
1.1.1 Superior Province.....	2
1.1.2 Wawa-Abitibi terrane.....	5
1.1.3 Michipicoten greenstone belt.....	7
1.1.4 Local geology of the Island Gold deposit area.....	10
1.1.5 Gold mineralization and veining.....	12
2.0 Objectives, purpose, and applications.....	15
2.1 Protoliths and metamorphism.....	15
2.2 Auriferous alteration.....	15
2.3 Mineral indicators and geochemical vectors for gold mineralization.....	16
2.4 Source(s) of sulphur and the gold-bearing fluid.....	17
2.5 Timing of gold mineralization.....	18
3.0 Methods.....	19
3.1 Sampling.....	19
3.1.1 Least-altered samples.....	19
3.1.2 Alteration envelopes and mineral indicators.....	19
3.1.3 Geochronology.....	20
3.1.4 Sulphur isotopes.....	20
3.2 Whole-rock geochemistry.....	20
3.2.1 Whole-rock geochemistry quality assurance / quality control (QA/QC).....	24
3.2.2 Isocon diagrams.....	28
3.2.3 Alteration strength groupings.....	30
3.2.4 Mass balance calculations.....	34
3.3 Petrography and point-counting.....	35
3.4 Scanning electron microscopy with energy dispersive spectroscopy (SEM-EDS).....	35

3.5	Scanning Electron Microscope Mineral Liberation Analyser® (SEM-MLA).....	35
3.6	Electron microprobe.....	36
3.7	Density .....	37
3.8	Sulphur isotopes.....	38
3.8.1	University of Waterloo – Environmental Isotope Laboratory .....	38
3.8.2	University of Maryland – Stable Isotope Laboratory.....	39
3.9	Laser ablation inductively coupled mass spectrometry (LA-ICP-MS).....	40
4.0	Results.....	42
4.1	Field relations, petrography, and scanning electron microscopy .....	42
4.1.1	Veins and gold mineralization ( $V_{GD}$ , $V_1$ - $V_2$ , $V_3$ , and $V_4$ ).....	43
4.1.2	Dacitic volcanic rocks (T2, V2, I2).....	45
4.1.3	Iron formation (IF) .....	52
4.1.4	Gabbro (I3G).....	53
4.1.5	Webb Lake stock: Tonalite–trondhjemite (I1JM).....	57
4.1.6	Gabbro/Lamprophyre (I2H).....	60
4.1.7	Quartz diorite .....	63
4.1.8	Silica-poor diorite–monzodiorite (I2M).....	65
4.1.9	Diabase–quartz diabase (I3DD) .....	68
4.1.10	Greenschist-facies metamorphism .....	69
4.2	Whole-rock geochemistry.....	103
4.2.1	Auriferous veins ( $V_{GD}$ and $V_1$ - $V_2$ veins).....	103
4.2.2	Dacitic volcanic rocks (T2, V2, I2).....	103
4.2.3	Iron formation (IF) .....	106
4.2.4	Gabbro (I3G).....	106
4.2.5	Webb Lake stock: Tonalite–trondhjemite (I1JM).....	108
4.2.6	Gabbro/Lamprophyre (I2H).....	110
4.2.7	Quartz diorite .....	111
4.2.8	Silica-poor diorite–monzodiorite (I2M).....	112
4.2.9	Diabase–quartz diabase (I3DD) .....	114
4.3	Mineral compositions.....	141
4.3.1	Biotite.....	141
4.3.2	Chlorite .....	141
4.3.3	White mica .....	142
4.3.4	Plagioclase .....	142
4.3.5	Carbonate minerals .....	143

4.4	Gold indicators and grade distribution .....	154
4.5	Sulphur isotopes.....	157
4.6	Laser ablation inductively coupled mass spectrometry (LA-ICP-MS).....	159
5.0	Discussion.....	163
5.1	Protoliths and genetic history.....	163
5.1.1	Dacitic volcanic rocks (T2, V2, I2).....	163
5.1.2	Iron formation (IF).....	163
5.1.3	Gabbro (I3G).....	164
5.1.4	Webb Lake stock: Tonalite–trondhjemite (I1JM).....	164
5.1.5	Gabbro/Lamprophyre (I2H).....	165
5.1.6	Quartz diorite .....	165
5.1.7	Silica-poor diorite–monzodiorite (I2M).....	166
5.1.8	Diabase–quartz diabase (I3DD).....	167
5.2	Greenschist-facies metamorphism .....	167
5.3	Auriferous quartz vein-related alteration .....	168
5.3.1	V <sub>GD</sub> and V <sub>1</sub> -V <sub>2</sub> vein-related alteration of dacitic volcanic rocks .....	168
5.3.2	V <sub>1</sub> -V <sub>2</sub> vein-related alteration of gabbro .....	171
5.3.3	V <sub>1</sub> -V <sub>2</sub> vein-related alteration of the Webb Lake stock.....	172
5.4	Comparison of auriferous alteration within different lithologies.....	173
5.5	Comparison with other orogenic gold deposits.....	174
5.6	Non-auriferous alteration .....	176
5.6.1	Carbonate-sericite alteration .....	176
5.6.2	V <sub>3</sub> vein-related alteration .....	177
5.6.3	Tourmalinization / V <sub>4</sub> veins .....	178
5.7	Source(s) of sulphur and gold-bearing fluids.....	179
5.8	Relative and absolute ages .....	183
6.0	Summary and conclusions .....	188
6.1	Protoliths and metamorphism .....	188
6.2	Vein-related alteration.....	189
6.3	Mineral indicators and geochemical vectors for gold mineralization .....	190
6.4	Source(s) sulphur and the gold-bearing fluid.....	191
6.5	Timing of gold mineralization .....	192
7.0	Suggested future work .....	193
8.0	References.....	195
	Appendix A. Supplementary information for mine geologists .....	209

Appendix B. Additional figures and tables .....	213
Appendix C. Grab sample information (Underground and surface).....	232
Appendix D. Drill core sample information .....	244
Appendix E. Point-counting results .....	254
Appendix F. SEM-MLA mineral modal proportion data.....	258
Appendix G. SEM-MLA thin section maps with false colours for minerals.....	261
Appendix H. Electron microprobe data and mineral formulae .....	265
Appendix I. Electron microprobe configurations and standards.....	286
Appendix J. Density measurements and QA/QC.....	289
Appendix K. Sulphur isotope data ( <sup>32</sup> S, <sup>34</sup> S): Environmental Isotope Laboratory.....	293
Appendix L. Sulphur isotope data ( <sup>32</sup> S, <sup>33</sup> S, <sup>34</sup> S, <sup>36</sup> S): Stable Isotope Laboratory .....	295
Appendix M. LA-ICP-MS data.....	297
Appendix N. Whole-rock geochemistry data including NRCan-provided standards .....	303
Appendix O. Whole-rock geochemistry QA/QC data (Lab-provided standards, duplicates, & blanks) ..	334
Appendix P. Whole-rock geochemistry QA/QC analysis of duplicates and lab-provided standards .....	482
Appendix Q. Whole-rock geochemistry QA/QC analysis of lab-provided blanks .....	487
Appendix R. Whole-rock geochemistry QA/QC analysis of NRCan-provided standards.....	492
Appendix S. Isocon results summary.....	501

## List of Figures

Figure 1. Tectonic framework of the North American continent.....	4
Figure 2. Superior Province, Wawa-Abitibi terrane, and Michipicoten greenstone belt .....	6
Figure 3. Geological map of the Michipicoten greenstone belt .....	9
Figure 4. Local geology map of the Island Gold deposit and surrounding area .....	11
Figure 5. Cross section of the Island Gold deposit .....	14
Figure 6A–C. K <sub>2</sub> O vs. S plots and alteration strength groupings .....	32
Figure 7A–C. Photographs of quartz veins .....	71
Figure 8A–D. Cross-polarized light photomicrographs of quartz veins .....	72
Figure 9A–C. Reflected light photomicrographs of gold and sulphide minerals.....	73
Figure 10A–C. Drill core and field photographs of dacite.....	74
Figure 11A–G. Mineral proportions in least-altered samples of various lithologies .....	75
Figure 12A–D. Photos of dacite variably altered by V <sub>1</sub> -V <sub>2</sub> auriferous quartz veining .....	76
Figure 13. Photo of dacite affected by non-auriferous carbonate-sericite alteration .....	77
Figure 14A–D. Photomicrographs of dacitic samples variably-altered by V <sub>1</sub> -V <sub>2</sub> veins .....	78
Figure 15A, B. Photomicrographs of dacitic samples subject to carbonate-sericite alteration.....	79
Figure 16A–C. Mineral modes in dacitic samples altered by auriferous quartz veins.....	80
Figure 17A, B. Mineral modes in samples of gabbro & Webb Lake stock altered by V <sub>1</sub> -V <sub>2</sub> veins .....	81
Figure 18. V <sub>2</sub> quartz veinlet and dacite-hosted alteration envelope (SEM-MLA image) .....	82
Figure 19. Locations of various dacite-hosted alteration envelopes studied in this thesis.....	83
Figure 20. Distribution of major alteration minerals in auriferous alteration envelopes .....	85
Figure 21A–D. Photos of outcrops and hand samples of iron formation.....	86
Figure 22A–D. Photomicrographs of samples of iron formation .....	87
Figure 23A–D. Photos of gabbro variably-altered by V <sub>1</sub> -V <sub>2</sub> veins.....	88
Figure 24A–D. Photomicrographs of gabbro variably-altered by V <sub>1</sub> -V <sub>2</sub> veins .....	89
Figure 25A–C. Hand sample and field photos of the Webb Lake stock.....	90
Figure 26A–D. Photos of the Webb Lake stock variably-altered by V <sub>1</sub> -V <sub>2</sub> veins .....	91
Figure 27. Quartz-Alkali Feldspar-Plagioclase (QAP) ternary diagram (point-counting).....	92
Figure 28A–D. Photomicrographs of variably-altered samples of the Webb Lake stock.....	93
Figure 29A–D. Field and hand sample photos of gabbro/lamprophyre.....	94
Figure 30. Alteration of gabbro/lamprophyre due to a white V <sub>3</sub> quartz vein with tourmaline .....	95
Figure 31A, B. Photomicrographs of gabbro/lamprophyre altered by a V <sub>3</sub> vein.....	96
Figure 32A–D. Field and hand sample photographs as well as photomicrographs of quartz diorite .....	97
Figure 33A–C. Hand sample and drill core photos of silica-poor diorite–monzodiorite.....	98
Figure 34A–C. Hand sample and field photos of silica-poor diorite–monzodiorite .....	99
Figure 35A, B. Photomicrographs of silica-poor diorite–monzodiorite altered by V <sub>3</sub> veins.....	100
Figure 36A–D. Hand sample and field photos of diabase–quartz diabase.....	101
Figure 37A, B. Photomicrographs of diabase–quartz diabase .....	102
Figure 38A, B. Dacitic samples plotted on mobile element classification diagrams .....	115
Figure 39A, B. Dacitic samples plotted on immobile element classification diagrams.....	116
Figure 40A–G. CI carbonaceous chondrite-normalized rare earth element diagrams with yttrium .....	117
Figure 41. Isocon diagram: Alteration of dacite by V <sub>1</sub> -V <sub>2</sub> veins .....	118
Figure 42. Isocon diagram: Alteration of dacite by a V <sub>GD</sub> vein .....	119
Figure 43. Isocon diagram: Non-auriferous carbonate-sericite alteration of dacite.....	120
Figure 44. Mass balance results histogram: Non-auriferous carbonate-sericite alteration .....	124
Figure 45. Quartz-Alkali Feldspar-Plagioclase (QAP) ternary diagram (CIPW Norm).....	126



Figure 46A–D. Geochemical classification plots for intrusive lithologies .....	129
Figure 47. Isocon diagram: Alteration of gabbro by V <sub>1</sub> -V <sub>2</sub> veins.....	130
Figure 48. Anorthite (An)-Orthoclase (Or)-Albite (Ab) ternary diagram: Webb Lake stock.....	132
Figure 49. Isocon diagram: Alteration of the Webb Lake stock by V <sub>1</sub> -V <sub>2</sub> veins .....	133
Figure 50. Isocon diagram: Alteration of gabbro/lamprophyre by a V <sub>3</sub> vein .....	135
Figure 51. Mass balance results histogram: Alteration of gabbro/lamprophyre by a V <sub>3</sub> vein .....	136
Figure 52. Isocon diagram: Alteration of silica-poor diorite–monzodiorite by a V <sub>3</sub> quartz vein .....	138
Figure 53. Mass balance results histogram: Alteration of silica-poor diorite–monzodiorite by V <sub>3</sub> veins	139
Figure 54A, B. Annite-Phlogopite-Eastonite-Siderophyllite (APSE) diagrams .....	145
Figure 55A–C. Chlorite classification diagrams .....	147
Figure 56A–C. Muscovite-Magnesium Celadonite-Ferrocaldonite (MMF) ternary diagrams .....	149
Figure 57A–C. Anorthite-Albite-Orthoclase (An-Ab-Or) ternary diagrams .....	151
Figure 58A–C. Magnesite-Siderite-Calcite (MSC) ternary diagrams.....	153
Figure 59. Distribution of gold grades in alteration strength groupings .....	156
Figure 60. δ <sup>34</sup> S vs Δ <sup>33</sup> S plot .....	158
Figure 61. Cathodoluminescent photomicrographs of zircons .....	160
Figure 62A, B. Geochronological results for the least-altered sample .....	161
Figure 63A–D. Geochronological results for the altered sample.....	162
Figure 64A–C. Drill core displaying alteration related to V <sub>1</sub> -V <sub>2</sub> veining.....	214
Figure 65A, B. Photos of chloritoid and garnet .....	215
Figure 66A–D. Photos of dacite variably-altered by V <sub>GD</sub> auriferous quartz veining.....	216
Figure 67. Photomicrographs of dacite variably-altered by V <sub>GD</sub> veins.....	217
Figure 68. Mineral proportions in dacites from various V <sub>1</sub> -V <sub>2</sub> vein-related alteration envelopes.....	218
Figure 69A, B. Geochronological results for the DD91 standard.....	226
Figure 70. Cathodoluminescent photomicrographs of zircons with spot locations .....	227

## List of Tables

Table 1. Summary of Actlabs analytical methods used for this thesis.....	24
Table 2. Alteration strength groupings .....	33
Table 3A, B. Alteration mineral proportions in variably-altered dacitic samples .....	84
Table 4. Summary of chemical enrichments and depletions due to alteration.....	121
Table 5. Mass balance results: Alteration of dacite by V <sub>1</sub> -V <sub>2</sub> veins .....	122
Table 6. Mass balance results: Alteration of dacite by V <sub>GD</sub> veins .....	123
Table 7. Mass balance results: Non-auriferous carbonate-sericite alteration of dacite.....	125
Table 8. Mass balance results: Alteration of gabbro by V <sub>1</sub> -V <sub>2</sub> veins.....	131
Table 9. Mass balance results: Alteration of the Webb Lake stock by V <sub>1</sub> -V <sub>2</sub> veins.....	134
Table 10. Mass balance results: Alteration of gabbro/lamprophyre by a V <sub>3</sub> vein.....	137
Table 11. Mass balance results: Alteration of silica-poor diorite–monzodiorite by V <sub>3</sub> veins.....	140
Table 12A, B. Summary of microprobe analyses of biotite.....	144
Table 13A, B. Summary of microprobe analyses of chlorite.....	146
Table 14A, B. Summary of microprobe analyses of white mica .....	148
Table 15A, B. Summary of microprobe analyses of plagioclase .....	150
Table 16A, B. Summary of microprobe analyses of carbonate minerals.....	152
Table 17A, B. Summary of concentrations of chemical species in each lithology .....	219
Table 18. Concentrations of chemical species in auriferous quartz veins .....	224
Table 19. Results & interpretations from this thesis & select information from other studies .....	228

## List of Abbreviations

An-Ab-Or: Anorthite-albite-orthoclase  
apfu: Atoms per formula unit  
APSE: Annite-phlogopite-siderophyllite-eastonite  
AR-FIMS: Aqua regia – Hg cold vapour flow injection technique  
AR-MS: Aqua regia – mass spectrometry  
Avg: Average  
bdl: Below detection limit  
C: Concentration  
Cert: Actual/known or certified value  
CL: Cathodoluminescence  
CV: Coefficient of variation  
CLLDZ: Cadillac Larder Lake deformation zone  
cm: Centimetres  
c.: Circa  
Dev: Deviation  
DL: Detection limit  
e.g.: For example  
FA-AA: Fire assay – atomic absorption finish  
FA-MS: Fire assay – mass spectrometry  
FA-GRA: Fire assay – gravimetric finish  
Fe<sub>2</sub>O<sub>3</sub>T: Total iron  
FUS-MS: Lithium metaborate/tetraborate fusion – mass spectrometry  
FUS-ICP: Lithium metaborate/tetraborate fusion – inductively coupled plasma atomic emission spectrometry  
GLDZ: Goudreau Lake Deformation Zone  
GSC: Geological Survey of Canada  
g/t: Grams per tonne  
HCl: Hydrochloric acid  
IR: Infrared detection  
J: Joules  
km: Kilometres  
kV: Kilovolts  
KSZ: Kapuskasing structural zone  
LA-ICP-MS: Laser ablation inductively coupled plasma mass spectrometry  
LOI: Loss on ignition  
LOQ: Limit of quantification  
m: Metres  
M: molar  
Max: Maximum  
MDF: Mass-dependent fractionation  
Meas: Measured value  
MIF: Mass-independent fractionation  
Min: Minimum  
mm: Millimetres  
MMF: Muscovite-magnesium celadonite-ferroceladonite

MSC: Magnesite-siderite-calcite  
MSc: Master's of Science  
MSWD: Mean square weighted deviation  
N/A: Not applicable  
nA: Nanoamperes  
nd: Not detected  
NRCan: Natural Resources Canada  
oz: Ounces  
PGNAA: Prompt gamma-neutron activation analysis  
ppb: Parts per billion  
ppm: Parts per million  
QAP: Quartz-alkali feldspar-plagioclase  
QA/QC: Quality assurance quality control  
Qtz: Quartz  
RD: Relative difference  
REE: Rare earth element  
RSD: Relative standard deviation  
SE: Standard error  
SEM-EDS: Scanning electron microscope – energy dispersive spectroscopy  
SEM-MLA: Scanning Electron Microscope – Mineral Liberation Analyser®  
SPDM: Silica-poor diorite–monzodiorite  
Std: Standard or reference material  
Standard: Standard or reference material  
TAS: Total alkali-silica  
TD-MS: Total digestion – mass spectrometry  
TITR: Titration  
TTG: Tonalite-trondhjemite-granodiorite  
µm: Micrometers  
VCDT: Vienna-Canyon Diablo Troilite  
vol%: Volume percent  
WDS: Wavelength-dispersive X-ray spectroscopy  
WLS: Webb Lake stock  
wt%: Mass percent  
~: Approximately  
#: Number  
ΔC: Change in concentration

## 1.0 Introduction

Orogenic gold deposits are the source of ~75% of the gold obtained throughout human history (Phillips, 2013). These economically important deposits are typically generated in mid-crustal rocks that have been subject to deformation and greenschist- to lower amphibolite-facies metamorphism. Gold is carried by hydrothermal fluids through orogeny-related, crustal-scale structures that act as conduits for these fluids (Groves, 1993; Goldfarb et al., 2001; Tomkins, 2013). Gold is deposited when changing chemical or mechanical conditions cause the gold-rich fluids to no longer be in equilibrium with their surroundings (Tomkins, 2013). However, the source and chemistry of these gold-bearing fluids, the chemical complexes that carry the gold in the fluids, the changes in conditions that cause the gold to precipitate, and the tectonic environments associated with such deposits are genetic aspects that are commonly unclear (Tomkins, 2013). A variety of genetic models have been proposed, many of which could be reasonable approximations for specific deposits but cannot be universally applied. As a result, detailed studies of individual orogenic gold deposits is crucial for developing genetic models that can be applied locally and regionally.

Greenstone belts within the Superior Province of the Canadian Shield host many world-class orogenic gold deposits and these deposits are significant economic drivers for many communities (Goldfarb et al., 2001). This study focuses on the Island Gold deposit located ~35 km north of Wawa, Ontario, and a 30-minute drive from the town of Dubreuilville (Figure 3). This deposit is situated ~100 km southeast of the Hemlo greenstone belt which contains the Hemlo gold deposit (Figure 2). The Island Gold mine is easily accessible by road and is owned and operated by Alamos Gold Inc. The Island Gold deposit has some of the highest-grade gold intersections in the Superior Province (Adam et al., 2017). It is located within the Goudreau Lake Deformation Zone (GLDZ) and this is thought to be the conduit that focused the fluids that resulted in gold mineralization. This deformation zone has been correlated with the large, gold-rich fault systems east of the Kapuskasing Structural Zone (Leclair et al., 1993). Some important areas of gold mineralization east of the Kapuskasing Structural Zone include the Kirkland Lake, Timmins, and Rouyn-Noranda mining camps (Figure 2). The Island Gold deposit therefore provides a unique opportunity to study orogenic ore-forming processes at an easily accessible, high-grade orogenic gold deposit at the less-studied western extent of this economically important fault zone.

This thesis integrates geochemistry, geochronology, petrography, scanning electron microscopy, and sulphur isotope analysis to identify the protoliths of altered lithologies, fully characterize the alteration associated with the auriferous hydrothermal fluids, provide effective indicators for gold mineralization, determine the age(s) of gold mineralization, and constrain the source of the auriferous fluid at the Island Gold deposit. This will assist with ore zone targeting, provide regional exploration vectors, update the genetic model and geological history of the deposit, and contribute to the understanding of orogenic gold deposits globally. A companion study has been conducted by Katia Jellicoe, a MSc student at the University of Waterloo, that focuses on the structural geology associated with the Island Gold deposit (Jellicoe, 2019).

The following thesis is divided into a total of seven sections. The remainder of the first section (1.1) provides the geological setting of the Island Gold deposit. The second section (2) outlines the research objectives of this thesis. Section 3 details the analytical methods used and Section 4 summarizes the results. Section 5 discusses the implications of the results and Section 6 presents the conclusions. Recommendations for future work are discussed in Section 7. All supplementary information is included in the Appendices.

## **1.1 Geological Setting**

### **1.1.1 Superior Province**

The Island Gold deposit is located within the Superior Province, which makes up a large portion of the Canadian Shield and extends from Quebec in the east to Manitoba in the west. The Superior Province is dominated by Mesoarchean to Neoarchean tonalitic-trondhjemitic-granodioritic (TTG) suites and also contains sublinear and anastomosing greenstone belts (Percival et al., 2012). These greenstone belts are composed of metavolcanic rocks as well as minor metasedimentary rocks (Percival et al., 2012). The Superior Province is divided into fault-bounded terranes that have been interpreted to represent north-directed terrane accretion between 2720 and 2680 Ma (Percival et al., 2012; Bédard and Harris, 2014). Archean rocks of the Superior Province are intruded by Proterozoic and Phanerozoic mafic dyke swarms.

The margins of the Superior Province are bounded by Proterozoic orogenic belts (Figure 1; Hoffman, 1988). Beginning at 1.9 Ga, the Paleoproterozoic Trans Hudson Orogen sutured the Hearne and Wyoming Provinces to the western and northern margins of the Superior Province (Berman et al., 2007). To the northeast, the New Quebec Orogen (2.17–1.77 Ga) welds the

southeastern part of the Rae Province to the Superior Province and the Torngat Orogen (~1.8 Ga) connects the Nain Province to the Superior Province (Machado et al., 1997; Van Kranendonk, 1996; Hoffman, 1988). To the south, the Superior Province is bounded by the 1.90–1.83 Ga Penokean Orogen as well as the younger 1.14 Ga Keweenawan rift (Hoffman, 1988). The Neoproterozoic Grenville Orogeny bounds the eastern margin of the Superior Province (Rivers et al., 2012). As a result of these orogens, in addition to those related to the amalgamation of the Superior Province itself, this province exhibits polyphase deformation. Large fault systems are concentrated in greenstone belts in the interior of the craton and are commonly associated with gold deposits (Percival et al., 2012) including the Island Gold deposit.

The mechanism for the amalgamation of the terranes that comprise the Superior Province is still debated (Bédard, 2006; Bédard, 2013; Wyman, 2013a; 2013b) and there are currently two dominant models. Subduction-driven accretion of terranes in the Archean Superior Province is proposed based on a uniformitarian model of plate tectonics that includes mid-ocean ridge spreading and subduction (Cawood et al., 2006, Warren, 2011, Wyman, 2013a). However, notable differences arise when examining Archean geology and comparing it to the Proterozoic and Phanerozoic Eons. These include the lack of high pressure-high temperature lithologies and adakites, presence of komatiites, and the dominance of TTG suites (Bédard, 2006). As a result, a second model that involves vertical or plume-driven tectonics was hypothesized for the Superior Province. This model uses mantle wind and plumes as the dominant forces that drove terranes northward to create the composite Superior Province (Bédard, 2006; Bédard and Harris, 2014). Others suggest that the Neoproterozoic was a transition period in the Superior Province where both subduction-driven and vertical tectonic processes were operating (Lin, 2005; Lin and Beakhouse, 2013). Due to this controversy, it is not clear whether one or parts of each of these models explains the history of the Superior Province.

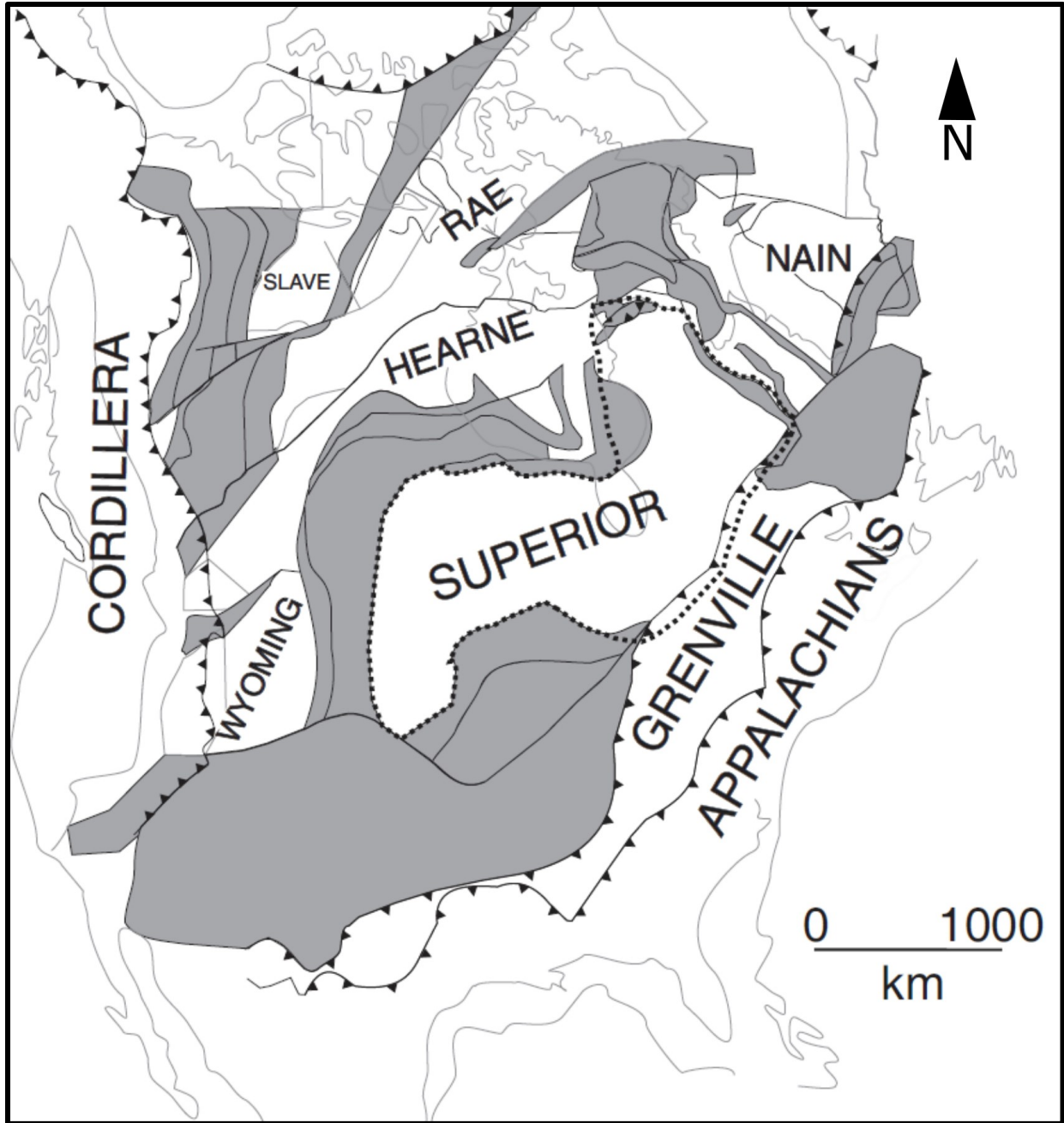


**Figure 1.** Tectonic framework of the North American continent. Paleoproterozoic domains related to the formation of Laurentia are shown in grey (Percival et al., 2012). Modified from Percival et al. (2012); After Hoffman (1989).

### 1.1.2 Wawa-Abitibi terrane

The Wawa-Abitibi terrane is one of the largest terranes in the Superior Province and is also a region of significant mineral wealth within the Superior Province (Figure 2). This terrane is composed of sublinear, east–west trending supracrustal belts enveloped by larger granitoid-dominated regions. Plutonic and volcanic rocks range in age from approximately 2.9 to 2.6 Ga and 2.9 to 2.7 Ga, respectively (Percival et al., 2012). In some cases, volcanic rocks are unconformably overlain by greywacke and conglomerate sedimentary rocks (Percival et al., 2012). Most authors agree that the Wawa and Abitibi terranes are broadly correlative (Percival and Easton, 2007) but earlier studies separated them into distinct subprovinces/terrane (Williams, 1989). The Kapuskasing uplift that exposes deeper gneissic crust (Percival et al., 2012) geographically separates the historical Wawa and Abitibi terranes. The Island Gold deposit is located within the Wawa-Abitibi terrane, west of this Kapuskasing Structural Zone (Figure 2).

Moving from the west towards east, the Wawa-Abitibi terrane is bounded to the north by the Western Wabigoon, Marmion and Opatica Terranes and to the south by the Minnesota River Valley Terrane, Pontiac Belt and Grenville Province (Percival et al., 2012). The Wawa-Abitibi terrane collided with the Winnipeg River-Marmion Terrane at 2690 Ma during the Shebandowanian Orogeny (Percival et al., 2012). This was followed by the collision with the Minnesota River Valley Terrane during the Minnesotan Orogeny which began at 2685 Ma (Percival et al., 2012). Geological histories at various localities within this terrane have been explained with reference to evolving oceanic environments including volcanic arcs, plateaus, accretionary margins and rifts (Thurston, 1994; Bédard and Ludden, 1997; Wyman and Kerrich, 2010).



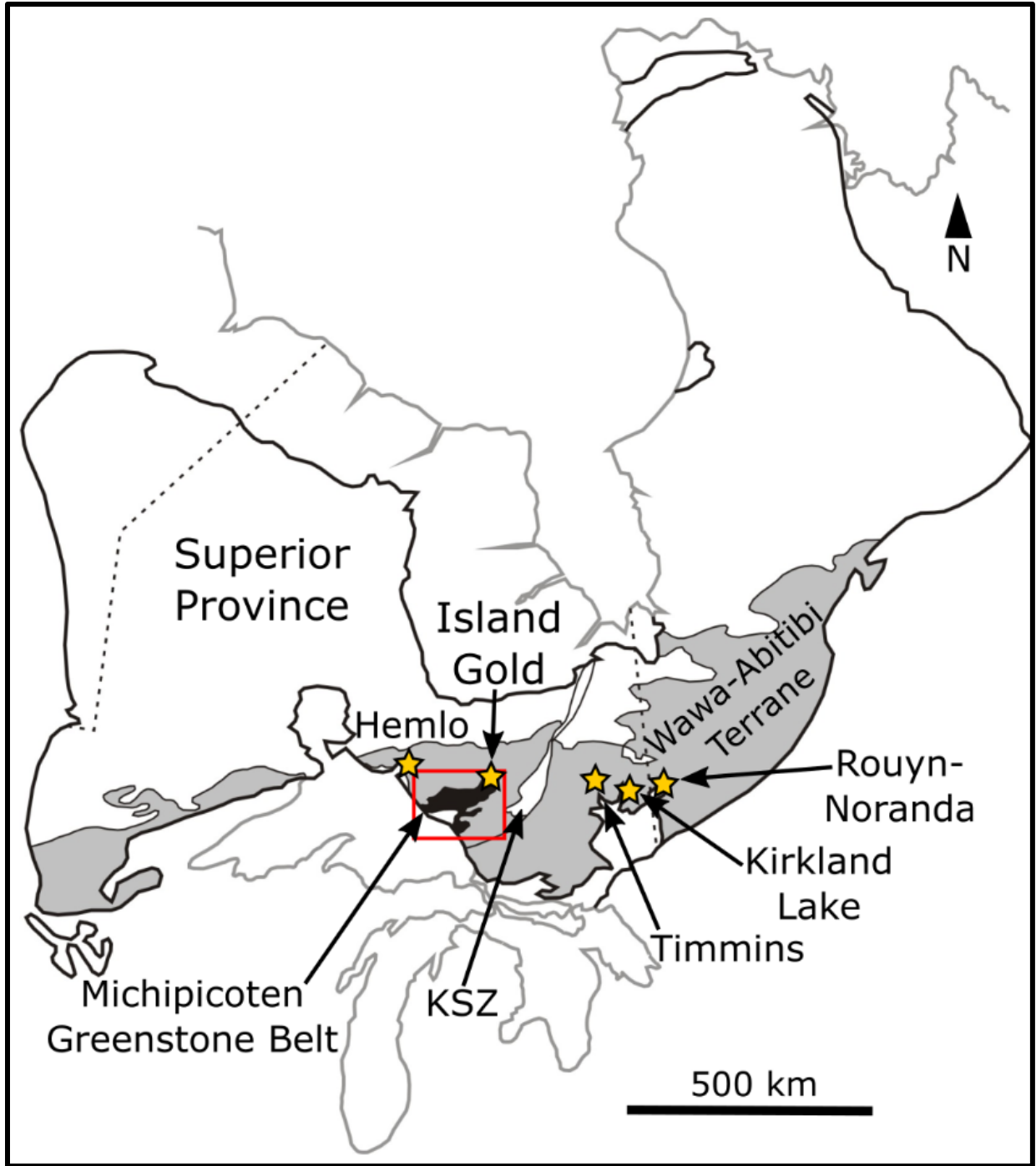


**Figure 2.** Position of the Michipicoten greenstone belt within the Wawa-Abitibi terrane of the Superior Province. Location of a variety of large gold camps as well as the Island Gold deposit (gold stars). The red rectangle outlines the extent of Figure 3. KSZ=Kapuskasing Structural Zone. Modified from Card (1990), Williams et al. (1991), and Jellicoe (2019).

### 1.1.3 Michipicoten greenstone belt

The Michipicoten greenstone belt is an approximately east-west trending belt within the Wawa Subprovince (Figure 2) and is dominantly composed of metamorphosed volcanic and sedimentary rocks as well as various intrusive rocks (Figure 3). The volcanic rocks are subdivided into three volcanic cycles of *c.* 2900, 2750 and 2700 Ma in age (Turek et al., 1984; 1992; Arias and Helmstaedt, 1990; Sage, 1994). The rocks of the first, second and third cycles of volcanism are part of the Hawk, Wawa and Catfish assemblages of Williams et al. (1991), respectively (Sage, 1994). These felsic–intermediate volcanic rocks are mineralogically and compositionally similar, making it challenging to distinguish which cycle they are from without geochronology (Sage, 1994). The bottom of each cycle is composed of ultramafic–mafic rocks and the sequence progressively becomes more felsic upwards through the cycle. Lower mafic and upper felsic portions of the cycles are often separated by discontinuities (Sage, 1994) but can be locally conformable (Sylvester et al., 1987). Ultramafic rocks in the 2900 Ma cycle consist of komatiites whereas mafic units in the younger cycles are tholeiitic basalts. The 2900 and 2750 Ma cycles are capped by an unconformity separating the volcanic rocks from overlying iron formations. These iron formations are interpreted to represent periods of relatively quiet sedimentation with hydrothermal input of iron from submarine vents in the sedimentary basin (Sage, 1994; Bekker et al., 2010). The supracrustal rocks are cut by dioritic–gabbroic intrusions as well as granitic stocks of various ages (Sage et al., 1996). This is likely a result of magmatism associated with each of the volcanic cycles.

The Doré metasedimentary rocks are extensive in the Michipicoten Greenstone Belt (Figure 3) and unconformably overlie the 2700 Ma cycle. Wacke and conglomerates with a wacke matrix comprise the majority of this unit. Clasts in the conglomerate consist of mainly felsic–intermediate volcanic rocks and granitic rocks (Sage, 1994). As discussed in Sage (1994), the clasts and matrix have U-Pb zircon ages that are equivalent to or slightly younger than the third cycle volcanic rocks (Turek et al., 1982; Turek et al., 1984; Corfu and Sage, 1987; Corfu and Sage, 1992; Turek et al., 1992). This suggests that the third cycle volcanic rocks and their intrusive equivalents are the source of the Doré metasedimentary rocks (Sage, 1994). Relatively undeformed diabase dykes of early Proterozoic age crosscut the deformed supracrustal rocks. The Michipicoten greenstone belt is bordered by granitoids that are mainly younger than rocks within the greenstone belt (Sage, 1994). Proximal to the margins of the greenstone belt, U-Pb

ages obtained from these external granitoids are younger than or of equivalent age to the 2750 Ma volcanic cycle (Turek et al., 1982). Approximately 25 km away from the eastern margin of the Michipicoten greenstone belt, 2920 Ma tonalitic gneisses are present (Moser et al., 1991). It is unclear how these distant older gneisses relate to the younger granitoids immediately surrounding the greenstone belt (Sage, 1994).

The Michipicoten greenstone belt reached amphibolite facies at its margins and only greenschist facies at the centre. This belt is interpreted to be an originally monoclinial sequence that was affected by both horizontal and vertical components of motion including thrusting, folding and shearing (Sage, 1994). It is unclear whether the higher metamorphic grade at the margins of the belt and the pervasive deformation are a result of subduction-related collision or vertical tectonic processes (Sage, 1994). Most studies published between 1970 and 1995 have interpreted the tectonic environment to involve an island arc transitioning into a continental arc (Sylvester et al., 1987; McGill, 1992; Sage, 1994). Both north-dipping (Williams, 1989) and south-dipping (Sage, 1994) subduction zones have also been hypothesized. More recently, vertical tectonics involving sagduction of the denser supracrustal rocks and diapirism of younger tonalites on either side have also been suggested (Lin and Beakhouse, 2013).

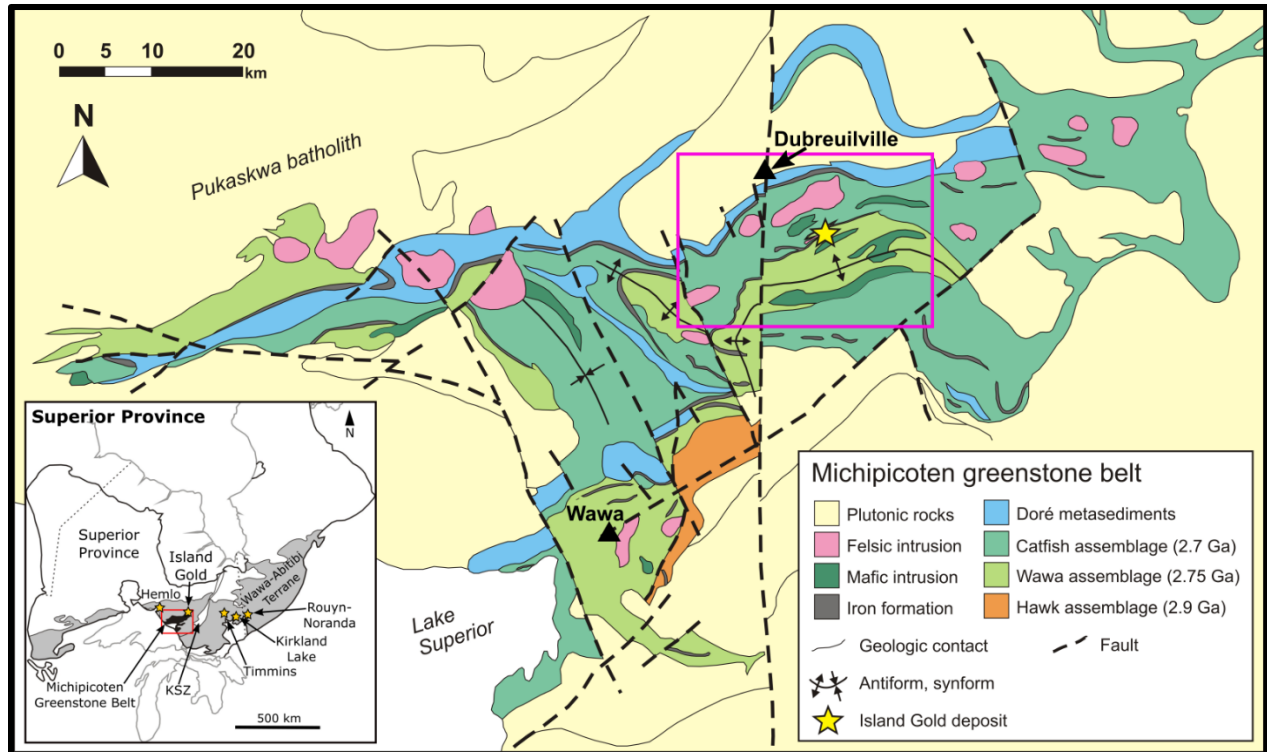


**Figure 3.** Geological map of the Michipicoten greenstone belt. Modified from Heather and Arias (1987), Williams et al. (1991), and Jellicoe (2019). The purple rectangle outlines the extent of Figure 4. Inset shows the location of the Michipicoten greenstone belt within the Superior Province map (modified from Card, 1990; Williams et al., 1991; Jellicoe, 2019).

#### 1.1.4 Local geology of the Island Gold deposit area

The Island Gold deposit is located within the Goudreau-Lochalsh gold district which is part of the Wawa gold camp. There are several closed gold mines and many gold showings located in or associated with the Goudreau Lake Deformation Zone (GLDZ) which is approximately 4.5 km wide and over 25 km in length (Heather and Arias, 1987; Figure 4). This deformation zone records sinistral deformation and, based on the association of gold deposits and showings with this deformation zone, it is thought to be the conduit that provided auriferous fluids to the district (Turcotte and Pelletier, 2008; Adam et al., 2017; Jellicoe, 2019). The GLDZ and the Island Gold deposit are located on the northern limb of a regional anticline in the northern portion of the Michipicoten greenstone belt (Figure 4). Rocks within the GLDZ have been metamorphosed to greenschist facies and were subject to various degrees of shearing and hydrothermal alteration (Heather and Arias, 1987).

The Island Gold deposit is hosted within felsic–intermediate volcanic rocks that were generated during the second cycle of volcanism (Arias and Helmstaedt, 1990). These volcanic rocks include tuffs, flows, intrusive rocks, and pyroclastic fragmental rocks (Adam et al., 2017). These second cycle volcanic rocks are capped to the north by the Goudreau Iron Range which separates the second cycle volcanic rocks from the third cycle volcanic rocks. All volcanic units in this area generally strike 070–090° and have subvertical dips (Adam et al., 2017).

Within the GLDZ, the trondhjemitic Webb Lake stock hosts the Magino deposit (Figure 4). Similar to the volcanic units, the Webb Lake stock strikes ENE (Figure 4) and dips steeply to the north (Figure 5). Other large intrusive bodies nearby include the Herman Lake nepheline-syenite intrusive complex and the Maskinonge Lake granodiorite stock (Figure 4). Various other smaller intrusive units of various ages have been identified at the Island Gold deposit but, in many cases, their protoliths are obscured due to metamorphism, deformation and alteration. Detailed geochemical and petrographic study has not yet been performed on many of these lithologies. Northerly-striking, undeformed diabase intrusions are also present.

Three distinct deformation events were identified in Jellicoe (2019) and are summarized below. The first regional compressional event (D1) developed the S1 cleavage and large F1 folds. North-side-up transpression (D2) resulted in the development of the S2 foliation and the GLDZ which are subparallel to each other. This deformation event was also synchronous with metamorphism and the emplacement of the gold-bearing quartz veins at the Island Gold deposit.

Dextral, south-side up transpression (D3) resulted in F3 folds and S3 cleavage which partially overprint and deform pre-existing structures (Jellicoe, 2019).

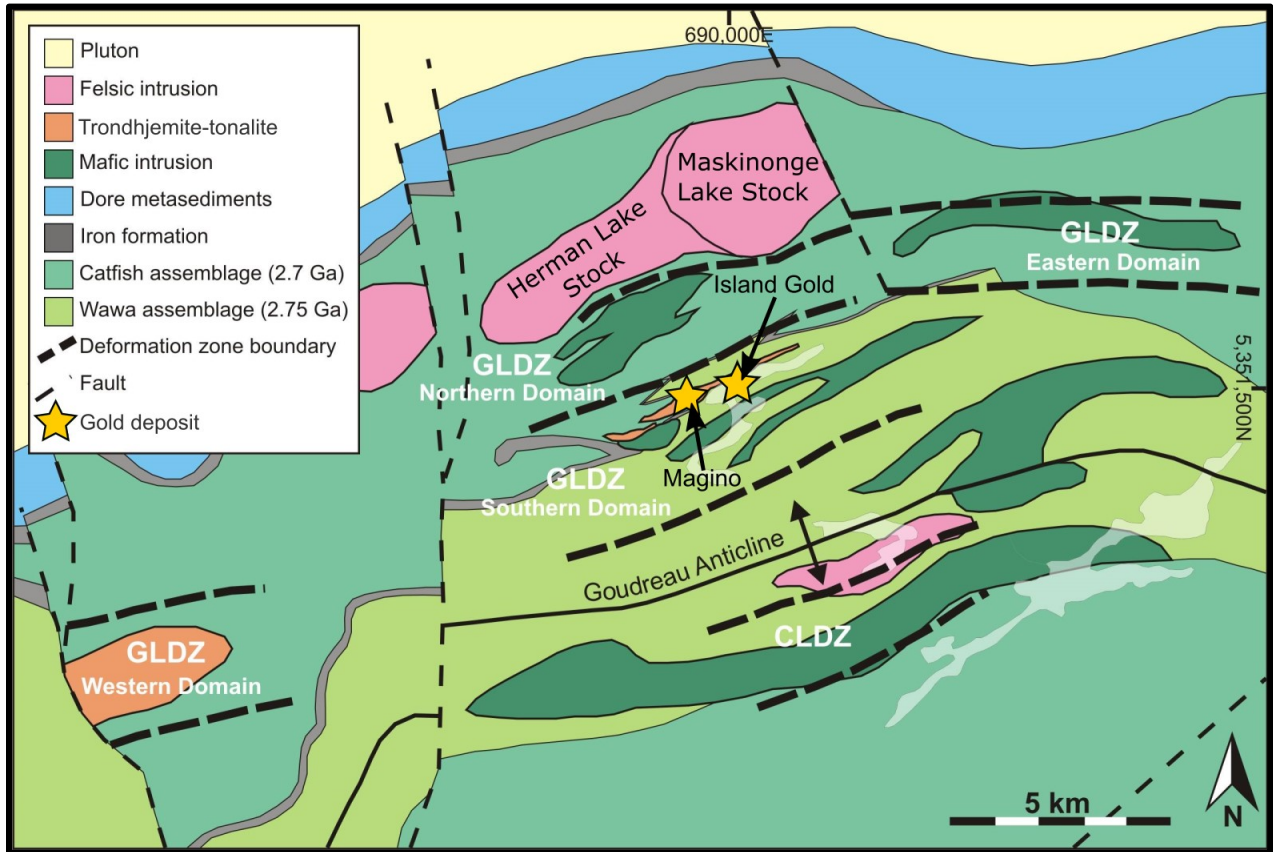


**Figure 4.** Local geology map of the Island Gold deposit and surrounding area. Modified from Heather and Arias (1987), Williams et al. (1991), and Jellicoe (2019). GLDZ: Goudreau Lake Deformation Zone. CLDZ: Cradle Lake Deformation Zone.

### 1.1.5 Gold mineralization and veining

At the Island Gold deposit, gold is concentrated within multiple, subparallel zones that have an east–northeast strike and a steep southerly dip (Figure 5). Between the 400 and 500 m levels, these major ore zones are inflected towards the south (Adam et al., 2017). These ore zones consist of two gold-bearing quartz ( $\pm$  carbonate) vein types ( $V_1$  and  $V_2$ ).  $V_1$  veins are shear veins while  $V_2$  veins are extensional veinlets. Both of these veins are believed to have formed during the same gold mineralization event, are intimately associated with each other, and cross-cut each other (Jellicoe, 2019). An envelope of hydrothermal alteration and high strain centres around  $V_1$ - $V_2$  veins and decreases in intensity moving outwards. It is difficult to differentiate the effects of a  $V_1$  vein versus a  $V_2$  vein on the surrounding wall rock due to their close association and as a result, the alteration associated with these veins is studied together in this thesis. The alteration that typically surrounds these gold-bearing quartz veins has been termed API (Alteration Package Island) by Alamos geologists. Mainly based on macroscopic study, API is thought to have been produced due to a combination of silicification, sericitization, feldspathization, carbonatization, sulphidization, chloritization, and biotitization (Adam et al., 2017). Prior to this thesis, the author is not aware of any petrographic and geochemical studies that focus primarily on the auriferous alteration at the Island Gold deposit. Alteration halos range up to 8 m in size (Adam et al., 2017) and the degree of alteration have been characterized using subjective terms ranging from very weak to very strong. A third vein type ( $V_3$ ) is also present but these are gold-barren, quartz-carbonate extensional veins that cross-cut ore zones (Jellicoe, 2019). Tourmaline ( $\pm$  quartz  $\pm$  carbonate) veins ( $V_4$ ) post-date  $V_3$  veins and invade/cross-cut all pre-existing structures and lithologies (Jellicoe, 2019). Unlike the gold-bearing quartz veins,  $V_3$  and  $V_4$  veins do not typically result in significant alteration of the surrounding wall rock.

Mine geologists have divided auriferous zones at the Island Gold deposit into two major areas of gold mineralization that are further subdivided: The Island Gold Zones (Main and Lower portions; Figure 5) and the Goudreau Zone. Other gold zones are also present on the property (Adam et al., 2017). The Goudreau Zone is unique from the Island Gold Zones because in addition to  $V_1$ - $V_2$  gold mineralization, this zone hosts a tightly-folded, gold-bearing, extensional quartz ( $\pm$  carbonate) vein ( $V_{GD}$  vein; Jellicoe, 2019). This vein set generally has a NNE-SSW strike and an average dip of  $30^\circ$  towards the east (Adam et al., 2017). Shears that host  $V_1$ - $V_2$  veins are observed offsetting  $V_{GD}$  veins (Jellicoe, 2019). For simplicity, quartz  $\pm$  carbonate veins

are often referred to simply as veins or quartz veins in this thesis. VGD, V1, V2, V3, and V4 vein types at the Island Gold deposit were identified in Jellicoe (2019). Subscripts are applied to these vein identifiers in this thesis (V<sub>GD</sub>, V<sub>1</sub>, V<sub>2</sub>, V<sub>3</sub>, and V<sub>4</sub>).

Hydrothermal alteration halos surround each of these vein types. The majority of the ore zones at this deposit (> 90%) are hosted by quartz veins within the felsic–intermediate volcanic rocks and a small amount (< 10%) are hosted by gabbro. Ore zones hosted by quartz veins in the Webb Lake stock are not common at the Island Gold deposit. However, this lithology is the main host lithology at the nearby Magino gold deposit (Turcotte and Pelletier, 2008) which is located to the west and along strike with the Goudreau Lake Deformation Zone.

Despite being hosted by different lithologies, gold mineralization within the Magino and Island Gold deposits are believed to have resulted from similar processes along the same major structures (Heather and Arias, 1992). Both of these deposits are classified as greenstone-hosted orogenic gold deposits (Adam et al., 2017; Turcotte and Pelletier, 2008). In the case of these two deposits, the structural conduit for auriferous fluids is believed to be the GLDZ. The Kremzar deposit is approximately one kilometre north of the GLDZ and is hosted within the third cycle mafic volcanic rocks and is controlled by a northwest-trending splay of the GLDZ (Adam et al., 2017).

At the end of 2016, the Island Gold Mine had estimated indicated and measured resources of 478,800 tonnes at 5.94 g/t Au (91,400 oz) as well as inferred resources estimated at 3,041,800 tonnes at 10.18 g/t Au (995,700 oz) (Adam et al., 2017). Simultaneously, proven and probable mineral reserves were estimated at 2,551,000 tonnes at 9.17 g/t Au (752,200 oz) (Adam et al., 2017).



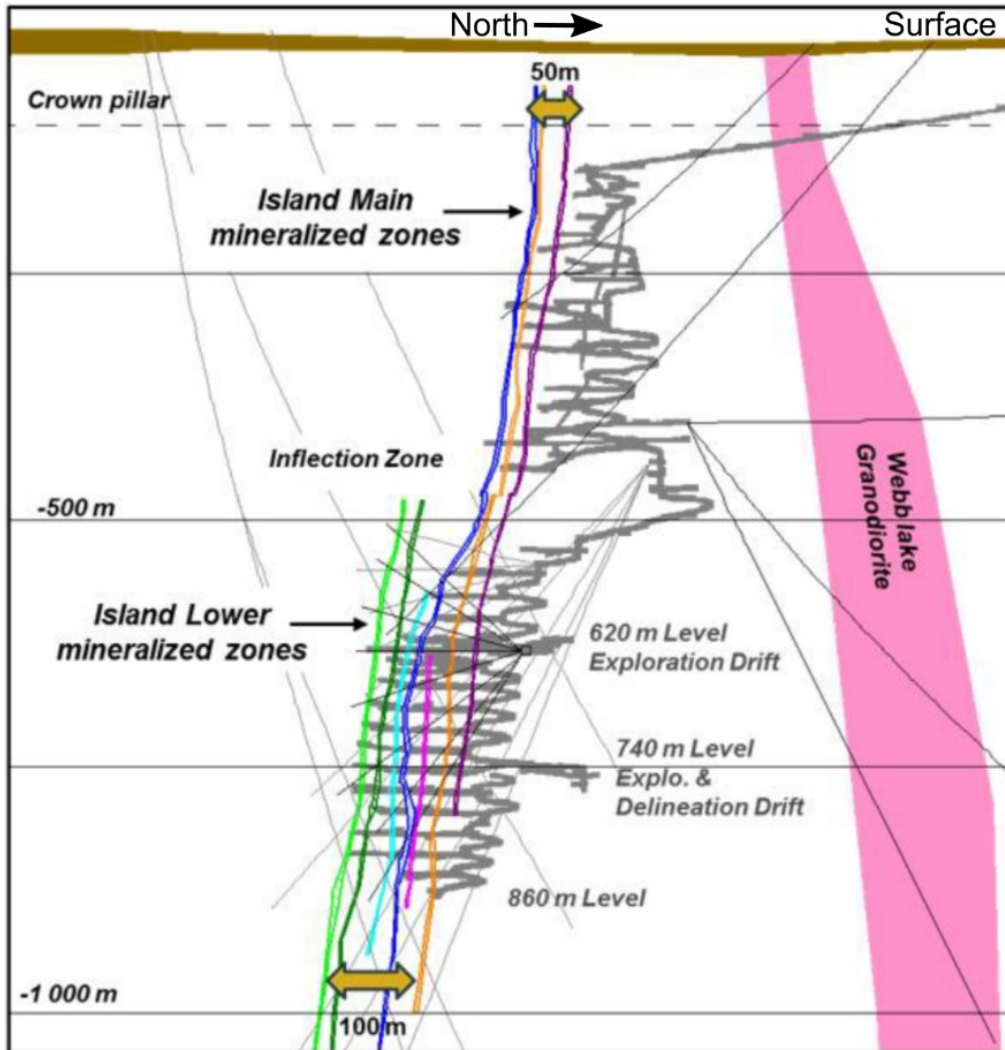


**Figure 5.** Cross section displaying a portion of the Island Gold deposit. The location of some of the existing ramps and drifts, major ore zones, and the Webb Lake stock are displayed. Modified from Adam et al. (2017).

## **2.0 Objectives, purpose, and applications**

The five main objectives of this thesis focusing on the Island Gold deposit are:

- 1) Determine the protoliths of major lithologies and the effects of metamorphism on these lithologies;
- 2) Characterize the alteration envelopes associated with various gold-bearing quartz veins and compare them with alteration at other orogenic gold deposits east of the Kapuskasing Structural Zone;
- 3) Establish mineralogical indicators and geochemical vectors for gold mineralization;
- 4) Constrain the source of the gold-bearing fluid using multiple sulphur isotopes; and
- 5) Determine the age(s) of gold mineralization.

### **2.1 Protoliths and metamorphism**

Due to the hydrothermal alteration associated with veining, deformation, and metamorphism it is often difficult to determine the protolith(s) of lithologies at the Island Gold deposit. However, identifying the protoliths of metamorphosed and altered lithologies is key to unravelling the full geological history, including the volcanic-sedimentary sequence, in order to target new deposits in the area. Through whole-rock geochemistry, petrography, scanning electron microscopy with energy dispersive spectroscopy (SEM-EDS), and electron microprobe analysis, this study identifies the protoliths or confirms previously identified protoliths of the various lithologies commonly encountered at the Island Gold deposit. This thesis also identifies the effects of metamorphism on these lithologies. Using mineral proportions and/or whole-rock geochemical data from least-altered samples of each lithology, an industry-standard geological name is assigned for each interpreted protolith.

### **2.2 Auriferous alteration**

Characterization of the alteration envelopes associated with the auriferous quartz vein corridors is the major focus of this thesis. Prior to this study, the alteration envelopes at the Island Gold deposit were mainly studied by mine geologists macroscopically and through limited geochemistry. Defining the signature of these alteration envelopes is crucial because they are significantly larger than the ore zones themselves. As a result, they are easier exploration targets and, if intersected, can be used to converge on ore zones.

This thesis identifies alteration mineral assemblages and geochemical vectors towards mineralized zones for each of the main host lithologies at this deposit (dacitic volcanic rocks, gabbro, and the Webb Lake stock). This will assist with the identification of weak alteration and

thereby help locate ore zones. The alteration envelopes are subdivided into zones based on the intensity of alteration and this is quantified using geochemistry. This addresses the use of the subjective terms currently used for describing the alteration halo surrounding the ore zones at the Island Gold deposit (strongly, moderately, and weakly-altered) by providing quantitative underpinning for these terms. This will also improve the consistency of mapping alteration envelopes and assist with the correlation of ore zones.

The alteration identified at the Island Gold deposit is also compared to the alteration described in previous studies of major orogenic gold deposits in the Timmins, Kirkland Lake, and Rouyn-Noranda mining camps (Figure 2; Dinel et al., 2008; Moritz and Crocket, 1991; Kishida and Kerrich, 1987; Martin, 2012; Bigot, 2012; Couture and Pilote, 1993) and similarities and differences are discussed. Similar to the first objective of this thesis (Section 2.1), analytical techniques used to achieve this second objective include: Whole-rock geochemistry, mass balance calculations, Isocon analysis (Grant, 1986; 2005), petrography, electron microprobe analysis, SEM-EDS, and SEM-MLA.

### **2.3 Mineral indicators and geochemical vectors for gold mineralization**

In samples that do not contain macroscopically-visible gold, it is useful to be aware of features that can be used to estimate gold concentrations. These are valuable for mine geologists especially when differentiating between lower grade ore and waste which is often challenging when working in wet and poorly lit conditions underground. This can be useful in a variety of grade control situations including but not limited to:

- a) Identification of prospective ore zones in drill core prior to assay;
- b) Estimating the grade of a face in order to facilitate further mine planning prior to receiving assay results; and
- c) Estimating gold-grade in oversized material or mislabelled/unlabelled stockpiles.

Gold grade is divided into three groups in this thesis: High-grade ( $> 4$  g/t Au), low-grade (1–4 g/t Au), and waste rock ( $< 1$  g/t Au). Key mineralogical and textural indicators that correspond with each of these groups are identified. The distribution of material in each of these groups within auriferous alteration envelopes is also presented. These objectives are accomplished using whole-rock geochemistry, Isocon analysis (Grant, 1986; 2005), petrography, electron microprobe analysis, SEM-EDS, and SEM-MLA.

## 2.4 Source(s) of sulphur and the gold-bearing fluid

The source of the auriferous fluid responsible for mineralization at the Island Gold deposit is unclear. The fluids responsible for mineralization in Archean orogenic gold deposits may have been sourced from the mantle, cooling crustal felsic intrusive bodies, meteoric water or generated through metamorphism (e.g. Phillips and Groves, 1983; Hronsky et al., 2012; Xue et al., 2013; Tomkins, 2013).

Hydrosulphide complexes are believed to transport gold in hydrothermal fluids (Zhu et al., 2011) and, as a result, sulphide minerals are genetically associated with orogenic gold deposits (Goldfarb et al., 2005). Ratios of sulphur isotopes ( $^{32}\text{S}$ ,  $^{33}\text{S}$ ,  $^{34}\text{S}$ , and  $^{36}\text{S}$ ) can be used to determine the source(s) from which the sulphur was derived and also constrain the temperatures of the fluid during infiltration (Xue et al., 2013; Lambert et al., 1984; Ohmoto and Rye, 1979). While most studies focus on  $\delta^{34}\text{S}$  ratios, other isotopes of sulphur can be used in Archean deposits to track the source of sulphur due to the potential for mass-independent fractionation (MIF) in the Archean. MIF of sulphur is only known to occur due to ultraviolet photolysis reactions in the low oxygen atmosphere of the Archean (Farquhar et al., 2001; Pavlov and Kasting, 2002). These photochemical reactions cause the dissociation of atmospheric  $\text{SO}_2$  to an oxidized species ( $\text{SO}_4^{2-}$  - negative  $\Delta^{33}\text{S}$ ) and a reduced species ( $\text{S}_8$  - positive  $\Delta^{33}\text{S}$ ) (Farquhar and Wing, 2003). These sulphur species are then transferred to meteoric waters and due to differences in solubility, some depositional environments become enriched in  $\text{S}_8$  while others are enriched in  $\text{SO}_4^{2-}$  (Maynard et al., 2013). As a result, some sedimentary rocks have dominantly positive  $\Delta^{33}\text{S}$  sulphur while others have negative  $\Delta^{33}\text{S}$  sulphur. Nonetheless, sulphur in or sourced from Archean sedimentary rocks often exhibits mass-independent fractionation (MIF) (Farquhar et al., 2000) where  $\Delta^{33}\text{S} \neq 0$ . Conversely, sulphur derived from post-Archean sedimentary rocks tends to show mass-dependent fractionation (MDF) (Farquhar et al., 2000) where  $\Delta^{33}\text{S} \approx 0$ . Similarly, juvenile sulphur derived from the Archean mantle (either directly or from igneous rocks of mantle parentage) also exhibits MDF (Farquhar et al., 2002; Xue et al., 2013) where  $\Delta^{33}\text{S} \approx 0$ . Non-zero  $\Delta^{36}\text{S}$  values are also indicative of MIF (Farquhar and Wing, 2003).

Comparing the sulphur isotopes of sulphide minerals from ore zones and veins to other sulphide-bearing lithologies locally is conducted to determine the potential source(s) of sulphur. If the sulphides at the Island Gold deposit are found to have MIF sulphur, this indicates that the

sulphur was at the Earth's surface at some point prior to the gold mineralization event(s) which likely occurred between *c.* 2680 Ma and 2672 Ma (Jellicoe, 2019). Constraining the source of the gold-bearing fluid will improve the understanding of the geological history of the Island Gold deposit and could contribute to the knowledge of orogenic gold deposits as a whole.

## **2.5 Timing of gold mineralization**

The age of gold mineralization at the Island Gold deposit has been bracketed by conducting geochronology on post-mineralization and pre-mineralization lithologies (Jellicoe, 2019). This study attempts to directly determine the age of gold mineralization by conducting an LA-ICP-MS geochronologic study of hydrothermally-altered and least-altered zircons from an ore zone. Altered zircons may show evidence of recrystallization, overgrowth, dissolution, and/or lead loss, which can be used to constrain the age of alteration and hence bracket the timing of gold mineralization (e.g. Schneider et al., 2012). The age of gold mineralization can help prioritize the exploration of structures and lithologies that pre-date this age as well as help target structures that were active during gold mineralization.

### **3.0 Methods**

In this section, major lithologies at the Island Gold deposit are referred to based on their interpreted protoliths (Section 5.1): Quartz ( $\pm$  carbonate) veins ( $V_{GD}$ ,  $V_1$ - $V_2$ , and  $V_3$ ), dacite, iron formation, gabbro, the Webb Lake stock, gabbro/lamprophyre, quartz diorite, silica-poor diorite–monzodiorite, and diabase–quartz diabase.

### **3.1 Sampling**

Samples were taken from drill core, wall rock in mine workings, and outcrops on surface. For all of the samples described below, macroscopic weathering and other contaminants were removed from each sample using a rock hammer or diamond rock saw.

#### **3.1.1 Least-altered samples**

To evaluate the protoliths of the various intrusive and volcanic rocks, samples of least-altered rocks were taken from outside, the margins, and within the GLDZ that correspond with more altered samples. These least-altered samples may have been subject to minor alteration and, in most cases, have been metamorphosed to greenschist facies.

#### **3.1.2 Alteration envelopes and mineral indicators**

Samples were taken moving progressively away from gold-bearing quartz veins towards areas unaffected by alteration related to the auriferous veins. When possible, grab samples with little or no vein-related hydrothermal alteration were also taken from outside of the alteration envelopes to act as representative “least-altered” samples. When selecting samples of altered wall rock, visible quartz veins and veinlets were preferentially avoided. This systematic sampling procedure was performed for alteration envelopes hosted by each of the three major ore-hosting lithologies at Island Gold (dacite, gabbro, and the Webb Lake stock). Furthermore, in order to identify if the alteration changed with varying distance (parallel to the GLDZ) or elevation, this was also undertaken for multiple dacite-hosted alteration envelopes with varying locations within the deposit. Alteration envelopes at approximately the same depth at the eastern and western margins of the mine workings were sampled for comparison. In addition, a near surface alteration envelope and one of the deepest intersected envelopes were sampled. These two alteration envelopes were situated at approximately the same location in relation to the strike of

the GLDZ. An alteration envelope located at the approximate centre of current mine workings was also sampled. Sporadic sampling of multiple dacite-hosted alteration envelopes was also conducted between the eastern and western, and upper and lower margins of the deposit. These samples were taken from underground mine workings and drill core. When studying a specific alteration (alteration related to  $V_{GD}$  veins for example), alteration envelopes were typically selected to avoid areas where alteration related to a different alteration event (e.g.  $V_1$ - $V_2$  veins) was also affecting the same rock. This practice ensures that the effects of one alteration event are not mistaken for the effects of another.

### **3.1.3 Geochronology**

To bracket the age(s) of gold mineralization at the Island Gold deposit, a sample of an intensely hydrothermally-altered dacite from an ore zone was collected. A sample of a least-altered equivalent from outside or at the outer margin of the same auriferous alteration envelope was also collected. Both samples were collected from underground mine workings on the same level. The least-altered sample was taken from a cross-cut, while the altered sample was collected from an attaching drift.

### **3.1.4 Sulphur isotopes**

Sulphide-rich samples of altered wall rock were taken from ore-zones hosted by each of the three main ore-hosting lithologies (dacite, gabbro, and the Webb Lake stock). Multiple samples from dacite-hosted ore zones distributed throughout the extent of the deposit were also collected. Furthermore, each type of auriferous quartz vein ( $V_{GD}$ ,  $V_1$  and  $V_2$  as identified in Jellicoe, 2019) was sampled. These sulphides, located in gold-bearing quartz veins and their associated alteration envelopes, are from the ore zones at Island Gold and are genetically linked to gold mineralization. Sulphide-rich iron formations and the silica-poor diorite-monzodiorite were also sampled. Samples were taken from underground workings, drill core, and surficial outcrops.

## **3.2 Whole-rock geochemistry**

A total of 94 samples were prepared at the University of Waterloo and then shipped to Activation Laboratories Ltd. (Actlabs) in Ancaster, Ontario for crushing and whole-rock

geochemical analyses. Crushing was conducted using a steel jaw crusher to a minimum of 90% (< 2 mm). A mechanically split portion (riffle) was then pulverized in a mild steel mill until > 95% of the sample was less than 74 µm. This pulverization method could result in the potential addition of a maximum of 0.2% Fe but does not introduce Ni or Cr. Cleaner sand was used between each sample (Actlabs, 2018a) to avoid cross contamination.

The following Actlabs packages/analyses were used: 4Lithores (4B and 4B2 Research)-Lithium Metaborate and Tetraborate Fusion-ICP and ICP/MS, Quant, 4F-B-PGNAA, 4F-CO2 Infrared, 4F-C, S Infrared, 4F-Hg Cold Vapour FIMS (HGFIMS), 4F-FeO Titration, Ultratrace 2-Aqua Regia-ICP-ICP/MS (As-Bi-Se-Sb-Te), Ultratrace 4-“Near Total” Digestion-ICP/MS (certain elements; Table 1), 1C-Exp 2-Fire Assay (Au, Pd, Pt), 1A3-Au Fire Assay-Gravimetric (if needed), Cu-Zn-Pb-Ni-As (if needed), 1A2-Au Fire Assay (Only sample numbers > T213; Appendix N) (Actlabs, 2018b). Table 1 summarizes the analytical techniques used to obtain concentrations of each analyte. In some cases, the concentration of the same analyte was measured using multiple methods. In Table 1, analyte-method pairs in bold were selected for use in this thesis. Whole-rock geochemical results, including those pertaining to QA/QC materials, were released as an Open File Report (Ciuffo et al., 2019) and are also reported in Appendix N and Appendix O.

Concentrations of major oxides and select trace elements (Table 1) were determined via lithium metaborate-tetraborate fusion followed by inductively coupled plasma atomic emission spectrometry (FUS-ICP). Samples were fused in an induction furnace after being mixed with lithium metaborate and tetraborate. The molten product was then dissolved in a solution of 5% nitric acid. Concentrations of analytes were then determined using Inductively Coupled Plasma Atomic Emission Spectrometers (Varian Vista 735 ICP or Thermo Jarrell-Ash ENVIRO II ICP). Seven CANMET and USGS certified reference materials were used to calibrate these spectrometers (Actlabs, 2018b). Loss on ignition (LOI) was determined by weighing the sample before and after roasting (Actlabs, 2018b).

Most trace elements concentrations were determined by fusing with lithium metaborate and tetraborate, diluting, and then analyzing with a Perkin Elmer Sciex ELAN 6000, 6100 or 9000 inductively coupled plasma mass spectrometer (recalibrated after every 40 samples; Actlabs, 2018b; FUS-MS).



Au, Pd, and Pt concentrations were determined via fire assay and inductively coupled plasma mass spectrometry (FA-MS). Litharge, silica, borax and soda ash are combined with the 30 g sample in a crucible. Ag is also added as a collector. Over the course of 60 minutes, the mixture is then heated in an assay furnace. The molten slag is then poured into a mould. The lead button from the base of the mould is transferred to a cupel which absorbs the lead from the bead. A hot nitric and hydrochloric acid solution is used to digest the bead and, after cooling, a Perkin Elmer Sciex ELAN 6000, 6100, or 9000 ICP/MS is used to determine the concentrations of Au, Pt, and Pd (Hoffman et al., 1998; Hoffman et al., 2002; Actlabs, 2018b). Samples returning Au concentrations greater than 30 ppm were repeated using the same fire assay process but with a gravimetric finish (FA-GRA). The gravimetric finish involves separating the Au from the Ag in the bead using nitric acid. The gold is then weighed gravimetrically (Hoffman et al., 1998; Actlabs, 2018b). For all samples with sample numbers greater than 213, gold concentrations were determined via the same fire assay process but with an atomic absorption finish (FA-AA; Appendix N). The bead is dissolved in aqua regia prior to being analyzed for gold via atomic absorption (Hoffman et al., 1998; Actlabs, 2018b). This technique was used to reduce cost, and these ten samples have low gold concentrations (< 0.1 ppm; Appendix N).

To determine the concentration of As, Bi, Sb, Se, and Te, aqua regia inductively coupled mass spectrometry (AR-MS) was used. Aqua regia is used to digest a 0.5 g sample for two hours. After dilution, the solution is analyzed using a Perkin Elmer SCIEX ELAN 6000, 6100, or 9000 ICP/MS (Actlabs, 2018b).

FeO was determined via titration (TITR) in an open system using a cold acid digestion of hydrofluoric acid and ammonium metavanadate in an open system. After digestion, ferrous ammonium sulphate is added. Potassium dichromate is used as the titrating agent. For samples with S concentrations greater than 10%, a hot digestion method is used instead (Wilson, 1955; Actlabs, 2018b).

The concentrations of certain elements (Table 1) were determined via “near total” digestion mass spectrometry (TD-MS). Four acids were used to digest a 0.25 g sample. First, hydrofluoric acid was used followed by nitric and perchloric acids. The sample was then dried by heating. Hydrochloric and nitric acid was used to bring the sample back into solution. Certain resistant minerals may not have been completely digested. Partial volatilization of As, Cr, and Sb

may have also occurred. A Perkin Elmer Sciex ELAN 6000, 6100, or 9000 ICP/MS was then used to determine the concentration of elements of interest (Actlabs, 2018b).

In order to measure the concentration of CO<sub>2</sub>, a 0.2 g sample was first decomposed using an ELTRA CW-800 (directly releasing CO<sub>2</sub>). This is conducted in a pure nitrogen environment within a resistance furnace at 1000°C. Prior to the detection of CO<sub>2</sub>, H<sub>2</sub>O was removed in a moisture trap. The concentration of CO<sub>2</sub> was determined via an infrared (IR) detector (Actlabs, 2018b).

Carbon and sulphur concentrations were determined via the following steps. A 0.2 g sample and accelerator material were subject to combustion in an induction furnace. SO<sub>2</sub> and CO<sub>2</sub> concentrations were measured via infrared (IR) detectors. Either a CS-2000 or an Eltra CS-800 was used in this process (Actlabs 2018b).

Boron concentrations were determined via prompt gamma neutron activation analysis (PGNAA). First, a 1 g sample is placed into a thermalized beam of neutrons. The doppler broadened prompt gamma ray was measured at 478 KeV with a GE detector and compared to the certified reference materials used for system calibration (Actlabs, 2018b).

The concentration of mercury is determined via cold vapour flow injection mercury technique (1G/AR-FIMS) using a Perkins Elmer FIMS 100. First, aqua regia was used to leach soluble compounds. An aliquot of the resulting solution is combined with a solution of potassium permanganate. The flow injection cold vapour mercury technique is then performed and the concentration of Hg is determined in the absorption cell by the absorption of light at 253.7 nm (Actlabs 2018b). Excluding Appendix N, Appendix O, and Appendix Q, concentrations below detection limit were replaced with values that are half of the detection limit in this thesis.

**Table 1.** Analytical methods used at Actlabs to obtain concentrations of chemical species. Bolded analyte-method pairs were selected for use in this thesis while those that are non-bolded are not used. AR-MS=Aqua Regia – Mass Spectrometry, FA-MS=Fire Assay – Mass Spectrometry, FA-GRA=Fire Assay – Gravimetric Finish, FUS-MS=Lithium Metaborate/Tetraborate Fusion – Mass Spectrometry, FUS-ICP=Lithium Metaborate/Tetraborate Fusion - Inductively Coupled Plasma Atomic Emission Spectrometry, TD-MS=Total Digestion – Mass Spectrometry, PGNAA=Prompt Gamma-Neutron Activation Analysis, TITR=Titration, IR=Infrared Detection, AR-FIMS=Aqua Regia – Hg Cold Vapour Flow Injection Technique (1G), FA-AA=Fire Assay – Atomic Absorption Finish.

FUS-MS	FUS-ICP	TD-MS	AR-MS	FA-MS	FA-GRA	FA-AA	PGNAA	TITR	IR	AR-FIMS
<b>Ag, As, Bi, Ce, Co, Cr, Cs, Cu, Dy, Eu, Er, Ga, Gd, Ge, Ho, Hf, In, La, Lu, Mo, Nb, Nd, Ni, Pr, Sm, Rb, Sb, Sn, Ta, Tb, Tl, Tm, Pb, Th, U, W, Y, Yb</b>	<b>SiO<sub>2</sub>, Al<sub>2</sub>O<sub>3</sub>, MnO, MgO, CaO, Na<sub>2</sub>O, K<sub>2</sub>O, TiO<sub>2</sub>, P<sub>2</sub>O<sub>5</sub>, Fe<sub>2</sub>O<sub>3</sub>(T), Ba, Be, LOI, Sc, Sr, V, Zr</b>	<b>Ag, Cd, Co, Cr, Cu, In, Li, Mn, Mo, Ni, Pb, Zn</b>	<b>As, Bi, Sb, Se, Te</b>	<b>Au, Pt, Pd</b>	<b>Au</b>	<b>Au</b>	<b>B, Mass</b>	<b>FeO</b>	<b>C, S, CO<sub>2</sub></b>	<b>Hg</b>

### 3.2.1 Whole-rock geochemistry quality assurance / quality control (QA/QC)

Quality assurance/quality control procedures undertaken for the validation of geochemical data are detailed in this section. Concentrations of chemical species in QA/QC materials in Appendix N and Appendix O are from Activation Laboratories Ltd. Measured concentrations of chemical species in lab (Actlabs)-provided reference materials, duplicates (duplicate analyses), and blanks used for geochemical QA/QC in this thesis are part of an open file report (Ciufu et al., 2019) and are also included in Appendix O. Measured concentrations of chemical species in NRCan-provided reference materials (STPL), that were also used for geochemical QA/QC in this thesis, are included in Appendix N. Based on analysis of these results (Sections 3.2.1.1 and 3.2.1.2; Appendices P to R), the geochemical data used in this thesis is considered fit for purpose. Concentrations of some chemical species determined via certain methods were not used in this thesis (besides being reported in the Appendix) and these analyte-method pairs are indicated in Appendices P and R. The term “standard(s)” is often used to refer to reference material(s) in this thesis.

#### 3.2.1.1 NRCan-provided reference materials

A total of 10 external pulp standards (seven “STPL-BAS” standards and three “STPL-PML-53” standards) provided by Natural Resources Canada were included with samples sent for geochemical analyses. This equates to a 9.4 : 1 sample to standard ratio. Both accuracy and precision are assessed separately for each of the two standard types. Accuracy is assessed for

each method-analyte pair and standard type by calculating percent relative difference using the following equation from Jenner (1996) and Piercey (2014) with modified variables:

$$RD = 100 * \frac{Avg - Std}{Std}$$

where ‘RD’ is percent relative difference; ‘Avg’ is the average of the measured values obtained in this study from analyses of the standard; and ‘Std’ is the ‘known/actual’ value for the standard.

The average of the measured values from previous analyses of each standard type for each analyte-method pair (Appendix R; Natural Resources Canada, personal communication, 2018) are used for the known values. The known average value for the STPL-BAS standard was calculated from 50 analyses while the known average value for STPL-PML-53 was calculated from 48 analyses (Appendix R; Natural Resources Canada, personal communication, 2018).

Precision is assessed for each analyte-method pair and standard type by determining percent relative standard deviation using the following equation from Jenner (1996) and Piercey (2014) with modified variables:

$$RSD = 100 * \frac{Std Dev}{Avg}$$

where ‘RSD’ is percent relative standard deviation; ‘Std Dev’ is the standard deviation of the measured values obtained in this study from analyses of the standard; and ‘Avg’ is the average of the measured values obtained in this study from analyses of the standard.

The results of QA/QC analysis of external standards are tabulated in Appendix R. It is indicated whether or not the average measured value for an analyte-method pair is near the detection limit (within ten times the detection limit (< 10x DL)). In many cases, RD or RSD values indicative of inaccuracy or imprecision are explained by concentrations of certain analytes being close to detection limit (Appendix R). Results from analyte-method pairs that were not used in this thesis are also indicated (Appendix R). Overall, results are consistent with historical analyses of these standards (Appendix R). For this geochemical dataset, the analysis of duplicates and lab-provided standards is recommended to quantify precision and accuracy

(Section 3.2.1.1; Appendix P) because it is likely that they can better represent true precision and accuracy than NRCan-provided standards. This is because the lab-provided standards include certified reference materials, are provided at various concentrations for a given analyte, and have a higher frequency of insertion than the NRCan-provided standards. Duplicate analyses are of samples submitted for this thesis from the Island Gold deposit. Subsequently, they will better reflect the analytical precision of samples from this dataset because they are from this location.

### 3.2.1.2 Lab-provided reference materials, duplicates, and method blanks

Standards, duplicates (duplicate analyses), and method blanks, provided by Actlabs as part of their quality control procedure, were also assessed (Appendix O). The frequency of each of these internal controls varies for each analyte-method pair and are summarized in Appendices P, Q, and R. Lab-provided standards include certified reference materials and in-lab standards that are traceable to certified reference materials (Actlabs, 2018b). Statistics to quantify precision and accuracy of data for each analyte-method pair are also displayed in these appendices. Detection limits (DL) and limits of quantification (LOQ; three times the detection limit) for each analyte-method pair are summarized in Appendix P.

Lab-provided standards are used to quantify accuracy. Average relative difference is determined for each method-analyte pair using the formula modified from Skoog and West (1963):

$$RD = \frac{\sum_{i=1}^n (100 * (Meas_i - Cert_i) / Cert_i)}{n}$$

where RD is average percent relative difference, 'Meas<sub>i</sub>' is the measured value for the i<sup>th</sup> standard for a given analyte-method pair, 'Cert<sub>i</sub>' is the corresponding 'known/actual' value for the i<sup>th</sup> standard; and 'n' is the total number of standards analyzed for a given analyte-method pair.

The results of QA/QC analysis of lab-provided standards are tabulated in Appendix P. The number of standards analyzed that have known values less than 10 times detection limit is noted for each analyte-method pair. Concentrations of LOI and Fe<sub>2</sub>O<sub>3</sub> were not determined in lab-provided standards and as a result the accuracy of LOI and Fe<sub>2</sub>O<sub>3</sub> are not quantified in Appendix P. Excluding LOI and Fe<sub>2</sub>O<sub>3</sub>, 82% of analyte-method pairs used in this thesis have

average RD values between -10 and 10%. Average RD values for all analyte-method pairs used in this thesis range from -48.4 to 77.7%. In many cases, average RD values indicative of inaccuracy for certain analyte-method pairs appear to be due to numerous standards having known values that are close to detection limit for these analytes. With the exception of As (-20.5%; AR-MS), Cr (-13.6%; TD-MS), and Sb (-48.4%; AR-MS), all analyte-method pairs used in this thesis with average RD values outside of the -10 to 10% range each have multiple standards with known values of their respective analyte below 10 times the detection limit (Appendix P).

Lab duplicates are used to assess precision by determining the average coefficient of variation equation as recommended in Stanley and Lawie (2007) and Abzalov (2008; 2011) and modified from Piercey (2014):

$$CV_{avg} = 100 * \sqrt{\frac{2}{n} * \sum_{i=1}^n \left( \frac{(A_i - B_i)^2}{(A_i + B_i)^2} \right)}$$

where ‘ $CV_{avg}$ ’ is the average coefficient of variation (%) for a given analyte-method pair; ‘ $A_i$ ’ is the original measured value for  $i^{th}$  duplicate pair; ‘ $B_i$ ’ is the corresponding duplicate measured value for  $i^{th}$  duplicate pair; and ‘ $n$ ’ is the total number of duplicate pairs.

The results of QA/QC analysis of internal lab duplicates are tabulated in Appendix P. The number of measured duplicate values that are less than 10 times detection limit is also noted for each analyte-method pair (Appendix P). No duplicate analyses of Au concentrations determined via FA-GRA were conducted and as a result the precision of this analyte-method pair is not quantified in Appendix P. Excluding Au (FA-GRA), 79% of analyte-method pairs used in this thesis have average CV values ranging from 0 to 10%. Average CV values for all analyte-method pairs used in this thesis range from 0 to 59.6%. In most cases, average CV values of analyte-method pairs indicative of imprecision appear to be due to duplicates with concentrations of respective analytes that are close to detection limit. With the exception of B (13.8%; PGNA), Cr (18.5%; TD-MS), and Ni (11.6%; TD-MS), all analyte-method pairs with average CV values above 10% that were used in this thesis have multiple duplicates with measured

values of their respective analyte below 10 times the detection limit (Appendix P). Results from analyte-method pairs that were not used in this thesis are also indicated (Appendix P).

A summary of the analysis of method blanks for each method-analyte pair is located in Appendix Q. Additional comments are included if blanks return measured concentrations that are higher than the LOQ (three times the detection limit; Appendix Q). The analyte-method pairs where analysis of blank(s) returned concentrations higher than LOQ include As (AR-MS), Bi (AR-MS), Au (FA-MS), Cr (TD-MS), Mn (TD-MS), and Zn (TD-MS). However, with the exception of Mn (TD-MS) and one As blank analyzed via AR-MS, concentrations determined via analysis of these blanks are relatively close to detection limit (Appendix Q). Of these six analyte-method pairs, concentrations of Mn determined via (TD-MS) were not used in this thesis while concentrations determined via the other five analyte-method pairs were used. No lab-provided method blanks were analyzed for C, Fe<sub>2</sub>O<sub>3</sub>, LOI, or S.

### 3.2.2 Isocon diagrams

Isocon diagrams introduced in Grant (1986) based on the equations in Gresens (1967) are used to determine and display chemical enrichments and depletions resulting from alteration. Isocon diagrams in this thesis were created using EASYGRESGRANT which is a Microsoft Excel spreadsheet developed by López-Moro (2012). These diagrams involve plotting the concentration of elements (ppm) and oxides (mass percent) in the altered sample ( $C_A$ ) against the concentration of the corresponding elements and oxides in the less-altered sample ( $C_{LA}$ ). The Isocon is a straight line through the origin that defines no relative change in mass (Grant, 1986). Chemical species that plot below the Isocon are assumed to have been lost during alteration while species plotting above the Isocon are gained (Grant, 2005). The slope of the Isocon is determined by the line of best fit (linear regression) through inferred immobile chemical species. Immobile species will have similar slopes ( $C_A/C_{LA}$ ) (Grant, 2005) and immobile elements for each Isocon diagram were selected based on the clustering of slope values. Species commonly identified and used as immobile elements in this study include Al<sub>2</sub>O<sub>3</sub>, Cr, Dy, Er, Gd, Hf, Ho, Lu, Nb, Sc, Ta, Tb, Th, TiO<sub>2</sub>, Tm, Y, Yb, and Zr. A number of studies also suggest that these elements and oxides are relatively immobile during alteration (e.g. Winchester and Floyd, 1977; Pearce, 1996; Hastie et al., 2007). Based on the clustering of slopes, each Isocon diagram used a number of immobile elements from this list and the immobile elements selected for each Isocon

diagram are summarized in Appendix S. To confirm that choice of immobile elements for each Isocon diagram is appropriate, a classical least-squares regression method is used. A correlation coefficient of greater than 0.999 is considered acceptable and is achieved for all Isocon diagrams. Constant mass and constant volume lines are also plotted for each diagram. Samples absent of macroscopically visible quartz veins were preferentially selected for Isocon analysis.

This method of selecting immobile elements that may vary from diagram to diagram minimizes a number of issues related to static immobile element selection. For example, an element may be immobile in circumstances of weak alteration and therefore can be used as an immobile element. However, this element may become mobile during strong alteration and should no longer be used as an immobile element. Furthermore, heterogeneities in samples can result in non-alteration-related apparent enrichments or depletions in certain elements even if these elements are immobile. For example, a less-altered sample with a large zircon grain ( $\text{ZrSiO}_4$ ) results in the altered sample having comparatively less zirconium when compared to the less-altered sample which does not contain this grain. In this example, this is due to mineralogical heterogeneity unrelated to alteration and is analogous to the ‘nugget effect’. If zirconium was used as an immobile element in this diagram, it would skew the slope of the Isocon line in this diagram but remains a valid immobile element choice for other altered/least-altered pairs. In many cases, the same immobile elements are selected between Isocon diagrams. Determining immobile elements on a case-by-case basis based on the clustering of slopes is more time consuming but prevents these errors. In the example above, zirconium will appear depleted but it will not affect the slope of this Isocon diagram and subsequent interpretations of enrichment or depletion for other chemical species. Multiple altered/less-altered pairs and associated Isocon diagrams are created and interpreted and only chemical species that are consistently enriched or depleted are deemed to be gained or lost, respectively. Therefore, non-alteration-related heterogeneities in a sample that result in pseudo enrichments and depletions are identified and discarded.

Chemical species that are selected as immobile for any given Isocon diagram are considered to be neither enriched nor depleted. In rare cases, certain chemical species are below detection limit in both the altered and least altered sample (most commonly: Ag, As, Mo, Se, Te, and Tl). For an altered/least-altered pair where this is the case, these chemical species are not plotted on its respective Isocon diagram. In addition, mass gains and losses for these chemical



species are considered inconclusive for that altered/less-altered pair. However, these chemical species can still be considered consistently gained or lost when examining the same type of alteration if other altered/less-altered pair(s) (where the concentration of that chemical species is not below detection limit for both samples in a pair) exhibit all gains or all losses of that chemical species, respectively. Chemical species that are determined to be gained or lost based on the examination of altered/least-altered pairs (as discussed above) are referred to as consistent gains and consistent losses in this thesis.

In order to quantify the magnitude of enrichment, mass balance calculations (discussed in Section 3.2.4) are also conducted after alteration groupings (Section 3.2.3) were established using the results from Isocon analysis. These mass balance calculations compare enrichments/depletions of chemical species in samples classified as strongly, moderately, weakly, and least-altered using static immobile element selection. Resulting enrichments and depletions from this mass balance method, in which the same immobile elements were selected for calculations, can be compared to the enrichments and depletions determined from the graphical Isocon method, in which different immobile elements were selected for each diagram on a case-by-case basis.

Constant volume lines are calculated using density values determined using the methods outlined in Section 3.7. In some Isocon diagrams, select concentrations of chemical species are arbitrarily scaled to avoid stacking/overlap. Arbitrarily scaling concentration data can change the slope of the best-fit Isocon (Mukherjee and Gupta, 2008.). To avoid this, the same Isocons (with identical slopes) are used in corresponding scaled and unscaled diagrams. In other words, the slopes of Isocons are determined prior to rescaling of any chemical species. For display purposes, some chemical species that are not discussed and are not consistently enriched or depleted in multiple altered/less-altered pairs are removed. Some elements included in the geochemical package (Be, Cd, Hg, In, Pt, Pd, Sn) were not examined via Isocon analysis because their concentrations are below detection limit for most samples.

### **3.2.3 Alteration strength groupings**

In order to compare variably-altered samples from alteration envelopes throughout the deposit, it was necessary to group samples based on strength of alteration. As a result, a preliminary geochemical study was conducted to determine chemical proxies for alteration.

Preliminary study of altered and least-altered pairs yielded that potassium oxide ( $K_2O$ ) and sulphur (S) consistently correlate with increasing alteration in all of the main ore-hosting lithologies (dacite, gabbro, and the Webb Lake stock; Table 4). These chemical species are also present in relatively low concentrations in the least-altered samples of these lithologies and are enriched significantly due to auriferous quartz vein-related alteration. These characteristics made them ideal candidates to be chemical proxies for strength of alteration.

Four alteration groups (Strongly-altered, moderately-altered, weakly-altered and least-altered) are defined based on concentrations of S and  $K_2O$  for each lithology (Figure 6), qualitative estimates of alteration strength, and proximity to gold-bearing quartz veins. The proposed groups correlate well with the estimated strength of alteration determined by macroscopic and microscopic examination. Boundaries between groupings were determined by averaging the chemical compositions of the nearest two points on either side of a proposed boundary. On Figure 6, vertical boundaries were determined by averaging  $K_2O$  concentrations while horizontal boundaries were determined by averaging S concentrations. Boundaries between alteration strength groupings are summarized in Table 2. These quantitative alteration strength groupings were only applied to select samples of dacite, gabbro, and the Webb Lake stock (the major pre-gold mineralization lithologies) that were sent for whole-rock geochemical analysis. For rocks and samples (including other lithologies) not classified via this quantitative method, these terms (e.g. least-altered, weakly-altered) are occasionally used to indicate the approximate strength of alteration based on qualitative estimates.

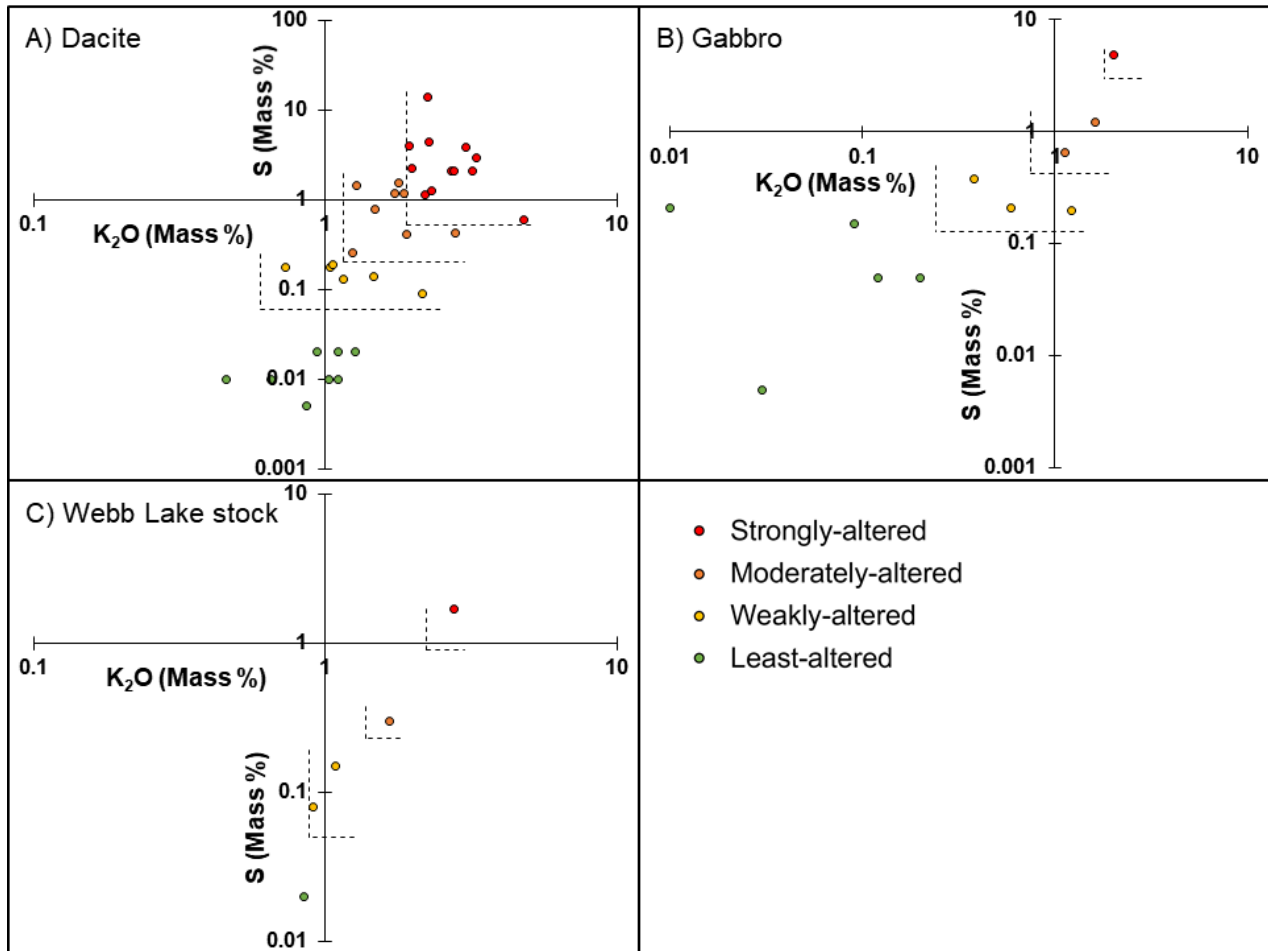


**Figure 6A–C.** Variably-altered samples of the three major ore-hosting lithologies plotted on separate  $K_2O$  vs.  $S$  plots. These diagrams are used to quantify the strength of alteration by subdividing samples into groups based on the  $K_2O$  and  $S$  enrichment. Boundaries between alteration groups are indicated using dashed lines and quantified in Table 2. Concentrations below detection limit are replaced with the detection limit for display purposes. A) Dacite: Strongly-altered (T56, T58, T71, T72, T86, T90, T105, T113, T157, T158, T162, T188), moderately-altered (T17, T20, T73, T85, T88, T114, T156, T186), weakly-altered (T13, T59, T115, T117, T118, T184), and least-altered (T8, T11, T65, T116, T154, T164, T183, T241). B) Gabbro: Strongly-altered (T142), moderately-altered (T141, T140), weakly-altered (T19, T87, T139), and least-altered (T14, T80, T89, T182, T200). C) Webb Lake stock: Strongly-altered (T195), moderately-altered (T194), weakly-altered (T6, T193), and least-altered (T192).

*Table 2. Boundaries between alteration strength groupings for each of the main ore-hosting lithologies.*

		<b>K<sub>2</sub>O (wt%)</b>	<b>S (wt%)</b>
<b>Dacite</b>	Strongly-altered	> 1.91	> 0.52
	Moderately-altered	1.15-1.91	0.20-0.52
	Weakly-altered	0.73-1.15	0.06-0.20
	Least-altered	< 0.73	< 0.20
<b>Gabbro</b>	Strongly-altered	> 1.82	> 3.02
	Moderately-altered	0.75-1.82	0.43-3.02
	Weakly-altered	0.24-0.75	0.13-0.43
	Least-altered	< 0.24	< 0.13
<b>Webb Lake stock</b>	Strongly-altered	> 2.22	> 0.99
	Moderately-altered	1.38-2.22	0.23-0.99
	Weakly-altered	0.88-1.38	0.05-0.23
	Least-altered	< 0.88	< 0.05

### 3.2.4 Mass balance calculations

In order to quantify the magnitude of gains and losses of chemical species due to alteration, mass balance calculations are performed. These calculations were conducted using an equation from Grant (1986) with modified variables:

$$\Delta C/C_{LA} = (\text{inverse of Isocon slope}) * (C_A/C_{LA}) - 1$$

where C=concentration,  $C_A$ =concentration in altered sample,  $C_{LA}$ =concentration in less-altered sample.

Gains and losses of chemical species were calculated for samples classified under each alteration strength grouping relative to less-altered samples. These calculations were performed separately for each lithology altered by  $V_1$ - $V_2$  veins. They were also conducted separately for dacite altered by  $V_{GD}$  veins. If multiple samples classified under a certain alteration grouping were present, their compositions were averaged. The chemical species that were frequently selected as immobile during Isocon analysis for a specific lithology were used as immobile elements for all mass balance calculations for that lithology. The slope of each Isocon was determined by averaging the values  $C_A/C_{LA}$  for each immobile element.

One sample of gabbro/lamprophyre altered by a  $V_3$  vein, one sample of silica-poor diorite–monzodiorite altered by  $V_3$  veins, and one dacitic sample subject to non-auriferous carbonate-sericite alteration were sampled. Due to the limited sampling of the alteration associated with  $V_3$  veins and this non-auriferous carbonate-sericite alteration, mass balance calculations were performed using the altered sample and a corresponding representative less-altered sample for each lithology. Immobile elements used in the corresponding Isocon diagram for each altered/less-altered pair were used for these calculations. The selection process for immobile elements for Isocon diagrams is discussed in Section 3.2.2. The slope values for Isocons used in these mass balance calculations are the same as the slope of the Isocon displayed in each corresponding Isocon diagram. The calculation of slope values for Isocon diagrams are also discussed in Section 3.2.2. Certain chemical species included in the geochemical package used for this thesis (Be, Cd, Hg, In, Pt, Pd, Sn) were not included in any mass balance calculations because their concentrations are below detection limit for most samples.

### **3.3 Petrography and point-counting**

Billets were cut using a rotary diamond saw from select samples and sent to Vancouver Petrographics Ltd. to be made into standard-sized (27 x 46 mm) polished thin sections for petrographic study. A total of 139 polished thin sections were created. Detailed transmitted and reflected light petrography and point-counting were conducted using a Nikon Eclipse LV100POL to identify minerals and textures. A Nikon Digital Sight DS-Fi2 camera coupled with NIS Elements Imaging Software was used to take most photomicrographs. In order to quantify mineral proportions, a thin section was subdivided into a 27-point by 15-point grid composed of 405 equally-spaced points. At each of these points, the mineral directly under the microscope crosshairs was identified and recorded. The mineral counts for each thin section were then normalized to 100%. Mineral modal proportions, in area percent, are assumed to be approximately equivalent to volume percent in this thesis. All point-counting data is presented in Appendix E.

### **3.4 Scanning electron microscopy with energy dispersive spectroscopy (SEM-EDS)**

An SEM-EDS at the Environmental Particle Analysis Laboratory (University of Waterloo) was used to identify minerals in polished thin sections that could not be identified using traditional reflected and transmitted light microscopy. This device is a Hitachi TM3000 Table-top SEM coupled with a Bruker QUANTAX 70 EDS. It was also used for microscopic imaging. Polished thin sections were affixed to the stage using double-sided carbon tape.

### **3.5 Scanning Electron Microscope Mineral Liberation Analyser<sup>®</sup> (SEM-MLA)**

SEM-MLA techniques were employed for mineral identification and determining mineral proportions for five variably-altered samples taken from a dacite-hosted alteration envelope (Appendix F). It is challenging to precisely determine the proportions of fine-grained quartz and feldspars in the volcanic rocks using transmitted light microscopy. As a result, SEM-MLA was used to identifying how the modal proportions of quartz and feldspar in dacitic rocks vary with changing alteration intensity. These analyses were conducted by staff at the Bruneau Centre's SEM-MLA Research Lab (Memorial University). The FEI MLA 650F SEM was used for this analysis. It is equipped with a Bruker electron backscatter diffraction system (EBSD) and an HKL Technology high throughput energy dispersive x-ray (EDX) system (CREAIT Network,

2018). The MLA software uses this equipment for the quantitative evaluation of a variety of characteristics including modal mineralogy, mineral associations, density distribution, mineral liberation, and grain sizes. It does this by automating imaging, movement of the stage, and X-ray acquisition of data (CREAIT Network, 2018). SEM-MLA thin section-scale images were also provided by this lab and feature false colours to help visualize changes in mineralogy (Appendix G; Figure 18). Mineral modal proportions, in area percent, (Appendix F) are assumed to be approximately equivalent to volume percent in this thesis.

### **3.6 Electron microprobe**

Six thin sections were selected for microprobe analysis at the Electron Microprobe Laboratory which is part of the Earth and Planetary Material Analysis Laboratory at Western University. These thin sections consisted of altered and less-altered pairs from a dacite-hosted, a gabbro-hosted, and a Webb Lake stock-hosted alteration envelope. A JEOL JXA-8530F field emission electron microprobe was used to conduct these analyses. This machine is equipped with a scanning electron microscope with energy-dispersive X-ray spectroscopy (SEM-EDS) which was used to quickly identify minerals and help select locations for wavelength-dispersive X-ray spectroscopic (WDS) analysis. WDS was used to acquire quantitative chemical data for key primary, metamorphic, and/or alteration-derived minerals. These minerals include biotite, white mica, chlorite, plagioclase, and carbonates. The following elements were detected: Si, Al, Ti, Na, Ca, K, Fe, Mg, Mn, F, and Cl. For carbonate minerals, C concentrations were also measured. Microprobe data is located in Appendix H. The microprobe was calibrated differently depending on the type of mineral being analysed. Three configurations were used for analyses of certain minerals and these configurations are summarized in Appendix I.

Atoms per formula unit (apfu; Appendix H) were calculated based on the following number of oxygens for each mineral: biotite (22), chlorite (28), white mica (11), and plagioclase (8). H<sub>2</sub>O values used in apfu calculations for biotite were calculated using the methods outlined in Tindle and Webb (1990). Biotite formulae are calculated using a Microsoft Excel spreadsheet by Andrew G. Tindle (Tindle, 2018a). Chlorite mineral formulae are calculated assuming full site occupancy when determining OH, Fe<sup>3+</sup> and Fe<sup>2+</sup> values. Chlorite formulae are calculated using an Excel spreadsheet program by Andrew G. Tindle (Tindle, 2018b). White mica formulae are calculated assuming all iron is ferrous using an Excel spreadsheet by John Brady (Brady,

2018b). Plagioclase formulae are calculated using an Excel spreadsheet by John Brady (Brady, 2018a). Mole proportions of Mg, Fe, and Ca were used to determine proportions of magnesite, siderite, and calcite for plotting on MSC ternary diagrams. These mole proportions were calculated for carbonate minerals assuming total iron is ferrous (Appendix H).

### 3.7 Density

The Archimedes method was used to determine the densities of certain samples which were used to plot constant volume lines on Isocon diagrams. The Archimedes Principle states that the buoyancy force equals the weight of the water the sample displaces. If the weight of the sample in air ( $m_a$ ) and the weight of the sample in deionized water ( $m_w$ ) are determined, the following equation can be used to determine the density of the sample ( $\rho_s$ ). The density of deionized water ( $\rho_w$ ) is assumed to be 0.9982 g/cm<sup>3</sup> at 20°C (Weast, 1972).

$$\rho_s = \frac{m_a}{m_a - m_w} * \rho_w$$

A representative piece of each sample selected for density measurement were first washed with deionized water and allowed to dry. These samples range in weight from 9 to 32 grams. A beaker was filled with deionized water. The suspension apparatus was set on the scale with the basket made of fishing line suspended in the beaker of water. The following steps were then repeated between each sample. First, the sample was placed on the scale and the weight in air ( $m_a$ ) was recorded. The sample was then placed in the basket suspended in the water-filled beaker and the weight was recorded ( $m_w$ ). This process was repeated for each sample. The scale used is a Sartorius Quintix124-1S which has a capacity of 120 g and a readability of 0.0001 g.

To assess accuracy and precision, the density of three known mineral samples (two quartz crystals and one apatite crystal) were measured after every ten samples. Quartz has an ideal density of 2.65 g/cm<sup>3</sup> (Mursky and Thompson, 1958) but is often noted to range from 2.5-2.7 g/cm<sup>3</sup> (e.g. Telford et al., 1990). The density of apatite ranges from 3.16 to 3.22 g/cm<sup>3</sup> (Mason and Berry, 1968). Due to microscopic inclusions or other imperfections in these mineral samples such as voids, measured densities may vary slightly from true densities. Average relative difference is used to assess accuracy using the RD equation described in Section 3.2.1.1. The RD



values determined from measurements of the two quartz crystal standards were -0.246% and -0.470%. All measurements of apatite fell within the apatite density range outlined above. Relative standard deviation is used to assess precision of repeat analysis of standards using the RSD equation described in Section 3.2.1.1. RSD values range from 0.192 to 0.227. To further assess precision, the density of seven samples were analysed a second time. All duplicate measurements fall within 2% precision control lines (Appendix J). Based on this QA/QC analysis, density measurements are considered fit for purpose. All the results of QA/QC analysis are summarized in Appendix J.

### **3.8 Sulphur isotopes**

#### **3.8.1 University of Waterloo – Environmental Isotope Laboratory**

Twenty select samples (Appendix K) were crushed at Actlabs using the same methodology outlined at the beginning of Section 3.2. These powdered samples were sent to the University of Waterloo-Environmental Isotope Laboratory to determine the  $\delta^{34}\text{S}$  value for each. The analytical process is summarized below (EIL, 2017). Samples and standards were weighed into tin capsules that also contained a few mg of  $\text{Nb}_2\text{O}_5$  which was added to aid in the conversion to  $\text{SO}_2$  gas. A 4010 Elemental Analyzer (Costech Instruments) coupled with a Isochrom (Micromass UK) Continuous Flow Isotope Ratio Mass Spectrometer (CFIRMS) was used for the conversion of samples to a gas (through combustion) and isotopic analyses. The  $\delta^{34}\text{S}$  values are the corrected ratios of  $^{34}\text{S}/^{32}\text{S}$ , measured against the Vienna-Canyon Diablo Troilite (VCDT) meteorite reference standard (EIL, 2017).

A number of international reference materials and in-house standards (calibrated using international reference materials: NBS-127, NBS-123, IAEA-SO-5, IAEA-SO-6, IAEA-S1 to-S3) were used to monitor data quality and make corrections. Sulphate standard reference materials are run with sulphate samples and sulphide standard reference materials are run with sulphide samples. Every 4<sup>th</sup> to 6<sup>th</sup> sample is repeated. At least 20% of the analyzed samples are standard reference materials which were used to normalize data and quantify accuracy and precision. They are also used to assess mass spectrometer drift or linearity issues during analysis. Based on this quality assurance-quality control protocol, an error of  $\pm 0.3\text{‰}$   $\delta^{34}\text{S}$  for standards is required (EIL, 2017). Results of this analysis (Appendix K) were used to help select samples to be sent to the University of Maryland for further isotopic analysis.

### 3.8.2 University of Maryland – Stable Isotope Laboratory

Ten select samples (Appendix L) were crushed using a steel pestle and mortar and sieved through a 2 mm mesh. Between each sample, the pestle, mortar, and sieve were cleaned thoroughly by washing and rinsing with water followed by ethanol. Pyrite grains were hand-picked from the material that passed through the 2 mm sieve with the aid of an Olympus SZX10 microscope and grains from each sample were placed in individually labelled glass vials. For samples that contained both pyrrhotite and pyrite, these sulphide minerals were separated and sent as different samples to be analyzed separately. Samples were then shipped to the Stable Isotope Laboratory at the University of Maryland for sulphur isotopic analyses and these analyses are summarized below.

Samples were then transferred to flasks. A solution consisting of 20 ml of acidic Cr (II) (0.3 M) and 10 ml HCl (5 M) was added to the flasks. The reaction proceeded for three hours, during which the solution was flushed with nitrogen gas. H<sub>2</sub>S gas was produced which passed through a water-cooled condenser, followed by a water trap (Milli-Q<sup>®</sup> water). A weakly acidic solution of AgNO<sub>3</sub> collected the silver sulfide (Ag<sub>2</sub>S). The solution containing the silver sulphide was allowed to sit for seven days after which the silver sulphide was removed and washed with Milli-Q<sup>®</sup> water. It was then soaked in a NH<sub>4</sub>OH solution (1 M) after which it was rinsed again using Milli-Q<sup>®</sup> water. The rinsing process was repeated ten times. For 48-72 hours, the silver sulphide was dried in an oven set to a temperature of 80°C, and then it was enfolded in aluminum foil. The silver sulphide was placed in a nickel capsule and in order to convert it to sulphur hexafluoride (SF<sub>6</sub>), the capsule was filled with fluorine gas and heated overnight at 250°C. Purification of sulphur hexafluoride was conducted via cryogenic distillation in a mixture of liquid nitrogen (-110°C) and mixed ethanol. A gas chromatography system (molecular sieve 5A column & a 1/8 in. 4.8 m Haysep Q column, 20 ml/min flow rate) was used for additional purification. The sulphur hexafluoride was frozen using liquid nitrogen out of the helium carrier flow and subsequently relocated into a glass tube. The conversion of silver sulphide to sulphur hexafluoride had a 94-100% recovery yield. The sulphur hexafluoride was analyzed using the ThermoFinnigan MAT 253 stable isotope ratio mass spectrometer which is capable of measuring <sup>36</sup>S, <sup>34</sup>S, <sup>33</sup>S, and <sup>32</sup>S. Vienna-Canyon Diablo Troilite (V-CDT) meteorite reference standard was used to normalize the data.  $\delta^{3xS} = \left(\frac{^{3xS}}{^{32S}}\right)_{\text{sample}} / \left(\frac{^{3xS}}{^{32S}}\right)_{\text{standard}} - 1$  (where x=3,4,6);  $\Delta^{33S} = \delta^{33S} -$

$((1+\delta^{34}\text{S})^{0.515}-1)$ ; and  $\Delta^{36}\text{S} = \delta^{36}\text{S} - ((1+\delta^{34}\text{S})^{1.90}-1)$  (Canfield et al., 1986; Farquhar et al., 2007b; Wu et al., 2018; Wu, personal communication, 2018).

After every four samples, an international reference silver sulphide (IAEA-S1) was also run to quantify uncertainty. IAEA-S1 was run a total of three times during the analyses and yielded  $\Delta^{33}\text{S} = 0.094 \pm 0.002\text{‰}$ ,  $\Delta^{36}\text{S} = -0.69 \pm 0.19\text{‰}$ , and  $\delta^{34}\text{S} = -0.30 \pm 0.07\text{‰}$  (2 SD; n=3). Long-term variation in standard IAEA-S1 at this laboratory from 2008–2017, has yielded the following results:  $\Delta^{33}\text{S} = 0.094 \pm 0.008\text{‰}$ ,  $\Delta^{36}\text{S} = -0.69 \pm 0.30\text{‰}$ , and  $\delta^{34}\text{S} = -0.30 \pm 0.20\text{‰}$  which are consistent with the values of IAEA-S1 reported in this study (Wu, personal communication, 2018).

### **3.9 Laser ablation inductively coupled mass spectrometry (LA-ICP-MS)**

To determine the age(s) of gold mineralization at the Island Gold deposit, U–Pb geochronology was performed on zircons from an intensely hydrothermally-altered dacitic sample in an ore zone and a least-altered equivalent nearby. The two samples were first crushed using a steel pestle and mortar and sieved through a 300  $\mu\text{m}$  mesh. Between samples, the pestle, mortar and sieve were cleaned thoroughly by washing followed by rinsing with ethanol. Clay minerals and small, light grains were removed from the sample material that passed through the 300  $\mu\text{m}$  sieve using water and a prospecting pan. After air drying each sample, a Frantz Isodynamic magnetic separator was used to remove most ferromagnesian minerals (e.g. garnet, magnetite, ilmenite) from each sample. Heavy minerals were separated by density using methylene iodide (MI) inside a fume hood. Due to the significant amount of pyrite in the hydrothermally-altered sample, it was necessary to use nitric acid to dissolve the pyrite. This sample was poured into a beaker containing a 5 molar (M) solution of nitric acid and this solution was heated on a hot plate to 80°C in a fume hood. The sample was then agitated gently until the reaction began. The reaction was allowed to proceed to completion (~45 minutes) after which the buoyant sulphur residue was removed from the surface. After the solution cooled, the mineral grains and nitric acid solution were poured through filter paper into a waste flask. During this entire process personal protective equipment was worn, lab equipment and samples were properly cleaned, waste chemicals were disposed of appropriately, and a complete procedure was followed (more detailed than the procedure summary discussed here).

Zircons were picked by hand using tweezers, with the aid of an Olympus SZX10 microscope equipped with an Olympus Highlight 3100 light source. Zircons were mounted in epoxy in 1" pucks, ground to roughly halfway through the grains, and polished to a 3  $\mu\text{m}$  finish.

The pucks were covered with a conductive gold coat and zircons were imaged using a Leo 1530 Field Emission Scanning Electron Microscope equipped with a cathodoluminescence detector. Gold coating and cathodoluminescence imaging was performed by Dr. Nina Heinig at the Waterloo Advanced Technology Laboratory. Centres and rims of grains were targeted on zircons from the least-altered sample and the altered sample. Based on cathodoluminescent images and reflected and transmitted light microscopic study (Nikon Eclipse LV100POL), fractures and inclusions of other minerals within zircons were avoided.

LA-ICP-MS U-Pb geochronology was performed at the Metal Isotope Geochemistry Laboratory at the University of Waterloo. An Analyte G2 laser system with a HelEx two-volume sample cell was used in conjunction with an Agilent 8800 quadrupole ICP-MS to conduct U-Pb geochronology. The elements and isotopes measured include  $^{206}\text{Pb}$ ,  $^{207}\text{Pb}$ ,  $^{238}\text{U}$ ,  $^{232}\text{Th}$ , and  $^{88}\text{Sr}$ . A  $\sim 25$   $\mu\text{m}$  in diameter spot size, fluence of 4  $\text{J}/\text{cm}^2$  (measured at sample surface), and a frequency of 5 Hz were used.

Zircons were ablated for 30s and aerosol was carried to the torch using  $\sim 1$  L/min He with an additional  $\sim 1$  L/min Ar added as a make up gas in a mixing bulb. Zircon standard DD85-17 was used as a primary standard ( $3002 \pm 2$  Ma; Tomlinson et al., 2003) and Archean standard DD91-1 ( $2682.4 \pm 1$  Ma; Davis 2002) was monitored as a secondary standard. Data was reduced using Iolite v 3.6 (Paton et al., 2011) and the U-Pb Geochronology4 data reduction scheme. No down-hole fractionation correction was applied and this, along with the different U concentrations between unknowns and standards, may explain some of the reverse discordance that is observed (Section 4.6). However, this is not expected to influence the  $^{207}\text{Pb}/^{206}\text{Pb}$  ages that are considered here. The secondary standard (DD91-1) yielded a  $^{207}\text{Pb}/^{206}\text{Pb}$  age of  $2682 \pm 6$  (MSWD = 0.50), which is within the uncertainty of the accepted value. Weighted mean  $^{207}\text{Pb}/^{206}\text{Pb}$  ages are reported with 95% confidence limits that include incorporation, in quadrature, of the uncertainty in the secondary reference zircons.

## **4.0 Results**

Section 4.1 outlines the results of field, petrographic, and scanning electron microscopic study. Section 4.2 presents findings based on analysis of whole-rock geochemical data. Section 4.3 summarizes the findings from the analysis of minerals via electron microprobe. Section 4.4 presents the results pertaining to gold indicators and the distribution of gold grades within the alteration envelopes associated with auriferous quartz veining. Results pertaining to gold indicators and distribution are outlined in Section 4.4. Results of multiple sulphur isotopic analyses of sulphide minerals are presented in Section 4.5 while findings pertaining to LA-ICP-MS are outlined in Section 4.6. Figures and tables pertaining to the sections discussed above are located at the end of each of these respective sections. Major lithological units at the Island Gold deposit are referred to based on their interpreted protoliths (discussed in Section 5.1): Dacite, iron formation, gabbro, the Webb Lake stock (tonalite-trondhjemite), gabbro/lamprophyre (protolith uncertain; Section 5.1.5), quartz diorite, silica-poor diorite–monzodiorite, and diabase–quartz diabase. However, it must be noted that these units have been subject to metamorphism and are believed to be the metamorphosed equivalents of these interpreted protoliths. Mine terms used to refer to these units are included in parentheses in the header for each of these lithologies when applicable.

### **4.1 Field relations, petrography, and scanning electron microscopy**

The results of field observations, hand sample analysis, petrography, SEM-EDS, and SEM-MLA are summarized in this chapter. First, results pertaining to vein types and gold mineralization at the Island Gold deposit are outlined in one section (Section 4.1.1). Each of the major lithologies at the Island Gold deposit then have a dedicated section where the results from these analyses are presented (Sections 4.1.2 to 4.1.9). If certain lithologies have results from both least-altered samples and samples subject to alteration related to quartz  $\pm$  carbonate veining, results pertaining to least-altered and altered samples are presented in separate sub-sections. Lastly, results related to metamorphism are summarized for all lithologies in Section 4.1.10. Specific mineral names determined via electron microprobe (Section 4.3) may also be included for minerals in certain mineral groups (carbonates, chlorite, plagioclase, and white mica) and lithologies (dacite, gabbro, and the Webb Lake stock) in this section.

#### 4.1.1 Veins and gold mineralization ( $V_{GD}$ , $V_1$ - $V_2$ , $V_3$ , and $V_4$ )

When applicable, the alteration associated with quartz veining is discussed in the corresponding alteration sub-section for each lithology (Sections 4.1.2 to 4.1.9).

##### 4.1.1.1 Field observations

White-coloured, semi-translucent  $V_{GD}$  extensional veins are present in the Goudreau Zone as shallowly dipping, folded quartz veins (Figure 7A). These veins crosscut and alter the dacite, gabbro, and Webb Lake stock.

White-grey, translucent  $V_1$  and  $V_2$  veins are observed throughout the deposit. A shear that hosted  $V_1$ - $V_2$  veins was observed offsetting and deforming a  $V_{GD}$  vein (Jellicoe, 2019; Figure 7A).  $V_1$ - $V_2$  veins were observed cross-cutting and altering the dacite, Webb Lake stock, and gabbro.  $V_2$  extensional veins are typically present as veinlets (< 1 cm across) while  $V_1$  shear veins are often much larger.  $V_1$  and  $V_2$  veins are closely associated with one another in shear zones and  $V_1$  veins often overprint  $V_2$  veins or vice versa. In many cases,  $V_1$  veins are a combination of subparallel  $V_1$  shear veins and small  $V_2$  veinlets (Figure 7B). For these reasons, it is impossible to macroscopically differentiate the effects of a  $V_1$  versus a  $V_2$  vein on the surrounding wall rock due to their close association. As a result, the alteration associated with these veins are studied together in this thesis. They are collectively referred to as  $V_1$ - $V_2$  veins.

In  $V_{GD}$ ,  $V_1$  and  $V_2$  veins, sulphide minerals were present in greater proportions at the margins of the veins or near fragments of wall rock encompassed by the veins. These veins often contain macroscopically visible gold. Envelopes of alteration that increase in intensity moving towards these gold-bearing veins (e.g. Figure 64) are also present and are described in detail for each lithology in its corresponding section. The strength of the foliation typically increases towards these veins as well. The highest concentrations of gold are located within these veins. Gold is also present in the alteration envelopes surrounding gold-bearing quartz veins and the concentration of gold decreases moving away from these veins.

Milky-white, opaque  $V_3$  veins were observed throughout the deposit (Figure 7C). These veins do not host gold mineralization. They are often present in shear zones associated with  $V_1$ - $V_2$  veining but are also situated outside of these shear zones as well. They were observed within all lithologies with the exception of the diabase–quartz diabase. These veins are often more abundant in more competent lithologies. They typically terminate within a few metres (e.g.

Figure 7B) but larger veins where terminations were not visible were also encountered in underground mine workings (e.g. Figure 7C). When these veins coincide with V<sub>1</sub>-V<sub>2</sub> veins, they are often oriented perpendicular or at a high-angle to and crosscut the V<sub>1</sub>-V<sub>2</sub> veins (Figure 7B). The alteration associated with V<sub>3</sub> veins is typically weak and is often indistinguishable. When visible, the alteration envelopes are also typically much smaller than those associated with the gold-bearing quartz veins at this deposit.

Tourmaline is typically present as semi-linear ribbons (Figure 7B; V<sub>4</sub> veins) or occasionally disseminated within various lithologies including V<sub>GD</sub>, V<sub>1</sub>, V<sub>2</sub>, and V<sub>3</sub> quartz veins. The semi-linear tourmaline ribbons commonly parallel the trajectory of these veins (Figure 7B) as well as various other contact surfaces. These tourmaline ribbons are referred to as V<sub>4</sub> veins in Jellicoe (2019). Tourmaline ribbons occasionally have minor quartz and carbonate minerals associated with them as well. Tourmaline was sporadically observed within all lithologies and vein types with the exception of the diabase-quartz diabase.

#### 4.1.1.2 Mineralogy

V<sub>GD</sub>, V<sub>1</sub>, V<sub>2</sub>, and V<sub>3</sub> quartz veins are typically composed of > 90 vol% quartz whereas V<sub>4</sub> veins are composed mostly of tourmaline as well as occasionally minor quartz. Some carbonate minerals (calcite ± dolomite ± ankerite) are also present (typically < 10 vol%) in all vein types (Figure 8). Fragments of wall rock are often included within quartz veins and, as a result, any minerals present in the wall rock are often present in small quantities within the veins. Minor tourmaline may be present in V<sub>GD</sub>, V<sub>1</sub>, V<sub>2</sub>, and V<sub>3</sub> veins but may also be completely absent.

The proportion of carbonate minerals is generally higher in V<sub>3</sub> veins than V<sub>GD</sub>, V<sub>1</sub>, and V<sub>2</sub> veins. The proportion of carbonate minerals is also slightly higher in V<sub>2</sub> veins than V<sub>1</sub> and V<sub>GD</sub> veins.

Gold grains, sulphide minerals (mainly pyrite ± pyrrhotite ± chalcopyrite), chlorite, white mica, and biotite are commonly present in variable but minor quantities within V<sub>GD</sub>, V<sub>1</sub>, and V<sub>2</sub> veins. Actinolite is occasionally observed within V<sub>GD</sub> and V<sub>1</sub>-V<sub>2</sub> veins as well. Based on SEM-EDS analyses, gold grains in V<sub>GD</sub>, V<sub>1</sub>, and V<sub>2</sub> veins also contain minor silver (< 15 weight %). Gold was observed mainly in these auriferous quartz veins but is also present in the alteration envelopes surrounding them. Besides gold itself (which has been discussed in this section), the

other alteration minerals present in the alteration envelopes surrounding these veins are discussed in Sections 4.1.2, 4.1.4, and 4.1.5.

#### **4.1.1.3 Textures**

All quartz vein types exhibit larger quartz grains (typically 0.2-2 mm) with undulose extinction and smaller quartz grains (typically < 0.2 mm) with weaker or no undulose extinction (Figure 8A-D). Quartz grains with undulose extinction are more common in V<sub>1</sub> veins than V<sub>GD</sub>, V<sub>2</sub>, and V<sub>3</sub> veins. In some cases, these smaller, less-strained grains have sub-polygonal to polygonal boundaries. When present, sulphide and carbonate minerals tend to be concentrated along the margins of quartz veins.

Gold is typically present as free gold along mineral grain boundaries within V<sub>GD</sub>, V<sub>1</sub>, and V<sub>2</sub> veins in the form of µm to mm-scale droplets, layers, or veinlets (Figure 9A, B; greater than ~90% of observed gold). Occasionally gold is present as inclusions within other minerals including quartz, carbonate minerals, white mica, and pyrite (e.g. Figure 9C; less than ~10% of observed gold). In all cases, observed gold was spatially associated with sulphide minerals within a few hundred µm. Less commonly, gold grains that are texturally-equivalent to those present within veins are observed within the altered wall rock outside of V<sub>GD</sub>, V<sub>1</sub>, and V<sub>2</sub> veins as well. Excluding gold (which has been discussed in this section), the textures of other alteration minerals present in the alteration envelopes surrounding these veins are discussed in Sections 4.1.2, 4.1.4, and 4.1.5.

Linear tourmaline ribbons (V<sub>4</sub> veins) are composed of groups of tourmaline grains with their long axes oriented subparallel to one another. Blocky/massive (Figure 34A) and radial tourmaline grains (Figure 32B, D) are also occasionally present within V<sub>4</sub> veins or disseminated within various other lithologies as well. When present, tourmaline typically overprints other minerals it coincides with.

### **4.1.2 Dacitic volcanic rocks (T2, V2, I2)**

#### **4.1.2.1 Field observations**

The dacitic volcanic rocks (referred to as dacite) are the most volumetrically significant protolith at the Island Gold deposit. As a result, this lithology hosts the majority of the ore zones at this deposit. These volcanic rocks are believed to be the oldest lithology within current mine



workings (Jellicoe, 2019) and are cross-cut or stratigraphically overlain by all other lithologies. At the Island Gold deposit, these rocks have been subject to greenschist-grade metamorphism and variable degrees of deformation and hydrothermal alteration. These volcanic rocks appear in a wide variety of forms including tuffs (Figure 10A-B), flows, pyroclastic breccias (Figure 10C), and hypabyssal intrusive units (Figure 10D). The tuffaceous units often contain lapilli (Figure 10B) and occasionally bomb-sized rock fragments that are mineralogically and chemically similar to the host tuff. Fragments may be composed of material equivalent to a tuff, flow, or hypabyssal intrusive.

A number of dacite-hosted alteration envelopes associated with auriferous quartz veins ( $V_{GD}$  and  $V_1$ - $V_2$ ; e.g. Figure 64A; Appendix B) at varying elevations and distances parallel to the GLDZ were sampled. Samples from within these auriferous alteration envelopes and quartz veins were subdivided into five quantitative groupings: Auriferous quartz veins, strongly-altered, moderately-altered, weakly-altered, and least-altered (Figure 12). These alteration strength groupings are discussed in detail in Section 3.2.3.

Deformation and alteration intensify towards gold-bearing quartz vein corridors. The alteration envelopes that surround these gold bearing quartz vein corridors are often approximately the same size on either side of the vein but this is not always the case. Alteration envelopes associated with  $V_1$ - $V_2$  veins were observed to range in size from millimetre scale up at least 10 m perpendicularly outwards from the nearest central quartz vein-wall rock contact. The central veins in the alteration envelopes studied range in size from millimetre scale to 1.5 m across. Larger gold-bearing veins were observed in underground mine workings but the extents of the alteration envelopes associated with these veins were not studied. Larger alteration envelopes are generally associated with the widest veins so alteration envelopes larger than 10 m in width are likely present. The alteration envelope associated with a  $V_{GD}$  extensional vein (~0.5 m apparent thickness) was observed to extend less than ~5 m perpendicularly outwards from the vein-wall rock contact. This is smaller than the alteration envelopes associated with  $V_1$ - $V_2$  shear veins of similar size. However, it is challenging to quantify the extent of alteration from a single quartz vein due to the presence of multiple quartz veins, which each have their own associated alteration envelope, within a single auriferous quartz vein corridor. Furthermore, alteration envelopes associated with neighbouring auriferous quartz vein corridors often overlap (particularly the weakly-altered portions which are the largest). In addition, continued post-

mineralization deformation has had an effect on the geometry of these alteration envelopes resulting in further variability in their shape and size. It is also difficult to quantify the size of quartz veins at the centre of alteration envelopes because these veins often pinch and swell. Occasionally no visible quartz veins are present at the centre of some alteration envelopes. Additionally, it is difficult to identify exactly where the weakly-altered outer margin of an alteration envelope ends and unaltered rock begins due to subtle differences in appearance.

A carbonate-sericite alteration zone that was not associated with quartz veining or gold mineralization was observed (Figure 13). This zone bears a resemblance to the alteration associated with auriferous zones but has a number of mineralogical and chemical differences that are discussed in the following sections. The alteration zone that was sampled and studied in this thesis was observed in drill core approximately 500 m SSW of the main Island Gold Zones. This type of alteration was not observed elsewhere during field work for this thesis. When present in the dacite, tourmaline ribbons are typically concentrated along the structural conduits such as enveloping surfaces of lithological contacts, shear zones, and quartz veins.

#### **4.1.2.2 Least-altered samples**

##### **4.1.2.2.1 Mineralogy**

The mineralogy of the dacite, in approximate order of abundance, consists of plagioclase (andesine), quartz, calcite, biotite, chlorite (ripidolite), white mica (muscovite and illite), and epidote. Accessory minerals (typically < 1 vol%) can include actinolite, apatite, chloritoid, grunerite, hematite, hornblende, ilmenite, magnetite, rutile, siderite, titanite, tourmaline, and zircon. Trace amounts of graphite were also detected by SEM-MLA but were not observed optically. In this case, the carbon coating is interpreted to have been mistaken for graphite during the automated SEM-MLA process. In a rare case, garnet was also observed in an interval of drill core composed of this lithology (Figure 65B). The volumetric proportions of minerals in a least-altered volcanic sample are displayed in Figure 11A.

##### **4.1.2.2.2 Textures**

Dacitic samples are often porphyritic and contain macroscopically-visible phenocrysts of quartz and plagioclase (< 1 cm) in an aphanitic groundmass (Figure 10A). Hypabyssal intrusive rocks are generally equigranular with a fine to medium grain size (typically <2 mm; Figure 10D).

Quartz phenocrysts observed in hand sample often have a blue colour and, based on SEM-EDS analysis, these phenocrysts have microscopic titanium-rich inclusions of rutile, titanite and/or ilmenite (discussed further in Appendix A). Plagioclase is typically anhedral–subhedral and are altered by white mica and epidote (Figure 14D). Potassium feldspar was not observed. Biotite and hornblende are usually anhedral and are partially altered or completely pseudomorphed by chlorite or actinolite. Similarly, carbonate minerals (mainly calcite) often replace hornblende and trace calcic pyroxene. Carbonates also infills irregular spaces between other mineral grains (Figure 14D) or are present as minor mm to cm-scale veinlets. Hematite alteration is occasionally associated with these calcite veinlets (Figure 10A). Actinolite, chlorite, epidote, carbonates, grunerite, hematite, ilmenite, magnetite, rutile, and titanite are intergrown with each other and often replace most other minerals (Figure 14D) excluding chloritoid, tourmaline, and garnet (when present). Chloritoid, tourmaline, and garnet overprint all other minerals. In rare cases, idioblastic to subidioblastic garnet was observed in drill core and appears to overprint all other minerals including chloritoid (Figure 65B). A timing relationship between tourmaline and garnet/chloritoid was not observed in this lithology. Chloritoid is typically randomly-oriented (Figure 65A). When present, tourmaline is typically concentrated along lithological contacts, shear planes, and the enveloping contact surfaces of veins/veinlets.

#### **4.1.2.2.3 Primary minerals**

Major primary minerals in the dacite include plagioclase (andesine), quartz, and biotite. Accessory primary minerals (typically < 1 vol%) can include apatite, hornblende, ilmenite, magnetite, and zircon. These minerals are often altered or overprinted by metamorphic minerals which are discussed cumulatively for all lithologies in Section 4.1.10.

#### **4.1.2.3 Altered samples**

##### **4.1.2.3.1 Mineralogy**

There are distinct changes in the mineral modes of variably-altered dacitic samples that have been subject to alteration related to auriferous quartz veins (Figure 16A-C). The mineral modes in Figure 16A were determined by averaging the mineral modes of dacitic samples that were classified within a specific alteration strength grouping (4 to 8 samples per group). It is challenging to differentiate between fine grained quartz and feldspar when point-counting. As a

result, these minerals are grouped together in this figure. Figure 16B is constructed based on SEM-MLA mineral proportion data from a representative dacite-hosted alteration envelope associated with a  $V_1$ - $V_2$  auriferous quartz vein. Quartz and feldspar can be easily differentiated using SEM-MLA analysis and their proportions are shown in Figure 16B. The mineral modes for a representative dacite-hosted alteration envelope associated with a  $V_{GD}$  auriferous quartz vein are shown in Figure 16C. Quartz and feldspars are grouped together in this figure. Averages (Table 3A) and ranges (Table 3B) of mineral proportions in dacitic samples classified under each alteration strength grouping and in quartz veins ( $V_1$ - $V_2$  and  $V_{GD}$ ) are displayed. Point-counting and SEM-MLA mineral proportion data are located in Appendix E and Appendix F, respectively.

Alteration minerals associated with  $V_1$ - $V_2$  gold-bearing quartz veins in the dacites include Ca-Mg-Fe carbonates, chlorite, quartz, sulphides (pyrite  $\pm$  pyrrhotite  $\pm$  chalcopyrite), white mica (muscovite), and trace amounts of rutile. The proportion of quartz steadily decreases while plagioclase modes increase when moving away from auriferous quartz veins towards least-altered material (Figure 16B). Strongly-altered dacite is dominated by white mica and pyrite but also has substantial amounts of carbonate minerals (Figure 16A, B). Trace amounts of chalcopyrite, closely associated with pyrite, are often present in this zone as well. In the moderate zone, the proportion of carbonate minerals increases while pyrite content decreases dramatically, and chlorite modes increase while white mica modes decrease (Figure 16A, B). Minor pyrrhotite often appears in the moderate zone as well (Figure 16A). The weak zone is characterised by substantial decreases in the amount of white mica, carbonates and sulphides and chlorite modes continue to increase (Figure 16A, B). Least-altered dacitic samples are characterized by the absence of pyrite and a decrease in the amount of chlorite relative to the weak zone (Figure 16 31A, B). Trace disseminated magnetite is often present in the weakly-altered and least-altered samples of the dacite. Trace potassium feldspar was identified via SEM-MLA in samples altered by  $V_1$ - $V_2$  veins (Figure 16B) but is present in insignificant proportions and was not verified optically. The mineralogy of least-altered samples is discussed in Section 4.1.2.2.1. A  $V_2$  veinlet was encountered in a dacitic sample weakly to moderately-altered by larger  $V_1$ - $V_2$  veins nearby. A thin section that includes this  $V_2$  veinlet and an associated cm-scale alteration envelope was analyzed by SEM-MLA. An SEM-MLA image of this thin section using false colours for minerals and displaying approximate boundaries between alteration zones is shown in Figure 18. Based on visual estimates, the alteration mineral assemblage and mineral

proportions are equivalent to the alteration associated with V<sub>1</sub>-V<sub>2</sub> combination veining on a larger scale. Photomicrographs of dacitic samples variably-altered by V<sub>GD</sub> and V<sub>1</sub>-V<sub>2</sub> veining are displayed in Figure 67 (Appendix B) and Figure 14, respectively.

Overall, the alteration mineral assemblage associated with V<sub>GD</sub> veins located in the Goudreau Zone is consistent with the alteration associated with V<sub>1</sub>-V<sub>2</sub> veins. However, there is a larger proportion of white mica and chlorite and a smaller amount of quartzofeldspathic minerals than typically observed in alteration envelopes associated with V<sub>1</sub>-V<sub>2</sub> veins (Figure 16). In addition, the largest concentration of carbonate minerals in alteration envelopes associated with V<sub>GD</sub> veins is typically in strongly-altered samples (Figure 16C) rather than in moderately-altered samples (Figure 16A, B). Furthermore, weakly-altered samples from the Goudreau Zone also have more white mica and chlorite than typically observed in weakly-altered samples associated with V<sub>1</sub>-V<sub>2</sub> veins elsewhere in the deposit (Figure 16).

A number of ore zones were sampled throughout the deposit and the locations of these ore zones relative to mine workings are displayed in Figure 19. Figures displaying the volumetric changes in mineralogy moving away from the centre of each of these zones are displayed in Figure 68 (Appendix B). Based on these results, alteration mineral assemblages associated with auriferous quartz veins are generally consistent along strike and at various depths within the deposit. However, there are a few notable variations in the proportions of these minerals between zones. The volumetric percentage of quartz in the strongly-altered sample from the deep zone associated with V<sub>1</sub>-V<sub>2</sub> veins (~1300 m depth) has more quartz and feldspar (64 vol%) when compared to the average quartzofeldspathic mineral content of all strongly-altered samples (46 vol%). Based on petrographic study, it is clear that this increase in quartzofeldspathic minerals can be attributed to silicification of this sample.

In addition, the strongly-altered sample from a V<sub>1</sub>-V<sub>2</sub> ore zone located approximately at the centre of current mine workings (~500 m depth) has more white mica (44 vol%) when compared to the white mica content in the average strongly-altered sample (33 vol%).

Furthermore, carbonate content is very low in the strongly-altered samples in both the central (< 1 vol%) and deep ore zones (~1 vol%) associated with V<sub>1</sub>-V<sub>2</sub> veins. However, carbonate content is commonly low in very strongly-altered samples directly proximal to auriferous quartz veins. These samples often contain small quartz veinlets and silicification rather than substantial carbonation. Moderately-altered samples associated with V<sub>1</sub>-V<sub>2</sub> veins are

typically composed of a substantial amount of carbonate minerals, but this was not verified petrographically in the central and deep ore zones.

An altered zone that was not associated with quartz veining or gold mineralization was also encountered. The mineralogy of this alteration is similar to the strongly-altered material associated with auriferous quartz veins but can be differentiated based on the lack of both sulphides and quartz veining/silicification. These zones are characterized by strong sericitization and the presence of substantial interstitial carbonates and carbonate veinlets.

#### **4.1.2.3.2 Textures**

V<sub>1</sub>-V<sub>2</sub> alteration-derived quartz, white mica (muscovite), sulphides, carbonates, rutile, and chlorite commonly overprint or alter primary and pre-existing metamorphic minerals present in the least-altered dacitic samples (which mainly consist of plagioclase, quartz, calcite, chlorite, biotite, and epidote; Figure 14A-C). When present, tourmaline overprints all minerals. In strongly-altered samples microscopic quartz veinlets may be present. Both chlorite and white mica commonly alter biotite and other minor ferromagnesian minerals (Figure 14A-C). Alteration-derived chlorite is intergrown with other alteration minerals. White mica commonly replaces chlorite (Figure 14B, C). Pyrite is the dominant sulphide mineral and is typically spatially associated with ferromagnesian minerals. When present, pyrrhotite and chalcopyrite are closely associated with pyrite. Ca-Mg-Fe carbonates are present as variably-shaped masses between other grains. Rutile typically replaces ilmenite and titanite. Many primary textures such as quartz and feldspar phenocrysts are no longer visible in moderately or strongly-altered samples (Figure 14). The strongly-altered samples typically have a stronger foliation (Figure 14A) and are often finer-grained than least-altered samples (Figure 14D). Furthermore, these strongly-altered samples often contain elongate minerals with preferential orientations (Figure 14A). The alteration minerals and textures discussed above are also observed in samples altered by V<sub>GD</sub> veins (Figure 67; Appendix B). Samples altered by V<sub>1</sub>-V<sub>2</sub> shear veins (Figure 12A) are typically more deformed than those in samples altered by V<sub>GD</sub> extensional veins (Figure 66A; Appendix B).

Besides the notable absence of quartz veining/silicification and pyrite, samples from the non-auriferous, sericite-carbonate alteration zones are texturally similar to samples from

alteration zones associated with auriferous veining (Figure 15). Similar to many V<sub>1</sub>-V<sub>2</sub> and V<sub>GD</sub> vein-related alteration zones, tourmaline was also observed within these samples (Figure 13).

#### **4.1.2.3.3 Carbonate-sericite, V<sub>GD</sub>, and V<sub>1</sub>-V<sub>2</sub>-vein related alteration minerals**

V<sub>GD</sub> vein-related alteration and V<sub>1</sub>-V<sub>2</sub> vein-related alteration of dacite both result in the same alteration mineral assemblage which replaces primary and pre-existing metamorphic minerals. These alteration minerals include Ca-Mg-Fe carbonate minerals, chlorite (ripidolite), quartz, sulphides (pyrite ± pyrrhotite ± chalcopyrite), and white mica (muscovite). Non-auriferous carbonate-sericite alteration minerals mainly include carbonate minerals and white mica which also commonly replace primary and pre-existing metamorphic minerals (Figure 15).

### **4.1.3 Iron formation (IF)**

#### **4.1.3.1 Field observations**

Iron formations separate the dacitic rocks from the mafic volcanic rocks to the north. In rare cases, iron formations are occasionally interbedded with dacitic rocks in drill core. Cross-cutting relationships between this lithology and intrusive lithologies at the Island Gold deposit were not observed. Massive sulphide and iron oxide-rich iron formations with no macroscopically visible layering (Figure 21A, C) and banded iron formations are present (Figure 21B). When visible, layers appear to be composed of iron oxides and sulphides alternating with chert, carbonate, and chlorite-rich layers. In one outcrop, the iron formation contains large dacite clasts stretched parallel to the foliation (Figure 21D).

#### **4.1.3.2 Mineralogy**

The mineralogy of the sulphide and iron oxide-rich layers of the iron formation consist of mainly hematite, magnetite, and pyrite. The proportions of minerals vary considerably within this layer grouping with layers ranging from mostly iron oxides (Figure 22A) to mainly sulphides (Figure 22B, D). Iron oxide and sulphide-rich layers are separated by layers with various proportions of quartz, carbonate minerals, chlorite, and plagioclase. Some layers are mainly composed of quartz (Figure 22C), others are dominantly composed of chlorite and biotite (Figure 22C), and others mostly consist of carbonate minerals (Figure 22D). Accessory minerals can

include chloritoid, epidote, ilmenite, white mica, and tourmaline. The heterogeneous and layered nature of this unit makes point-counting analyses unsuitable.

#### **4.1.3.3 Textures**

Iron oxide and sulphide-rich layers in the iron formation range from fine to coarse-grained whereas silicate-rich layers are typically fine grained. Iron oxides and sulphide minerals are present as massive bands (Figure 22A, B, D). Carbonates are interstitial or are present as minor mm to cm-scale carbonate veinlets. Hematite alteration is occasionally associated with these carbonate veinlets. Plagioclase feldspar is anhedral and is typically altered by chlorite, epidote, carbonates, and white mica. Biotite is often replaced or pseudomorphed by chlorite but, in some cases, biotite appears to overprint chlorite (Figure 22C). Carbonates, chlorite, epidote, ilmenite, and white mica commonly replace or overprint most other minerals with the exception of chloritoid and tourmaline. When present, tourmaline and randomly oriented chloritoid grains overprint all minerals. A timing relationship between chloritoid and tourmaline was not observed in this lithology.

##### **4.1.3.3.1 Primary minerals**

Major primary minerals in the banded to massive iron formations include carbonate minerals, hematite, magnetite, plagioclase, pyrite, and quartz. Proportions of minerals vary considerably depending on the layer being observed. Primary clay minerals were not observed but may have been the precursors of the chlorite and biotite-rich layers prior to metamorphism.

#### **4.1.4 Gabbro (I3G)**

##### **4.1.4.1 Field observations**

Gabbro is common at the Island Gold deposit and is present as sills and dykes that cross-cut the dacitic rocks. These rocks have been subject to metamorphism and variable degrees of deformation and hydrothermal alteration. This lithology is distinguished based on its deep green colour due to significant chlorite content (Figure 23D). This lithology hosts a small proportion of the ore at the Island Gold deposit (< 10%). A gabbro-hosted alteration envelope associated with V<sub>1</sub>-V<sub>2</sub> auriferous veining was sampled (Figure 23). Samples from this alteration envelope and other samples of this lithology were taken throughout the deposit and were subdivided into five



quantitative groupings: Auriferous quartz veins, strongly-altered, moderately-altered, weakly-altered, and least-altered (Figure 23; Section 3.2.3). This gabbro also hosted  $V_{GD}$  veins in the Goudreau Zone. However, both  $V_{GD}$  and  $V_1$ - $V_2$  veining were present in this location so it was impossible to discern the effects of  $V_{GD}$  veining alone on this lithology. As a result of this, the effects of  $V_{GD}$  veins on this lithology were not studied.

Similar to ore zones hosted by other lithologies, deformation and alteration intensify towards gold-bearing quartz veining (Figure 23) and alteration envelopes observed were approximately the same width on either side of the vein. The auriferous quartz vein at the centre of the alteration envelope sampled consists of a small group of veins/veinlets each of which are less than 0.1 m across. The total extent of this alteration envelope hosted by this lithology could not be determined because a contact with dacite was encountered ~2.4 m up-hole from the auriferous veins (~1.4 m perpendicular distance from the vein-wall rock contact) while still in a weakly-altered zone of the alteration envelope. However, the start of the moderately-altered zone appears to be approximately the same perpendicular distance from the vein contact as in a dacite-hosted zone associated with a quartz vein of similar size (~1.9 m versus ~2.2 m, respectively). The challenges summarized in Section 4.1.2.1 regarding the quantification of quartz vein and alteration envelope sizes/extents were also encountered when studying this gabbro-hosted ore zone.

#### **4.1.4.2 Least-altered samples**

##### **4.1.4.2.1 Mineralogy**

The mineralogy of the gabbro, in approximate order of abundance, consists of chlorite (ripidolite), quartz, epidote, carbonates (mainly calcite), actinolite, titanite, plagioclase (oligoclase–andesine), and hornblende. Accessory minerals can include chloritoid, hematite, ilmenite, magnetite, clinopyroxene, rutile, tourmaline, and white mica (phengite). The proportions of minerals in a representative least-altered sample of gabbro are displayed in Figure 11B. The compositions of select minerals were determined by microprobe (Section 3.6). In one case, garnet was also observed in a hand sample.

#### **4.1.4.2.2 Textures**

Least-altered samples of the gabbro (Figure 23D; Figure 24D) are typically equigranular and medium-grained (1-3 mm). Carbonate minerals are interstitial (Figure 24D) or are present as mm to cm-scale carbonate veinlets (Figure 23D). Hematite alteration is occasionally associated with these calcite veinlets. Plagioclase is anhedral and is typically replaced by chlorite, epidote, calcite, and white mica (Figure 24D). Potassium feldspar was not observed. Hornblende and pyroxene are often pseudomorphed by actinolite, chlorite, and calcite. Actinolite, calcite, chlorite, epidote, ilmenite, quartz, rutile, titanite, and white mica are often intergrown and commonly overprint most other minerals (Figure 24D) excluding chloritoid, tourmaline, and garnet (when present). Chloritoid, tourmaline, and garnet overprint all other minerals. Idioblastic garnet was only observed in one hand sample and appears to overprint all other minerals including chloritoid. A timing relationship between tourmaline and garnet/chloritoid was not observed.

#### **4.1.4.2.3 Primary minerals**

In the majority of the least-altered gabbroic samples, the breakdown and replacement of primary plagioclase and ferromagnesian minerals due to metamorphism is fairly pervasive. As a result, the proportion of primary minerals is low relative to most other lithologies. When present, major primary minerals consist of plagioclase, clinopyroxene, and hornblende. Accessory primary minerals can include ilmenite, magnetite, and quartz.

Due to the low proportions of primary minerals, it is not appropriate to classify this lithology by point-counting to determine mineral modes and plotting on conventional mineralogical classification plots such as the Quartz-Alkali Feldspar-Plagioclase (QAP) ternary diagram. Instead, geochemistry is used in Section 4.2.4.1 to suggest a likely classification.

#### **4.1.4.3 Altered samples**

##### **4.1.4.3.1 Mineralogy**

Figure 17A illustrates the volumetric changes in the mineralogy of the gabbro with varying intensities of alteration. It is challenging to accurately differentiate between fine grained quartz and feldspar so these minerals are grouped together in this figure. However, based on petrographic estimates, quartz content decreases while plagioclase content increases with

increasing alteration. However, quartz content is typically higher immediately proximal to V<sub>1</sub>-V<sub>2</sub> veins/veinlets. Alteration minerals associated with this auriferous corridor include biotite, calcite, chlorite (ripidolite), plagioclase (oligoclase), quartz, rutile, white mica (phengite), and sulphides (pyrite ± pyrrhotite ± chalcopyrite). The strongly-altered sample contains significant biotite, calcite, and pyrite (Figure 17A). In the moderate zone, the amount of carbonate minerals decreases slightly, pyrite content decreases substantially, the amount of biotite decreases, and chlorite content decreases relative to the strong zone (Figure 17A). Minor pyrrhotite is often present in the moderate zone as well. Relative to the moderate zone, the weak zone is characterized by substantial decreases in biotite, calcite, and sulphides and chlorite content increases (Figure 17A). Least-altered samples are characterized by a decrease in biotite, calcite, chlorite, and white mica relative to weakly-altered samples. There is also an increase in the proportions of actinolite, epidote, hornblende, and titanite relative to altered samples (Figure 17A).

#### 4.1.4.3.2 Textures

Alteration-derived biotite, calcite, chlorite, plagioclase (oligoclase), quartz, rutile, white mica (phengite), and sulphides commonly replace primary and pre-existing metamorphic minerals that are present in the least-altered samples of gabbro (Figure 24A–C). When present, tourmaline overprints all minerals. In altered samples, microscopic quartz veinlets may be present. Quartz content increases directly adjacent to veins/veinlets, but away from these veinlets, quartz is replaced by plagioclase. Biotite frequently replaces chlorite (Figure 24A–C) and primary ferromagnesian minerals. Alteration-derived chlorite is intergrown with other alteration-derived minerals (Figure 24A–C). When present, white mica replaces feldspar and chlorite grains. Rutile replaces ilmenite and titanite. Pyrite is the dominant sulphide mineral and is typically spatially associated with other ferromagnesian minerals (Figure 24A-C). When present, pyrrhotite and chalcopyrite are spatially associated with pyrite. Interstitial calcite is present as variably shaped masses. Primary and metamorphic minerals such as pyroxene, hornblende, and actinolite were not observed in moderately or strongly-altered samples. The strongly-altered samples (Figure 24A) typically have a stronger foliation than less-altered samples (Figure 24D). These strongly-altered samples have more elongated and preferentially oriented minerals compared to less-altered samples (Figure 24).

#### **4.1.4.3.3 V<sub>1</sub>-V<sub>2</sub> vein-related alteration minerals**

Minerals that form in the gabbro as a result of V<sub>1</sub>-V<sub>2</sub> veining include biotite, calcite, chlorite (ripidolite), plagioclase (oligoclase), quartz, rutile, sulphides (pyrite ± pyrrhotite ± chalcopyrite) and, occasionally, minor white mica and these minerals commonly replace primary and pre-existing metamorphic minerals.

### **4.1.5 Webb Lake stock: Tonalite–trondhjemite (I1JM)**

#### **4.1.5.1 Field observations**

The Webb Lake stock is a relatively minor lithology at the Island Gold deposit but does host economic gold grades if it is located adjacent to an auriferous quartz vein. However, the Webb Lake stock hosts the majority of the ore at the Magino deposit to the west of the Island Gold deposit (Turcotte and Pelletier, 2008; Figure 4). The competency contrast between this intrusive body and the volcanic rocks that surround it is interpreted to have concentrated strain resulting in the emplacement of the auriferous veins at the Island Gold deposit (Jellicoe, 2019). The Webb Lake stock cross-cuts both the dacite and gabbro. The Webb Lake stock has been subject to metamorphism and variable intensities of deformation and hydrothermal alteration. The samples studied in this thesis were taken from the outer margins of this Webb Lake intrusion. Based on visual estimates, samples closer to the periphery of the intrusion (Figure 25A) have more ferromagnesian minerals than those nearer to the centre (Figure 25C). Tourmaline veining occasionally invades the foliation and earlier quartz veining within this lithology (Figure 25B).

An alteration envelope associated with a V<sub>1</sub>-V<sub>2</sub> auriferous vein and hosted by this lithology at the Island Gold deposit was sampled (Figure 26). The Webb Lake stock also hosted V<sub>GD</sub> veins in areas near the Goudreau Zone but these areas were inaccessible during site visits. As a result, the effect of V<sub>GD</sub> veins on this lithology was not studied. Samples from this alteration envelope and other samples of this lithology were taken throughout the deposit and were subdivided into five quantitative groupings: Auriferous quartz veins, strongly-altered, moderately-altered, weakly-altered, and least-altered (Figure 26; Section 3.2.3). Similar to ore zones hosted by other lithologies, deformation and alteration intensify towards the gold-bearing quartz vein. The auriferous quartz vein at the centre of the alteration envelope is approximately 0.6 m across. The outer boundary of the alteration envelope is relatively sharp and easier to

identify than the outer boundaries of alteration envelopes hosted by dacite or gabbro. The perpendicular distance between the upper vein-wall rock contact and least-altered material was approximately 1.6 m. The perpendicular distance between the lower vein-wall rock contact and least-altered material was approximately 4.0 m. This alteration envelope is asymmetrical although other Webb Lake stock-hosted alteration envelopes were approximately symmetrical. Both ~1.6 m and ~4.0 m extents are appreciably smaller than those from alteration envelopes associated with V<sub>1</sub>-V<sub>2</sub> veins and hosted by dacite or gabbro. The challenges discussed in Section 4.1.2.1 regarding the quantification of quartz vein and alteration envelope sizes/extents were also encountered when studying Webb Lake stock-hosted ore zones.

#### **4.1.5.2 Least-altered and weakly-altered samples**

##### **4.1.5.2.1 Mineralogy**

The mineralogy of the least-altered sample of the Webb Lake stock (Figure 25A; Figure 28D) in order of abundance is as follows: Plagioclase (albite–oligoclase), quartz, chlorite (ripidolite), biotite, white mica (phengite ± muscovite), epidote, and calcite. Accessory minerals can include actinolite, apatite, chloritoid, hematite, hornblende, ilmenite, pyrite, pyroxene, rutile, titanite, tourmaline, and zircon. The proportions of minerals in a least-altered sample of the Webb Lake stock are displayed in Figure 11C. The proportions of ferromagnesian minerals in point-counted samples classified as weakly and least-altered range from 9–20 vol%. These samples were taken from the outer margins of this Webb Lake intrusion. Based on visual estimates, samples away from the margins of the intrusion had fewer ferromagnesian minerals.

##### **4.1.5.2.2 Textures**

The Webb Lake stock (Figure 25A; Figure 28D) is equigranular with a medium to coarse grain size (1–8 mm). Similar to quartz in the dacite, quartz often has a blue colour and phenocrysts have microscopic titanium-rich inclusions of rutile and/or ilmenite. Calcite is interstitial (Figure 28D) or present as carbonate veinlets that are millimetres to centimetres in width. Hematite alteration is occasionally associated with these calcite veinlets. Feldspars are subhedral to euhedral and are typically altered by fine grained epidote, white mica, and calcite (Figure 28D). Trace hornblende and pyroxene are often pseudomorphed by actinolite, chlorite, and calcite. Biotite is partially or completely replaced by chlorite (Figure 28D). When present

actinolite, calcite, chlorite, epidote, ilmenite, rutile, and titanite are intergrown and often overprint most other minerals excluding chloritoid and tourmaline which are occasionally present in this lithology. Chloritoid and tourmaline overprint all other minerals. A timing relationship between tourmaline and chloritoid was not observed.

#### **4.1.5.2.3 Primary minerals**

Major primary minerals in the Webb Lake stock, in approximate order of abundance, include plagioclase (albite–oligoclase), quartz, and biotite. Accessory primary minerals include apatite, hornblende, ilmenite, pyroxene, and zircon.

Based on mineral modes determined via petrographic point counting techniques, three samples of this lithology plot in the tonalite field of a QAP diagram (Figure 27). Difficulty accurately distinguishing between plagioclase compositions petrographically makes point-counting techniques inappropriate for plotting on the Anorthite-Albite-Orthoclase ternary diagram. As a result, geochemistry and CIPW Normative calculations are used to determine the modal proportions of these feldspar end-members for this ternary diagram (Section 4.2.5.1).

#### **4.1.5.3 Altered samples**

##### **4.1.5.3.1 Mineralogy**

Figure 17B highlights the changes in mineral proportions in the Webb Lake stock with varying intensities of alteration related to V<sub>1</sub>-V<sub>2</sub> veining. The alteration assemblage present in this alteration envelope includes biotite, Ca-Mg-Fe carbonates, quartz, rutile, sulphides (pyrite ± pyrrhotite ± chalcopyrite), and white mica (muscovite/phengite). Plagioclase content steadily increases while quartz content generally decreases moving from the V<sub>1</sub>-V<sub>2</sub> auriferous veins to least-altered material (Figure 17B). The strong alteration zone of the Webb Lake stock contains significant proportions of white mica, carbonate minerals, and pyrite (Figure 17B). In the moderate zone, biotite content increases significantly while pyrite and carbonate content decrease relative to the strong zone. Some chlorite is also present in the moderate zone (Figure 17B). Minor pyrrhotite and chalcopyrite closely associated with pyrite are generally restricted to auriferous quartz veins in addition to strongly and moderately-altered samples. Sulphide minerals are typically only present in trace amounts beyond the moderate zone (Figure 17B). The weak zone is characterized by a decrease in the amount of white mica, biotite, and carbonates as well

as an increase in the amount of chlorite relative to the moderate zone (Figure 17B). In least-altered samples, white mica content decreases while the proportions of epidote and chlorite increase (Figure 17B). The mineralogy of the least-altered samples is discussed in Section 4.1.5.2.

#### **4.1.5.3.2 Textures**

Alteration-derived biotite, Ca-Mg-Fe carbonates, quartz, white mica (muscovite/phengite), and sulphides (pyrite  $\pm$  pyrrhotite  $\pm$  chalcopyrite) commonly overprint and/or alter the primary and pre-existing metamorphic minerals present in the least-altered samples of the Webb Lake stock (mainly plagioclase, quartz, calcite, chlorite, biotite, and epidote). When present, tourmaline overprints all minerals it coincides with. In altered samples, quartz is present as subhedral grains as well as interstitial anhedral grains (Figure 28A). In strongly-altered samples microscopic quartz veinlets are occasionally present. White mica often replaces chlorite grains and feldspars. Rutile commonly replaces ilmenite and titanite. Biotite frequently alters chlorite in moderately and strongly altered samples (Figure 28A, B). Pyrite is the dominant sulphide mineral and typically concentrates near ferromagnesian minerals (Figure 28A). When present, pyrrhotite and chalcopyrite are closely associated with pyrite. Ca-Mg-Fe carbonates are present as interstitial masses or replace primary and pre-existing metamorphic Ca-bearing minerals (Figure 28). The strongly-altered samples typically have a stronger foliation and are often finer-grained than less-altered samples (Figure 28).

#### **4.1.5.3.3 V<sub>1</sub>-V<sub>2</sub> vein-related alteration minerals**

Alteration of the Webb Lake stock as a result of V<sub>1</sub>-V<sub>2</sub> veining resulted in the growth of biotite, Ca-Mg-Fe carbonates, chlorite (ripidolite), quartz, rutile, sulphides (pyrite  $\pm$  pyrrhotite  $\pm$  chalcopyrite), and white mica (muscovite  $\pm$  phengite) at the expense of primary and pre-existing metamorphic minerals.

### **4.1.6 Gabbro/Lamprophyre (I2H)**

#### **4.1.6.1 Field observations**

The gabbro/lamprophyre (Figure 29A; protolith uncertain; likely gabbro or lamprophyre; discussed in Section 5.1.5) occurs as sills and dykes that have been metamorphosed and

deformed. In many cases, it is challenging to distinguish between the gabbro, silica-poor diorite–monzodiorite, and gabbro/lamprophyre macroscopically. Intrusions of the gabbro/lamprophyre cross-cut the dacite and gabbro. Dacitic xenoliths are occasionally present within intrusions of the gabbro/lamprophyre (Figure 29B). The gabbro/lamprophyre, Webb Lake stock, and the quartz diorite were not observed in the same area so a definitive timing relationship could not be determined. However,  $V_1$ - $V_2$  veins do crosscut the Webb Lake stock while these veins were not observed crosscutting the gabbro/lamprophyre.

The gabbro/lamprophyre is commonly oriented parallel to gold-bearing quartz vein corridors associated with  $V_1$ - $V_2$  auriferous veins. As a result, clear, high-angle cross-cutting relationships between auriferous veins and this lithology are rarely observed. However, despite being located directly adjacent to  $V_1$ - $V_2$  quartz veins with visible gold, this lithology typically does not exhibit the typical alteration features that gold-hosting lithologies (dacite, gabbro, and the Webb Lake stock) commonly exhibit when near  $V_1$ - $V_2$  veins. In addition, despite the contact between gabbro/lamprophyre and auriferous quartz veins being parallel to the approximate strike of both, these auriferous quartz veins abruptly end at the contact with this lithology indicating that gabbro/lamprophyre cross-cuts these veins and their associated alteration envelopes. Based on the presence of a strong foliation in this lithology, particularly when present in gold-bearing quartz vein corridors, it is evident that this lithology has been subject to deformation after emplacement (Figure 29A).  $V_3$  non-auriferous quartz veins cross-cut, alter (Figure 29C), and occasionally brecciate this intrusion (Figure 29D). Occasionally, slightly larger and more intense alteration aureoles (< 0.2 m away from the quartz vein-gabbro contact) are present in this lithology when it is located directly adjacent to  $V_1$ - $V_2$  veining with intermixed  $V_3$  veins (e.g. Figure 30). This stronger alteration is not present when this lithology is located adjacent to  $V_1$ - $V_2$  veins that are not associated with any visible  $V_3$  veining. Tourmaline may be present or absent in these  $V_3$  veins. When present in the gabbro/lamprophyre, tourmaline veins/ribbons are often concentrated at the contact between gabbro/lamprophyre and neighbouring lithologies (e.g. Figure 30).



## **4.1.6.2 Least-altered samples**

### **4.1.6.2.1 Mineralogy**

The mineralogy of the gabbro/lamprophyre (Figure 29A; Figure 31), in approximate order of abundance, consists of quartz, oligoclase–andesine, carbonate minerals, chlorite, and white mica. Accessory minerals can include actinolite, epidote, hematite, rutile, titanite, tourmaline, and zircon. The proportions of minerals in a representative least-altered sample of gabbro/lamprophyre are displayed in Figure 11D. It is challenging to accurately differentiate between fine-grained quartz and feldspar so they are grouped together in this figure. However, based on visual estimates, there is a larger proportion of quartz than plagioclase in this lithology.

### **4.1.6.2.2 Textures**

The gabbro/lamprophyre is typically equigranular with mainly a fine to medium grain size (<5 mm; Figure 31B). Carbonate minerals are present as subhedral grains, interstitial anhedral grains (Figure 31B), or minor mm- to cm-scale carbonate veinlets. Hematite alteration is occasionally associated with these carbonate veinlets. Plagioclase feldspars are anhedral and are typically replaced by chlorite, epidote, carbonates, and white mica (Figure 31B). Potassium feldspar was not observed. Actinolite, carbonates, chlorite, epidote, quartz, titanite, rutile, and white mica are intergrown and often replace most other minerals excluding tourmaline (Figure 31B). When present, tourmaline overprints all minerals and is typically concentrated along microstructural conduits such as shear planes and veinlets.

### **4.1.6.2.3 Primary minerals**

The breakdown and replacement of primary plagioclase and ferromagnesian minerals is pervasive in all samples of the gabbro/lamprophyre. Trace primary zircon was also optically identified. Based on the chemical composition (Section 4.2.6) and the metamorphic mineral assemblage (Section 4.1.10), likely primary minerals are discussed in Section 5.1.5.

Due to the low proportions of primary minerals, it is not appropriate to classify this lithology by point-counting to determine mineral modes and subsequently use this data to plot on conventional mineralogical classification plots such as the Quartz-Alkali Feldspar-Plagioclase (QAP) ternary diagram. Instead, geochemistry is used in Section 4.2.6.1 to suggest a likely classification.

### **4.1.6.3 Altered samples**

#### **4.1.6.3.1 Mineralogy**

The mineralogy of a sample of the gabbro/lamprophyre altered by a proximal V<sub>3</sub> vein consists mainly of quartz, plagioclase, carbonate minerals, chlorite, and white mica. Based on visual petrographic estimates, this sample (T213), which has been altered by a non-auriferous V<sub>3</sub> vein, has notable increases in the amount of white mica ( $\pm$  minor fuchsite) compared to least-altered samples. In addition, epidote content decreases relative to least-altered samples and only trace amounts are present in the altered sample. Chlorite content decreases but this mineral still makes up a large proportion of the sample. Proportions of other minerals, including sulphides, remain similar to the proportions in least-altered samples.

#### **4.1.6.3.2 Textures**

White mica and large carbonate grains commonly replace the minerals in the least-altered samples of the gabbro/lamprophyre (Figure 31A), with the exception of tourmaline (when present). White mica grains are often randomly oriented and the long axes of these minerals are often not parallel to the dominant foliation (Figure 31A). On average, carbonate mineral grains in altered samples are larger than those in least-altered samples (Figure 31). Carbonates are interstitial or are present as subhedral–euhedral grains (Figure 31A). Plagioclase feldspars are anhedral and are altered by chlorite, epidote, carbonates, and white mica. This altered sample has an overall coarser-grain size than most least-altered samples (Figure 31).

#### **4.1.6.3.3 V<sub>3</sub>-vein related alteration minerals**

The minerals that form in gabbro/lamprophyre as a result of V<sub>3</sub> vein-related alteration and replace primary and pre-existing metamorphic minerals are mainly white mica ( $\pm$  fuchsite) and carbonates.

### **4.1.7 Quartz diorite**

#### **4.1.7.1 Field observations**

Xenoliths of the red/pink-coloured quartz diorite were identified within an intrusion of silica-poor diorite–monzodiorite on the 620 level (Figure 32A). These xenoliths contain visible carbonate ( $\pm$  quartz  $\pm$  tourmaline) veinlets and have been subject to metamorphism and

deformation. This quartz diorite also occurs on the 600 level in the form of a dyke cross-cutting the dacite but the location of this occurrence on this level was not accessible. This intrusion was not encountered elsewhere in mine workings and was not encountered proximal to auriferous quartz veining.

#### **4.1.7.2 Mineralogy**

The mineralogy of a quartz diorite sample (T215; Figure 32B–D), in approximate order of abundance, consists of plagioclase (albite), quartz, carbonate minerals, hematite, and chlorite. Accessory minerals include biotite, epidote, magnetite, titanite, tourmaline, white mica, and zircon. Despite the pink colouration of this intrusive lithology, potassium feldspar is absent and plagioclase makes up the majority of this intrusion. There is also a substantial amount of hematite. The proportions of minerals in a representative quartz diorite sample are displayed in Figure 11E.

#### **4.1.7.3 Textures**

The quartz diorite is generally equigranular with typically a medium grain size (1–5 mm; Figure 32C, D). Carbonate minerals are interstitial (Figure 32D) or present as parallel mm to cm-scale carbonate veinlets (Figure 32A, B). Microscopic hematite inclusions (< 10 µm) are present along fracture surfaces or as inclusions within plagioclase grains (Figure 32C). In addition, larger anhedral–euhedral magnetite and hematite grains are also present. Plagioclase feldspars are typically subhedral–euhedral and are weakly-altered by chlorite, epidote, carbonates, and white mica (Figure 32D). Trace amounts of biotite are replaced or pseudomorphed by chlorite. Carbonates, chlorite, epidote, hematite, magnetite, quartz, titanite, and white mica are intergrown and replace most other minerals (Figure 32C, D) excluding tourmaline. Tourmaline typically overprints all minerals and is concentrated along microstructural conduits such as quartz-carbonate veinlets and grain boundaries (Figure 32B).

#### **4.1.7.4 Primary minerals**

Major primary minerals in the quartz diorite, in approximate order of abundance, include plagioclase (albite) and quartz. Accessory primary minerals can include biotite, magnetite, and

zircon. Based on mineral modes determined via petrographic point counting techniques, this lithology plots in the quartz diorite field of the QAP diagram (Figure 27).

#### **4.1.8 Silica-poor diorite–monzodiorite (I2M)**

##### **4.1.8.1 Field observations**

Silica-poor dioritic–monzodioritic intrusions are commonly present as sills and dykes that have been subject to metamorphism and deformation. These diorite–monzodiorite intrusions cross-cut the dacite and gabbro. A sharp contact between the silica-poor diorite–monzodiorite and the gabbro/lamprophyre was observed in drill core (Figure 33C) but the cross-cutting relationship is unclear. In a few cases within underground workings, the silica-poor diorite–monzodiorite appears to cross-cut the gabbro/lamprophyre. However, due to difficulty differentiating between the gabbro/lamprophyre and silica-poor diorite–monzodiorite in this setting, these cross-cutting relationships are ambiguous. Additionally, both of these lithologies are relatively minor and commonly parallel each other within mine workings so clear, high-angle, cross-cutting relationships were not observed. The silica-poor diorite–monzodiorite is notably less deformed than the gabbro and gabbro/lamprophyre when these lithologies are located in the same area and compared.

Large, volumetrically significant and partially resorbed xenoliths of quartz diorite were observed within this intrusive lithology as well (Figure 32A). Silica-poor dioritic–monzodioritic samples may be grey-coloured (Figure 33A) or have a slight pink–red colouration (Figure 33B) which is a less intense variety of the distinct pink–red colour of the hematite-rich quartz diorite lithology. Particularly when present in gold-bearing quartz vein corridors, it is evident that this lithology has been subject to some deformation after emplacement. The silica-poor diorite–monzodiorite and the Webb Lake stock were not observed to occur in the same area so a definitive timing relationship could not be determined. However,  $V_1$ - $V_2$  veins crosscut the Webb Lake stock while these veins were not observed crosscutting the silica-poor diorite–monzodiorite despite the silica-poor diorite–monzodiorite commonly paralleling  $V_1$ - $V_2$  auriferous veins. As a result, clear, high-angle cross-cutting relationships between auriferous veins and this lithology are rarely observed. However, despite being located directly adjacent to  $V_1$ - $V_2$  quartz veins with visible gold, this lithology does not exhibit the alteration features that gold-hosting lithologies (dacite, gabbro, and the Webb Lake stock) commonly exhibit when near  $V_1$ - $V_2$  veins. In

addition, despite the contacts between the silica-poor diorite–monzodiorite and auriferous quartz veins typically being parallel to their approximate strikes, these auriferous quartz veins abruptly end at the contact with this lithology indicating that the silica-poor diorite–monzodiorite cross-cuts these veins and their associated alteration envelopes (Figure 34C). In many cases, small alteration aureoles (10 cm perpendicular distance from the quartz vein-diorite–monzodiorite contact) are present in this lithology when it is directly adjacent to  $V_3$  veins or  $V_1$ - $V_2$  veins with intermixed  $V_3$  veins (Figure 34A). This alteration is typically not present when this lithology is located adjacent to  $V_1$ - $V_2$  veins that are not associated with any visible  $V_3$  veining (e.g. Figure 34C). Tourmaline may be present or absent from these  $V_3$  veins. When present, tourmaline veins/ribbons are often concentrated at the contact between the silica-poor diorite–monzodiorite and the host-rock that it intrudes.

#### **4.1.8.2 Least-altered samples**

##### **4.1.8.2.1 Mineralogy**

The mineralogy of the silica-poor diorite–monzodiorite, in approximate order of abundance, consists of plagioclase (oligoclase), carbonate minerals, biotite, chlorite, epidote, magnetite, and orthoclase. Accessory minerals can include hematite, pyrite, quartz, rutile, titanite, tourmaline, white mica, and zircon. The proportions of minerals in a representative least-altered silica-poor diorite–monzodiorite sample are displayed in Figure 11F.

##### **4.1.8.2.2 Textures**

The silica-poor diorite–monzodiorite is typically equigranular and medium-grained (1–5 mm; Figure 35B). It is also characterized by substantial carbonate content (~25 vol%; Figure 11F). Carbonate minerals take the form of xenoblastic interstitial grains, larger subidioblastic grains (Figure 35B), and as mm- to cm-scale carbonate veinlets. Hematite alteration is occasionally associated with these carbonate veinlets. Plagioclase is typically subhedral and altered by chlorite, epidote, carbonates, and white mica (Figure 35B). Biotite is often altered by chlorite but, in some cases, biotite appears to overprint chlorite (Figure 35B). Magnetite is closely associated with hematite. Carbonates, biotite, chlorite, epidote, hematite, quartz, rutile, titanite, white mica, and occasionally magnetite are often intergrown and commonly replace

most other minerals excluding tourmaline (Figure 35B). Tourmaline overprints all minerals and, when present, is typically concentrated along structures such as shear planes and veinlets.

#### **4.1.8.2.3 Primary minerals**

Major primary minerals in the silica-poor diorite–monzodiorite, in approximate order of abundance, include plagioclase (oligoclase), biotite, magnetite, and orthoclase. Accessory primary minerals can include pyrite, quartz, white mica, and zircon. Some of the biotite is primary while some is likely alteration-derived. This is made apparent by the presence of some unaltered biotite grains in least-altered samples overprinting pre-existing chlorite (Figure 35B). It is unclear whether these unaltered biotite grains formed during metamorphism or due to another alteration event. Based on mineral modes determined via petrographic point counting techniques, this lithology plots in the diorite field of the QAP diagram (Figure 27).

#### **4.1.8.3 Altered samples**

##### **4.1.8.3.1 Mineralogy**

The mineralogy of a silica-poor diorite–monzodiorite sample altered by a  $V_3$  vein (Figure 34B; Figure 35), in approximate order of abundance, consists mainly of plagioclase, carbonate minerals, chlorite, magnetite, and orthoclase. Based on visual petrographic estimates, this sample (T245) altered by non-auriferous  $V_3$  veins displays notable increases in the amount of chlorite and white mica when compared to least-altered samples. In addition, biotite and epidote modes are significantly lower in the altered sample relative to least-altered samples. Proportions of other minerals remain similar to the proportions in least-altered samples. Based on macroscopic visual estimates, silica-poor dioritic–monzodioritic samples altered by  $V_3$  veins with adjacent  $V_1$ - $V_2$  veins have more white mica (Figure 34A) than silica-poor dioritic–monzodioritic samples altered by  $V_3$  veins with no adjacent  $V_1$ - $V_2$  veins (Figure 34B).

##### **4.1.8.3.2 Textures**

Some white mica, carbonate, and chlorite grains overprint or alter primary and pre-existing metamorphic minerals present in the least-altered samples of silica-poor diorite–monzodiorite. White mica grains are often randomly oriented and not parallel to the dominant foliation (Figure 35A). Biotite is present only in minor quantities and is often located at the core

of grains that are almost entirely replaced by chlorite (Figure 35A). Plagioclase is typically subhedral and altered by chlorite, epidote, carbonates, and white mica (Figure 35A). Pyrite is the dominant sulphide mineral and typically concentrates near ferromagnesian minerals (Figure 35A). Carbonates are interstitial or overgrow primary and metamorphic minerals. On average, this altered sample has a finer grain size than other least-altered samples.

#### **4.1.8.3.3 V<sub>3</sub>-vein related alteration minerals**

The minerals that form in the silica-poor diorite–monzodiorite as a result of V<sub>3</sub> vein-related alteration and replace primary and pre-existing metamorphic minerals are mainly white mica, carbonate minerals, and chlorite.

### **4.1.9 Diabase–quartz diabase (I3DD)**

#### **4.1.9.1 Field observations**

Diabase–quartz diabase dykes at the Island Gold deposit are typically aphanitic at the margins and medium grained closer to the centre. Unlike the other lithologies at this deposit, the diabase–quartz diabase has not been subject to substantial metamorphism or deformation (Figure 36A). These intrusions occasionally host xenoliths of granitoid rock that do not correspond with any lithologies observed at the Island Gold deposit (Figure 36B). These mafic intrusions crosscut the dacite, iron formation, gabbro, Webb Lake stock, gabbro/lamprophyre, and silica-poor diorite–monzodiorite. This lithology sharply cuts V<sub>1</sub>-V<sub>2</sub> auriferous quartz veins and V<sub>3</sub> veins at a high-angle and shows no evidence of quartz vein-related alteration (Figure 36C, D). North of the Island Gold deposit, the diabase–quartz diabase dykes also cross-cut the mafic volcanic rocks and large intrusive bodies such as the Herman Lake Stock and the Maskinonge Lake Stock.

#### **4.1.9.2 Mineralogy**

The mineralogy of the diabase–quartz diabase, in approximate order of abundance, consists of plagioclase (andesine–labradorite), clinopyroxene, orthopyroxene, magnetite, actinolite, chlorite, biotite, quartz, hornblende, and epidote. Accessory minerals include carbonate minerals, and white mica. Proportions of minerals in a representative diabase–quartz diabase sample are displayed in Figure 11G. Carbonate mineral content is low in this lithology compared to most other lithologies at this deposit (Figure 11).

#### **4.1.9.3 Textures**

The diabase–quartz diabase is equigranular and fine to medium-grained (< 3 mm; Figure 36; Figure 37). Plagioclase is typically euhedral and slightly replaced by fine-grained chlorite, epidote, carbonates, and white mica (Figure 37). Quartz is also present and is unstrained. Potassium feldspars were not observed. Anhedra–subhedral magnetite is disseminated throughout these rocks as well (Figure 37). Pyroxene is subhedral–euhedral and grains are often slightly altered around their margins by actinolite and chlorite (Figure 37). Minor hornblende was often altered by actinolite and chlorite as well. Biotite typically overprints or is intergrown with this actinolite and chlorite alteration of both pyroxene and hornblende (Figure 37). Chlorite often alters the edges of biotite grains as well (Figure 37). Minor actinolite, biotite, carbonates, chlorite, epidote, and white mica alter or overprint most other minerals (Figure 37).

#### **4.1.9.4 Primary minerals**

Major primary minerals in the diabase–quartz diabase, in approximate order of abundance, consist of plagioclase (andesine–labradorite), clinopyroxene, orthopyroxene, magnetite, quartz, and hornblende. Based on mineral modes determined via petrographic point counting techniques, this lithology plots on the boundary of the quartz gabbro/quartz diorite and gabbro/diorite fields of the QAP diagram (Figure 27). Based on SEM-EDS analyses of plagioclase in this lithology, a larger proportion the plagioclase plots closer to the anorthite endmember than albite member ( $An > 50\%$ ) which supports the gabbroic classifications.

#### **4.1.10 Greenschist-facies metamorphism**

All lithologies at the Island Gold deposit were affected by metamorphism. Least-altered samples of all lithologies have metamorphic minerals which typically replace primary minerals. Depending on the protolith, these main metamorphic minerals may include actinolite, carbonates (mainly calcite), chlorite (ripidolite), chloritoid, epidote, hematite, ilmenite, magnetite, quartz, sodic plagioclase, titanite, and white mica (Sections 4.1.1 to 4.1.9). Textural relationships of these metamorphic minerals are summarized in this section based on observations detailed in Sections 4.1.1 to 4.1.9. Many of these minerals are typical greenschist-facies metamorphic minerals. These metamorphic minerals occasionally overprint or replace minerals derived from auriferous quartz vein-related alteration as well. However, alteration assemblages produced as a



result of gold mineralization appear well-preserved and are only weakly affected by later metamorphism. Occasionally, biotite may also be derived from metamorphism in the iron formation, silica-poor diorite-monzodiorite, and diabase-quartz diabase as it is sometimes observed intergrown with or overprinting metamorphic minerals in these lithologies (e.g. Figure 35). Ilmenite, magnetite, and titanite are typically present in trace amounts and replace primary iron-bearing minerals. Primary magnetite and ilmenite are also present in most lithologies but based on petrographic observations these minerals are dominantly metamorphic. Rutile is occasionally present in some least-altered samples but is more common in samples altered by quartz veins. This suggests rutile is mainly produced by quartz vein-related alteration but trace amounts may be produced due to metamorphism as well. Although not a greenschist-facies mineral, metamorphic grunerite is present in trace amounts in one least-altered dacitic sample.

Ferromagnesian minerals such as pyroxene, hornblende, and biotite are often replaced by chlorite and actinolite. Epidote, carbonates, and white mica typically replace plagioclase. In mafic-ultramafic lithologies, quartz and sodic plagioclase often overprint primary minerals indicating quartz and sodic plagioclase formed as a result of metamorphism in these lithologies. Hematite is occasionally associated with carbonate veinlets which are common throughout the deposit but have no observed spatial correlation with ore zones. Carbonate minerals, including those within these carbonate veinlets, were likely a product of metamorphism because they overprint primary minerals but are often overprinted by alteration minerals associated with  $V_1$ - $V_2$  and  $V_{GD}$  veins. The close association of hematite with these carbonate veinlets suggests that hematite can be metamorphic in origin. Chloritoid is sporadically present, and it overprints other metamorphic minerals and is often randomly oriented, suggesting that it also post-dates most deformation and represents late metamorphic growth. In rare cases, garnet is present and was observed closely associated with and replacing chloritoid. Based on this overprinting relationship, it is likely that garnet was generated after chloritoid potentially during late metamorphism as well. Alternatively, chloritoid and garnet may have been produced during a later alteration event unrelated to metamorphism.

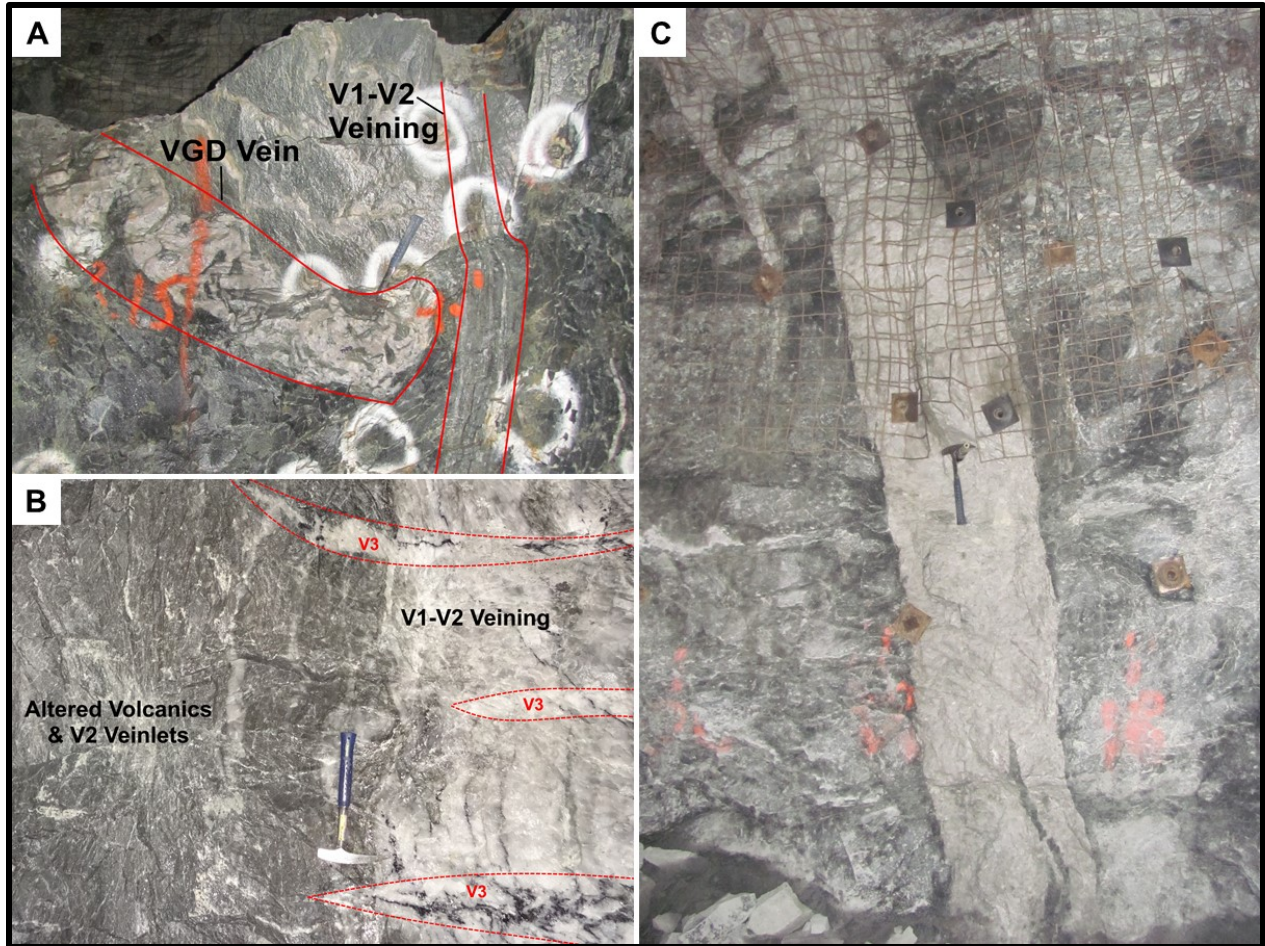


**Figure 7A–C.** Photos of various quartz veins at the Island Gold deposit. A) Folded  $V_{GD}$  auriferous quartz veining (left) and  $V_1$ - $V_2$  auriferous quartz veining (right). B)  $V_1$ - $V_2$  auriferous quartz veining (right), altered dacite with  $V_2$  veinlets (left), and  $V_3$  veins (outlined in red). Tourmaline (black ribbons) invades into pre-existing structures. C) Large  $V_3$  non-auriferous quartz vein in dacite.



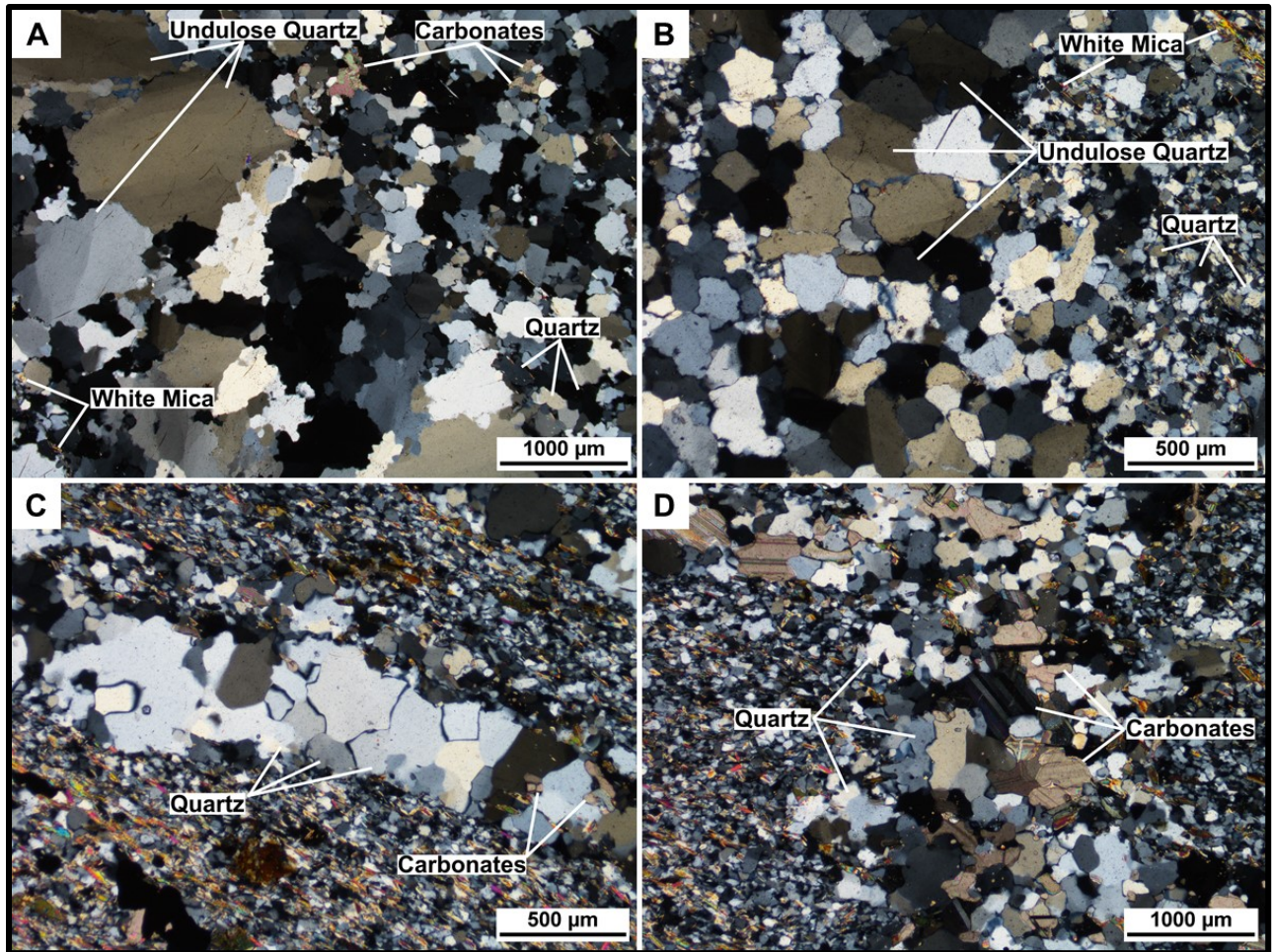


**Figure 8A–D.** Cross-polarized light photomicrographs of quartz veins. A) A  $V_{GD}$  vein displaying both larger quartz grains with undulose extinction and smaller quartz grains without undulose extinction. B) a  $V_1$ - $V_2$  vein displaying both larger quartz grains with undulose extinction and smaller quartz grains without undulose extinction. C) A  $V_2$  gold-bearing quartz veinlet intruding through an altered dacite. This vein is subparallel to the dominant foliation. D) A  $V_3$  non-auriferous quartz veinlet intruding through an altered dacitic sample. This vein is approximately perpendicular to the dominant foliation.

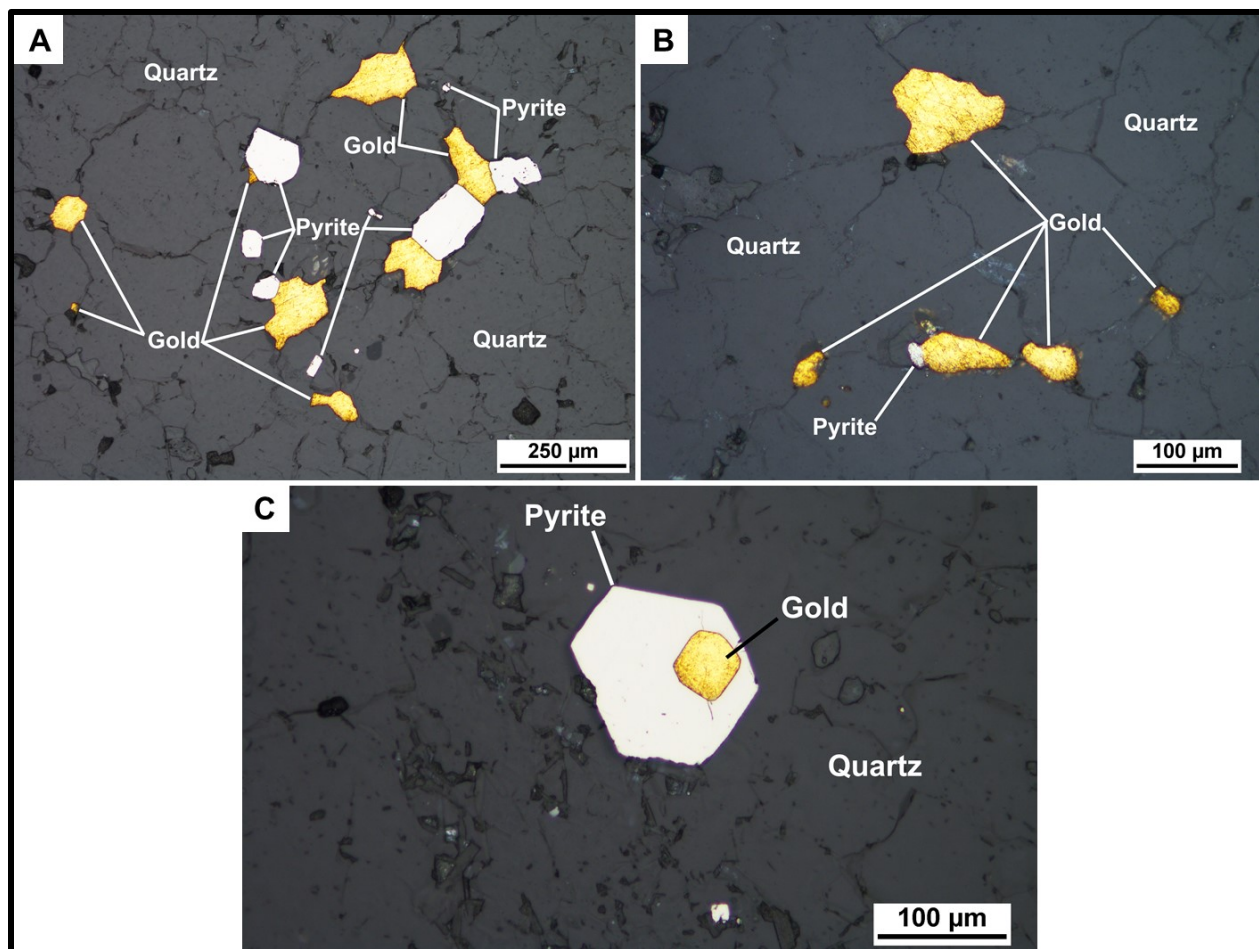


**Figure 9A–C.** Reflected light photomicrographs of gold and sulphide minerals in quartz veins. Grey-coloured minerals are mainly quartz. A) A reflected light photomicrograph of gold associated with sulphides. B) Free gold spatially associated with minor sulphides. C) Gold inclusion in pyrite.



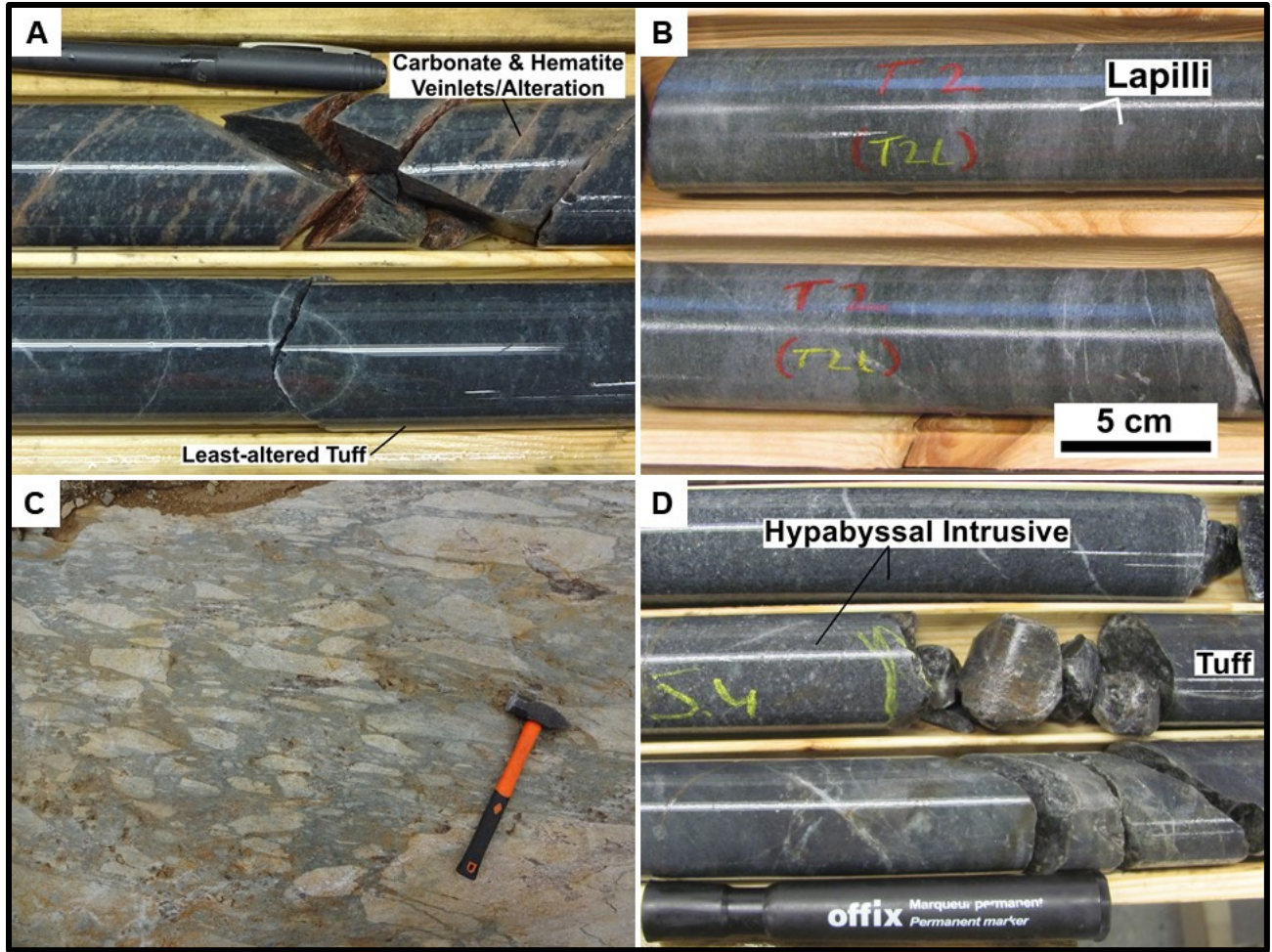


**Figure 10A–C.** Drill core and field photos of dacite. *A)* Least-altered dacitic tuff (bottom) and carbonate veinlets with hematite alteration (top). *B)* Dacitic lapilli tuff. *C)* Dacitic pyroclastic breccia. *D)* Contact between a dacitic sub-volcanic intrusive and an extrusive tuff.

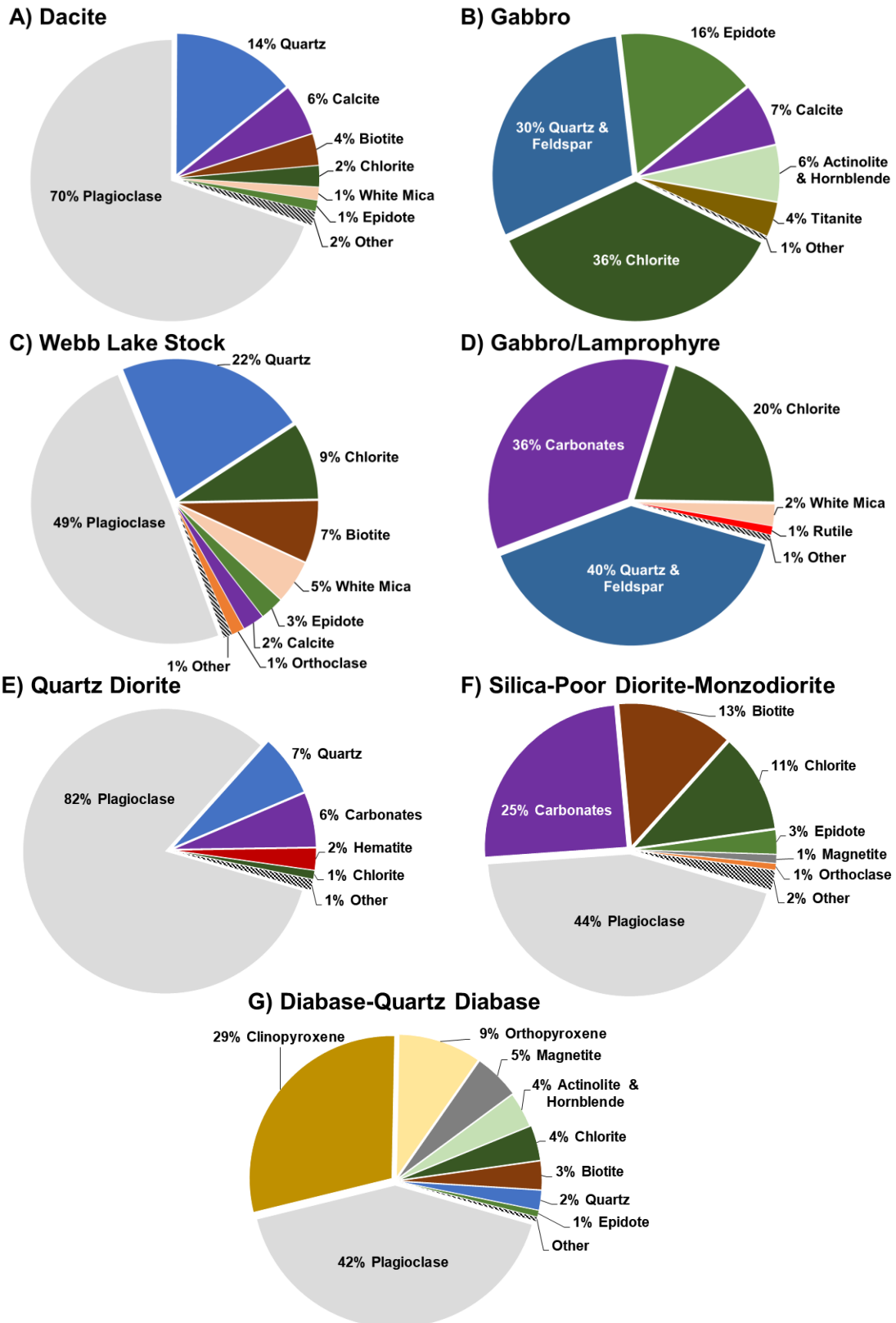


**Figure 11A–G.** Volumetric mineral proportions in least-altered samples of lithologies at the Island Gold deposit. Proportions were determined via SEM-MLA for dacite (T241) and point-counting for gabbro (T182), Webb Lake stock (T192), gabbro/lamprophyre (T239), quartz diorite (T215), diorite–monzodiorite (T66) and diabase (T83).

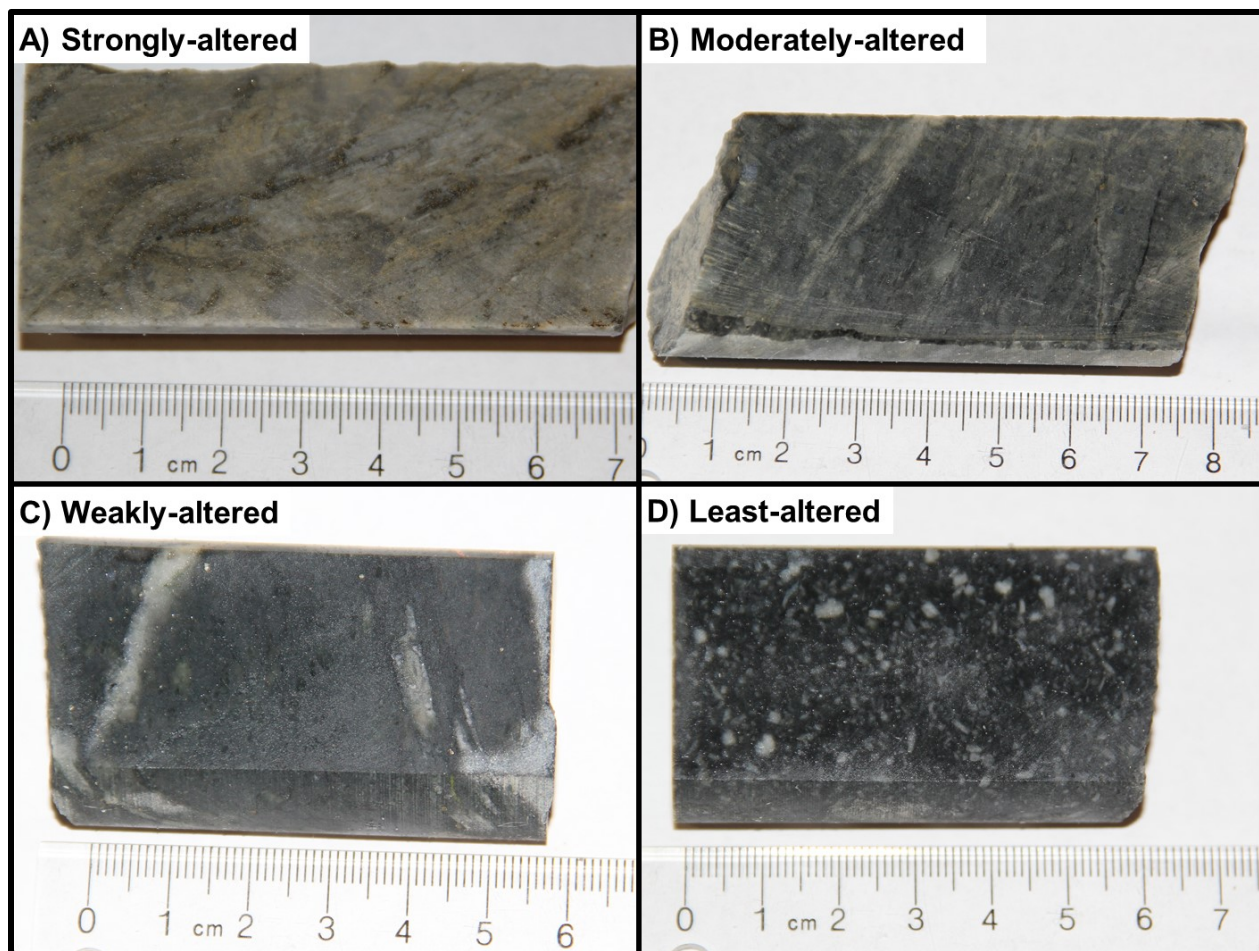


**Figure 12A–D.** Dacitic samples variably altered by  $V_1$ - $V_2$  auriferous quartz veining. T188 (A), T186 (B), T184 (C), and T241 (D).



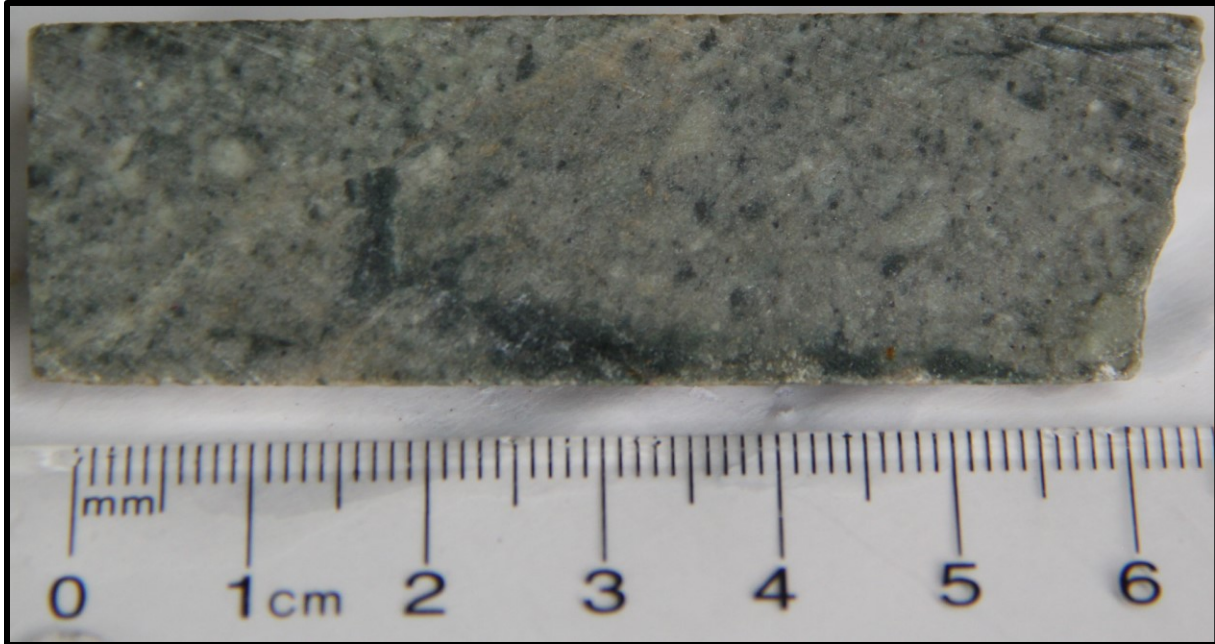


**Figure 13.** *Dacite affected by non-auriferous carbonate-sericite alteration (T218). Dark-coloured minerals include both chlorite and tourmaline.*



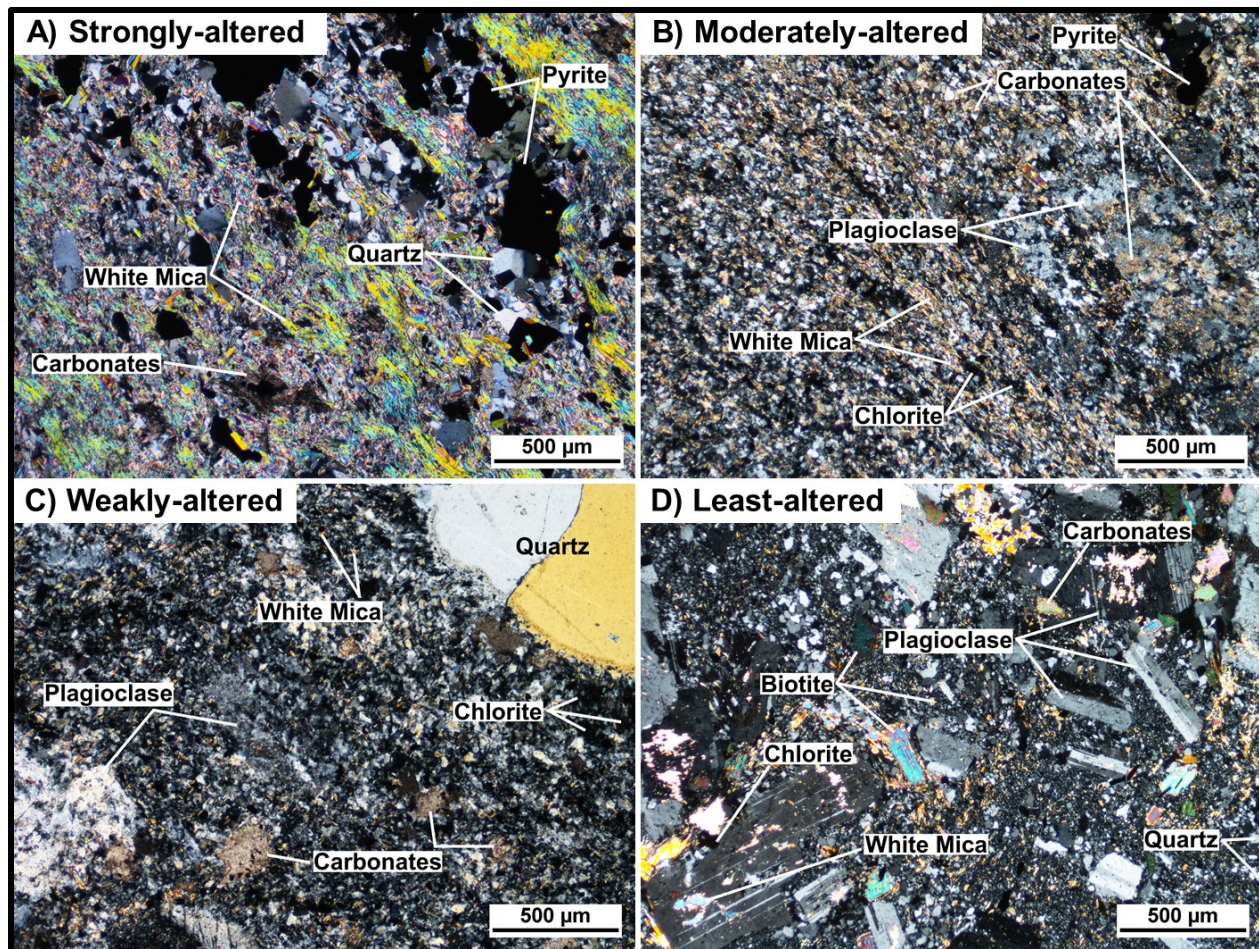


**Figure 14A–D.** Cross-polarized light photomicrographs of dacitic samples variably-altered by  $V_1$ - $V_2$  veins. T188 (A), T186 (B), T184 (C), and T241 (D).



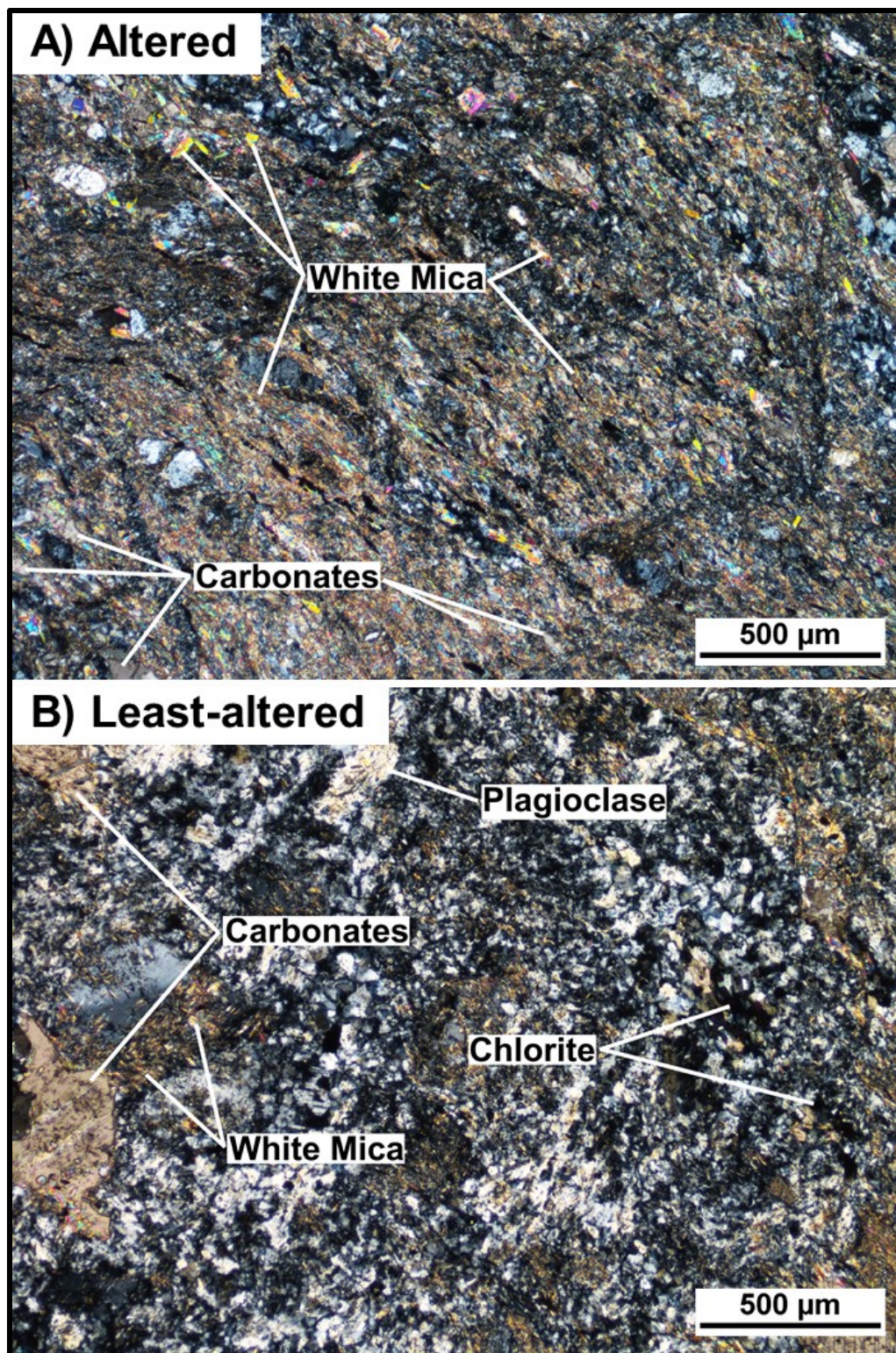


*Figure 15A, B. Cross-polarized light photomicrographs of a dacitic sample subject to carbonate-sericite alteration (T218) and a least-altered equivalent (T220).*

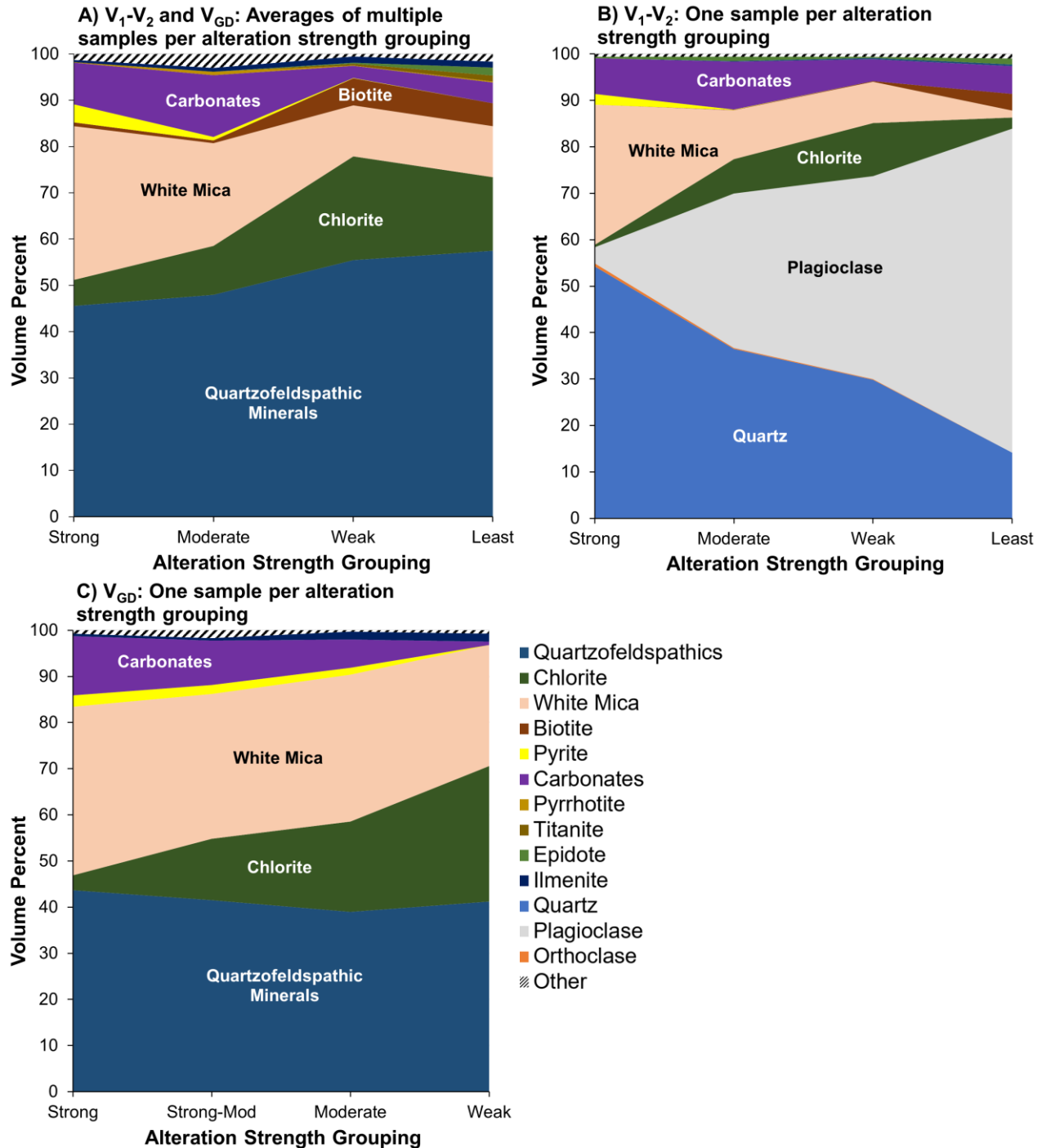


**Figure 16A–C.** Mineral proportions in dacitic samples variably- altered by auriferous quartz veins. *A) Average mineral proportions (point-counting) in strongly- altered (T56, T58, T72, T105, T113, T157, T162, T188), moderately- altered (T73, T85, T114, T156, T186), weakly- altered (T59, T115, T118, T184), and least- altered (T8, T154, T164, T241) dacitic samples from throughout the deposit that were altered by  $V_1$ - $V_2$  or  $V_{GD}$  quartz veins. B) Mineral proportions (SEM-MLA) of variably- altered samples from a  $V_1$ - $V_2$  vein-related alteration envelope (T188, T186, T184). The least- altered sample (T241) was taken from elsewhere in the study area but is believed to have the same protolith as the altered samples. C) Mineral proportions (point-counting) of variably- altered samples from a  $V_{GD}$  vein-related alteration envelope (T105, T113, T114, T115). The “Strong-Mod” sample (T113) is classified as strongly- altered but is less altered than the “Strong” sample (T105).*



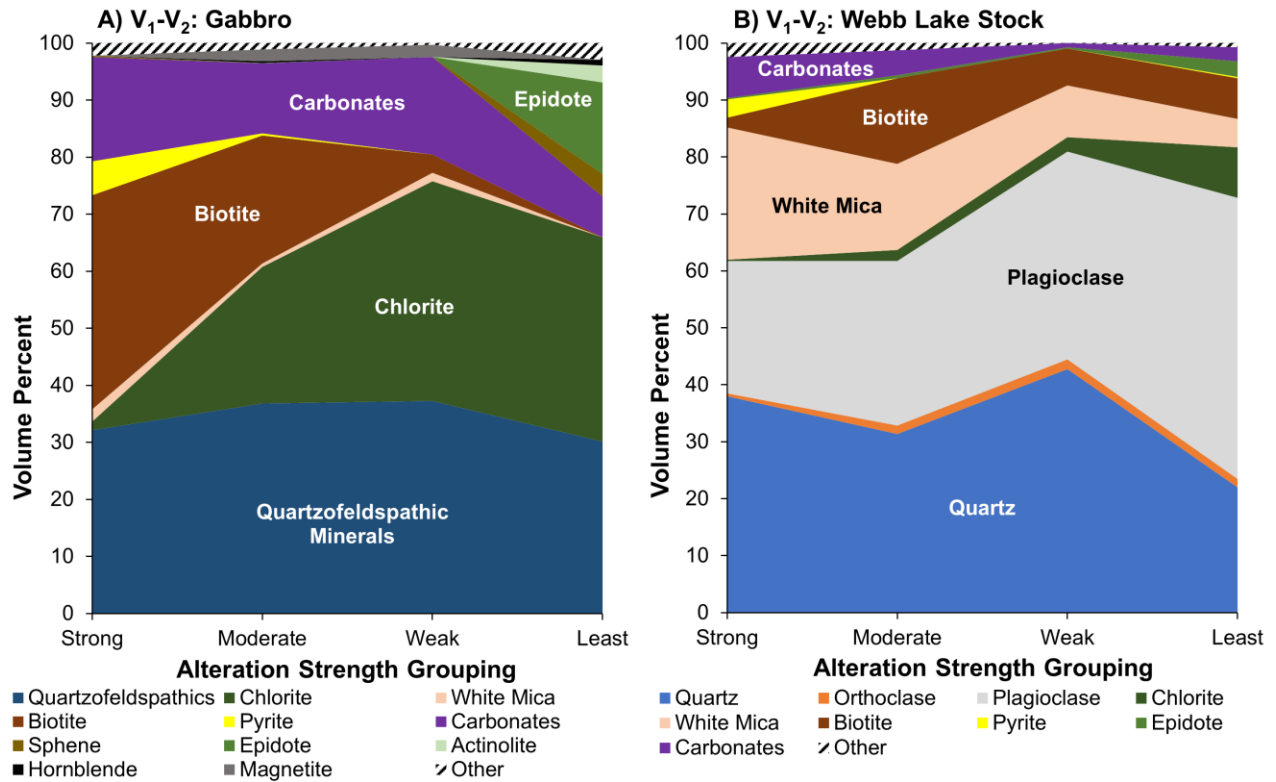


**Figure 17A, B.** A) Mineral proportions in variably-altered samples from a gabbro-hosted alteration envelope (T142, T141, T140, T139) associated with V<sub>1</sub>-V<sub>2</sub> veining. The least-altered sample (T182) was taken from elsewhere in the study area but is believed to have the same protolith as the altered samples. The mineralogy of the two moderately-altered samples (T141 and T140) were averaged. B) Mineral proportions in variably-altered samples from a Webb Lake stock-hosted alteration envelope (T195, T194, T193, T192) associated with an auriferous V<sub>1</sub>-V<sub>2</sub> vein. All mineral proportions are determined via point-counting.

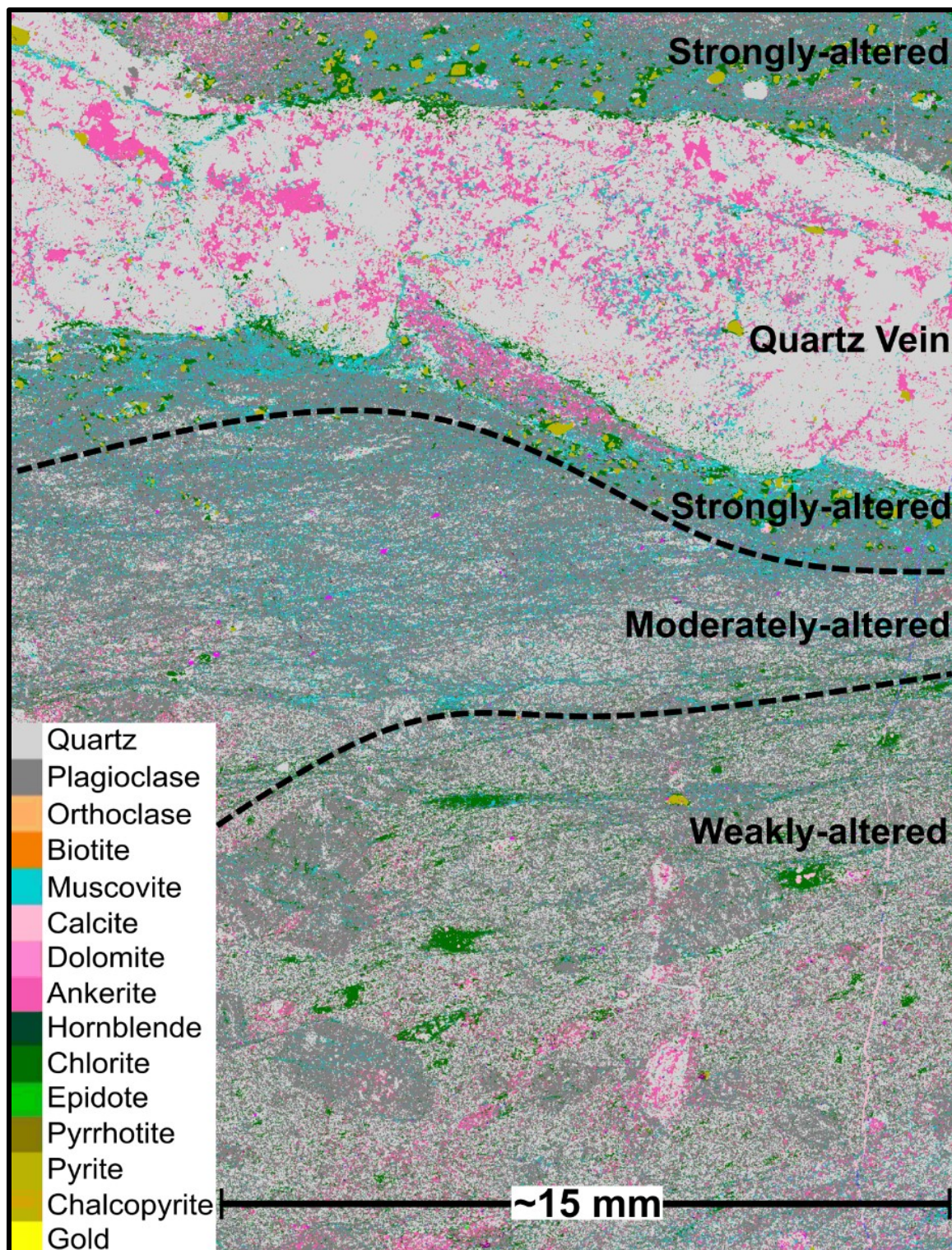


**Figure 18.** An SEM-MLA image using false colours to represent minerals of a  $V_2$  quartz veinlet and an associated miniature dacite-hosted alteration envelope. Approximate boundaries between alteration strength groupings are displayed. This image was produced by the Bruneau Centre's SEM-MLA Research Lab (Memorial University) and modified for this thesis (Section 3.5).

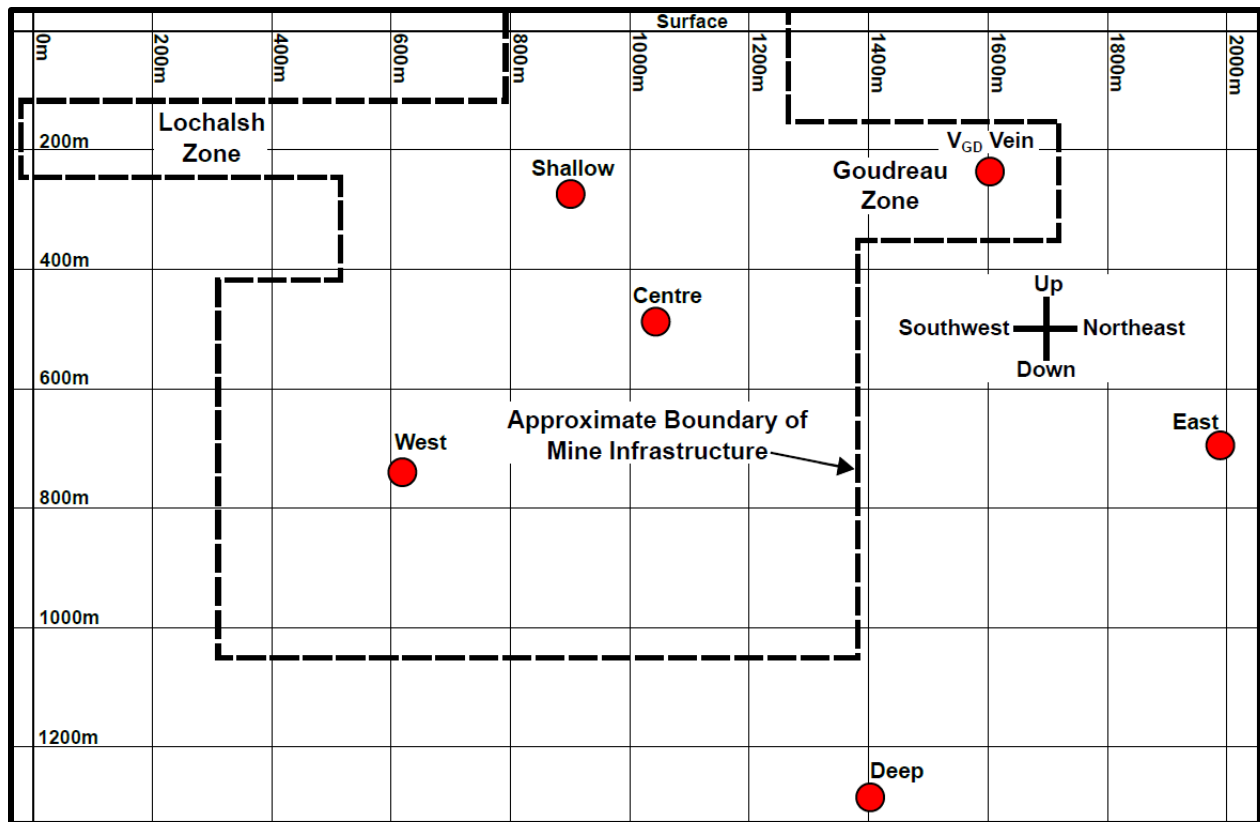


**Figure 19.** Vertical cross-section facing northwest parallel to the strike of the GLDZ displaying the approximate locations of the dacite-hosted ore zones and associated alteration envelopes that are studied in this thesis. Unless otherwise indicated, the ore zones and alteration envelopes are associated with  $V_1$ - $V_2$  auriferous veins. The approximate boundaries of mine infrastructure around the time field work was conducted are indicated.



**Table 3A, B.** Averages (A) and ranges (B) of mineral proportions of strongly-altered (T56, T58, T72, T105, T113, T157, T162, T188), moderately-altered (T73, T85, T114, T156, T186), weakly-altered (T59, T115, T118, T184), and least-altered (T8, T154, T164, T241) dacitic samples that were point-counted and classified under each alteration strength grouping. Alteration is associated with  $V_1$ - $V_2$  and  $V_{GD}$  auriferous quartz veins. All major minerals are displayed and values are expressed in volume percent. Min=Minimum, Max=Maximum.

<b>A) Averages</b>	<b>Strongly altered</b>	<b>Moderately altered</b>	<b>Weakly altered</b>	<b>Least altered</b>
<b>Biotite</b>	0.8	0.6	5.9	5.0
<b>Carbonates</b>	9.0	13.3	2.7	4.4
<b>Chlorite</b>	5.6	10.6	22.3	15.9
<b>Epidote</b>	0.1	0.0	0.2	1.7
<b>Pyrite</b>	3.9	0.7	0.1	0.0
<b>Pyrrhotite</b>	0.0	0.7	0.1	0.2
<b>Quartzfeldspathics</b>	45.6	48.0	55.5	57.5
<b>White Mica</b>	33.2	22.1	11.0	11.0

<b>B) Ranges</b>	<b>Strongly-altered</b>		<b>Moderately-altered</b>		<b>Weakly-altered</b>		<b>Least-altered</b>	
	<b>Min</b>	<b>Max</b>	<b>Min</b>	<b>Max</b>	<b>Min</b>	<b>Max</b>	<b>Min</b>	<b>Max</b>
<b>Biotite</b>	0.0	3.5	0.0	2.7	0.0	15.1	0.0	16.5
<b>Carbonates</b>	0.0	18.3	6.2	28.1	0.5	8.9	0.2	9.4
<b>Chlorite</b>	0.2	13.3	5.7	19.5	13.6	29.4	1.7	30.9
<b>Epidote</b>	0.0	0.2	0.0	0.0	0.0	0.7	0.0	5.2
<b>Pyrite</b>	1.5	11.1	0.2	1.5	0.0	0.2	0.0	0.0
<b>Pyrrhotite</b>	0.0	0.0	0.0	1.7	0.0	0.2	0.0	1.0
<b>Quartzfeldspathics</b>	37.8	63.5	38.0	66.4	41.2	66.4	46.4	69.1
<b>White Mica</b>	20.0	44.4	12.1	33.3	3.0	26.2	1.5	19.0

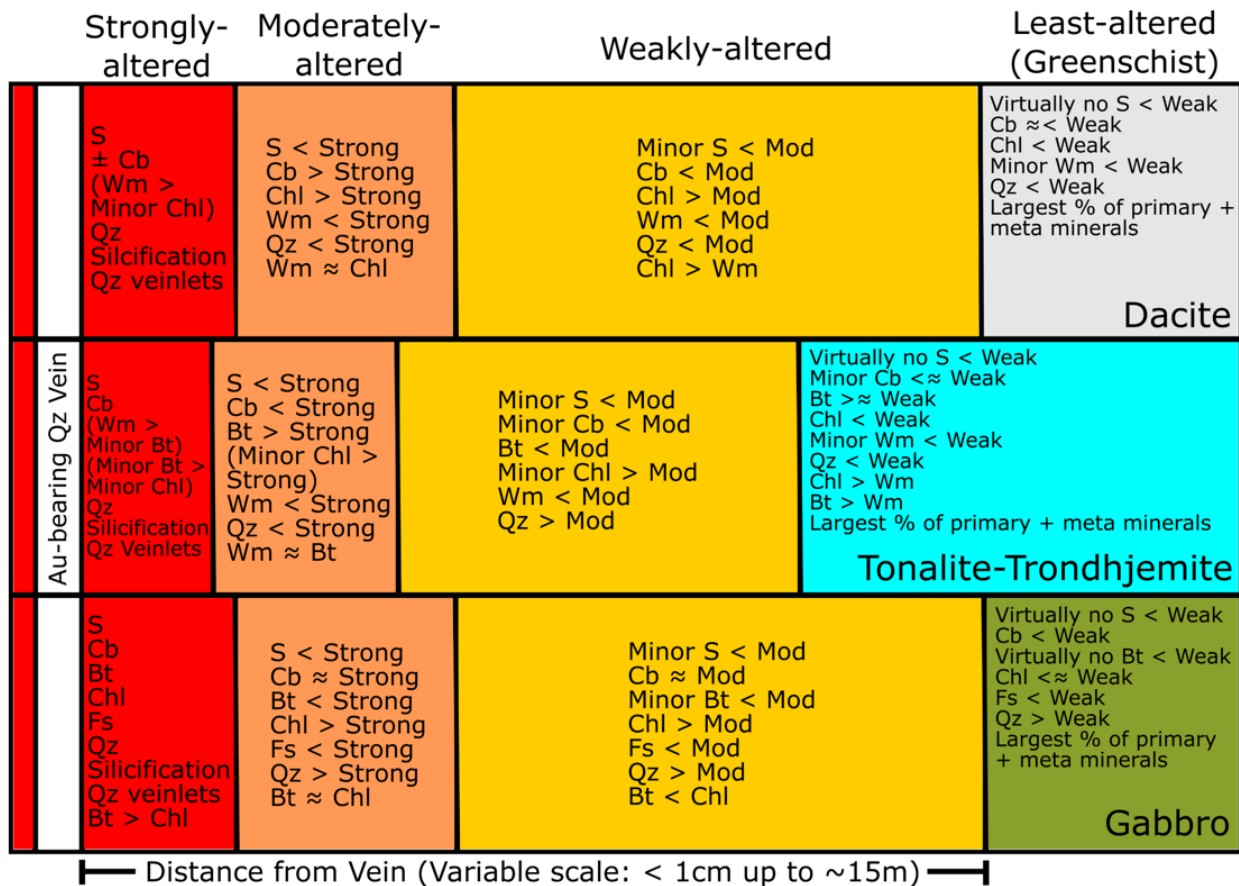


**Figure 20.** Summary of the modal proportions of major alteration minerals in each of the alteration strength groupings for each of the main ore-hosting lithologies. For example, “S < Strong” in the moderately-altered zone hosted by gabbro indicates that there is a lower amount of sulphide minerals in the gabbro-hosted moderately-altered zone compared to the gabbro-hosted strongly-altered zone. Key mineral proportion relationships that define each zone are also included. The dacite and gabbro-hosted alteration envelopes studied in this thesis were marginally wider than those hosted by the Webb Lake stock (tonalite-trondhjemite) and this is qualitatively reflected in this figure. Bt=Biotite, Cb=Carbonates, Chl=Chlorite, Fs=Feldspar, Qz=Quartz, S=Sulphides, Wm=White Mica, meta=Metamorphic.



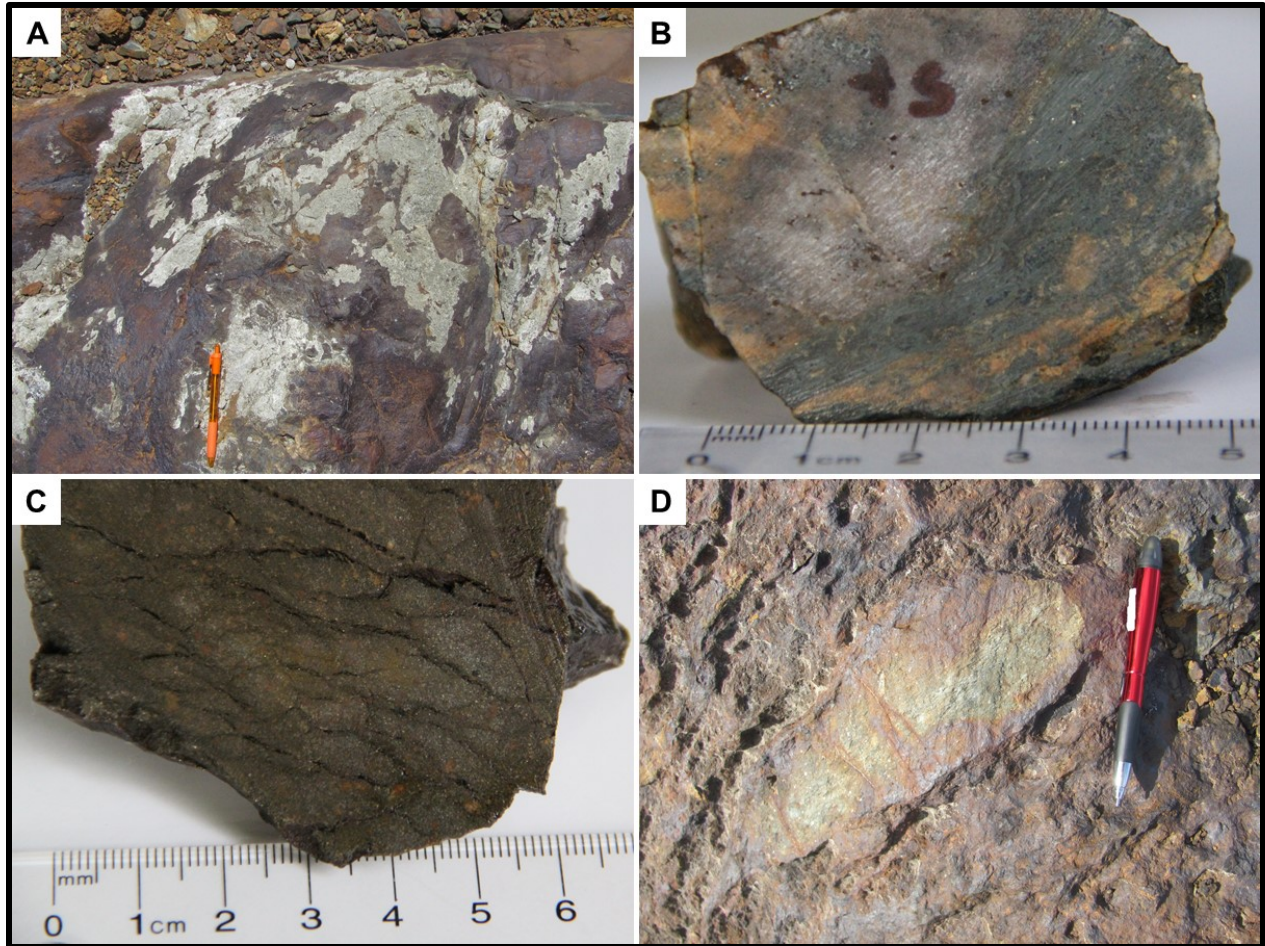


**Figure 21A–D.** Photos of outcrops and hand samples of iron formation. A) Outcrop of pyrite-rich iron formation. B) Sample of iron formation with chert-rich, carbonate-rich, and chlorite/biotite rich layers (T38). C) Sample of pyrite and iron oxide-rich iron formation with substantial carbonate and chlorite content as well (T37). D) Clast of dacitic rock in a pyrite-rich iron formation.



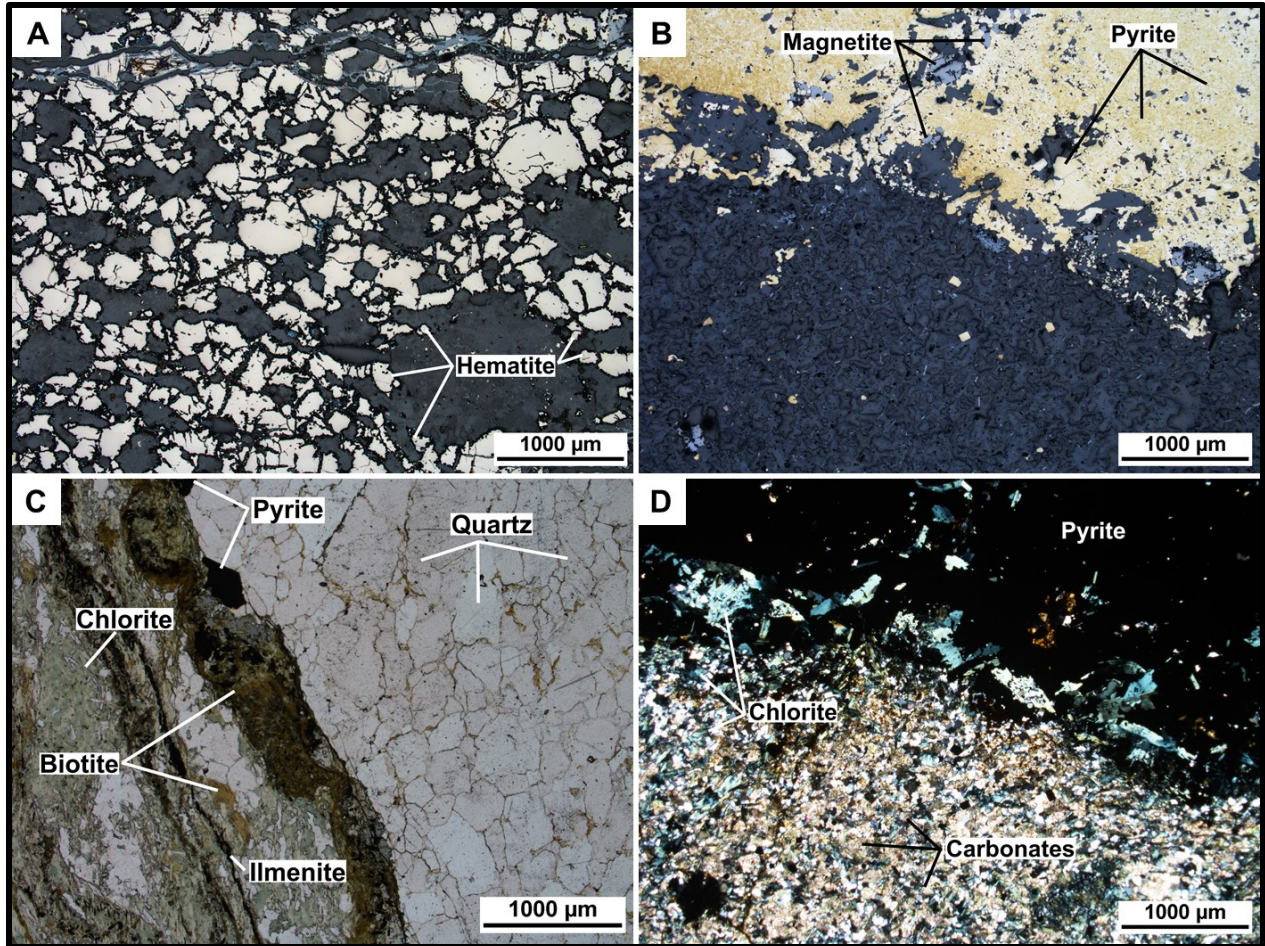


**Figure 22A–D.** Photomicrographs of samples of iron formation. *A*) A reflected light photomicrograph of a hematite-rich layer (T24). *B*) A reflected light photomicrograph displaying a pyrite-rich layer (top) and a carbonate rich layer (bottom) (T37). Same photo location as *D*. *C*) A plane-polarized light displaying a chlorite and biotite-rich layer (left) and quartz-rich layer (right) (T38). *D*) A cross-polarized light photomicrograph displaying a pyrite-rich layer (top) and a carbonate rich layer (bottom) (T37).



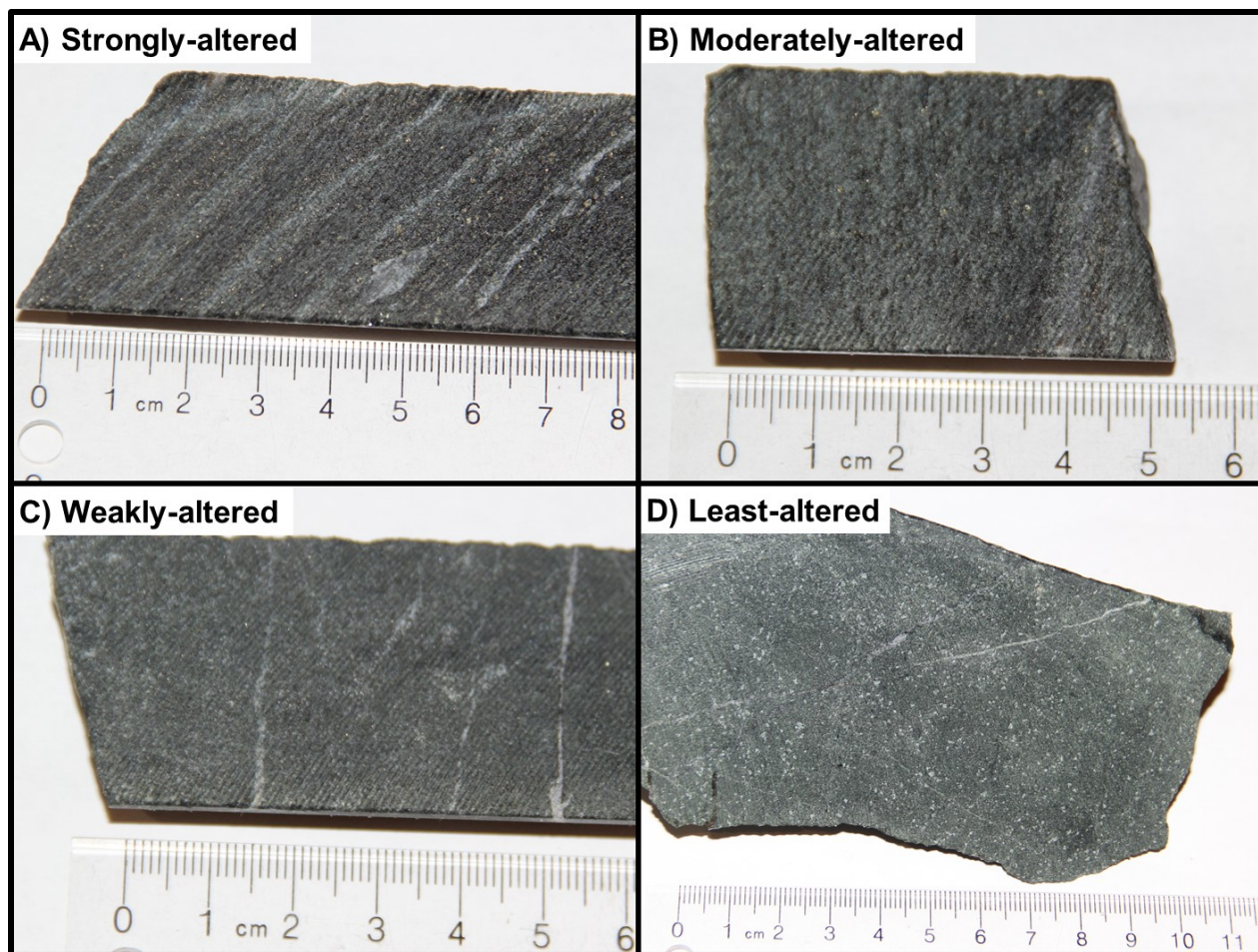


**Figure 23A–D.** Variably-altered samples of gabbro classified in each alteration strength grouping. T142 (A), T141 (B), T139 (C), and T182 (D).



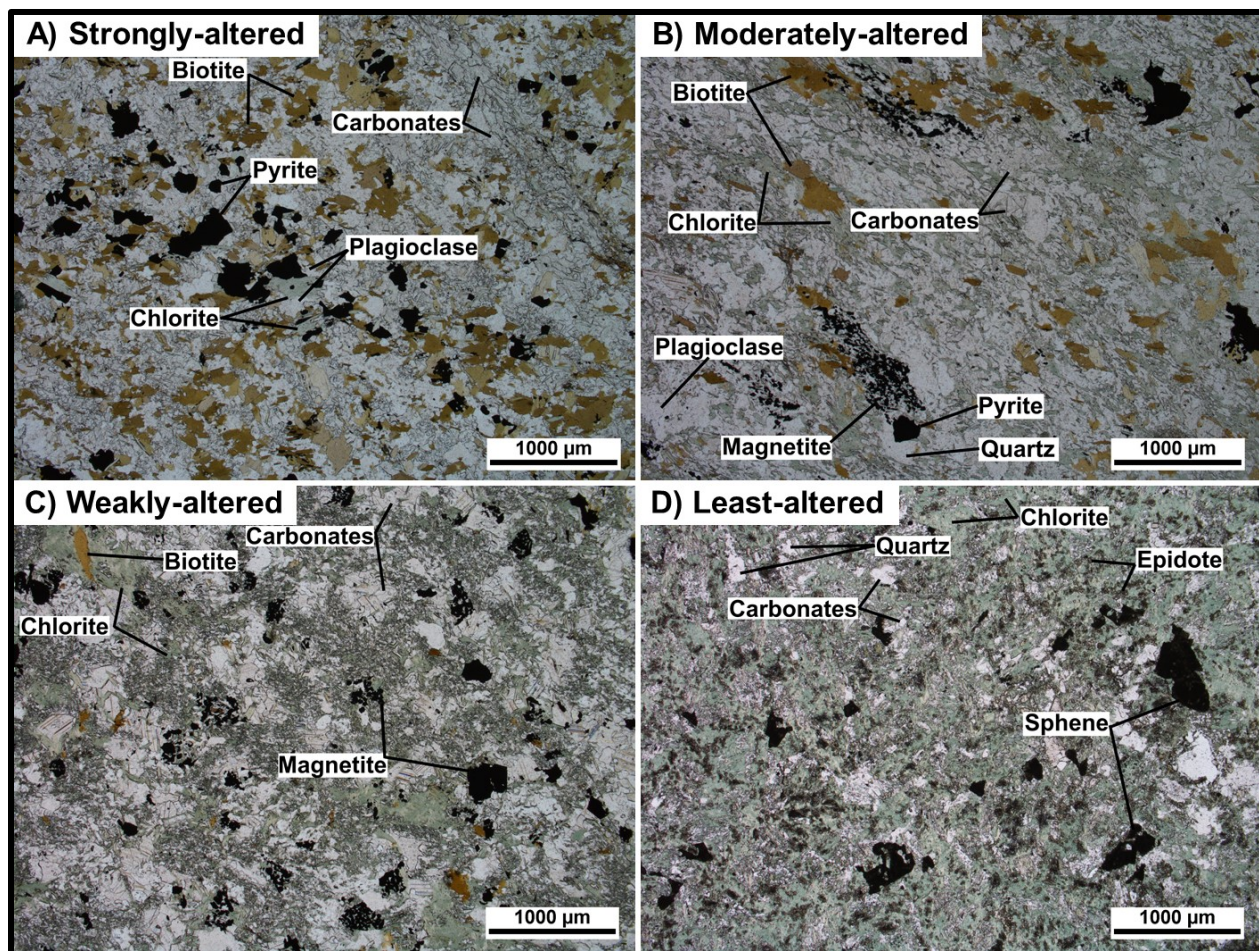


**Figure 24A–D.** Plane-polarized light photomicrographs of strongly-altered (T142), moderately-altered (T140), weakly-altered (T139), and least-altered (T182) samples of gabbro.



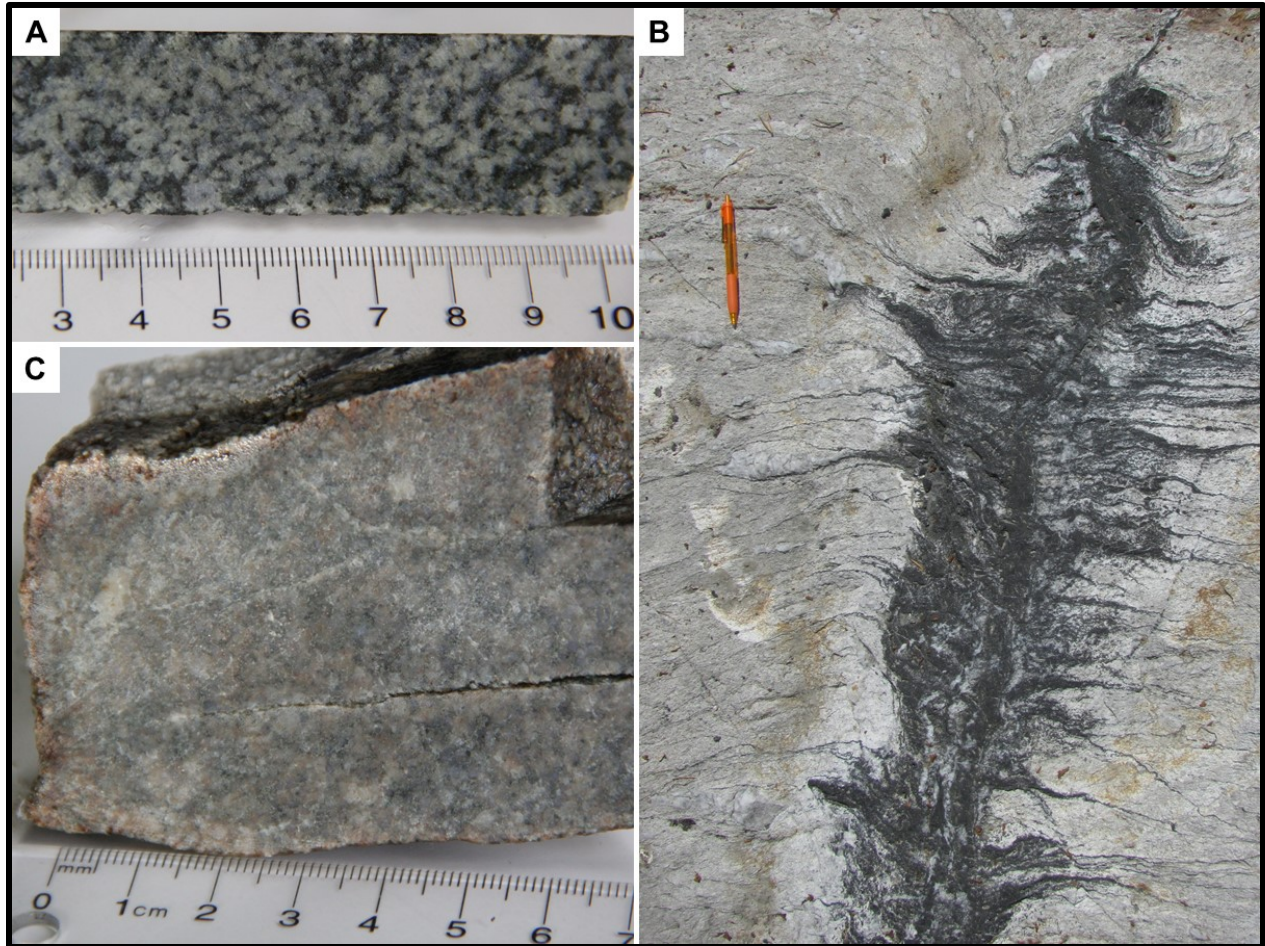


**Figure 25A–C.** Hand sample and field photos of the Webb Lake stock. A) A least-altered sample of the Webb Lake stock taken near to the margins of the stock (T192). B) A weakly-altered sample of the Webb Lake stock (T6) with fewer ferromagnesian minerals than T192 (A). This sample is from closer to the centre of the stock than T192. C) Tourmaline invading pre-existing structures and the foliation of the Webb Lake stock.

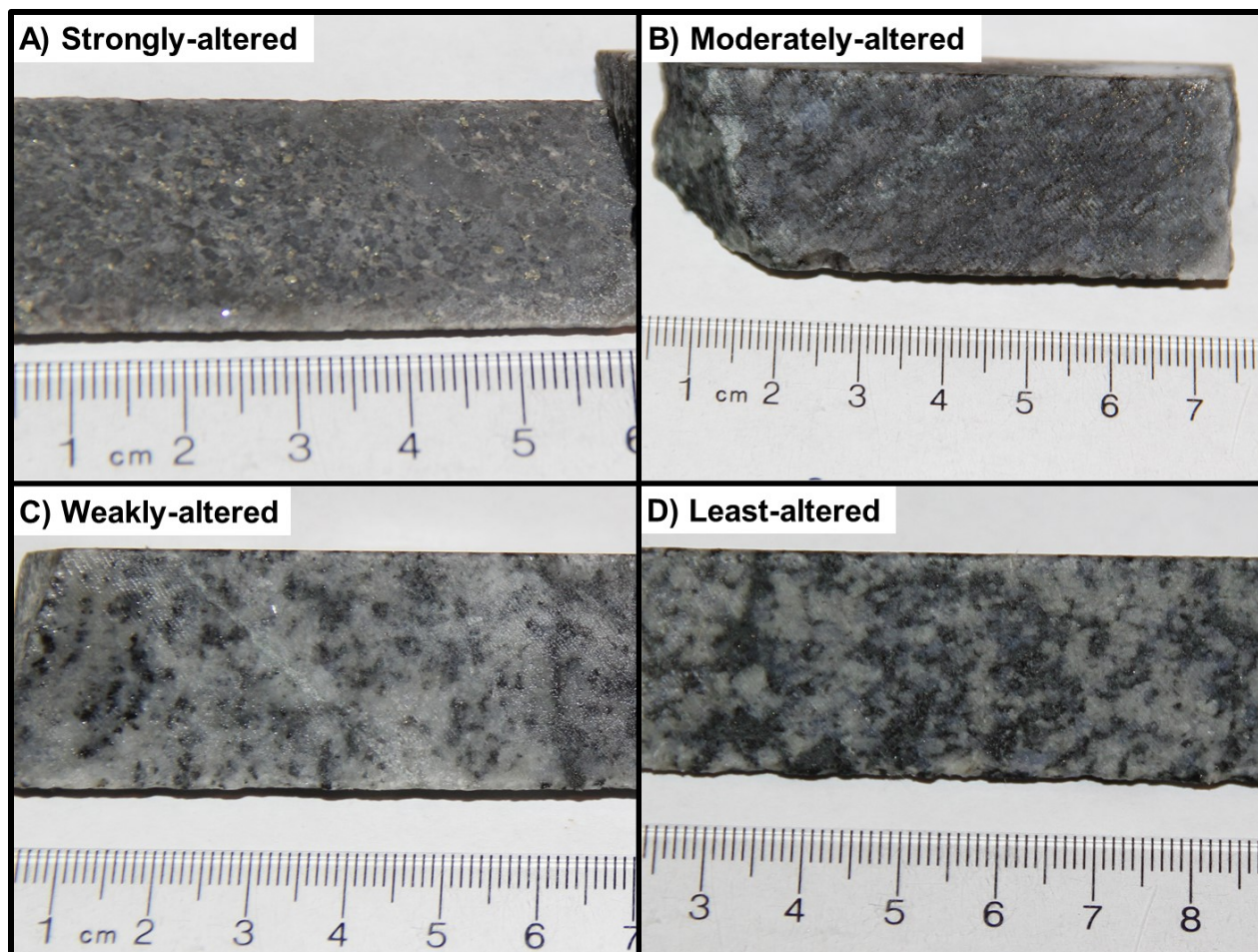


**Figure 26A–D.** Variably-altered samples of the Webb Lake stock classified under each alteration strength grouping. T195 (A), T194 (B), T193 (C), and T192 (D).

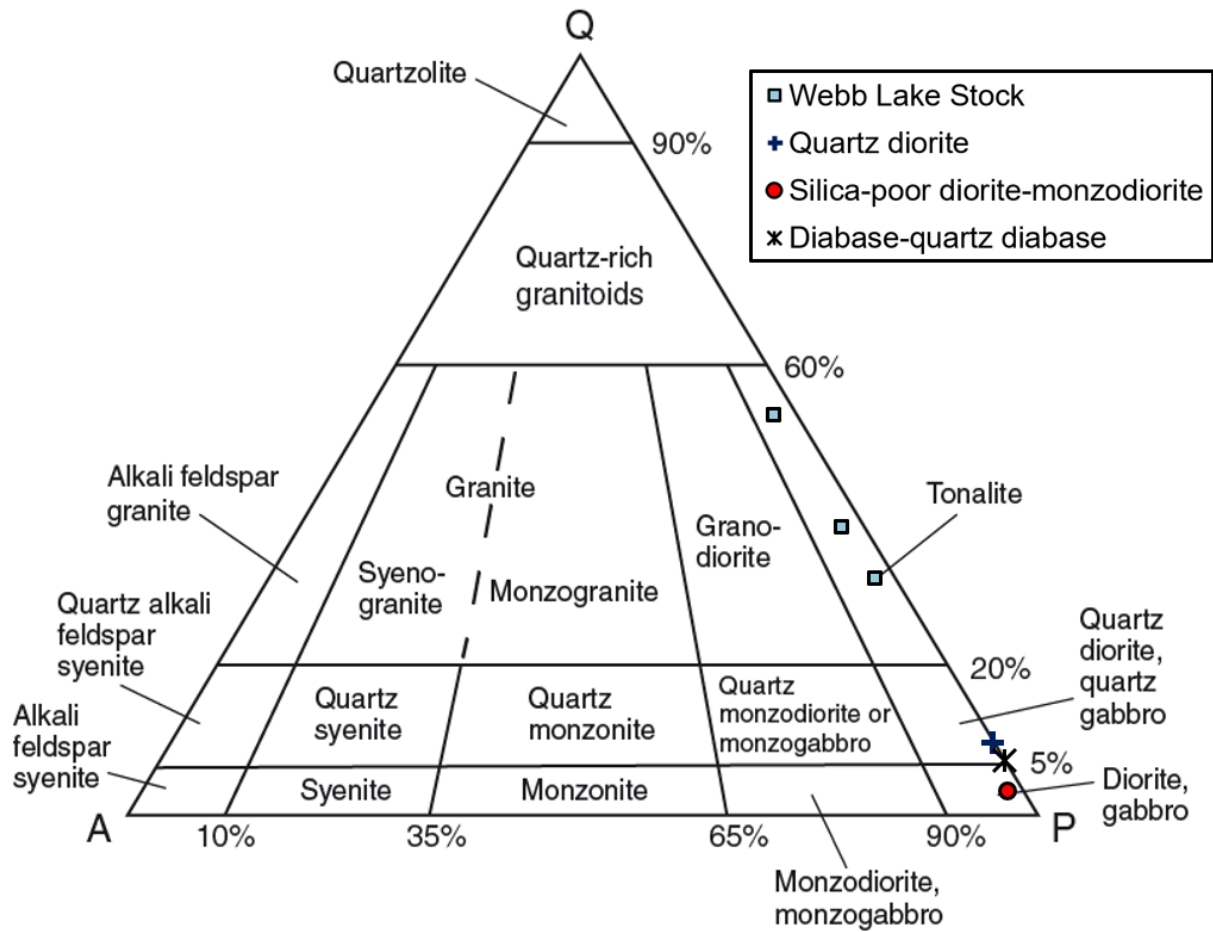


**Figure 27.** Least-altered and weakly-altered intrusive samples plotted on a Quartz-Alkali Feldspar-Plagioclase (QAP) ternary diagram. Modal mineralogy was determined via petrographic point-counting techniques. The following representative samples were used for each lithology: Webb Lake stock (T6, T192, T193), quartz diorite (T215), silica-poor diorite-monzodiorite (T66), and diabase-quartz diabase (T83). Modified from Streckeisen (1976a).



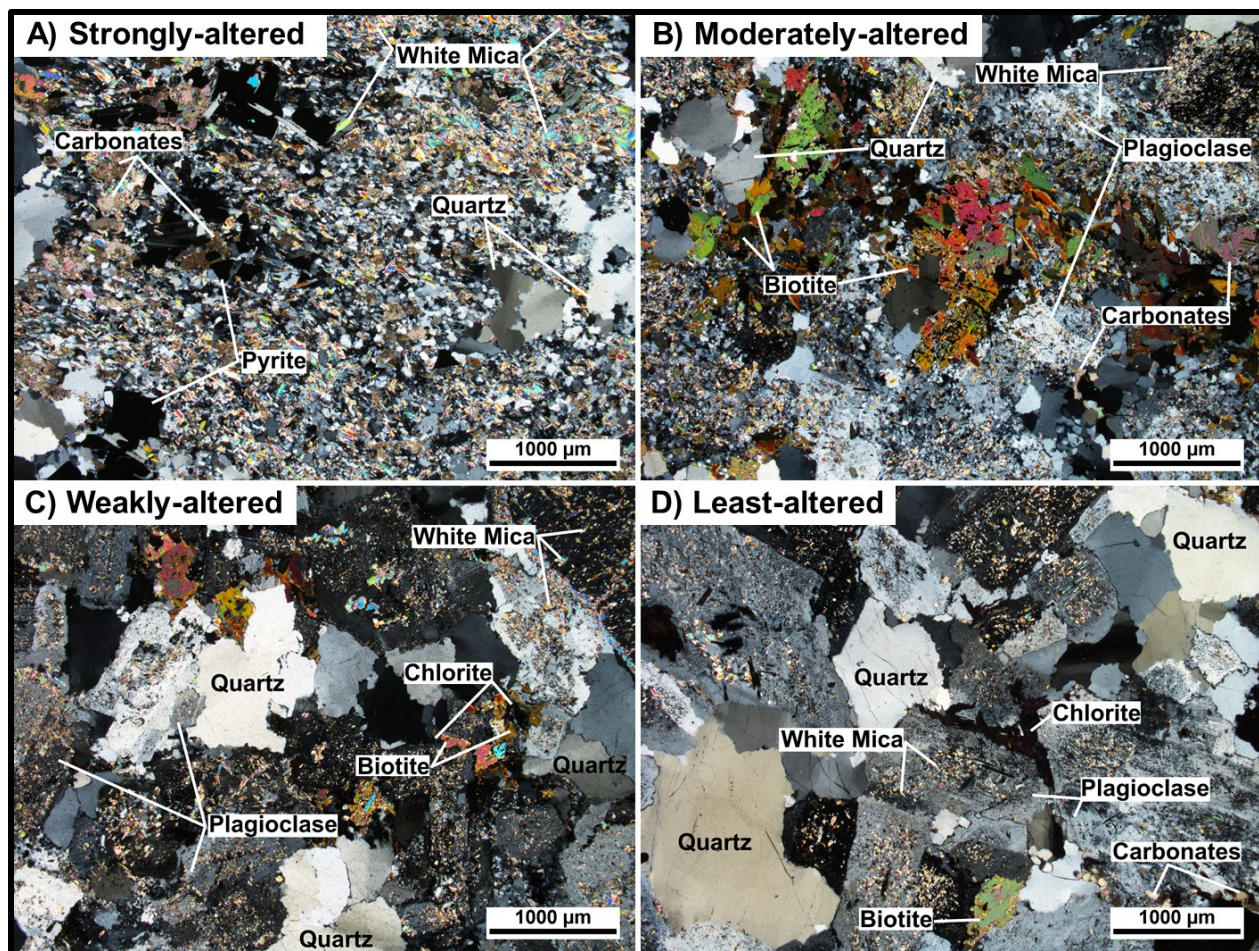


**Figure 28A–D.** Cross-polarized light photomicrographs of variably-altered samples of the Webb Lake stock. T195 (A), T194 (B), T193 (C), and T192 (D).



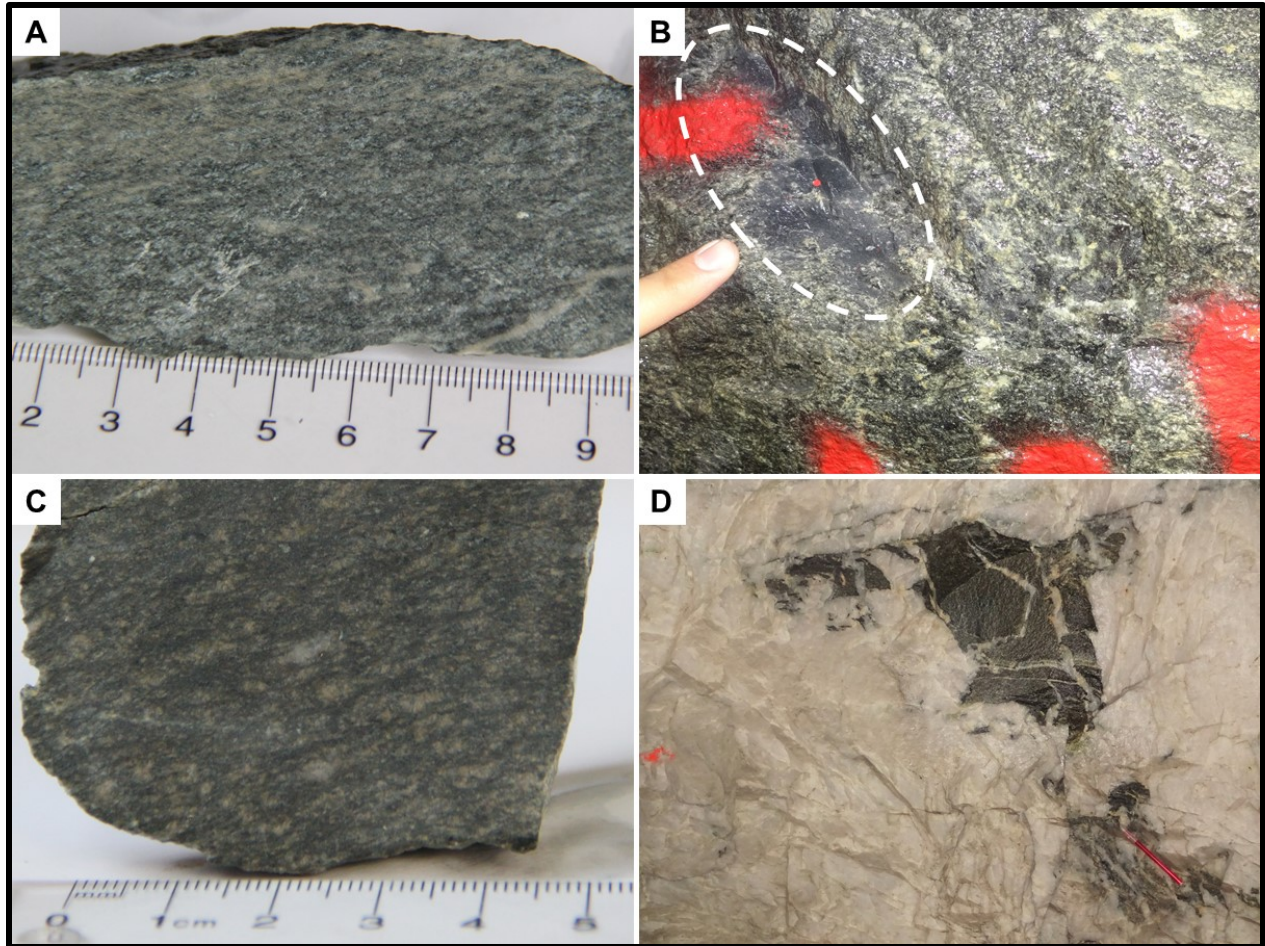


**Figure 29A–D.** Field and hand sample photos of gabbro/lamprophyre. A) A least-altered sample of gabbro/lamprophyre (T81). B) A dacitic xenolith within an intrusion of gabbro/lamprophyre. C) An altered sample of gabbro/lamprophyre (T213) that was brecciated and included within a  $V_3$  vein shown in D. D) A brecciated fragment of gabbro/lamprophyre within a large  $V_3$  extensional vein.

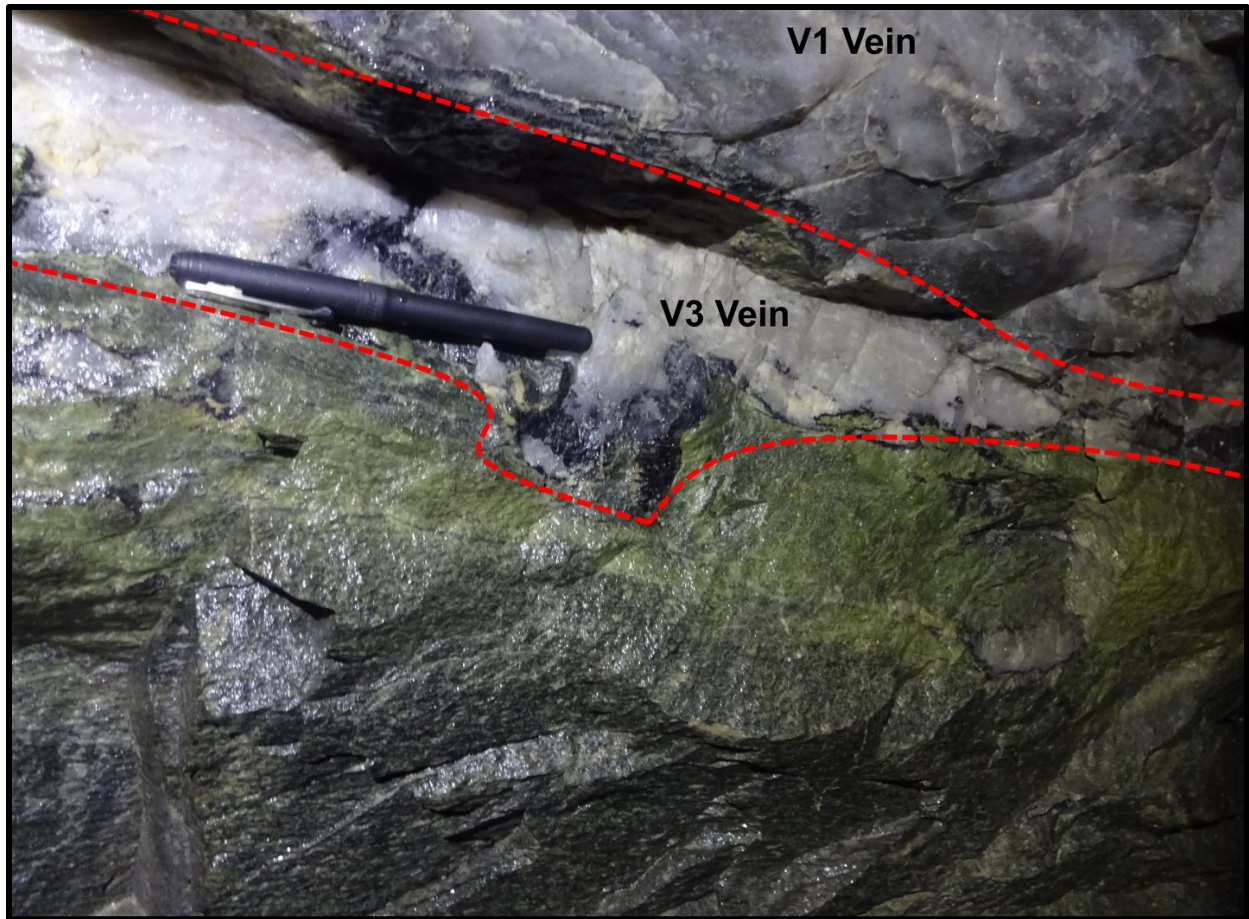


**Figure 30.** Anomalously strong alteration of gabbro/lamprophyre due to a white  $V_3$  quartz vein with tourmaline. A smoky  $V_1$  vein is located above the  $V_3$  vein and the altered portion of gabbro/lamprophyre is directly below the  $V_3$  vein. Alteration decreases moving downwards and away from the  $V_3$  vein. In this photo, black-coloured tourmaline is concentrated within the  $V_3$  vein and at the contact between the  $V_3$  vein and gabbro/lamprophyre.



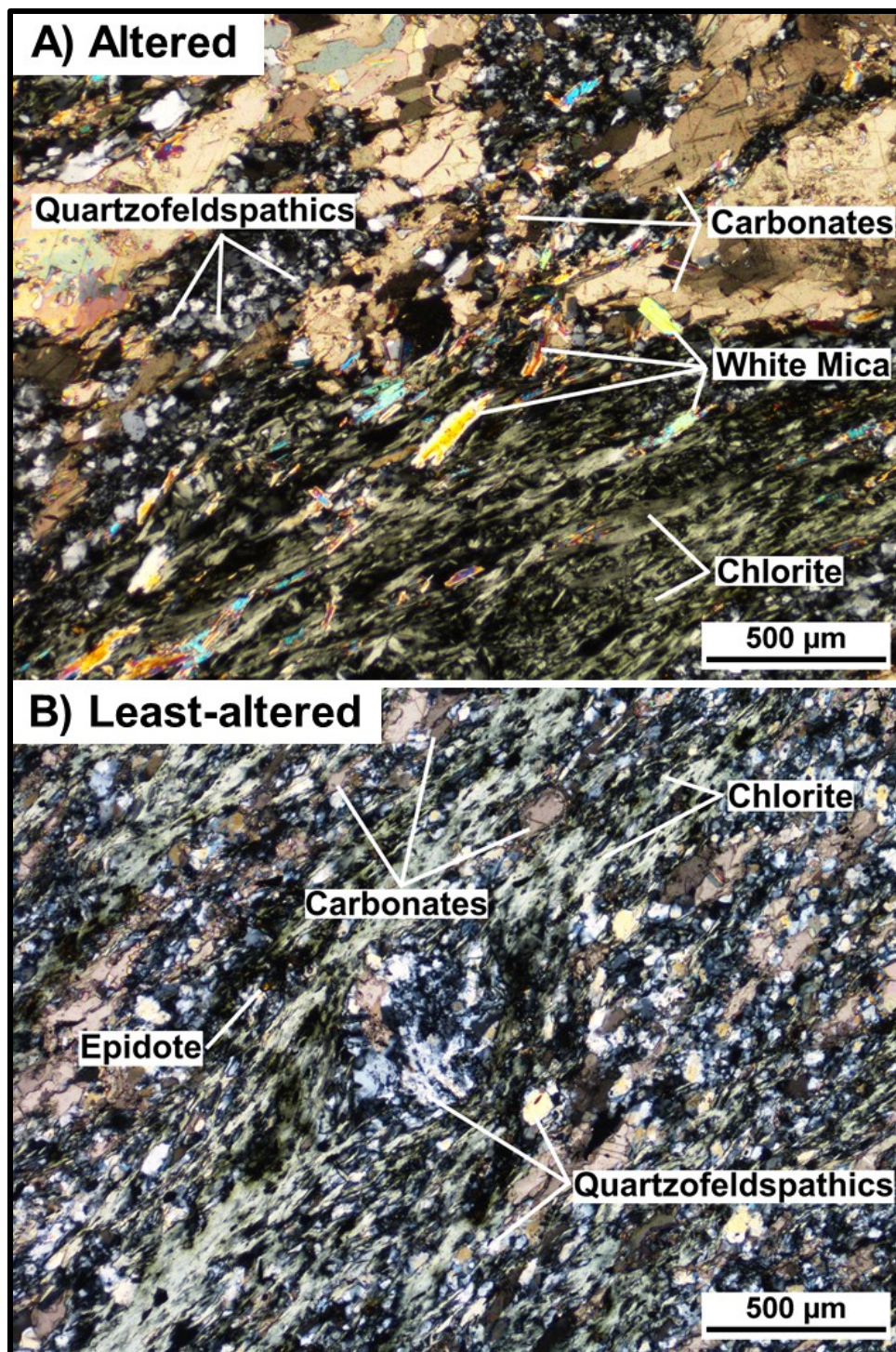


*Figure 31A, B. Cross-polarized light photomicrographs of a sample of gabbro/lamprophyre subject to alteration by a proximal  $V_3$  vein (A, T213) and a least-altered equivalent (B, T63).*



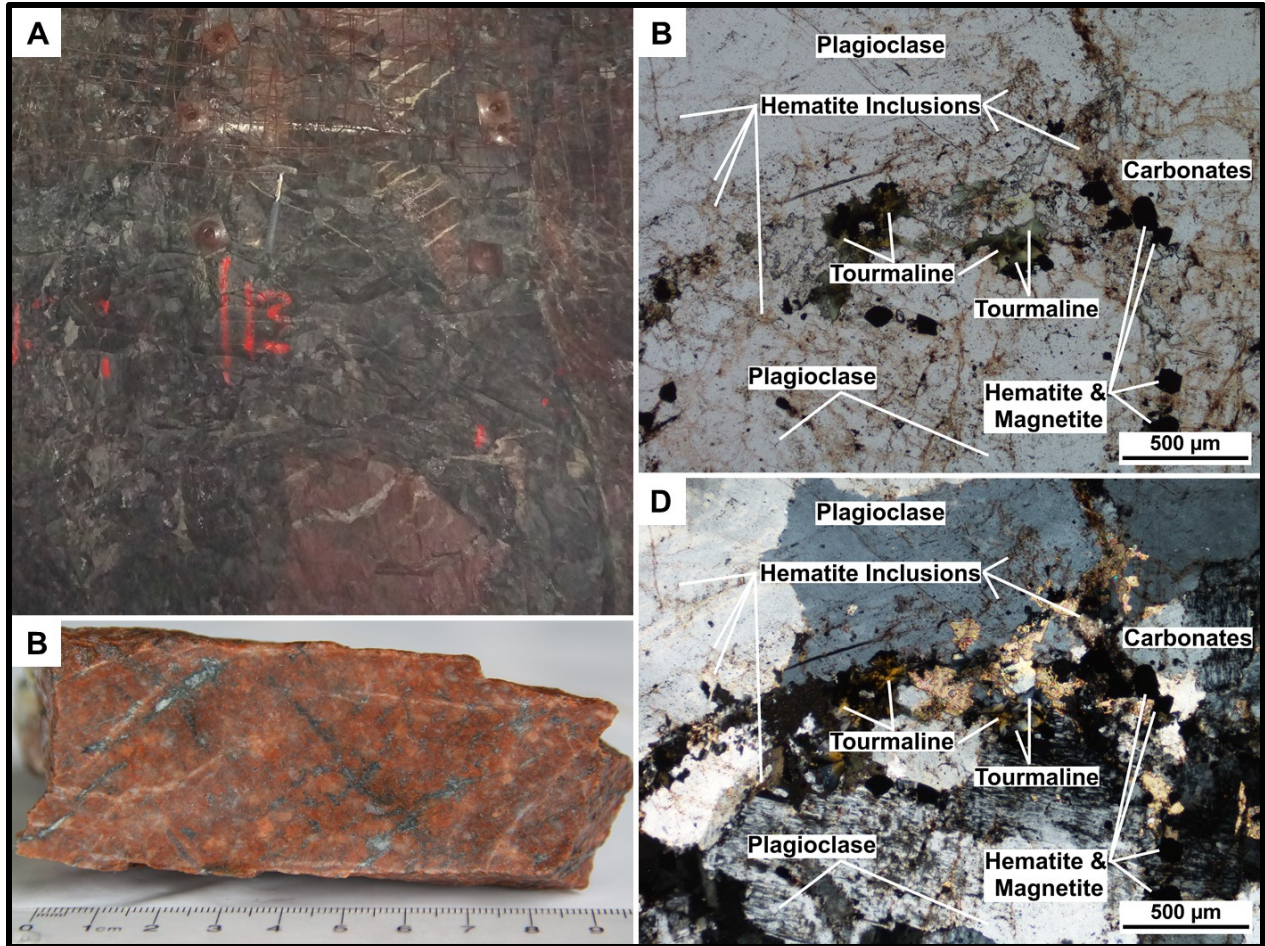


**Figure 32A–D.** Field and hand sample photographs as well as photomicrographs of quartz diorite. *A)* Hematite-rich quartz diorite xenoliths (pink–red colour) in an intrusion of silica-poor diorite–monzodiorite. Subparallel carbonate ( $\pm$  quartz and tourmaline) veinlets are concentrated in many of the xenoliths as well. *B)* A hand sample of quartz diorite (T215). *C)* A plane-polarized light photomicrograph of a sample of quartz diorite (T215). *D)* A cross-polarized light photomicrograph of a sample of quartz diorite (same thin section and photo location as D; T215).

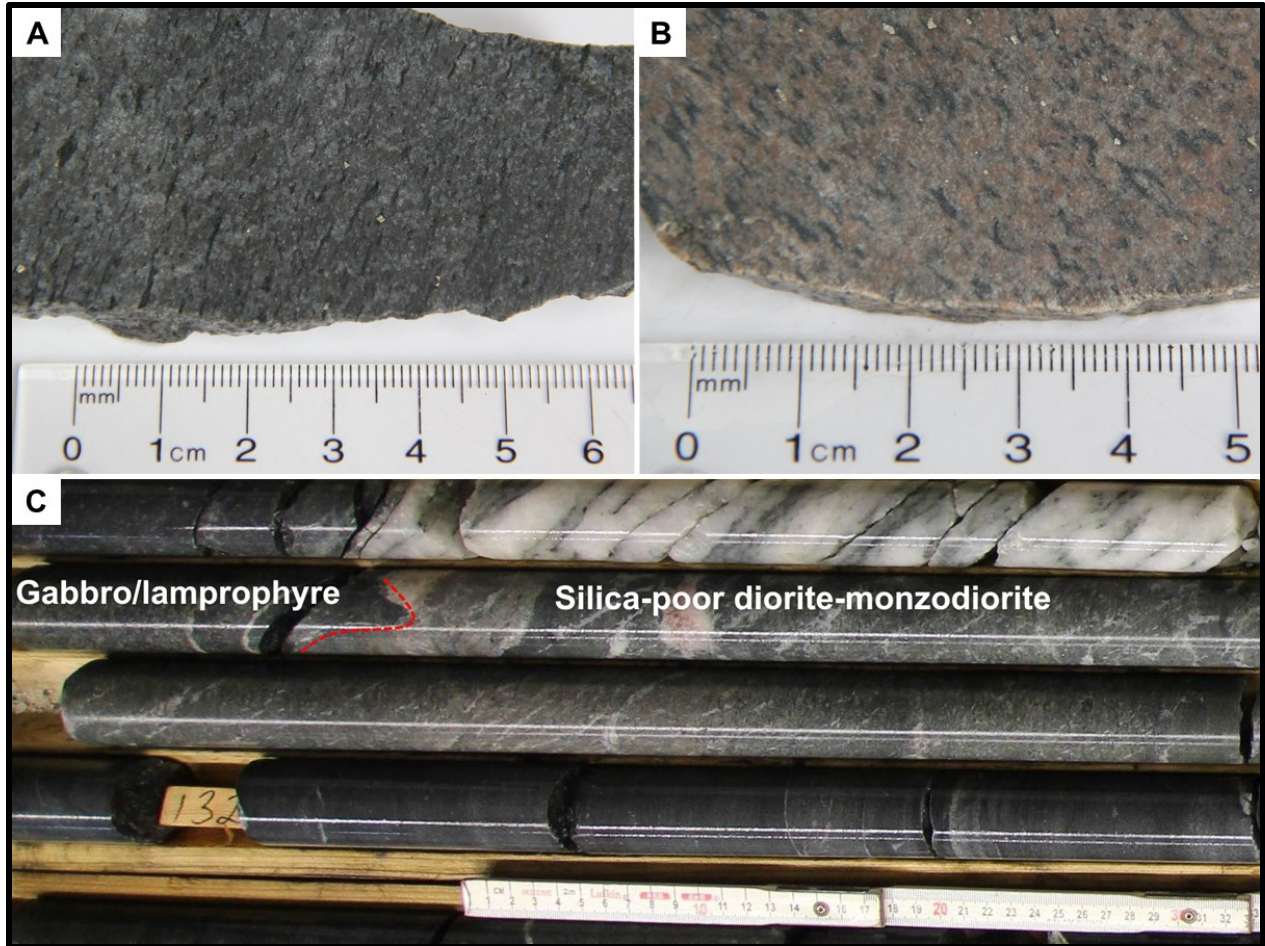


**Figure 33A–C.** Hand sample and drill core photos of silica-poor diorite–monzodiorite. A) A grey least-altered sample of silica-poor diorite–monzodiorite (T216). B) A hematite-rich, pink-coloured, least-altered sample of silica-poor diorite–monzodiorite (T228). C) Contact between silica-poor diorite–monzodiorite and gabbro/lamprophyre in drill core.



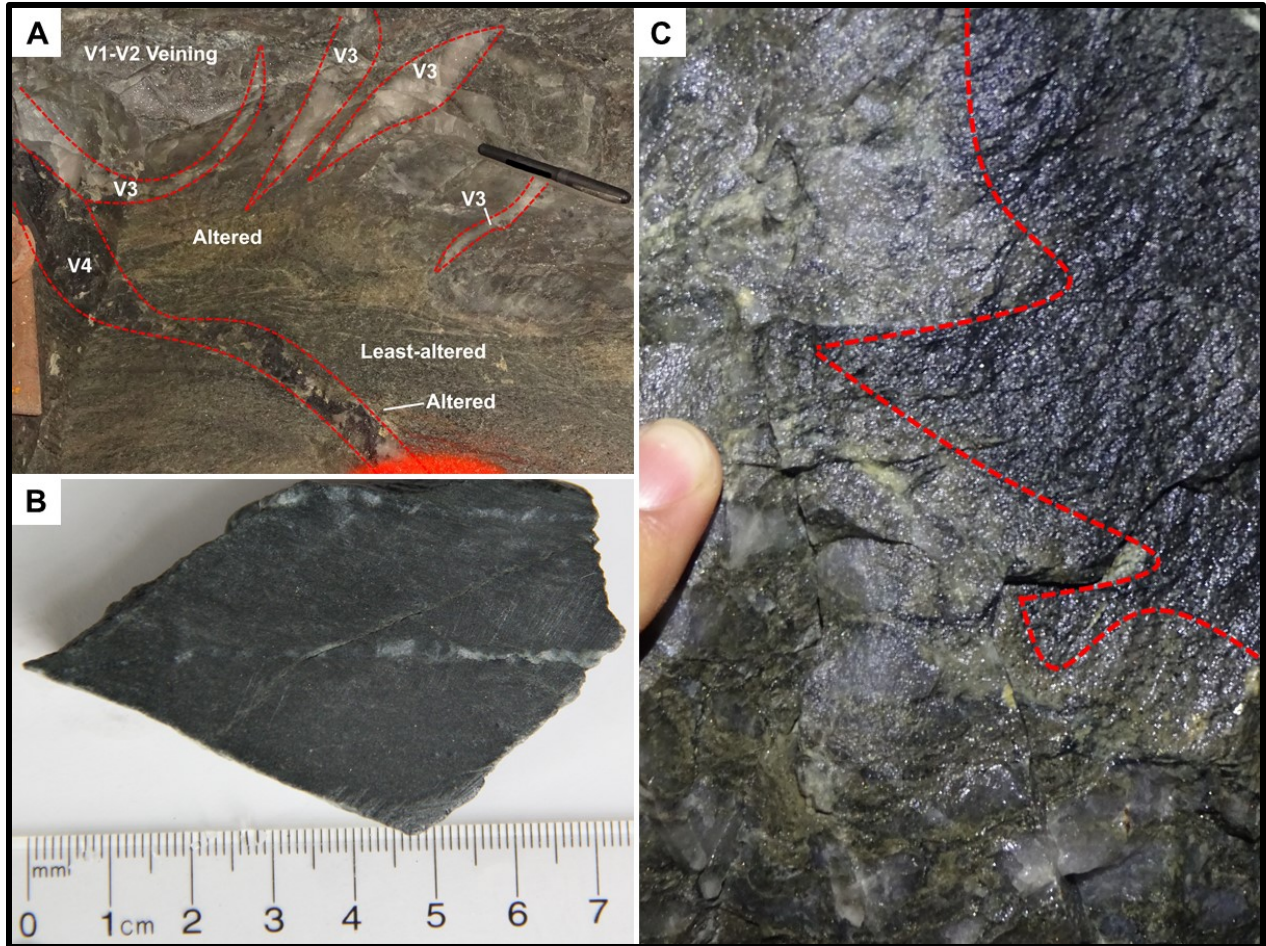


**Figure 34A–C.** Hand sample and field photos of silica-poor diorite–monzodiorite. *A)* Altered silica-poor diorite–monzodiorite adjacent to  $V_1$ – $V_2$  veining with abundant  $V_3$  veining. The alteration intensifies approaching the  $V_3$  veins. Some tourmaline is visible within  $V_3$  veins and is present as a  $V_4$  vein as well. *B)* Sample of silica-poor diorite–monzodiorite altered by  $V_3$  veins.  $V_3$  veinlets are visible in the sample (T245). *C)* The red dashed line parallels the approximate location of the sharp contact between least-altered silica-poor diorite–monzodiorite (right) and  $V_1$ – $V_2$  veining/strongly-altered dacite (left).



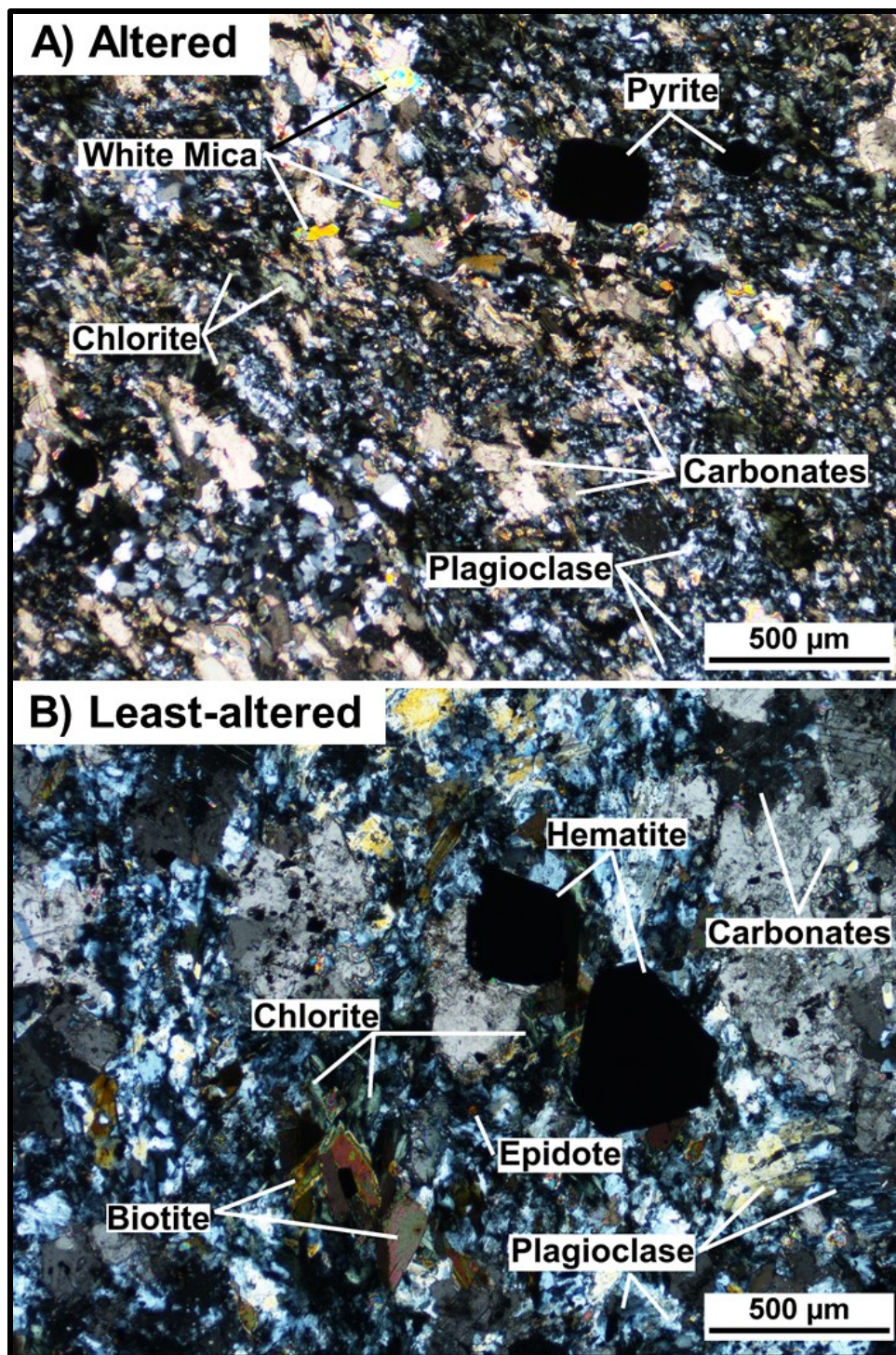


*Figure 35A, B. A cross-polarized light photomicrograph of a sample of silica-poor diorite-monzodiorite altered by proximal V<sub>3</sub> veins (A; T245) as well as a least-altered equivalent (B; T66).*



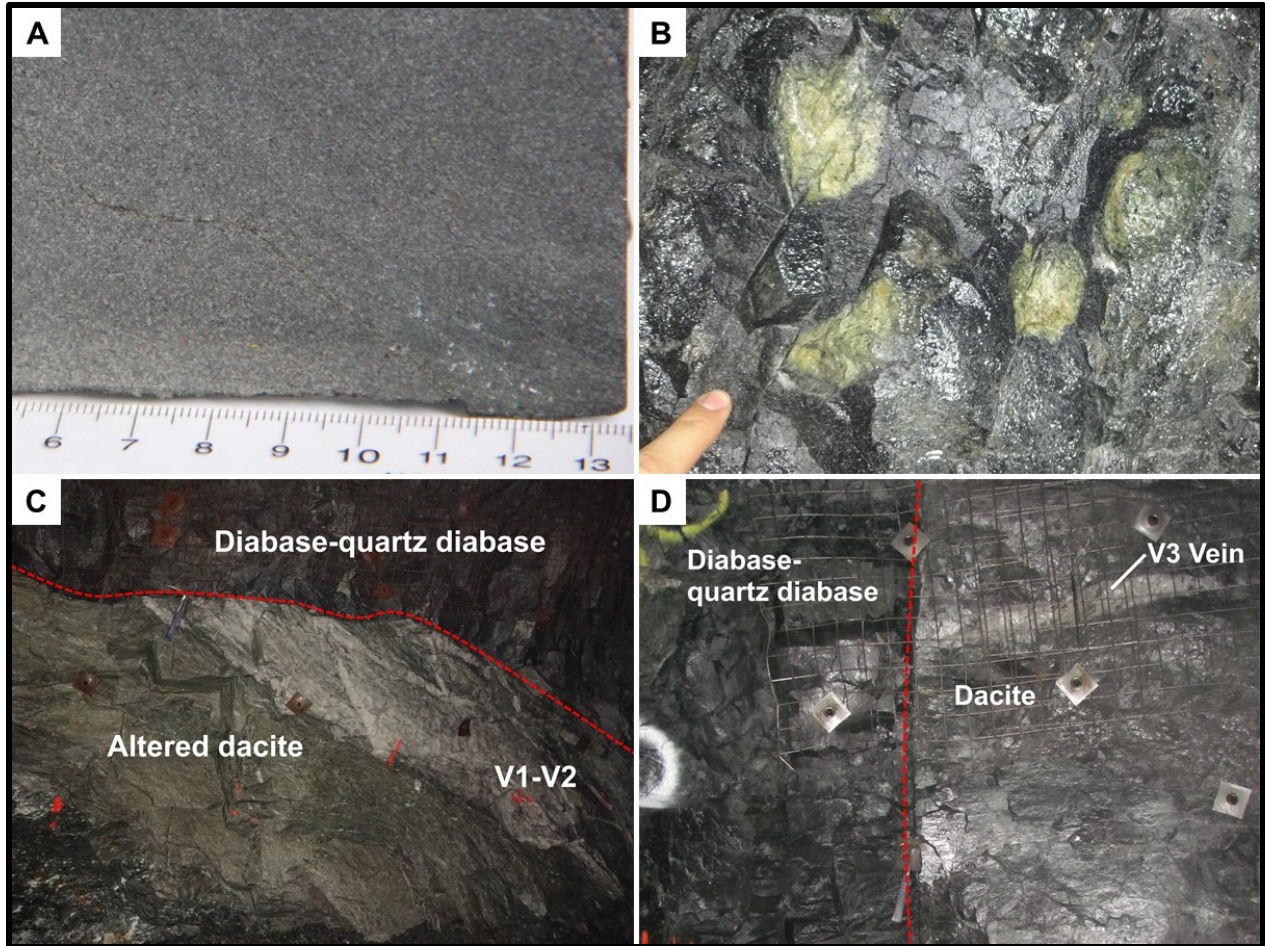


**Figure 36A–D.** Hand sample and field photos of diabase–quartz diabase. A) Hand sample of diabase–quartz diabase (T12). B) Unidentified granitoid xenoliths within a large diabase–quartz diabase intrusion. C) Diabase–quartz diabase (top) sharply cross-cutting  $V_1$ – $V_2$  auriferous veins (bottom right) and altered dacite (bottom left). The contact between the diabase–quartz diabase and the rock that it intrudes through is outlined in red. D) A Diabase–quartz diabase intrusion sharply cross-cutting a  $V_3$  vein and dacite.



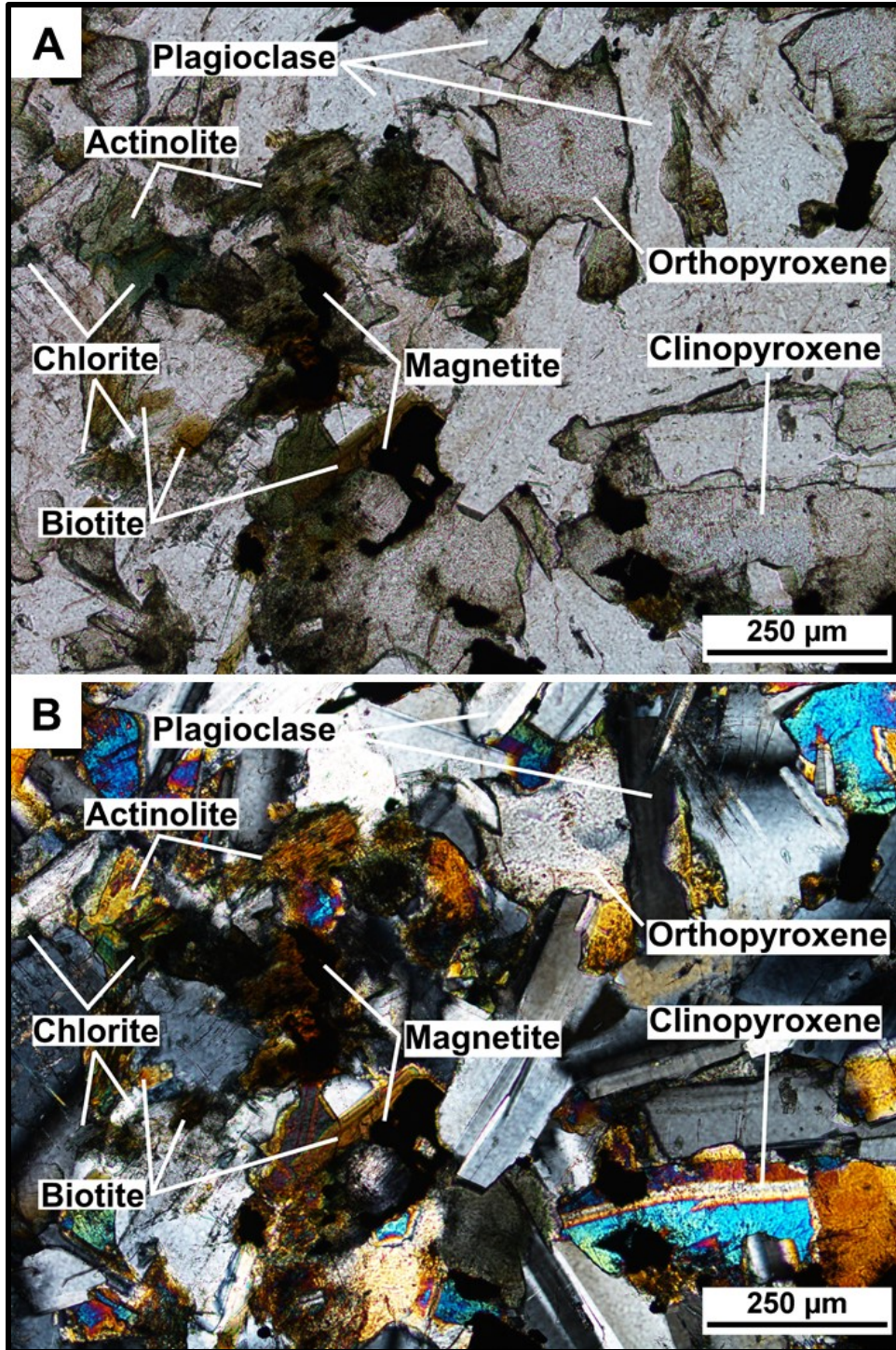


*Figure 37A, B. Photomicrographs of diabase–quartz diabase (T83). A) Plane-polarized light. B) Cross-polarized light (same thin section and photo location as A).*

## 4.2 Whole-rock geochemistry

In this section, the results of whole-rock geochemical study are summarized for nine lithologies: quartz ( $\pm$  carbonate) veins, dacite, iron formation, gabbro, the Webb Lake stock, gabbro/lamprophyre, quartz diorite, silica-poor diorite–monzodiorite, and diabase–quartz diabase. If certain lithologies have results from both least-altered samples and samples subject to alteration related to quartz  $\pm$  carbonate veining, results pertaining to least-altered and altered samples are presented in separate sub-sections.

Major element concentrations in least-altered samples from each lithology at the Island Gold deposit are summarized in Table 17A, B. Averages and ranges are based off of the following least-altered and weakly-altered samples of each lithology: Dacite (8 samples: T8, T11, T65, T116, T154, T164, T183, T241), iron formation (2 samples: T24, T37), gabbro (5 samples: T14, T80, T89, T182, T200), Webb Lake stock (3 samples: T6, T192, T193), gabbro/lamprophyre (5 samples: T15, T63, T81, T239, T240), quartz diorite (1 sample: T215), silica-poor diorite–monzodiorite (5 samples: T16, T66, T216, T228, T242), and diabase-quartz diabase (2 samples: T12, T83). Diagrams used to classify least-altered samples in this section (4.2) also use these samples. T6 and T193 (Webb Lake stock) are classified as weakly-altered (Section 3.2.3).

### 4.2.1 Auriferous veins ( $V_{GD}$ and $V_1$ - $V_2$ veins)

The compositions of  $V_{GD}$  and  $V_1$ - $V_2$  veins are summarized in Table 18 in Section 4.2. Samples of  $V_{GD}$  and  $V_1$ - $V_2$  quartz veins are characterized by high concentrations of  $SiO_2$  (80.4–96.6 wt%). These samples also have economic concentrations of gold ranging from 2.1 to 50.5 ppm.

### 4.2.2 Dacitic volcanic rocks (T2, V2, I2)

#### 4.2.2.1 Least-altered samples

Concentrations of chemical species in least-altered dacitic volcanic samples are summarized in Table 17. These dacitic samples are sodium rich (2.1–5.8 wt%  $Na_2O$ ) and potassium poor (0.5–1.3 wt%  $K_2O$ ). The four least-altered dacitic samples have smooth negatively-sloping chondrite-normalized REE patterns with no Eu or Ce anomalies. Chondrite-normalized patterns of the heavy REE (Ho–Lu) are flat (Figure 40).

On a Total-Alkali Silica (TAS) diagram, least-altered samples of this lithology consistently plot within the dacite field (Figure 38A; Le Bas et al., 1986). They also plot within the dacite and rhyodacite fields of the R<sub>1</sub>-R<sub>2</sub> multi-cationic plot (Figure 38B; De La Roche et al., 1980). However, these samples have been subject to metamorphism. To verify the classifications suggested by these plots, immobile element classifications plots were also used. These least-altered samples plot within both the dacite/rhyolite and the andesite/basaltic andesite fields of the Co-Th plot (Figure 39A; Hastie et al., 2007). They also plot within the andesite/basaltic andesite field of the Nb/Y-Zr/Ti plot (Figure 39B; Pearce, 1996).

#### **4.2.2.2 Altered samples**

Average concentrations of chemical species in volcanic samples classified under each alteration strength grouping and altered by proximal V<sub>1</sub>-V<sub>2</sub> veins are presented alongside mass balance calculations in Table 5. Similarly, average concentrations of chemical species in volcanic samples classified under each alteration strength grouping and altered by proximal V<sub>GD</sub> veins are presented in Table 6. Average concentrations of these chemical species in equivalent least-altered samples are also included in these tables for comparison. Concentrations of chemical species in a dacitic sample (T218) subject to non-auriferous carbonate-sericite alteration are displayed in Appendix N. Concentrations of select chemical species in T218 are also displayed alongside mass balance calculations in Table 7.

##### **4.2.2.2.1 Isocon diagrams**

Isocon diagrams (Grant, 1986; Section 3.2.2) are used in this section in order to determine and display consistent chemical enrichments and depletions as a result of the alteration of the dacite. An Isocon diagram was constructed for each altered/less-altered pair from volcanic-hosted alteration envelopes associated with V<sub>1</sub>-V<sub>2</sub> auriferous veins at the locations shown in Figure 19. A volcanic-hosted alteration envelope associated with a V<sub>GD</sub> vein in the Goudreau Zone is also examined via Isocon diagram analysis (Figure 42). Chemical gains and losses determined by examining the Isocon diagrams of altered/less-altered pairs from each alteration envelope are summarized in Table 4 and Appendix S. The chemical gains/losses for each alteration envelope are based on multiple altered/less-altered pairs from the same alteration

envelope (Table 4). The chemical gains/losses that are verified by multiple altered/less-altered pairs from the same alteration envelope are more reliable (discussed in Section 3.2.2).

An average Isocon diagram was created to summarize chemical gains/losses as a result of alteration related to  $V_1$ - $V_2$  veins throughout the deposit. A representative altered/less-altered pair was selected from each of the five  $V_1$ - $V_2$  vein-related alteration envelopes outlined in Figure 19. An Isocon diagram was then constructed based on the average chemical composition of altered samples and the average chemical composition of less-altered samples (Figure 41). Chemical gains and losses that were consistently observed in each alteration envelope associated with  $V_1$ - $V_2$  veins are displayed. Chemical species that are typically enriched in dacite due to alteration related to  $V_{GD}$  or  $V_1$ - $V_2$  veins include As, Au, Bi,  $K_2O$ , Rb, S, Se, Te, Tl, and W while depletions include  $Na_2O$  and Sr (Table 4).

Carbonate-sericite volcanic-hosted alteration zones that are gold-barren are occasionally observed at the Island Gold deposit. This type of alteration has a superficial resemblance to auriferous alteration and the mineralogy of these zones is discussed in Section 4.1.2. A representative Isocon diagram that displays the chemical gains/losses that consistently occur based on multiple altered/less-altered pairs associated with this type of alteration is displayed in Figure 43 and summarized in Table 4. Notably, there is no consistent enrichment in As, Te, Tl, or W and no consistent loss of Sr or  $Na_2O$  (Table 4). Enrichments and depletions of these chemical species are commonly associated with auriferous quartz veining at the Island Gold deposit (Table 4).

#### **4.2.2.2 Mass balance calculations**

Mass balance calculations (Section 3.2.4) are used in this section to quantify the magnitude of enrichment and depletion of chemical species due to the alteration of dacite. The chemical compositions of samples classified under each alteration strength grouping were first averaged and then compared to the average chemical composition of least-altered samples taken from throughout the deposit. Calculations were performed separately for dacitic samples altered by  $V_1$ - $V_2$  veining (Table 5) and for dacitic samples altered by  $V_{GD}$  veins (Table 6). Average concentrations of chemical species (C) for samples classified in each alteration strength grouping as well as the calculated concentration changes ( $\Delta C$ ) of chemical species are displayed. Concentration changes of chemical species relative to their concentration in the least-altered

sample are also displayed in this table ( $\Delta C/C_{LA}$ ).  $Al_2O_3$ , Hf, Nb, Th,  $TiO_2$ , Y, and Zr were selected as immobile for calculations involving samples altered by  $V_1$ - $V_2$  veining.  $Al_2O_3$ , Th,  $TiO_2$  and Zr were selected as immobile for samples altered by  $V_{GD}$  veins. Chemical species that are significantly enriched in strongly-altered samples due to  $V_1$ - $V_2$  vein-related alteration include Au, S, W, As, Te, Bi,  $K_2O$ , B, Rb,  $Fe_2O_3$ , Cs, Mo, and LOI (Table 5). Similarly, chemical species that are notably enriched due to  $V_{GD}$  vein-related alteration include Au, As, S, Te, Bi, W,  $K_2O$ , B,  $Fe_2O_3$ , Rb,  $CO_2$ , C, Cs, Cu, and LOI (Table 6).

Mass balance was also used to compare the magnitude of gains/losses associated with the non-auriferous carbonate-sericite alteration to the alteration associated with auriferous quartz veins. The chemical compositions of the representative altered and least-altered samples, used in the Isocon diagram displayed in Figure 43 (Section 4.2.2.2.1), are used for these calculations. Only gains/losses of chemical species that are observed to be consistently enriched or depleted in Section 4.2.2.2.1 are displayed. Concentration changes of chemical species relative to their concentration in the least-altered sample ( $\Delta C/C_{LA}$ ) are displayed in Figure 44 and summarized in Table 7. Altered and least-altered concentrations as well as the calculated concentration changes ( $\Delta C$ ) of chemical species are also displayed in Table 7. Despite this intense alteration, concentration changes are negligible for many of the chemical species that are consistently and significantly enriched due to alteration associated with  $V_1$ - $V_2$  and  $V_{GD}$ . For example,  $\Delta C$  is only 0.01 ppm for both Au and S. Chemical species that are significantly enriched due to carbonate-sericite alteration include C,  $CO_2$ , LOI, B, and CaO (Table 7).

### **4.2.3 Iron formation (IF)**

Compositions of least-altered iron formation samples are summarized in Table 17. Relative to other lithologies at the Island Gold deposit, samples of iron formation are characterized by high average concentrations of  $Fe_2O_3$  (43.8 wt%), FeO (18.5 wt%), and S (30.8 wt%).

### **4.2.4 Gabbro (I3G)**

#### **4.2.4.1 Least-altered samples**

This lithology has 44.1–48.7 wt%  $SiO_2$  and is generally characterized by higher total iron (12.0–14.4 wt%  $Fe_2O_3T$ ) and  $TiO_2$  (0.6–1.2 wt%) concentrations than the gabbro/lamprophyre

(Table 17B). They also have lower average MgO (6.7 wt%), Cr (132 ppm), and Ni (115 ppm) concentrations when compared to gabbro/lamprophyre (Table 17A). Least-altered samples are also potassium deficient (0.01–0.12 wt% K<sub>2</sub>O). Four representative least-altered samples have flat chondrite-normalized REE patterns with a slight negative Eu anomaly in T89, a slight positive Eu anomaly in T200, and no Ce anomalies (Figure 40B).

Least-altered samples with mineral modes determined via CIPW Norm calculations fall in the tonalite and gabbro fields of the QAP diagram (Figure 45). Least-altered samples with the most primary textures (T182 and T200) plot closer to the plagioclase apex in the lower tonalite and gabbro fields of the QAP diagram (Figure 45). On a TAS diagram modified for intrusive lithologies, these samples fall in the subalkalic gabbro field (Figure 46A; Middlemost, 1994). The least-altered samples of this lithology fall in the gabbro-norite, gabbro-diorite, and diorite fields of the R<sub>1</sub>, R<sub>2</sub> multi-cationic plot (Figure 46B; De La Roche et al., 1980) and in the quartz diorite and tonalite fields of the P-Q diagram (Figure 46C; Debon and Le Fort, 1983). However, these samples have also been subject to significant metamorphism. As a result, immobile element plots are also used to support these classifications. On the immobile element ratio plot that was modified for intrusive lithologies, these samples all plot in the gabbro field (Figure 46D; Nb/Y, Zr/TiO<sub>2</sub>; Pearce, 1996).

#### **4.2.4.2 Altered samples**

Average concentrations of chemical species in gabbroic samples classified under each alteration strength grouping and altered by proximal V<sub>1</sub>-V<sub>2</sub> veins are presented alongside mass balance calculations in Table 8. The average concentrations of chemical species in equivalent least-altered samples are also included for comparison.

##### **4.2.4.2.1 Isocon diagrams**

Isocon diagrams (Section 3.2.2) are used in this section in order to determine and display consistent chemical enrichments and depletions as a result of alteration related to V<sub>1</sub>-V<sub>2</sub> veining. Isocon diagrams were constructed for altered/less-altered pairs from a gabbro-hosted alteration envelope associated with V<sub>1</sub>-V<sub>2</sub> auriferous quartz veining. Results of the analysis of these diagrams are summarized in Table 4 and Appendix S. An Isocon diagram for a representative altered/less-altered pair is displayed in Figure 47. Only chemical species that consistently exhibit

gains/losses based on Isocon analysis of multiple altered/less-altered pairs are displayed. Chemical species that are consistently enriched in gabbro due to alteration related to V<sub>1</sub>-V<sub>2</sub> veins include Au, B, Ba, Cs, K<sub>2</sub>O, Li, MnO, Pb, Rb, S, Sm, Sr, and Te. Consistent depletions include Bi, Ge, Na<sub>2</sub>O, P<sub>2</sub>O<sub>5</sub>, Sb, and Tl (Table 4).

#### **4.2.4.2.2 Mass balance calculations**

Mass balance calculations (Section 3.2.4) are used in this section to quantify the magnitude of enrichment and depletion of chemical species due to the V<sub>1</sub>-V<sub>2</sub> vein-related alteration of gabbro. The chemical composition of samples classified under each alteration strength grouping from the same gabbro-hosted alteration envelope were first averaged and then compared to the average chemical composition of least-altered samples taken from throughout the deposit. Mass balance calculations were performed and the results are summarized in Table 8. Al<sub>2</sub>O<sub>3</sub>, Er, Nb, and Zr were selected as immobile for calculations. Chemical species that are significantly enriched in the strongly-altered sample due to V<sub>1</sub>-V<sub>2</sub> vein-related alteration include Au, S, B, Bi, K<sub>2</sub>O, As, Ba, Te, Rb, W, Se, Cs, and Tl (Table 8).

### **4.2.5 Webb Lake stock: Tonalite–trondhjemite (I1JM)**

#### **4.2.5.1 Least-altered samples**

This felsic intrusion (66.2–71.5 wt% SiO<sub>2</sub>) is rich in sodium (4.5–4.9 wt % Na<sub>2</sub>O) and is comparatively potassium poor (0.9–1.1 wt % K<sub>2</sub>O; Table 17). Al<sub>2</sub>O<sub>3</sub> concentrations range from 13.9–15.3 wt% while CaO concentrations range from 2.7–4.5 wt%. These are generally consistent with Archean tonalite-trondhjemite-granodiorites (TTG; Barker, 1979; Moyen and Martin, 2012). The sum of the average MgO, TiO<sub>2</sub>, Fe<sub>2</sub>O<sub>3</sub>T, and MnO concentrations for Webb Lake stock samples equates to 5.2 wt% (Table 17) while Archean TTGs typically have ≤5.0 wt% (Moyen and Martin, 2012). A least-altered and a weakly-altered sample of the Webb Lake stock have smooth chondrite-normalized REE patterns with steep negative slopes (left of Y), no Eu or Ce anomalies, and heavy REE patterns are flat (Figure 40C).

Least-altered and weakly-altered samples with mineral modes determined via CIPW Norm calculations fall in the tonalite field of the QAP diagram (Figure 45). Difficulty distinguishing the composition of each plagioclase makes point-counting techniques inappropriate for plotting on the Anorthite-Albite-Orthoclase ternary diagram. Using mineral



modes determined by CIPW Norm calculations, these samples plot in the trondhjemite field of the Anorthite-Albite-Orthoclase ternary diagram (Figure 48). On a TAS diagram modified for intrusive lithologies these samples plot in the granodiorite and granite fields (Figure 46A). Least-altered and weakly-altered samples of this lithology fall in the granodiorite field of the R<sub>1</sub>, R<sub>2</sub> multi-cationic plot (Figure 46B) and the tonalite field of the P-Q classification diagram (Figure 46C). On the immobile element ratio plot, that was modified for intrusive lithologies, these samples all plot in the diorite-gabbro diorite field (Figure 46D; Nb/Y, Zr/TiO<sub>2</sub>). A tonalite field is not delineated on this diagram.

#### **4.2.5.2 Altered samples**

Concentrations of chemical species in representative samples of the Webb Lake stock classified under each alteration strength grouping and altered by proximal V<sub>1</sub>-V<sub>2</sub> veins are presented alongside mass balance calculations in Table 9. The average concentrations of chemical species in equivalent least-altered samples are also included for comparison.

##### **4.2.5.2.1 Isocon diagrams**

Isocon diagrams (Section 3.2.2) are used in this section in order to determine and display consistent chemical enrichments and depletions as a result of alteration related to V<sub>1</sub>-V<sub>2</sub> veining. Isocon diagrams were constructed for altered/less-altered pairs from a Webb Lake stock-hosted alteration envelope associated with V<sub>1</sub>-V<sub>2</sub> auriferous quartz veining. Results of the analysis of these diagrams are summarized in Table 4 and Appendix S. An Isocon diagram for a representative altered/less-altered pair is displayed in Figure 49. Only chemical species that consistently exhibit gains/losses based on Isocon analysis of multiple altered/less-altered pairs are displayed. Chemical species that are consistently enriched in the Webb Lake stock due to alteration related to V<sub>1</sub>-V<sub>2</sub> veins include Ag, As, Au, B, Bi, C, CO<sub>2</sub>, Cu, Fe<sub>2</sub>O<sub>3</sub>, Ge, K<sub>2</sub>O, LOI, Mo, Rb, S, Se, Ta, Te, U, and W. Consistent depletions include CaO, Co, Fe<sub>2</sub>O<sub>3</sub>T, FeO, MnO, Na<sub>2</sub>O, Sc, SiO<sub>2</sub>, and Sm (Table 4).

##### **4.2.5.2.2 Mass balance calculations**

Mass balance calculations (Section 3.2.4) are used in this section to quantify the magnitude of enrichment and depletion of chemical species due to the V<sub>1</sub>-V<sub>2</sub> vein-related

alteration of the Webb Lake stock. The chemical compositions of samples classified under each alteration strength grouping from the same Webb Lake stock-hosted alteration envelope were compared to the chemical composition of the least-altered sample taken just outside of the alteration envelope. Mass balance calculations were performed and the results are summarized in Table 9.  $\text{Al}_2\text{O}_3$  and Y were selected as immobile for calculations. Chemical species that are significantly enriched in the strongly-altered sample due to  $V_1$ - $V_2$  vein-related alteration include As, S, Au, Te, Mo, B, W, Bi,  $\text{Fe}_2\text{O}_3$ , Cu,  $\text{K}_2\text{O}$ , Ag, and Rb (Table 9).

#### **4.2.6 Gabbro/Lamprophyre (I2H)**

##### **4.2.6.1 Least-altered samples**

The gabbro/lamprophyre at the Island Gold deposit contains 40.9–46.8 wt%  $\text{SiO}_2$  and has a low concentration of  $\text{K}_2\text{O}$  (0.08–0.39 wt%). This unit is also characterized by high MgO (8.0–10.7 wt%), Cr (282–576 ppm), Ni (119–472 ppm), and  $\text{CO}_2$  (11.5–15.7 wt%) concentrations compared to most other lithologies at the Island Gold deposit (Table 17). Four representative least-altered samples have smooth, steep, negatively-sloping chondrite-normalized REE patterns with no Eu or Ce anomalies and flat heavy REE patterns (Figure 40D).

Least-altered samples with mineral modes determined via CIPW Norm calculations fall in the tonalite field of the QAP diagram (Figure 45). One sample also plots in the granodiorite field (Figure 45). On a TAS diagram modified for intrusive lithologies these samples fall in the gabbro diorite and subalkalic gabbro fields (Figure 46A). The least-altered samples of this lithology plot within the gabbro-diorite, gabbro-norite, and gabbro fields on a  $R_1$ ,  $R_2$  multicationic plot (Figure 46B) and in the quartz diorite and gabbro fields of the P-Q diagram (Figure 46C). On the immobile element ratio plot, that was modified for intrusive lithologies, these samples all plot in the diorite and gabbro-diorite field (Figure 46D; Nb/Y, Zr/ $\text{TiO}_2$ ).

##### **4.2.6.2 Altered samples**

Concentrations of chemical species in a sample of gabbro/lamprophyre (T213) altered by a  $V_3$  vein are displayed in Appendix N. Concentrations of select chemical species in T213 are also displayed alongside mass balance calculations in Table 10.

#### 4.2.6.2.1 Isocon diagrams

Isocon diagrams (Section 3.2.2) are used in this section in order to determine and display consistent chemical enrichments and depletions as a result of alteration related to  $V_3$  veining. Two Isocon diagrams were constructed in which a sample of gabbro/lamprophyre altered by  $V_3$  quartz veining is compared to representative least-altered equivalents. Only chemical species that were enriched or depleted in both altered/least-altered pairs are displayed in the representative Isocon diagram in Figure 50. Results are summarized in Table 4 and Appendix S.

The following chemical species were consistently enriched: As, Au, B, Ba, Bi, Ce, Cr, Cs, Ga, Ge,  $K_2O$ , La, Li, Mo, Rb, Sb, Sr, V, W, and Zn. The chemical species that are consistently depleted are Ag, C, CaO, Co,  $CO_2$ , Dy, Er, LOI, Lu, MgO, MnO,  $Na_2O$ , Ni, Pb, Se,  $SiO_2$ , Tb, Tm, Y, and Yb.

#### 4.2.6.2.2 Mass balance calculations

Mass balance calculations (Section 3.2.4) are used in this section to quantify the magnitude of enrichment and depletion of chemical species due to the  $V_3$  vein-related alteration of gabbro/lamprophyre. The chemical compositions of the representative altered and least-altered samples, used in the Isocon diagram displayed in Section 4.2.6.2.1 (Figure 50), are used for these calculations. Only gains/losses of chemical species that are observed to be consistently enriched or depleted (from Section 4.2.6.2.1) are displayed. Relative concentration changes determined via mass balance calculations are displayed graphically in Figure 51 and numerically in Table 10. Concentration changes associated with  $V_3$  vein-related alteration are small for most chemical species that are consistently and significantly enriched due to alteration associated with  $V_1$ - $V_2$  and  $V_{GD}$  veins. For example, there is a concentration gain of only 0.05 ppm for Au (Table 10). Chemical species that are significantly enriched in the altered sample due to  $V_3$  vein-related alteration include Ba, As, W, and Sr (Table 10).

#### 4.2.7 Quartz diorite

A single sample of the quartz diorite is characterized by high  $SiO_2$  (65.5 wt%),  $Al_2O_3$  (16.7 wt%), and  $Na_2O$  (8.9 wt%), in addition to low  $K_2O$  (0.05 wt%) concentrations relative to other rock types at the Island Gold deposit (Table 17). The quartz diorite is also plotted on a chondrite-normalized REE diagram (Figure 40E). This sample has a smooth, steep, negative

slope that shallows rapidly in the middle REEs and becomes positive in the latter half of the heavy REEs (Figure 40E). This pattern has no Eu or Ce anomalies.

Using CIPW-calculated mineral modes, this lithology plots as a quartz diorite on a QAP ternary diagram (Figure 45). On a TAS diagram modified for intrusive lithologies, this sample falls in the quartz monzonite field (Figure 46A). When plotted on the  $R_1$ ,  $R_2$  multi-cationic plot (Figure 46B), it falls in the quartz syenite field. This sample does not plot within any of the defined fields on the P-Q diagram (Figure 46C). On the immobile element ratio plot that was modified for intrusive lithologies, this sample plots in the syenite field (Figure 46D; Nb/Y, Zr/TiO<sub>2</sub>).

## **4.2.8 Silica-poor diorite–monzodiorite (I2M)**

### **4.2.8.1 Least-altered samples**

The silica-poor diorite–monzodiorite has the lowest SiO<sub>2</sub> content out of all the chemically analyzed lithologies at the Island Gold deposit (37.9–45.9 wt%; Table 17). It is also characterized by high Na<sub>2</sub>O (3.4–5.5 wt%) and CaO (9.9–13.6 wt%) concentrations relative to most lithologies at the Island Gold deposit (Table 17). Four representative least-altered samples have a smooth, negatively-sloping, chondrite-normalized REE patterns with no Eu or Ce anomalies (Figure 40F). Their slopes become shallower to the right of Y. When compared to the REE patterns of other lithologies, the silica-poor diorite–monzodiorite generally exhibits the highest concentrations of REEs relative to the other rock types at the Island Gold deposit.

Least-altered samples with mineral modes determined via CIPW Norm calculations fall in the quartz diorite and diorite fields of the QAP diagram (Figure 45). All of the least-altered samples are also plotted on a TAS diagram modified for intrusive lithologies and these samples fall in the monzo-diorite, monzo-gabbro, and foid-gabbro fields (Figure 46A). On the  $R_1$ ,  $R_2$  multi-cationic plot (Figure 46B), the least-altered samples of this lithology fall in the theralite and essexite fields. These same samples do not plot within any of the defined fields on the P-Q diagram (Figure 46C). On the immobile element ratio plot that was modified for intrusive lithologies, these samples all plot in the monzonite and diorite, as well as gabbro-diorite fields (Figure 46D; Nb/Y, Zr/TiO<sub>2</sub>).

#### 4.2.8.2 Altered samples

Concentrations of chemical species in a silica-poor dioritic–monzodioritic sample (T245) altered by  $V_3$  veining are displayed in Appendix N. Concentrations of select chemical species in T245 are also displayed alongside mass balance calculations in Table 11.

##### 4.2.8.2.1 Isocon diagrams

Isocon diagrams (Section 3.2.2) are used in this section in order to determine and display consistent chemical enrichments and depletions as a result of alteration related to  $V_3$  veining. Two Isocon diagrams were constructed in which a sample of silica-poor diorite–monzodiorite altered by  $V_3$  quartz veining is compared to representative least-altered equivalents. Only chemical species that were consistently enriched or depleted in both altered/least-altered pairs are displayed in the representative Isocon diagram (Figure 52). Results are summarized in Table 4 and Appendix S.

The following chemical species were consistently enriched: As, Au, CaO, FeO, Hf, Li, S, Sc, Te, and W. Conversely, the chemical species consistently depleted are: B, Ba, C,  $CO_2$ , Cr, Cs, Cu,  $Fe_2O_3$ , Ga,  $K_2O$ , LOI, Mo,  $Na_2O$ , Ni, Pb, Rb, Sb, Se, Sr, and U.

##### 4.2.8.2.2 Mass balance calculations

Mass balance calculations (Section 3.2.4) are used in this section to quantify the magnitude of enrichment and depletion of chemical species due to the  $V_3$  vein-related alteration of the silica-poor diorite–monzodiorite.

The chemical compositions of the representative altered and least-altered samples, used in the Isocon diagram displayed in Section 4.2.8.2.1 (Figure 52), are used for these calculations. Only gains/losses of chemical species that are observed to be consistently enriched or depleted in Section 4.2.8.2.1 are displayed. Relative concentration changes of chemical species are displayed graphically in Figure 53 and numerically in Table 11. Concentration changes associated with this alteration are small for many of the chemical species that are consistently and significantly enriched due to alteration associated with  $V_1$ - $V_2$  and  $V_{GD}$ . For example, there is a concentration gain of only 0.07 and 0.15 ppm for Au and S, respectively (Table 11). Chemical species that are significantly enriched in the altered sample due to  $V_3$  vein-related alteration include W and As (Table 11).

#### 4.2.9 Diabase–quartz diabase (I3DD)

Relative to other lithologies at the Island Gold deposit, two samples of the diabase–quartz diabase have high average concentrations of total iron (1.4 wt% Fe<sub>2</sub>O<sub>3</sub>T), CaO (9.5 wt%), and TiO<sub>2</sub> (1.4 wt%; Table 17). Chondrite-normalized REE patterns have shallow negative slopes with minor Eu anomalies (Figure 40G). Right of Y, the slopes become flat or slightly positive.

Least-altered samples with mineral modes determined via CIPW Norm calculations fall in the quartz gabbro field of the QAP diagram (Figure 45). On a TAS diagram modified for intrusive lithologies, these samples fall in the subalkalic gabbro and gabbro diorite fields (Figure 46A). These samples plot in the gabbro-diorite field on the R<sub>1</sub>, R<sub>2</sub> multi-cationic plot (Figure 46B) and the quartz diorite field of the P-Q diagram (Figure 46C). On the immobile element ratio plot that was modified for intrusive lithologies, these samples plot in the alkali gabbro and gabbro fields (Figure 46D; Nb/Y, Zr/TiO<sub>2</sub>).



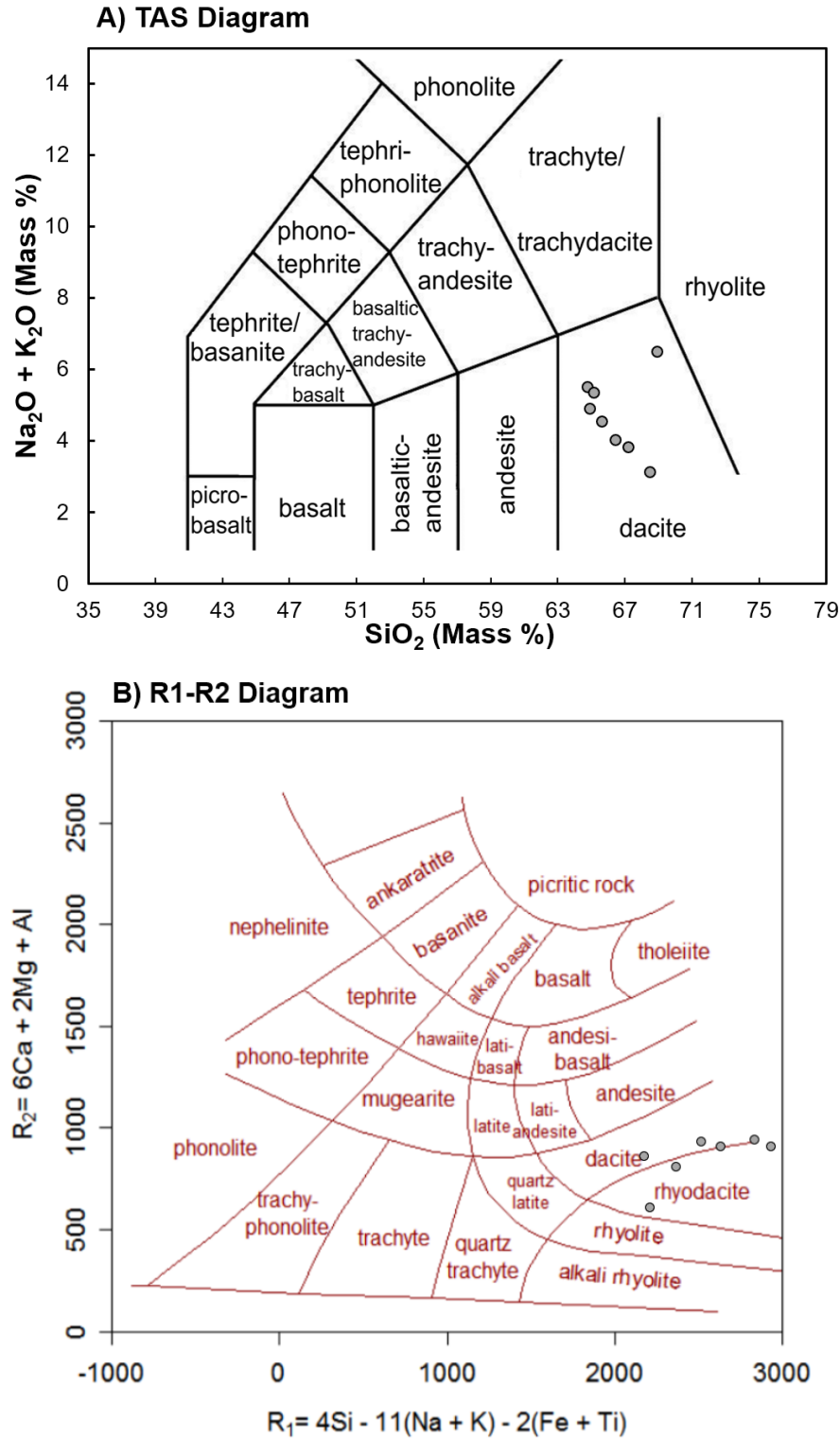


**Figure 38A, B.** Least-altered dacitic samples (T8, T11, T65, T116, T154, T164, T183, T241) plotted on mobile element classification diagrams. A) Total Alkali Silica (TAS) diagram. Concentrations of oxides are normalized on a volatile-free basis to 100% before plotting. Modified from Le Bas et al. (1986) and Janoušek (2018). B) Least-altered dacitic samples (T8, T11, T65, T116, T154, T164, T183, T241) plotted on the R<sub>1</sub>-R<sub>2</sub> multicationic plot modified from De La Roche et al. (1980) and Janoušek (2018).

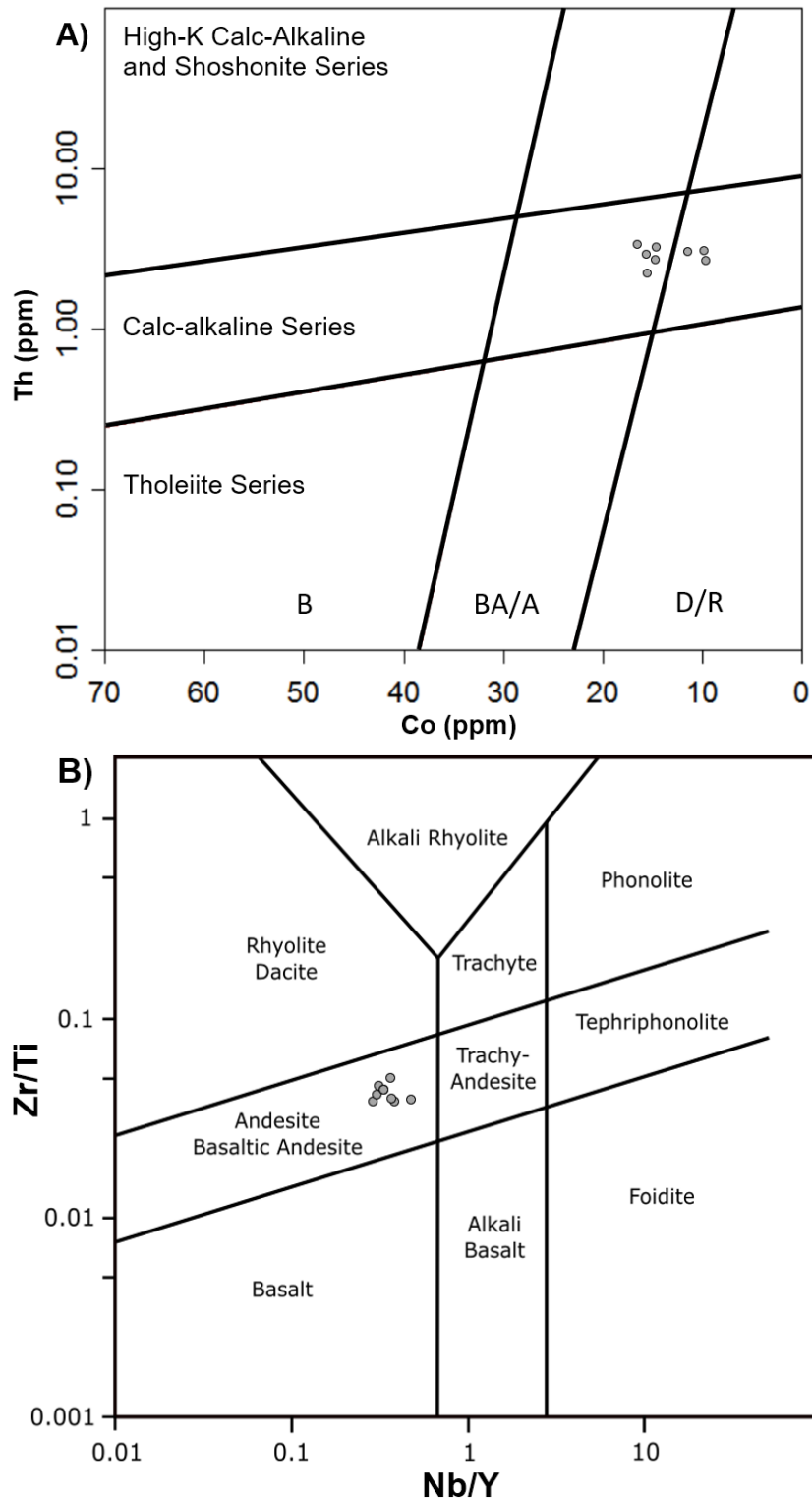


**Figure 39A, B.** Least-altered dacitic samples (T8, T11, T65, T116, T154, T164, T183, T241) plotted on classification diagrams designed to classify volcanic rocks using relatively immobile elements. A) Co-Th diagram modified from Hastie et al. (2007) and Janoušek (2018). B=Basalt, BA/A=Basaltic Andesite/Andesite, D/R=Dacite/Rhyolite. B) Nb/Y-Zr/Ti diagram modified from Pearce (1996). This diagram is originally from Winchester and Floyd (1977) and was later revised in Pearce (1996). Modified from Janoušek (2018).

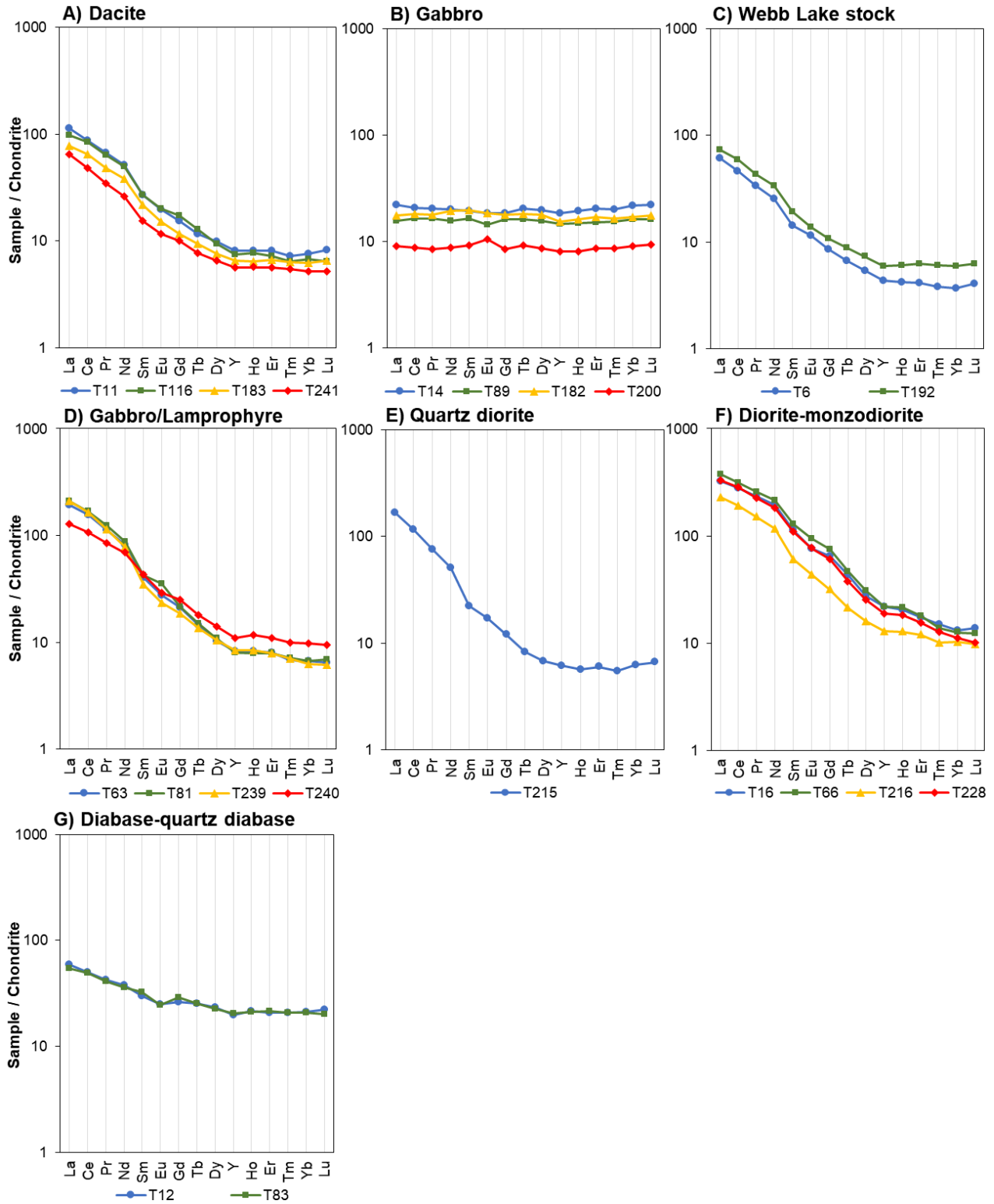


**Figure 40A–G.** Representative least-altered intrusive and volcanic samples of various lithologies at the Island Gold deposit plotted on CI carbonaceous chondrite-normalized rare earth element diagrams with yttrium. The y-axis uses a  $\log_{10}$  scale. Chondrite chemistry is from McDonough and Sun (1995).

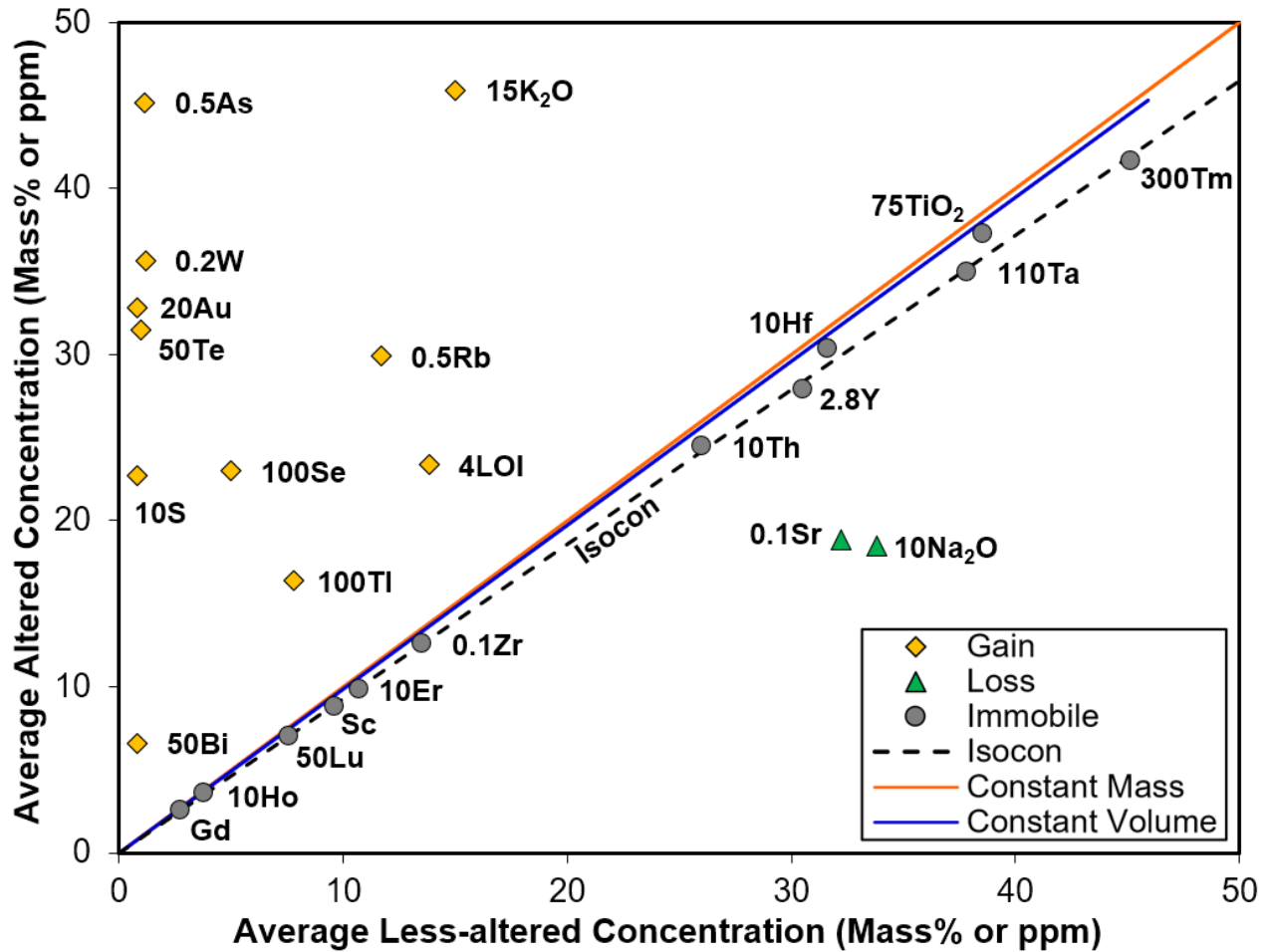


**Figure 41.** Isocon diagram displaying the average chemistry of five altered dacitic samples (T58, T72, T157, T162, T188) from five ore zones dispersed throughout the deposit plotted against the average chemistry of five corresponding less-altered dacitic samples (T59, T65, T154, T164, T184). These ore zones and associated alteration envelopes are associated with  $V_1$ - $V_2$  auriferous veins. In addition to chemical species determined to be relatively immobile for this average altered/average less-altered pair, only chemical species that are consistently enriched or depleted, based on the study of multiple altered/less-altered pairs, are displayed. Concentrations of elements are arbitrarily scaled to avoid stacking/overlap. This is achieved by multiplying both the concentration of the chemical species in the altered sample and the concentration of the chemical species in the less-altered sample by the scale factor/multiplier shown beside each chemical species. LOI=Loss on ignition,  $Fe_2O_3T$ =Total Iron. The methods used to construct these diagrams are detailed in Section 3.2.2.

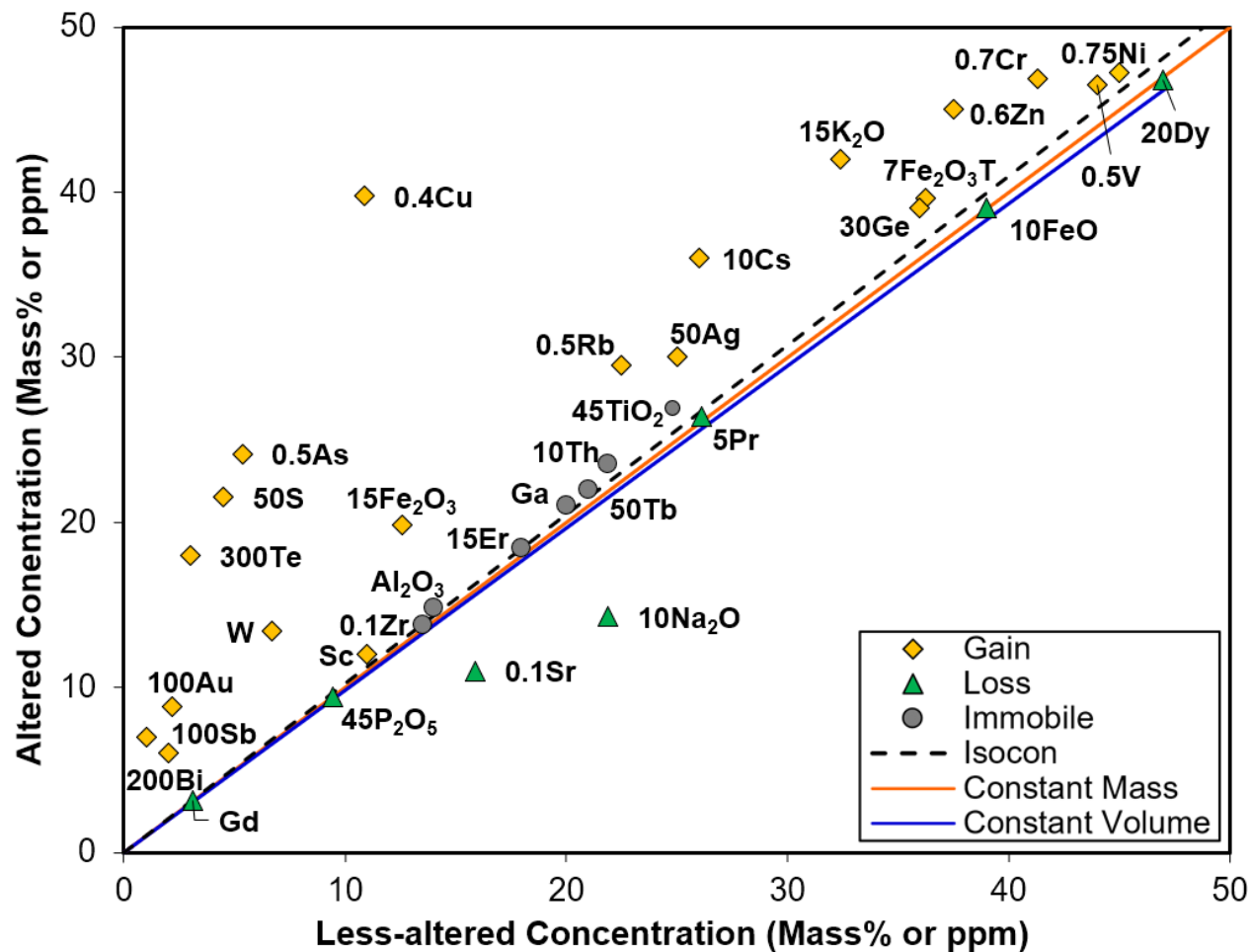


**Figure 42.** Isocon diagram displaying an altered dacitic sample (T115) plotted against a less-altered dacitic sample (T114) from same alteration envelope. This alteration envelope is from the Goudreau Zone and is associated with a  $V_{GD}$  auriferous vein. In addition to chemical species determined to be relatively immobile for this altered/less-altered pair, only chemical species that are consistently enriched or depleted, based on the study of multiple altered/less-altered pairs, are displayed. Concentrations of elements are arbitrarily scaled to avoid stacking/overlap. This is achieved by multiplying both the concentration of the chemical species in the altered sample and the concentration of the chemical species in the less-altered sample by the scale factor/multiplier shown beside each chemical species. LOI=Loss on ignition,  $Fe_2O_3T$ =Total Iron. The methods used to construct these diagrams are detailed in Section 3.2.2.

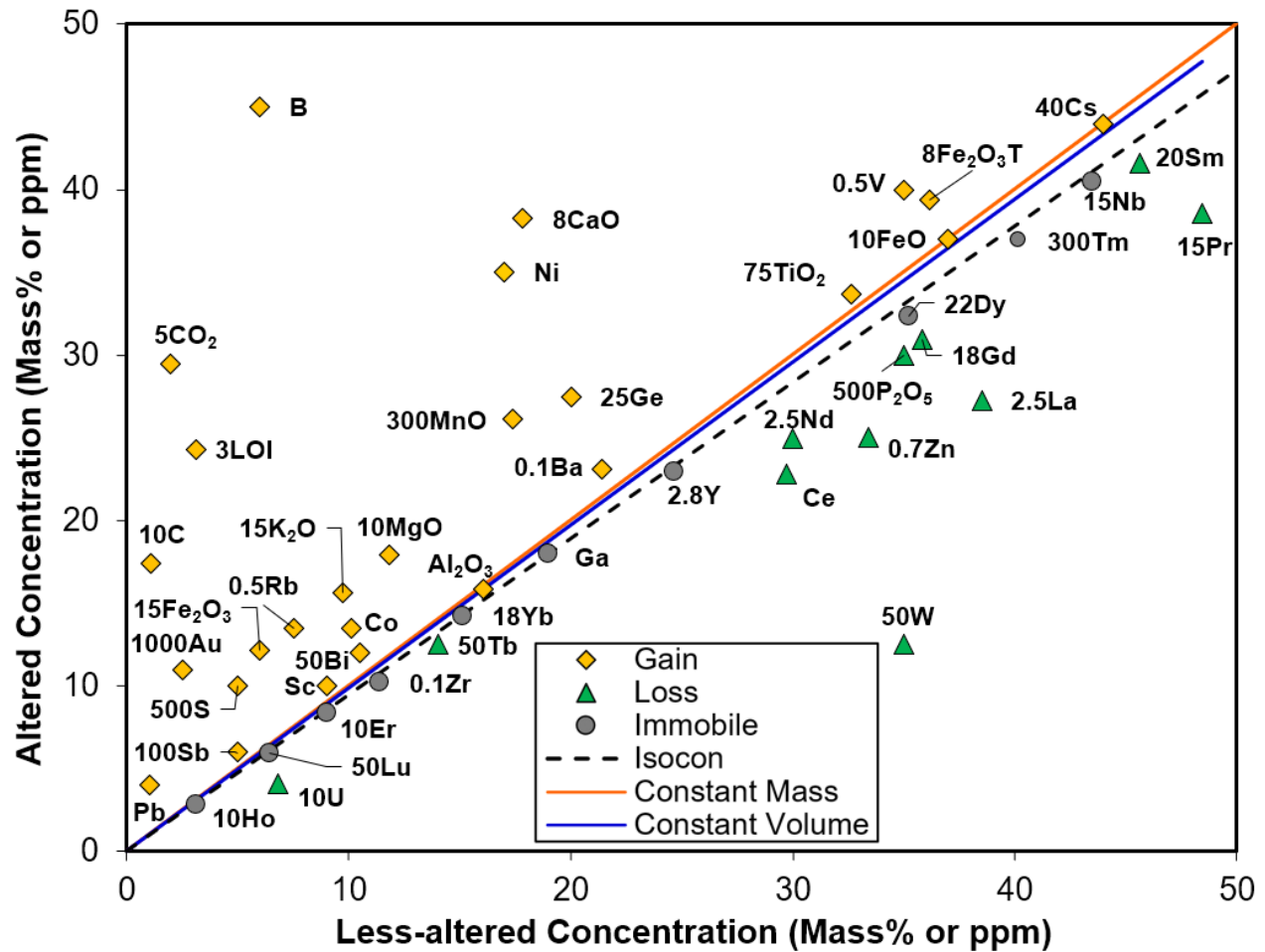


**Figure 43.** Isocon diagram displaying an altered dacitic sample (T218) plotted against a representative least-altered dacitic sample (T241). This carbonate-sercite alteration zone is not associated with quartz veining or appreciable gold mineralization but has a superficial resemblance to the alteration associated with gold-bearing quartz veins. In addition to chemical species determined to be relatively immobile for this altered/least-altered pair, only chemical species that are consistently enriched or depleted, based on the study of multiple altered/least-altered pairs, are displayed. Concentrations of elements are arbitrarily scaled to avoid stacking/overlap. This is achieved by multiplying both the concentration of the chemical species in the altered sample and the concentration of the chemical species in the less-altered sample by the scale factor/multiplier shown beside each chemical species. LOI=Loss on ignition, Fe<sub>2</sub>O<sub>3</sub>T=Total Iron. The methods used to construct these diagrams are detailed in Section 3.2.2.



**Table 4.** Summary of chemical enrichments and depletions associated with different lithologies, alteration envelopes, and vein types located throughout the Island Gold deposit. Elements and oxides that are consistently enriched or depleted based on the examination of multiple altered/less-altered pairs (Isocon analysis; Appendix S) are displayed. The number of altered/less-altered pairs that these gains and losses were determined from are indicated in the right-most column. Gains and losses in rows labelled “All” correspond with consistent gains and losses associated with the indicated vein type(s) throughout the deposit. Gains and losses in rows labelled “Most” correspond with consistent gains and losses associated with the indicated vein type(s) throughout the deposit with the exception of one or two altered/less-altered pairs where the indicated gains/losses are not observed. If a lithology is not listed, all altered/less-altered pairs associated with the indicated vein type(s) are considered. Descriptive terms for the approximate location within the deposit where dacitic altered/less-altered pairs affected by auriferous quartz veining were taken from are included. The locations of each of the alteration envelopes described using these terms are shown in Figure 19. LOI=Loss on ignition, Fe<sub>2</sub>O<sub>3</sub>T=Total Iron. Methods are discussed in Sections 3.2.2, 3.2.4, and 4.2.

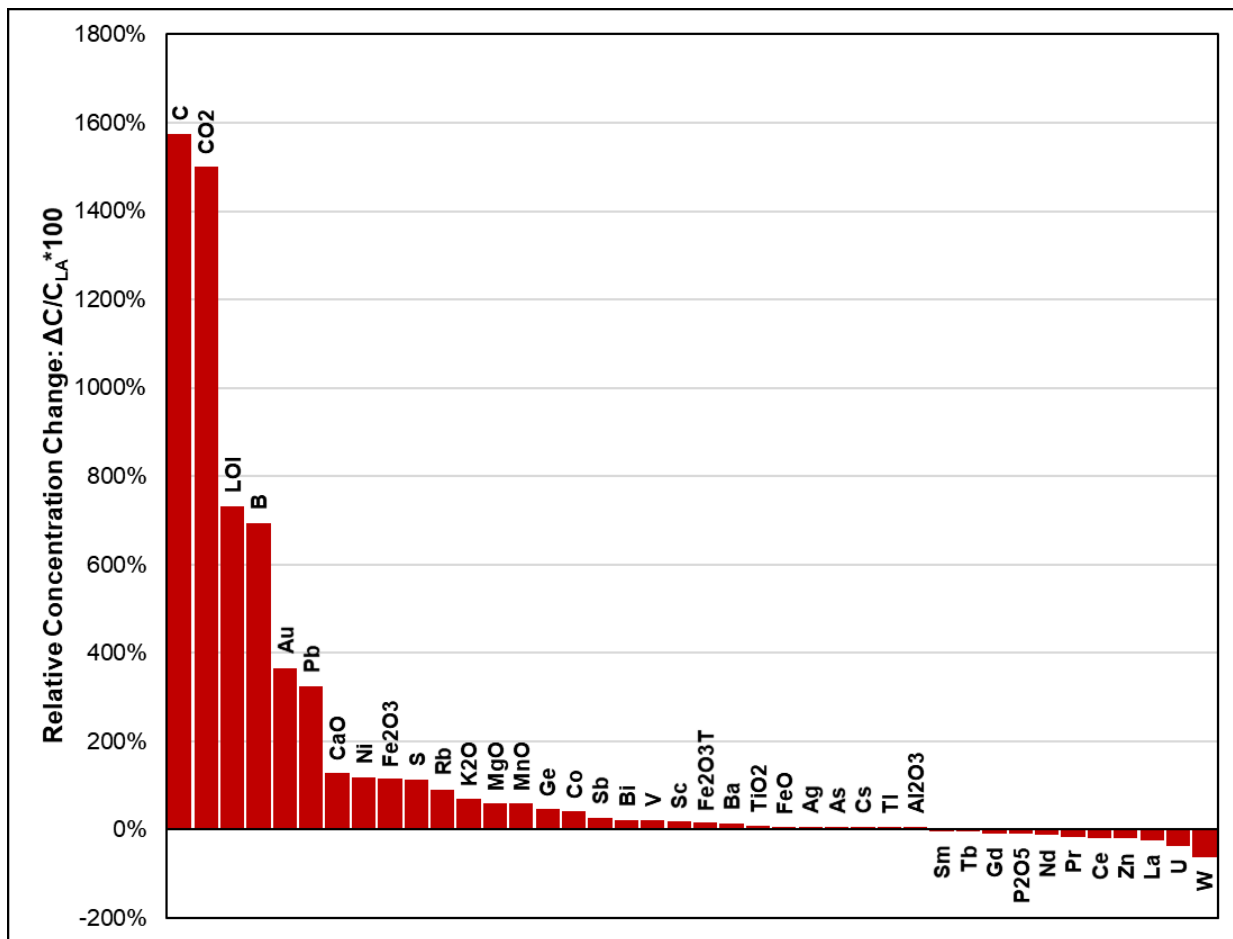
	Enrichments / Gains	Depletions / Losses	Number of Altered/ Less-Altered Pairs
Dacite, East (V <sub>1</sub> -V <sub>2</sub> veins)	As, Au, Bi, Co, Fe <sub>2</sub> O <sub>3</sub> , Fe <sub>2</sub> O <sub>3</sub> T, K <sub>2</sub> O, LOI, Mo, Ni, Pb, Rb, S, Se, Te, Tl	P <sub>2</sub> O <sub>5</sub> , SiO <sub>2</sub> , Sr, U	3
Dacite, West (V <sub>1</sub> -V <sub>2</sub> veins)	Al <sub>2</sub> O <sub>3</sub> , As, Au, Bi, Co, Ge, K <sub>2</sub> O, LOI, Rb, S, Sc, Ta, Te, V, W	Mo, Na <sub>2</sub> O, P <sub>2</sub> O <sub>5</sub> , Sr	3
Dacite, Shallow (V <sub>1</sub> -V <sub>2</sub> veins)	Ag, As, Au, B, C, CaO, CO <sub>2</sub> , Cr, Cs, Fe <sub>2</sub> O <sub>3</sub> T, Ga, K <sub>2</sub> O, La, LOI, MnO, Nd, Ni, P <sub>2</sub> O <sub>5</sub> , Rb, S, Sb, Se, SiO <sub>2</sub> , Sm, Te, Tl, U, W	Cu, Li, Na <sub>2</sub> O, Sr	3
Dacite, Deep (V <sub>1</sub> -V <sub>2</sub> veins)	Ag, As, Au, Ba, C, CO <sub>2</sub> , Cu, Ge, Hf, K <sub>2</sub> O, La, LOI, Mo, Pb, Rb, S, Sb, SiO <sub>2</sub> , Te, Tl, U, W, Zn	B, Co, Fe <sub>2</sub> O <sub>3</sub> T, FeO, MgO, MnO, Na <sub>2</sub> O, Ni, Sc, TiO <sub>2</sub> , Tm, V	2
Dacite, Centre (V <sub>1</sub> -V <sub>2</sub> veins)	As, Au, B, Ba, Bi, Cr, Cs, Ge, K <sub>2</sub> O, Li, Lu, Mo, Rb, S, Sc, SiO <sub>2</sub> , Te, TiO <sub>2</sub> , Tl, V, W, Yb	C, CaO, CO <sub>2</sub> , Eu, Na <sub>2</sub> O, Ni, Sr	2
All Dacites (V <sub>1</sub> -V <sub>2</sub> veins)	As, Au, K <sub>2</sub> O, Rb, S, Se, Te		13
Most Dacites (V <sub>1</sub> -V <sub>2</sub> veins)	As, Au, Bi, K <sub>2</sub> O, LOI, Rb, S, Se, Te, Tl, W	Na <sub>2</sub> O, Sr	13
Dacite, Goudreau Zone (V <sub>GD</sub> vein)	Ag, As, Au, Bi, Cr, Cs, Cu, Fe <sub>2</sub> O <sub>3</sub> , Fe <sub>2</sub> O <sub>3</sub> T, Ge, K <sub>2</sub> O, Mo, Ni, Rb, S, Sb, Sc, Te, V, W, Zn	Dy, FeO, Gd, Na <sub>2</sub> O, P <sub>2</sub> O <sub>5</sub> , Pr, Sr	3
All Dacites (V <sub>1</sub> -V <sub>2</sub> and V <sub>GD</sub> veins)	As, Au, K <sub>2</sub> O, Rb, S, Se, Te		16
Most Dacites (V <sub>1</sub> -V <sub>2</sub> and V <sub>GD</sub> veins)	As, Au, Bi, K <sub>2</sub> O, Rb, S, Se, Te, Tl, W	Na <sub>2</sub> O, Sr	16
Dacite, (Non-auriferous Sericitization/Carbonation)	Al <sub>2</sub> O <sub>3</sub> , Au, B, Ba, Bi, C, CaO, Co, CO <sub>2</sub> , Cs, Fe <sub>2</sub> O <sub>3</sub> , Fe <sub>2</sub> O <sub>3</sub> T, FeO, Ge, K <sub>2</sub> O, LOI, MgO, MnO, Ni, Pb, Rb, S, Sb, Sc, TiO <sub>2</sub> , V	Ag, As, Ce, Gd, La, Nd, P <sub>2</sub> O <sub>5</sub> , Pr, Sm, Tb, Tl, U, W, Zn	2
Gabbro (V <sub>1</sub> -V <sub>2</sub> Veins)	Au, B, Ba, Cs, K <sub>2</sub> O, Li, MnO, Pb, Rb, S, Sm, Sr, Te	Bi, Ge, Na <sub>2</sub> O, P <sub>2</sub> O <sub>5</sub> , Sb, Tl	3
Webb Lake Stock (V <sub>1</sub> -V <sub>2</sub> Veins)	Ag, As, Au, B, Bi, C, CO <sub>2</sub> , Cu, Fe <sub>2</sub> O <sub>3</sub> , Ge, K <sub>2</sub> O, LOI, Mo, Rb, S, Se, Ta, Te, U, W	CaO, Co, Fe <sub>2</sub> O <sub>3</sub> T, FeO, MnO, Na <sub>2</sub> O, Sc, SiO <sub>2</sub> , Sm	3
Gabbro/Lamprophyre (V <sub>3</sub> Veins)	As, Au, B, Ba, Bi, Ce, Cr, Cs, Ga, Ge, K <sub>2</sub> O, La, Li, Mo, Rb, Sb, Sr, V, W, Zn	Ag, C, CaO, Co, CO <sub>2</sub> , Dy, Er, LOI, Lu, MgO, MnO, Na <sub>2</sub> O, Ni, Pb, Se, SiO <sub>2</sub> , Tb, Tm, Y, Yb	2
Diorite-Monzodiorite (V <sub>3</sub> Veins)	As, Au, CaO, FeO, Hf, Li, S, Sc, Te, W	B, Ba, C, CO <sub>2</sub> , Cr, Cs, Cu, Fe <sub>2</sub> O <sub>3</sub> , Ga, K <sub>2</sub> O, LOI, Mo, Na <sub>2</sub> O, Ni, Pb, Rb, Sb, Se, Sr, U	2
All (V <sub>1</sub> -V <sub>2</sub> veins)	Au, K <sub>2</sub> O, Rb, S, Te		22
Most (V <sub>1</sub> -V <sub>2</sub> veins)	As, Au, K <sub>2</sub> O, Rb, S, Se, Te, W	Na <sub>2</sub> O	22
All (V <sub>1</sub> -V <sub>2</sub> and V <sub>GD</sub> veins)	Au, K <sub>2</sub> O, Rb, S, Te		19
Most (V <sub>1</sub> -V <sub>2</sub> and V <sub>GD</sub> veins)	As, Au, K <sub>2</sub> O, Rb, S, Se, Te, W	Na <sub>2</sub> O	19

**Table 5.** Results of mass balance calculations based on the chemistry of dacitic samples variably altered by  $V_1$ - $V_2$  veining. Average concentrations of chemical species (C) for samples classified under each alteration strength grouping as well as the calculated concentration changes ( $\Delta C$ ) of chemical species are displayed. Concentration changes of chemical species relative to their average concentration in the least-altered samples are displayed ( $\Delta C/C_{LA}$ ). All altered samples are altered by  $V_1$ - $V_2$  veins. Calculations were performed using an equation from Grant (1986) with modified variables:  $\Delta C/C_{LA} = (\text{slope of Isocon}) * (C_A/C_{LA}) - 1$ . C=Concentration,  $C_A$ =Concentration in altered sample,  $C_{LA}$ =Concentration in least-altered sample. LOI=Loss on Ignition,  $Fe_2O_3T$ =Total Iron. The following samples were used for each alteration strength grouping: Strongly-altered (T58, T72, T86, T157, T162, T188), moderately-altered (T17, T20, T73, T85, T88, T156, T186), weakly-altered (T13, T59, T117, T118, T184), least-altered (T8, T11, T65, T116, T154, T164, T183, T241).

	Strongly-altered			Moderately-altered			Weakly-altered			Least-altered
	C	$\Delta C$	$\Delta C/C_{LA}$	C	$\Delta C$	$\Delta C/C_{LA}$	C	$\Delta C$	$\Delta C/C_{LA}$	C
Au (ppm)	1.644	1.805	28592%	0.547	0.610	9659%	0.047	0.042	660%	0.006
S (wt%)	2.24	2.45	18678%	0.98	1.09	8275%	0.16	0.16	1187%	0.01
W (ppm)	183.9	200.6	9523%	7.7	6.5	310%	5.6	3.7	175%	2.1
As (ppm)	92.3	100.7	9474%	28.7	31.2	2940%	3.0	2.1	195%	1.1
Te (ppm)	0.55	0.59	3607%	0.08	0.07	445%	0.02	0.01	52%	0.02
Se (ppm)	0.2	0.2	341%	0.2	0.1	238%	0.1	0.0	3%	0.1
Bi (ppm)	0.14	0.12	283%	0.12	0.10	236%	0.03	-0.01	-15%	0.04
K <sub>2</sub> O (wt%)	3.08	2.47	266%	1.61	0.89	96%	1.09	0.19	21%	0.93
B (ppm)	45	35	252%	54	47	336%	15	2	11%	14
Rb (ppm)	62	45	193%	35	16	68%	24	2	8%	23
Fe <sub>2</sub> O <sub>3</sub> (wt%)	1.52	0.98	142%	2.22	1.81	262%	0.65	-0.02	-3%	0.69
Cs (ppm)	2.6	1.5	115%	1.7	0.6	45%	1.4	0.1	6%	1.3
Mo (ppm)	1.7	1.0	110%	0.9	0.2	20%	0.9	0.1	6%	0.9
LOI (wt%)	5.46	2.87	91%	4.91	2.39	76%	2.80	-0.26	-8%	3.15
Pb (ppm)	5	2	75%	6	4	108%	4	1	39%	3
Tl (ppm)	0.14	0.07	72%	0.08	0.00	-3%	0.06	-0.03	-37%	0.09
C (wt%)	0.69	0.32	72%	0.96	0.64	145%	0.48	0.05	11%	0.44
CO <sub>2</sub> (%)	2.40	1.10	71%	3.28	2.15	139%	1.65	0.15	10%	1.55
Cu (ppm)	45.7	16.5	49%	37.8	8.7	26%	38.6	5.9	17%	33.9
Ge (ppm)	1.4	0.5	43%	1.1	0.2	15%	1.0	0.0	-2%	1.1
Ba (ppm)	298	90	38%	209	-3	-1%	219	-13	-6%	239
Ag (ppm)	0.65	0.18	35%	0.46	-0.01	-2%	0.48	-0.04	-7%	0.53
Co (ppm)	15.2	3.0	22%	14.7	2.9	21%	11.8	-1.5	-11%	13.7
Ga (ppm)	21	4	18%	19	3	13%	20	1	5%	19
Al <sub>2</sub> O <sub>3</sub> (wt%)	15.8	2.0	13%	14.3	0.8	5%	15.4	0.5	3%	15.4
SiO <sub>2</sub> (wt%)	63.63	5.78	9%	62.19	5.72	9%	64.63	2.22	3%	64.34
U (ppm)	0.61	0.02	4%	0.63	0.06	10%	0.61	-0.01	-2%	0.65
Dy (ppm)	1.97	0.07	4%	1.84	-0.02	-1%	2.05	0.02	1%	2.09
Zr (ppm)	124	4	3%	120	2	2%	133	5	3%	132
TiO <sub>2</sub> (wt%)	0.497	0.015	3%	0.462	-0.011	-2%	0.517	0.001	0%	0.532
V (ppm)	77	2	3%	75	1	2%	83	3	4%	83
Tb (ppm)	0.36	0.01	3%	0.34	-0.01	-2%	0.38	0.01	2%	0.39
Hf (ppm)	3.0	0.1	2%	2.9	0.0	-1%	3.0	-0.1	-4%	3.3
Ho (ppm)	0.36	0.00	1%	0.36	0.01	3%	0.38	-0.01	-1%	0.39
Cr (ppm)	41	0	0%	33	-8	-18%	41	-2	-5%	45
Gd (ppm)	2.53	0.01	0%	2.41	-0.06	-2%	2.77	0.08	3%	2.78
Sm (ppm)	3.24	0.01	0%	3.02	-0.16	-5%	3.48	0.02	1%	3.56
Eu (ppm)	0.91	0.00	0%	0.86	-0.04	-4%	1.00	0.02	2%	1.01
Th (ppm)	2.55	-0.02	-1%	2.47	-0.05	-2%	2.70	-0.05	-2%	2.83
Ta (ppm)	0.32	0.00	-1%	0.31	-0.01	-2%	0.33	-0.02	-4%	0.36
Y (ppm)	9.9	-0.2	-2%	9.8	0.0	0%	10.9	0.1	1%	11.1
La (ppm)	19.15	-0.35	-2%	18.21	-0.93	-4%	21.16	0.34	2%	21.45
Sc (ppm)	9	0	-2%	9	0	-1%	9	0	-4%	10
Tm (ppm)	0.141	-0.004	-2%	0.146	0.006	4%	0.153	-0.001	-1%	0.159
Nd (ppm)	17.6	-0.5	-3%	16.3	-1.5	-8%	19.6	0.3	2%	19.9
Ce (ppm)	39.8	-1.2	-3%	38.1	-2.2	-5%	45.0	1.3	3%	45.0
Er (ppm)	0.99	-0.03	-3%	1.00	0.01	1%	1.07	-0.01	-1%	1.12
Pr (ppm)	4.55	-0.18	-3%	4.29	-0.35	-7%	5.17	0.14	3%	5.19
Fe <sub>2</sub> O <sub>3</sub> T (wt%)	4.54	-0.33	-6%	6.44	1.92	36%	4.69	-0.50	-9%	5.33
Yb (ppm)	0.91	-0.07	-6%	0.96	0.02	2%	0.99	-0.04	-4%	1.07
Lu (ppm)	0.139	-0.012	-7%	0.148	0.001	1%	0.154	-0.007	-4%	0.166
P <sub>2</sub> O <sub>5</sub> (wt%)	0.14	-0.01	-8%	0.13	-0.02	-10%	0.18	0.02	12%	0.17
Nb (ppm)	3.1	-0.5	-13%	3.4	-0.1	-4%	3.8	-0.1	-1%	3.9
Ni (ppm)	30	-6	-15%	26	-10	-25%	30	-8	-20%	38
CaO (wt%)	3.22	-0.75	-17%	4.80	1.11	26%	4.90	0.74	17%	4.30
Sb (ppm)	0.07	-0.02	-22%	0.05	-0.04	-40%	0.15	0.06	67%	0.09
Li (ppm)	25	-8	-23%	26	-7	-20%	29	-7	-18%	36
Sr (ppm)	197	-85	-28%	244	-26	-9%	259	-35	-12%	302
FeO (wt%)	2.7	-1.2	-28%	3.8	0.1	3%	3.6	-0.4	-10%	4.2
MnO (wt%)	0.07	-0.04	-34%	0.11	0.02	14%	0.07	-0.04	-38%	0.11
Na <sub>2</sub> O (wt%)	1.97	-1.51	-41%	3.09	-0.19	-5%	3.64	0.08	2%	3.67
MgO (wt%)	0.88	-1.03	-52%	1.48	-0.33	-17%	1.67	-0.28	-14%	2.00
Zn (ppm)	44.9	-93.1	-65%	82.8	-49.3	-35%	62.9	-77.8	-55%	142.6

**Table 6.** Results of mass balance calculations based on the chemistry of dacitic samples variably altered by  $V_{GD}$  veining. Average concentrations of chemical species (C) for samples classified under each alteration strength grouping as well as the calculated concentration changes ( $\Delta C$ ) of chemical species are displayed. Concentration changes of chemical species relative to their average concentration in the least-altered samples are displayed ( $\Delta C/C_{LA}$ ). All altered samples are altered by  $V_{GD}$  veins. Calculations were performed using an equation from Grant (1986) with modified variables:  $\Delta C/C_{LA} = (\text{slope of Isocon}) * (C_A/C_{LA}) - 1$ . C=Concentration,  $C_A$ =Concentration in altered sample,  $C_{LA}$ =Concentration in least-altered sample. LOI=Loss on Ignition.  $Fe_2O_3T$ =Total Iron. The following samples were used for each alteration strength grouping: Strongly-altered (T105, T113), moderately-altered (T114), weakly-altered (T115), least-altered (T8, T11, T65, T116, T154, T164, T183, T241).

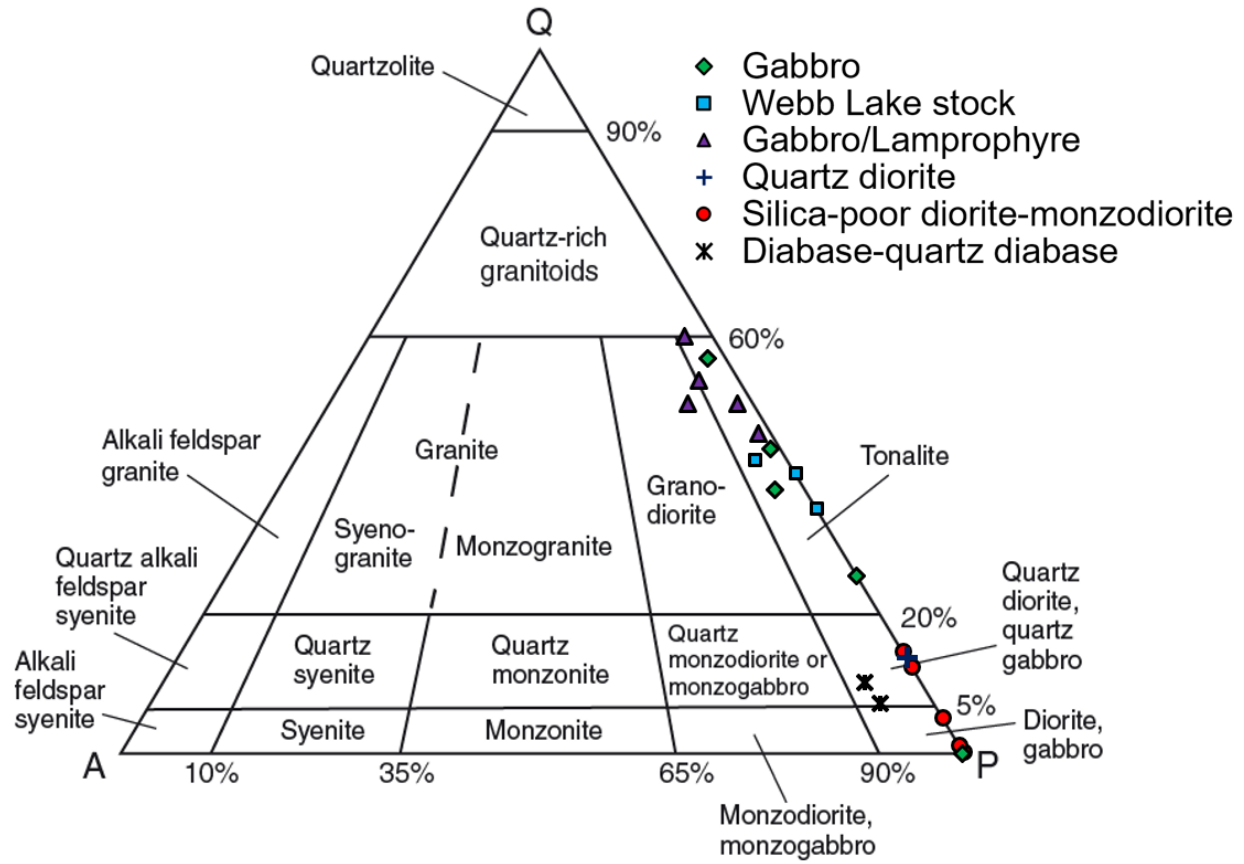
	Strongly-altered			Moderately-altered			Weakly-altered			Least-altered
	C	$\Delta C$	$\Delta C/C_{LA}$	C	$\Delta C$	$\Delta C/C_{LA}$	C	$\Delta C$	$\Delta C/C_{LA}$	C
Au (ppm)	2.545	2.722	43117%	0.088	0.084	1325%	0.022	0.018	277%	0.006
As (ppm)	194.5	207.4	19523%	48.3	48.3	4545%	10.7	10.5	990%	1.1
S (wt%)	1.68	1.78	13580%	0.43	0.43	3248%	0.09	0.08	642%	0.01
Te (ppm)	0.23	0.23	1417%	0.06	0.05	277%	0.01	-0.01	-33%	0.02
Bi (ppm)	0.26	0.24	576%	0.03	-0.01	-26%	0.01	-0.03	-74%	0.04
W (ppm)	12.8	11.6	551%	13.4	11.6	550%	6.7	5.1	244%	2.1
K <sub>2</sub> O (wt%)	2.51	1.76	189%	2.80	1.93	208%	2.16	1.41	152%	0.93
B (ppm)	34	22	158%	19	5	35%	21	9	65%	14
Fe <sub>2</sub> O <sub>3</sub> (wt%)	1.64	1.06	154%	1.32	0.66	95%	0.84	0.22	32%	0.69
Rb (ppm)	51	31	134%	59	37	161%	45	26	111%	23
CO <sub>2</sub> (wt%)	3.29	1.98	128%	2.91	1.43	92%	3.60	2.35	152%	1.55
C (wt%)	0.94	0.56	127%	0.83	0.40	91%	1.07	0.71	161%	0.44
Cs (ppm)	2.8	1.6	122%	3.6	2.4	178%	2.6	1.5	112%	1.3
Cu (ppm)	66.0	36.8	109%	99.4	67.7	200%	27.2	-4.5	-13%	33.9
Cr (ppm)	83	43	97%	67	23	52%	59	19	42%	45
LOI (wt%)	5.49	2.73	87%	5.53	2.51	80%	6.01	3.36	107%	3.15
Mo (ppm)	1.5	0.7	84%	0.5	-0.4	-42%	0.5	-0.3	-38%	0.9
Ni (ppm)	64	30	77%	63	26	68%	60	27	69%	38
Ge (ppm)	1.6	0.7	63%	1.3	0.3	27%	1.2	0.2	24%	1.1
MgO (wt%)	2.73	0.93	47%	3.21	1.28	64%	2.84	1.08	54%	2.00
Co (ppm)	17.5	5.0	37%	14.9	1.6	11%	17.8	5.6	41%	13.7
Ag (ppm)	0.65	0.17	31%	0.60	0.08	15%	0.50	0.01	2%	0.53
Ba (ppm)	281	62	26%	377	146	61%	338	127	53%	239
P <sub>2</sub> O <sub>5</sub> (wt%)	0.20	0.04	25%	0.21	0.05	28%	0.21	0.06	36%	0.17
CaO (wt%)	4.87	0.91	21%	4.45	0.24	6%	5.50	1.65	38%	4.30
Nb (ppm)	4.4	0.7	19%	4.9	1.1	28%	4.2	0.6	16%	3.9
Tm (ppm)	0.173	0.026	16%	0.171	0.016	10%	0.185	0.042	26%	0.159
Sc (ppm)	11	2	16%	12	2	21%	11	2	18%	10
Li (ppm)	39	6	16%	35	0	-1%	30	-4	-10%	36
Fe <sub>2</sub> O <sub>3</sub> T (wt%)	5.75	0.83	16%	5.66	0.45	8%	5.18	0.27	5%	5.33
Pb (ppm)	4	1	15%	1	-2	-69%	4	1	33%	3
TiO <sub>2</sub> (wt%)	0.568	0.077	14%	0.597	0.078	15%	0.553	0.067	13%	0.532
Er (ppm)	1.19	0.15	14%	1.23	0.14	12%	1.20	0.18	16%	1.12
V (ppm)	88	11	13%	93	12	15%	88	13	15%	83
Ho (ppm)	0.41	0.05	12%	0.42	0.04	9%	0.43	0.07	19%	0.39
Dy (ppm)	2.15	0.21	10%	2.34	0.30	14%	2.35	0.45	22%	2.09
Gd (ppm)	2.82	0.24	9%	3.15	0.44	16%	3.12	0.60	22%	2.78
Y (ppm)	11.3	1.0	9%	12.1	1.3	11%	12.9	2.9	26%	11.1
Se (ppm)	0.1	0.0	7%	0.1	0.0	2%	0.1	0.0	8%	0.1
Yb (ppm)	1.06	0.07	7%	1.07	0.03	3%	1.13	0.16	15%	1.07
Tb (ppm)	0.38	0.02	6%	0.44	0.06	17%	0.42	0.07	18%	0.39
Ta (ppm)	0.35	0.02	6%	0.41	0.06	18%	0.37	0.05	13%	0.36
Zr (ppm)	131	8	6%	138	9	7%	135	14	10%	132
Ga (ppm)	19	0	2%	21	2	11%	20	2	12%	19
SiO <sub>2</sub> (wt%)	61.13	1.19	2%	61.57	-1.42	-2%	60.27	0.91	1%	64.34
Lu (ppm)	0.156	0.001	1%	0.155	-0.007	-4%	0.162	0.010	6%	0.166
Al <sub>2</sub> O <sub>3</sub> (wt%)	14.3	0.0	0%	14.9	-0.2	-1%	14.0	-0.2	-1%	15.4
Sm (ppm)	3.26	-0.07	-2%	3.74	0.26	7%	3.56	0.29	8%	3.56
Eu (ppm)	0.91	-0.03	-3%	1.09	0.11	11%	1.04	0.12	12%	1.01
Nd (ppm)	17.8	-0.8	-4%	20.9	1.5	8%	19.4	1.2	6%	19.9
Pr (ppm)	4.61	-0.25	-5%	5.28	0.21	4%	5.23	0.48	9%	5.19
FeO (wt%)	3.7	-0.2	-5%	3.9	-0.2	-5%	3.9	0.0	1%	4.2
Ce (ppm)	39.7	-2.5	-6%	45.5	1.5	3%	43.7	2.3	5%	45.0
Hf (ppm)	2.8	-0.2	-8%	2.9	-0.3	-9%	2.9	-0.1	-3%	3.3
Sb (ppm)	0.08	-0.01	-9%	0.07	-0.02	-24%	0.01	-0.08	-88%	0.09
U (ppm)	0.55	-0.06	-9%	0.61	-0.02	-3%	0.57	-0.03	-4%	0.65
La (ppm)	18.05	-2.10	-10%	20.30	-0.71	-3%	19.80	-0.01	0%	21.45
Th (ppm)	2.24	-0.43	-15%	2.35	-0.43	-15%	2.19	-0.46	-16%	2.83
MnO (wt%)	0.09	-0.02	-19%	0.09	-0.02	-21%	0.10	-0.01	-7%	0.11
Na <sub>2</sub> O (wt%)	1.97	-1.57	-43%	1.43	-2.21	-60%	2.19	-1.30	-35%	3.67
Zn (ppm)	74.5	-62.8	-44%	75.0	-66.0	-46%	62.5	-75.0	-53%	142.6
Sr (ppm)	142	-150	-50%	110	-189	-63%	159	-130	-43%	302
Ti (ppm)	0.03	-0.06	-70%	0.03	-0.06	-72%	0.03	-0.06	-70%	0.09



**Figure 44.** Relative concentration changes of chemical species between an altered dacitic sample (T218) within a non-economic, carbonate-sericite alteration zone and a representative least-altered dacitic sample (T241). Chemical gains/losses are expressed as a percentage relative to the least-altered sample. Only chemical species that are consistently enriched or depleted, based on the study of multiple altered/least-altered pairs, are displayed. Calculations were performed using the following equation from Grant (1986) with modified variables:  $\Delta C/C_{LA} = (\text{slope of isocon}) * (C_A/C_{LA}) - 1$ . The slope of the Isocon in Figure 43 was used. C=Concentration,  $C_A$ =Concentration in altered sample,  $C_{LA}$ =Concentration in least-altered sample. LOI=Loss on Ignition,  $Fe_2O_3T$ =Total Iron.

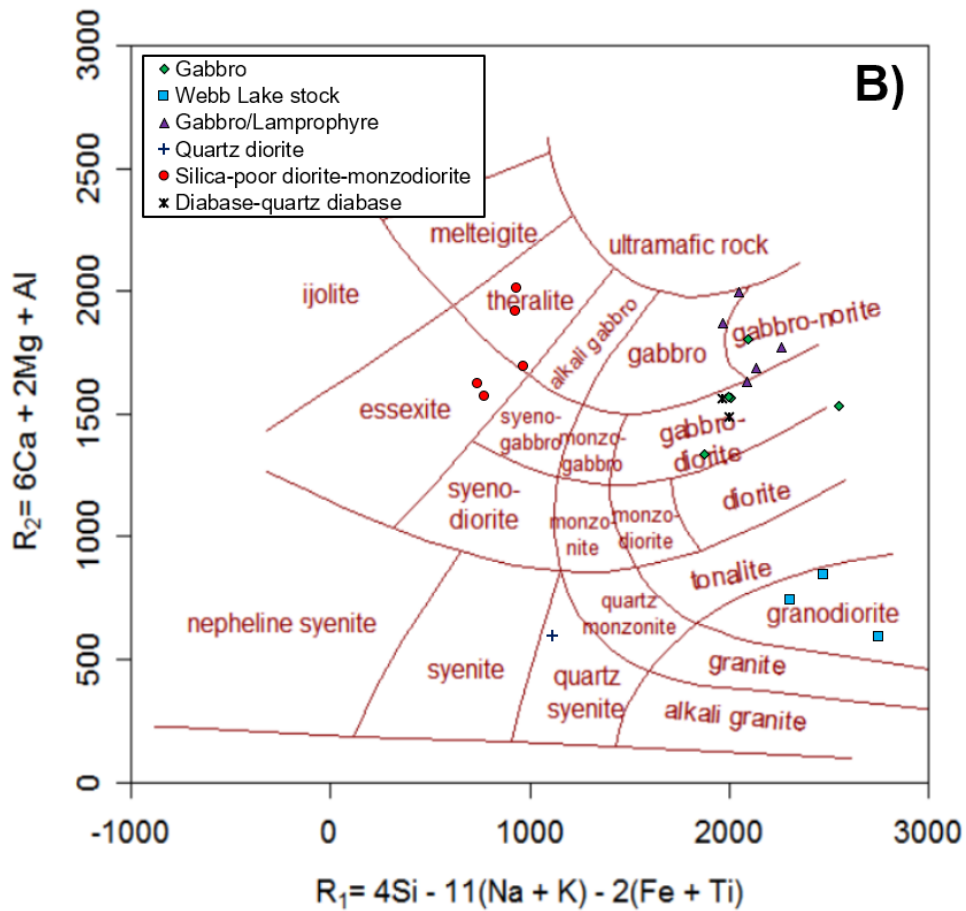
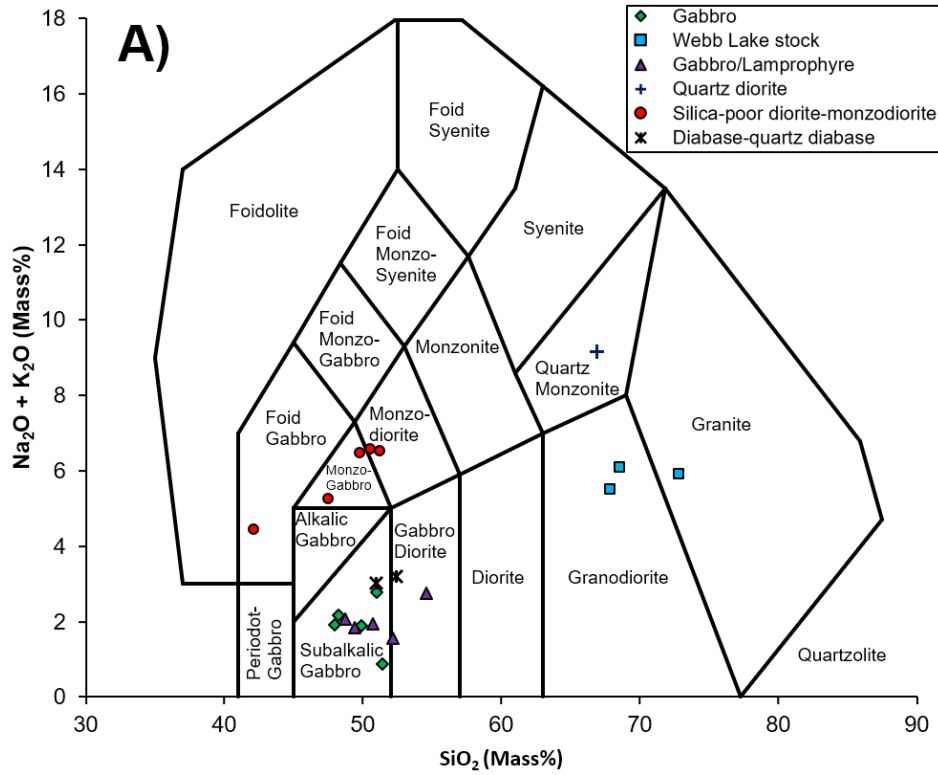
**Table 7.** Concentrations of chemical species in an altered dacitic sample (T218) within a non-economic carbonate-sericite alteration zone and a least-altered dacitic sample (T241). Concentration changes of chemical species between the least-altered and altered samples are also displayed. Relative concentration changes are expressed as a percentage relative to the least-altered sample. Only chemical species that are consistently enriched or depleted, based on the study of multiple altered/least-altered pairs, are displayed. Calculations were performed using the following equation from Grant (1986) with modified variables:  $\Delta C/C_{LA} = (\text{slope of isocon}) * (C_A/C_{LA}) - 1$ . The slope of the Isocon in Figure 43 was used. C=Concentration,  $C_A$ =Concentration in altered sample,  $C_{LA}$ =Concentration in least-altered sample. LOI=Loss on Ignition,  $Fe_2O_3T$ =Total Iron.

	Units	Least-altered (T241)	Altered (T218)	Relative Concentration Change: $\Delta C/C_{LA} * 100$ (%)	Concentration Change: $\Delta C$
C	wt%	0.11	1.74	1575.3%	1.73
CO <sub>2</sub>	wt%	0.39	5.89	1499.5%	5.85
LOI	wt%	1.03	8.09	731.9%	7.54
B	ppm	6	45	694.3%	41.66
Au	ppm	0.0025	0.011	366.0%	0.01
Pb	ppm	1	4	323.6%	3.24
CaO	wt%	2.23	4.78	127.0%	2.83
Ni	ppm	17	35	118.1%	20.07
Fe <sub>2</sub> O <sub>3</sub>	wt%	0.4	0.81	114.5%	0.46
S	wt%	0.01	0.02	111.8%	0.01
Rb	ppm	15	27	90.6%	13.60
K <sub>2</sub> O	wt%	0.65	1.04	69.5%	0.45
MgO	wt%	1.18	1.79	60.7%	0.72
MnO	wt%	0.058	0.087	58.9%	0.03
Ge	ppm	0.8	1.1	45.6%	0.37
Co	ppm	10.1	13.5	41.6%	4.20
Sb	ppm	0.05	0.06	27.1%	0.01
Bi	ppm	0.21	0.24	21.0%	0.04
V	ppm	70	80	21.0%	14.73
Sc	ppm	9	10	17.7%	1.59
Fe <sub>2</sub> O <sub>3</sub> T	wt%	4.52	4.92	15.3%	0.69
Ba	ppm	214	231	14.3%	30.65
TiO <sub>2</sub>	wt%	0.435	0.449	9.3%	0.04
FeO	wt%	3.7	3.7	5.9%	0.22
Ag	ppm	0.25	0.25	5.9%	0.01
As	ppm	0.05	0.05	5.9%	0.00
Cs	ppm	1.1	1.1	5.9%	0.07
Tl	ppm	0.025	0.025	5.9%	0.00
Al <sub>2</sub> O <sub>3</sub>	wt%	16.05	15.88	4.8%	0.77
Sm	ppm	2.28	2.08	-3.4%	-0.08
Tb	ppm	0.28	0.25	-5.4%	-0.02
Gd	ppm	1.99	1.72	-8.5%	-0.17
P <sub>2</sub> O <sub>5</sub>	wt%	0.07	0.06	-9.2%	-0.01
Nd	ppm	12	9.99	-11.8%	-1.42
Pr	ppm	3.23	2.57	-15.7%	-0.51
Ce	ppm	29.7	22.8	-18.7%	-5.55
Zn	ppm	47.7	35.7	-20.7%	-9.89
La	ppm	15.4	10.9	-25.0%	-3.86
U	ppm	0.68	0.41	-36.1%	-0.25
W	ppm	0.7	0.25	-62.2%	-0.44



**Figure 45.** Least-altered and weakly-altered intrusive samples (Section 4.2) plotted on a Quartz-Alkali Feldspar-Plagioclase (QAP) ternary diagram. Modal mineralogy determined using the standard CIPW Norm calculations for gabbro, gabbro/lamprophyre, and diabase-quartz diabase. The CIPW Norm modification that includes biotite is used for all other lithologies because substantial primary biotite was observed in these samples. Calculations were conducted using GCDkit (Janoušek et al., 2006) using the methods outlined in Hutchison (1975). This diagram is modified from Streckeisen (1976a).





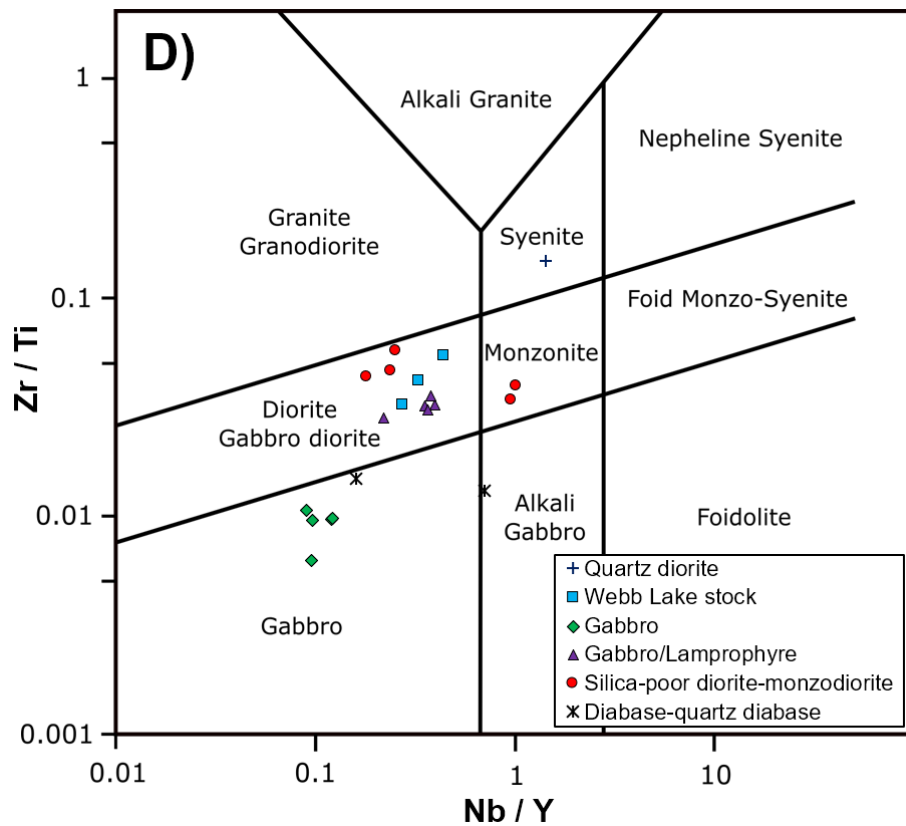
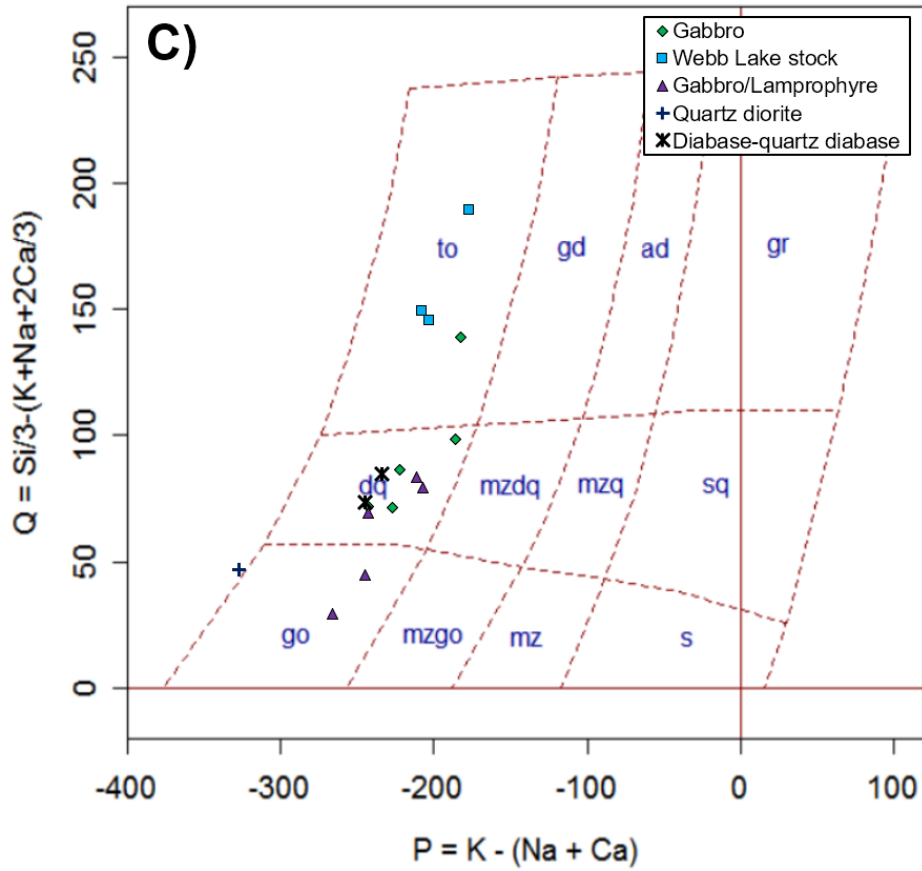


**Figure 46A–D.** *Least-altered and weakly-altered samples (Section 4.2) of the various intrusive lithologies at the Island Gold deposit plotted on classification diagrams. This caption applies to the figures on the previous two pages. A) A TAS diagram for intrusive lithologies. Modified from Middlemost (1994). B)  $R_1$ - $R_2$  multicationic plot modified from De La Roche et al. (1980) and Janoušek (2018). C) A P-Q multicationic plot modified from Debon and Le Fort (1983) and Janoušek (2018). to=Tonalite, gd=Granodiorite, ad=Adamellite, gr=Granite, dq=Quartz Diorite, mzdq=Quartz Monzodiorite, mzq=Quartz Monzonite, sq=Quartz Syenite, go=Gabbro, mzgo=Monzogabbro, mz=Monzonite, s=Syenite. D) A modified Nb/Y-Zr/Ti diagram modified from Pearce (1996) and Janoušek (2018). This diagram is originally from Winchester and Floyd (1977) and was later revised in Pearce (1996). This diagram is designed to classify extrusive igneous rocks based on ratios of relatively immobile element ratios. It has been modified for intrusive rocks by replacing extrusive rocks with their respective intrusive equivalent.*

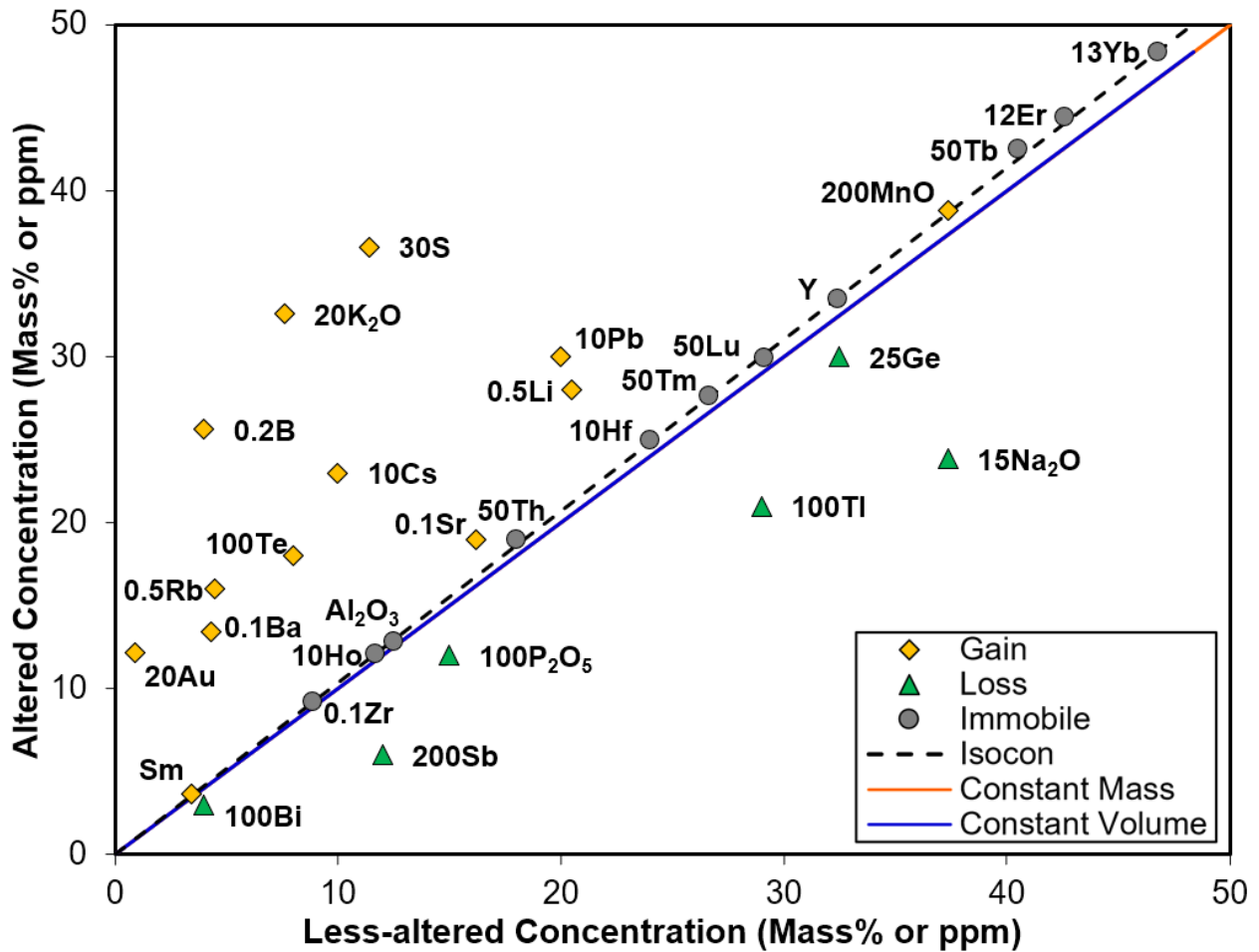


**Figure 47.** Isocon diagram displaying an altered gabbroic sample (T141) plotted against a less-altered gabbroic sample (T139) from the same alteration envelope. This alteration envelope is associated with  $V_1$ - $V_2$  auriferous quartz veining. In addition to chemical species determined to be relatively immobile for this altered/less-altered pair, only chemical species that are consistently enriched or depleted, based on the study of multiple altered/less-altered pairs, are displayed. Concentrations of elements are arbitrarily scaled to avoid stacking/overlap. This is achieved by multiplying both the concentration of the chemical species in the altered sample and the concentration of the chemical species in the less-altered sample by the scale factor/multiplier shown beside each chemical species. LOI=Loss on Ignition,  $Fe_2O_3T$ =Total Iron. The methods used to construct these diagrams are detailed in Section 3.2.2.

**Table 8.** Results of mass balance calculations based on the chemistry of samples of gabbro altered by  $V_1$ - $V_2$  veining. Average concentrations of chemical species (C) for samples classified under each alteration strength grouping as well as the calculated concentration changes ( $\Delta C$ ) of chemical species are displayed. Concentration changes of chemical species relative to their average concentration in the least-altered samples are displayed ( $\Delta C/C_{LA}$ ). Calculations were performed using the following equation from Grant (1986) with modified variables:  $\Delta C/C_{LA} = (\text{slope of Isocon}) * (C_A/C_{LA}) - 1$ . C=Concentration,  $C_A$ =Concentration in altered sample,  $C_{LA}$ =Concentration in least-altered sample. LOI=Loss on Ignition,  $Fe_2O_3T$ =Total Iron. The following samples were used for each alteration strength grouping: Strongly-altered (T142), moderately-altered (T140, T141), weakly-altered (T139), least-altered (T14, T80, T89, T182, T200).

	Strongly-altered			Moderately-altered			Weakly-altered			Least-altered
	C	$\Delta C$	$\Delta C/C_{LA}$	C	$\Delta C$	$\Delta C/C_{LA}$	C	$\Delta C$	$\Delta C/C_{LA}$	C
Au (ppm)	6.780	5.713	28566%	0.531	0.384	1918%	0.044	0.014	71%	0.020
S (wt%)	4.81	3.97	4273%	0.94	0.62	665%	0.38	0.20	218%	0.09
B (ppm)	95	78	3568%	93	69	3130%	20	13	611%	2
Bi (ppm)	0.35	0.29	2860%	0.04	0.02	166%	0.04	0.02	211%	0.01
K <sub>2</sub> O (wt%)	2.01	1.61	1788%	1.38	0.96	1062%	0.38	0.21	229%	0.09
As (ppm)	130.0	103.7	1679%	3.9	-3.3	-53%	0.1	-6.1	-99%	6.2
Ba (ppm)	213	168	1353%	118	77	621%	43	21	170%	12
Te (ppm)	0.47	0.37	1319%	0.15	0.08	294%	0.08	0.03	122%	0.03
Rb (ppm)	37	29	1204%	26	17	708%	9	5	192%	2
W (ppm)	30.0	22.7	847%	16.4	9.8	365%	11.3	6.1	228%	2.7
Se (ppm)	1.2	0.9	681%	0.1	-0.1	-71%	0.1	-0.1	-70%	0.1
Cs (ppm)	1.9	1.3	518%	1.9	1.1	441%	1.0	0.5	199%	0.3
Tl (ppm)	0.19	0.11	235%	0.23	0.12	257%	0.29	0.18	370%	0.05
Pb (ppm)	4	2	142%	3	1	63%	2	0	11%	1
Li (ppm)	70	25	74%	52	6	16%	41	-2	-6%	34
Mo (ppm)	1.0	0.2	41%	0.5	-0.2	-37%	0.5	-0.2	-35%	0.6
La (ppm)	5.95	1.34	36%	4.67	-0.14	-4%	4.63	-0.08	-2%	3.69
Zr (ppm)	88	20	36%	92	15	28%	89	15	26%	55
Ce (ppm)	15.0	3.2	34%	13.0	0.4	4%	12.7	0.4	5%	9.4
Hf (ppm)	2.4	0.4	28%	2.5	0.3	20%	2.4	0.3	18%	1.6
Pr (ppm)	2.08	0.36	26%	2.01	0.13	9%	1.98	0.15	10%	1.40
Nd (ppm)	10.0	1.5	22%	10.5	1.0	15%	10.1	0.9	13%	6.9
Ta (ppm)	0.17	0.02	16%	0.16	-0.01	-5%	0.16	0.00	0%	0.12
Sm (ppm)	3.05	0.34	15%	3.59	0.49	22%	3.43	0.43	19%	2.24
Th (ppm)	0.49	0.05	14%	0.36	-0.09	-24%	0.36	-0.08	-23%	0.36
Na <sub>2</sub> O (wt%)	2.26	0.21	12%	1.82	-0.32	-19%	2.49	0.24	14%	1.70
Ho (ppm)	0.97	0.08	11%	1.18	0.16	21%	1.17	0.17	23%	0.74
Lu (ppm)	0.474	0.036	10%	0.585	0.080	22%	0.582	0.089	24%	0.364
U (ppm)	0.13	0.01	10%	0.10	-0.03	-28%	0.09	-0.03	-30%	0.10
Tm (ppm)	0.443	0.033	10%	0.549	0.076	22%	0.533	0.074	22%	0.341
Gd (ppm)	3.71	0.28	10%	4.41	0.49	17%	4.31	0.49	17%	2.86
Dy (ppm)	4.60	0.34	9%	5.65	0.74	21%	5.46	0.70	20%	3.55
Y (ppm)	25.9	1.7	8%	32.9	4.8	24%	32.4	5.0	25%	20.2
Sr (ppm)	223	13	7%	187	-34	-19%	162	-50	-28%	176
Yb (ppm)	2.98	0.17	7%	3.62	0.40	17%	3.60	0.45	19%	2.35
Er (ppm)	2.84	0.16	7%	3.67	0.54	24%	3.55	0.52	23%	2.25
Tb (ppm)	0.69	0.04	7%	0.84	0.09	17%	0.81	0.08	16%	0.55
LOI (wt%)	8.46	0.45	7%	7.87	-0.72	-11%	8.74	0.10	2%	6.70
C (wt%)	1.59	0.04	3%	1.44	-0.22	-16%	1.86	0.14	11%	1.31
CO <sub>2</sub> (wt%)	5.45	0.12	3%	4.75	-0.87	-19%	6.15	0.30	7%	4.49
Eu (ppm)	1.00	0.01	2%	1.19	0.07	8%	1.19	0.10	11%	0.83
Fe <sub>2</sub> O <sub>3</sub> (wt%)	1.98	0.02	1%	2.32	0.11	7%	1.74	-0.30	-18%	1.66
P <sub>2</sub> O <sub>5</sub> (wt%)	0.10	0.00	1%	0.13	0.01	13%	0.15	0.03	39%	0.08
TiO <sub>2</sub> (wt%)	1.147	-0.003	0%	1.411	0.100	10%	1.383	0.104	11%	0.973
Nb (ppm)	2.4	-0.1	-3%	2.7	-0.1	-4%	2.7	0.0	0%	2.1
Ga (ppm)	18	-1	-5%	18	-2	-14%	19	-1	-8%	16
V (ppm)	285	-19	-7%	341	-1	0%	331	-2	-1%	260
SiO <sub>2</sub> (wt%)	47.85	-5.82	-13%	46.96	-10.57	-23%	46.02	-10.45	-23%	46.29
MnO (wt%)	0.18	-0.03	-17%	0.19	-0.03	-18%	0.19	-0.03	-19%	0.18
CaO (wt%)	8.60	-1.67	-19%	7.77	-3.04	-34%	8.40	-2.41	-27%	8.95
Al <sub>2</sub> O <sub>3</sub> (wt%)	12.5	-3.1	-23%	13.1	-3.7	-27%	12.5	-3.9	-28%	13.6
Fe <sub>2</sub> O <sub>3</sub> T (%)	11.65	-2.90	-23%	14.22	-1.94	-15%	13.75	-2.05	-16%	12.75
Sc (ppm)	30	-8	-25%	37	-5	-16%	36	-6	-17%	34
FeO (wt%)	8.7	-2.6	-26%	10.7	-1.8	-18%	10.8	-1.6	-16%	10.0
Ag (ppm)	0.25	-0.09	-30%	0.25	-0.11	-37%	0.25	-0.11	-35%	0.30
Ge (ppm)	1.1	-0.4	-31%	1.3	-0.4	-29%	1.3	-0.3	-24%	1.3
Co (ppm)	35.3	-21.2	-42%	39.5	-21.0	-41%	37.5	-21.9	-43%	51.1
Zn (ppm)	66.7	-40.2	-42%	139.5	9.5	10%	142.0	14.0	14%	96.6
Ni (ppm)	72	-54	-47%	70	-62	-54%	71	-60	-52%	115
MgO (wt%)	4.18	-3.37	-49%	4.82	-3.24	-47%	4.83	-3.14	-46%	6.90
Cr (ppm)	80	-83	-55%	90	-83	-55%	89	-81	-54%	151
Sb (ppm)	0.07	-0.09	-59%	0.04	-0.12	-82%	0.06	-0.10	-68%	0.15
Cu (ppm)	28.2	-110.7	-82%	65.6	-84.6	-63%	62.4	-85.9	-64%	134.5

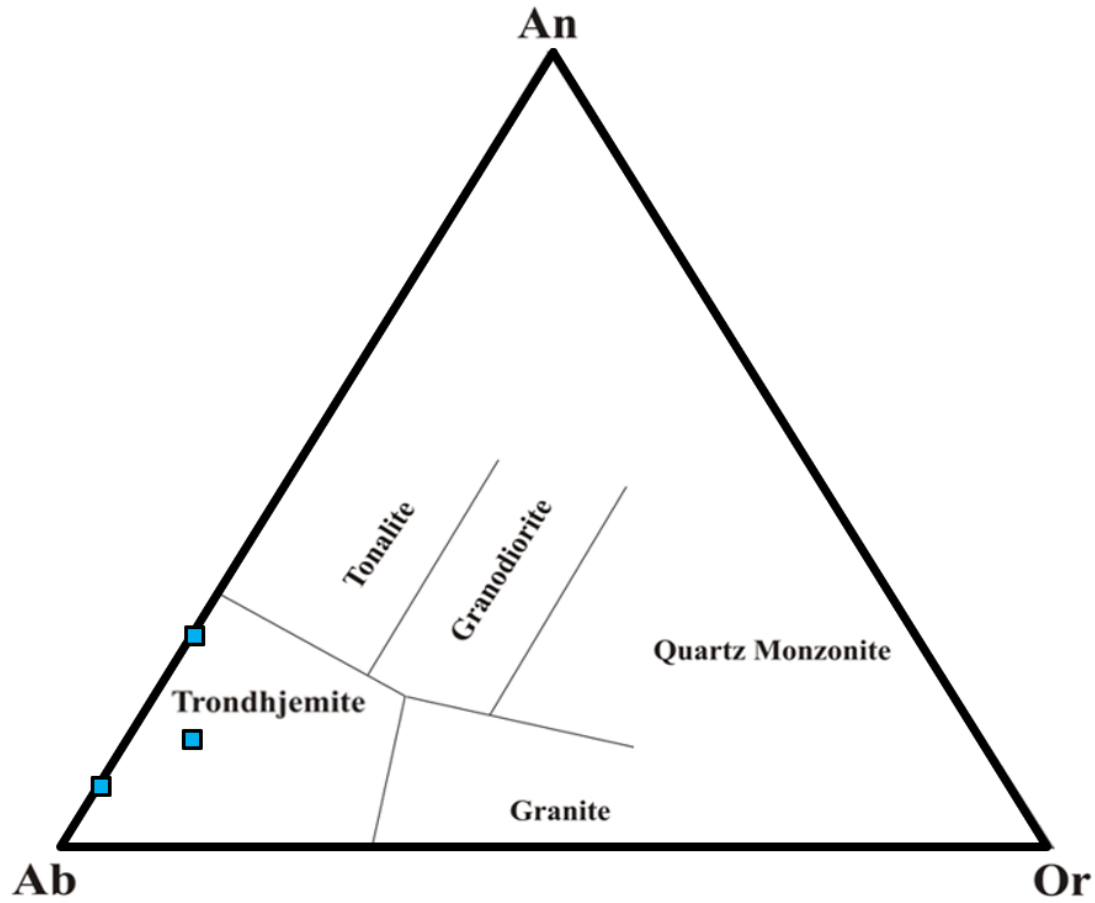


**Figure 48.** Least-altered and weakly-altered samples of the Webb Lake stock (T6, T192, T193) plotted on an Anorthite (An) – Orthoclase (Or) – Albite (Ab) ternary diagram modified from Barker (1979). Endmember proportions were determined using CIPW Norm calculations modified to include biotite and hornblende (Hutchison, 1975).



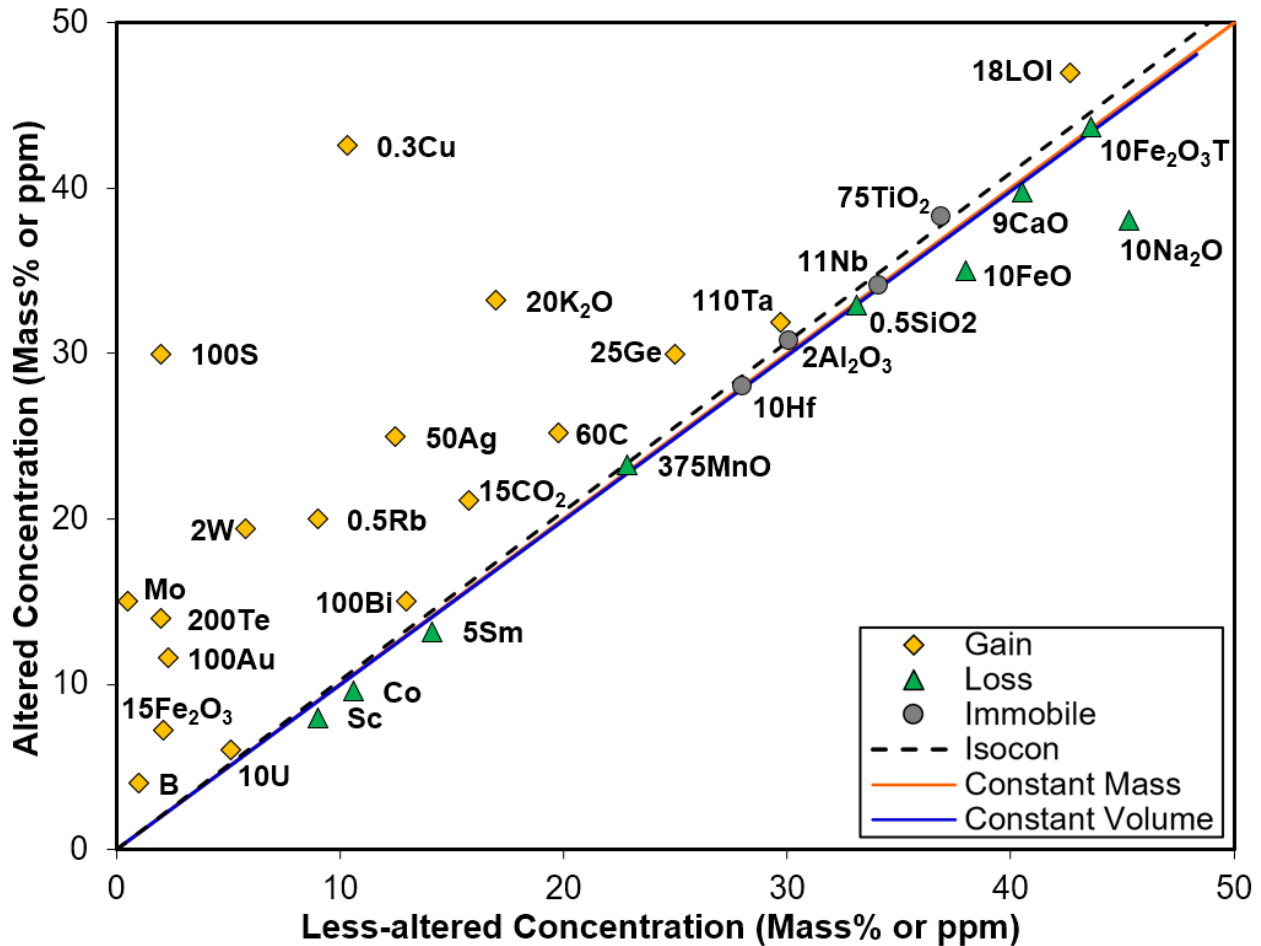


**Figure 49.** Isocon diagram displaying an altered sample of the Webb Lake stock (T194) plotted against a least-altered sample of the Webb Lake stock (T192) from the same alteration envelope. This alteration envelope is associated with  $V_1$ - $V_2$  auriferous quartz veining. In addition to chemical species determined to be relatively immobile for this altered/least-altered pair, only chemical species that are consistently enriched or depleted, based on the study of multiple altered/less-altered pairs, are displayed. Concentrations of elements are arbitrarily scaled to avoid stacking/overlap. This is achieved by multiplying both the concentration of the chemical species in the altered sample and the concentration of the chemical species in the less-altered sample by the scale factor/multiplier shown beside each chemical species. LOI=Loss on Ignition,  $Fe_2O_3T$ =Total Iron. The methods used to construct these diagrams are detailed in Section 3.2.2.

**Table 9.** Results of mass balance calculations based on the chemistry of samples of the Webb Lake stock altered by  $V_1$ - $V_2$  veining. Average concentrations of chemical species (C) for samples classified under each alteration strength grouping as well as the calculated concentration changes ( $\Delta C$ ) of chemical species are displayed. Concentration changes of chemical species relative to their concentration in the least-altered sample are displayed ( $\Delta C/C_{LA}$ ). Calculations were performed using the following equation from Grant (1986) with modified variables:  $\Delta C/C_{LA} = (\text{slope of Isocon}) * (C_A/C_{LA}) - 1$ . C=Concentration,  $C_A$ =Concentration in altered sample,  $C_{LA}$ =Concentration in least-altered sample. LOI=Loss on Ignition,  $Fe_2O_3T$ =Total Iron. The following samples were used for each alteration strength grouping: Strongly-altered (T195), moderately-altered (T194), weakly-altered (T193), least-altered (T192).

	Strongly-altered			Moderately-altered			Weakly-altered			Least-altered
	C	$\Delta C$	$\Delta C/C_{LA}$	C	$\Delta C$	$\Delta C/C_{LA}$	C	$\Delta C$	$\Delta C/C_{LA}$	C
As (ppm)	73.5	72.7	145371%	0.1	0.0	2%	0.1	0.0	13%	0.1
S (wt%)	1.68	1.64	8213%	0.30	0.28	1424%	0.15	0.15	748%	0.02
Au (ppm)	1.480	1.442	6268%	0.116	0.095	412%	0.052	0.036	155%	0.023
Te (ppm)	0.62	0.60	6036%	0.07	0.06	611%	0.06	0.06	578%	0.01
Mo (ppm)	18.0	17.3	3463%	15.0	14.7	2948%	0.5	0.1	13%	0.5
B (ppm)	15	14	1384%	4	3	306%	1	0	-43%	1
W (ppm)	43.3	39.9	1378%	9.7	7.0	240%	3.0	0.5	17%	2.9
Bi (ppm)	0.96	0.82	631%	0.15	0.02	17%	0.17	0.06	48%	0.13
Fe <sub>2</sub> O <sub>3</sub> (wt%)	0.93	0.78	557%	0.48	0.35	248%	0.57	0.50	360%	0.14
Cu (ppm)	204.0	167.5	487%	142.0	109.9	319%	67.5	41.9	122%	34.4
K <sub>2</sub> O (wt%)	2.78	1.90	224%	1.66	0.84	98%	1.09	0.38	45%	0.85
Ag (ppm)	0.80	0.54	217%	0.50	0.26	103%	0.25	0.03	13%	0.25
Rb (ppm)	48	30	164%	40	23	126%	20	5	26%	18
Se (ppm)	0.1	0.0	98%	0.1	0.0	2%	0.1	0.0	13%	0.1
Sb (ppm)	0.06	0.03	98%	0.02	-0.01	-32%	0.06	0.04	126%	0.03
LOI (wt%)	4.67	2.25	95%	2.61	0.28	12%	1.74	-0.40	-17%	2.37
CO <sub>2</sub> (wt%)	1.89	0.82	78%	1.41	0.38	36%	0.87	-0.07	-6%	1.05
C (wt%)	0.59	0.25	77%	0.42	0.10	29%	0.25	-0.05	-14%	0.33
Ge (ppm)	1.5	0.5	48%	1.2	0.2	22%	1.0	0.1	13%	1.0
Nb (ppm)	4.6	1.5	47%	3.1	0.0	2%	2.2	-0.6	-20%	3.1
U (ppm)	0.72	0.20	40%	0.60	0.10	20%	1.17	0.81	159%	0.51
Cs (ppm)	1.4	0.4	39%	1.6	0.6	63%	0.7	-0.2	-21%	1.0
Cr (ppm)	19	5	34%	55	42	299%	53	46	328%	14
Pb (ppm)	4	1	32%	3	0	2%	3	0	13%	3
Ta (ppm)	0.36	0.09	32%	0.29	0.02	9%	0.33	0.10	38%	0.27
Ba (ppm)	336	69	26%	258	-2	-1%	222	-13	-5%	264
Hf (ppm)	3.2	0.4	13%	2.8	0.0	2%	2.1	-0.4	-15%	2.8
TiO <sub>2</sub> (wt%)	0.519	0.022	4%	0.511	0.027	6%	0.229	-0.233	-47%	0.492
Ga (ppm)	20	1	4%	19	0	2%	19	2	13%	19
Lu (ppm)	0.161	0.004	3%	0.140	-0.013	-8%	0.125	-0.014	-9%	0.155
Al <sub>2</sub> O <sub>3</sub> (wt%)	15.5	0.3	2%	15.4	0.6	4%	13.9	0.6	4%	15.0
Th (ppm)	2.35	0.04	2%	2.15	-0.11	-5%	4.19	2.44	107%	2.29
Zn (ppm)	63.5	0.4	1%	62.2	0.8	1%	29.1	-29.5	-47%	62.4
MgO (wt%)	1.46	0.00	0%	1.57	0.16	11%	0.74	-0.60	-42%	1.44
V (ppm)	73	0	0%	73	2	3%	32	-36	-50%	72
Yb (ppm)	0.97	0.00	0%	0.87	-0.08	-8%	0.75	-0.11	-12%	0.96
P <sub>2</sub> O <sub>5</sub> (wt%)	0.12	0.00	-1%	0.14	0.02	19%	0.05	-0.06	-53%	0.12
Li (ppm)	17	0	-1%	18	1	8%	10	-6	-34%	17
Y (ppm)	9.3	-0.2	-2%	8.9	-0.4	-4%	8.0	-0.4	-4%	9.4
SiO <sub>2</sub> (wt%)	65.18	-1.69	-3%	65.85	0.72	1%	71.52	14.63	22%	66.19
Er (ppm)	0.98	-0.03	-3%	0.92	-0.07	-7%	0.74	-0.16	-16%	1.00
Fe <sub>2</sub> O <sub>3</sub> T (wt%)	4.27	-0.13	-3%	4.37	0.08	2%	2.46	-1.58	-36%	4.36
Ho (ppm)	0.32	-0.01	-4%	0.32	0.00	-1%	0.25	-0.05	-14%	0.33
Tm (ppm)	0.145	-0.007	-4%	0.133	-0.015	-10%	0.110	-0.026	-17%	0.150
Pr (ppm)	3.80	-0.24	-6%	3.63	-0.31	-8%	4.10	0.63	16%	4.00
Eu (ppm)	0.73	-0.06	-7%	0.71	-0.06	-8%	0.42	-0.31	-40%	0.78
Tb (ppm)	0.30	-0.02	-7%	0.30	-0.02	-5%	0.24	-0.05	-15%	0.32
Gd (ppm)	2.02	-0.16	-7%	2.00	-0.13	-6%	1.75	-0.18	-8%	2.16
Ce (ppm)	33.2	-3.0	-8%	31.8	-3.6	-10%	37.8	6.8	19%	35.9
Ni (ppm)	12	-1	-9%	14	1	9%	6	-6	-48%	13
Sm (ppm)	2.61	-0.25	-9%	2.64	-0.15	-5%	2.56	0.06	2%	2.83
Dy (ppm)	1.65	-0.17	-9%	1.66	-0.11	-6%	1.36	-0.26	-15%	1.80
Nd (ppm)	14.0	-1.4	-9%	13.8	-1.3	-8%	14.5	1.1	7%	15.3
Tl (ppm)	0.10	-0.01	-10%	0.12	0.01	11%	0.08	-0.02	-18%	0.11
La (ppm)	15.80	-1.76	-10%	15.20	-1.96	-11%	18.90	3.96	23%	17.40
Sc (ppm)	8	-1	-12%	8	-1	-10%	4	-4	-50%	9
MnO (wt%)	0.05	-0.01	-12%	0.06	0.00	3%	0.03	-0.02	-39%	0.06
Co (ppm)	9.3	-1.4	-13%	9.6	-0.8	-8%	5.0	-4.9	-47%	10.6
FeO (wt%)	3.0	-0.8	-22%	3.5	-0.2	-6%	1.7	-1.9	-49%	3.8
CaO (wt%)	3.49	-1.05	-23%	4.42	-0.01	0%	2.65	-1.51	-33%	4.50
Sr (ppm)	228	-99	-31%	174	-148	-46%	159	-145	-45%	325
Zr (ppm)	76	-47	-38%	68	-53	-43%	44	-72	-59%	122
Na <sub>2</sub> O (wt%)	2.08	-2.47	-55%	3.81	-0.66	-15%	4.74	0.83	18%	4.53



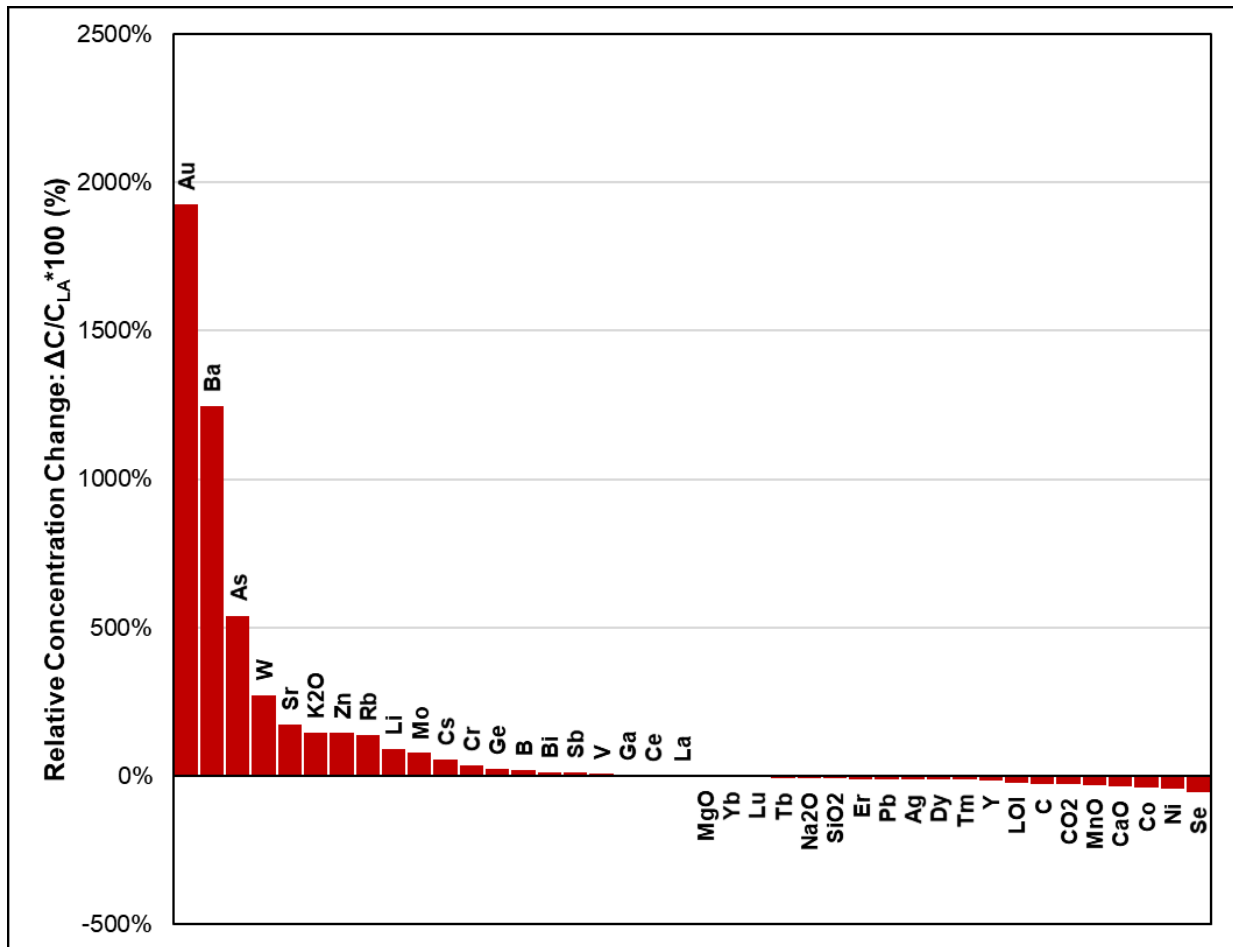


**Figure 51.** Relative concentration changes of chemical species between a representative least-altered sample of gabbro/lamprophyre (T239) and a sample of gabbro/lamprophyre (T213) altered by a  $V_3$  quartz vein. Chemical gains/losses are expressed as a percentage relative to the least-altered sample. Only chemical species that are consistently enriched or depleted, based on the study of multiple altered/least-altered pairs, are displayed. Calculations were performed using the following equation from Grant (1986) with modified variables:  $\Delta C/C_{LA} = (\text{slope of isocon}) * (C_A/C_{LA}) - 1$ . The slope of the Isocon in Figure 50 was used. C=Concentration,  $C_A$ =Concentration in altered sample,  $C_{LA}$ =Concentration in least-altered sample. LOI=Loss on Ignition.  $Fe_2O_3T$ =Total Iron.

**Table 10.** Concentration and relative concentration changes of chemical species between a sample of gabbro/lamprophyre altered by a  $V_3$  vein and a least-altered sample of gabbro/lamprophyre. Relative concentration changes are expressed as a percentage relative to the least-altered sample. Only chemical species that are consistently enriched or depleted, based on the study of multiple altered/least-altered pairs, are displayed. Calculations were performed using the following equation from Grant (1986) with modified variables:  $\Delta C/C_{LA} = (\text{slope of isocon}) * (C_A/C_{LA}) - 1$ . The slope of the Isocon in Figure 50 was used.  $C$ =Concentration,  $C_A$ =Concentration in altered sample,  $C_{LA}$ =Concentration in least-altered sample.  $LOI$ =Loss on Ignition.  $Fe_2O_3T$ =Total Iron.

		Least-altered (T239)	Altered (T213)	Relative Concentration Change: $\Delta C/C_{LA} * 100$ (%)	Concentration Change: $\Delta C$
<b>Au</b>	ppm	0.0025	0.057	1927.6%	0.05
<b>Ba</b>	ppm	22	333	1246.1%	274.13
<b>As</b>	ppm	1.6	11.5	539.2%	8.63
<b>W</b>	ppm	5.1	21.3	271.4%	13.84
<b>Sr</b>	ppm	131	402	172.9%	226.49
<b>K<sub>2</sub>O</b>	wt%	0.22	0.61	146.6%	0.32
<b>Zn</b>	ppm	60.1	165	144.1%	86.63
<b>Rb</b>	ppm	6	16	137.1%	8.23
<b>Li</b>	ppm	39	84	91.5%	35.70
<b>Mo</b>	ppm	0.5	1	77.9%	0.39
<b>Cs</b>	ppm	0.4	0.7	55.6%	0.22
<b>Cr</b>	ppm	343	522	35.3%	121.21
<b>Ge</b>	ppm	1	1.4	24.5%	0.25
<b>B</b>	ppm	9	12	18.6%	1.67
<b>Bi</b>	ppm	0.22	0.28	13.2%	0.03
<b>Sb</b>	ppm	0.04	0.05	11.2%	0.00
<b>V</b>	ppm	101	121	6.5%	6.60
<b>Ga</b>	ppm	13	15	2.6%	0.34
<b>Ce</b>	ppm	99.9	114	1.5%	1.48
<b>La</b>	ppm	49.4	55.6	0.1%	0.04
<b>MgO</b>	wt%	9.3	10.07	-3.7%	-0.34
<b>Yb</b>	ppm	1	1.08	-4.0%	-0.04
<b>Lu</b>	ppm	0.151	0.16	-5.8%	-0.01
<b>Tb</b>	ppm	0.49	0.51	-7.4%	-0.04
<b>Na<sub>2</sub>O</b>	wt%	1.37	1.42	-7.8%	-0.11
<b>SiO<sub>2</sub></b>	wt%	41.44	42.78	-8.2%	-3.40
<b>Er</b>	ppm	1.26	1.26	-11.1%	-0.14
<b>Pb</b>	ppm	3	3	-11.1%	-0.33
<b>Ag</b>	ppm	0.25	0.25	-11.1%	-0.03
<b>Dy</b>	ppm	2.56	2.52	-12.5%	-0.32
<b>Tm</b>	ppm	0.172	0.167	-13.7%	-0.02
<b>Y</b>	ppm	13.2	12.7	-14.4%	-1.91
<b>LOI</b>	wt%	18.21	15.94	-22.2%	-4.03
<b>C</b>	wt%	4.62	3.77	-27.4%	-1.27
<b>CO<sub>2</sub></b>	wt%	15.7	12.6	-28.6%	-4.49
<b>MnO</b>	wt%	0.161	0.125	-31.0%	-0.05
<b>CaO</b>	wt%	12.73	9.28	-35.2%	-4.48
<b>Co</b>	ppm	32.5	22.2	-39.3%	-12.76
<b>Ni</b>	ppm	472	298	-43.9%	-206.99
<b>Se</b>	ppm	0.1	0.05	-55.5%	-0.06

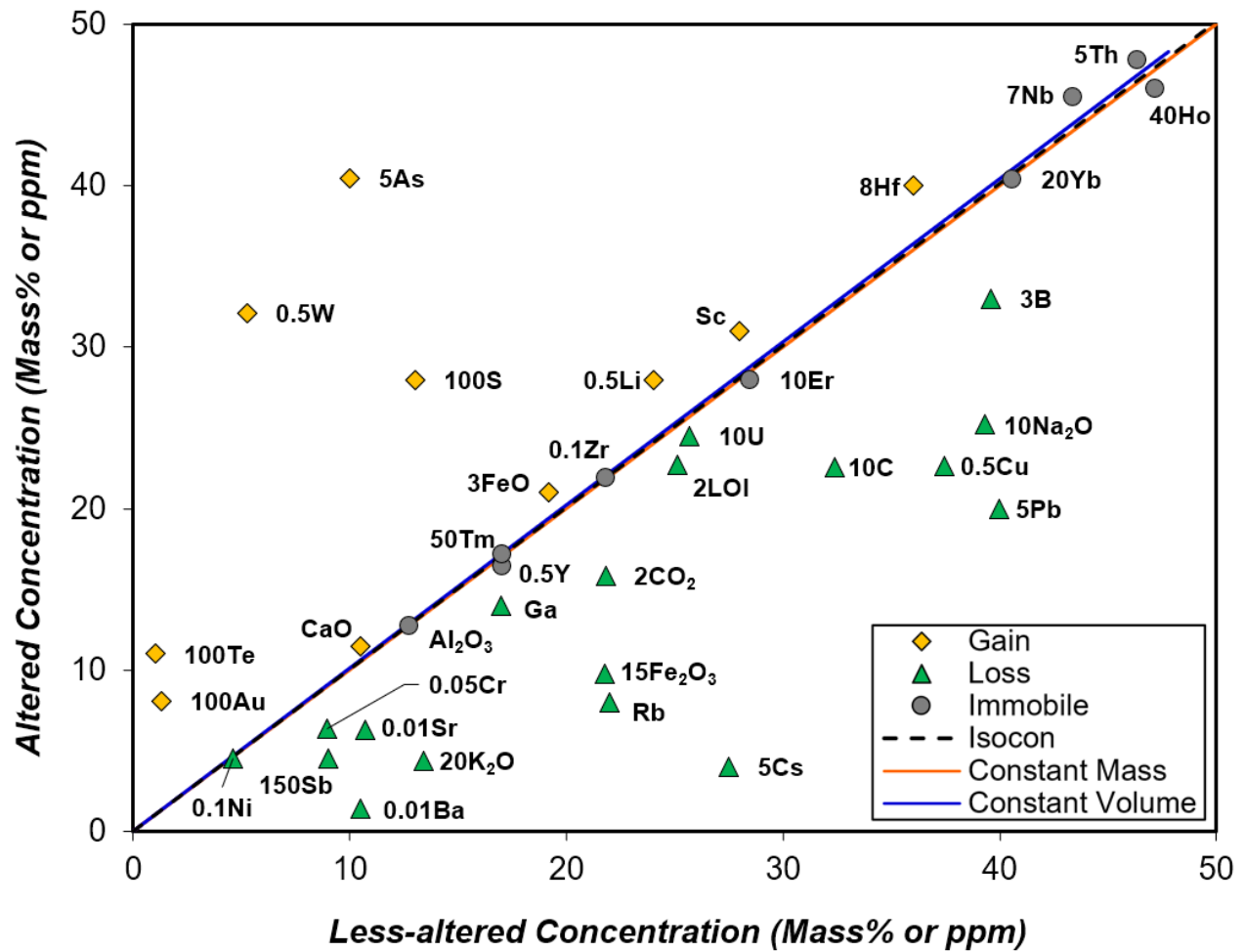


**Figure 52.** Isocon diagram displaying an altered sample of silica-poor diorite–monzodiorite (T245) plotted against a least-altered sample of silica-poor diorite–monzodiorite (T66). The altered sample is altered by a  $V_3$  quartz vein. Concentrations of elements are arbitrarily scaled to avoid stacking/overlap. This is achieved by multiplying both the concentration of the chemical species in the altered sample and the concentration of the chemical species in the least-altered sample by the scale factor/multiplier shown beside each chemical species. In addition to chemical species determined to be relatively immobile for this altered/least-altered pair, only chemical species that are consistently enriched or depleted, based on the study of multiple altered/least-altered pairs, are displayed. LOI=Loss on Ignition,  $Fe_2O_3T$ =Total Iron. The methods used to construct these diagrams are detailed in Section 3.2.2.



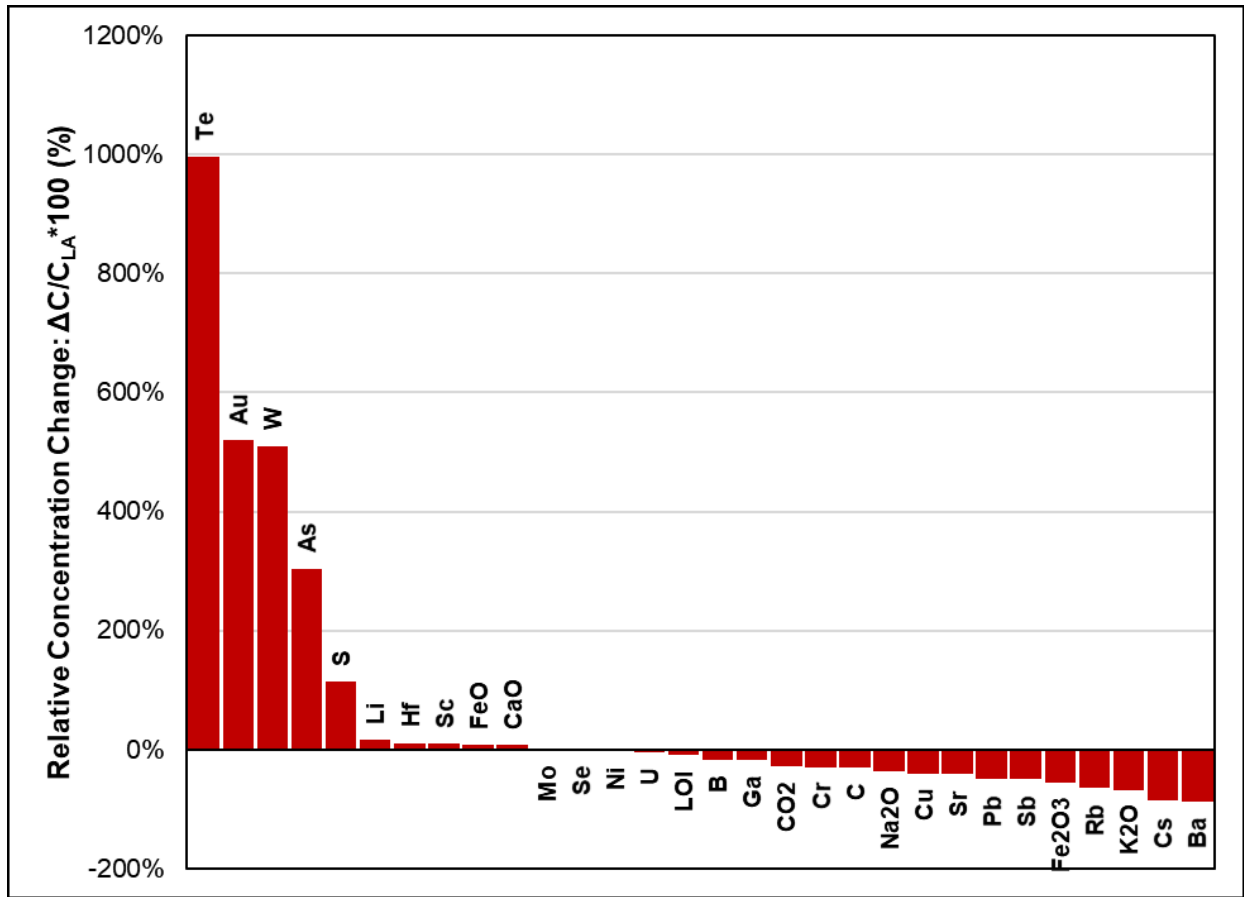


**Figure 53.** Relative concentration changes of chemical species between a representative least-altered sample of silica-poor diorite-monzodiorite (T66) and a sample of silica-poor diorite-monzodiorite (T245) altered by a  $V_3$  quartz vein. Chemical gains/losses are expressed as a percentage relative to the least-altered sample. Only chemical species that are consistently enriched or depleted, based on the study of multiple altered/least-altered pairs, are displayed. Calculations were performed using an equation from Grant (1986) with modified variables:  $\Delta C/C_{LA} = (\text{slope of isocon}) * (C_A/C_{LA}) - 1$ . The slope of the Isocon in Figure 52 was used. C=concentration,  $C_A$ =concentration in altered sample,  $C_{LA}$ =concentration in least-altered sample. LOI=Loss on ignition.  $Fe_2O_3T$ =Total Iron.

**Table 11.** Concentration and relative concentration changes of chemical species between a sample of silica-poor diorite–monzodiorite altered by a V<sub>3</sub> vein and a least-altered sample of silica-poor diorite–monzodiorite. Concentration change for oxides, C, S, and LOI are expressed in weight percent (wt%). Concentration change for all other chemical species are expressed in parts per million (ppm). Relative concentration changes are expressed as a percentage relative to the least-altered sample. Only chemical species that are consistently enriched or depleted, based on the study of multiple altered/least-altered pairs, are displayed. Calculations were performed using the following equation from Grant (1986) with modified variables:  $\Delta C/C_{LA} = (\text{slope of isocon}) * (C_A/C_{LA}) - 1$ . The slope of the Isocon in Figure 52 was used. C=Concentration, C<sub>A</sub>=Concentration in altered sample, C<sub>LA</sub>=Concentration in least-altered sample. LOI=Loss on Ignition. Fe<sub>2</sub>O<sub>3</sub>T=Total Iron.

	Units	Least-altered (T66)	Altered (T245)	Relative Concentration Change: $\Delta C/C_{LA} * 100$ (%)	Concentration Change: $\Delta C$
Te	ppm	0.01	0.11	996.0%	0.10
Au	ppm	0.013	0.081	520.8%	0.07
W	ppm	10.5	64.3	510.2%	53.57
As	ppm	2	8.1	303.5%	6.07
S	wt%	0.13	0.28	114.6%	0.15
Li	ppm	48	56	16.2%	7.80
Hf	ppm	4.5	5	10.7%	0.48
Sc	ppm	28	31	10.3%	2.89
FeO	wt%	6.4	7	9.0%	0.57
CaO	wt%	10.51	11.44	8.5%	0.89
Mo	ppm	0.5	0.5	-0.4%	0.00
Se	ppm	0.05	0.05	-0.4%	0.00
Ni	ppm	46	45	-2.5%	-1.16
U	ppm	2.57	2.45	-5.0%	-0.13
LOI	wt%	12.55	11.36	-9.8%	-1.23
B	ppm	13.2	11	-17.0%	-2.24
Ga	ppm	17	14	-17.9%	-3.05
CO <sub>2</sub>	wt%	10.9	7.92	-27.6%	-3.01
Cr	ppm	179	127	-29.3%	-52.46
C	wt%	3.24	2.26	-30.5%	-0.99
Na <sub>2</sub> O	wt%	3.93	2.52	-36.1%	-1.42
Cu	ppm	74.9	45.3	-39.7%	-29.76
Sr	ppm	1071	628	-41.6%	-445.27
Pb	ppm	8	4	-50.2%	-4.01
Sb	ppm	0.06	0.03	-50.2%	-0.03
Fe <sub>2</sub> O <sub>3</sub>	wt%	1.45	0.65	-55.3%	-0.80
Rb	ppm	22	8	-63.8%	-14.03
K <sub>2</sub> O	wt%	0.67	0.22	-67.3%	-0.45
Cs	ppm	5.5	0.8	-85.5%	-4.70
Ba	ppm	1051	139	-86.8%	-912.50

### 4.3 Mineral compositions

Six thin sections were selected for electron probe microanalysis of key minerals (biotite, white mica, chlorite, epidote, plagioclase, and carbonates). These thin sections consisted of altered and least-altered pairs from a dacite-hosted (T157 and T154), a Webb Lake stock-hosted (T195 and T192), and a gabbro-hosted (T141 and T139) ore zone. The least-altered gabbro sample (T139) is actually classified as a weakly-altered sample (Section 4.2.4.2) but, for simplicity, is referred to as a least-altered sample in this section. Altered samples of these lithologies are altered by  $V_1$ - $V_2$  auriferous veins. All electron microprobe results are located in Appendix H.

#### 4.3.1 Biotite

Compositions of biotite from the gabbro and Webb Lake stock are summarized in Table 12 and plotted on a biotite classification diagram in Figure 54. Compositions of biotite in altered and least-altered gabbro samples are similar and plot close to the centre of the biotite field on the Annite-Phlogopite-Eastonite-Siderophyllite (APSE) diagram (Figure 54A). However, biotite in the altered sample generally has slightly lower  $Fe/(Fe+Mg)$  than biotite in the least-altered sample (Figure 54A). Biotite from the least-altered Webb Lake stock sample have similar compositions to biotite in the gabbro (Figure 54B). Biotite from altered samples of the Webb Lake stock have significantly lower  $Fe/(Fe+Mg)$  values (Figure 54B), more fluorine (Table 12) and less potassium (Table 12) than biotite in least-altered samples of the Webb Lake stock. These compositional differences affirm the presence of both primary biotite and alteration-derived biotite in the Webb Lake stock.

#### 4.3.2 Chlorite

Compositions of chlorite from the dacite, Webb Lake stock, and gabbro are summarized in Table 13 and plotted on a chlorite classification diagram in Figure 55. Chlorite within individual samples exhibit minimal compositional variation (Table 13). Most measured compositions are consistent with the chlorite end-member ripidolite (Figure 55A–C). Chlorite in altered samples of the dacite and Webb Lake stock tends to be more enriched in silica and magnesium when compared to chlorite in least-altered equivalents (Table 13). Chlorite in least-altered and altered samples of the gabbro is compositionally similar (Table 13).

### 4.3.3 White mica

Compositions of white mica are summarized in Table 14 and plotted on a ternary classification diagram in Figure 56. The altered gabbroic sample did not contain any white mica. White Mica within individual samples exhibits minimal compositional variation (Table 14) and all plot in the muscovite phengite fields (Figure 56). Similarly, when comparing white mica in altered and least-altered equivalents, the composition of the mica does not change substantially. Slight increases in magnesium and titanium as well as decreases in calcium and iron are noted in altered samples when compared to equivalent least-altered samples (Table 14). White mica in both altered and least-altered dacitic samples is consistent with muscovite (Figure 56A). White mica in the least-altered gabbroic sample is phengite (Figure 56B). White mica in the altered and least-altered samples of the Webb Lake stock both cluster on the phengite-muscovite boundary with analyses plotting in both fields. White mica in the least-altered sample is mainly consistent with phengite while white mica in the altered sample is mostly muscovite (Figure 56C). Considering that there are distinct compositional groupings of white mica in the dacite and Webb Lake stock, this supports the hypothesis that there are two generations of muscovite with the later related to alteration associated with V<sub>1</sub>-V<sub>2</sub> veining.

### 4.3.4 Plagioclase

Compositions of plagioclase are summarized in Table 15 and plotted on a Anorthite-Albite-Orthoclase (An-Ab-Or) feldspar classification diagram in Figure 57. With the exception of the altered gabbroic sample, analyses of plagioclase show substantial variation in concentrations of SiO<sub>2</sub>, Al<sub>2</sub>O<sub>3</sub>, Na<sub>2</sub>O, and CaO. Plagioclase compositions from in all samples are mostly consistent with oligoclase and andesine (Figure 57A–C). Plagioclase in the altered dacitic sample is mainly oligoclase while plagioclase in the least-altered equivalent is comparatively sodium and silica-poor and is mainly andesine (Figure 57A). Plagioclase in the least-altered gabbro has a wide range of compositions ranging from oligoclase to andesine while plagioclase in the altered sample clusters exclusively in the oligoclase field of the An-Ab-Or diagram (Figure 57B). Plagioclase in the altered sample of the Webb Lake stock is mainly consistent with andesine while plagioclase in the least-altered sample of the Webb Lake stock is more sodium and silica-rich and ranges from oligoclase to albite (Figure 57C).

#### 4.3.5 Carbonate minerals

Compositions of carbonate minerals are summarized in Table 16 and plotted on a ternary classification diagram in Figure 58. Some carbonates within the same samples were subdivided into different groups because they have distinctly different compositions. Carbonate minerals in the least-altered dacitic sample cluster near the calcite end-member on the Magnesite-Siderite-Calcite (MSC) ternary diagram (Figure 58A). Carbonates in the altered dacitic sample were subdivided into two groups. Carbonate B has significantly higher concentrations of magnesium and iron than Carbonate A. Carbonate A is calcite and Carbonate B is magnesio-ferro-calcite (Figure 58A).

Within each of the samples of gabbro, carbonates compositions show little chemical variation (Table 16) and are both consistent with calcite (Figure 58B). Analyses of carbonates in the least-altered sample of the Webb Lake stock are compositionally similar and are consistent with calcite (Figure 58C). Carbonates in the altered samples of the Webb Lake stock display significant compositional variation and as a result have been subdivided into four groups (Carbonate C–F; Figure 58C). Calcium content increases moving sequentially from Carbonate C to Carbonate F. Carbonate C and D cluster farthest from the calcite end-member with Carbonate D being closer than Carbonate C. Carbonates C and D are magnesio-ferro-calcites. Carbonate E and F are calcites. Carbonate F has lower average silica and aluminum and has slightly higher average iron and magnesium than Carbonate E (Table 16A).

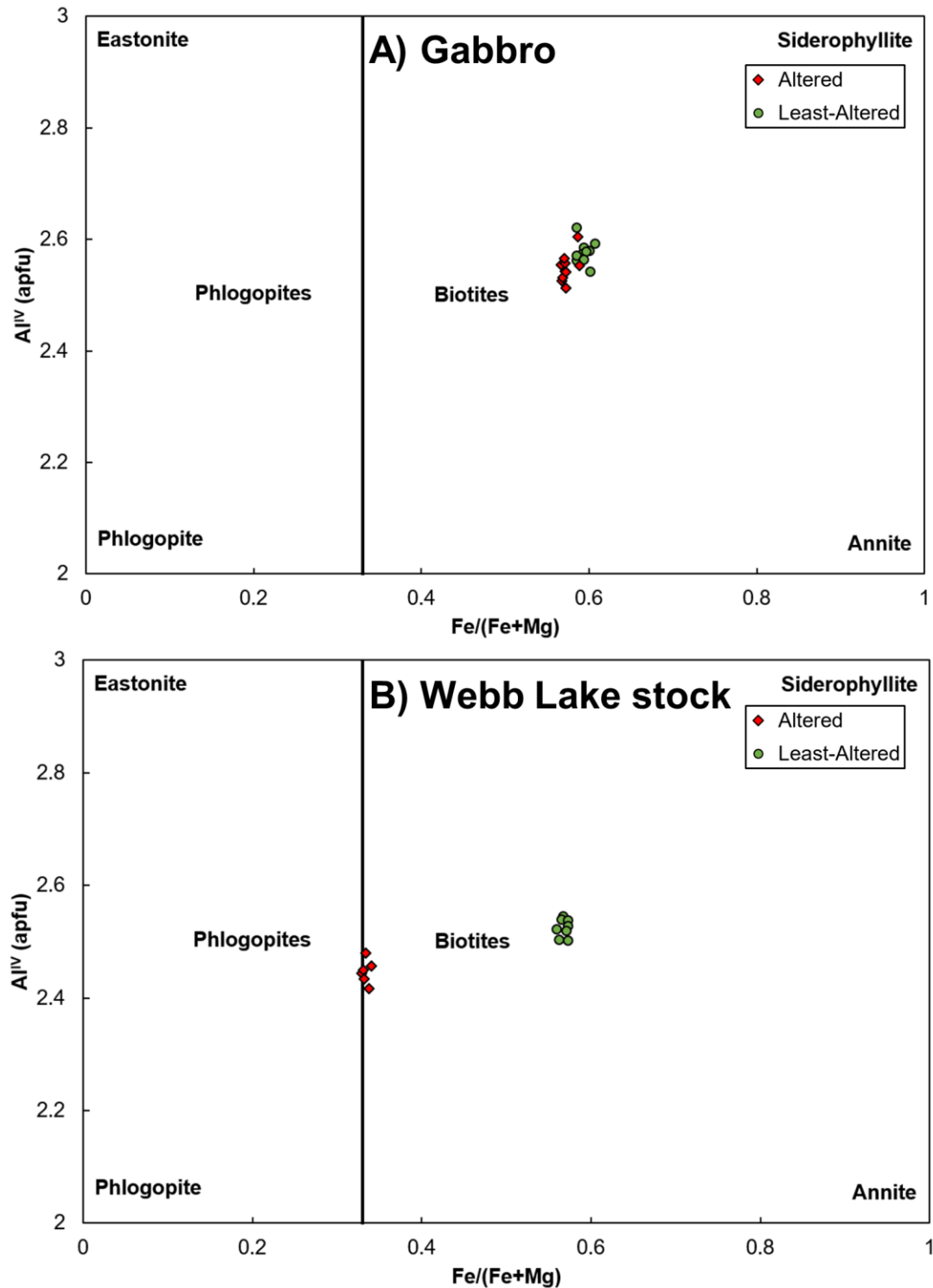
**Table 12A, B.** Summary of microprobe analyses of biotite measured in mass percent. A) Average concentrations of chemical species based on analyses of biotite in each sample. The number of microprobe spot locations analyzing this mineral in each sample are also shown (#). B) Minimum (min) and maximum (max) measured concentrations of oxides and elements in biotite in each sample. bdl=Below detection limit.

<b>A) Averages</b>													
	SiO <sub>2</sub>	Al <sub>2</sub> O <sub>3</sub>	Na <sub>2</sub> O	MgO	F	TiO <sub>2</sub>	CaO	FeO	MnO	K <sub>2</sub> O	Cl	Total	#
Webb Lake	35.39	17.59	0.11	9.02	0.38	1.86	0.00	21.12	0.11	9.76	0.03	95.21	8
Altered Webb Lake	37.41	17.92	0.18	14.91	1.09	1.29	0.02	13.34	0.07	9.60	0.04	95.41	6
Gabbro	35.14	18.18	0.19	8.48	0.24	1.77	0.00	22.10	0.07	9.60	0.23	95.83	10
Altered Gabbro	35.36	18.02	0.12	8.90	0.13	1.79	0.00	21.34	0.10	9.61	0.21	95.48	10

<b>B) Ranges</b>													
	SiO <sub>2</sub>	Al <sub>2</sub> O <sub>3</sub>	Na <sub>2</sub> O	MgO	F	TiO <sub>2</sub>	CaO	FeO	MnO	K <sub>2</sub> O	Cl	Total	
Webb Lake Min	35.21	17.43	0.07	8.89	0.24	1.79	bdl	20.41	0.09	9.66	0.03	94.93	
Webb Lake Max	35.57	17.84	0.18	9.14	0.55	1.93	bdl	21.50	0.12	9.87	0.04	95.59	
Altered Webb Lake Min	37.19	17.75	0.14	14.58	0.99	1.24	bdl	13.13	0.06	9.05	0.03	95.10	
Altered Webb Lake Max	37.67	18.02	0.21	15.27	1.21	1.34	0.04	13.64	0.09	9.81	0.05	95.62	
Gabbro Min	34.62	17.73	0.09	8.28	0.12	1.74	bdl	21.73	0.06	9.26	0.06	94.76	
Gabbro Max	35.55	18.41	0.44	8.78	0.41	1.80	0.01	22.91	0.08	9.84	0.41	96.41	
Altered Gabbro Min	34.94	17.65	0.09	8.60	0.02	1.66	bdl	20.82	0.08	9.40	0.11	94.78	
Altered Gabbro Max	35.81	18.26	0.18	9.15	0.30	1.99	0.04	21.89	0.13	9.75	0.43	96.33	





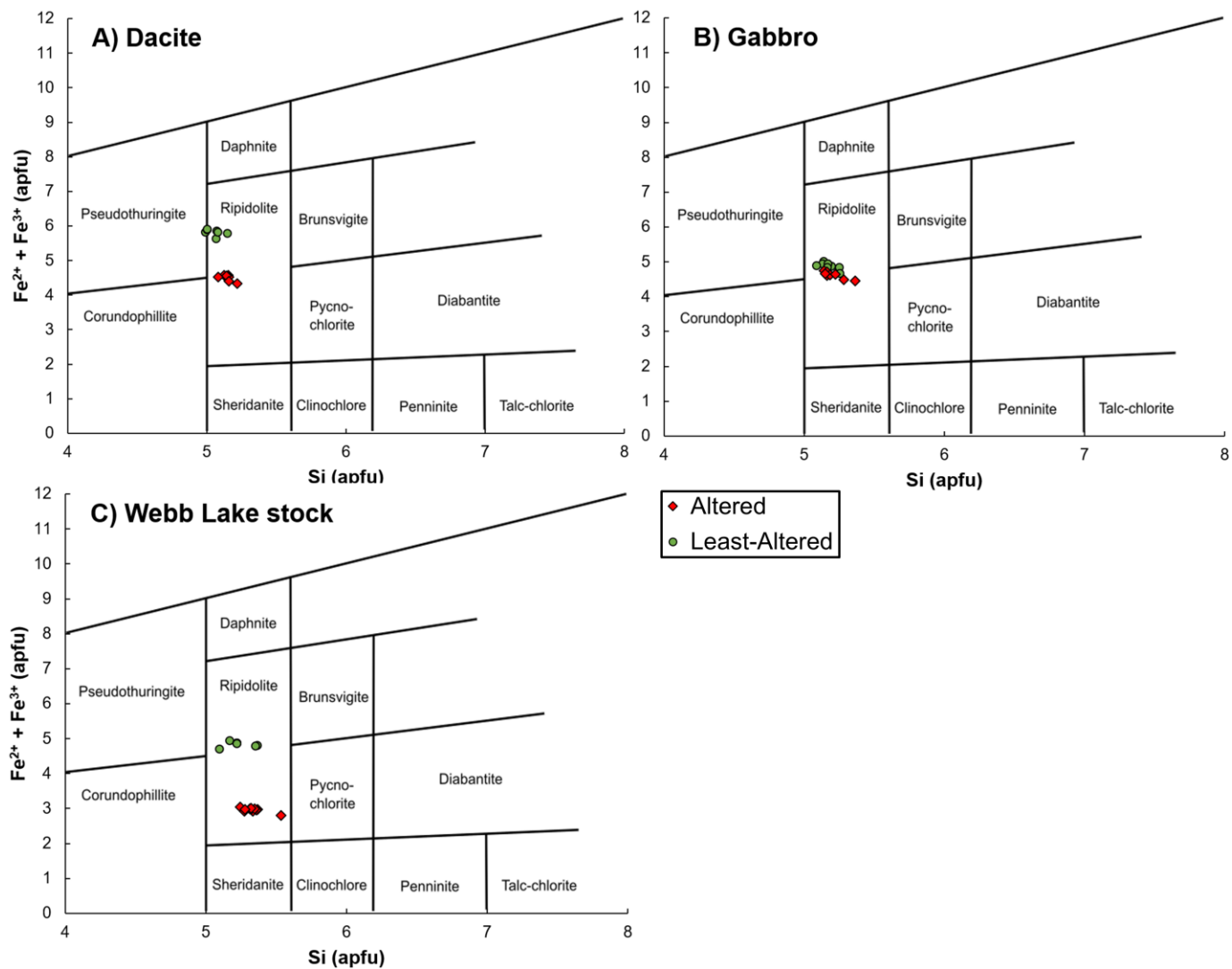
**Figure 54A, B.** Biotite compositions from altered and less-altered samples plotted on Annite-Phlogopite-Eastonite-Siderophyllite (APSE) diagrams. Atoms per formula unit (apfu) values are calculated on a 22-oxygen basis. Modified from Deer et al. (1992).

**Table 13A, B.** Summary of microprobe analyses of chlorite measured in mass percent. A) Average concentrations of chemical species based on analyses of chlorite in each sample. The number of microprobe spot locations analyzing this mineral in each sample are also shown (#). B) Minimum (min) and maximum (max) measured concentrations of oxides and elements in chlorite in each sample. bdl=Below detection limit.

<b>A) Averages</b>													
	SiO <sub>2</sub>	Al <sub>2</sub> O <sub>3</sub>	Na <sub>2</sub> O	MgO	F	TiO <sub>2</sub>	CaO	FeO	MnO	K <sub>2</sub> O	Cl	Total	#
Dacite	22.90	23.33	0.09	8.45	0.02	0.05	0.08	31.47	0.19	0.04	0.04	86.62	7
Altered Dacite	24.32	23.64	0.04	13.22	0.05	0.06	0.01	25.39	0.12	0.02	0.01	86.87	7
Webb Lake	24.36	22.08	0.05	12.87	0.07	0.06	0.02	26.84	0.22	0.01	0.01	86.56	7
Altered Webb Lake	26.32	22.73	0.02	19.80	0.14	0.06	0.01	17.45	0.14	0.07	0.01	86.68	11
Gabbro	24.28	22.94	0.05	12.56	0.02	0.05	0.00	27.35	0.13	0.03	0.03	87.43	10
Altered Gabbro	24.50	22.85	0.04	13.26	0.03	0.06	0.04	25.96	0.19	0.05	0.03	86.98	8

<b>B) Ranges</b>													
	SiO <sub>2</sub>	Al <sub>2</sub> O <sub>3</sub>	Na <sub>2</sub> O	MgO	F	TiO <sub>2</sub>	CaO	FeO	MnO	K <sub>2</sub> O	Cl	Total	
Dacite Min	22.67	22.60	0.03	8.37	bdl	0.03	bdl	30.57	0.15	0.01	0.03	85.46	
Dacite Max	23.07	23.72	0.18	8.63	0.10	0.06	0.32	32.08	0.21	0.13	0.07	87.34	
Altered Dacite Min	23.94	23.41	0.00	12.75	bdl	0.02	bdl	24.82	0.10	0.01	0.01	86.32	
Altered Dacite Max	25.05	24.00	0.15	13.75	0.11	0.12	0.08	25.69	0.15	0.05	0.03	87.70	
Webb Lake Min	23.74	21.11	bdl	12.44	0.01	0.03	bdl	26.13	0.19	0.00	0.01	85.95	
Webb Lake Max	25.03	23.49	0.16	13.39	0.11	0.07	0.05	27.40	0.23	0.03	0.03	87.07	
Altered Webb Lake Min	25.69	22.42	bdl	19.39	0.05	0.04	bdl	16.90	0.10	0.00	0.00	86.13	
Altered Webb Lake Max	27.93	23.12	0.05	20.16	0.23	0.13	0.04	17.78	0.16	0.47	0.03	87.74	
Gabbro Min	23.96	22.32	0.00	12.24	bdl	0.03	bdl	26.42	0.11	0.00	0.01	86.61	
Gabbro Max	24.94	23.82	0.16	13.00	0.08	0.07	0.03	27.89	0.15	0.09	0.05	87.80	
Altered Gabbro Min	24.10	22.21	0.01	12.92	bdl	0.02	bdl	25.19	0.18	0.01	0.01	86.30	
Altered Gabbro Max	25.36	23.16	0.10	13.87	0.09	0.09	0.25	26.78	0.21	0.11	0.06	87.56	



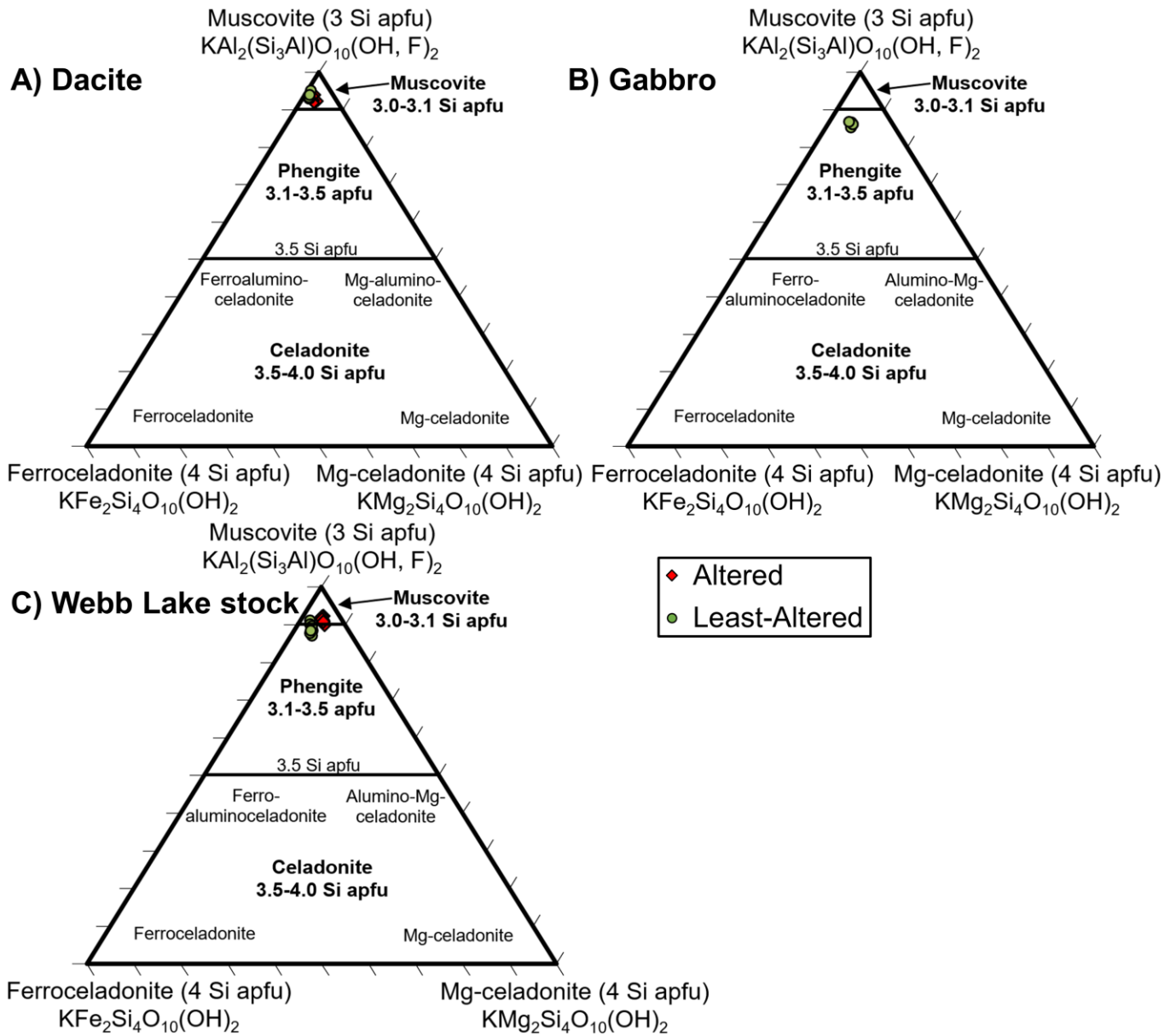
**Figure 55A–C.** Chlorite compositions from altered and least-altered equivalents plotted on chlorite classification diagrams modified from Hey (1954). Atoms per formula unit (apfu) values are calculated on a 28-oxygen basis.

**Table 14A, B.** Summary of microprobe analyses of white mica measured in mass percent. A) Average concentrations of chemical species based on analyses of white mica in each sample. The number of microprobe spot locations analyzing this mineral in each sample are also shown (#). B) Minimum (min) and maximum (max) measured concentrations of oxides and elements in white mica in each sample. bdl=Below detection limit.

<b>A) Averages</b>													
	SiO <sub>2</sub>	Al <sub>2</sub> O <sub>3</sub>	Na <sub>2</sub> O	MgO	F	TiO <sub>2</sub>	CaO	FeO	MnO	K <sub>2</sub> O	Cl	Total	#
Dacite	45.40	36.98	1.37	0.27	0.06	0.16	0.13	1.97	0.01	9.28	0.01	95.61	10
Altered Dacite	45.96	36.50	1.18	0.53	0.15	0.28	0.03	1.74	0.00	9.81	0.00	96.14	13
Webb Lake	45.16	34.56	0.49	0.73	0.12	0.09	0.13	2.89	0.01	10.69	0.00	94.83	7
Altered Webb Lake	45.93	35.72	0.62	0.98	0.10	0.36	0.01	1.53	0.01	10.73	0.00	95.94	9
Gabbro	46.75	33.63	0.65	1.05	0.07	0.27	0.06	3.25	0.01	10.68	0.01	96.40	7

<b>B) Ranges</b>													
	SiO <sub>2</sub>	Al <sub>2</sub> O <sub>3</sub>	Na <sub>2</sub> O	MgO	F	TiO <sub>2</sub>	CaO	FeO	MnO	K <sub>2</sub> O	Cl	Total	
Dacite Min	44.67	36.37	1.18	0.20	bdl	0.14	0.02	1.64	bdl	8.35	bdl	94.71	
Dacite Max	46.00	38.26	1.62	0.33	0.21	0.18	0.68	2.17	0.02	9.66	0.03	96.13	
Altered Dacite Min	45.14	36.06	1.00	0.36	bdl	0.19	0.00	1.44	bdl	9.52	bdl	95.07	
Altered Dacite Max	46.68	37.10	1.34	0.73	0.21	0.34	0.14	1.99	0.01	10.12	0.01	96.90	
Webb Lake Min	44.67	33.13	0.39	0.48	0.05	0.04	0.00	2.63	bdl	10.54	bdl	94.30	
Webb Lake Max	45.64	36.02	0.55	0.92	0.30	0.14	0.59	3.19	0.03	10.81	0.01	95.85	
Altered Webb Lake Min	45.67	35.01	0.56	0.83	0.02	0.12	bdl	1.27	bdl	10.63	bdl	95.50	
Altered Webb Lake Max	46.26	36.25	0.68	1.18	0.19	0.96	0.02	1.65	0.02	10.83	0.01	96.26	
Gabbro Min	45.87	33.14	0.43	0.90	bdl	0.15	bdl	3.01	bdl	10.23	bdl	95.71	
Gabbro Max	48.03	33.94	1.12	1.15	0.19	0.38	0.24	3.44	0.01	10.97	0.01	97.80	



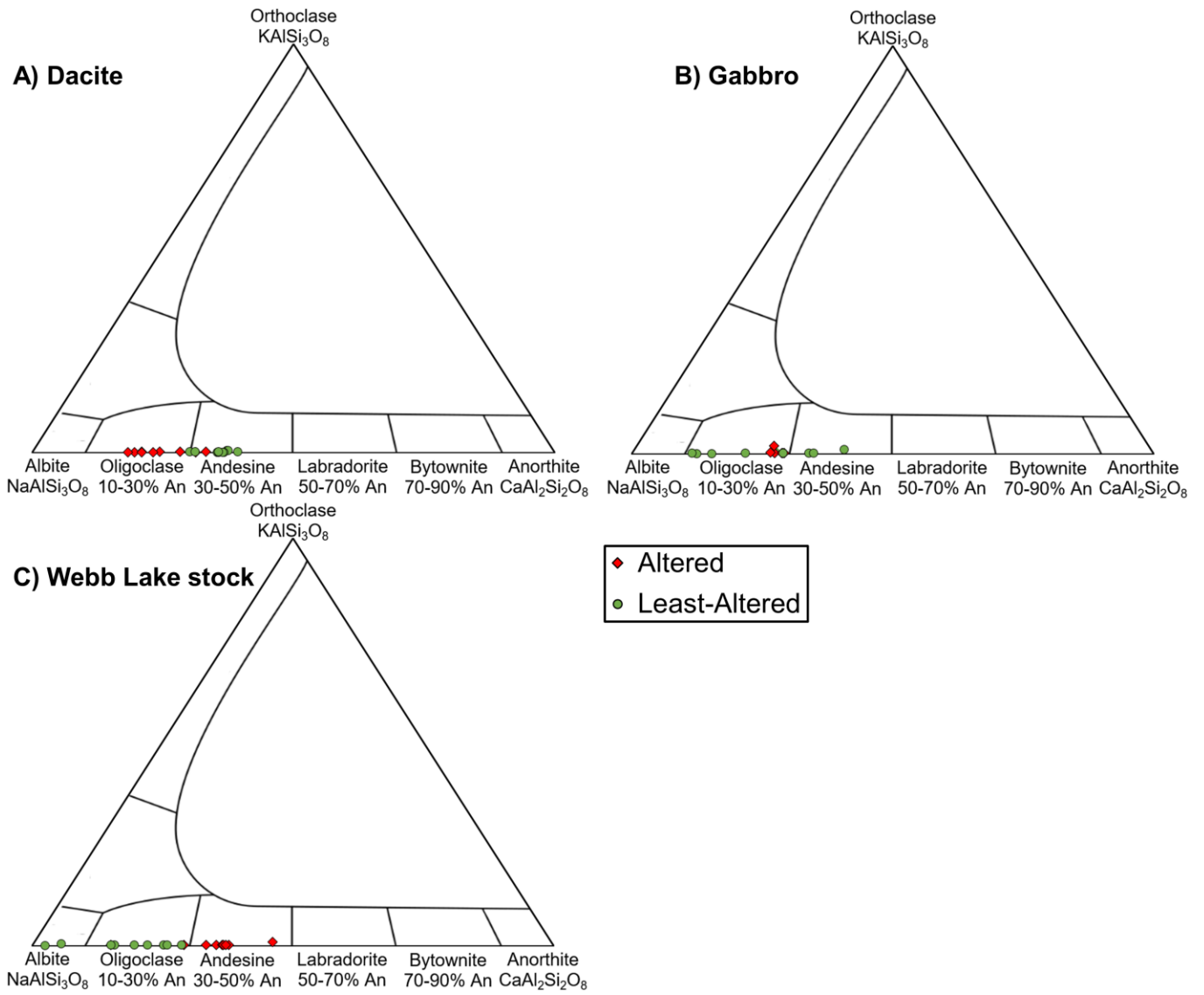
**Figure 56A–C.** Compositions of white mica from altered and least-altered equivalents plotted on Muscovite-Magnesium Celadonite-Ferroceladonite (MMF) ternary diagrams modified from Tappert et al. (2013). The location of the phengite series, ferroaluminoceladonite, and Mg-aluminoceladonite are also included. The proportions of Si, Mg, and Fe in atoms per formula unit (apfu) are used to plot on this diagram. Apfu are calculated on an 11-oxygen basis.

**Table 15A, B.** Summary of microprobe analyses of plagioclase measured in mass percent. A) Average concentrations of chemical species based on analyses of plagioclase in each sample. The number of microprobe spot locations analyzing this mineral in each sample are also shown (#). B) Minimum (min) and maximum (max) measured concentrations of oxides and elements in plagioclase in each sample. bdl=Below detection limit.

<b>A) Averages</b>	<b>SiO<sub>2</sub></b>	<b>Al<sub>2</sub>O<sub>3</sub></b>	<b>Na<sub>2</sub>O</b>	<b>MgO</b>	<b>F</b>	<b>TiO<sub>2</sub></b>	<b>CaO</b>	<b>FeO</b>	<b>MnO</b>	<b>K<sub>2</sub>O</b>	<b>Cl</b>	<b>Total</b>	<b>#</b>
Dacite	58.97	26.12	7.33	0.00	0.02	0.01	7.30	0.12	0.01	0.05	0.00	99.92	11
Altered Dacite	62.43	24.02	8.76	0.00	0.03	0.00	5.12	0.11	0.00	0.04	0.00	100.49	9
Webb Lake	63.85	22.52	9.49	0.00	0.05	0.00	3.69	0.02	0.01	0.05	0.00	99.67	9
Altered Webb Lake	60.04	25.57	7.50	0.02	0.00	0.00	7.00	0.05	0.01	0.07	0.00	100.26	9
Gabbro	62.37	24.30	8.71	0.01	0.02	0.01	5.20	0.25	0.01	0.07	0.00	100.92	8
Altered Gabbro	61.12	24.58	8.32	0.00	0.04	0.01	5.80	0.15	0.00	0.10	0.00	100.10	7

<b>B) Ranges</b>	<b>SiO<sub>2</sub></b>	<b>Al<sub>2</sub>O<sub>3</sub></b>	<b>Na<sub>2</sub>O</b>	<b>MgO</b>	<b>F</b>	<b>TiO<sub>2</sub></b>	<b>CaO</b>	<b>FeO</b>	<b>MnO</b>	<b>K<sub>2</sub>O</b>	<b>Cl</b>	<b>Total</b>
Dacite Min	56.67	24.93	6.71	bdl	bdl	bdl	6.29	0.05	bdl	0.03	bdl	99.35
Dacite Max	60.87	28.05	8.03	0.01	0.09	0.02	7.85	0.33	0.02	0.11	0.01	100.38
Altered Dacite Min	60.11	23.10	7.66	bdl	bdl	bdl	3.86	0.04	bdl	0.02	bdl	100.11
Altered Dacite Max	64.28	25.47	9.55	0.01	0.09	0.01	6.89	0.28	0.01	0.05	0.01	101.04
Webb Lake Min	61.01	19.79	8.19	bdl	bdl	bdl	0.52	bdl	bdl	0.03	bdl	99.33
Webb Lake Max	67.90	24.48	11.42	0.01	0.12	0.01	5.95	0.04	0.02	0.11	0.02	100.10
Altered Webb Lake Min	56.85	22.36	6.06	bdl	bdl	bdl	3.13	bdl	bdl	0.05	bdl	99.95
Altered Webb Lake Max	65.02	27.79	9.76	0.11	0.01	0.01	9.39	0.11	0.02	0.17	0.03	100.50
Gabbro Min	57.79	21.87	6.67	bdl	bdl	bdl	2.43	0.16	bdl	0.03	bdl	100.49
Gabbro Max	65.83	27.17	10.37	0.02	0.10	0.04	8.25	0.39	0.02	0.21	0.01	101.56
Altered Gabbro Min	60.73	24.28	8.11	bdl	bdl	bdl	5.48	0.08	bdl	0.05	bdl	99.87
Altered Gabbro Max	61.44	24.92	8.53	0.01	0.12	0.02	6.06	0.24	0.02	0.35	0.01	100.37



**Figure 57A–C.** Feldspar compositions from altered and least-altered equivalents plotted on Anorthite-Albite-Orthoclase (An-Ab-Or) ternary classification diagrams modified from Deer et al. (1963). Proportions of each end-member are calculated based on the molar proportions of Ca, Na, and K, respectively

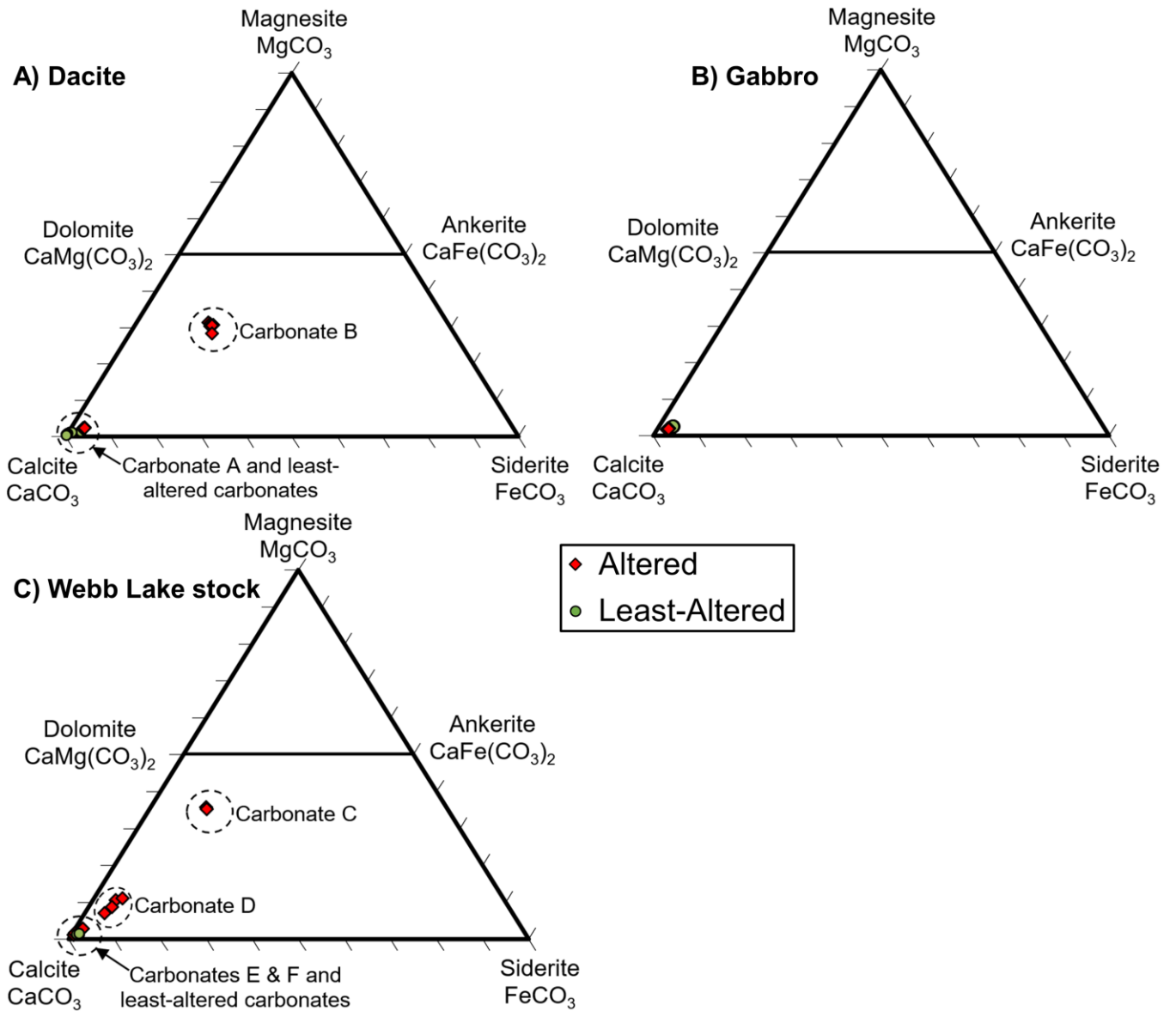


**Table 16A, B.** Summary of microprobe analyses of carbonate minerals measured in mass percent. Averages, ranges, and standard deviations for carbonate minerals with distinctly different compositions within the same sample are provided separately. A) Average concentrations of chemical species based on analyses of carbonate minerals in each sample. The number of microprobe spot locations analyzing this mineral in each sample are also shown (#). B) Minimum (min) and maximum (max) measured concentrations of oxides and elements in carbonate minerals in each sample. Cb=Carbonate, bdl=Below detection limit.

<b>A) Averages</b>		SiO <sub>2</sub>	Al <sub>2</sub> O <sub>3</sub>	Na <sub>2</sub> O	MgO	F	TiO <sub>2</sub>	CaO	FeO	MnO	K <sub>2</sub> O	Cl	CO <sub>2</sub>	Total	#
Dacite		0.08	0.05	0.02	0.26	0.07	0.01	55.19	0.51	0.35	0.01	0.00	43.47	100.01	8
Altered Dacite Cb A		0.05	0.01	0.02	0.94	0.16	0.00	52.15	2.01	0.62	0.01	0.00	44.11	100.02	8
Altered Dacite Cb B		0.15	0.06	0.04	12.41	0.06	0.02	29.90	12.31	1.26	0.02	0.00	43.90	100.11	6
Webb Lake		0.11	0.05	0.01	0.49	0.25	0.01	53.69	1.18	0.59	0.00	0.00	43.66	99.94	9
Altered Webb Lake Cb C		0.12	0.00	0.03	14.92	0.04	0.00	30.55	9.16	0.54	0.01	0.00	44.71	100.05	2
Altered Webb Lake Cb D		4.50	2.57	0.01	3.63	0.20	0.02	46.04	3.55	0.68	0.03	0.01	38.87	100.02	4
Altered Webb Lake Cb E		2.07	1.09	0.10	0.55	0.25	0.07	52.57	0.41	0.76	0.17	0.00	41.97	99.90	2
Altered Webb Lake Cb F		0.04	0.04	0.00	1.18	0.06	0.00	53.30	1.24	0.60	0.17	0.00	43.41	100.02	1
Gabbro		0.02	0.01	0.00	0.97	0.16	0.01	52.27	2.14	0.66	0.00	0.00	43.86	100.04	8
Altered Gabbro		0.02	0.02	0.02	0.76	0.07	0.01	52.86	1.65	0.72	0.01	0.00	43.97	100.09	8

<b>B) Ranges</b>		SiO <sub>2</sub>	Al <sub>2</sub> O <sub>3</sub>	Na <sub>2</sub> O	MgO	F	TiO <sub>2</sub>	CaO	FeO	MnO	K <sub>2</sub> O	Cl	CO <sub>2</sub>	Total
Dacite Min		0.03	bdl	bdl	0.06	bdl	bdl	52.12	0.11	0.15	bdl	bdl	42.58	99.91
Dacite Max		0.19	0.14	0.05	0.50	0.32	0.04	56.74	2.06	0.78	0.02	0.01	44.51	100.13
Altered Dacite Cb A Min		bdl	bdl	0.00	0.89	bdl	bdl	51.58	1.93	0.52	bdl	bdl	43.71	99.77
Altered Dacite Cb A Max		0.11	0.03	0.05	0.99	0.69	0.02	52.45	2.13	0.72	0.04	0.01	44.98	100.19
Altered Dacite Cb B Min		0.02	0.02	bdl	11.49	bdl	bdl	29.56	11.53	1.14	0.00	bdl	43.49	99.85
Altered Dacite Cb B Max		0.37	0.17	0.10	12.74	0.35	0.05	30.33	13.09	1.45	0.04	0.01	44.40	100.24
Webb Lake Min		bdl	bdl	bdl	0.45	bdl	bdl	53.08	0.96	0.54	bdl	bdl	42.34	99.73
Webb Lake Max		0.49	0.30	0.03	0.57	0.67	0.03	55.28	1.32	0.66	0.01	0.01	44.39	100.11
Altered Webb Lake Cb C Min		0.07	bdl	0.01	14.84	bdl	bdl	30.44	9.05	0.48	0.00	bdl	44.69	100.00
Altered Webb Lake Cb C Max		0.16	0.00	0.04	15.01	0.08	0.00	30.65	9.26	0.60	0.01	0.01	44.73	100.10
Altered Webb Lake Cb D Min		3.71	2.20	bdl	2.77	bdl	bdl	44.06	2.96	0.66	0.02	0.01	38.26	99.88
Altered Webb Lake Cb D Max		5.72	2.96	0.03	4.28	0.42	0.05	47.90	4.23	0.70	0.04	0.02	39.71	100.29
Altered Webb Lake Cb E Min		1.21	0.69	0.03	0.44	0.23	0.01	52.28	0.41	0.74	0.14	0.00	41.03	99.89
Altered Webb Lake Cb E Max		2.93	1.49	0.18	0.66	0.27	0.13	52.86	0.42	0.78	0.20	0.01	42.91	99.90
Altered Webb Lake Cb F Min		0.04	0.04	bdl	1.18	0.06	bdl	53.30	1.24	0.60	0.17	0.00	43.41	100.02
Altered Webb Lake Cb F Max		0.04	0.04	bdl	1.18	0.06	bdl	53.30	1.24	0.60	0.17	0.00	43.41	100.02
Gabbro Min		bdl	bdl	bdl	0.90	bdl	bdl	52.04	2.03	0.62	bdl	bdl	43.51	99.78
Gabbro Max		0.08	0.03	0.02	1.03	0.53	0.04	52.66	2.29	0.70	0.01	0.01	44.16	100.38
Altered Gabbro Min		bdl	0.01	bdl	0.71	bdl	bdl	52.27	1.50	0.65	bdl	bdl	43.09	99.91
Altered Gabbro Max		0.05	0.04	0.03	0.83	0.22	0.03	53.24	1.81	0.81	0.05	0.00	44.60	100.53



**Figure 58A–C.** Carbonate mineral compositions from altered and least-altered equivalents plotted on Magnesite-Siderite-Calcite (MSC) ternary diagrams. The location of the intermediate carbonates, dolomite and ankerite, are also included. Mole proportions of Mg, Fe, and Ca (Appendix H) are used to plot on this diagram. Total iron is assumed to be all ferrous iron.

#### 4.4 Gold indicators and grade distribution

Economic gold grades at the Island Gold deposit are located in  $V_{GD}$  and  $V_1$ - $V_2$  veins and their associated alteration envelopes. Lithologies that can host economic gold grades if they coincide with an auriferous zone include dacite, iron formation, gabbro, and the Webb Lake stock. However, iron formation was not observed to coincide with an area of  $V_{GD}$  or  $V_1$ - $V_2$  veining so the results outlined below may not apply to this lithology. Alteration minerals associated with auriferous quartz veining at the Island Gold deposit mainly include biotite, Ca-Mg-Fe carbonates, chlorite (ripidolite), plagioclase, quartz, sulphides (pyrite  $\pm$  pyrrhotite  $\pm$  chalcopyrite), and white mica (muscovite  $\pm$  phengite; Section 4.1, 4.3).

Gold grade is divided into three groups in this thesis: high-grade ( $> 4$  g/t Au), low-grade (1–4 g/t Au), and waste rock ( $< 1$  g/t Au; Figure 59). High-grade samples are restricted to auriferous quartz veins and a portion of the strongly-altered zone directly adjacent to these veins. All high-grade samples contain macroscopically visible  $V_{GD}$  or  $V_1$ - $V_2$  veins/veinlets, quartz flooding and/or silicification. These samples also typically have the highest proportion of alteration-derived minerals.

Low-grade samples are present in auriferous quartz veins, as well as the entire strongly-altered zone (Figure 59). Grades  $> 1$  g/t are typically not found in the moderately-altered zone. Most low-grade samples contained macroscopically visible  $V_{GD}$  or  $V_1$ - $V_2$  veins/veinlets, quartz flooding and/or silicification. All low-grade samples that did not have these features were samples of strongly-altered rocks that contained greater than 3 vol% sulphide minerals.

All samples of waste material ( $< 1$  g/t Au) did not have macroscopically visible  $V_{GD}$  or  $V_1$ - $V_2$  veins/veinlets, quartz flooding and/or silicification. In addition, these samples had less than 3 vol% sulphide minerals. Waste rock samples also typically have lower proportions of alteration minerals than both high-grade and low-grade samples (Section 4.1). The moderately-altered zone contains mostly 0.1–1 g/t Au whereas samples taken from the weak or least-altered zones have concentrations of gold usually  $> 0.1$  g/t (Figure 59).

In summary, macroscopically visible  $V_{GD}$  or  $V_1$ - $V_2$  veins/veinlets, quartz flooding and/or silicification are the most reliable indicators for economic gold grades at the Island Gold deposit. Sulphide minerals are also useful and easily recognizable mineral indicators that can be used to differentiate between potential low-grade material and waste that do not contain macroscopically visible  $V_{GD}$  or  $V_1$ - $V_2$  veins/veinlets, quartz flooding and/or silicification. Proportions of other

alteration minerals can be used to help discern which zone of an alteration envelope a sample is located in (Section 4.1; Figure 16, Figure 17, Figure 20), which in turn can be used to estimate gold grade. However, proportions of these minerals alone do not correspond reliably enough with gold content to be used to differentiate between cut-off grades. Subtle increases in the proportions of chlorite and carbonate minerals relative to unaltered rock mark the outer edge of alteration envelopes associated with gold-bearing quartz veins. However, the weakly-altered outer margins of these alteration envelopes are challenging to identify because chlorite and carbonates are also metamorphic minerals.

Increasing strength of alteration due to  $V_{GD}$  or  $V_1$ - $V_2$  veining in pre-gold mineralization lithologies or increasing proportions of these vein types in a given sample typically corresponds with increasing gold content. Outside of auriferous quartz veins themselves, the most reliable geochemical vectors/indicators for alteration/gold mineralization that are consistent for all lithologies are  $K_2O$ , Rb, S, and Te enrichment as well as  $Na_2O$  depletion (Table 4). Other common geochemical enrichments include As, Se, and W (Table 4). Copper concentration is consistently enriched in Webb Lake stock-hosted ore zones (Table 4). As a result, even trace amounts of chalcopyrite or other copper-bearing minerals may be a useful indicator for economic gold grades within this lithology.

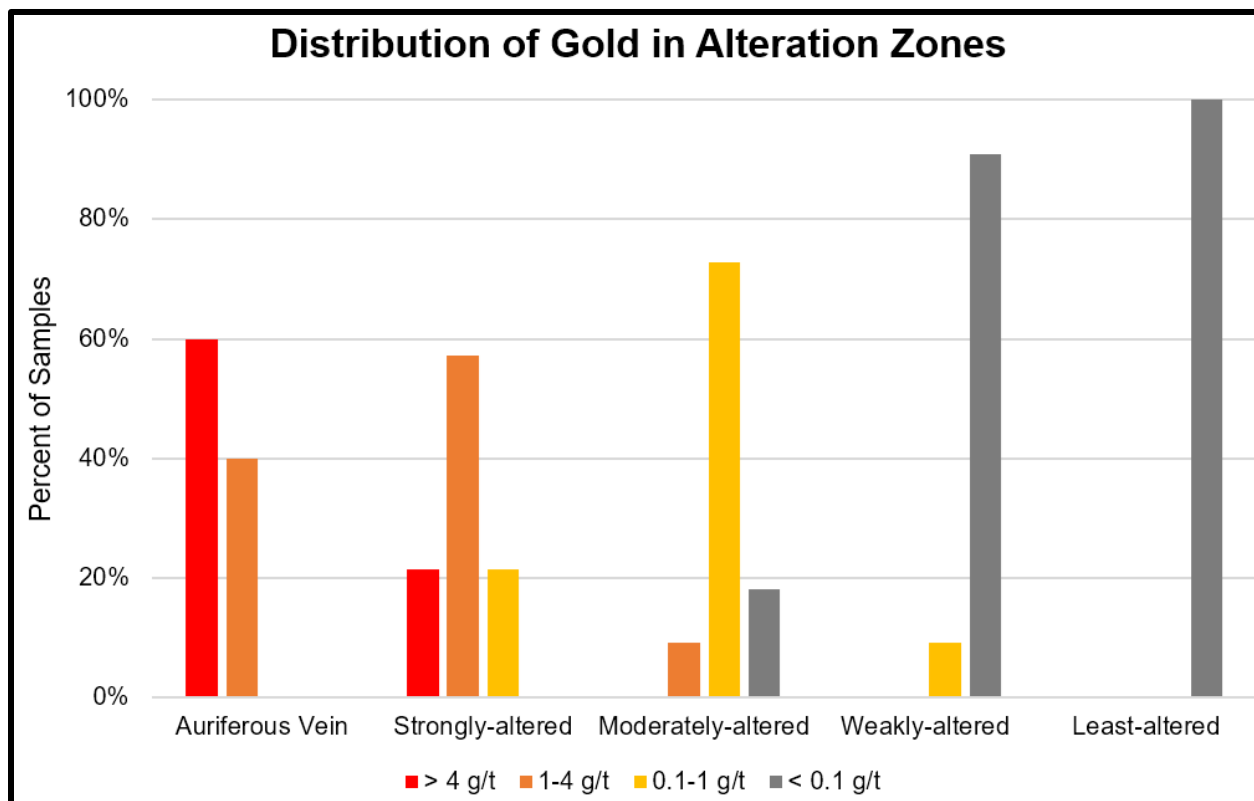


**Figure 59.** Samples of dacite, gabbro, the Webb Lake stock, as well as  $V_{GD}$  and  $V_1$ - $V_2$  auriferous quartz veins are subdivided into five groupings: Auriferous vein, strongly-altered, moderately-altered, weakly-altered, and least-altered. This histogram displays the proportion of samples, within each of these groupings, which fall into each of the gold-grade intervals outlined in the legend. Gold grade groupings used in this thesis are as follows: > 4 g/t is considered high grade, 1-4 g/t is considered low grade, and < 1.0 g/t is considered waste.

## 4.5 Sulphur isotopes

Results of sulphur isotope analyses from the University of Maryland are summarized in this section and in Figure 60. A complete list of all sulphur isotope data is presented in Appendix K and Appendix L. Two analyses of sulphur in pyrite-rich iron formations are similar (-1.33‰ and -0.46‰) while one value deviates significantly (19.60‰). All of their  $\Delta^{33}\text{S}$  and  $\Delta^{36}\text{S}$  values are consistent with  $\Delta^{33}\text{S}$  values ranging from -0.508‰ to -0.551‰ (Figure 60), and  $\Delta^{36}\text{S}$  values ranging from 0.7‰ to 0.8‰ (Appendix L).

Sulphur in  $V_1$  and  $V_2$  quartz veins and their associated alteration envelopes display fairly consistent  $\delta^{34}\text{S}$  and  $\Delta^{33}\text{S}$  values.  $\delta^{34}\text{S}$  values range from 1.22‰ to 2.92‰, and  $\Delta^{33}\text{S}$  values range from -0.057‰ to -0.033‰. These  $\delta^{34}\text{S}$  and  $\Delta^{33}\text{S}$  value ranges include samples of both pyrite and pyrrhotite from ore zones hosted by each of the three major host lithologies (dacite, tonalite–trondhjemite and gabbro).  $\Delta^{36}\text{S}$  values range from 0.06‰ to -0.05‰, excluding one pyrite sample from a gabbro-hosted alteration envelope which has an anomalously high value of 0.8‰.

Pyrite from a  $V_{\text{GD}}$  vein has a  $\delta^{34}\text{S}$  value of 2.00‰ and a  $\Delta^{36}\text{S}$  value of -0.05‰. These are consistent with the ranges of these values found in sulphides from auriferous zones throughout the deposit. However, the  $\Delta^{33}\text{S}$  value of this sample is 0.143‰ and this differs from the samples taken from auriferous quartz vein corridors zones associated with  $V_1$  and  $V_2$  vein types even if analytical uncertainty is considered.

Pyrite from a silica-poor diorite–monzodiorite intrusive that commonly parallels auriferous quartz vein corridors at this deposit has a  $\delta^{34}\text{S}$  value of 1.92‰ which is within the range of values found in sulphide minerals from auriferous quartz veins throughout the deposit. However, this is not the case for the  $\Delta^{33}\text{S}$  value of 0.806‰ and the  $\Delta^{36}\text{S}$  value of -0.1‰ which both differ significantly from these ranges.

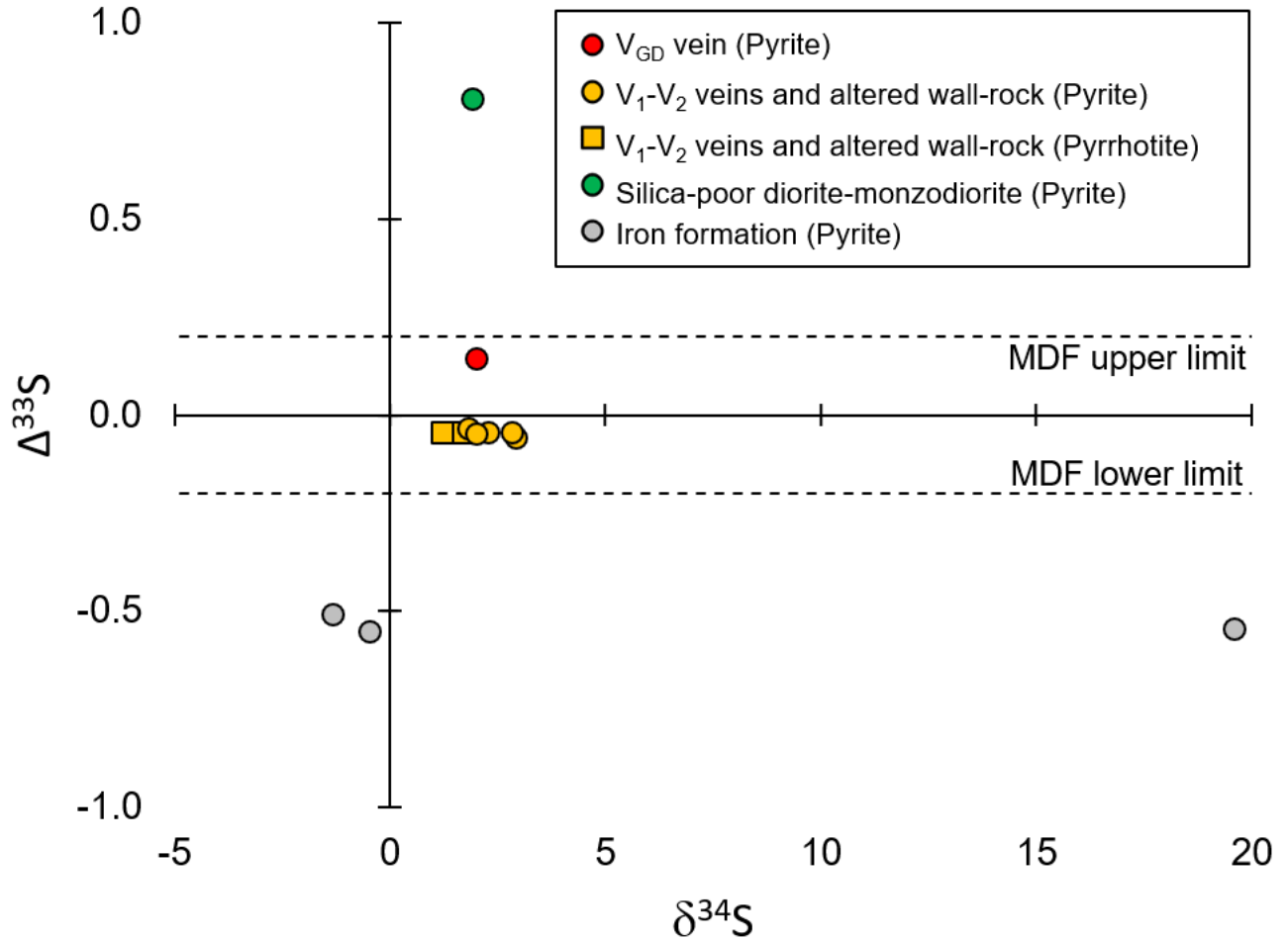


**Figure 60.**  $\delta^{34}\text{S}$  vs  $\Delta^{33}\text{S}$  plot of samples from auriferous quartz vein corridors and various other sulphide-bearing lithologies at the Island Gold deposit. Sulphides include both pyrrhotite and pyrite. Dashed lines indicate approximate upper and lower limits for  $\Delta^{33}\text{S}$  values that can be produced exclusively by MDF processes (Farquhar and Wing, 2003). Sulphides that plot outside of these points show evidence of MIF. Sulphides that plot within these bounds may have been produced through via MDF processes alone or are a combination of MDF and MIF sulphur.



#### 4.6 Laser ablation inductively coupled mass spectrometry (LA-ICP-MS)

U-Pb zircon geochronology was performed on zircons from an intensely hydrothermally-altered dacitic sample and a least-altered equivalent nearby. The alteration envelope, from which this altered sample was taken, centred around V<sub>1</sub>-V<sub>2</sub> auriferous quartz veining. As is common in ore zones related to V<sub>1</sub>-V<sub>2</sub> veins, some V<sub>3</sub> non-auriferous quartz veins and tourmaline were also present in this alteration envelope. The least-altered sample was taken from outside or at the outer margin of the alteration envelope. Zircons in both samples exhibit distinct oscillatory and sector zoning in cathodoluminescence (CL) images (Figure 61). Zircons in the least-altered sample were larger (typically <300 µm) and subhedral–euhedral (Figure 61A). Zircons in the altered sample are smaller (typically <200 µm), anhedral–subhedral, and often fractured (Figure 61B–C). Occasionally, some of these zircons have an anomalous mottled/uniform/homogeneous appearance in CL images where the oscillatory and sector zoning (Figure 61B–D) is indistinct. These anomalous areas of indistinct zonation are present as portions of zircons, rims, or affect entire zircon grains (Figure 61B–D). Centres of zircons and edges were targeted for U-Pb analysis on zircons from both the altered and least-altered sample. The spot locations where each analysis was conducted are displayed in Figure 70 (Appendix B). Geochronological results are summarized in Appendix M, Figure 62, and Figure 63.

47 analyses of zircons from the least-altered sample yielded a weighted mean <sup>207</sup>Pb/<sup>206</sup>Pb age of 2735 ± 8 Ma (MSWD = 1.04; Figure 62). This age is interpreted to represent the crystallization age of the dacite.

Excluding spot locations located on the anomalous rims and grains discussed above, 37 spots on zircons from the altered sample yielded a weighted mean <sup>207</sup>Pb/<sup>206</sup>Pb age of 2738 ± 9 Ma (MSWD = 0.53, Figure 63D), which is within uncertainty of zircon from the least-altered sample and is interpreted to represent the crystallization age of the dacite. Spot locations located on the mottled CL portions of zircons in the altered sample yielded Proterozoic ages that range from approximately *c.* 975 to 1499 Ma (Figure 63B). Some reverse discordance is observed in least-altered samples, altered samples, and standards (Figure 62A, Figure 63A–C, Figure 69A) and may be related to down-hole fractionation. Similarly, many of the Proterozoic ages plot above concordia (Figure 63B) and therefore the results should be treated with caution. Nonetheless, there is a significant Proterozoic population at *c.* 1.1–1.2 Ga (Figure 63A, B).

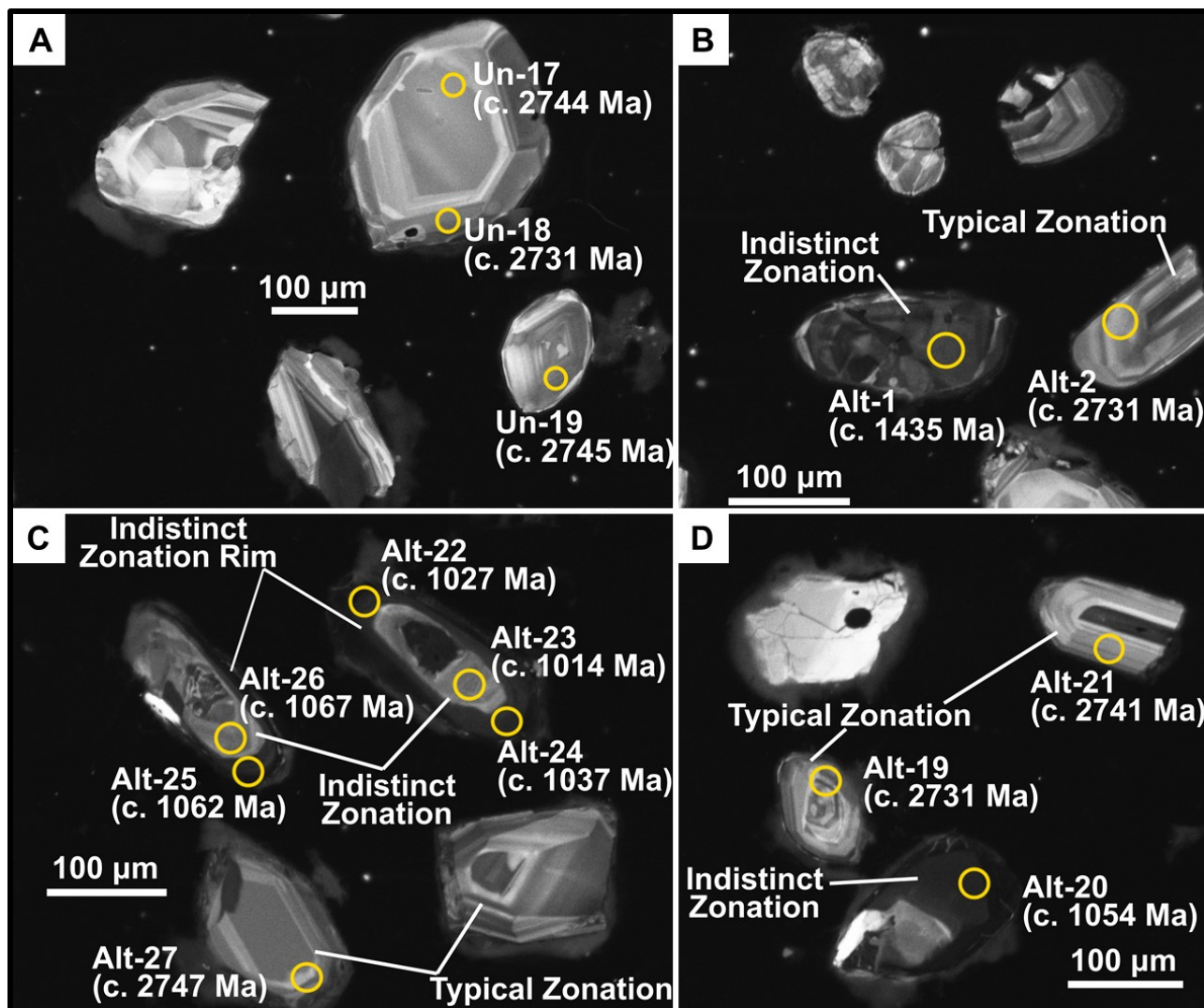


**Figure 61.** Cathodoluminescent photomicrographs of zircons from an altered dacite and a least-altered equivalent. Spot locations and  $^{207}\text{Pb}/^{206}\text{Pb}$  ages are displayed when applicable. A) Large, euhedral-subhedral zircons from the least-altered sample displaying typical distinct zonation. B) Subhedral-anhedral zircons from the altered sample. Some zircons display indistinct zonation while others display typical distinct zonation. C) Subhedral zircons from the altered sample. Some zircons display indistinctly zoned cores and rims while others display typical distinct zonation. Spot locations on zircons and corresponding approximate ages are displayed when applicable. D) Anhedral-subhedral zircons from the altered sample. Some zircons display distinct zonation while others display typical distinct zonation.

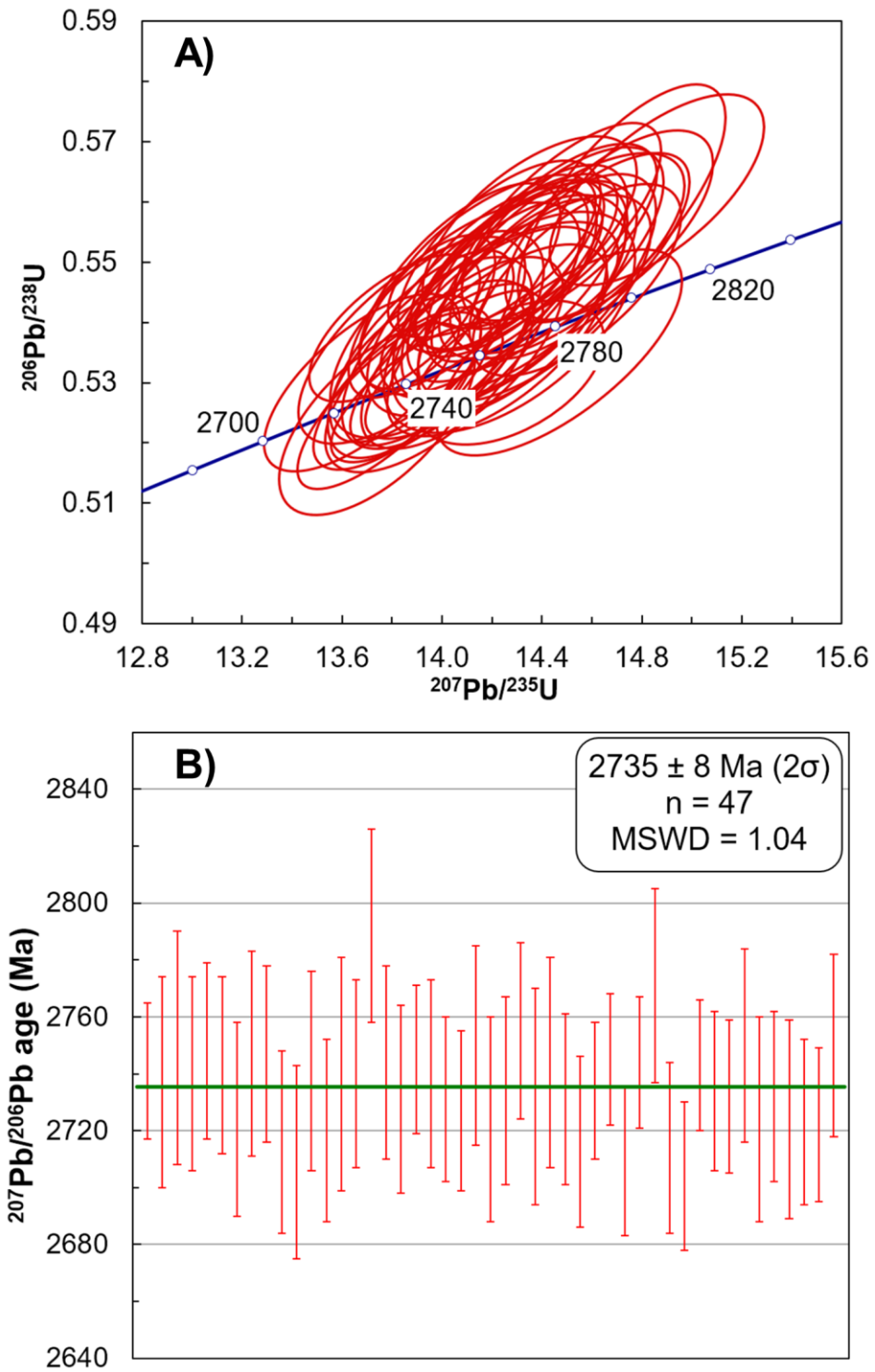


**Figure 62A, B.** Geochronological results for the least-altered sample. A) Wetherill concordia diagram (Wetherill, 1956) for 47 analyses of zircons from the least-altered sample. Error ellipses for each data point are  $2\sigma$ . B)  $^{207}\text{Pb}/^{206}\text{Pb}$  weighted mean age diagram for analyses of Archean zircons from the altered sample. MSWD=Mean Square Weighted Deviation.

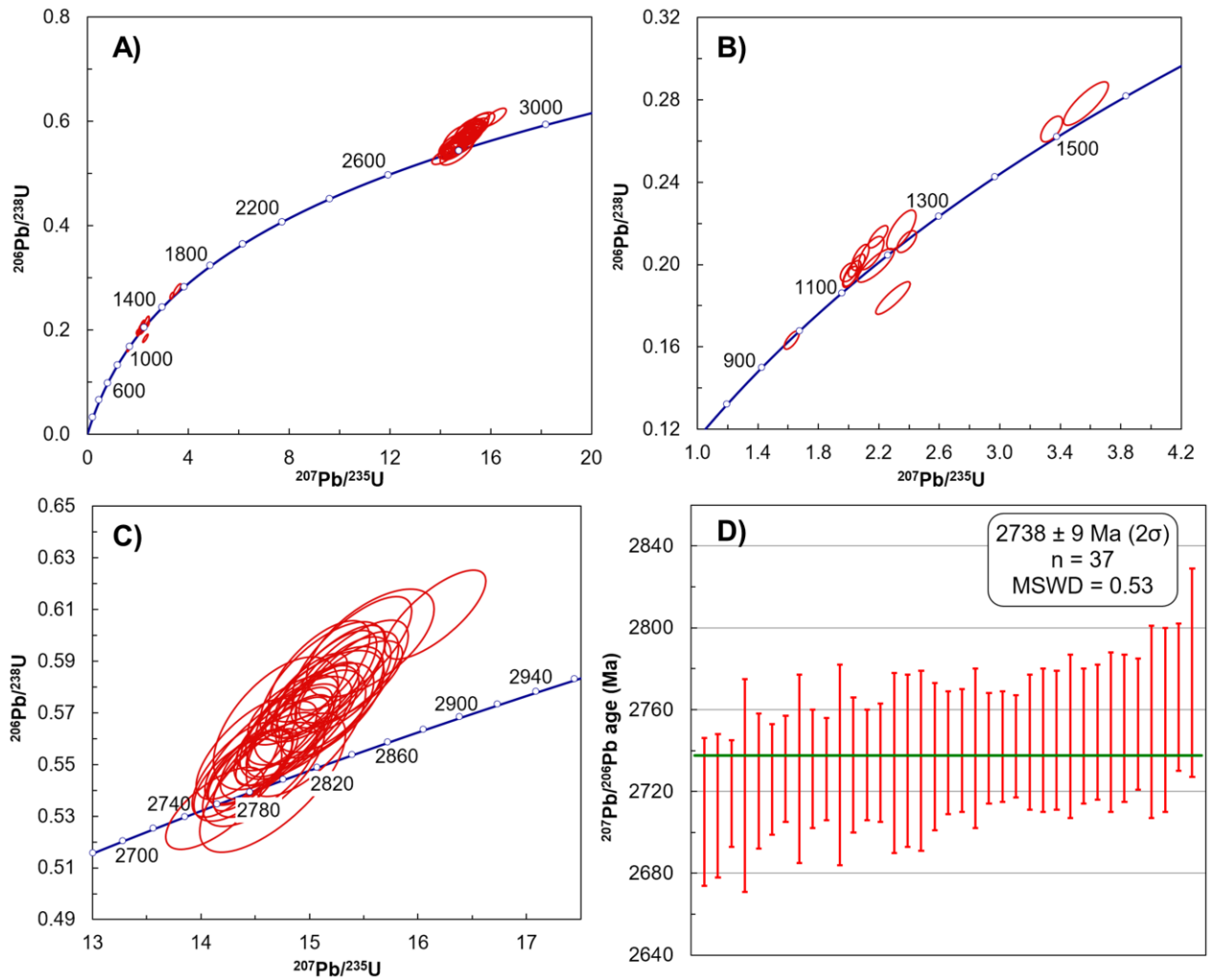


**Figure 63A–D.** Geochronological results for the altered sample. A) Wetherill concordia diagram (Wetherill, 1956) for 51 analyses of zircons from the altered sample. Note the Archean and smaller Proterozoic age groups. Error ellipses for each data point are  $2 \times \text{sigma}$ . B) Wetherill concordia diagram for 14 Proterozoic-aged analyses of zircons from the altered sample. Error ellipses for each data point are  $2 \times \text{sigma}$ . C) Wetherill concordia diagram for 37 Archean-aged analyses of zircons from the altered sample. Error ellipses for each data point are  $2 \times \text{sigma}$ . D)  $^{207}\text{Pb}/^{206}\text{Pb}$  weighted mean age diagram for Archean-aged analyses of zircons from the altered sample.  $\text{MSWD} = \text{Mean Square Weighted Deviation}$ .

## **5.0 Discussion**

### **5.1 Protoliths and genetic history**

The interpreted protoliths of each of the major lithologies at the Island Gold deposit based on field relationships, petrology and geochemistry are discussed below for each rock type. The interpreted geological significance of each rock type is also discussed when applicable.

#### **5.1.1 Dacitic volcanic rocks (T2, V2, I2)**

This lithology is interpreted to be volcanic in origin due to the presence of tuffs (often with lapilli and/or bombs), flows, pyroclastic breccias, and compositionally equivalent hypabyssal intrusive units (Figure 10). The bulk composition of these volcanic rocks are broadly dacitic based on the TAS diagram and the  $R_1$ - $R_2$  diagram (Figure 38A, B). Considering that silica is generally considered mobile during metamorphism (e.g. Ague, 1991) these diagrams may not be appropriate if silica was substantially mobilized in least-altered samples. The immobile elements are suggestive of an andesite–basaltic andesite or a dacite/rhyolite protolith (Figure 39A, B). However, the presence of a large proportion of primary minerals in many least-altered samples of this lithology (e.g. Figure 14D) suggest that the standard classification of volcanic rocks using the TAS diagram can still be used with reasonable certainty.

Archean volcanic rocks in the Superior Province are thought to be generated by volcanism related to either subduction-related processes (e.g. Wyman et al., 2002; Percival et al., 2012) or non-subduction, plume/delamination-related tectonic processes (e.g. Bédard, 2006; Bédard and Harris, 2014). Therefore, the dacitic volcanic rocks at the Island Gold deposit are not diagnostic of either tectonic process.

#### **5.1.2 Iron formation (IF)**

The iron formation at the Island Gold deposit is consistent with Algoma-type iron formations (e.g. Gross, 1980) as indicated by its limited spatial extent, Archean age, and association with volcanic rocks in a greenstone belt. This agrees with previous studies which have also classified the Michipicoten iron formation as an Algoma-type iron formation (Sage, 1994). These iron formations are thought to have formed due to periodic oxidation of iron in seawater resulting in the precipitation of iron oxides followed by periods of regular, iron-oxide-poor sedimentation. Biological and non-biological mechanisms that caused the oxidation of iron

are still debated (Bekker et al., 2010). As discussed in Section 5.7, the sulphides in these banded iron formations are believed to have a biogenic signature, which suggests that early organisms may have had a role in the genesis of these iron formations.

### **5.1.3 Gabbro (I3G)**

This mafic intrusive rock contains few primary minerals and mostly greenschist-facies assemblages (Section 4.1.10). With the exception of the Q-P plot (Figure 46C), both mobile and immobile element plots consistently indicate that the protolith is a gabbro (Figure 46). The chondrite-normalized REE profile of this lithology is flat (Figure 40B) which is characteristic of transitional mid oceanic ridge basalts (Schilling et al., 1983) or low-K (tholeiitic) island arc rocks (e.g. Gill, 1981). Given the absence of unambiguous Archean ophiolites (Warren, 2011) and the significant volume of dacitic volcanic rocks at the Island Gold deposit and surrounding area, a mid ocean ridge origin is unlikely and it is more probable that this lithology is related to an island arc setting.

### **5.1.4 Webb Lake stock: Tonalite–trondhjemite (I1JM)**

With the exception of chlorite replacing primary biotite, the least-altered and weakly-altered samples of the Webb Lake stock appear to be composed mostly of primary minerals. These samples plot in the tonalite field of the QAP diagram (Figure 27) and the trondhjemite field of the Anorthite-Albite-Orthoclase diagram (Figure 48). The amount of ferromagnesian minerals in most samples is > 10 vol%, which is consistent with a tonalite (Barker, 1979). However, some samples, particularly those farther from the margins of the Webb Lake stock contain < 10 vol% ferromagnesian minerals and are therefore considered trondhjemite. In summary, the Webb Lake stock ranges from tonalitic to trondhjemitic in composition at the Island Gold deposit.

The REE patterns of least-altered samples of the Webb Lake stock, including the lack of Eu anomalies, are typical of Archean tonalite-trondhjemite-granodiorites (TTGs) (Moyen and Martin, 2012). The genesis of Archean TTGs is still widely debated and both subduction and non-subduction genetic models are considered (Moyen and Martin, 2012). Therefore, this rock type is not diagnostic of a particular geodynamic setting.

### 5.1.5 Gabbro/Lamprophyre (I2H)

This lithology has a similar appearance to the gabbro discussed in Section 5.1.3. Key mineralogical, textural, and chemical differences that can be used to differentiate between these lithologies are summarized in Appendix A. This lithology contains few primary minerals and mostly greenschist-facies assemblages (Section 4.1.10). Based on the chemical composition and metamorphic mineral assemblage, interpreted primary minerals likely consisted mainly of Ca-rich plagioclase, hornblende, pyroxene, and potentially olivine.

Mobile and immobile element plots are consistent with gabbro or diorite classifications (Figure 46). This lithology may be a gabbro or silica-poor gabbro based on the low concentrations of SiO<sub>2</sub>. Yet, the high proportion of volatiles (LOI of 7.5–18.1 wt%), high average Cr (405 ppm), Ni (317 ppm), Th (6 ppm), and Na<sub>2</sub>O (1.6 wt%) content, low average Si content (43.5 wt%), and occurrence as dykes suggest that a low-K lamprophyre is another potential alternative (Streckeisen et al., 2002). Based on the relatively high average Na<sub>2</sub>O (1.6 wt%) and CaO (10.6 wt%), but low K<sub>2</sub>O (0.2 wt%), this sodic-calcic lamprophyre likely had low proportions of primary potassium-rich minerals (e.g. biotite or potassium feldspar). Therefore, it would be classified as spessartite which is dominated by hornblende and plagioclase (Streckeisen et al., 2002). However, lamprophyres are typically enriched in potassium (Streckeisen et al., 2002), so a gabbroic classification is still plausible.

This REE pattern of least-altered samples of this lithology is similar to that of ocean island basalts (Wilson, 1989), and continental flood basalts (Hooper and Hawkesworth, 1993). It is also similar to the REE pattern of lamprophyres (e.g. Zhilong et al., 2002) including those in the Superior Province (e.g. Stern and Hanson, 1992). Therefore, the protolith of this lithology is interpreted to be either a lamprophyre (spessartite) or a gabbro. Neither of these lithologies are restricted to a certain tectonic setting.

### 5.1.6 Quartz diorite

This lithology appears less affected by metamorphism than many other lithologies at the Island Gold deposit and is classified as a quartz diorite based on mineralogy (Figure 27). Mobile and immobile element chemical classification plots suggest a quartz monzonite, quartz syenite, and syenite classification (Figure 46). However, the extremely low potassium content (0.05 wt% K<sub>2</sub>O) and absence of primary potassium feldspar discount these potential classifications. The



quartz-carbonate veins observed in the quartz diorite xenoliths but not the silica-poor diorite–monzodiorite (Figure 32A) likely formed due to competency differences between the two lithologies. The quartz diorite is brittle relative to the silica-poor diorite–monzodiorite and as a result, the quartz diorite fractured rather than deforming when stress was applied. Dioritic rocks are present in a wide range of tectonic environments and as a result are not diagnostic of a specific geological setting.

### **5.1.7 Silica-poor diorite–monzodiorite (I2M)**

The silica-poor diorite–monzodiorite may have a similar appearance to the gabbro and gabbro/lamprophyre discussed in Sections 5.1.3 and 5.1.5. Key mineralogical, textural, and chemical differences that can be used to differentiate between these lithologies are summarized in Appendix A. The variability in the appearance and chemical composition of the silica-poor diorite–monzodiorite may be caused by variable magmatic assimilation of earlier lithologies (e.g. Figure 32A). This unit is classified as a diorite based on its current mineralogical composition (Figure 27). Primary potassium feldspars may have been present in greater proportions in the protolith but have since been replaced by biotite and white mica. As a result, a monzodiorite protolith could also be possible. Mobile element and immobile element plots suggest a wide range of classifications that broadly agree with diorite or monzodiorite. These include monzodiorite, monzogabbro, foid-bearing gabbro, foid-bearing monzogabbro, monzonite, diorite, and gabbro-diorite (Figure 46A–D). The presence of primary oligoclase and lack of significant proportions of ferromagnesian minerals is inconsistent with a gabbro. The low silica content (37.9 to 45.9 wt%) suggests the potential for primary feldspathoids that may have been replaced during metamorphism and alteration. However, no feldspathoid minerals were observed, so a silica-poor diorite–monzodiorite is an appropriate name for the likely protolith.

This intrusion may be related to other silica-undersaturated intrusions in the area, such as the Herman Lake nepheline syenite intrusive complex that was dated at  $2671 \pm 17/-10$  Ma (Corfu and Sage, 1992). This age is similar to that obtained from this silica-poor diorite–monzodiorite at the Island Gold deposit ( $2672.2 \pm 3.5$  Ma; Jellicoe, 2019). Low degrees of partial melting of the alkali-rich, subcontinental lithospheric mantle lherzolite due to lithospheric extension can generate silica-undersaturated magmas equivalent to a nepheline syenite (Laporte et al., 2014).

### **5.1.8 Diabase–quartz diabase (I3DD)**

This lithology is classified as a gabbro–quartz gabbro based on the QAP diagram (Figure 27). This intrusion is typically fine-grained (Figure 36A), particularly at its margins, which is consistent with a diabase–quartz diabase and supports the classification by Sage (1994). Mobile and immobile element classification plots suggest gabbro, alkali gabbro, gabbro-diorite, and quartz diorite classifications (Figure 46A–D) which broadly support this diabase/gabbro classification. This lithology may correspond with the Matachewan dyke swarm which occurred at 2473 ±16/-9 (Heaman, 1997) and has been previously documented in this area (e.g. Jellicoe, 2019). Average concentrations of SiO<sub>2</sub>, alkalis (Na<sub>2</sub>O + K<sub>2</sub>O), Fe<sub>2</sub>O<sub>3</sub>T, MgO, Ni, and Cr in the diabase–quartz diabase fall within the concentration ranges of Matachewan dykes in Ciborowski et al. (2015). Chondrite-normalized rare-earth element patterns of diabase–quartz diabase samples from this thesis (Figure 40G) are consistent with those of those of known Matachewan dykes (Ciborowski et al., 2015) suggesting the diabase–quartz diabase at the Island Gold deposit is part of the Matachewan dyke swarm. These rare-earth element patterns are similar to those of enriched mid-ocean ridge basalts (MORBs), ocean island basalts (OIBs), and continental flood basalts (Schilling et al., 1983; Wilson, 1989; Hooper and Hawkesworth, 1993). However, the setting of these dykes is not characteristic of MORBs or OIBs. Flood basalts, on the other hand, have been linked to the Matachewan Large Igneous Province which includes the Matachewan dyke swarm (Ciborowski et al., 2015). The Matachewan dykes are believed to be related to a mantle plume that resulted in rifting and continental break-up (Ciborowski et al., 2015).

## **5.2 Greenschist-facies metamorphism**

The abundance of typical greenschist-facies metamorphic minerals such as chlorite, actinolite, and epidote at the Island Gold deposit is consistent with regional greenschist-facies metamorphism which has previously been interpreted in the Michipicoten greenstone belt (e.g. Sage, 1994). The margins of the Michipicoten greenstone belt reached amphibolite-facies conditions (Ayres, 1978) but at the Island Gold deposit, the vast majority of samples do not show evidence for metamorphism exceeding greenschist-facies conditions. The sporadic, late, randomly-oriented chloritoid and, in rare cases garnet (often associated with chloritoid; Figure 65), likely formed at the end or after regional deformation. This is because these minerals are typically not preferentially-oriented. These minerals may have formed during the later stages of

regional metamorphism because these minerals often overprint other metamorphic minerals. However, the distribution of rocks bearing these minerals and their metamorphic significance is not clear. Alternatively, the gabbro and chloritoid may be related to an alteration event unrelated to regional metamorphism.

Metamorphism continued after the formation of the gold-bearing quartz veins but appears to have had only a minor effect on the alteration assemblages generated as a result of gold mineralization. Greenschist-facies assemblages are easily observed in the gabbro and gabbro/lamprophyre and are less obvious in the quartz diorite and silica-poor diorite–monzodiorite. The quartz diorite and silica-poor diorite–monzodiorite may have been emplaced after peak metamorphism. The diabase–quartz diabase intrusions have been affected the least by metamorphism and only display minor growth of metamorphic minerals, typically at the margins of primary minerals. Therefore, the intrusion of the diabase–quartz diabase is interpreted to post-date regional greenschist-facies metamorphism, which occurred during D2 deformation (Jellicoe, 2019).

### **5.3 Auriferous quartz vein-related alteration**

#### **5.3.1 $V_{GD}$ and $V_1$ - $V_2$ vein-related alteration of dacitic volcanic rocks**

$V_{GD}$  and  $V_1$ - $V_2$  veining resulted in the growth of the same alteration minerals. Besides the larger proportion of white mica and chlorite and lower proportions of quartz and feldspar in samples altered by  $V_{GD}$  veins compared to samples altered by  $V_1$ - $V_2$  veins, the alteration mineral assemblages associated with these vein types are very similar (Figure 16). These differences in the proportion of minerals may be attributed to protolith compositional differences or differences in the extent of alteration. Besides minerals in samples altered by  $V_1$ - $V_2$  veins typically exhibiting more deformation, samples altered by  $V_1$ - $V_2$  veins and those altered by  $V_{GD}$  veins are also texturally equivalent. The alteration envelopes associated with  $V_1$ - $V_2$  veins tend to be larger (Section 4.1.2.1). This is interpreted to be due to the shearing associated with  $V_1$ - $V_2$  veining creating more structural conduits which can accommodate the movement of hydrothermal fluids further outward from the central vein. Furthermore, with the exception of LOI, Se, and Tl, all chemical species that were typically enriched (As, Au, Bi,  $K_2O$ , Rb, S, Te and W) and depleted ( $Na_2O$  and Sr) as a result of alteration associated with  $V_1$ - $V_2$  veining were also enriched and depleted as a result of alteration related to  $V_{GD}$  veining (Table 4). Based on mass balance

calculations, these chemical species also generally had the greatest magnitude of enrichment/depletion relative their concentrations in least-altered samples (Table 5, Table 6). The consistency of the mineralogy, textures, and chemistry of samples altered by  $V_{GD}$  veins and samples altered by  $V_1$ - $V_2$  veins suggests that these veins were produced under comparable conditions by a hydrothermal fluid of similar composition. The same mineralogical and chemical vectors can be used when exploring for gold mineralization related to  $V_{GD}$  and  $V_1$ - $V_2$  vein types.

The addition of  $K_2O$  during alteration resulted in the growth of muscovite in altered samples and the addition of sulphur generated Fe-sulphide minerals at the expense of primary and metamorphic Fe-bearing minerals. This is consistent with the lower Fe content in chlorite in altered samples (Figure 55A; Table 13). This is also supported by pyrite clusters near pre-existing iron-bearing minerals (e.g. Figure 18).

There is not a continuous increase in the proportion of carbonate minerals with increasing alteration because there are generally more carbonate minerals in the moderately-altered zone than either the strongly-altered or weakly-altered zones (Figure 16A, B). This is because strongly-altered rocks are directly proximal to quartz veins. Silicification is a significant alteration type adjacent to quartz veins and results in less carbonate minerals adjacent to these veins compared to the moderately-altered zone. As a result, despite carbonates being major alteration minerals,  $CO_2$  (a major constituent of carbonate minerals) does not consistently correlate with increasing alteration (Table 4) because strongly-altered samples often contain less  $CO_2$  than moderately-altered samples.

Plagioclase in the least-altered sample is andesine while plagioclase in the altered sample ranges from oligoclase to andesine (Figure 57A). This suggests that alteration resulted in either the replacement of Ca with Na in relict primary andesine producing oligoclase or the formation of some alteration-derived oligoclase. In addition, the proportion of plagioclase in altered samples is significantly lower than in least-altered samples indicating that alteration related to  $V_1$ - $V_2$  veining resulted in the significant breakdown of primary plagioclase. As a result,  $Na_2O$  depletion due to alteration is probably a result of the breakdown of primary andesine and the removal of sodium by the hydrothermal fluid.

Significant alteration-derived quartz is generally restricted to the strongly-altered zones and hence  $SiO_2$  is not consistently enriched due to alteration across entire alteration envelopes (Table 4). Given the enrichment in Au, As, Bi, Rb, Se, Te, and Tl (Table 4), these elements were

likely associated with the Au-bearing fluid(s), however, these elements were not introduced in large enough quantities to result in the formation of visible minerals that contain these chemical species as a major structural component (e.g. tellurides). Similarly, the fluid likely resulted in the removal of Sr which was not present in a significant amount prior to alteration to form any minerals with Sr as a major structural component.

### **5.3.1.1 Deposit-scale variations in V<sub>1</sub>-V<sub>2</sub> vein-related alteration**

The mineralogy and chemistry of dacitic samples taken from alteration envelopes associated with V<sub>1</sub>-V<sub>2</sub> veining in the dacitic volcanic rocks are consistent throughout the deposit (Sections 4.1.2.3.1 and 4.2.2.2.1) with some minor differences. These minor anomalous gains and losses of a variety of chemical species were observed in each alteration envelope. These are attributed to limited sampling of individual alteration envelopes resulting in apparent gains and losses due to non-alteration-related sample heterogeneities.

Increased silicification is noted in the strongly-altered sample from the deepest alteration envelope studied (Figure 68; Appendix B). This tentatively suggests that silicification may be a more dominant alteration type in deeper ore zones associated with V<sub>1</sub>-V<sub>2</sub> veining. The strongly-altered sample from a V<sub>1</sub>-V<sub>2</sub> ore zone located approximately at the centre of current mine workings (~500m depth; Figure 19) has more white mica (44 vol%) when compared to the white mica content in the average strongly-altered sample (33 vol%). This is probably the result of V<sub>3</sub> veining and/or a protolith more enriched in aluminum. The low amount of carbonate minerals noted in strongly-altered samples from both the central (<1 vol%) and deep ore zones (1 vol%) (Figure 19), is attributed to these samples being taken from the portion of the strongly-altered zone directly adjacent to V<sub>1</sub>-V<sub>2</sub> veining. Low proportions of carbonates are often present in the portion of the strongly-altered zone that is proximal to auriferous quartz veining. The moderately-altered zone and the distal portion of the strongly-altered zone typically have more carbonate minerals. Besides these minor differences in mineral proportions discussed above, the overall signature of the alteration in dacite-hosted alteration envelopes related to auriferous quartz veining remains consistent with varying distance parallel to the GLDZ and elevation.

### 5.3.2 V<sub>1</sub>-V<sub>2</sub> vein-related alteration of gabbro

Gains of K<sub>2</sub>O due to alteration associated with V<sub>1</sub>-V<sub>2</sub> veining in gabbro-hosted alteration envelopes at the Island Gold deposit is due to the increased amount of biotite in alteration zones (Figure 17A). Higher sulphide mineral proportions in altered zones (Figure 17A) results from the introduction of S. Similar to the dacite, there is not a continuous increase in the proportion of carbonate minerals with increasing alteration. In this case, fewer carbonate minerals were observed in the moderately-altered sample compared to the strongly-altered and weakly-altered samples (Figure 17A). As a result, despite calcite being a major alteration mineral, increasing CO<sub>2</sub> and CaO content do not consistently correspond with increasing alteration (Table 4).

The restricted range of plagioclase compositions (oligoclase) in the altered sample relative to the large range of plagioclase compositions (oligoclase to andesine) in the less-altered sample (Figure 57B) indicates that plagioclase generated via metamorphism was replaced by oligoclase during alteration related to V<sub>1</sub>-V<sub>2</sub> veining. Plagioclase modes also increase in altered samples. Na<sub>2</sub>O depletion in altered samples (Figure 47) is due to the breakdown of sodic, metamorphic-derived oligoclase (almost albite; Figure 57B) and sodium-bearing amphibole.

Alteration-derived quartz is restricted to the strongly-altered zone and hence SiO<sub>2</sub> is not consistently enriched due to alteration across entire alteration envelopes (Table 4). Gold is present mainly as free gold in the quartz veins and altered wall rock and is interpreted to have been introduced by the fluid that generated the V<sub>1</sub>-V<sub>2</sub> veins. The larger proportion of tourmaline in altered samples is due to mass gains in B (Figure 47). This may be because the post-V<sub>1</sub>-V<sub>2</sub> fluid that caused the formation of tourmaline utilized pre-existing structural conduits including the shear zones where V<sub>1</sub>-V<sub>2</sub> veining occurs. As a result, there is generally a positive correlation with tourmaline content and alteration intensity because alteration intensity increases when moving towards the centre of the shear zone.

Additionally, the auriferous hydrothermal fluid was likely enriched in Ba, Cs, Li, MnO, Pb, Rb, Sm, Sr, and Te resulting in the addition of these chemical species to altered samples (Table 4). The fluid likely removed Bi, Ge, P<sub>2</sub>O<sub>5</sub>, Sb, and Tl (Table 4). Unlike the dacitic volcanic lithology, only one alteration envelope hosted gabbro was studied and it is unclear how representative this single transect of a gabbro-hosted V<sub>1</sub>-V<sub>2</sub> vein-related alteration envelope is for the entire deposit.

### 5.3.3 V<sub>1</sub>-V<sub>2</sub> vein-related alteration of the Webb Lake stock

Unlike the dacite and gabbro, evidence of K<sub>2</sub>O influx due to V<sub>1</sub>-V<sub>2</sub> vein-related alteration (Figure 49) resulted in significant growth of both white mica and biotite in the Webb Lake stock. Carbonate mineral growth is attributed to gains of C and CO<sub>2</sub> (Figure 49) while sulphide mineral formation results in consistent S enrichment in altered samples (Table 4). The mass loss of FeO and simultaneous mass gain of ferric iron due to alteration (Figure 49) suggests the conversion of ferrous iron to ferric iron and this indicates that the gold-bearing fluid was relatively oxidizing. There is also a loss of total iron but this is typically negligible relative to the more significant gains of Fe<sub>2</sub>O<sub>3</sub> and losses of FeO (e.g. Figure 49). Increasing concentrations of sulphide minerals in altered samples (Table 4) indicates that the gold-bearing fluid was also sulphur-bearing. The spatial association of alteration-derived sulphide minerals with iron-bearing minerals such as biotite and chlorite indicates that iron was sourced from these minerals for sulphide mineral growth. This is supported by lower concentrations of Fe in biotite (Table 12) and chlorite (Table 13) in altered samples. Na<sub>2</sub>O depletion due to alteration is likely due to the breakdown of sodic plagioclase (albite and oligoclase) in altered samples (Figure 57C).

Similar to gabbro and dacite-hosted alteration envelopes, alteration-derived quartz is restricted to the strongly-altered zone and hence SiO<sub>2</sub> is not enriched due to alteration (Table 4). Similar to dacite and gabbro-hosted ore zones, gold is present mainly as free gold in the quartz veins and altered wall rock and is interpreted to have been introduced by the fluid that generated the V<sub>1</sub>-V<sub>2</sub> veins. Presence of trace chalcopyrite, particularly in strongly-altered samples, explains the enrichment in Cu (Table 4). Breakdown of primary and metamorphic calcium-bearing minerals such as epidote and hornblende and removal of CaO by the hydrothermal fluid accounts for the loss of CaO (Table 4). The larger amount of tourmaline typically observed in altered samples can be attributed to an influx of B (Table 4). However, the B-rich fluid that produced the tourmaline post-dates V<sub>1</sub>-V<sub>2</sub> veins and the same reasons for tourmaline enrichment as discussed in Section 5.3.2 also apply here.

Additionally, the hydrothermal fluid was likely enriched in Ag, As, Bi, Ge, Mo, Rb, Se, Ta, Te, U, and W resulting in the addition of these elements to altered samples (Figure 49). The fluid likely resulted in the removal of Co, MnO, Sc, SiO<sub>2</sub>, and Sm resulting in losses of these elements due to alteration (Table 4). However, only one alteration envelope hosted by the Webb Lake stock was studied and it is unclear if these results can be extrapolated to the entire deposit.



#### 5.4 Comparison of auriferous alteration within different lithologies

Alteration related to V<sub>1</sub>-V<sub>2</sub> veining at the Island Gold deposit results in the significant and consistent enrichment of Au, K<sub>2</sub>O, Rb, S, and Te in all altered/less-altered pairs studied, regardless of their protolith (Table 4; Section 4.2). With the exception of a single dacitic altered/less-altered pair, Na<sub>2</sub>O depletion also consistently occurs due to V<sub>1</sub>-V<sub>2</sub> veining (Table 4). The consistent enrichment and depletion of these elements suggests that alteration envelopes associated with V<sub>1</sub>-V<sub>2</sub> veins throughout the deposit were all generated by the same fluid.

Alteration minerals associated with V<sub>1</sub>-V<sub>2</sub> auriferous quartz veining mainly consist of biotite, Ca-Mg-Fe carbonates, chlorite (ripidolite), plagioclase, quartz, sulphides (pyrite ± pyrrhotite ± chalcopyrite), and white mica (muscovite ± phengite) (Section 4.1 and 4.3). The mineralogical changes between each zone and key mineralogical relationships that help define alteration zones in each pre-gold mineralization lithology are summarized in Figure 20. White mica is the dominant potassic mica in alteration envelopes hosted by the dacite and the Webb Lake stock (Figure 16A–C; Figure 17B). This is interpreted to be due to the simultaneous addition of potassium and the breakdown of primary plagioclase thereby providing the chemical components necessary for the growth of white mica (mainly K, Al, Si, and O). White mica is an insignificant alteration mineral in gabbro-hosted alteration envelopes (Figure 17A) when compared to dacite and Webb Lake stock-hosted alteration envelopes (Figure 16A–C; Figure 17B). Instead, biotite is the dominant potassic mineral and is likely the result of gabbro containing less Al and more Fe and Mg than the dacite and Webb Lake stock (Table 17). Significant growth of plagioclase due to alteration exclusively occurs in the gabbro (Section 4.1.4.3). Biotite is also a minor alteration mineral in the Webb Lake stock (Figure 17B), perhaps suggesting that the conversion of plagioclase to white mica was not as pervasive as in the dacite and, as a result, some alteration-derived biotite formed. Chlorite that is clearly alteration-derived was not identified in Webb Lake stock-hosted alteration envelopes but, based on slight differences in the chemistry of chlorite in altered and least-altered samples (Section 4.3.2), it may be present in minor proportions.

Carbonates in altered samples of gabbro are almost exclusively calcite (Figure 58B) whereas carbonates in altered dacitic and Webb Lake stock samples are a combination of calcite and Ca-Mg-Fe carbonates (Figure 58A, C). This suggests that calcite forms preferentially when the lithology contains significant CaO (as is the case with the gabbro; Table 17). Besides these

differences in mineralogy, which are likely due to differences in protolith composition, the alteration mineral assemblages in V<sub>1</sub>-V<sub>2</sub> alteration envelopes hosted by the dacite, gabbro, and Webb Lake stock are relatively consistent.

V<sub>GD</sub> veins were generated as a result of an earlier event as indicated by structural (Jellicoe, 2019) and isotopic evidence (Section 5.7). The alteration related to V<sub>GD</sub> veins was studied through the examination of one dacite-hosted alteration envelope. The mineral assemblage is consistent to that observed in dacite-hosted alteration envelopes associated with V<sub>1</sub>-V<sub>2</sub> veins (Figure 16). Similarly, the same consistent and significant enrichments and depletions of chemical species observed as a result of alteration of dacites by V<sub>1</sub>-V<sub>2</sub> veins also occur as a result of alteration related to V<sub>GD</sub> veins (Table 4). Although V<sub>GD</sub> veins are a result of an earlier auriferous veining event, the mineralogical and chemical signature of the alteration is almost identical to that of V<sub>1</sub>-V<sub>2</sub> veins. It is therefore extrapolated that gabbro or Webb Lake stock-hosted alteration envelopes associated with V<sub>GD</sub> veins would have the same mineralogical and chemical signature as those associated with V<sub>1</sub>-V<sub>2</sub> veins. This reaffirms that the same geochemical and mineralogical vectors towards V<sub>1</sub>-V<sub>2</sub> auriferous zones can be employed when exploring for V<sub>GD</sub> auriferous zones.

The gabbro/lamprophyre and silica-poor diorite–monzodiorite post-date and cross-cut the V<sub>1</sub>-V<sub>2</sub> veins (e.g. Figure 34C). Multiple samples of the gabbro/lamprophyre and silica-poor diorite–monzodiorite were taken from intrusions that were located directly adjacent or near V<sub>1</sub>-V<sub>2</sub> auriferous veining. The lack of substantial enrichment of these samples in Au, K<sub>2</sub>O, Rb and S further supports that V<sub>GD</sub> and V<sub>1</sub>-V<sub>2</sub>-related alteration did not affect these lithologies. Similarly, the absence of notable alteration and key alteration minerals further affirms this interpretation.

## **5.5 Comparison with other orogenic gold deposits**

Many aspects of the mineralogical and chemical signature associated with gold mineralization at the Island Gold deposit are commonly featured in other orogenic gold deposits throughout the world. These aspects include the presence of biotite, carbonates, chlorite, plagioclase, sericite, and sulphides in the auriferous alteration assemblage. Additional features commonly include chemical enrichments of As, Au, K, S, Te, and W as a result of auriferous quartz veining (Groves et al., 1998). This supports the interpretation that the Island Gold deposit is an orogenic gold deposit (e.g. Adam et al., 2017).

The large fault systems east of the Kapuskasing Structural Zone (KSZ) that host major orogenic gold deposits have been correlated with the Goudreau Lake Deformation Zone (GLDZ) which hosts the Island Gold deposit (Leclair et al., 1993). Studies of a number of gold deposits east of the KSZ near Timmins (Hoyle Pond, Dome), Kirkland Lake (Kerr-Addison, Young-Davidson, Beattie), and Rouyn-Noranda (Francoeur 3) (Figure 2) were reviewed. These deposits are typically characterized by enrichments in Au, K<sub>2</sub>O, Rb, and S (Dinel et al., 2008; Moritz and Crocket, 1991; Kishida and Kerrich, 1987; Martin, 2012; Bigot, 2012; Couture and Pilote, 1993) which is consistent with the Island Gold deposit (Table 4). Other common enrichments in these deposits east of the KSZ often include As, Ba, CO<sub>2</sub> (and/or volatiles/LOI), SiO<sub>2</sub>, and W (Dinel et al., 2008; Moritz and Crocket, 1991; Kishida and Kerrich, 1987; Martin, 2012; Bigot, 2012; Couture and Pilote, 1993). These enrichments also commonly occurred due to auriferous vein-related alteration at the Island Gold deposit but did not consistently occur in each host lithology and all altered/less-altered pairs (Table 4). Sodium enrichment in the wall-rock around auriferous quartz veins is common in orogenic gold deposits east of the KSZ in the Wawa-Abitibi terrane (e.g. Dinel et al., 2008; Kishida and Kerrich, 1987; Martin, 2012; Couture and Pilote, 1993). However, sodium depletion occurs at the Island Gold deposit (Table 4) and some deposits east of the KSZ such as the Beattie Gold deposit (Bigot, 2012) as well.

Gold mineralization-related alteration minerals in the deposits discussed above that are located east of the KSZ in the Wawa-Abitibi terrane typically include carbonate minerals, chlorite, sericite and/or potassium feldspar, plagioclase, quartz, and sulphide minerals (Dinel et al., 2008; Moritz and Crocket, 1991; Kishida and Kerrich, 1987; Martin, 2012; Bigot, 2012; Couture and Pilote, 1993; Smith et al., 1987a). Biotite is not typically an alteration mineral at these deposits but is an alteration mineral in gabbro and Webb Lake stock-hosted ore zones at the Island Gold deposit. In addition, potassium feldspar was not a major alteration mineral in any lithologies at Island Gold. All of the other minerals discussed above are significant alteration minerals at the Island Gold deposit (Section 4.1).

These differences in the mineralogical and chemical signature of alteration at the Island Gold deposit relative to the auriferous alteration at these other orogenic gold deposits suggests that alteration envelopes around auriferous veins in these deposits can vary and no single model fits for all deposits. However, the overall similarity of the auriferous alteration at Island Gold relative to these deposits east of the KSZ may support the correlation of the GLDZ with fault

systems east of the KSZ (as proposed in Leclair et al., 1993) and, at least suggests a similar genetic process for these orogenic gold deposits.

## **5.6 Non-auriferous alteration**

### **5.6.1 Carbonate-sericite alteration**

The gold-barren, carbonate-sericite alteration zone that was observed in drill core approximately 500 m SSW of the main Island Gold Zones has a notable absence of sulphidization and silicification/quartz veining which allows it to be distinguished from alteration envelopes associated with auriferous  $V_{GD}$  or  $V_1$ - $V_2$  quartz veins. Similarly, the fluid responsible is probably different than the auriferous fluid responsible for mineralization at the Island Gold deposit and reasons for this are discussed below. Considering the significant intensity of this carbonate-sericite alteration (Figure 13, Figure 15), mass gains of Au (0.01 ppm) and S (0.01 ppm; Table 7) are negligible compared to the typical enrichments observed due to alteration associated with auriferous quartz veining (e.g. Table 5, Table 6). In addition, unlike the alteration associated with auriferous quartz veins, consistent sodium depletion was not observed (Table 4).

Based on the most consistent and significant enrichments relative to least-altered concentrations, this hydrothermal alteration was likely generated from a fluid especially enriched in C,  $CO_2$ , Ca, and K (Table 4; Table 7). This is reflected by the presence of carbonate minerals and sericite in the altered sample (Figure 15). Tourmaline was observed in greater proportions in the altered sample which explains the elevated boron content relative to the least-altered sample (Table 7). It is unclear whether tourmaline post-dates this alteration or is related to the carbonate-sericite alteration event and is simply a late alteration mineral phase. Tourmaline was confirmed to post-date the alteration associated with  $V_{GD}$ ,  $V_1$ - $V_2$ , and  $V_3$  quartz veins through the examination of multiple alteration envelopes (Section 5.6.3). The tourmaline was occasionally present in these vein types and their associated alteration envelopes while in other occasions it was completely absent. In the case of this carbonate-sericite alteration zone, only one zone was encountered in drill core during site visits so it could not be confirmed that the tourmaline is unrelated to this carbonate-sericite alteration. Similarly, this alteration was not observed to coincide with any other lithologies or any auriferous zones. As a result, the source of this fluid and the timing of this uncommon alteration at the Island Gold deposit is unclear.

### 5.6.2 V<sub>3</sub> vein-related alteration

Alteration resulting from V<sub>3</sub> veining in the silica-poor diorite–monzodiorite and gabbro/lamprophyre was studied to confirm that it is distinctly different from the alteration related to auriferous quartz veins and, subsequently, provide further evidence that these lithologies post-date gold mineralization. Auriferous quartz veining (V<sub>GD</sub> and V<sub>1</sub>-V<sub>2</sub>) at the Island Gold deposit results in the significant and consistent enrichment of Au, K<sub>2</sub>O, Rb, S, and Te in all altered/least-altered pairs studied, regardless of their protolith (Table 4). The fluid that generated the V<sub>3</sub> veins was not derived from the same fluid that generated the V<sub>GD</sub> and V<sub>1</sub>-V<sub>2</sub> veins because Au, K<sub>2</sub>O, Rb, S, and Te are not all consistently enriched in altered/least-altered pairs subject to alteration by V<sub>3</sub> veins (Table 4). For comparison, a sample of gabbro directly adjacent to V<sub>1</sub>-V<sub>2</sub> auriferous veins exhibited significant mass gains of Au (5.7 ppm), K<sub>2</sub>O (1.6 wt%), Rb (29 ppm), S (4.0 wt%), and Te (0.37 ppm) relative to a least-altered sample of gabbro (Table 8). Starting with the gabbro/lamprophyre, consistent mass gains in Au, K<sub>2</sub>O, and Rb were observed but consistent gains of S and Te were not observed due to alteration related to V<sub>3</sub> veining (Table 4). In addition, despite the altered sample being directly adjacent to a V<sub>3</sub> vein, gains of Au (0.05 ppm), K<sub>2</sub>O (0.32 wt%), and Rb (8.23 ppm) were relatively minor. Similarly, in the silica-poor diorite–monzodiorite, consistent mass gains in Au, S, and Te were observed but despite the altered sample being directly adjacent to a V<sub>3</sub> vein, the concentration gains were relatively insignificant (0.07 ppm, 0.15 wt%, and 0.10 ppm, respectively). These are minor compared to the typical gains related to auriferous quartz veining (e.g. Table 8). Furthermore, K<sub>2</sub>O and Rb were both consistently depleted as a result of this alteration (Table 4). As a result, V<sub>3</sub> veins could not have been generated from the same fluid as V<sub>GD</sub> or V<sub>1</sub>-V<sub>2</sub> veins.

Based on macroscopic observation, the small alteration envelopes associated with V<sub>3</sub> veins often have notable variations in intensity and mineralogy even within the same lithology. In many cases, there were no macroscopically visible alteration envelopes associated with these veins (Figure 7C) while in other cases, the alteration envelope, although relatively small compared to those associated with V<sub>GD</sub> and V<sub>1</sub>-V<sub>2</sub> veining, was clearly visible. Particularly when V<sub>3</sub> veins are hosted in an intrusion of gabbro/lamprophyre or silica-poor diorite–monzodiorite, and this intrusion is overprinting part of an alteration envelope associated with auriferous quartz veining, the V<sub>3</sub> vein-related alteration appears more intense (Figure 30, Figure 34A, B). However, these more intense alteration envelopes may be related to the tourmalinization event as

tourmaline is also present in these veins (Figure 30, Figure 34A, B; Section 5.6.3). Regardless, the alteration associated with  $V_3$  veins is different from the  $V_{GD}$  and  $V_1$ - $V_2$  veins which both have consistent mineralogical and textural alteration envelopes irrespective of their spatial location, as long as they are located within the same lithology. The inconsistency of the  $V_3$  vein-related alteration suggests the composition of the vein-filling fluid in  $V_3$  veins varies from one vein to the next and is dependent on the host rock, which is not always the same. This is thought to explain the varying intensity of alteration and why the chemical gains and losses determined from study of silica-poor dioritic–monzodioritic altered/least-altered pairs are different from those determined via study of altered/least-altered pairs of gabbro/lamprophyre (Table 4).  $V_3$  veins are interpreted as extensional veins (Jellicoe, 2019) and are typically relatively small and discontinuous. As a result, unlike the large, continuous, extensional  $V_{GD}$  veins and shear-related  $V_1$ - $V_2$  vein systems and associated structures that are the conduits that provided the auriferous external fluid to the deposit (Jellicoe, 2019), the fluids within  $V_3$  veins are more likely to have been locally sourced. This suggests that local dissolution-precipitation may have been the vein-filling process which does not require an external fluid source (e.g. Kenis, 2004). In summary,  $V_3$  veins resulted in minor alteration and local remobilization of certain elements which vary depending on the host rock in which the veins formed.

Alteration related to  $V_3$  veins was studied primarily in the silica-poor diorite–monzodiorite and gabbro/lamprophyre which post-date  $V_{GD}$  and  $V_1$ - $V_2$  veining. This is because the intensity of the alteration related to  $V_{GD}$  and  $V_1$ - $V_2$  veining is more intense than the alteration related to  $V_3$  veins. This makes  $V_3$  vein-related alteration often indistinguishable in pre-gold mineralization lithologies because they are often at least weakly-altered by  $V_1$ - $V_2$  veins within mine workings. In addition, in any given pre-gold mineralization lithology, it is not known if alteration is directly-related to a  $V_3$  vein or is partly related to variations in  $V_{GD}$ / $V_1$ - $V_2$  vein-related alteration. Non-auriferous,  $V_3$  vein-related alteration was not the main focus of this thesis and was only studied in a limited number of samples.

### **5.6.3 Tourmalinization / $V_4$ veins**

Tourmaline is sporadically present in all lithologies, with the exception of diabase–quartz diabase intrusions, and manifests as disseminated tourmaline crystals or clusters of tourmaline that concentrates in ribbons along existing structures (e.g. Figure 25B). These ribbons of

tourmaline are referred to as V<sub>4</sub> veins (Jellicoe, 2019) and occasionally have minor quartz and carbonate minerals associated with them (e.g. Figure 25B). Based on this information, a boron-rich hydrothermal fluid that preferentially propagated along pre-existing structures is interpreted to be responsible for tourmalinization and V<sub>4</sub> veins. Tourmaline overprints primary and metamorphic minerals as well as V<sub>GD</sub>, V<sub>1</sub>-V<sub>2</sub>, and V<sub>3</sub> vein-related alteration minerals indicating that it post-dates these veins (Section 4.1). Tourmalinization is likely unrelated to the main gold mineralization events because least-altered rocks which contain tourmaline still have gold grades that are equivalent to other least-altered samples without any tourmaline. In many cases, tourmaline ribbons/veins have no visible alteration envelope. However, if they coincide with existing veins, they occasionally result in intensification of the surrounding alteration envelopes (e.g. Figure 30, Figure 34A). This suggests that the boron-bearing fluid may have resulted in the local remobilization of some elements. Sampling of tourmaline-related alteration envelopes that are sufficiently isolated from and unaffected by other alteration events was not conducted in this thesis. Further investigation of the tourmalinization event is recommended in Section 7.0.

## **5.7 Source(s) of sulphur and gold-bearing fluids**

Potential sources of the sulphur and gold introduced to the Island Gold deposit by the auriferous fluids include: the mantle, meteoric water, igneous rocks, and/or sedimentary rocks (e.g. Phillips and Groves, 1983; Hronsky et al., 2012; Xue et al., 2013; Tomkins, 2013; Agangi et al., 2016). Mass-independent fractionation (MIF) of sulphur is only known to occur on Earth due to surficial processes in the Archean (Farquhar et al., 2001) and subsequently can be used to determine whether sulphur in Archean ore deposits was sourced from meteoric water or sedimentary rocks with incorporated sulphur that was once present in the Archean atmosphere.

Determining the source(s) of sulphur can also be used to identify potential source(s) of gold. Sulphide minerals are intimately associated with the auriferous quartz veins (Section 4.1) and there are inclusions of gold within the pyrite grains (refractory gold) at the Island Gold deposit (Figure 9C). This suggests gold and sulphur were introduced to the deposit by the same fluid. Furthermore, sulphide complexes commonly transport gold in hydrothermal fluids (Loucks and Mavrogenes, 1999). Although this demonstrates that gold and sulphur were likely carried by the same fluid, it is possible that they have different sources. For example, the fluid could have been derived from the mantle, the cooling of an igneous body or dehydration reactions due to



metamorphism while gold may have been scavenged later from certain lithologies as this fluid percolated through them or propagated along structural conduits. Alternatively, the gold could have been derived from any of these potential fluid sources along with the fluid itself (Phillips and Groves, 1983; Hronsky et al., 2012; Xue et al., 2013; Tomkins, 2013; Agangi et al., 2016).

The non-zero  $\Delta^{33}\text{S}$  and  $\Delta^{36}\text{S}$  values of sulphides from iron formations (Section 4.5) within the study area are consistent with MIF sulphur. MIF sulphur has been documented in a wide variety of Archean sedimentary rocks (e.g. Farquhar et al., 2000; Hou et al., 2007). The negative  $\Delta^{33}\text{S}$  values in sulphides from iron formations at the Island Gold deposit indicate that the sulphur was sourced from a negative  $\Delta^{33}\text{S}$  reservoir. These iron formations would have been enriched in the oxidized species ( $\text{SO}_4^{2-}$ ) produced by photochemical oxidation of volcanic sulphur species in the Archean atmosphere (Farquhar et al., 2001). The range of  $\delta^{34}\text{S}$  values in sulphides from iron formations (-1.33‰ to 19.60‰; Figure 60) suggests sulphur isotope fractionation that is characteristic of a relatively low sulphate reservoir which is typical in the Archean (Canfield and Raiswell, 1999). This variation in  $\delta^{34}\text{S}$  values is suggestive of a later reduction process that caused this fractionation. Previous studies have interpreted this fractionation to be due to biological processes such as microbial sulphate reduction (e.g. Goodwin et al., 1976; Lambert and Donnelly, 1992). Microbial reduction would result in MDF (Farquhar et al., 2000) and, as a result, this secondary process would not result in a significant change in the  $\Delta^{33}\text{S}$  value.

The  $\Delta^{33}\text{S}$  and  $\Delta^{36}\text{S}$  values of sulphides from  $V_1$  and  $V_2$  vein types and their associated alteration envelopes are all very close to zero and these values are considered to reflect dominantly mass-dependent fractionation (e.g. Farquhar et al., 2000; Xue et al., 2013). One  $\Delta^{36}\text{S}$  value from an altered gabbroic sample has an anomalous  $\Delta^{36}\text{S}$  value indicative of MIF sulphur (Section 4.5). However, unlike  $\Delta^{33}\text{S}$ , there is more uncertainty associated with  $\Delta^{36}\text{S}$  values based on historical analyses of the standard IAEA-S1 at this lab ( $\pm 0.008\text{‰}$  for  $\Delta^{33}\text{S}$  versus  $\pm 0.30\text{‰}$  for  $\Delta^{36}\text{S}$ ; Wu, personal communication, 2018). As a result,  $\Delta^{33}\text{S}$  is given priority over  $\Delta^{36}\text{S}$  when differentiating between MIF and MDF sulphur. The consistent slightly negative  $\Delta^{33}\text{S}$  value may also suggest a small contribution from a source with negative  $\Delta^{33}\text{S}$ . A second alternative involves the mixing of two sulphur sources: one with positive  $\Delta^{33}\text{S}$  and one with negative  $\Delta^{33}\text{S}$ . However, the small range of  $\Delta^{33}\text{S}$  values for these samples, as well as the probability of the mixing of two sources producing values equivalent to MDF ( $\Delta^{33}\text{S} \approx 0$ ), makes this interpretation unlikely.

Continuing with the first interpretation, the minimal MIF sulphur indicates that meteoric water and the metamorphism of sedimentary rocks were not the dominant sources of sulphur. Instead, sulphur of mantle parentage is more probable. The negative  $\Delta^{33}\text{S}$  sulphur could have been incorporated due to limited leaching of sulphide-rich iron formations (which have negative  $\Delta^{33}\text{S}$  values; Figure 60) as the fluid moved up and along the GLDZ. Sulphide-rich iron formations separate the first and second cycles of volcanism and the second and third cycles of volcanism in the Michipicoten greenstone belt (Sage, 1994). These iron formations are volumetrically minor compared to other lithologies within the Michipicoten greenstone belt (Sage, 1994). However, the high sulphide content in the iron formations studied in this thesis (e.g. Figure 22A) suggests they are likely a significant reservoir of sulphur in this greenstone belt because other observed lithologies typically contain relatively low amounts of sulphur.

In summary, most of the sulphur associated with the main gold-mineralization event at the Island Gold deposit is most likely originally of mantle/igneous parentage, sourced from: (1) a sulphur-rich mantle fluid, (2) an exsolved sulphur-bearing fluid from a crystallizing intrusive body, and/or (3) the leaching of sulphur from igneous rocks during fluid propagation. The gold may be derived from the same source of the sulphur or leached during the movement of the sulphur-bearing fluid through the crust.

The  $\Delta^{33}\text{S}$  value obtained from pyrite in a  $V_{\text{GD}}$  vein is well outside the range of  $\Delta^{33}\text{S}$  values found in sulphides associated with  $V_1$  and  $V_2$  auriferous quartz veins (Figure 60), even if analytical uncertainty is considered. This indicates that the sulphur in  $V_{\text{GD}}$  veins has a different source than the sulphur present in the  $V_1$  and  $V_2$  veins. The  $V_{\text{GD}}$  veins are interpreted to have formed prior to the formation of the  $V_1$  and  $V_2$  veins (Jellicoe, 2019). These findings suggest that  $V_{\text{GD}}$  veins formed from a unique fluid source which supports that the  $V_{\text{GD}}$  veins formed separately from  $V_1$ - $V_2$  veins. The  $\Delta^{36}\text{S}$  value of negative 0.05‰ is consistent with MDF sulphur. However, as discussed earlier in this section, there is notable uncertainty associated with  $\Delta^{36}\text{S}$  values relative to  $\Delta^{33}\text{S}$  values. The positive  $\Delta^{33}\text{S}$  value of 0.143‰ obtained from pyrite in a  $V_{\text{GD}}$  vein falls close to the upper limit of the MDF field. In the absence of MIF and processes related to metabolic activity, only small deviations of  $\Delta^{33}\text{S}$  from 0‰ of  $\pm 0.05$ ‰ are possible (Farquhar et al., 2007a). Larger deviations from zero can result from either metabolic processes or MIF. Firstly, metabolic mixing of MDF sulphur reservoirs with large differences in  $\delta^{34}\text{S}$  (Farquhar et al., 2007a) can cause  $\Delta^{33}\text{S}$  deviations from 0‰ of  $\pm 0.2$ ‰ (Farquhar and Wing, 2003). As a

result, it is possible that MDF sulphur may have been affected by processes related to surficial microbial metabolism producing this intermediate  $\Delta^{33}\text{S}$  value. However, this is unlikely because all of the sulphides that fall within the MDF field (Figure 60) have a very narrow range of  $\delta^{34}\text{S}$  values (1.2–1.9‰) and therefore only a maximum difference of 1.7‰. Mixing of components with a difference of this magnitude will not produce a  $\Delta^{33}\text{S}$  value as large as 0.143 (Farquhar et al., 2007a). Furthermore, non-zero  $\Delta^{33}\text{S}$  values produced due to this metabolic mixing process are not common (Farquhar and Wing, 2003). Alternatively, this  $\Delta^{33}\text{S}$  value could have been produced from the mixing of a typical MDF sulphur source ( $\Delta^{33}\text{S} \approx 0$ ) and a positive  $\Delta^{33}\text{S}$  MIF sulphur source. Regardless of whether this non-zero  $\Delta^{33}\text{S}$  value was produced by MDF sulphur affected by near-surface metabolic activity or MIF, the sulphur must have been present at or near surface prior to the gold mineralization event. This contribution from surficial sulphur suggests that leaching of sulphur from sedimentary units as the auriferous fluid propagated through structural conduits was taking place. Alternatively, metamorphism of a combination of igneous and sedimentary rocks could produce a sulphur-rich fluid with this isotopic signature. Juvenile MDF sulphur ( $\Delta^{33}\text{S} \approx 0$ ) could have been present in the fluid originally or leached from igneous rocks of mantle parentage during fluid propagation. These interpretations should be used with caution because only one sample from the  $V_{\text{GD}}$  vein type was analyzed. Although analytical uncertainties associated with  $\delta^{34}\text{S}$  and  $\Delta^{33}\text{S}$  are small (Section 3.8.2), additional sulphur isotopic analyses of sulphides from these veins are recommended to confirm these findings.

The silica-poor diorite–monzodiorite typically hosts minor disseminated pyrite regardless of its proximity to ore zones (e.g. Figure 33A, B). The sulphur in this pyrite has a unique isotopic signature (Figure 60) which suggests that it is from a different source than sulphur from the ore zones. This also supports the interpretation that this lithology post-dates gold-mineralization because, despite being commonly found adjacent and parallel to auriferous veins, the sulphides in the veins have different  $\Delta^{33}\text{S}$  and  $\Delta^{36}\text{S}$  values when compared to the silica-poor diorite–monzodiorite (Section 4.5). The positive  $\Delta^{33}\text{S}$  value of pyrite from the silica-poor diorite–monzodiorite suggests MIF took place but this sulphur was sourced from a reduced MIF sulphur reservoir (Farquhar et al., 2000). This sulphur was originally derived from an Archean sedimentary source but is not derived from the same reservoir as the oxidized sulphur in the banded iron formations which exhibits negative  $\Delta^{33}\text{S}$  values. A possible source of this sulphur is melting and assimilation of a sulphide-rich sedimentary rock with positive  $\Delta^{33}\text{S}$  values during

pluton transport and emplacement. Partially melted xenoliths have been observed in this lithology (Figure 32) which supports that this intrusive did melt and assimilate earlier lithologies. However, there are no known sedimentary rocks in the region with appropriate positive  $\Delta^{33}\text{S}$  values. This may be because extensive multiple sulphur isotopic studies of lithologies in the Michipicoten greenstone belt have not been conducted.

Previous multiple sulphur isotopic studies of Archean gold deposits in the Yilgarn Craton, Superior Province, and Kaapvaal Craton and have yielded contrasting results and interpretations. Some studies have found that MDF sulphur dominates which suggests a mantle/igneous source of sulphur and, by association, gold (e.g. Xue et al., 2013). Other studies have found that most of the deposits examined display varying contributions from MIF sulphur. This is interpreted to be a result of the metamorphism of a combination of sedimentary and igneous rocks (e.g. Agangi et al., 2016; Selvaraja et al., 2017). Results from this study of the Island Gold deposit largely support a mantle/igneous source of sulphur for sulphides associated with  $V_1$  and  $V_2$  veins. However, sulphides from  $V_{GD}$  veins are composed of MDF sulphur affected by surficial metabolic activity or a combination of surficial MIF sulphur in addition to juvenile MDF sulphur. This is likely due to metamorphism and/or leaching of sulphur from a combination of sedimentary rocks and mantle-derived igneous rocks.

## 5.8 Relative and absolute ages

The voluminous dacitic rocks are crosscut or stratigraphically overlain by all lithologies and, as a result, they are the oldest lithology at the Island Gold deposit. Previous U-Pb zircon geochronological studies of the felsic–intermediate volcanic rocks of the Wawa Assemblage yielded ages ranging from  $2749 \pm 2$  to  $2728 \pm 2.7$  Ma (Turek et al., 1982, 1992). The age of  $2735 \pm 8$  Ma obtained in this study from a least-altered dacitic sample (Section 4.6) falls within this range. Similarly, the age of  $2738 \pm 9$  Ma obtained from an altered dacitic sample in an ore zone is also consistent with these previous studies (excluding spot locations situated on the anomalous uniform CL crystals and rims described in Section 4.6 and discussed later in this section). These two ages from this study are identical within error. As a result, the zircons in these samples are believed to have crystallized at approximately the same time.

Banded iron formation layers are occasionally interlayered with the dacitic rocks. The larger Michipicoten iron formation caps the cycle 2 felsic–intermediate volcanic rocks (Sage,

1994), separating them from the mafic volcanic rocks to the north of the Island Gold deposit. A U-Pb age of  $2728.8 \pm 2.7$  Ma was obtained from the felsic–intermediate volcanic rocks of the Wawa Assemblage, directly below the Morrison No. 1 iron range (Turek et al., 1988, 1992). This iron range is interpreted to be part of the Michipicoten iron formation (Sage, 1994) and is located north of the Island Gold deposit. A U-Pb date obtained from the felsic–intermediate volcanic portion of the overlying Catfish Assemblage is  $2717 \pm 11$  Ma (Smith et al., 1987b). As a result, the Michipicoten iron formation was deposited between *c.* 2729 and *c.* 2717 Ma. In summary, some iron formation layers are of similar age to the dacitic rocks, however, the majority are younger.

The gabbro at the Island Gold deposit crosscuts the dacite (Section 4.1.4.1) and therefore, is younger. This lithology may have been emplaced during multiple intrusion events but samples taken throughout the deposit are mineralogically and chemically equivalent. Although the gabbro was not directly observed cross-cutting the iron formation, minor iron formations are occasionally found interbedded within the dacite and as a result, it is likely that this gabbroic intrusion, at the least, post-dates these minor iron formations. The relative timing between the larger Michipicoten iron formation that stratigraphically overlies the second cycle dacite (Sage, 1994) and the gabbro is not known because cross-cutting relationships were not observed.

The Webb Lake stock intrudes the dacite, iron formations, and gabbro (Section 4.1.5.1) and therefore, post-dates these lithologies. The Webb Lake stock was dated at  $2724 \pm 4.3$  (Jellicoe, 2019). This age, and the age of the dacite, effectively bracket the age of the Michipicoten iron formation.

The dacite, gabbro, and the Webb Lake stock were observed to host  $V_{GD}$  and  $V_1$ - $V_2$  veins if they were located in an auriferous zone (Section 4.1). Iron formation was not observed near occurrences of  $V_{GD}$  or  $V_1$ - $V_2$  veins, but because the Webb Lake stock post-dates the iron formation and hosts these auriferous veins, it is likely that iron formation pre-dates these veins as well. Shearing associated with the emplacement of  $V_1$ - $V_2$  veins is observed deforming the  $V_{GD}$  veins (Figure 7A). As a result, the  $V_{GD}$  veins are older than the  $V_1$ - $V_2$  veins (Jellicoe, 2019).  $V_1$  and  $V_2$  veins are believed to have formed synchronously (Jellicoe, 2019) based on contradicting and often ambiguous cross-cutting relationships (Section 4.1.1.1).

The gabbro/lamprophyre is observed cross-cutting the dacite and gabbro. It is not cross-cut or altered by  $V_1$ - $V_2$  veins despite being commonly found within these auriferous quartz vein

corridors (Section 4.1.6.1). It also does not contain economic gold grades despite being directly adjacent to these veins (Section 5.6.2). Therefore, this lithology intruded after the auriferous quartz veining events and is younger than the lithologies discussed above in this section.

The quartz diorite was directly observed as xenoliths within the silica-poor diorite–monzodiorite (Figure 32A) and as a result, the quartz diorite is younger than the diorite–monzodiorite. The quartz diorite is also present as a separate intrusive body on the 600 level but was not directly observed because it was inaccessible during site visits. A cross-cutting relationship between this minor lithology and the gabbro/lamprophyre was not observed. However, based on the fresh appearance of the quartz diorite in thin section and lack of significant deformation (Figure 32B, D), it qualitatively appears that this lithology has been subject to less metamorphism and deformation and as a result, is possibly younger than the gabbro/lamprophyre (Figure 29A). The quartz diorite was not observed adjacent to auriferous quartz veins so a timing relationship could not be determined. However, if this lithology is younger than the gabbro/lamprophyre, it must also post-date the  $V_{GD}$  and  $V_1$ - $V_2$  veins.

Similar to the gabbro/lamprophyre, the silica-poor diorite–monzodiorite cross-cuts  $V_1$ - $V_2$  auriferous veins and is not altered by them (Figure 34C). It also does not have notable gold enrichment when directly adjacent to these veins. As a result, the silica-poor diorite–monzodiorite intruded after the formation of the  $V_1$ - $V_2$  auriferous veins. The silica-poor diorite–monzodiorite appears to ambiguously cross-cuts the gabbro/lamprophyre in a few cases. However, both of these intrusions are relatively minor and commonly parallel each other within mine workings so clear, high-angle, cross-cutting relationships are rare. The silica-poor diorite monzodiorite and the quartz diorite xenoliths within appear to have been subject to less metamorphism (have a larger proportion of primary minerals) and appear less deformed than the gabbro/lamprophyre (Figure 33A, B; Figure 32; Figure 29A). This tentatively suggests that the silica-poor diorite–monzodiorite is younger than the gabbro/lamprophyre but this warrants further investigation (Section 7.0). Besides the gabbro/lamprophyre, the silica-poor diorite–monzodiorite is younger than the quartz diorite and all of the lithologies and veins types discussed above in this section. The silica-poor diorite–monzodiorite has been dated at  $2672.2 \pm 3.5$  Ma (Jellicoe, 2019).

$V_3$  quartz veins post-date all of the lithologies and veins discussed above in this section, because these non-auriferous extensional veins were observed in all lithologies and cross-cut

V<sub>GD</sub> and V<sub>1</sub>-V<sub>2</sub> veins (Section 4.1.1.1). It is interpreted that the tourmaline post-dates the structures and the lithologies it occurs in. Tourmalinization, including the formation of the tourmaline ribbons (V<sub>4</sub> veins) is believed to post-date V<sub>3</sub> veining as these ribbons invade V<sub>3</sub> veins (Jellicoe, 2019; e.g. Figure 30). Tourmaline is probably not present in the diabase–quartz diabase because this unit post-dates the tourmalinization event. Alternatively, the diabase–quartz diabase is relatively undeformed and simply does not contain structures for a B-rich fluid to propagate along and precipitate tourmaline. If the second alternative is true, tourmalinization may have occurred after the intrusion of the diabase–quartz diabase.

Diabase–quartz diabase dykes have only been subject to minor greenschist-grade metamorphism and sharply cut all other lithologies and quartz vein types. Therefore, this lithology is the youngest. The age of these dykes is uncertain as both late Archean and Proterozoic diabase dykes are located in the area (Sage, 1994). These are interpreted to be part of the Matachewan dyke swarm (Jellicoe, 2019; Section 5.1.8) which has been dated at 2473 ± 16/-9 Ma (Heaman, 1997). The stratigraphy, relative timing relationships, absolute timing, and associated interpretations regarding the lithologies discussed above are summarized in Table 19 (Appendix B).

The spot locations situated on the uniform CL zircons/rims in the altered dacitic sample that yielded anomalous Proterozoic ages ranging from *c.* 975 to 1499 Ma (Section 4.6) are believed to have formed due to one or multiple alteration event(s). It was originally suspected that these anomalous zircons/rims formed as a result of the intense alteration related to the emplacement of the V<sub>1</sub>-V<sub>2</sub> auriferous quartz veins. However, the cause of this zircon growth/alteration is not related to gold mineralization because the silica-poor diorite–monzodiorite intrusive lithology, that cross-cuts the V<sub>1</sub>-V<sub>2</sub> gold-bearing veins and post-dates gold mineralization, yielded a U-Pb age of 2672.2 ± 3.5 (Jellicoe, 2019). The smaller, anhedral, and often fractured zircons in the altered sample (e.g. Figure 61B–D) suggest that zircon dissolution rather than growth/alteration resulted from the emplacement of the V<sub>1</sub>-V<sub>2</sub> veins.

These anomalous CL zircons may be a result of the intrusion of the diabase–quartz diabase dykes in the area that have Proterozoic ages (Leech et al., 1963; Sage, 1994). However, these dykes typically do not cause significant visible alteration of the surrounding wall-rock and as a result, it is likely that the alteration associated with the uniform CL zircons was not caused by these dykes. In addition, the diabase–quartz diabase intrusions were not observed directly



proximal to either sample location. However, diabase–quartz diabase dykes were observed within the drift from which the altered sample was taken. The diabase–quartz diabase dykes observed within mine workings are believed to be part of the Matachewan dyke swarm (Jellicoe, 2019) which are Paleoproterozoic (Heaman, 1997). If this interpretation is correct, zircon growth/alteration resulting from these dykes would not have produced Meso–Neoproterozoic aged zircon. However, younger Proterozoic diabase dykes have been observed in the Michipicoten greenstone belt as well (Leech et al., 1963; Sage, 1994) so it is possible that these dykes are younger than believed.

Alternatively, these Proterozoic-age zircons could be a result of the emplacement of the  $V_3$  extensional veins, or later tourmalinization, both of which tend to concentrate within the shear zones that host the  $V_1$ - $V_2$  veins. Both  $V_3$  veins and tourmaline were observed within the ore zone from which the altered sample was taken. However, these events are believed to pre-date the intrusion of the diabase–quartz diabase dykes because neither tourmaline nor  $V_3$  veins were observed within the diabase–quartz diabase. Alternatively, these zircons could be related to the alteration event that resulted in the sporadic growth of chloritoid in certain areas and lithologies (Section 5.2). These Proterozoic-age zircons could also be a result of an unrecognized fluid pulse along, or reactivation of, the shear zone that hosts these auriferous quartz veins. At the Young-Davidson deposit, monazite U-Pb ages are consistent with a Paleoproterozoic alteration event at  $1730 \pm 5$  Ma (Zhang et al., 2014) and were attributed to late hydrothermal reactivation. Although these are two temporally unrelated events, a similar process may have taken place at the Island Gold deposit resulting in the generation of these anomalous Meso–Neoproterozoic ages. However, the specific timing of the Proterozoic alteration event(s) recorded by zircon at the Island Gold site cannot be resolved with the current data set.

## 6.0 Summary and conclusions

The five main objectives of this thesis focusing on the Island Gold deposit were:

- 1) Determine the protoliths of major lithologies and effects of metamorphism;
- 2) Characterize the alteration envelopes associated with various gold-bearing quartz veins and compare to the alteration at other orogenic gold deposits east of the Kapuskasing Structural Zone;
- 3) Establish mineralogical indicators and geochemical vectors for gold mineralization;
- 4) Constrain the source of the gold-bearing fluid using sulphur isotopes; and
- 5) Determine the age(s) of gold mineralization.

The conclusions pertaining to each of these objectives are summarized in order below.

### 6.1 Protoliths and metamorphism

The interpreted protoliths of lithologies observed at the Island Gold deposit are listed below in order from oldest to youngest. Mine terms used to refer to these units are included in parentheses when applicable.

- 1) Dacitic volcanic rocks: Tuffs, hypabyssal intrusives, flows, and pyroclastic breccias (T2, I2, V2)
- 2) Banded-massive iron formation (IF)
- 3) Gabbro (I3G)
- 4) Tonalite–trondhjemite (Webb Lake stock: I1JM)
- 5) Lamprophyre (Spessartite) or gabbro (Sub-volcanic equivalent to ocean island basalt or continental flood basalt) (I2H)
- 6) Quartz diorite
- 7) Silica-poor diorite–monzodiorite (I2M)
- 8) Diabase–quartz diabase (I3DD)

Protoliths 1 to 4 (above) are pre-gold mineralization lithologies. A stratigraphic chart that summarizes the timing, textures, and mineralogy for each lithology is included in Appendix B (Table 19). The interpreted primary minerals in each lithology prior to metamorphism and alteration is also included. All lithologies at the Island Gold deposit were affected by some degree of greenschist-grade metamorphism. Least-altered samples of all lithologies often contain

metamorphic minerals (e.g. actinolite, carbonates, chlorite, chloritoid, epidote, hematite, ilmenite, magnetite, quartz, sodic plagioclase, titanite, and white mica) which commonly replace primary minerals. Metamorphism appears to have had a weaker effect on the quartz diorite and the silica-poor diorite–monzodiorite compared to most other lithologies at this deposit, tentatively suggesting that these two lithologies were emplaced after peak metamorphism. The diabase–quartz diabase intrusions have been affected the least by metamorphism and this indicates that they post-date the main greenschist-grade metamorphic event which occurred during D2 deformation (Jellicoe, 2019).

## 6.2 Vein-related alteration

Alteration related to  $V_1$ - $V_2$  veining at the Island Gold deposit results in the significant and consistent enrichment of Au,  $K_2O$ , Rb, S, and Te and typically  $Na_2O$  depletion in alteration envelopes hosted by dacite, gabbro, and the Webb Lake stock. The consistent enrichment and depletion of these elements supports that  $V_1$ - $V_2$  veins hosted by these lithologies precipitated from the same gold-rich fluid. Additional chemical enrichments and depletions specific to each lithology are summarized in Table 4. Alteration minerals associated with  $V_1$ - $V_2$  auriferous quartz veining mainly consist of biotite, Ca-Mg-Fe carbonates, chlorite, plagioclase, quartz, sulphides (pyrite  $\pm$  pyrrhotite  $\pm$  chalcopyrite), and white mica (muscovite  $\pm$  phengite). The alteration mineral assemblage varies depending on the lithology being altered (Table 19; Appendix B). The minerals in alteration envelopes associated with  $V_1$ - $V_2$  veining remain consistent with varying distance parallel to the GLDZ and elevation. Silicification of the alteration envelope may increase with depth.

The chemical and mineralogical signature of alteration related to  $V_{GD}$  veins in the dacite is similar to the alteration related to  $V_1$ - $V_2$  veins in the same lithology. It is therefore extrapolated that gabbro or Webb Lake stock-hosted alteration envelopes associated with  $V_{GD}$  veins would have similar mineralogical and chemical signatures as those associated with  $V_1$ - $V_2$  veins.

$V_3$  non-auriferous veins resulted in minor alteration and inconsistent local remobilization of various elements (Table 4) that are dependent on the host lithology in which they form. When present, small alteration envelopes associated with these veins often have notable variations in intensity and mineralogy even within the same lithology. The fluids that generated  $V_3$  veins were

likely locally sourced and the fluid composition is a direct product of the surrounding wall rock composition. Conversely,  $V_1$ - $V_2$  and  $V_{GD}$  veins were generated from exotic, gold-enriched fluids that propagated along structural conduits, resulting in consistent and predictable alteration zones.

Alteration envelopes associated with auriferous quartz veins ( $V_1$ - $V_2$  and  $V_{GD}$ ) are relatively symmetrical and range from a few centimetres to 10 m or more perpendicularly outwards from a central vein. Alteration envelopes associated with  $V_{GD}$  veins are generally smaller than those associated with  $V_1$ - $V_2$  veins of comparable size. Similarly, alteration envelopes hosted by the Webb Lake stock are smaller than those hosted by the dacite or gabbro.  $V_3$  veins have no visible alteration envelope or small alteration envelopes that are typically less than 0.2 m perpendicularly outwards from the vein/wall rock contact.

Orogenic gold deposits east of the Kapuskasing Structural Zone (KSZ) such as Hoyle Pond, Dome, Kerr-Addison, Young-Davidson, and Francoeur 3 generally have similar alteration mineral assemblages and chemical enrichments associated with auriferous quartz vein-related alteration. One notable difference is sodium enrichment is more common at these deposits but sodium depletion consistently occurs at the Island Gold deposit. Furthermore, potassium feldspar was not a significant alteration mineral in any lithologies at the Island Gold deposit but is often an alteration mineral at these other deposits. These notable differences in the mineralogical and chemical signature of alteration suggests that alteration envelopes around auriferous veins in orogenic gold deposits can vary and no single model fits for all deposits. Aside from these differences, the alteration mineral assemblages and chemical signatures of the alteration observed in these gold deposits east of the KSZ are similar to those identified at the Island Gold deposit. This overall consistency of the alteration between these deposits and the Island Gold deposit may support the correlation of the Goudreau Lake Deformation Zone with major fault systems east of the KSZ (as proposed in Leclair et al., 1993) and, at least suggests a similar genetic process for these orogenic gold deposits.

### **6.3 Mineral indicators and geochemical vectors for gold mineralization**

The most reliable geochemical vectors towards mineralized zones include Au,  $K_2O$ , Rb, S, and Te enrichment. Other geochemical vectors include As, Se, and W enrichment and  $Na_2O$  depletion. Smoky quartz veins, veinlets, and flooding are the most reliable indicators for economic gold grades at the Island Gold deposit. In low-grade samples (< 4 g/t), pyrite correlates

well with gold grade. Proportions of alteration minerals such as biotite, carbonates, chlorite, quartz, sericite, and sulphides can be used as an approximate guide to help discern which zone of an alteration envelope a sample is from. This can be used to help provide a general estimate of gold grade (Section 4.1; Section 4.4; Figure 20; Figure 59). However, proportions of these minerals alone do not correspond reliably enough with gold content to differentiate between units with different cut-off grades. Increased proportions of chlorite and carbonate minerals relative to unaltered rock can be used to identify the weakly-altered outer margins of alteration envelopes associated with auriferous quartz veins.

#### **6.4 Source(s) sulphur and the gold-bearing fluid**

Despite the availability of sources of MIF sulphur in nearby iron formations, the majority of the sulphur in, and associated with, the auriferous V<sub>1</sub> and V<sub>2</sub> veins exhibits MDF. This indicates that most of the sulphur has a mantle or igneous parentage and did not come into contact with Archean atmosphere. The auriferous fluid that produced these veins was likely derived from the mantle, exsolved from a cooling intrusive body, or the dehydration of igneous rocks due to metamorphism. The gold was likely originally enriched in this fluid or sourced from the leaching of igneous rocks during fluid movement. A small amount of MIF sulphur may have been incorporated due to leaching of sedimentary units during fluid propagation.

Despite their alteration envelopes having similar chemical and mineralogical signatures, the V<sub>GD</sub> veins formed earlier than the V<sub>1</sub>-V<sub>2</sub> veins as a result of a separate gold mineralization event due to a unique gold-bearing fluid with a different sulphur source. The sulphur was likely derived from either MDF sulphur subject to near-surface metabolic processes or a combination of juvenile MDF and positive  $\Delta^{33}\text{S}$  MIF sulphur sources. The MIF and surficial MDF sulphur would have been leached from sedimentary units as the auriferous fluid propagated through structural conduits or originally enriched in the fluid (assuming the fluid was of metamorphic origin). The juvenile MDF sulphur could have been present in the fluid originally or leached from igneous rocks during fluid propagation.

The unique isotopic signature of pyrite in the silica-poor diorite–monzodiorite supports the interpretation that this lithology post-dates gold mineralization and that these sulphide minerals did not form due to remobilization of existing sulphides from ore zones. Similar to

sulphur in the  $V_{GD}$  veins, the sulphur in this lithology suggests the presence of a positive  $\Delta^{33}S$  MIF sedimentary sulphur source that is located down-dip or parallel to the GLDZ.

## **6.5 Timing of gold mineralization**

Gold mineralization at the Island Gold deposit is younger than the Archean U-Pb LA-ICP-MS ages of  $2738 \pm 9$  Ma and  $2735 \pm 8$  Ma obtained from zircons in altered and least-altered dacitic samples. These ages are consistent with previous geochronological studies of the dacite. The spot locations yielding Proterozoic ages ranging from *c.* 975 to 1499 Ma, located on the anomalous, uniform CL zircons/rims in the altered sample, are believed to have formed due to alteration unrelated to auriferous quartz veining. The cause(s) of the alteration event(s) that resulted in the generation of these Proterozoic U-Pb ages are uncertain.

## 7.0 Suggested future work

Additional microprobe study of the minerals in least-altered samples of iron formation, gabbro/lamprophyre, quartz diorite, silica-poor diorite–monzodiorite, and diabase–quartz diabase is recommended. This will help classify observed minerals in these lithologies that are challenging to accurately classify using petrography and SEM-EDS techniques alone (e.g. carbonate minerals). This may further refine the interpreted protoliths of these lithologies and subsequently, their genetic history.

Alteration envelopes hosted by the gabbro and Webb Lake stock that are associated with  $V_{GD}$  veins should be studied petrographically and geochemically. This will confirm the interpretation in this thesis that alteration envelopes associated with  $V_{GD}$  veins and hosted by the gabbro and Webb Lake stock are chemically and mineralogically similar to alteration envelopes associated with  $V_1$ - $V_2$  veins. This was proven to be the case for dacite-hosted alteration envelopes.

As employed in this thesis for the study of a dacite-hosted alteration envelope, SEM-MLA techniques are recommended instead of point-counting for any further mineral modal proportion analyses. This method is believed to be more accurate and precise than point-counting, particularly for determining the modal proportions of accessory minerals. It is suggested that SEM-MLA analyses are also performed on a gabbro-hosted and a Webb Lake stock-hosted alteration envelope associated with  $V_1$ - $V_2$  veining to more accurately determine the modal proportions of minerals determined via point-counting techniques in this study.

Analysis of tourmalinization/ $V_4$  veins and related alteration to determine the source of the boron-rich fluid and determine if it remobilizes existing gold is another potential avenue to study. Conducting work to better constrain the timing of the tourmalinization event is also suggested. Similarly, the non-auriferous sericite-carbonate alteration zone that was encountered warrants additional study in order to determine the relative timing and source of the fluid that generated this alteration zone. The mineralogical and chemical signature of this carbonate-sericite alteration and whether or not it is related to the tourmalinization event should be confirmed via examination of multiple carbonate-sericite alteration zones. Likewise, further study of chloritoid and its spatial distribution is also recommended to determine whether or not the chloritoid formed during late metamorphism or if it is a product of an alteration event unrelated to metamorphism.



Identify and photograph an unambiguous cross-cutting relationship between the silica-poor diorite-monzodiorite and the gabbro/lamprophyre. This will definitively determine the timing relationship between these two lithologies. Similarly, better constraining the timing of the quartz diorite relative to other lithologies at the Island Gold deposit by studying additional occurrences of the quartz diorite within mine workings is recommended. Absolute dating of the quartz diorite and gabbro/lamprophyre is also suggested.

It was originally suspected that the anomalous indistinct zircons and zircon rims in the altered sample were a result of the intense alteration related to the emplacement of V<sub>1</sub>-V<sub>2</sub> veins. This study has shown that this is due to a Proterozoic post-gold mineralization event and, as a result, the age of gold mineralization could not be directly determined. It is possible that the alteration rims due to V<sub>1</sub>-V<sub>2</sub> veining (if any) are too thin to be analyzed through traditional LA-ICP-MS of polished zircons. Altered zircon rims, interpreted to be a result of hydrothermal fluids related to gold mineralization, can be < 3 µm across (Schneider et al., 2012). Therefore, LA-ICP-MS depth profiling may be able to resolve the ages of narrow rims. The Proterozoic ages recorded by zircon in dacite at the Island Gold deposit suggest a Proterozoic alteration event. Further study is needed to determine the cause and identify the specific timing of the alteration event that resulted in the Meso–Neoproterozoic ages recorded by zircon in this sample from the Island Gold deposit.

Some of the rutile in alteration envelopes associated with auriferous veins at the Island Gold deposit is also believed to have formed due to alteration related to gold mineralization. As a result, U-Pb dating of rutile is suggested to determine the age(s) of gold mineralization at the Island Gold deposit.

## 8.0 References

- Abzalov, M. 2008. Quality Control of Assay Data: A Review of Procedures for Measuring and Monitoring Precision and Accuracy. *Exploration and Mining Geology*, **17**: 131-144.
- Abzalov, M. 2011. Sampling Errors and Control of Assay Data Quality in Exploration and Mining Geology. *In Applications and Experiences of Quality Control*. Edited by O. Ivanov. InTech Open Access Publishing, Rijeka, Croatia, pp. 611-644.
- Actlabs. 2018a. Sample Preparation [online]: Available from <http://www.actlabs.com/page.aspx?menu=74&app=243&cat1=617&tp=2&lk=no> [cited 15 January 2018].
- Actlabs. 2018b. Methods [online]: Available from <http://www.actlabs.com/list.aspx?menu=64&app=226&cat1=549&tp=12&lk=no> [cited 15 January 2018].
- Adam, D., LeBlanc, L.G., Bélisle, M., Ramcharan, and Vincent, R. 2017. Island Gold Mine Technical Report and Expansion Case Preliminary Economic Assessment, Dubreuilville, Ontario, Canada, Technical Report according to National Instrument 43-101 and Form 43-101F1. Richmond Mines Inc., Rouyn-Noranda, Québec.
- Agangi, A., Hofmann, A., Eickmann, B., Marin-Carbonne, J., and Reddy, S.M. 2016. An atmospheric source of S in Mesoarchean structurally-controlled gold mineralisation of the Barberton Greenstone Belt. *Precambrian Research*, **285**: 10-20.
- Ague, J.J. 1991. Evidence for major mass transfer and volume strain during regional metamorphism of pelites. *Geology*, **19 (8)**: 855-858.
- Ashley, P.M., Dudley, R.L., Lesh, R.H., Marr, J.M., and Ryall, A.W. 1988. The Scuddles Cu-Zn prospect, an Archean volcanogenic massive sulfide deposit, Golden Grove district, Western Australia. *Economic Geology*, **83**: 918-951.
- Arias, Z.G., and Helmstaedt, H. 1990. Grant 343 Structural Evolution of the Michipicoten (Wawa) Greenstone Belt, Superior Province: Evidence for an Archean Fold and Thrust Belt. *In Geoscience Research Grant Program Summary of Research 1989-1990*. Edited by V.G. Milne. Ontario Geological Survey, Miscellaneous Paper 150, pp. 107-114.
- Ayres, L.D. 1978. Metamorphism in the Superior Province of Northwestern Ontario and its relationship to crustal development. *In Metamorphism in the Canadian Shield*. Edited by J.A. Fraser and W.W. Heywood. Geological Survey of Canada Paper 78-10, pp. 25-36.
- Barker, F. 1979. Trondhjemite: Definition, environment and hypotheses of origin. *In Trondhjemites, Dacites, and Related Rocks*. Edited by F. Barker. Elsevier, Developments in Petrology, Amsterdam, Vol. 4, pp. 1-12.

- Bigot, L. 2012. Gold Mineralizations at the Syenite-hosted Beattie Gold Deposit at Duparquet, Neoproterozoic Abitibi Belt, Quebec, Canada. M.Sc. thesis, Université du Québec à Montréal, Montréal, Quebec.
- Bédard, L.P., and Ludden, J.N. 1997. Nd-isotope evolution of Archean plutonic rocks in the Opatica, Abitibi and Pontiac subprovinces, Quebec, Canada. *Canadian Journal of Earth Sciences*, **34**: 286-299.
- Bédard, J.H. 2006. A catalytic delamination-driven model for coupled genesis of Archean crust and sub-continental lithospheric mantle. *Geochimica et Cosmochimica Acta*, **70**: 1188-1214.
- Bédard, J.H. 2013. How many arcs can dance on the head of a plume? A 'Comment' on: A critical assessment of Neoproterozoic 'plume only' geodynamics: Evidence from the Superior province, by Derek Wyman, *Precambrian Research*, 2012. *Precambrian Research*, **229**: 189-197.
- Bédard, J.H., and Harris, L.B. 2014. Neoproterozoic disaggregation and reassembly of the Superior craton. *Geology*, **42**: 951-954
- Bekker, A., Slack, J.F., Planavsky, N., Krapež, N., Hofmann, A., Konhauser, K.O., and Rouxel, O.J. 2010. Iron Formation: The Sedimentary Product of a Complex Interplay among Mantle, Tectonic, Oceanic, and Biospheric Processes. *Economic Geology*, **105 (3)**: 467-508.
- Berman, R.G., Davis, W.J., and Pehrsson, S. 2007. Collisional Snowbird tectonic zone resurrected: Growth of Laurentia during the 1.9 Ga accretionary phase of the Hudsonian orogeny. *Geology*, **35**: 911-914.
- Brady, J. 2018a. Recalculation of a feldspar analysis (all Fe as FeO) and solving for Fe+3 [online]: Available from [https://serc.carleton.edu/research\\_education/equilibria/mineralformulaerecalculation.html](https://serc.carleton.edu/research_education/equilibria/mineralformulaerecalculation.html) [cited 10 May 2018].
- Brady, J. 2018b. Recalculation of an EDS/WDS mica analysis using stoichiometry to place limits on Fe+3 [online]: Available from [https://serc.carleton.edu/research\\_education/equilibria/mineralformulaerecalculation.html](https://serc.carleton.edu/research_education/equilibria/mineralformulaerecalculation.html) [cited 10 May 2018].
- Bryan, S.E. 2006. Petrology and Geochemistry of the Quaternary Caldera-forming, Phonolitic Granadilla Eruption, Tenerife (Canary Islands). *Journal of Petrology*, **47 (8)**: 1557-1589.
- Canfield, D.E., Raiswell, R., Westrich, J.T., Reaves, C.M., and Berner, R.A. 1986. The use of chromium reduction in the analysis of reduced inorganic sulphur in sediments and shale. *Chemical Geology*, **54**: 149-155.

- Canfield, D.E., and Raiswell, R. 1999. The evolution of the sulphur cycle. *American Journal of Science*, **299**: 697-723.
- Card, K.D. 1990. A review of the Superior Province of the Canadian Shield, a product of Archean accretion. *Precambrian Research*, **48**: 99-156.
- Cawood, A., Kröner, A., and Pisarevsky, S. 2006. Precambrian plate tectonics: Criteria and Evidence. *GSA Today*, **16**: 4-11.
- Ciborowski, T.J.R., Kerr, A.C., Ernst, R.E., McDonald, I., Minifie, M.J., Harlan, S.S., and Millar, I.L. 2015. The Early Proterozoic Matachewan Large Igneous Province: Geochemistry, Petrogenesis, and Implications for Earth Evolution. *Journal of Petrology*, **56 (8)**: 1459-1494.
- Ciufo, T., Mercier-Langevin, P., Yakymchuk, C., Lin, S., Bécu, V., Lauzière, K. 2019. Whole-rock litho-geochemistry of the Archean Island Gold deposit Ontario, Canada. Geological Survey of Canada, Open File 8524, 1 .zip file.
- Corfu, F., and Sage, R.P. 1987. A precise U-Pb zircon age for a Trondhjemite clast in the Dore Conglomerate, Wawa, Ontario. *In Proceedings and Abstracts, Institute on Lake Superior Geology Annual Meeting, Wawa, Ontario, Vol. 33, Part 1, pp. 18.*
- Corfu, F., and Sage R.P. 1992. U-Pb age constraints for deposition of clastic metasedimentary rocks and late tectonic plutonism, Michipicoten Belt, Superior Province. *Canadian Journal of Earth Sciences*, **29**: 1640-1651.
- Couture, J.-F., and Pilote, P. 1993. The Geology and Alteration Patterns of a Disseminated, Shear Zone-Hosted Mesothermal Gold Deposit: The Francoeur 3 Deposit, Rouyn-Noranda, Quebec. *Economic Geology*, **88**: 1664-1684.
- Core Research Equipment & Instrument Training (CREAIT) Network. 2018. The Scanning Electron Microscope (SEM) [online]: Available from <https://www.mun.ca/research/resources/creait/physical-sci/maf/sem/mla.php> [cited 20 May 2018].
- Cross, W., Iddings, J.P., Pirrson, L.V., and Washington, H.S. 1902. A quantitative chemico-mineralogical classification and nomenclature of igneous rocks. *Journal of Geology*, **10**: 555-590.
- Davidson, A. 1995. A review of the Grenville orogen in its North American type area. *AGSO Journal of Australian Geology & Geophysics*, **16 (1/2)**: 3-24.
- Davis, D.W. 2002. U-Pb geochronology of Archean metasedimentary rocks in the Pontiac and Abitibi subprovinces, Quebec, constraints on timing, provenance and regional tectonics. *Precambrian Research*, **115 (1)**: 97-117.

- Debon, F., and Le Fort, P. 1983. A chemical-mineralogical classification of common plutonic rocks and associations. *Transactions of Royal Society of Edinburgh, Earth Sciences* **73**: 135–149.
- Debon, F., and Lefort, P. 1988. A Cationic Classification of Common Plutonic Rocks and Their Magmatic Associations: Principles, Method, Applications. *Bulletin de Mineralogie*, **111**: 493-510.
- Deer, W.A., Howie, R.A., and Zussman, J. 1963. *Rock-forming minerals, Vol. 1. Ortho- and ring silicates*. Longman, London, England.
- Deer, W.A., Howie, R.A., and Zussman, J. 1992. *An introduction to the rock forming minerals*, 2<sup>nd</sup> ed. Longman Scientific and Technical, New York, New York.
- De La Roche, H., Leterrier, J., Grandclaude, P., and Marchal, M., 1980. A classification of volcanic and plutonic rocks using R<sub>1</sub> R<sub>2</sub>-diagram and major element analyses – Its relationships with current nomenclature. *Chemical Geology*, **29**: 183-210.
- Dinel, E., Fowler, A.D., Ayer, J., Still, A., Tylee, K., and Barr, E. 2008. Litho-geochemical and Stratigraphic Controls on Gold Mineralization within the Metavolcanic Rocks of the Hoyle Pond Mine, Timmins, Ontario. *Economic Geology*, **103**: 1341-1363.
- Environmental Isotope Laboratory (EIL). 2017. <sup>34</sup>S Isotope Analysis: Equipment, data report guide and precision details. *Received by Tyler Ciufu*.
- Farquhar, J., Bao, H., and Thiemens, M. 2000. Atmospheric Influence of Earth's Earliest Sulfur Cycle. *Science*, **289 (5480)**, 756-758.
- Farquhar, J., Savarino, J., Airieau, S., and Thiemens, M.H. 2001. Observation of wavelength-sensitive mass-independent sulfur isotope effects during SO<sub>2</sub> photolysis: application to the early atmosphere. *Journal of Geophysical Research: Planets*, **106 (E12)**: 32829-32839.
- Farquhar, J., Wing, B.A., McKeegan, K.D., Harris, J.W., Cartigny, P., and Thiemens, M.H. 2002. Mass-Independent Sulfur of Inclusions in Diamond and Sulfur Recycling on Early Earth. *Science*, **298**: 2369-2372.
- Farquhar, J., and Wing, B.A. 2003. Multiple sulfur isotopes and the evolution of the atmosphere. *Earth and Planetary Science Letters*, **213**: 1-13.
- Farquhar, J., Johnston, D.T., and Wing, B.A. 2007a. Implications of conservation of mass effects on mass-dependent isotope fractionations: Influence of network structure on sulfur isotope phase space of dissimilatory sulfate reduction. *Geochimica et Cosmochimica Acta*, **71**: 5862–5875.

- Farquhar, J., Sang-Tae, K., and Masterson, A. 2007b. Implications from sulfur isotopes of the Nakhla meteorite for the origin of sulfate on Mars. *Earth and Planetary Science Letters*, **264** (1-2): 1-8.
- Franklin, J.M., Kasarda, J., and Poulson, K.H. 1975. Petrology and chemistry of the alteration zone of the Mattabi massive sulfide deposit. *Economic Geology*, **70**: 63-79.
- Gill, J.B. 1981. *Orogenic Andesites and Plate Tectonics*. Springer-Verlag, Berlin, Germany.
- Goldfarb, R.J., Groves, D.I., and Gardoll, S. 2001. Orogenic gold and geologic time: a global synthesis. *Ore Geology Reviews*, **18**: 1-75.
- Goldfarb, R.J., Baker, T., Dubé, B., Groves, D.I., Hart, C.J.R., and Gosselin, P. 2005. Distribution, Character, and Genesis of Gold Deposits in Metamorphic Terranes. *In* *Economic Geology 100th Anniversary Volume*. Edited by J.W. Hedenquist, J.F.H. Thompson, R.J. Goldfarb, and J.P. Richards. Society of Economic Geologists, Littleton, Colorado, USA, pp. 407-450.
- Goodwin, A.M., Monster, J., and Thode, H.G. 1976. Carbon and sulfur isotope abundances in Archean iron-formations and early Precambrian life. *Economic Geology*, **71**: 870-891.
- Grant, J.A. 1986. The Isocon Diagram—A Simple Solution to Gresens' Equation for Metasomatic Alteration. *Economic Geology*, **81**: 1976-1982.
- Grant, J.A. 2005. Isocon analysis: a brief review of the method and applications. *Physics and Chemistry of the Earth*, **30**: 997-1004.
- Gresens, R.L. 1967. Composition-volume relationships of metasomatism. *Chemical Geology*, **2**: 47-55.
- Gross, G.A. 1980. A Classification of Iron Formations based on Depositional Environments. *Canadian Mineralogist*, **18**: 215-222.
- Groves, D.I. 1993. The crustal continuum model for late-Archaeon lode-gold deposits of the Yilgarn Block, Western Australia. *Mineralium Deposita*, **28**: 366-374.
- Groves, D.I., Goldfarb, R.J., Gebre-Mariam, M., Hagemann, S.G., and Robert, F. 1998. Orogenic gold deposits: A proposed classification in the context of their crustal distribution and relationship to other gold deposit types. *Ore Geology Reviews*, **13**: 7-27.
- Hastie, A.R., Kerr, A.C., Pearce, J.A., and Mitchell S.F. 2007. Classification of altered volcanic island arc rocks using immobile trace elements: development of the Th-Co discrimination diagram. *Journal of Petrology*, **48**: 2341-2357.
- Heaman, L.M. 1997. Global mafic magmatism at 2.45 Ga: Remnants of an ancient large igneous province? *Geology*, **25**: 299-302.

- Heather, K.B., and Arias, Z.G. 1987. 024: Geological Setting of Gold Mineralization in the Goudreau-Lochalsh Area, District of Algoma. *In* Summary of Field Work and Other Activities 1987, by the Ontario Geological Survey. *Edited by* R.B. Barlow, M.E. Cherry, A.C. Colvine, B.O. Dressler and O.L. White. Ontario Geological Survey, Miscellaneous Paper 137, pp. 155-162.
- Heather, K.B., and Arias, Z. 1992. Geological and Structural Setting of Gold Mineralization in the Goudreau-Lochalsh Area, Wawa Gold Camp. Ontario Geological Survey, Open File Report 5832.
- Hey, M.H. 1954. A new review of the chlorites. *The Mineralogical Magazine*, **224**: 277–292.
- Hoffman, P.F. 1988. United Plates of America, The Birth of a Craton: Early Proterozoic Assembly and Growth of Laurentia. *Annual Review of Earth and Planetary Sciences*, **16**: 543-603.
- Hoffman, P.F. 1989. Precambrian geology and tectonic history of North America. *In* *Geology of North America - An Overview*. *Edited by* A.W. Bally and A.R. Palmer. Geological Society of America, pp. 447-512.
- Hoffman, E.L., Clark, J.R., and Yeager, J.R. 1998. Gold analysis – Fire Assaying and alternative methods. *Exploration and Mining Geology*, **7**: 155-160.
- Hoffman, E.L., and Dunn, B. 2002. Sample Preparation and Bulk Analytical Methods for PGE. *In* CIM Special Volume 54 The Geology, Geochemistry and Mineral Beneficiation of Platinum Group Elements. *Edited by* L.J. Cabri. Canadian Institute of Mining, Metallurgy and Petroleum, Montreal, Quebec, Vol. 54, pp. 1-11.
- Hooper, P.R., and Hawkesworth, C.J. 1993. Isotopic and geochemical constraints on the origin and evolution of the Columbia River Basalt. *Journal of Petrology*, **34**: 1203-1246.
- Hou, K., Li, Y., and Wan, D. 2007. Constraints on the Archean atmospheric oxygen and sulfur cycle from mass-independent sulfur records from Anshan-Benxi BIFs, Liaoning Province, China. *Science in China Series D: Earth Sciences*, **50 (10)**: 1471-1478.
- Hronsky, J., Groves, D.I., Loucks, R.R., and Begg, G.C. 2012. A unified model for gold mineralisation in accretionary orogens and implications for regional-scale exploration targeting methods. *Mineralium Deposita*, **47**: 339-358.
- Hutchison, C.S. 1975. The norm, its variations, their calculation and relationships. *Schweizerische mineralogische und petrographische Mitteilungen*, **55**: 243–256.
- Irvine, T.N., and Baragar, W.R.A. 1971. A guide to the chemical classification of the common volcanic rocks: *Canadian Journal of Earth Sciences*, **8**: 523-548.

- Ishikawa, Y., Sawaguchi, T., Iwaya, S., and Horiuchi, M. 1976. Delineation of prospecting targets for Kuroko deposits based on modes of volcanism of underlying dacite and alteration halos. *Mining Geology*, **26**: 105-117.
- Janoušek, V., Farrow, C.M., and Erban, V. 2006. Interpretation of Whole-rock Geochemical Data in Igneous Geochemistry: Introducing Geochemical Data Toolkit (GCDkit). *Journal of Petrology*, **47** (6): 1255-1259.
- Janoušek, V. Diversity and processes modifying composition of the igneous rocks. Czech Geological Survey. Available from <http://www.geology.cz/projekt681900/english/learning-resources/ETIO%201%20Classification%20and%20diversification%20of%20magmas.pdf> [cited 25 March 2018]
- Jellicoe, K. 2019. Structural Controls and Deformation History of the Orogenic Island Gold Deposit, Michipicoten Greenstone Belt, Ontario. M.Sc. thesis, Department of Earth and Environmental Sciences, The University of Waterloo, Waterloo, Ontario.
- Jenner, G.A. 1996. Trace element geochemistry of igneous rocks: Geochemical nomenclature and analytical geochemistry. *In* Trace Element Geochemistry of Volcanic Rocks: Applications for Massive Sulfide Exploration, 12, *Edited by* D.A. Wyman. Geological Association of Canada, Short Course Notes, St. John's, Newfoundland, Vol. 12, pp. 51-77.
- Kenis, I. 2004. Brittle-Ductile Deformation Behaviour in the Middle Crust as Exemplified by Mullions (Former "Boudins") in the High Ardenne Slate Belt, Belgium. *Edited by* Gullentops, F. Leuven University Press, Leuven, Belgium.
- Kishida, A., and Kerrich, R. 1987. Hydrothermal Alteration Zoning and Gold Concentration at the Kerr-Addison Archean Lode Gold Deposit, Kirkland Lake, Ontario. *Economic Geology*, **82**: 649-690.
- Lambert, I.B., Phillips, G.N., and Groves, D.I. 1984. Sulfur isotope compositions and genesis of Archaean gold mineralization, Australia and Zimbabwe. *In* Gold'82: The Geology, Geochemistry and Genesis of Gold Deposits. *Edited by* R.P. Foster. Geological Society of Zimbabwe Special Publication No. 1, A.A. Balkema Publishers, Rotterdam, Netherlands, pp. 373-387.
- Lambert, I.B., and T. H. Donnelly. 1992. Global Oxidation and a Supercontinent in the Proterozoic: Evidence from Stable Isotopic Trends. *In* Early Organic Evolution: Implications for Mineral and Energy Resources. *Edited by* M.G. Schidlowski, S. Golubic, M.M. Kimberly, D.M. McKirdy and P.A. Trudinger. Springer-Verlag, New York, pp. 408-415.



- Laporte, D., Lambart, S., Schiano, P., and Ottolini, L. 2014. Experimental derivation of nepheline syenite and phonolite liquids by partial melting of upper mantle peridotites. *Earth and Planetary Science Letters*, 404: 319-331.
- Large, R.R., Gemmell, J.B., and Paulick, H. 2001. The Alteration Box Plot: A Simple Approach to Understanding the Relationship between Alteration Mineralogy and Lithogeochemistry Associated with Volcanic-Hosted Massive Sulfide Deposits. *Economic Geology*, **96**: 957-971.
- Le Bas, M.J., Le Maitre, R.W., Streckeisen, A., and Zanettin, B. 1986. A Chemical Classification of Volcanic Rocks Based on the Total Alkali-Silica Diagram. *Journal of Petrology*, **27** (3): 745-750.
- Leclair, A.D., Ernst, R.E., and Hattori, K. 1993. Crustal-scale auriferous shear zones in the central Superior Province, Canada. *Geology*, **21** (5): 399-402.
- Leech, G.B., Lowden, J.A., Stockwell, C.H., and Wanless, R.K. 1963. Age determinations and geological studies. Geological Survey of Canada Paper 63-17, Ottawa, Ontario, pp. 140.
- Lin, S. 2005. Synchronous vertical and horizontal tectonism in the Neoproterozoic: Kinematic evidence from a synclinal keel in the northwestern Superior craton, Canada. *Precambrian Research*, **139** (3): 181-194.
- Lin, S., and Beakhouse, G.P. 2013. Synchronous vertical and horizontal tectonism at late stages of Archean cratonization and genesis of Hemlo gold deposit, Superior craton, Ontario, Canada. *Geology*, **41** (3): 359-362.
- López-Moro, F.J. 2012. EASYGRESGRANT—A Microsoft Excel spreadsheet to quantify volume changes and to perform mass-balance modeling in metasomatic systems. *Computers & Geosciences*, **39**: 191-196.
- Loucks, R.R., and Mavrogenes, J.A. 1999. Gold Solubility in Supercritical Hydrothermal Brines Measured in Synthetic Fluid Inclusions. *Science*, **284**: 2159-2163.
- Machado, N., Clark, T., David, J., and Goulet, N. 1997. U–Pb ages for magmatism and deformation in the New Quebec Orogen. *Canadian Journal of Earth Sciences*, **34** (5): 716-723.
- Martin, R.D. 2012. Syenite-hosted gold mineralization and hydrothermal alteration at the Young-Davidson deposit, Matachewan, Ontario. M.Sc. thesis, The University of Waterloo, Waterloo, Ontario.
- Mason, B., and Berry, L.G. 1968. *Elements of Mineralogy*. W.H. Freeman and Company, San Francisco, California.

- Maynard, J.B., Sutton, S.J., Rumble III, D., and Bekker, A. 2013. Mass-independently fractionated sulfur in Archean paleosols: A large reservoir of negative  $\Delta^{33}\text{S}$  anomaly on the early Earth. *Chemical Geology*, **362**: 74-81.
- McDonough, W.F., and Sun, S.S. 1995. Composition of the Earth. *Chemical Geology*, **120**: 223-253.
- McGill, G.E., and Shradly, C.H. 1988. Structure of the Southwestern Michipicoten Greenstone Belt, Ontario: Evidence for Archean Accretion. *In Workshop on the Growth of Continental Crust, Lunar and Planetary Institute, Houston, Texas*, pp. 98-100.
- McGill, G.E. 1992. Structure and kinematics of a major tectonic contact, Michipicoten Greenstone Belt, Ontario. *Canadian Journal of Earth Sciences*, **29**: 2118-2132.
- Middlemost, E.A.K. 1994. Naming materials in the magma/igneous rock system. *Earth-Science Reviews*, **37**: 215-224.
- Moritz, R.P., and Crocket, J.H. 1991. Hydrothermal wall-rock alteration and the formation of the gold-bearing quartz-fuchsite vein at the Dome Mine, Timmins area, Ontario, Canada. *Economic Geology*, **86 (3)**: 620-643.
- Moser, D.E., Krogh, T.E., Heaman, L. M., Hanes, J.A., and Helmstaedt, H. 1991. *In Program with Abstracts, GAC-AGC-MAC-AMC-SEG Annual Meeting, Toronto, Ontario*, pp. A86
- Moyen, J.F., and Martin, H. 2012. Forty years of TTG research. *Lithos*, **148**: 312-336.
- Mukherjee, P.K., and Gupta, P.K. 2008. Arbitrary scaling in ISOCON method of geochemical mass balance: an evaluation of the graphical approach. *Geochemical Journal*, **42**: 247-253.
- Mursky, G.A., and Thompson, R.M. 1958. A specific gravity index for minerals. *The Canadian Mineralogist*, **6 (2)**: 273-287.
- Natural Resources Canada. 2018. Historical STPL-BAS and STPL-PML-53 standards results compilation. *Received by T. Ciufu*.
- Ohmoto, H., and Rye, R. 1979. Isotopes of Sulfur and Carbon. *In Geochemistry of Hydrothermal Ore deposits*, 2nd edition. *Edited by H.L. Barnes*. New York, Wiley, pp. 509-567.
- Paton, C., Hellstrom, J., Paul, B., Woodhead, J., and Hergt, J. 2011. Iolite: Freeware for the visualisation and processing of mass spectrometric data. *Journal of Analytical Atomic Spectrometry*, **26(12)**: 2508-2518.

- Pavlov, A.A., and Kasting, J.F. 2002. Mass independent fractionation of sulfur isotopes in Archaean sediments: Strong evidence for an anoxic Archaean atmosphere. *Astrobiology*, **2**: 27-41.
- Pearce, J.A., and Norry, M.J. 1979. Petrogenetic Implications of Ti, Zr, Y, and Nb Variations in Volcanic Rocks. *Contributions to Mineralogy and Petrology*, **69**: 33-47.
- Pearce, J.A. 1996. A user's guide to basalt discrimination diagrams. *In Trace Element Geochemistry of Volcanic Rocks: Applications for Massive Sulphide Exploration. Edited by D.A. Wyman. Geological Association of Canada, Short Course Notes, St. John's, Newfoundland, Vol. 12, pp. 79-113.*
- Percival, J.A., and Easton, R.M. 2007. Geology of the Canadian Shield in Ontario: an update. Ontario Geological Survey, Sudbury Ontario, Open File Report 6196, Geological Survey of Canada, Open File 5511, Ontario Power Generation, Report 06819-REP-01200-10158-R00.
- Percival, J.A., Skulski, T., Sanborn-Barrie, M., Stott, G.M., Leclair, A.D., Corkery, M.T., and Boily, M. 2012. Geology and tectonic evolution of the Superior Province, Canada. Chapter 6 *In Tectonic Styles in Canada: The LITHOPROBE Perspective. Edited by J.A. Percival, F.A. Cook and R.M. Clowes. Geological Association of Canada, Special Paper 49, pp. 321-378.*
- Phillips, G.N., and Groves, D.I. 1983. The nature of Archaean gold-bearing fluids as deduced from gold deposits of Western Australia. *Journal of the Geological Society of Australia*, **30**: 25-39.
- Phillips, G.N. 2013. Australian and global setting for gold in 2013. *In World Gold 2013. The Australian Institute of Mining and Metallurgy, Brisbane, Australia, pp. 15-21.*
- Piercey, S.J. 2014. Modern Analytical Facilities 2. A Review of Quality Assurance and Quality Control (QA/QC) Procedures for Lithochemical Data. *Geoscience Canada*, **41**: 75-88.
- Poulsen, K.H., Robert, F., and Dubé, B. 2000. Geological Classification of Canadian Gold Deposits. Geological Survey of Canada, Bulletin 540, Ottawa, Ontario, pp. 1-106.
- Rivers, T., Culshaw, N., Hynes, A., Indares, A., Jamieson, R., and Martignole, J. 2012. The Grenville Orogen – A post-LITHOPROBE perspective. Chapter 3 *In Tectonic Styles in Canada: the LITHOPROBE Perspective. Edited by J.A. Percival, F.A. Cook, and R.M. Clowes. Geological Association of Canada, Special Paper 49, pp. 97-236.*
- Sage, R.P. 1993. Geology of Agounie, Bird, Finan and Jacobson Townships, District of Algoma, Ontario. Ministry of Northern Development and Mines, Ontario Geological Survey, Open File Report 5588.

- Sage, R.P. 1994. Geology of the Michipicoten Greenstone Belt. Ministry of Northern Development and Mines, Ontario Geological Survey, Open File Report 5888.
- Sage, R.P., Lightfoot, P.C., and Doherty, W. 1996. Geochemical characteristics of granitoid rocks from within the Archean Michipicoten Greenstone Belt, Wawa Subprovince, Superior Province, Canada: implications for source regions and tectonic evolution. *Precambrian Research*, **76**: 155-190.
- Schilling, J.G., Zajac, M., Evans, R., Johnston, T., White, W., Devine, J.D., and Kingsley, R. 1983. Petrologic and geochemical variations along the Mid-Atlantic Ridge from 29°N to 73°N. *American Journal of Science* **283**: 510-586.
- Schneider, D.A., Bachtel, J., and Schmitt, A.K. 2012. Zircon alteration in wall rock of Pamour and Hoyle Pond Au deposits, Abitibi Greenstone Belt: Constraints on timescales of fluid flow from depth-profiling techniques. *Economic Geology*, **107**: 1043-1072.
- Seifert, W., Rhede, D., Thomas, R., Förster, H.J., Lucassen, F., Dulski, P., and Wirth, R. 2011. Distinctive properties of rock-forming blue quartz: inferences from a multi-analytical study of submicron mineral inclusions. *Mineralogical Magazine*, **75**: 2519-2534.
- Selvaraja, V., Fiorentini, M.L., LaFlamme, C.K., Wing, B.A., and Hao, T.H. 2017. Anomalous sulfur isotopes trace volatile pathways in magmatic arcs. *Geology*, **45**: 419-422.
- Skoog, D.A., and West, D.M. 1963. *Fundamentals of analytical chemistry*. Holt, Rinehart and Winston, New York, New York.
- Smith, E.J., Kesler, S.E., and Van Hees, E.H.P. 1987a. Relationship of Fluid Inclusion Geochemistry to Wall-Rock Alteration and Lithochemical Zonation at the Hollinger-McIntyre Gold Deposit, Porcupine District, Canada. *Journal of Geochemical Exploration*, **29**: 434.
- Smith, P.E., Tatsumoto, M., and Farquhar, R.M. 1987b. Zircon Lu - Hf systematics and evolution of the Archean crust in the Superior Province, Canada; *Contributions to Mineralogy and Petrology*, **97**: 93-104.
- Stanley, C.R., and Lawie, D. 2007. Average relative error in geochemical determinations: Clarification, calculation, and a plea for consistency. *Exploration and Mining Geology*, **16**: 267-275.
- Stern, R.A., and Hanson, G.N. 1992. Origin of Archean lamprophyre dykes, Superior Province, Canada: rare earth element and Nd-Sr isotopic evidence. *Contributions to Mineralogy and Petrology*, **111**: 514-526.
- Streckeisen, A.L. 1976a. To each plutonic rock its proper name. *Earth-Science Reviews*, **12**: 1-33.

- Streckeisen, A.L. 1976b. Classification of the common igneous rocks by means of their chemical composition: a provisional attempt. *Neues Jahrbuch für Mineralogie, Monatshefte*, **1**: 1-15.
- Streckeisen, A., Zanettin, B., Le Bas, M.J., Bonin, B., Bateman, P., Bellieni, G., Dudek, A., Efremova, S., Keller, J., Lameyre, J., Sabine, P.A., Schmid, R., Sørensen, H., and Woolley, A.R. 2002. *Igneous Rocks: A Classification and Glossary of Terms*. Edited by R.W. Le Maitre. Cambridge University Press, Cambridge, United Kingdom.
- Sylvester, P.J., Attoh, K., and Schulz, K.J. 1987. Tectonic setting of late Archean bimodal volcanism in the Michipicoten (Wawa) greenstone belt, Ontario. *Canadian Journal of Earth Sciences*, **24**: 1120-1134.
- Tappert, M.C., Rivard, B., Giles, D., Tappert, R., and Mauger, A. 2013. The mineral chemistry, near-infrared, and mid-infrared reflectance spectroscopy of phengite from the Olympic Dam IOCG deposit, South Australia. *Ore Geology Reviews*, **53**: 26-38.
- Telford, W.M., Geldart, L.P., and Sheriff, R.E. 1990. *Applied Geophysics*, Second Edition. Cambridge University Press, New York, New York.
- Thurston, P.C. 1994. Archean volcanic patterns. *In Archean Crustal Evolution*. Edited by K.C. Condie. *Developments in Precambrian Geology*, Elsevier, Amsterdam, Vol. 11, pp. 45-84.
- Tindle, A.G., and Webb, P.C. 1990. Estimation of lithium contents in trioctahedral micas using microprobe data: application to micas from granitic rocks. *European Journal of Mineralogy*, **2**: 595-610.
- Tindle, A.G. 2018a. Biotite etc. Formula Unit Calculations - with optional calculated Li<sub>2</sub>O [online]: Available from <http://www.open.ac.uk/earth-research/tindle/AGTWebData/Mica-bio.xls> [cited May 10, 2018].
- Tindle, A.G., 2018b. Chlorite formula unit calculator and variety namer (Chlorite.xls) [online]: Available from <http://www.open.ac.uk/earth-research/tindle/AGTWebData/Chlorite.xls> [cited May 10, 2018].
- Turcotte, B., and Pelletier, C. 2008. Technical Report and Mineral Resource Estimate for the Magino Mine (according to Regulation 43-101 and Form 43-101F1). Golden Goose Resources Inc., Montréal, Québec, Canada.
- Tomkins, A.G. 2013. On the source of orogenic gold. *Geology*, **41**: 1255-1256.
- Tomlinson, K.Y., Davis, D.W., Stone, D., and Hart, T.R. 2003. U-Pb age and Nd isotopic evidence for Archean terrane development and crustal recycling in the south-central Wabigoon subprovince, Canada. *Contributions to Mineralogy and Petrology*, **144**: 684-702.

- Turek, A., Smith, P.E., and Van Schmus, W.R. 1982. Rb-Sr and U-Pb ages of volcanics and granite emplacement in the Michipicoten Belt-Wawa, Ontario; *Canadian Journal of Earth Sciences*, **19**: 1608-1626.
- Turek, A., Smith, P.E., and Van Schmus, W.R. 1984. U-Pb zircon ages and the evolution of the Michipicoten plutonic-volcanic terrane of the Superior Province, Ontario. *Canadian Journal of Earth Sciences*, **21**: 457-464.
- Turek, A., Van Schmus, W.R., and Sage, R.P. 1988. Extended volcanism in the Michipicoten Greenstone Belt, Wawa, Ontario. *In* Program with Abstracts, GAC-MAC-CSPGAGC-AMC-SCGP Annual Meeting, St. John's, Newfoundland, Vol. 13, pp. A127.
- Turek, A., Sage, R.P., and Van Schmus, W.R. 1992. Advances in the U-Pb zircon geochronology of the Michipicoten Greenstone Belt, Superior Province, Ontario. *Canadian Journal of Earth Sciences*, **29**: 1154-1165.
- Van Kranendonk, M. J. 1996. Tectonic evolution of the Paleoproterozoic Torngat Orogen: Evidence from pressure-temperature-time-deformation paths in the North River map area, Labrador. *Tectonics*, **15**: 843-869.
- Warren, H.B. 2011. Plate tectonics began in Neoproterozoic time and plumes from deep mantle have never operated. *Lithos*, **123**: 1-20.
- Weast, R.C. 1972. *CRC Handbook of Chemistry and Physics*, 53<sup>rd</sup> edition. CRC Press, Cleveland, Ohio.
- Wetherill, G.W. 1956. Discordant uranium-lead ages. *Transaction of the American Geophysical Union*, **37 (3)**: 320-326.
- Williams, H.R. 1989. Subprovince accretion tectonics in the south-central Superior Province. *Canadian Journal of Earth Science*, **27**: 570-581.
- Williams, H.R., Scott, G.M., Heather, K.B., Muir, T.L., Sage, R.P. 1991. Wawa Subprovince. Chapter 12 *in* *Geology of Ontario*. Edited by P.C. Thurston, H.R. Williams, R.H. Sutcliffe, and G.M. Stott. Ontario Geological Survey, Special Volume 4, Part 1, pp. 485-539.
- Wilson, A.D. 1955. A new method for the determination of ferrous iron in rocks and minerals. *Bulletin of the Geological Survey of Great Britain*, Vol. 9, pp. 56-58.
- Wilson, M. 1989. Chapter 9 *in* *Igneous Petrogenesis: A Global Tectonic Approach*. Unwin Hyman, London.

- Winchester, J.A., and Floyd, P.A. 1977. Geochemical discrimination of different magma series and their differentiation products using immobile elements. *Chemical Geology*, **20**: 325-343.
- Winter, J.D. 2010. *Principles of Igneous and Metamorphic Petrology*, Second Edition. Pearson Prentice Hall, Upper Saddle River, N.J.
- Wu, N. 2018. University of Maryland Stable Isotope Laboratory methods and data evaluation. *Received by T. Ciufu*.
- Wu, N., Farquhar, J., Dottin III, J.W., and Magalhaes, N. 2018. Sulfur isotope signatures of eucrites and diogenites. *Geochimica et Cosmochimica Acta*, **223**: 1-13.
- Wyman, D.A., Kerrich, R., and Polat, A. 2002. Assembly of Archean cratonic mantle lithosphere and crust: plume-arc interaction in the Abitibi-Wawa subduction-accretion complex. *Precambrian Research*, **115**: 37-62.
- Wyman, D., and Kerrich, R. 2010. Mantle plume volcanic arc interaction: consequences for magmatism, metallogeny, and cratonization in the Abitibi and Wawa subprovinces, Canada. *Canadian Journal of Earth Sciences*, **47**: 565-589.
- Wyman, D.A. 2013a. A critical assessment of Neoproterozoic “plume only” geodynamics: Evidence from the Superior Province. *Precambrian Research*, **229**: 3-19.
- Wyman, D.A. 2013b. A reply to “How many arcs can dance on the head of a plume?” by Jean Bédard, *Precambrian Research*, 2012. *Precambrian Research*, **229**: 198-202.
- Xue, Y., Campbell, I., Ireland, T.R., Holden, P., and Armstrong, R. 2013. No mass-independent sulfur isotope fractionation in auriferous fluids supports a magmatic origin for Archean gold deposits. *Geology*, **41**: 791-794.
- Zhang, J., Linnen, R., Lin, S., Davis, D., and Martin, R. 2014. Paleoproterozoic hydrothermal reactivation in a neoproterozoic orogenic lode-gold deposit of the southern Abitibi subprovince: U-Pb monazite geochronological evidence from the Young-Davidson mine, Ontario. *Precambrian Research*, **249**: 263-272.
- Zhilong, H., Chongqiang, L., Hailing, Y., Cheng, X., Runsheng, H., Yunhua, X., Bo, Z., and Wenbo, L. 2002. The geochemistry of lamprophyres in the Laowangzhai gold deposits, Yunnan Province, China: Implications for its characteristics of source region. *Geochemical Journal*, **36**: 91-112.
- Zhu, Y., An, F., and Tan, J. 2011. Geochemistry of hydrothermal gold deposits: A review. *Geoscience Frontiers*, **2**: 367-374.

**Appendix A**  
**Supplementary information for mine geologists**



### **Differentiating between the gabbro, gabbro/lamprophyre, and silica-poor diorite–monzodiorite**

In many cases, it is challenging to distinguish between the gabbro, gabbro/lamprophyre, and silica-poor diorite–monzodiorite at the Island Gold deposit macroscopically. This problem is exacerbated when examining dust-covered walls in the damp, poorly-lit conditions typical of underground mine workings. Key mineralogical, textural, and chemical differences between these lithologies that can be used to help distinguish between them are discussed below.

The silica-poor diorite–monzodiorite is composed of less chlorite when compared to the gabbro and gabbro/lamprophyre. This results in the silica-poor diorite–monzodiorite generally having a lighter colour than either of these two lithologies. The silica-poor diorite–monzodiorite also often has a large proportion of biotite which is not present in the gabbro/lamprophyre and was only observed in the gabbro if it was altered by nearby auriferous quartz veins. Furthermore, the silica-poor diorite–monzodiorite often has a slight pink colouration due to hematite and this is diagnostic when comparing this lithology to the gabbro or gabbro/lamprophyre. Lastly, when these three lithologies are located in the same area, the silica-poor diorite–monzodiorite is typically less deformed than both the gabbro and the gabbro/lamprophyre. When compared to the gabbro, the gabbro/lamprophyre has a larger proportion of carbonate minerals and quartzofeldspathic minerals, but less epidote and chlorite.

Despite the substantial amount of carbonate minerals in the gabbro/lamprophyre, this lithology typically has no reaction or only a weak reaction with HCl. This lithology is also usually non-magnetic. These features can be used to distinguish it from the gabbro and silica-poor diorite–monzodiorite which both often react with HCl and are magnetic. The silica-poor diorite–monzodiorite is typically magnetic and often reacts with dilute HCl. The gabbro may be either magnetic or non-magnetic but consistently reacts with dilute HCl. These basic field tests may be useful in helping differentiate between these lithologies.

The higher concentration of magnesium, chromium, and nickel in the gabbro/lamprophyre when compared to the gabbro and silica-poor diorite–monzodiorite can be used to chemically differentiate the gabbro/lamprophyre from these lithologies. Gabbro/lamprophyre also has lower aluminum than both the gabbro and the silica-poor diorite–monzodiorite. The gabbro/lamprophyre also has comparatively lower titanium and total iron when compared to the gabbro. Furthermore, the

gabbro/lamprophyre has lower concentrations of the elements niobium, yttrium, and zirconium compared to the silica-poor diorite–monzodiorite. These elements are often considered to be relatively immobile (e.g. Winchester and Floyd, 1977; Pearce, 1996). It has been proposed that the silica-poor diorite–monzodiorite may be an altered version of gabbro/lamprophyre. However, the significant chemical differences between the two lithologies, including the different concentrations of immobile elements, suggest that these lithologies have two distinct protoliths.

When compared to the chemistry of the gabbro, the silica-poor diorite–monzodiorite is characterized by high calcium, potassium, and sodium, and these relationships can be used to chemically differentiate these two lithologies. The silica-poor diorite–monzodiorite also has comparatively lower iron, cobalt, and nickel when compared to the gabbro. Furthermore, silica-poor dioritic–monzodioritic samples also have higher concentrations of the elements niobium, thorium, and zirconium than gabbro. These elements are often considered to be immobile elements (e.g. Winchester and Floyd, 1977; Pearce, 1996; Hastie et al., 2007) which indicates that these lithologies have two distinct protoliths as well.

### **Blue Quartz**

Large quartz phenocrysts within the dacitic volcanic rocks and the Webb Lake stock are commonly observed at the Island Gold deposit. Previous studies have attributed the blue colour of quartz to inclusions of titanium-rich minerals causing Rayleigh scattering of light (Seifert et al., 2011). This is likely responsible for the blue-coloured quartz grains commonly observed at the Island Gold deposit because titanium-rich micro-inclusions of ilmenite and rutile were observed within these grains.

### **Summary of hydrochloric acid and magnetism field test observations for altered samples**

The results of dilute hydrochloric acid (HCl) and magnetism tests on altered samples for a number of lithologies at the Island Gold deposit are summarized below. A summary of the results of these field tests on least-altered samples of each lithology is located in Table 19 (Appendix B).

Samples of dacite altered by nearby V<sub>1</sub>-V<sub>2</sub> veining are typically non-magnetic but occasionally may be weakly magnetic due to the presence of pyrrhotite in moderately and strongly-altered samples. Primary magnetite occasionally results in weak magnetism in weakly-altered and least-altered samples. Samples altered by V<sub>GD</sub> veins are all non-magnetic. Dacitic samples altered by V<sub>1</sub>-V<sub>2</sub> veins react with dilute hydrochloric acid (HCl). In most cases, strongly and moderately-altered samples have the strongest reaction but occasionally, silicified strongly-altered samples have no reaction or only a weak reaction with HCl. Samples altered by V<sub>GD</sub> veins also react with HCl. The intensity of the reaction increases with increasing alteration strength. These samples are also non-magnetic. Dacitic samples altered by non-auriferous carbonate-sericite alteration strongly react with HCl. These samples are also magnetic.

Samples of gabbro altered by V<sub>1</sub>-V<sub>2</sub> veins react vigorously with HCl and are magnetic. The strength of the reaction remained relatively consistent with varying intensities of alteration. The strength of magnetism decreased with increasing alteration strength. Samples of the Webb Lake stock altered by V<sub>1</sub>-V<sub>2</sub> veins react with HCl and the intensity of the reaction increases with increasing alteration strength. Altered samples are non-magnetic. A sample of the gabbro/lamprophyre altered by a proximal V<sub>3</sub> vein is non-magnetic and has no reaction or only a very weak reaction with HCl. A sample of the silica-poor diorite–monzodiorite altered by a proximal V<sub>3</sub> vein is non-magnetic and has a vigorous reaction with HCl.

**Appendix B**  
**Additional figures and tables**

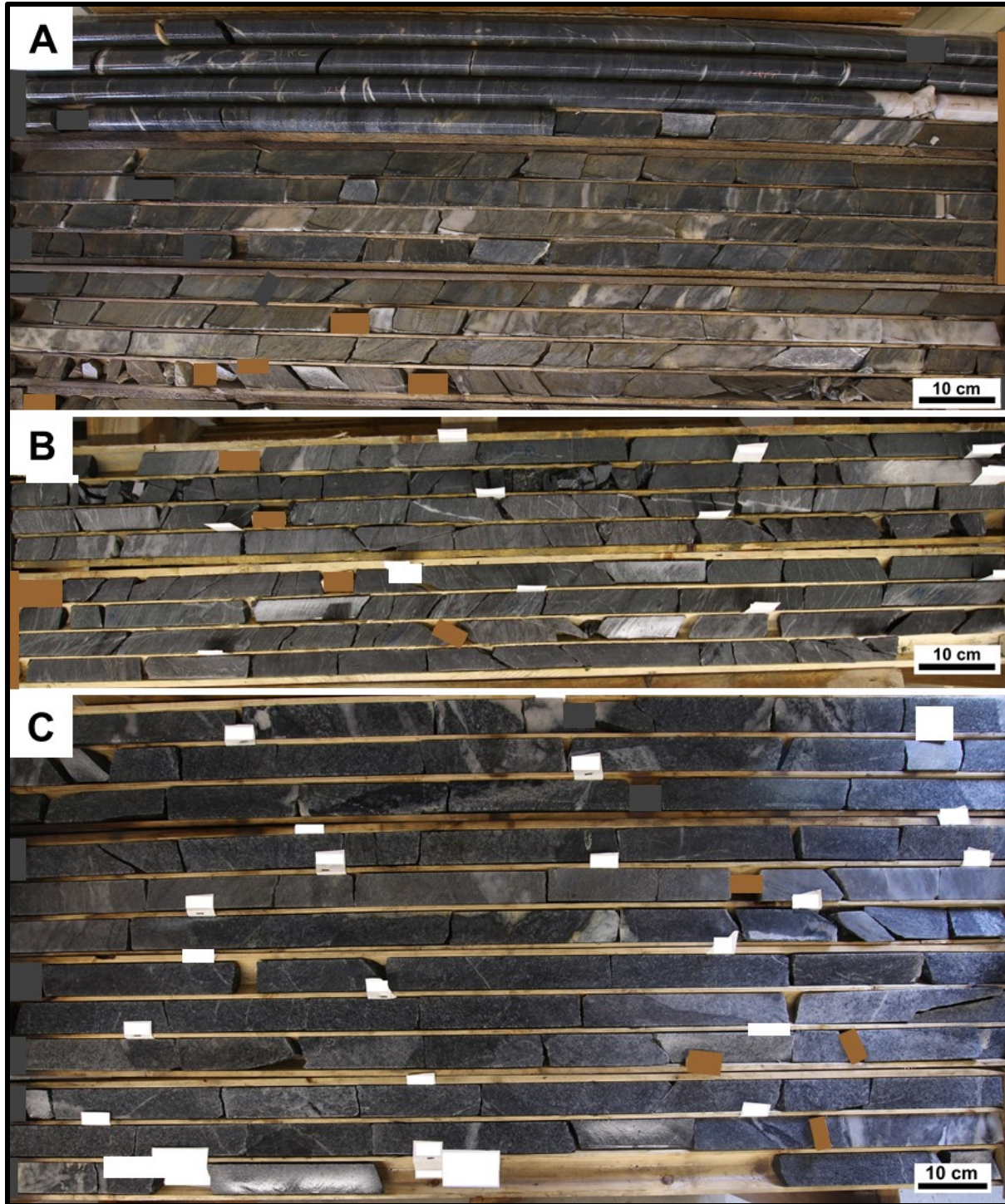


*Figure 64A–C. Drill core displaying alteration related to  $V_1$ - $V_2$  veining. A) Dacite-hosted alteration. B) Gabbro-hosted alteration. C) Webb Lake stock-hosted alteration.*



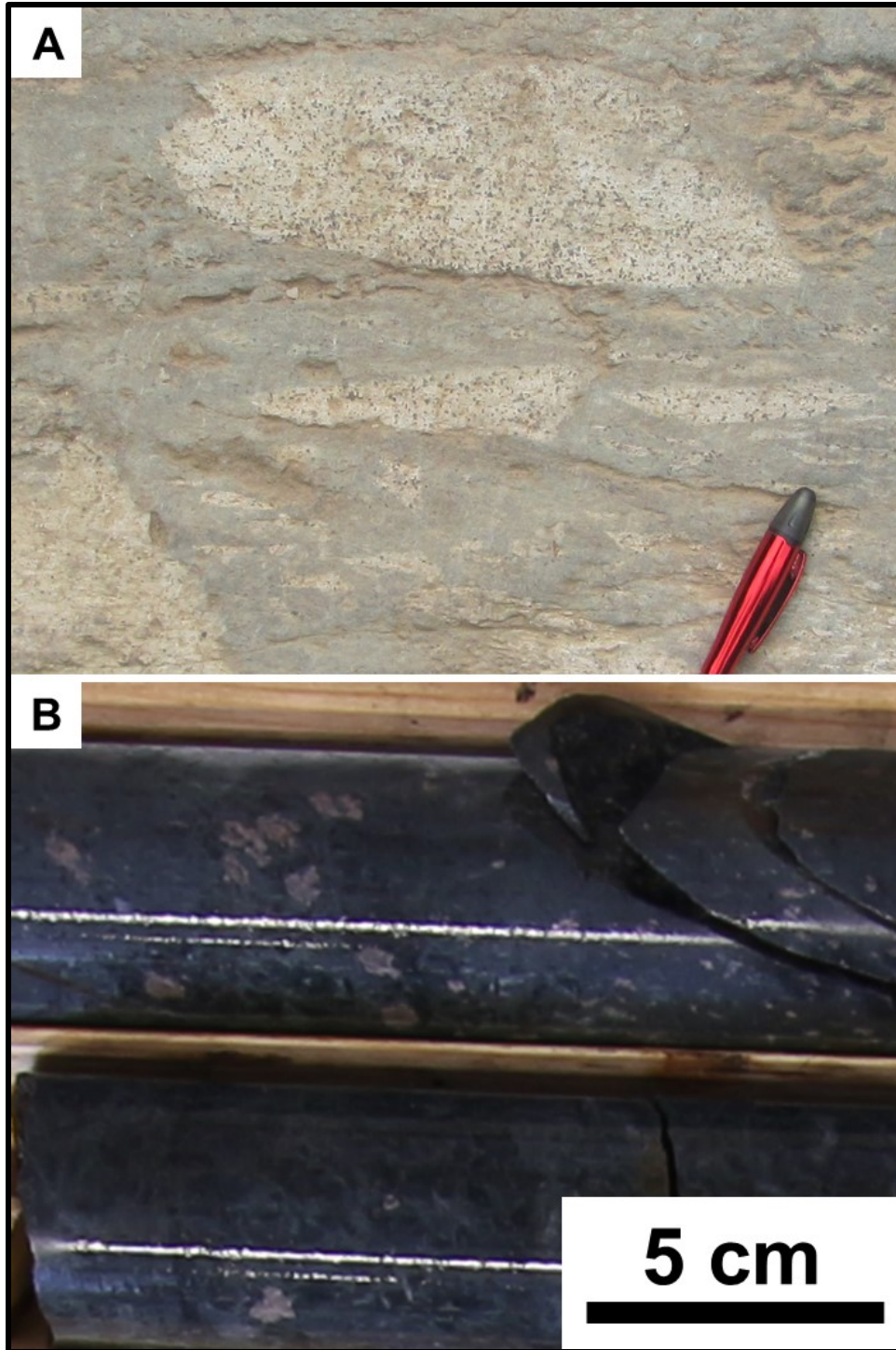


*Figure 65A, B. Photos of chloritoid and garnet. A) Dacitic pyroclastic breccia with randomly-oriented, disseminated chloritoid (black-coloured minerals) concentrated in the fragments. B) Dacitic tuff with lapilli subject to chloritoid alteration (green-black minerals) with pink-coloured garnet overprinting the chloritoid.*

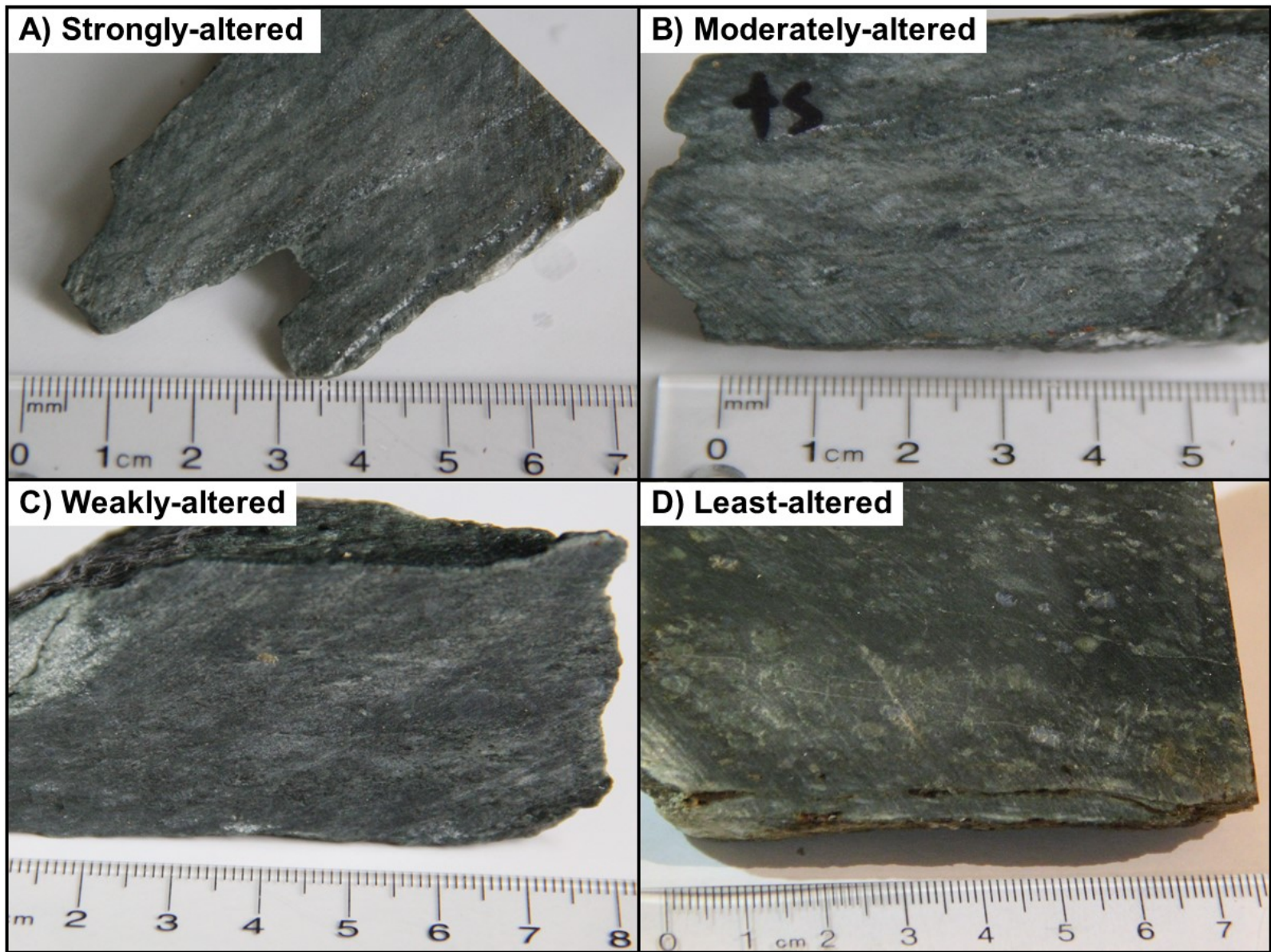


*Figure 66A–D. Dacitic samples variably altered by  $V_{GD}$  auriferous quartz veining (T113, T114, T115) and a representative least-altered sample (T183).*



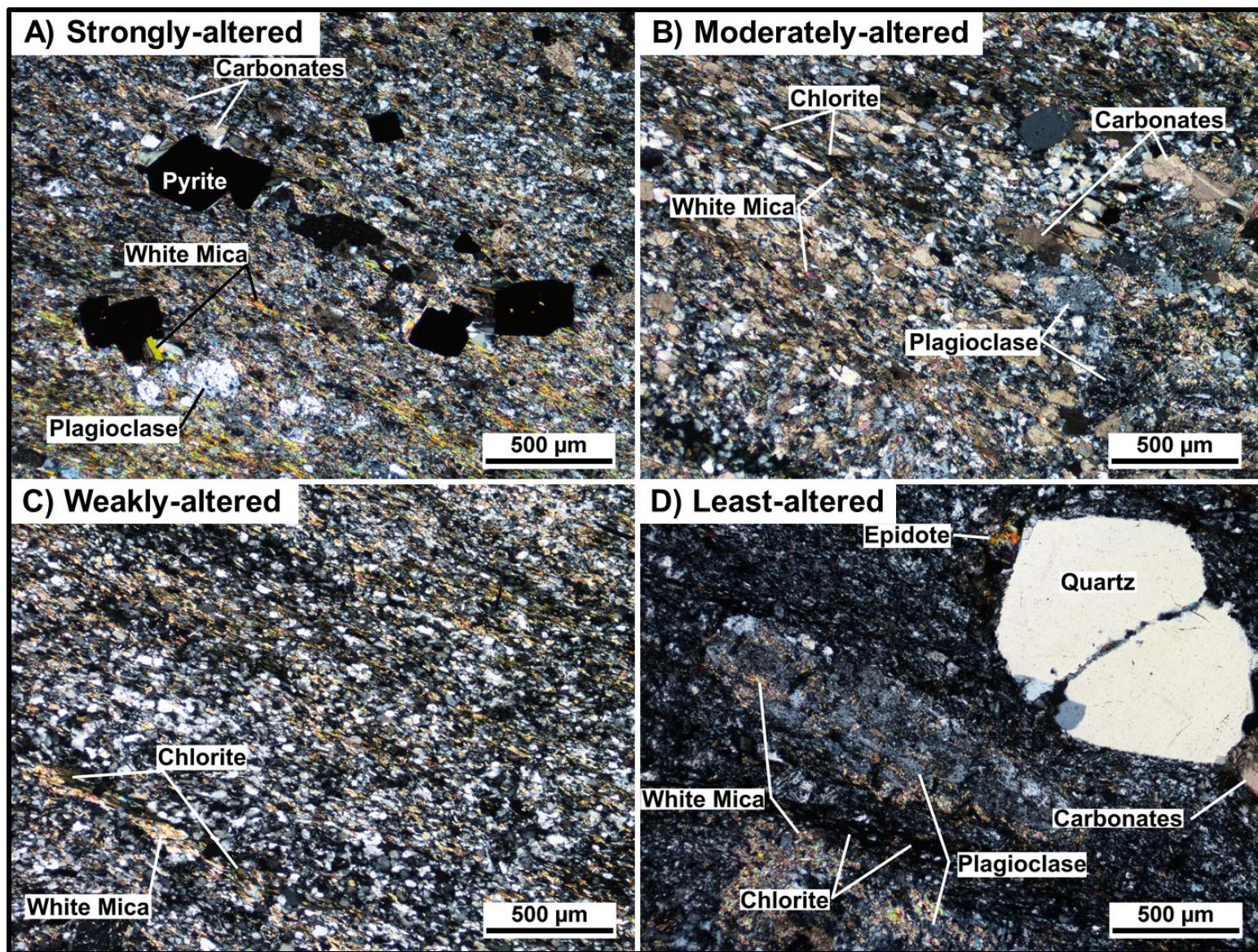


**Figure 67.** Cross-polarized light photomicrographs of dacitic samples variably-altered by  $V_{GD}$  veins (T105, T114, T115) and a representative least-altered sample (T11).



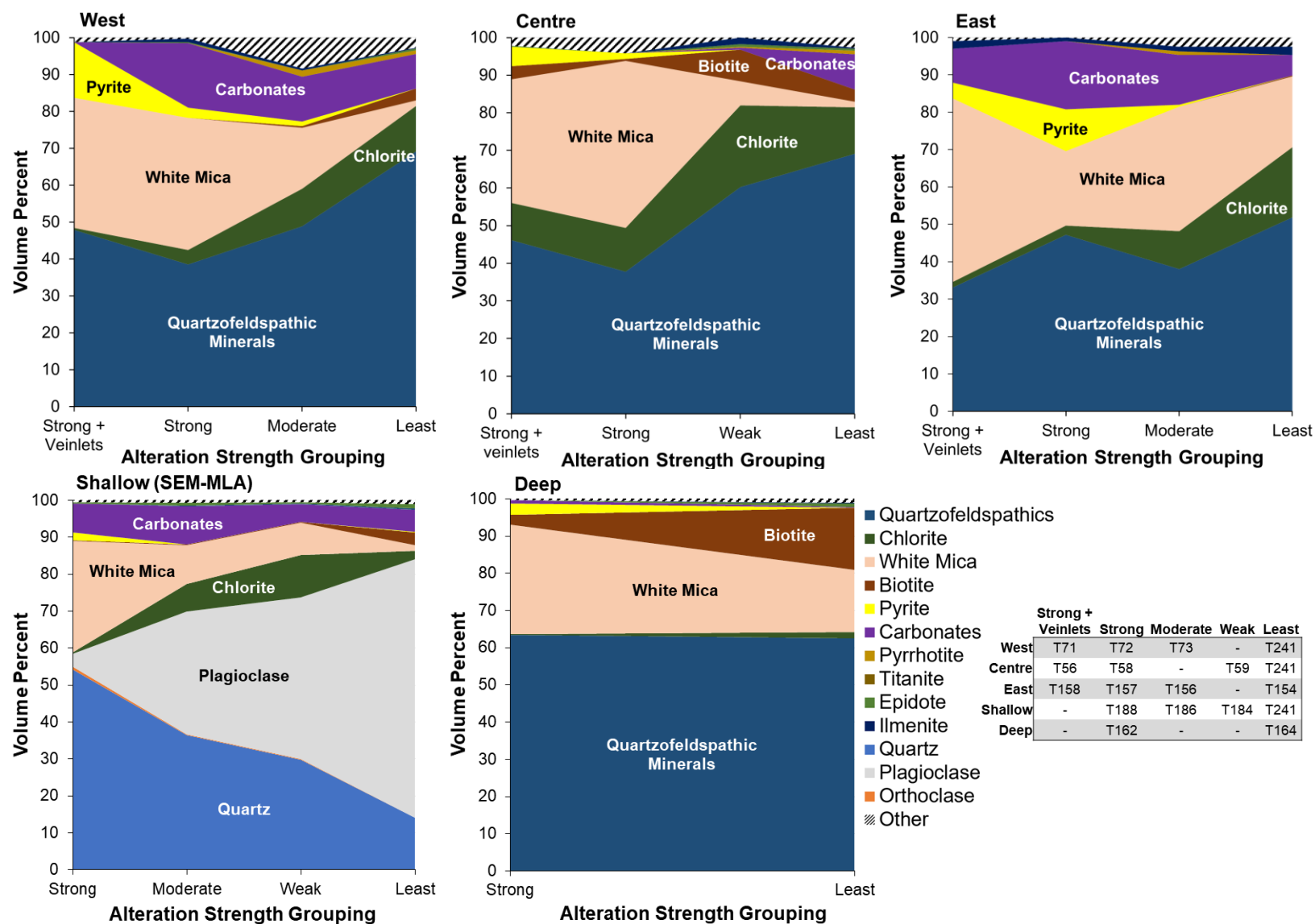


**Figure 68.** Mineral proportions in dacitic samples variably-altered by  $V_1$ - $V_2$  veining from various ore zones taken from throughout the deposit. Mineral proportions were determined via point-counting with the exception the shallow zone where they were determined via SEM-MLA. Ore zone locations are summarized in Figure 19. When not available locally, mineral proportions in a least-altered sample (T241) taken from elsewhere in the deposit are used.

**Table 17A, B.** Averages and ranges of concentrations of chemical species in least-altered samples of each lithology. Averages are based off of the following samples for each lithology: Dacite (8 samples: T8, T11, T65, T116, T154, T164, T183, T241), iron formation (2 samples: T24, T37), gabbro (5 samples: T14, T80, T89, T182, T200), Webb Lake stock (3 samples: T6 (weakly-altered), T192, T193 (weakly-altered)), gabbro/lamprophyre (5 samples: T15, T63, T81, T239, T240), quartz diorite (1 sample: T215), silica-poor diorite–monzodiorite (5 samples: T16, T66, T216, T228, T242), and diabase–quartz diabase (2 samples: T12, T83). LOI=Loss on Ignition. Fe<sub>2</sub>O<sub>3</sub>T=Total Iron, %=Mass Percent, Min=Minimum, Max=Maximum, IF=Iron Formation, WLS=Webb Lake Stock, Qtz Diorite=Quartz Diorite, Gabbro/Lamp=Gabbro/Lamprophyre, SPDM=Silica-Poor Diorite–Monzodiorite, Diabase=Diabase–Quartz Diabase.

A)	Dacite	IF	Gabbro	WLS	Gabbro / Lamp	Qtz Diorite	SPDM	Diabase
Averages								
SiO <sub>2</sub> (%)	64.34	5.80	46.29	67.98	43.51	65.46	42.77	51.60
Al <sub>2</sub> O <sub>3</sub> (%)	15.35	0.76	13.62	14.73	9.77	16.68	12.03	13.15
Fe <sub>2</sub> O <sub>3</sub> (%)	0.69	43.84	1.66	0.24	0.42	0.76	1.73	2.19
MnO (%)	0.112	1.275	0.181	0.047	0.159	0.035	0.162	0.228
MgO (%)	2.00	1.33	6.90	1.20	9.49	0.52	6.59	5.12
CaO (%)	4.30	4.10	8.95	3.54	10.60	2.30	11.25	9.52
Na <sub>2</sub> O (%)	3.67	0.06	1.70	4.75	1.55	8.92	4.46	2.55
K <sub>2</sub> O (%)	0.93	0.03	0.09	0.95	0.19	0.05	0.75	0.56
TiO <sub>2</sub> (%)	0.532	0.029	0.973	0.377	0.630	0.202	0.730	1.366
P <sub>2</sub> O <sub>5</sub> (%)	0.17	0.03	0.08	0.09	0.33	0.08	0.56	0.16
LOI (%)	3.15	21.28	6.70	2.49	14.65	2.15	11.06	0.19
Fe <sub>2</sub> O <sub>3</sub> T (%)	5.33	64.35	12.75	3.60	7.20	2.21	7.76	15.15
C (%)	0.44	1.72	1.31	0.39	3.82	0.51	3.29	0.10
S (%)	0.01	30.80	0.09	0.08	0.03	0.02	0.31	0.09
CO <sub>2</sub> (%)	1.55	5.91	4.49	1.31	13.26	1.74	11.25	0.30
FeO (%)	4.2	18.5	10.0	3.0	6.1	1.3	5.4	11.7
Ag (ppm)	0.5	0.3	0.3	0.5	0.6	0.6	0.8	0.7
As (ppm)	1.1	49.9	6.2	2.2	2.1	1.9	5.3	2.5
Au (ppb)	6	48	20	31	8	6	15	6
B (ppm)	14	6	2	6	10	176	10	0
Ba (ppm)	239	8	12	242	45	123	584	196
Be (ppm)	1	1	1	1	1	1	2	1
Bi (ppm)	0.04	0.04	0.01	0.11	0.12	0.29	0.22	0.18
Cd (ppm)	0.3	0.1	0.1	0.1	0.1	0.1	0.1	0.5
Ce (ppm)	45.04	4.97	9.45	34.03	92.34	72.00	150.84	30.30
Co (ppm)	13.7	20.6	51.1	8.2	36.3	3.9	28.1	50.1
Cr (ppm)	45	14	151	30	405	17	188	62
Cs (ppm)	1.3	0.1	0.3	1.0	0.4	0.2	10.2	0.8
Cu (ppm)	33.9	86.7	134.5	47.2	21.0	12.4	43.7	179.0
Dy (ppm)	2.09	0.77	3.55	1.50	2.74	1.68	5.64	5.67
Er (ppm)	1.12	0.54	2.25	0.80	1.36	0.96	2.35	3.39
Eu (ppm)	1.006	0.499	0.831	0.615	1.590	0.972	3.678	1.395
Ga (ppm)	19	2	16	19	14	20	14	20
Gd (ppm)	2.78	0.66	2.86	1.87	4.23	2.39	10.40	5.51
Ge (ppm)	1.1	0.3	1.3	1.0	1.0	0.7	1.3	1.7
Hf (ppm)	3.3	0.2	1.6	2.7	3.0	4.3	4.3	2.9
Hg (ppb)	3	6	3	3	3		3	3
Ho (ppm)	0.39	0.17	0.74	0.27	0.48	0.31	0.93	1.17
In (ppm)	0.1	0.1	0.1	0.1	0.1	0.1	0.1	0.2

A) Averages	Gabbro / Qtz							
	Dacite	IF	Gabbro	WLS	Lamp	Diorite	SPDM	Diabase
La (ppm)	21.45	2.83	3.69	16.90	44.10	40.10	68.72	13.50
Li (ppm)	36	1	34	23	55	4	42	6
Lu (ppm)	0.166	0.091	0.364	0.127	0.184	0.163	0.270	0.521
Mo (ppm)	1	4	1	1	1	1	1	1
Nb (ppm)	3.9	0.1	2.1	2.8	4.6	13.7	12.1	13.9
Nd (ppm)	19.9	2.4	6.9	13.8	36.9	23.5	73.8	16.8
Ni (ppm)	38	67	115	11	317	10	67	45
Pb (ppm)	3	6	1	3	4	4	8	6
Pd (ppb)	0.3	0.8	2.9	0.3	2.5		5.1	0.3
Pr (ppm)	5.19	0.58	1.40	3.75	10.27	7.00	18.46	3.89
Pt (ppb)	0.3	0.4	3.2	0.3	1.3		3.5	0.6
Rb (ppm)	23	1	2	21	5	1	36	18
Sb (ppm)	0.09	1.01	0.15	0.04	0.04	0.05	0.10	0.05
Sc (ppm)	10	2	34	7	18	2	24	42
Se (ppm)	0.1	0.4	0.1	0.1	0.1	0.1	0.1	0.1
Sm (ppm)	3.56	0.52	2.24	2.50	5.94	3.32	13.81	4.63
Sn (ppm)	1	1	1	1	1	1	1	1
Sr (ppm)	302	34	176	249	372	376	980	156
Ta (ppm)	0.36	0.01	0.12	0.28	0.28	0.75	0.51	4.39
Tb (ppm)	0.39	0.11	0.55	0.27	0.53	0.30	1.21	0.92
Te (ppm)	0.02	0.15	0.03	0.05	0.02	0.01	0.02	0.03
Th (ppm)	2.83	0.17	0.36	2.83	6.03	23.90	10.21	2.80
Tl (ppm)	0.09	0.07	0.05	0.13	0.03	0.03	0.10	0.09
Tm (ppm)	0.159	0.087	0.341	0.118	0.187	0.136	0.302	0.513
U (ppm)	0.65	0.23	0.10	0.70	1.12	4.50	2.67	0.65
V (ppm)	83	19	260	55	116	40	176	350
W (ppm)	2.1	0.3	2.7	2.6	7.5	1.5	7.2	2.6
Y (ppm)	11.1	7.2	20.2	8.1	13.8	9.6	27.4	31.6
Yb (ppm)	1.07	0.57	2.35	0.77	1.17	1.00	1.83	3.37
Zn (ppm)	142.6	33.3	96.6	46.7	80.7	9.9	73.9	141.0
Zr (ppm)	132	12	55	99	119	177	191	114

B) Ranges	Dacite		Dacite		Gabbro		WLS		Gabbro /	
	Min	Max	IF Min	IF Max	Min	Max	Min	Max	Lamp Min	Lamp Max
SiO <sub>2</sub> (%)	63.01	68.19	3.53	8.07	44.08	48.67	66.19	71.52	40.85	46.80
Al <sub>2</sub> O <sub>3</sub> (%)	14.19	16.05	0.55	0.97	11.90	16.56	13.86	15.28	9.01	10.45
Fe <sub>2</sub> O <sub>3</sub> (%)	0.25	1.37	42.57	45.10	0.21	3.14	0.01	0.57	0.23	0.68
MnO (%)	0.058	0.287	0.793	1.756	0.136	0.210	0.033	0.061	0.113	0.230
MgO (%)	0.87	2.85	0.40	2.25	4.82	9.92	0.74	1.44	8.01	10.65
CaO (%)	2.23	5.11	1.93	6.27	6.50	10.11	2.65	4.50	9.39	12.73
Na <sub>2</sub> O (%)	2.06	5.79	0.05	0.07	0.82	2.31	4.53	4.99	1.16	2.27
K <sub>2</sub> O (%)	0.46	1.27	0.02	0.03	0.01	0.20	0.85	1.09	0.08	0.39
TiO <sub>2</sub> (%)	0.435	0.649	0.016	0.042	0.620	1.217	0.229	0.492	0.575	0.679
P <sub>2</sub> O <sub>5</sub> (%)	0.07	0.26	0.03	0.03	0.06	0.10	0.05	0.12	0.26	0.42
LOI (%)	1.03	5.86	16.15	26.40	2.94	11.46	1.74	3.37	7.53	18.21
Fe <sub>2</sub> O <sub>3</sub> T (%)	4.52	6.17	62.22	66.47	11.44	14.37	2.46	4.36	6.01	8.14
C (%)	0.11	0.88	0.59	2.84	0.01	2.37	0.25	0.60	3.27	4.62
S (%)	0.01	0.02	27.00	34.60	0.01	0.21	0.02	0.15	0.01	0.06
CO <sub>2</sub> (%)	0.39	3.35	2.06	9.75	0.01	8.25	0.87	2.02	11.50	15.70
FeO (%)	3.7	4.9	15.4	21.5	8.8	11.1	1.7	3.8	5.2	6.7

B) Ranges	Dacite		IF		Gabbro		WLS		Gabbro /	
	Min	Max	Min	Max	Min	Max	Min	Max	Lamp Min	Lamp Max
Ag (ppm)	0.3	0.9	0.3	0.3	0.3	0.5	0.3	1.1	0.3	1.7
As (ppm)	0.1	4.0	4.1	95.6	0.2	16.7	0.1	6.4	0.1	6.2
Au (ppb)	1	12	35	60	5	51	18	52	3	18
B (ppm)	6	25	3	9	0	5	1	15	2	22
Ba (ppm)	149	398	3	13	4	18	222	264	12	87
Be (ppm)	1	1	1	1	1	1	1	1	1	1
Bi (ppm)	0.01	0.21	0.01	0.06	0.01	0.01	0.03	0.17	0.01	0.29
Cd (ppm)	0.1	1.8	0.1	0.1	0.1	0.1	0.1	0.1	0.1	0.1
Ce (ppm)	29.70	55.20	4.11	5.82	5.31	12.60	28.40	37.80	65.70	103.00
Co (ppm)	9.8	16.7	1.5	39.6	38.9	62.5	5.0	10.6	30.8	41.1
Cr (ppm)	19	68	13	15	44	259	14	53	282	576
Cs (ppm)	0.5	2.7	0.1	0.1	0.1	0.4	0.7	1.3	0.2	0.7
Cu (ppm)	0.8	88.3	73.9	99.4	45.6	208.0	34.4	67.5	3.0	45.2
Dy (ppm)	1.60	2.68	0.55	0.99	2.12	4.82	1.33	1.80	2.49	3.43
Er (ppm)	0.90	1.42	0.39	0.69	1.38	3.22	0.66	1.00	1.24	1.74
Eu (ppm)	0.655	1.340	0.493	0.505	0.590	1.040	0.417	0.782	1.320	1.990
Ga (ppm)	16	21	1	2	14	17	19	20	13	15
Gd (ppm)	1.99	3.49	0.52	0.80	1.68	3.66	1.71	2.16	3.72	4.94
Ge (ppm)	0.8	1.4	0.3	0.3	1.2	1.6	1.0	1.0	0.8	1.1
Hf (ppm)	3.0	3.6	0.1	0.3	0.9	2.2	2.1	3.2	2.7	3.6
Hg (ppb)	3	9	3	10	3	3	3	3	3	3
Ho (ppm)	0.31	0.54	0.12	0.22	0.44	1.05	0.23	0.33	0.43	0.64
In (ppm)	0.1	0.1	0.1	0.1	0.1	0.1	0.1	0.1	0.1	0.1
La (ppm)	15.40	26.90	2.36	3.30	2.12	5.22	14.40	18.90	30.40	49.70
Li (ppm)	14	81	1	1	10	65	10	41	33	86
Lu (ppm)	0.128	0.220	0.074	0.108	0.223	0.546	0.100	0.155	0.151	0.232
Mo (ppm)	1	2	2	6	1	1	1	1	1	1
Nb (ppm)	2.8	5.5	0.1	0.1	1.2	2.9	2.2	3.1	3.8	5.2
Nd (ppm)	12.0	24.9	2.0	2.7	4.0	9.1	11.7	15.3	31.5	40.1
Ni (ppm)	17	61	51	83	59	268	6	14	119	472
Pb (ppm)	1	6	6	6	1	2	3	3	2	5
Pd (ppb)	0.3	0.3	0.8	0.8	0.8	7.6	0.3	0.3	1.9	3.0
Pr (ppm)	3.23	6.64	0.50	0.66	0.78	1.87	3.14	4.10	7.87	11.50
Pt (ppb)	0.3	0.5	0.3	0.5	1.3	5.9	0.3	0.3	1.1	1.5
Rb (ppm)	15	32	1	1	1	5	18	25	2	12
Sb (ppm)	0.01	0.44	0.02	1.99	0.02	0.54	0.03	0.06	0.01	0.07
Sc (ppm)	9	13	1	2	17	43	4	9	15	21
Se (ppm)	0.1	0.1	0.2	0.6	0.1	0.3	0.1	0.1	0.1	0.1
Sm (ppm)	2.28	4.60	0.43	0.60	1.35	2.91	2.11	2.83	5.13	6.40
Sn (ppm)	1	1	1	1	1	1	1	1	1	1
Sr (ppm)	159	445	19	48	100	225	159	325	131	631
Ta (ppm)	0.28	0.44	0.01	0.01	0.08	0.16	0.25	0.33	0.26	0.30
Tb (ppm)	0.28	0.50	0.09	0.13	0.33	0.73	0.24	0.32	0.46	0.65
Te (ppm)	0.01	0.05	0.13	0.16	0.01	0.04	0.01	0.09	0.01	0.05
Th (ppm)	2.16	3.28	0.16	0.17	0.29	0.44	2.00	4.19	4.81	7.14
Tl (ppm)	0.03	0.14	0.03	0.11	0.03	0.14	0.08	0.20	0.03	0.03
Tm (ppm)	0.127	0.205	0.066	0.108	0.213	0.490	0.094	0.150	0.169	0.244
U (ppm)	0.34	1.04	0.22	0.23	0.08	0.12	0.42	1.17	1.01	1.37
V (ppm)	67	99	18	20	127	345	32	72	90	132
W (ppm)	0.3	6.8	0.3	0.3	0.5	6.1	1.8	3.0	0.3	16.2
Y (ppm)	8.8	14.4	6.3	8.0	12.5	28.7	6.8	9.4	12.6	17.3

B) Ranges	Dacite		Dacite		Gabbro		WLS		Gabbro /	
	Min	Max	IF Min	IF Max	Min	Max	Min	Max	Lamp Min	Lamp Max
Yb (ppm)	0.84	1.41	0.46	0.68	1.46	3.50	0.59	0.96	1.00	1.57
Zn (ppm)	47.7	692.0	22.8	43.7	80.7	118.0	29.1	62.4	60.1	97.5
Zr (ppm)	114	148	11	12	23	77	44	132	103	131

B) Ranges	Qtz		Qtz		SPDM		Diabase	
	Diorite Min	Diorite Max	SPDM Min	SPDM Max	Diabase Min	Diabase Max		
SiO <sub>2</sub> (%)	65.46	65.46	37.89	45.91	50.87	52.33		
Al <sub>2</sub> O <sub>3</sub> (%)	16.68	16.68	11.36	12.77	12.82	13.48		
Fe <sub>2</sub> O <sub>3</sub> (%)	0.76	0.76	1.22	2.46	1.72	2.66		
MnO (%)	0.035	0.035	0.147	0.205	0.223	0.232		
MgO (%)	0.52	0.52	5.64	7.75	4.96	5.28		
CaO (%)	2.30	2.30	9.87	13.62	9.17	9.87		
Na <sub>2</sub> O (%)	8.92	8.92	3.39	5.49	2.49	2.60		
K <sub>2</sub> O (%)	0.05	0.05	0.26	1.72	0.52	0.60		
TiO <sub>2</sub> (%)	0.202	0.202	0.641	0.839	1.354	1.377		
P <sub>2</sub> O <sub>5</sub> (%)	0.08	0.08	0.35	0.83	0.15	0.17		
LOI (%)	2.15	2.15	7.73	13.71	0.17	0.20		
Fe <sub>2</sub> O <sub>3</sub> T (%)	2.21	2.21	7.10	8.56	14.96	15.33		
C (%)	0.51	0.51	1.91	4.10	0.06	0.13		
S (%)	0.02	0.02	0.03	0.77	0.04	0.13		
CO <sub>2</sub> (%)	1.74	1.74	6.53	14.00	0.18	0.41		
FeO (%)	1.3	1.3	4.5	6.4	11.4	11.9		
Ag (ppm)	0.6	0.6	0.3	1.5	0.6	0.7		
As (ppm)	1.9	1.9	2.0	8.6	0.7	4.2		
Au (ppb)	6	6	3	24	3	9		
B (ppm)	176	176	7	13	0	0		
Ba (ppm)	123	123	148	1051	192	200		
Be (ppm)	1	1	1	3	1	1		
Bi (ppm)	0.29	0.29	0.06	0.40	0.11	0.24		
Cd (ppm)	0.1	0.1	0.1	0.1	0.1	0.9		
Ce (ppm)	72.00	72.00	99.20	192.00	30.00	30.60		
Co (ppm)	3.9	3.9	25.0	34.5	49.6	50.6		
Cr (ppm)	17	17	122	268	57	66		
Cs (ppm)	0.2	0.2	0.8	32.7	0.7	0.9		
Cu (ppm)	12.4	12.4	23.5	74.9	155.0	203.0		
Dy (ppm)	1.68	1.68	3.67	7.61	5.57	5.76		
Er (ppm)	0.96	0.96	1.75	2.85	3.32	3.46		
Eu (ppm)	0.972	0.972	2.060	5.280	1.380	1.410		
Ga (ppm)	20	20	13	17	19	21		
Gd (ppm)	2.39	2.39	5.91	14.90	5.25	5.77		
Ge (ppm)	0.7	0.7	0.9	1.6	1.7	1.7		
Hf (ppm)	4.3	4.3	3.4	5.4	2.6	3.1		
Hg (ppb)			3	3	3	3		
Ho (ppm)	0.31	0.31	0.66	1.18	1.16	1.17		
In (ppm)	0.1	0.1	0.1	0.1	0.1	0.2		
La (ppm)	40.10	40.10	45.30	88.60	12.90	14.10		
Li (ppm)	4	4	30	63	4	7		
Lu (ppm)	0.163	0.163	0.223	0.337	0.497	0.545		
Mo (ppm)	1	1	1	1	1	2		
Nb (ppm)	13.7	13.7	6.2	20.7	5.0	22.7		

B) Ranges	Qtz	Qtz	SPDM	SPDM	Diabase	Diabase
	Diorite Min	Diorite Max	Min	Max	Min	Max
Nd (ppm)	23.5	23.5	46.0	97.8	16.4	17.2
Ni (ppm)	10	10	40	99	44	45
Pb (ppm)	4	4	6	9	5	6
Pd (ppb)			3.2	7.0	0.3	0.3
Pr (ppm)	7.00	7.00	11.90	23.80	3.82	3.96
Pt (ppb)			2.7	4.2	0.3	1.0
Rb (ppm)	1	1	13	104	17	19
Sb (ppm)	0.05	0.05	0.02	0.19	0.01	0.09
Sc (ppm)	2	2	15	32	41	43
Se (ppm)	0.1	0.1	0.1	0.2	0.1	0.1
Sm (ppm)	3.32	3.32	8.00	19.10	4.44	4.82
Sn (ppm)	1	1	1	2	1	1
Sr (ppm)	376	376	790	1238	154	158
Ta (ppm)	0.75	0.75	0.24	0.89	0.32	8.46
Tb (ppm)	0.30	0.30	0.72	1.69	0.91	0.92
Te (ppm)	0.01	0.01	0.01	0.06	0.01	0.04
Th (ppm)	23.90	23.90	9.27	11.10	1.87	3.72
Tl (ppm)	0.03	0.03	0.03	0.40	0.03	0.16
Tm (ppm)	0.136	0.136	0.238	0.368	0.512	0.513
U (ppm)	4.50	4.50	2.40	3.05	0.47	0.82
V (ppm)	40	40	129	229	349	351
W (ppm)	1.5	1.5	0.8	15.8	0.3	5.0
Y (ppm)	9.6	9.6	18.9	34.2	31.1	32.1
Yb (ppm)	1.00	1.00	1.52	2.13	3.34	3.40
Zn (ppm)	9.9	9.9	54.2	103.0	138.0	144.0
Zr (ppm)	177	177	146	218	107	120

**Table 18.** Average concentrations and concentration ranges of chemical species based on whole-rock geochemistry of auriferous quartz veins. Select trace elements that often appear to be enriched or depleted due to auriferous alteration at the Island Gold deposit are also displayed. Averages and ranges are based off of samples T100 and T104 for  $V_{GD}$  veins and T159, T187, and T196 for  $V_1$ - $V_2$  veins. LOI=Loss On Ignition,  $Fe_2O_3T$ =Total Iron, %=Mass Percent, ppm=Parts per Million, ppb=Parts per Billion.

	$V_{GD}$ Average	$V_{GD}$ Minimum	$V_{GD}$ Maximum	$V_1$ - $V_2$ Average	$V_1$ - $V_2$ Minimum	$V_1$ - $V_2$ Maximum
SiO <sub>2</sub> (%)	88.50	80.35	96.64	93.36	88.37	97.20
Al <sub>2</sub> O <sub>3</sub> (%)	2.17	0.40	3.94	2.55	0.69	5.08
Fe <sub>2</sub> O <sub>3</sub> (%)	0.52	0.01	1.04	0.97	0.46	1.83
MnO (%)	0.045	0.015	0.075	0.014	0.011	0.016
MgO (%)	0.66	0.06	1.25	0.17	0.09	0.22
CaO (%)	2.57	0.99	4.14	0.67	0.44	0.91
Na <sub>2</sub> O (%)	0.31	0.03	0.59	0.21	0.04	0.48
K <sub>2</sub> O (%)	0.21	0.09	0.32	0.60	0.17	1.21
TiO <sub>2</sub> (%)	0.190	0.007	0.372	0.084	0.020	0.175
P <sub>2</sub> O <sub>5</sub> (%)	0.02	0.01	0.03	0.02	0.01	0.04
LOI (%)	2.37	0.85	3.89	1.26	0.64	1.87
Fe <sub>2</sub> O <sub>3</sub> T (%)	2.40	0.30	4.49	1.26	0.90	1.94
C (%)	0.56	0.21	0.91	0.14	0.09	0.20
S (%)	0.84	0.04	1.63	0.48	0.18	0.97
CO <sub>2</sub> (%)	1.92	0.76	3.08	0.49	0.29	0.69
FeO (%)	1.8	0.4	3.1	0.3	0.1	0.4
Ag (ppm)	0.4	0.3	0.6	1.1	0.3	2.1
As (ppm)	95.8	16.6	175.0	30.9	3.8	55.2
Au (ppb)	17550	10500	24600	18697	2110	50500
B (ppm)	4	2	5	12	5	23
Ba (ppm)	46	12	80	70	17	163
Be (ppm)	1	1	1	1	1	1
Bi (ppm)	0.11	0.02	0.19	0.54	0.02	1.57
Cd (ppm)	0.1	0.1	0.1	0.1	0.1	0.1
Ce (ppm)	3.11	0.93	5.29	6.43	0.81	13.10
Co (ppm)	7.4	0.5	14.2	2.6	1.1	4.7
Cr (ppm)	38	37	39	55	9	81
Cs (ppm)	0.3	0.1	0.5	0.3	0.1	0.4
Cu (ppm)	31.5	12.9	50.1	28.5	5.4	74.5
Dy (ppm)	0.67	0.09	1.24	0.36	0.18	0.66
Er (ppm)	0.44	0.06	0.82	0.18	0.08	0.35
Eu (ppm)	0.148	0.023	0.272	0.154	0.051	0.286
Ga (ppm)	4	1	7	4	1	8
Gd (ppm)	0.70	0.12	1.27	0.41	0.15	0.77
Ge (ppm)	2.8	2.7	2.8	2.6	1.8	3.2
Hf (ppm)	0.3	0.1	0.5	0.5	0.1	1.0
Hg (ppb)	3	3	3	3	3	3
Ho (ppm)	0.15	0.02	0.28	0.07	0.03	0.12
In (ppm)	0.1	0.1	0.1	0.1	0.1	0.1
La (ppm)	1.15	0.20	2.10	3.07	0.35	6.35
Li (ppm)	9	1	18	4	3	5
Lu (ppm)	0.076	0.010	0.141	0.030	0.008	0.062
Mo (ppm)	1	1	1	14	1	35
Nb (ppm)	0.4	0.1	0.6	0.5	0.1	1.0
Nd (ppm)	1.9	0.5	3.3	2.8	0.5	5.7
Ni (ppm)	9	2	15	7	3	10



	V <sub>GD</sub> Average	V <sub>GD</sub> Minimum	V <sub>GD</sub> Maximum	V <sub>1-V2</sub> Average	V <sub>1-V2</sub> Minimum	V <sub>1-V2</sub> Maximum
<b>Pb (ppm)</b>	2	1	3	1	1	2
<b>Pd (ppb)</b>	0.3	0.3	0.3	0.4	0.3	0.7
<b>Pr (ppm)</b>	0.42	0.10	0.74	0.73	0.10	1.49
<b>Pt (ppb)</b>	0.3	0.3	0.3	0.3	0.3	0.3
<b>Rb (ppm)</b>	5	2	8	10	3	19
<b>Sb (ppm)</b>	0.10	0.05	0.15	0.05	0.02	0.09
<b>Sc (ppm)</b>	6	1	11	2	1	4
<b>Se (ppm)</b>	0.1	0.1	0.1	0.1	0.1	0.2
<b>Sm (ppm)</b>	0.50	0.06	0.94	0.51	0.14	0.99
<b>Sn (ppm)</b>	1	1	1	1	1	1
<b>Sr (ppm)</b>	34	11	56	28	8	56
<b>Ta (ppm)</b>	0.03	0.01	0.06	0.05	0.02	0.09
<b>Tb (ppm)</b>	0.11	0.02	0.20	0.06	0.03	0.11
<b>Te (ppm)</b>	0.67	0.45	0.88	1.95	0.34	3.75
<b>Th (ppm)</b>	0.09	0.03	0.15	0.38	0.06	0.84
<b>Tl (ppm)</b>	0.03	0.03	0.03	0.03	0.03	0.03
<b>Tm (ppm)</b>	0.071	0.009	0.132	0.027	0.010	0.054
<b>U (ppm)</b>	0.06	0.05	0.07	0.08	0.02	0.17
<b>V (ppm)</b>	50	3	97	15	7	26
<b>W (ppm)</b>	6.0	0.8	11.2	748.4	9.2	1550.0
<b>Y (ppm)</b>	4.4	0.6	8.1	1.9	1.0	3.5
<b>Yb (ppm)</b>	0.51	0.06	0.95	0.18	0.06	0.38
<b>Zn (ppm)</b>	16.0	0.3	31.7	21.6	11.8	34.5
<b>Zr (ppm)</b>	14	4	23	14	5	24

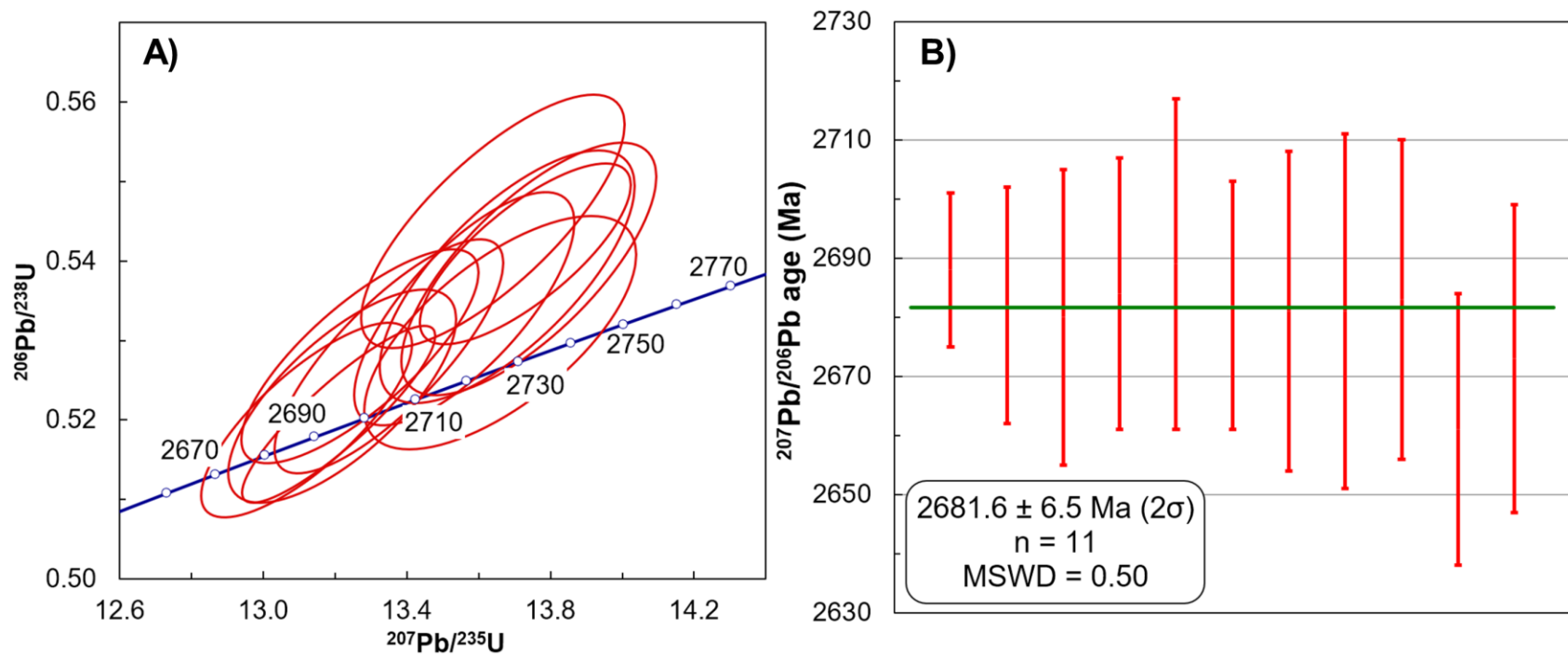


**Figure 69A, B.** A) Wetherill concordia diagram (Wetherill, 1956) with analyses of the DD91 standard. Error ellipses for each data point are 2\*sigma. B)  $^{207}\text{Pb}/^{206}\text{Pb}$  weighted mean age diagram for analyses of the DD91 standard (2682 Ma reference age). MSWD=Mean Square Weighted Deviation.

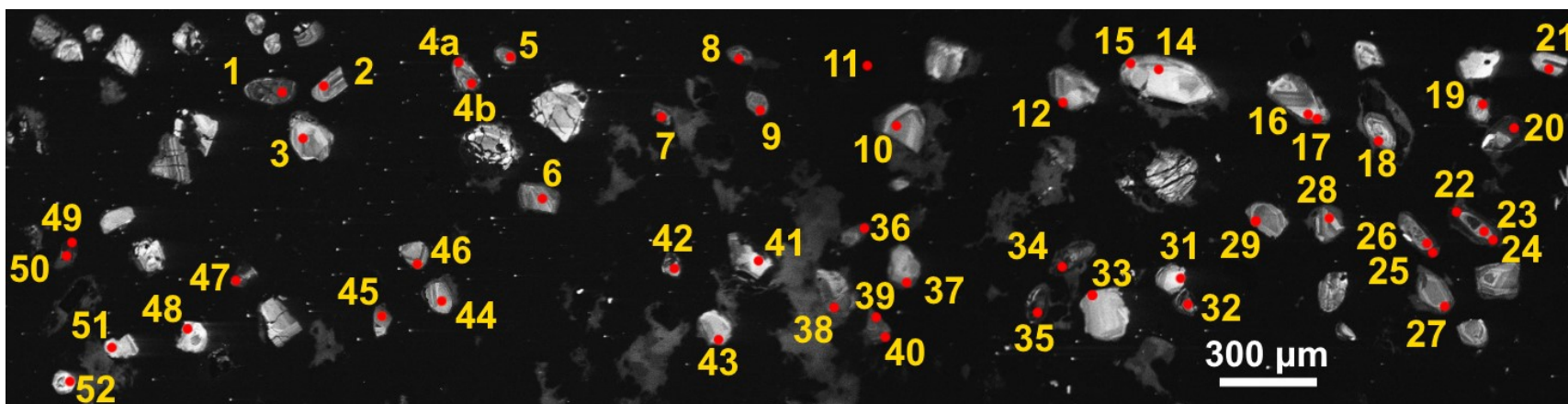
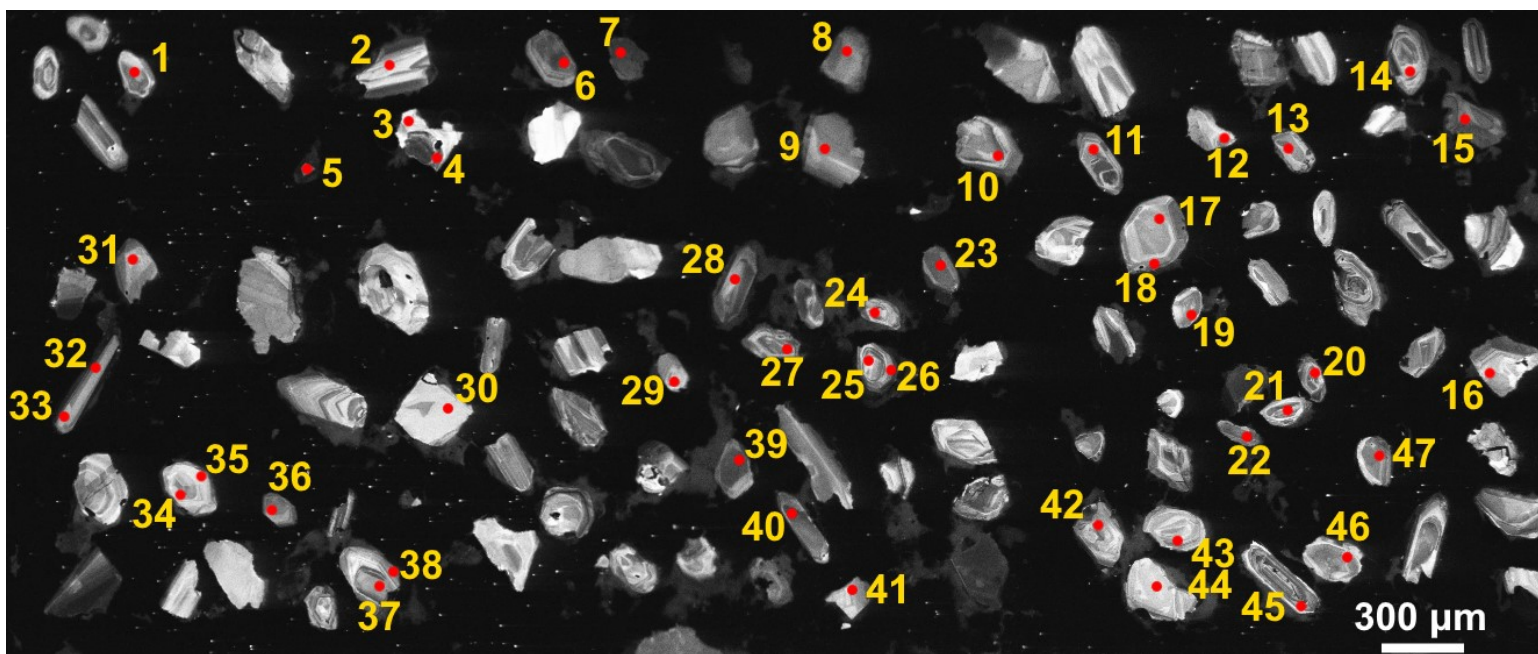


**Figure 70.** Cathodoluminescent photomicrographs displaying LA-ICP-MS analysis locations on zircons from the least-altered sample (top) and zircons from the altered sample (bottom).

**Table 19.** Summary of some of the results and interpretations from this thesis. Some pertinent information from other studies is also included.

Lithology/Vein Textures	Lithology/Vein Features of Least-altered samples	Mineralogy of Least-altered Samples	Interpreted Primary Minerals	Quartz Vein-related Alteration	Timing
<b>Dacitic volcanic rocks (T2, V2, I2): Tuffs, hypabbysal intrusives, flows, and pyroclastic breccias</b>	<ul style="list-style-type: none"> <li>• Tuffs often contain lapilli to bomb-sized fragments.</li> <li>• Porphyritic–equigranular.</li> <li>• Fine–medium grain size.</li> <li>• Non–moderately magnetic.</li> <li>• No–weak reaction with HCl.</li> </ul>	<ul style="list-style-type: none"> <li>• Plagioclase (andesine), quartz, calcite, biotite, chlorite (ripidolite), white mica (muscovite and illite), and epidote.</li> <li>• Accessory minerals (typically &lt; 1 vol%): Actinolite, apatite, chloritoid, grunerite, hematite, hornblende, ilmenite, magnetite, rutile, siderite, titanite, tourmaline, and zircon.</li> </ul>	<ul style="list-style-type: none"> <li>• Plagioclase (andesine), quartz, and biotite.</li> <li>• Accessory minerals (typically &lt; 1 vol%): Apatite, hornblende, ilmenite, magnetite, and zircon.</li> </ul>	<ul style="list-style-type: none"> <li>• <b>V<sub>GD</sub> and V<sub>1</sub>–V<sub>2</sub> Auriferous Veining:</b></li> <li>• Ca–Mg–Fe carbonate minerals, chlorite (ripidolite), quartz, sulphides (pyrite ± pyrrhotite and chalcopyrite), rutile, and white mica (muscovite).</li> <li>• Gains: As, Au, Bi, K<sub>2</sub>O, Rb, S, Se, Te, Tl, W.</li> <li>• Losses: Na<sub>2</sub>O, Sr.</li> </ul>	<ul style="list-style-type: none"> <li>• Cross-cut/overlain by all other lithologies. Oldest lithology.</li> <li>• U–Pb: 2749 ± 2 to 2728 ± 2.7 Ma (Turek at al., 1982, 1992).</li> <li>• U–Pb: 2735 ± 8 Ma and 2738 ± 9 Ma (this study).</li> <li>• Pre–D1 deformation (Jellicoe, 2019).</li> </ul>
<b>Iron formation (IF)</b>	<ul style="list-style-type: none"> <li>• Banded/layered or massive.</li> <li>• 5 main layer groups: Sulphide-rich layers, iron oxide-rich layers, chert-rich layers, carbonate-rich layers, and chlorite-rich layers.</li> <li>• Fine–coarse grained.</li> <li>• Non–strongly magnetic.</li> <li>• No–strong reaction with HCl.</li> </ul>	<ul style="list-style-type: none"> <li>• Sulphide and iron oxide-rich layers: Hematite, magnetite, and pyrite.</li> <li>• Sulphide and iron oxide-poor layers: Quartz, carbonate minerals, chlorite, plagioclase.</li> <li>• Accessory minerals: Chloritoid, epidote, ilmenite, white mica, and tourmaline.</li> </ul>	<ul style="list-style-type: none"> <li>• Clay minerals, carbonate minerals, hematite, magnetite, plagioclase, pyrite, pyrrhotite, and quartz.</li> </ul>	<ul style="list-style-type: none"> <li>• Not studied</li> </ul>	<ul style="list-style-type: none"> <li>• Thin layers interbedded with dacite are of equivalent age to dacite.</li> <li>• Larger Michipicoten iron formation overlies/post-dates dacite.</li> <li>• Formed after underlying dacite (U–Pb: 2728.8 ± 2.7 Ma; Turek et al., 1988, 1992) but before the Webb Lake stock (U–Pb: 2724 ± 4.3; Jellicoe, 2019).</li> <li>• Pre–D1 deformation (Jellicoe, 2019).</li> </ul>
<b>Gabbro (I3G)</b>	<ul style="list-style-type: none"> <li>• Sills and dykes.</li> <li>• Equigranular.</li> <li>• Medium grain size.</li> <li>• Non–strongly magnetic.</li> <li>• Moderate–strong reaction with HCl.</li> </ul>	<ul style="list-style-type: none"> <li>• Chlorite (ripidolite), quartz, epidote, calcite, actinolite, titanite, plagioclase (oligoclase–andesine), and hornblende.</li> <li>• Accessory minerals: Chloritoid, hematite, ilmenite, magnetite, phengite, pyroxene, rutile, and tourmaline.</li> </ul>	<ul style="list-style-type: none"> <li>• Plagioclase, pyroxene, and hornblende.</li> <li>• Accessory minerals: Ilmenite, magnetite, and quartz.</li> </ul>	<ul style="list-style-type: none"> <li>• <b>V<sub>1</sub>–V<sub>2</sub> Auriferous Veining:</b></li> <li>• Biotite, calcite, chlorite (ripidolite), plagioclase (oligoclase), quartz, rutile, sulphides (pyrite ± pyrrhotite and chalcopyrite), ± minor white mica.</li> <li>• Gains: Au, B, Ba, Cs, K<sub>2</sub>O, Li, MnO, Pb, Rb, S, Sm, Sr, Te.</li> <li>• Losses: Bi, Ge, Na<sub>2</sub>O, P<sub>2</sub>O<sub>5</sub>, Sb, Tl.</li> </ul>	<ul style="list-style-type: none"> <li>• Cross-cuts dacite and likely cross-cuts iron formations. Post-dates these lithologies.</li> <li>• Formed after dacitic volcanic rocks (Youngest U–Pb age: 2728.8 ± 2.7 Ma; Turek et al., 1988, 1992) but before the Webb Lake stock (U–Pb: 2724 ± 4.3; Jellicoe, 2019).</li> <li>• Likely pre–D1 deformation.</li> </ul>

Lithology/Vein Textures	Lithology/Vein Features of Least-altered samples	Mineralogy of Least-altered Samples	Interpreted Primary Minerals	Quartz Vein-related Alteration	Timing
<b>Tonalite–trondhemite (I1JM: Webb Lake stock)</b>	<ul style="list-style-type: none"> <li>• Large intrusive body with associated dykes.</li> <li>• Phaneritic, equigranular.</li> <li>• Medium–coarse grain size.</li> <li>• Non-magnetic.</li> <li>• No–weak reaction with HCl.</li> </ul>	<ul style="list-style-type: none"> <li>• Plagioclase (albite–oligoclase), quartz, chlorite (ripidolite), biotite, white mica (phengite ± muscovite), epidote, and calcite.</li> <li>• Accessory minerals: Actinolite, apatite, chloritoid, hematite, hornblende, ilmenite, pyrite, pyroxene, rutile, titanite, tourmaline, and zircon.</li> </ul>	<ul style="list-style-type: none"> <li>• Plagioclase (albite–oligoclase), quartz, and biotite.</li> <li>• Accessory minerals: Apatite, hornblende, ilmenite, pyroxene, and zircon.</li> </ul>	<ul style="list-style-type: none"> <li>• <b>V<sub>1</sub>–V<sub>2</sub> Auriferous Veining:</b></li> <li>• Biotite, Ca–Mg–Fe carbonates, chlorite (ripidolite), quartz, rutile, sulphides (pyrite ± pyrrhotite and chalcopyrite), and white mica (muscovite ± phengite).</li> <li>• Gains: Ag, As, Au, B, Bi, C, CO<sub>2</sub>, Cu, Fe<sub>2</sub>O<sub>3</sub>, Ge, K<sub>2</sub>O, LOI, Mo, Rb, S, Se, Ta, Te, U, W.</li> <li>• Losses: CaO, Co, Fe<sub>2</sub>O<sub>3</sub>T, FeO, MnO, Na<sub>2</sub>O, Sc, SiO<sub>2</sub>, Sm.</li> </ul>	<ul style="list-style-type: none"> <li>• Cross-cuts dacite, iron formations, and gabbro. Post-dates these lithologies.</li> <li>• U–Pb: 2724 ± 4.3 (Jellicoe, 2019).</li> <li>• Syn-D1 deformation (Jellicoe, 2019).</li> </ul>
<b>V<sub>GD</sub> veins: Auriferous quartz-carbonate extensional veins</b>	<ul style="list-style-type: none"> <li>• Shallowly-dipping.</li> <li>• Semi-opaque, white.</li> <li>• Large, consistent alteration envelopes.</li> <li>• Non-magnetic.</li> <li>• No–weak reaction with HCl.</li> </ul>	<ul style="list-style-type: none"> <li>• Quartz and carbonate minerals.</li> <li>• Common accessory minerals: Actinolite, biotite, chlorite, tourmaline, sulphide minerals, white mica, free gold, and others depending on host lithology.</li> </ul>	<ul style="list-style-type: none"> <li>• N/A</li> </ul>	<ul style="list-style-type: none"> <li>• N/A</li> </ul>	<ul style="list-style-type: none"> <li>• Cross-cuts/alters dacite, iron formations, gabbro, and Webb Lake stock. Post-dates these lithologies.</li> <li>• Prior to or early D2 deformation (Jellicoe, 2019).</li> </ul>
<b>V<sub>1</sub>–V<sub>2</sub> veins: Auriferous quartz-carbonate shear-related veins</b>	<ul style="list-style-type: none"> <li>• Steeply-dipping.</li> <li>• White-grey, translucent.</li> <li>• Large, consistent alteration envelopes.</li> <li>• Non-magnetic.</li> <li>• No–weak reaction with HCl.</li> </ul>	<ul style="list-style-type: none"> <li>• Quartz and carbonate minerals.</li> <li>• Common accessory minerals: Actinolite, biotite, chlorite, tourmaline, sulphide minerals, white mica, free gold, and others depending on host lithology.</li> </ul>	<ul style="list-style-type: none"> <li>• N/A</li> </ul>	<ul style="list-style-type: none"> <li>• N/A</li> </ul>	<ul style="list-style-type: none"> <li>• Cross-cuts/alters dacite, iron formations, gabbro, and the Webb Lake stock. V<sub>1</sub>–V<sub>2</sub> vein-bearing shears deform V<sub>GD</sub> veins. Post-dates these lithologies/veins.</li> <li>• Late-D2 deformation (Jellicoe, 2019).</li> </ul>
<b>Lamprophyre: Spessartite or Gabbro: Sub-volcanic equivalent to OIB or CFB (I2H)</b>	<ul style="list-style-type: none"> <li>• Dykes and sills.</li> <li>• Equigranular.</li> <li>• Fine–medium grain size.</li> <li>• Non-magnetic.</li> <li>• No–weak reaction with HCl.</li> </ul>	<ul style="list-style-type: none"> <li>• Quartz, plagioclase (oligoclase–andesine), carbonate minerals, chlorite, and white mica.</li> <li>• Accessory minerals: Actinolite, epidote, hematite, rutile, tourmaline, and zircon.</li> </ul>	<ul style="list-style-type: none"> <li>• Plagioclase, hornblende, pyroxene, and potentially olivine.</li> <li>• Accessory minerals: Zircon.</li> </ul>	<ul style="list-style-type: none"> <li>• <b>V<sub>3</sub> Non-auriferous Veining:</b></li> <li>• White mica (± fuchsite) and carbonates.</li> <li>• Gains: As, Au, B, Ba, Bi, Ce, Cr, Cs, Ga, Ge, K<sub>2</sub>O, La, Li, Mo, Rb, Sb, Sr, V, W, Zn.</li> <li>• Losses: Ag, C, CaO, Co, CO<sub>2</sub>, Dy, Er, LOI, Lu, MgO, MnO, Na<sub>2</sub>O, Ni, Pb, Se, SiO<sub>2</sub>, Tb, Tm, Y, Yb.</li> </ul>	<ul style="list-style-type: none"> <li>• Cross-cuts V<sub>1</sub>–V<sub>2</sub> veins and all earlier lithologies/veins. Post-dates these lithologies/veins.</li> <li>• Likely late-D2 deformation.</li> </ul>

Lithology/Vein Textures	Lithology/Vein Features of Least-altered samples	Mineralogy of Least-altered Samples	Interpreted Primary Minerals	Quartz Vein-related Alteration	Timing
<b>Quartz diorite</b>	<ul style="list-style-type: none"> <li>• Dyke and xenoliths in intrusion of silica-poor diorite–monzodiorite.</li> <li>• Distinct pink–red colour due to hematite.</li> <li>• Phaneritic, equigranular.</li> <li>• Medium grain size.</li> <li>• Weakly magnetic</li> <li>• Weak reaction with HCl.</li> </ul>	<ul style="list-style-type: none"> <li>• Plagioclase (albite), quartz, carbonate minerals, hematite, and chlorite.</li> <li>• Accessory minerals: Biotite, epidote, magnetite, titanite, tourmaline, white mica, and zircon.</li> </ul>	<ul style="list-style-type: none"> <li>• Plagioclase (albite), and quartz.</li> <li>• Accessory minerals: Biotite, magnetite, and zircon.</li> </ul>	<ul style="list-style-type: none"> <li>• Not studied</li> </ul>	<ul style="list-style-type: none"> <li>• Present as xenoliths within diorite–monzodiorite. Pre-dates this lithology.</li> <li>• Limited extent. Timing uncertain.</li> <li>• Insignificant alteration, metamorphism, and deformation suggests it post-dates the gabbro/lamprophyre.</li> <li>• Likely late or post-D2 deformation.</li> </ul>
<b>Silica-poor diorite–monzodiorite (I2M)</b>	<ul style="list-style-type: none"> <li>• Dykes and sills.</li> <li>• Often has a weak to distinct pink colour.</li> <li>• Phaneritic, equigranular.</li> <li>• Medium grain size.</li> <li>• Weakly–strongly magnetic.</li> <li>• Weak–strong reaction with HCl.</li> </ul>	<ul style="list-style-type: none"> <li>• Plagioclase (oligoclase), carbonate minerals, biotite, chlorite, epidote, magnetite, and orthoclase.</li> <li>• Accessory minerals: Hematite, pyrite, quartz, rutile, titanite, tourmaline, white mica, and zircon.</li> </ul>	<ul style="list-style-type: none"> <li>• Plagioclase (oligoclase), biotite, magnetite, and orthoclase.</li> <li>• Accessory minerals: Pyrite, quartz, white mica, and zircon</li> </ul>	<ul style="list-style-type: none"> <li>• <b>V<sub>3</sub> Non-auriferous Veining:</b></li> <li>• White mica, carbonate minerals, and chlorite</li> <li>• Gains: As, Au, CaO, FeO, Hf, Li, S, Sc, Te, W.</li> <li>• Losses: B, Ba, C, CO<sub>2</sub>, Cr, Cs, Cu, Fe<sub>2</sub>O<sub>3</sub>, Ga, K<sub>2</sub>O, LOI, Mo, Na<sub>2</sub>O, Ni, Pb, Rb, Sb, Se, Sr, U.</li> </ul>	<ul style="list-style-type: none"> <li>• Contains quartz diorite xenoliths.</li> <li>• Cross-cuts V<sub>1</sub>-V<sub>2</sub> veins and earlier lithologies/veins. Post-dates these lithologies and vein types.</li> <li>• Believed to post-date gabbro/lamprophyre.</li> <li>• U-Pb: 2672.2 ± 3.5 Ma (Jellicoe, 2019).</li> <li>• Late or post D2 deformation (Jellicoe, 2019).</li> </ul>
<b>V<sub>3</sub> veins: Non-auriferous, quartz-carbonate extensional veins</b>	<ul style="list-style-type: none"> <li>• Milky-white, opaque.</li> <li>• Typically, short and discontinuous.</li> <li>• No to small envelope.</li> <li>• Inconsistent alteration.</li> <li>• Non-magnetic.</li> <li>• No–weak reaction with HCl.</li> </ul>	<ul style="list-style-type: none"> <li>• Quartz and carbonate minerals.</li> <li>• Varies depending on host lithology.</li> </ul>	<ul style="list-style-type: none"> <li>• N/A</li> </ul>	<ul style="list-style-type: none"> <li>• N/A</li> </ul>	<ul style="list-style-type: none"> <li>• Sporadically present in all lithologies except Diabase.</li> <li>• Cross-cuts V<sub>GD</sub> and V<sub>1</sub>-V<sub>2</sub> veins.</li> <li>• Post-dates diorite–monzodiorite and all prior lithologies/veins.</li> <li>• Syn-D3 deformation (Jellicoe, 2019).</li> </ul>

Lithology/Vein Textures	Lithology/Vein Features of Least-altered samples	Mineralogy of Least-altered Samples	Interpreted Primary Minerals	Quartz Vein-related Alteration	Timing
<b>Tourmalinization / V<sub>4</sub> veins</b>	<ul style="list-style-type: none"> <li>• Semi-linear ribbons (V<sub>4</sub> veins; Jellicoe et al., 2018) or disseminated alteration minerals.</li> <li>• Tourmaline ribbons invade pre-existing structural conduits.</li> </ul>	<ul style="list-style-type: none"> <li>• Tourmaline (<math>\pm</math> minor quartz/carbonate minerals if present as a distinct vein).</li> </ul>	<ul style="list-style-type: none"> <li>• N/A</li> </ul>	<ul style="list-style-type: none"> <li>• N/A</li> </ul>	<ul style="list-style-type: none"> <li>• Invades V<sub>3</sub> veins and all other pre-existing lithologies/veins. Post-dates these lithologies.</li> <li>• Late or post-D<sub>3</sub> deformation (Jellicoe, 2019).</li> </ul>
<b>Diabase–quartz diabase (I3DD)</b>	<ul style="list-style-type: none"> <li>• Dykes.</li> <li>• Fine–medium grain size.</li> <li>• Aphanitic–phaneritic, equigranular.</li> <li>• Strongly magnetic.</li> </ul>	<ul style="list-style-type: none"> <li>• Plagioclase (andesine–labradorite), clinopyroxene, orthopyroxene, magnetite, actinolite, chlorite, biotite, quartz, hornblende, and epidote.</li> <li>• Accessory minerals: Carbonate minerals and white mica.</li> </ul>	<ul style="list-style-type: none"> <li>• Plagioclase (andesine–labradorite), clinopyroxene, orthopyroxene, magnetite, quartz, and hornblende.</li> </ul>	<ul style="list-style-type: none"> <li>• N/A</li> </ul>	<ul style="list-style-type: none"> <li>• Sharply cross-cuts all lithologies and vein types.</li> <li>• Timing of all diabase dykes uncertain.</li> <li>• Potentially multiple generations.</li> <li>• Mainly Matachewan dyke swarm (2473 <math>\pm</math> 16/-9 Ma; Heaman, 1997).</li> <li>• Post-D<sub>3</sub> deformation (Jellicoe, 2019).</li> </ul>

## **Appendix C**

### **Grab sample information (Underground and surface)**

Spatial data: UTM Zone 16U, North American 1983 datum. Elevation is measured in metres above sea level (m ASL). Additional sample information as well as most of the data presented in this appendix are also presented in an open file report (Ciufu et al., 2019).



ID	Lithology	Brief Sample Description	Easting	Northing	Elevation (m ASL)	Thin Section	Geochemistry	Geochronology	SEM-MLA	32S	33S	34S	36S	32S	34S	Microprobe
T5	Tonalite-Trondhjemite	Weakly-altered Webb Lake Stock, tonalitic-trondhjemitic intrusive rock. Chlorite and carbonate alteration. Altered by nearby V <sub>1</sub> -V <sub>2</sub> veins.	688860	5351125	380-400	1										
T6	Tonalite-Trondhjemite	Weakly-altered Webb Lake Stock, tonalitic-trondhjemitic intrusive rock. Chlorite and carbonate alteration. Altered by nearby V <sub>1</sub> -V <sub>2</sub> veins.	688860	5351125	380-400	1	1									
T7	Tonalite-Trondhjemite	Weakly-altered Webb Lake Stock, tonalitic-trondhjemitic intrusive rock. Chlorite and carbonate alteration. Altered by nearby V <sub>1</sub> -V <sub>2</sub> veins.	689950	5351700	380-400	1										
T8	Felsic-intermediate volcanic rock	Least-altered felsic-intermediate volcanic rock with feldspar and blue quartz phenocrysts.	689950	5351700	380-400	1	1									
T9	Diabase-Quartz Diabase	Diabase-Quartz Diabase dyke.	690700	5352230	380-400	1	1									
T11	Felsic-intermediate volcanic rock	Least-altered felsic-intermediate volcanic rock with feldspar and blue quartz phenocrysts.	690460	5352335	380-400	1	1									
T12	Diabase-Quartz Diabase	Diabase-Quartz Diabase dyke.	690350	5352510	380-400	1	1									
T17	Felsic-intermediate volcanic rock	Moderately-altered felsic-intermediate volcanic rock. <3% pyrite, moderately-strongly foliated, non-magnetic. Chlorite, sericite, pyrite, and carbonate alteration. Altered by nearby V <sub>1</sub> -V <sub>2</sub> veins.	690673	5351573	-361	1	1							1		
T19	Mafic intrusive rock	Weakly-altered mafic intrusive rock consisting of mostly chlorite and small carbonate veinlets. Altered by nearby V <sub>1</sub> -V <sub>2</sub> veins.	690517	5351529	-361	1	1									

ID	Lithology	Brief Sample Description	Easting	Northing	Elevation (m ASL)	Thin Section	Geochemistry	Geochronology	SEM-MLA	S		Microprobe
										<sup>32</sup> S	<sup>34</sup> S	
T20	Felsic-intermediate volcanic rock	Moderately-altered felsic-intermediate volcanic rock. <3% pyrite, moderately-strongly foliated, non-magnetic. Chlorite, sericite, pyrite, and carbonate alteration. Altered by nearby V <sub>1</sub> -V <sub>2</sub> veins.	690477	5351533	-361	1	1				1	
T21	Felsic-intermediate volcanic rock	Felsic-intermediate volcanic rock with randomly-oriented chloritoid grains.	690800	5352600	380-400	1	1					
T24	Iron Formation	Sulphide-rich iron formation.	690800	5352600	380-400	1	1			1	1	
T27	Felsic-intermediate volcanic rock	Felsic-intermediate volcanic rock with feldspar and blue quartz phenocrysts, intruded/brecciated by chlorite-rich rock.	692170	5352770	380-400	1	1				1	
T28	Felsic-intermediate volcanic rock	Felsic-intermediate volcanic rock with feldspar and blue quartz phenocrysts, intruded/brecciated by chlorite-rich rock.	692170	5352770	380-400	1						
T29	Felsic-intermediate volcanic rock	Chlorite-rich matrix component of fragmental felsic-intermediate tuff (sample of matrix only).	692275	5352470	380-400	0	1					
T31	Felsic-intermediate volcanic rock	Chloritoid-rich felsic-intermediate volcanic fragment encompassed by a more chlorite-rich matrix (sample of clast only).	692275	5352470	380-400	1	1					
T32	Felsic intrusive rock	Altered felsic intrusive rock.	692330	5352330	380-400	1	1					
T36	Felsic-intermediate volcanic rock	Altered felsic-intermediate volcanic rock with feldspar and blue quartz phenocrysts.	694700	5352400	380-400	1						
T37	Iron formation	Sulphide-rich iron formation.	690635	5350620	380-400	1	1			1	1	
T38	Iron formation	Banded iron formation with chert, carbonate, chlorite, and biotite-rich layers.	690635	5350620	380-400	1	1					
T39	Mafic intrusive rock	Mafic intrusive rock with small, sulfide-bearing quartz veinlets.	692170	5352770	380-400	1	1					

ID	Lithology	Brief Sample Description	Easting	Northing	Elevation (m ASL)	Thin Section	Geochemistry	Geochronology	SEM-MLA	<sup>32</sup> S	<sup>33</sup> S	<sup>34</sup> S	<sup>36</sup> S	<sup>32</sup> S	<sup>34</sup> S	Microprobe
T40	Breccia	Altered and deformed breccia consisting of felsic to intermediate clasts and a magnetic, chlorite-rich matrix.	692170	5352770	380-400	1										
T41	Breccia	Altered and deformed breccia consisting of felsic to intermediate clasts and a magnetic, chlorite-rich matrix.	692170	5352770	380-400	1										
T42	Felsic-intermediate intrusive rock	Altered and strongly-deformed felsic-intermediate intrusive rock.	692170	5352770	380-400	1	1									
T43	Felsic-intermediate intrusive rock	Felsic-Intermediate volcanic rock with feldspar and blue quartz phenocrysts, appears to be intruded/brecciated by chlorite-rich rock.	692170	5352770	380-400	1	1									
T45	Felsic intrusive rock	Felsic intrusive rock.	691650	5352930	380-400	1	1									
T46	Felsic rock	Altered felsic fragment with minor disseminated pyrite content.	692170	5352770	380-400	1										
T47	Mafic intrusive rock	Altered, pyrite-bearing, chlorite-rich intrusive rock with a strong foliation.	692170	5352770	380-400	1										
T48	Felsic intrusive rock	Felsic-intrusive rock.	691750	5351540	380-400	1										
T56	Felsic-intermediate volcanic rock	Strongly-altered felsic-intermediate volcanic rock, some quartz veining present, ~8% pyrite, strongly-foliated, weakly magnetic outside of quartz veins, weak reaction with HCl. Silica, pyrite, sericite, and carbonate alteration. Altered by nearby V <sub>1</sub> -V <sub>2</sub> veins.	690813	5351716	-90	1	1								1	
T58	Felsic-intermediate volcanic rock	Strongly-altered felsic-intermediate volcanic rock, ~3% disseminated pyrite, strongly-foliated, non-magnetic, weak reaction with HCl. Sericite, silica, pyrite, carbonate, and chlorite alteration alteration. Altered by nearby V <sub>1</sub> -V <sub>2</sub> veins.	690813	5351715	-90	1	1								1	

ID	Lithology	Brief Sample Description	Easting	Northing	Elevation (m ASL)	Thin Section	Geochemistry	Geochronology	SEM-MLA	<sup>32</sup> S	<sup>33</sup> S	<sup>34</sup> S	<sup>36</sup> S	<sup>32</sup> S	<sup>34</sup> S	Microprobe
T59	Felsic-intermediate volcanic rock	Weakly-altered felsic-intermediate volcanic rock, carbonate veinlets/flooding, trace pyrite, moderately-foliated, non-magnetic, strong reaction with HCl. Carbonate, chlorite, and minor pyrite alteration. Altered by nearby V <sub>1</sub> -V <sub>2</sub> veins.	690814	5351714	-90	1	1									
T66	Diorite-Monzodiorite	Grey with slight pink colour, some hematite content, relatively equigranular and homogeneous, mineral grains <1mm across, ~1% disseminated euhedral pyrite, weak-moderate foliation, moderately-magnetic, weak reaction with HCl.	690576	5351551	-361	1	1									
T70	Felsic-intermediate volcanic rock	Strongly-altered felsic-intermediate volcanic rock, ~13% disseminated and stringers of disseminated fine-grained pyrite, strongly-foliated, non-magnetic, moderate-weak reaction with HCl. Silica, pyrite, sericite, carbonate, and chlorite alteration. Altered by nearby V <sub>1</sub> -V <sub>2</sub> veins.	690446	5351535	-361	1										
T71	Felsic-intermediate volcanic rock	Strongly-altered felsic-intermediate volcanic rock with some V <sub>1</sub> -V <sub>2</sub> veining. Pyrite densely concentrated at the contact between quartz veinlets and volcanic rock. Dense stringers and disseminated pyrite ~20%, strongly-foliated, non-magnetic, strong reaction with HCl in carbonate-rich areas of V <sub>1</sub> -V <sub>2</sub> veins, no reaction elsewhere. Silica, pyrite, sericite, and carbonate alteration.	690446	5351535	-361	1	1			1				1		
T72	Felsic-intermediate volcanic rock	Strongly-altered felsic-intermediate volcanic rock, visible blue quartz phenocrysts, 10% pyrite, strongly-foliated, non-magnetic, weak reaction with HCl. Silica, pyrite, sericite, and carbonate alteration. Altered by nearby V <sub>1</sub> -V <sub>2</sub> veins.	690446	5351535	-361	1	1							1		

ID	Lithology	Brief Sample Description	Easting	Northing	Elevation (m ASL)	Thin Section	Geochemistry	Geochronology	SEM-MLA	<sup>32</sup> S	<sup>33</sup> S	<sup>34</sup> S	<sup>36</sup> S	<sup>32</sup> S	<sup>34</sup> S	Microprobe
T73	Felsic-intermediate volcanic rock	Moderately-altered felsic-intermediate volcanic rock, ~4% sulfides (2% pyrite, 2% pyrrhotite), strongly-foliated, weakly magnetic due to pyrrhotite, moderate reaction with HCl. Sericite, chlorite, carbonate, and sulphide alteration. Altered by nearby V <sub>1</sub> -V <sub>2</sub> veins.	690444	5351534	-361	1	1			2				1		
T76	Felsic-intermediate volcanic rock	Moderately-strongly-altered felsic-intermediate volcanic rock, quartz +/- carbonate flooding/veining, sub-mm across tourmaline seams, ~1% pyrite, strongly-foliated, non-magnetic, strong-moderate reaction with HCl. Sericite, carbonate, chlorite, and pyrite alteration. Altered by nearby V <sub>1</sub> -V <sub>2</sub> veins.	690895	5351706	-235	1										
T77	Felsic-intermediate volcanic rock	Moderately-altered felsic-intermediate volcanic rock, ~1% disseminated pyrite, strongly-foliated, non-magnetic, moderate reaction with HCl. Sericite, carbonate, chlorite, and pyrite alteration. Altered by nearby V <sub>1</sub> -V <sub>2</sub> veins.	690895	5351706	-235	1										
T78	Felsic-intermediate volcanic rock	Moderately-strongly-altered felsic-intermediate volcanic rock, ~3% disseminated pyrite, strongly-foliated, non-magnetic, strong reaction with HCl. Carbonate, sericite, chlorite, and pyrite alteration. Altered by nearby V <sub>1</sub> -V <sub>2</sub> veins.	690895	5351705	-235	1										
T79	Felsic-intermediate volcanic rock	Weakly-altered felsic-intermediate volcanic rock, blue quartz phenocrysts, sulfide barren, strongly-foliated, non-magnetic, strong reaction with HCl. Chlorite and carbonate alteration. Altered by nearby V <sub>1</sub> -V <sub>2</sub> veins.	690895	5351704	-235	1										
T80	Gabbro	Least-altered gabbro, trace disseminated pyrite, non-magnetic, strong reaction with HCl.	690557	5351594	-340	1	1									
T81	Gabbro / Lamprophyre	Ultramafic-mafic intrusive rock, some large 1-8mm across carbonate grains present, sulfide barren, non-magnetic, weak reaction with HCl.	690568	5351589	-340	1	1									

ID	Lithology	Brief Sample Description	Easting	Northing	Elevation (m ASL)	Thin Section	Geochemistry	Geochronology	SEM-MLA	S		Microprobe
										<sup>32</sup> S	<sup>34</sup> S	
T82	Gabbro / Lamprophyre and felsic-intermediate volcanic rock	Contact between ultramafic-mafic intrusive rock and felsic-intermediate volcanic rock, linear tourmaline ribbons on contact, carbonate veinlets and pods, non-magnetic, strong reaction with HCl in carbonate veinlets, weak elsewhere.	690568	5351589	-340	1						
T83	Diabase-Quartz Diabase	Diabase dyke, appears undeformed, weak foliation, moderately-magnetic, no reaction with HCl.	690809	5351715	-90	1	1					
T85	Felsic-intermediate volcanic rock	Moderately-altered felsic-intermediate volcanic rock, some V <sub>1</sub> -V <sub>2</sub> veinlets, ~4% pyrite, weakly magnetic in some places, weak reaction with HCl. Sericite, silica, carbonate, pyrite, and chlorite alteration.	690394	5351501	-275	1	1				1	
T86	Felsic-intermediate volcanic rock	Strongly-altered felsic-intermediate volcanic rock, some minor V <sub>1</sub> -V <sub>2</sub> veinlets, tourmaline ribbons, ~4% pyrite, non-magnetic, strong reaction with HCl. Silica, sericite, carbonate, and pyrite alteration.	690394	5351501	-275	1	1				1	
T87	Gabbro	Weakly-altered gabbro, trace pyrite, moderately-magnetic, moderate reaction with HCl. Chlorite, carbonate, and minor pyrite alteration. Altered by nearby V <sub>1</sub> -V <sub>2</sub> veins.	690394	5351500	-275	1	1					
T88	Felsic-intermediate volcanic rock	Moderately-altered felsic-intermediate volcanic rock, trace pyrite, strongly-foliated, layered appearance, strongly-magnetic in more mafic layers, moderately-magnetic elsewhere, moderate reaction with HCl. Carbonate, sericite, chlorite, and pyrite alteration. Altered by nearby V <sub>1</sub> -V <sub>2</sub> veins.	690395	5351499	-275	1	1					
T89	Gabbro	Least-altered gabbro, non-magnetic, weakly to moderately-foliated, weak-moderate reaction with HCl.	690569	5351568	-275	1	1					

ID	Lithology	Brief Sample Description	Easting	Northing	Elevation (m ASL)	Thin Section	Geochemistry	Geochronology	SEM-MLA	<sup>32</sup> S	<sup>33</sup> S	<sup>34</sup> S	<sup>36</sup> S	<sup>32</sup> S	<sup>34</sup> S	Microprobe
T90	Felsic-intermediate volcanic rock	Strongly-altered felsic-intermediate volcanic rock with V <sub>1</sub> -V <sub>2</sub> veining, strongly-foliated, ~12% disseminated and stringer pyrite, non-magnetic, no reaction with HCl. Silica, sericite, and pyrite alteration.	690545	5351544	-275	1	1							1		
T94	Tonalite-Trondhjemite	Likely a moderately-altered sample of the Webb Lake Stock (uncertain) altered by both V <sub>1</sub> -V <sub>2</sub> and V <sub>GD</sub> veins. Prominent pink minerals (either K-spar or hematite), minor quartz veining, blue quartz phenocrysts, weakly-moderately foliated, non-magnetic, strong reaction with HCl, sulfide barren. Chlorite, carbonate, sericite, and silica alteration.	691182	5352156	200	1	1									
T98	Gabbro	Moderately-altered gabbro altered by both V <sub>1</sub> -V <sub>2</sub> and V <sub>GD</sub> veins, chloritic schist with abundant quartz-carbonate veinlets, 1% disseminated pyrite, strongly-foliated, non-magnetic, weak-moderate reaction with HCl outside veinlets, strong reaction within veinlets. Carbonate, chlorite, silica, and pyrite alteration.	691186	5352160	200	1	1							1		
T99	Gabbro	Strongly-altered gabbro altered by both V <sub>1</sub> -V <sub>2</sub> and V <sub>GD</sub> veins, quartz-carbonate veinlets, 15% disseminated pyrite, strongly-foliated, non-magnetic, strong reaction with HCl. Carbonate, chlorite, silica, and pyrite alteration.	691186	5352160	200	1	1							1		
T100	Auriferous quartz-carbonate vein	V <sub>GD</sub> quartz-carbonate vein, white, semi-opaque, folded, subhorizontal, small fragments of the gabbroic host-rock are included in the vein, pyrite is concentrated at the margins of the vein or within the gabbroic rock, ~8% pyrite, non-magnetic, weak-moderate reaction with HCl in V <sub>GD</sub> vein, strong reaction in gabbro adjacent to vein.	691186	5352160	200	1	1				1			1		

ID	Lithology	Brief Sample Description	Easting	Northing	Elevation (m ASL)	Thin Section	Geochemistry	Geochronology	SEM-MLA	<sup>32</sup> S	<sup>33</sup> S	<sup>34</sup> S	<sup>36</sup> S	<sup>32</sup> S	<sup>34</sup> S	Microprobe
T101	Felsic-intermediate volcanic rock	Strongly-altered gabbro directly below V <sub>GD</sub> vein and proximal to V <sub>1</sub> -V <sub>2</sub> veins. Significant quartz carbonate veining, pyrite concentrated near small quartz carbonate veins, ~5% pyrite, strongly-foliated, non-magnetic, strong reaction with HCl. Chlorite, carbonate, silica, and pyrite alteration.	691186	5352160	200	1	1							1		
T102	Felsic-intermediate volcanic rock	Weakly-altered felsic-intermediate volcanic rock, trace cubic pyrite, moderately-strongly-foliated, non-magnetic, strong reaction with HCl. Carbonate, chlorite, sericite, and pyrite alteration. Altered by both V <sub>1</sub> -V <sub>2</sub> and V <sub>GD</sub> veins.	691186	5352159	200	1	1									
T104	Auriferous quartz-carbonate vein	V <sub>GD</sub> quartz-carbonate vein, subhorizontal quartz vein, trace pyrite concentrated near contacts with felsic-intermediate volcanic rock fragments within vein, non-magnetic, no reaction with HCl.	691187	5352176	200	1	1									
T105	Felsic-intermediate volcanic rock	Strongly-altered felsic-intermediate volcanic rock directly adjacent to a V <sub>GD</sub> vein, ~4% disseminated pyrite, strongly-foliated, seams of possible tourmaline or chlorite are also present, non-magnetic, strong-moderate reaction with HCl. Sericite, silica, carbonate, pyrite, and chlorite alteration.	691187	5352176	200	1	1							1		
T112	Gabbro	Weakly-moderately-altered gabbro, quartz-carbonate veinlets, trace disseminated fine-grained pyrite, strongly-foliated, non-magnetic, strong reaction with HCl. Chlorite, carbonate, and pyrite alteration. Altered by nearby V <sub>GD</sub> and V <sub>1</sub> -V <sub>2</sub> veining.	691191	5352174	200	1										
T113	Felsic-intermediate volcanic rock	Strongly-altered felsic-intermediate volcanic rock, minor quartz-carbonate veinlets, ~3% pyrite, strongly-foliated, non-magnetic, strong reaction with HCl. Sericite, carbonate, pyrite, and silica alteration. Altered by nearby V <sub>GD</sub> veining.	691187	5352176	200	1	1							1		



ID	Lithology	Brief Sample Description	Easting	Northing	Elevation (m ASL)	Thin Section	Geochemistry	Geochronology	SEM-MLA	S		Microprobe
										<sup>32</sup> S	<sup>34</sup> S	
T114	Felsic-intermediate volcanic rock	Moderately-altered felsic-intermediate volcanic rock, ~2% disseminated fine-grained pyrite, strongly-foliated, non-magnetic, strong reaction with HCl. Carbonate, sericite, chlorite, and pyrite alteration. Altered by nearby V <sub>GD</sub> veining.	691186	5352176	200	1	1					
T115	Felsic-intermediate volcanic rock	Weakly-altered felsic-intermediate volcanic rock, some carbonate veinlets, strongly-foliated, non-magnetic, strong reaction with HCl. Carbonate, sericite, silica, and pyrite alteration. Altered by nearby V <sub>GD</sub> veining.	691186	5352176	200	1	1					
T116	Felsic-intermediate volcanic rock	Least-altered felsic-intermediate volcanic rock, macroscopically visible blue quartz phenocrysts, sulphide barren, moderately-foliated, non-magnetic, weak reaction with HCl.	691214	5352095	200	1	1					
T119	Auriferous quartz-carbonate vein	V <sub>1</sub> -V <sub>2</sub> quartz with minor carbonate vein with tourmaline ribbons, visible gold, intrudes through strongly-altered felsic-intermediate volcanic rock. Pyrite is concentrated at the margins of the vein and near fragments of the wall-rock within the vein.	691185	5352178	-360	1						
T127	Felsic-intermediate volcanic rock	Strongly-altered felsic-intermediate volcanic rock, minor quartz-carbonate veinlets, ~3-4% pyrite, strongly-foliated, non-magnetic, moderate reaction with HCl. Sericite, carbonate, pyrite, and silica alteration. Altered by nearby V <sub>1</sub> -V <sub>2</sub> veining.	690766	5351588	-385					1		
T128	Felsic-intermediate volcanic rock	Strongly-altered felsic-intermediate volcanic rock, minor quartz-carbonate veinlets, ~3-4% pyrite, strongly-foliated, non-magnetic, moderate reaction with HCl. Sericite, carbonate, pyrite, and silica alteration. Altered by nearby V <sub>1</sub> -V <sub>2</sub> veining.	690764	5351592	-385			1				
T129	Felsic-intermediate volcanic rock	Least-altered felsic-intermediate volcanic rock with quartz and feldspar phenocrysts, moderately-foliated, non-magnetic, weak reaction with HCl.	690565	5351588	-385			1				

ID	Lithology	Brief Sample Description	Easting	Northing	Elevation (m ASL)	Thin Section	Geochemistry	Geochronology	SEM-MLA	<sup>32</sup> S	<sup>33</sup> S	<sup>34</sup> S	<sup>36</sup> S	<sup>32</sup> S	<sup>34</sup> S	Microprobe
T134	Nepheline syenite	Herman Lake Intrusive Complex nepheline syenite, medium-coarse grained, relatively unaltered.	687326	5354240	388	1	1									
T136	Nepheline syenite	Herman Lake Intrusive Complex nepheline syenite, coarse-grained, pink potassium feldspar or potentially hematite-staining visible.	688580	5354645	423	1										
T138	Granodiorite	Medium-grained granodiorite from the Maskinonge Lake Intrusion.	688313	5356171	466	1										
T165	Intermediate intrusive rock	Intermediate intrusive rock located in a small shear zone intruding through mafic volcanic rocks.	688630	5353737	406	1	1									
T168	Gabbro	Medium-coarse grained gabbro intruding through mafic volcanic rocks.	688939	5353169	437	1										
T170	Basalt	Fine-grained mafic volcanic rock.	689378	5352918	427	1										
T173	Diabase-Quartz Diabase	Medium-grained, mafic intrusive rock intruding in felsic-intermediate volcanic rocks.	692330	5351391	404	1										
T178	Auriferous quartz-carbonate vein	Gold-bearing V <sub>1</sub> -V <sub>2</sub> vein with fuchsite.	690686	5351577	-396	2										
T182	Gabbro	Least-altered gabbro, medium-grained, intruding through felsic-intermediate volcanic rock.	697448	5351475	417	1	1									
T183	Felsic-intermediate volcanic rock	Least-altered felsic-intermediate volcanic rock, some chlorite and carbonate alteration.	696682	5351495	410	1	1									
T189	Granodiorite	Medium-grained Maskinonge Lake granodiorite.	688198	5356123	479	1	1									
T197	Felsic-intermediate volcanic rock	Strongly-altered felsic-intermediate volcanic rock, near both a large diabase intrusion and V <sub>1</sub> -V <sub>2</sub> veining. Sericite, carbonate, silica, and pyrite alteration.	690802	5351600	-392	1										
T199	Iron Formation	Sulphide-rich iron formation.	685546	5349403	402					1						
T200	Gabbro	Least-altered gabbro, medium-grained, intruding through felsic-intermediate volcanic rock.	692869	5350600	387	1	1									

ID	Lithology	Brief Sample Description	Easting	Northing	Elevation (m ASL)	Thin Section	Geochemistry	Geochronology	SEM-MLA	<sup>32</sup> S	<sup>33</sup> S	<sup>34</sup> S	<sup>36</sup> S	<sup>32</sup> S	<sup>34</sup> S	Microprobe
T208	Porphyritic felsic intrusive rock	Porphyritic felsic intrusive with large feldspar phenocrysts. Potentially a sample of the Webb Lake Stock but uncertain.	692321	5352445	414	1										
T213	Gabbro / Lamprophyre	Hydrothermally-altered mafic-ultramafic intrusive rock altered by a V <sub>3</sub> non-auriferous quartz vein.	690666	5351577	-394.557	1	1									
T215	Quartz Diorite	Xenoliths of a coarse-grained, hematite-rich, felsic intrusive rock within a larger dioritic-monzodioritic intrusion. Weakly-magnetic, weak reaction with HCl.	690912	5351666	-231.065	1	1									
T216	Diorite-Monzodiorite	Diorite-monzodiorite hosting the sample described in T215, grey colour, minor hematite content, strongly-magnetic, moderate reaction with HCl.	690912	5351666	-231.065	1	1									
T228	Diorite-Monzodiorite	Diorite-monzodiorite with significant hematite content, mainly composed of biotite/chlorite, plagioclase, and carbonate minerals. Moderately-strongly-foliated, strongly-magnetic, weak reaction with HCl.	690641	5351572	-394.67	1	1									
T229	Non-auriferous quartz-carbonate vein and Gabbro / Lamprophyre	V <sub>3</sub> non-auriferous quartz vein in contact with an altered mafic-ultramafic intrusive rock. The intrusive rock exhibits fuchsite, sericite, and carbonate alteration at the contact with the vein which decreases in intensity moving away from the vein.	690677	5351574	-393.609	1										
T243	Quartz Diorite	Coarse-grained, felsic intrusive rock with substantial hematite content, weakly-magnetic, weak reaction with HCl.	690907	5351672	-209.775	1										
T244	Diorite-Monzodiorite	Deformed diorite-monzodiorite, taken adjacent to sample 245, some hematite content, moderately-foliated, non-magnetic, moderate reaction with HCl.	690876	5351624	-644	1										
T245	Diorite-Monzodiorite	Diorite-monzodiorite altered by V <sub>3</sub> non-auriferous quartz veins. This sample is located adjacent to T244. Abundant carbonate veinlets, strongly-foliated, non-magnetic, strong reaction with HCl. Chlorite, carbonate, and minor sericite alteration.	690876	5351624	-644	1	1									

## **Appendix D**

### **Drill core sample information**

Additional sample information as well as most of the data presented in this appendix are also presented in an open file report (Ciufu et al., 2019). Additional spatial data pertaining to drill holes in Ciufu et al. (2019) is from Alamos Gold Inc. and Richmond Mines Inc.

ID	Lithology	Brief Sample Description	Hole ID	From (m)	To (m)	Thin Section	Geochemistry	Geochronology	SEM-MLA	S		Microprobe
										<sup>32</sup> S	<sup>34</sup> S	
T13	Felsic-intermediate volcanic rock	Felsic-intermediate volcanic rock with lapilli sized volcanic fragments of similar composition.	740-477-09	79.5	80.1	1	1					
T14	Gabbro	Least-altered gabbro, carbonate veinlets, chlorite alteration, non-magnetic, strong reaction with HCl.	740-477-09	69	69.5	1	1					
T15	Gabbro / Lamprophyre	Mafic-ultramafic intrusive rock, non-magnetic, no reaction with HCl.	740-477-09	128.8	129.1	1	1					
T16	Diorite-Monzodiorite	Diorite-Monzodiorite, grey-pink colour, some hematite content, moderately-magnetic, moderate reaction with HCl.	740-477-09	130.5	130.9	1	1			1	1	
T50	Mafic-ultramafic intrusive rock	Altered mafic-ultramafic intrusive rock, exact lithology uncertain, ~1% disseminated pyrite, non-magnetic, strong-moderate reaction with HCl. Strong chlorite and carbonate alteration.	740-471-18	166	166.8	1	1					
T62	Gabbro	Gabbro, sulfide barren, strongly-foliated, non-magnetic, strong reaction with HCl. Chlorite and carbonate alteration.	740-477-30	189.5	189.8	1						
T63	Gabbro / Lamprophyre	Weakly deformed ultramafic-mafic intrusive rock, sulfide barren, grain sizes <1mm, non-magnetic, very weak reaction with HCl.	740-477-30	189.8	190.4	1	1					
T65	Felsic-intermediate volcanic rock	Least-altered felsic-intermediate volcanic rock with ~5% feldspathic and blue quartz phenocrysts, small carbonate veinlets, sulfide barren, some hematite alteration around carbonate veinlets, moderately-magnetic due to trace magnetite, no reaction with HCl outside of small carbonate veinlets.	740-477-30	190.2	192.15	1	1					
T106	Gabbro	Gabbro with ~50% randomly oriented chloritoid grains, trace pyrrhotite and pyrite, weakly-foliated, non-magnetic, strong reaction with HCl.	740-477-39	540	540.8	1	1					

ID	Lithology	Brief Sample Description	Hole ID	From (m)	To (m)	Thin Section	Geochemistry	Geochronology	SEM-MLA	32 S	33 S	34 S	36 S	32 S	34 S	Microprobe
T107	Felsic-intermediate volcanic rock	Felsic-intermediate volcanic rock with lapilli of similar composition, sulphide barren, contains randomly-oriented chloritoid grains, aphanitic groundmass, non-magnetic.	740-477-39	548.2	548.4	1										
T108	Felsic-intermediate volcanic rock	Least-altered felsic-intermediate volcanic rock (sub-volcanic hypabyssal intrusive rock), relatively homogenous and equigranular, weakly-altered, sub-phaneritic (grains 1mm or less across), trace very fine-grained disseminated pyrite, non-magnetic, no reaction with HCl.	740-477-16	130.6	131.4	1										
T109	Felsic-intermediate volcanic rock	Weakly-altered felsic-intermediate volcanic rock, porphyritic with quartz and plagioclase phenocrysts and an aphanitic groundmass, minor millimetre wide quartz carbonate veinlets with trace tourmaline concentrated within, weak to moderate foliation, non-magnetic outside of veinlets/fracture fill, ~1% disseminated pyrrhotite or magnetite grains outside of veinlets, weak-moderate reaction with HCl, strong reaction in veinlets. Altered by nearby V <sub>1</sub> -V <sub>2</sub> veins.	740-477-16	127.8	128.8	1										
T110	Felsic-intermediate volcanic rock	Weakly-altered felsic-intermediate volcanic rock (sub-volcanic hypabyssal intrusive rock), relatively equigranular, ~1% pyrite, non-magnetic, minor barren smoky quartz veins in some samples, moderate reaction with HCl. Altered by nearby V <sub>1</sub> -V <sub>2</sub> veins.	740-471-35	252.8	253.5	1										
T117	Felsic-intermediate volcanic rock	Weakly-altered felsic-intermediate volcanic rock (sub-volcanic hypabyssal intrusive rock), ~1% pyrite, appears relatively homogeneous and equigranular, grain size is less than 2mm across, weak-moderate foliation, non-magnetic, no reaction with HCl. Altered by nearby V <sub>1</sub> -V <sub>2</sub> veins.	740-465-02	13.3	14.6	1	1									

ID	Lithology	Brief Sample Description	Hole ID	From (m)	To (m)	Thin Section	Geochemistry	Geochronology	SEM-MLA	32 S	33 S	34 S	36 S	32 S	34 S	Microprobe	
T118	Felsic-intermediate volcanic rock	Weakly-altered felsic-intermediate volcanic rock, quartz and feldspar phenocrysts (<3 mm across), ~1% pyrite, weakly-moderately-foliated, non-magnetic, weak reaction with HCl. Altered by nearby V <sub>1</sub> -V <sub>2</sub> veins.	740-465-02	15.5	16.2	1	1										
T125	Mafic-ultramafic intrusive rock	Mafic-ultramafic intrusive rock, lithology uncertain.	740-465-44	77	79.9	1											
T126	Mafic-ultramafic intrusive rock	Mafic-ultramafic intrusive rock, lithology uncertain, Altered and deformed version of T125, chlorite and carbonate alteration, strongly-foliated.	740-465-44	79.9	80.3	1											
T139	Gabbro	Weakly-altered gabbro, trace disseminated sulfides, ~1% disseminated magnetite, <2mm wide carbonate veinlets/seams, weakly-foliated, strongly-magnetic, moderate-strong reaction with HCl. Chlorite, carbonate, and pyrite alteration. Altered by nearby V <sub>1</sub> -V <sub>2</sub> veins.	740-465-46	168.3	169	1	1										1
T140	Gabbro	Moderately-altered gabbro, ~1-2% disseminated pyrite, <2mm scale carbonate veinlets/seams, moderately-foliated, strongly-magnetic, weak reaction with HCl. Chlorite, carbonate, biotite, and pyrite alteration. Altered by nearby V <sub>1</sub> -V <sub>2</sub> veins.	740-465-46	174.4	175	1	1										
T141	Gabbro	Moderately-altered gabbro, 1-2mm thick carbonate veinlets, ~2-3% disseminated pyrite, strongly-foliated, moderately-magnetic, strong reaction with HCl. Chlorite, carbonate, biotite, pyrite, and silica alteration. Altered by nearby V <sub>1</sub> -V <sub>2</sub> veins.	740-465-46	175.5	176.2	1	1										1

ID	Lithology	Brief Sample Description	Hole ID	From (m)	To (m)	Thin Section	Geochemistry	Geochronology	SEM-MLA	<sup>32</sup> S	<sup>33</sup> S	<sup>34</sup> S	<sup>36</sup> S	<sup>32</sup> S	<sup>34</sup> S	Microprobe
T142	Gabbro	Strongly-altered gabbro, ~5-7% disseminated pyrite and pyrrhotite, 1 mm to 1 cm across quartz-carbonate veinlets, strongly-foliated, weakly-magnetic, strong reaction with HCl. Carbonate, biotite, silica, pyrite, and chlorite alteration. Altered by nearby V <sub>1</sub> -V <sub>2</sub> veins.	740-465-46	176.2	177	1	1			1						
T154	Felsic-intermediate volcanic rock	Least-altered felsic-intermediate volcanic rock, quartz and feldspar phenocrysts, some lapilli-sized fragments of similar composition, moderately-foliated, non-magnetic, moderate reaction with HCl.	GD-620-01	712.8	713.5	1	1									1
T155	Felsic-intermediate volcanic rock	Weakly-altered felsic-intermediate volcanic rock, quartz and feldspar phenocrysts, some small carbonate veinlets with orange straining - perhaps ankerite or hematite, ~1% pyrite, moderately-foliated, non-magnetic, strong reaction with HCl. Chlorite, carbonate, pyrite, and minor sericite alteration. Altered by nearby V <sub>1</sub> -V <sub>2</sub> veins.	GD-620-01	723.2	724.3	1										
T156	Felsic-intermediate volcanic rock	Moderately-altered felsic-intermediate volcanic rock, quartz and feldspar phenocrysts, ~1-3% pyrite and pyrrhotite, some disseminated magnetite, some hematite alteration, strongly-foliated, moderately-magnetic, moderate reaction with HCl. Carbonate, sericite, chlorite, and pyrite alteration. Altered by nearby V <sub>1</sub> -V <sub>2</sub> veins.	GD-620-01	727.7	728.5	1	1									
T157	Felsic-intermediate volcanic rock	Strongly-altered felsic-intermediate volcanic rock, ~3-5% pyrite, strongly-foliated, non-magnetic, strong reaction to HCl. Sericite, carbonate, pyrite, chlorite, and silica alteration. Altered by nearby V <sub>1</sub> -V <sub>2</sub> veins.	GD-620-01	728.5	728.9	1	1									1



ID	Lithology	Brief Sample Description	Hole ID	From (m)	To (m)	Thin Section	Geochemistry	Geochronology	SEM-MLA	32S	33S	34S	36S	32S	34S	Microprobe
T158	Felsic-intermediate volcanic rock	Strongly-altered felsic-intermediate volcanic rock with quartz veining/flooding, ~5-7% pyrite, strongly-foliated, non-magnetic, weak-moderate reaction with HCl. Sericite, silica, pyrite, and carbonate alteration. Altered by nearby V <sub>1</sub> -V <sub>2</sub> veins.	GD-620-01	728.9	729.7	1	1									
T159	Auriferous quartz-carbonate vein	V <sub>1</sub> -V <sub>2</sub> smoky quartz-carbonate vein with visible gold flecks, contains some actinolite, chlorite, sericite, and pyrite, some tourmaline seams/ribbons, non-magnetic, no reaction with HCl. Altered by nearby V <sub>1</sub> -V <sub>2</sub> veins.	MH3-7	1400.2	1401.4	1	1									
T161	Felsic-intermediate volcanic rock	Strongly-altered felsic-intermediate volcanic rock, ~5% disseminated pyrite, strongly-foliated, non-magnetic, moderate reaction with HCl. Sericite, carbonate, pyrite, and chlorite alteration. Altered by nearby V <sub>1</sub> -V <sub>2</sub> veins.	MH3-7	1406.1	1407.3	1										
T162	Felsic-intermediate volcanic rock	Strongly-altered felsic-intermediate volcanic rock, ~3% disseminated pyrite, strongly-foliated, non-magnetic, no reaction with HCl except in small carbonate seams. Sericite, pyrite, carbonate, and silica alteration. Altered by nearby V <sub>1</sub> -V <sub>2</sub> veins.	MH3-7	1409.3	1410.4	1	1									
T163	Felsic-intermediate volcanic rock	Weakly-moderately-altered felsic-intermediate volcanic rock, small discontinuous carbonate veinlets, ~1-2% disseminated pyrite, moderately-foliated, non-magnetic, strong reaction with HCl. Altered by nearby V <sub>1</sub> -V <sub>2</sub> veins.	MH3-7	1412.4	1413.6	1										
T164	Felsic-intermediate volcanic rock	Least-altered felsic-intermediate volcanic rock with lapilli of similar composition, a few small carbonate veinlets, weakly-foliated, strongly-magnetic, no reaction with HCl except in the carbonate seams.	MH3-7	1418.5	1419.7	1	1									

ID	Lithology	Brief Sample Description	Hole ID	From (m)	To (m)	Thin Section	Geochemistry	Geochronology	SEM-MLA	<sup>32</sup> S	<sup>33</sup> S	<sup>34</sup> S	<sup>32</sup> S	<sup>34</sup> S	Microprobe
T184	Felsic-intermediate volcanic rock	Weakly-altered felsic-intermediate volcanic rock with quartz and feldspar phenocrysts, minor carbonate veinlets, trace pyrite, moderately-foliated, non-magnetic, weak reaction with HCl. Chlorite, carbonate, weak pyrite, and weak sericite alteration. Altered by nearby V <sub>1</sub> -V <sub>2</sub> veins.	PR-UG-144	69.4	70	1	1		1						
T185	Felsic-intermediate volcanic rock	Weakly-altered felsic-intermediate volcanic rock with quartz and feldspar phenocrysts, minor carbonate veinlets, trace pyrite, moderately-foliated, non-magnetic, no reaction with HCl. Chlorite, minor pyrite, and minor sericite alteration. Altered by nearby V <sub>1</sub> -V <sub>2</sub> veins.	PR-UG-144	72	72.6	1									
T186	Felsic-intermediate volcanic rock	Moderately-altered felsic-intermediate volcanic rock with quartz and feldspar phenocrysts, ~1-2% pyrite in stringers/bands and disseminated, strongly-foliated, weakly-magnetic, moderate-strong reaction with HCl. Carbonate, sericite, chlorite, and pyrite alteration. Altered by nearby V <sub>1</sub> -V <sub>2</sub> veins.	PR-UG-144	78.2	79	1	1		2						
T187	Auriferous quartz-carbonate vein	V <sub>1</sub> -V <sub>2</sub> quartz-carbonate vein with visible gold flecks/droplets, lots of sericite clots in the quartz vein, pyrite stringers and disseminated cubes associated with the sericite-rich areas, non-magnetic, no reaction with HCl.	PR-UG-144	81.1	82.2	1	1								
T188	Felsic-intermediate volcanic rock	Strongly-altered felsic-intermediate volcanic rock, clusters and stringers of cubic pyrite (~3-5%), strongly-foliated, non-magnetic, weak reaction with HCl. Sericite, pyrite, silica, and carbonate alteration. Altered by nearby V <sub>1</sub> -V <sub>2</sub> veins.	PR-UG-144	82.2	82.8	1	1		1						

ID	Lithology	Brief Sample Description	Hole ID	From (m)	To (m)	Thin Section	Geochemistry	Geochronology	SEM-MLA	<sup>32</sup> S	<sup>33</sup> S	<sup>34</sup> S	<sup>32</sup> S	<sup>34</sup> S	Microprobe
T192	Tonalite-trondhjemite	Least-altered Webb Lake Stock, tonalitic-trondhjemitic intrusive rock, some small <1 mm thick carbonate veinlets, trace sulfides, weakly-foliated, non-magnetic, no reaction with HCl outside of carbonate veinlets.	SH-4	430	431.5	1	1								1
T193	Tonalite-trondhjemite	Weakly-altered Webb Lake Stock, tonalitic-trondhjemitic intrusive rock, some <1 mm scale carbonate seams, ~1% pyrite, weakly-foliated, non-magnetic, weak reaction with HCl, non-magnetic. Chlorite, carbonate, biotite, sericite, and pyrite alteration. Altered by nearby V <sub>1</sub> -V <sub>2</sub> veins.	SH-4	444.5	445.3	1	1								
T194	Tonalite-trondhjemite	Moderately-altered Webb Lake Stock, tonalitic-trondhjemitic intrusive rock, some small <1 mm across carbonate veinlets, ~2-4% disseminated pyrite, moderately-foliated, non-magnetic, moderate reaction with HCl. Chlorite, sericite, biotite, carbonate, and pyrite alteration. Altered by nearby V <sub>1</sub> -V <sub>2</sub> veins.	SH-4	445.3	445.9	1	1								
T195	Tonalite-trondhjemite	Strongly-altered Webb Lake Stock, tonalitic-trondhjemitic intrusive rock, some <1 mm across carbonate veinlets, ~5-7% disseminated pyrite and chalcopyrite, moderately-strongly-foliated, non-magnetic, weak-moderate reaction with HCl. Sericite, silica, sulphide, and carbonate alteration. Altered by nearby V <sub>1</sub> -V <sub>2</sub> veins.	SH-4	446	446.9	1	1			2					1
T196	Auriferous quartz-carbonate vein	Smokey V <sub>1</sub> -V <sub>2</sub> auriferous quartz-carbonate vein, visible gold droplets/flecks, sericite seams and clots, ~1-2% pyrite and chalcopyrite, non-magnetic, some <1 mm across carbonate seams, no reaction with acid outside of these carbonate seams.	SH-4	446.9	447.4	1	1								

ID	Lithology	Brief Sample Description	Hole ID	From (m)	To (m)	Thin Section	Geochemistry	Geochronology	SEM-MLA	<sup>32</sup> S	<sup>33</sup> S	<sup>34</sup> S	<sup>36</sup> S	<sup>32</sup> S	<sup>34</sup> S	Microprobe
T218	Felsic-intermediate volcanic rock	Intensely-altered felsic-intermediate volcanic rock with quartz and feldspar phenocrysts, abundant tourmaline seams, lacking quartz veinlets, no quartz veining nearby, some small <2 mm across carbonate veinlets, ~1-2% disseminated magnetite, sulphide barren, minerals are stretched and deformed, strongly-foliated, strongly-magnetic, strong reaction with HCl. Sericite and carbonate alteration.	GD-465-02	48.1	49.5	1	1									
T219	Felsic-intermediate volcanic rock	Weakly-moderately-altered felsic-intermediate volcanic rock with quartz and feldspar phenocrysts, abundant tourmaline seams, minor V <sub>3</sub> non-auriferous quartz-carbonate veining, ~1-2% disseminated magnetite, trace pyrite, moderately-foliated, strongly-magnetic, moderate reaction to HCl. Sericite and carbonate alteration.	GD-465-02	46.6	47.4	1										
T220	Felsic-intermediate volcanic rock	Least-altered felsic-intermediate volcanic rock with quartz and feldspar phenocrysts, minor lapilli of similar composition are also present, trace cubic pyrite, ~1-2% disseminated magnetite, a few tourmaline seams/ribbons, lack of deformation, moderate-strong magnetism, no reaction with HCl.	GD-465-02	42.2	43.3	1										
T226	Gabbro	Gabbro, magnetite inclusions in garnet with chloritoid.	MH9-2	1272.5	1272.6	1										
T233	Felsic-intermediate volcanic rock	Felsic-intermediate volcanic rock with hematite alteration and quartz and feldspar phenocrysts	LC-415-04	253.1	253.2	1										
T237	Felsic intrusive rock	Felsic intrusive rock, protolith uncertain.	MH9-2	1562.3	1562.4	1										
T238	Mafic intrusive rock	Mafic xenolith or mafic intrusive rock intruding through felsic intrusive rock (T237). Protolith uncertain.	MH9-2	1562.4	1562.5	1										

ID	Lithology	Brief Sample Description	Hole ID	From (m)	To (m)	Thin Section	Geochemistry	Geochronology	SEM-MLA	<sup>32</sup> S	<sup>33</sup> S	<sup>34</sup> S	<sup>32</sup> S	<sup>34</sup> S	Microprobe
T239	Gabbro / Lamprophyre	Mafic-ultramafic intrusive rock, weakly-foliated, medium-coarse-grained, non-magnetic, no reaction with HCl.	700-496-10	9.4	10	1	1								
T240	Gabbro / Lamprophyre	Mafic-ultramafic intrusive rock, medium-grained, non-magnetic, no reaction with HCl.	MH4	261	261.8	1	1								
T241	Felsic-intermediate volcanic rock	Least-altered felsic-intermediate volcanic rock with feldspar and quartz phenocrysts and an aphanitic groundmass.	620-517-24	22.7	23.6	1	1		1						
T242	Diorite-Monzodiorite	Diorite-Monzodiorite, weakly-moderately foliated, moderately-strongly-magnetic, strong reaction with HCl.	620-517-24	61	62	1	1								

**Appendix E**  
**Point-counting results**

All values are in area percent. Methods are described in Section 3.3.

<b>Mineral(s)</b>	<b>T6</b>	<b>T8</b>	<b>T15</b>	<b>T56</b>	<b>T58</b>	<b>T59</b>	<b>T66</b>	<b>T71</b>	<b>T72</b>	<b>T73</b>	<b>T80</b>	<b>T83</b>	<b>T85</b>	<b>T100</b>	<b>T104</b>	<b>T105</b>
Quartz	25.2	0.2	11.9	23.0	19.0	9.9	0.5	26.2	13.6	20.0	11.6	2.2	4.4	95.6	91.9	18.3
Potassium Feldspar	1.5	3.5	0.2	0.0	0.0	0.0	0.7	0.0	0.0	2.0	0.0	0.0	0.0	0.0	0.0	0.7
Plagioclase	40.7	1.0	0.2	0.7	0.2	0.5	44.4	11.6	0.5	0.2	15.1	41.7	0.0	0.0	0.0	4.7
Feldspar (undifferentiated)	0.0	0.0	1.5	0.0	0.0	0.0	0.0	0.0	0.0	1.5	5.2	0.0	0.2	0.0	0.0	1.7
Quartzofeldspathics (undifferentiated)	0.0	41.7	13.3	22.5	18.5	49.9	0.0	10.1	24.4	25.2	4.2	0.0	61.7	0.0	0.0	18.3
Total (sum of above)	67.4	46.4	27.2	46.2	37.8	60.2	45.7	47.9	38.5	48.9	36.0	44.0	66.4	95.6	91.9	43.7
Actinolite	0.0	0.0	0.0	0.0	0.0	0.0	0.0	0.0	0.0	0.0	0.0	2.5	0.0	0.0	0.0	0.0
Augite	0.0	0.0	0.5	0.0	0.0	0.0	0.0	0.0	0.0	0.0	0.2	29.1	1.0	0.0	0.0	0.0
Biotite	0.0	0.0	0.0	3.5	0.5	8.4	13.1	0.0	0.0	0.5	0.0	3.2	2.7	0.0	0.0	0.0
Carbonates	4.4	2.7	33.6	0.0	0.0	0.5	24.7	0.0	17.5	12.1	19.0	0.0	6.9	3.2	2.0	12.8
Chalcopyrite	0.0	0.0	0.0	0.0	0.0	0.0	0.0	0.0	0.0	0.0	0.0	0.0	0.0	0.0	0.0	0.0
Chlorite	15.1	30.9	30.4	9.9	11.6	21.7	11.1	0.5	4.0	10.1	42.2	4.0	7.7	0.7	2.2	3.2
Chloritoid	0.0	0.0	0.0	0.0	0.0	0.0	0.0	0.0	0.2	0.0	0.0	0.0	0.2	0.0	0.0	0.0
Epidote	1.7	5.2	0.0	0.2	0.0	0.7	2.7	0.0	0.2	0.0	0.5	0.7	0.0	0.0	0.0	0.0
Fuchsite	0.0	0.0	0.0	0.0	0.0	0.0	0.0	0.0	0.0	0.0	0.0	0.0	0.0	0.0	0.0	0.0
Grunerite	0.0	0.0	0.0	0.0	0.0	0.0	0.0	0.0	0.0	0.0	0.0	0.0	0.0	0.0	0.0	0.0
Hematite	0.0	0.0	0.0	0.0	0.0	0.0	0.0	0.0	0.0	0.0	0.0	0.0	0.0	0.0	0.0	0.0
Hornblende	0.0	0.0	0.0	0.0	0.0	0.0	0.0	0.0	0.0	0.0	0.0	1.5	0.0	0.0	0.0	0.0
Ilmenite	0.0	2.5	0.0	0.0	0.0	1.7	0.0	0.0	1.0	0.5	1.5	0.0	0.2	0.0	0.0	0.5
Magnetite	0.0	0.0	0.0	0.7	0.0	0.0	1.0	0.5	0.0	0.0	0.0	5.2	1.0	0.0	0.0	0.0
Orthopyroxene	0.0	0.0	0.0	0.0	0.0	0.0	0.0	0.0	0.0	0.0	0.0	9.4	0.0	0.0	0.0	0.0
Pyrite	0.5	0.0	0.0	5.2	1.5	0.0	0.5	15.1	2.7	1.2	0.2	0.0	0.2	0.5	0.0	2.5
Pyrrhotite	0.0	0.0	0.0	0.0	0.0	0.2	0.0	0.0	0.0	1.7	0.0	0.0	1.0	0.0	0.0	0.0
Rutile	0.2	0.5	1.5	1.2	3.7	0.0	0.2	0.2	0.0	0.2	0.2	0.0	0.2	0.0	0.0	0.0
White Mica	10.1	6.7	6.9	32.8	44.4	6.4	0.5	35.3	35.8	16.5	0.0	0.5	12.1	0.0	4.0	36.5
Titanite	0.5	5.2	0.0	0.0	0.0	0.0	0.2	0.0	0.0	0.0	0.0	0.0	0.0	0.0	0.0	0.5
Tourmaline	0.0	0.0	0.0	0.2	0.0	0.0	0.0	0.5	0.0	8.1	0.0	0.0	0.2	0.0	0.0	0.2
Zircon	0.0	0.0	0.0	0.0	0.5	0.0	0.2	0.0	0.0	0.0	0.0	0.0	0.0	0.0	0.0	0.0

<b>Mineral(s)</b>	<b>T113</b>	<b>T114</b>	<b>T115</b>	<b>T118</b>	<b>T139</b>	<b>T140</b>	<b>T141</b>	<b>T142</b>	<b>T154</b>	<b>T156</b>	<b>T157</b>	<b>T158</b>	<b>T159</b>	<b>T162</b>
Quartz	4.0	0.7	0.7	0.7	2.5	3.7	4.9	5.2	8.1	4.7	11.6	16.0	94.3	2.0
Potassium Feldspar	0.5	0.0	0.2	1.5	0.0	0.0	0.0	0.0	0.0	0.0	0.0	0.0	0.0	0.0
Plagioclase	1.7	0.5	1.2	1.5	34.8	36.5	28.4	26.9	0.2	0.0	0.2	0.0	0.0	0.0
Feldspar (undifferentiated)	1.0	1.0	0.2	2.5	0.0	0.0	0.0	0.0	13.1	1.2	1.2	3.5	0.0	0.0
Quartzofeldspathics (undifferentiated)	34.3	36.8	38.8	47.9	0.0	0.0	0.0	0.0	30.4	32.1	34.1	13.6	0.0	61.5
Total (sum of above)	41.5	39.0	41.2	54.1	37.3	40.2	33.3	32.1	51.9	38.0	47.2	33.1	94.3	63.5
Actinolite	0.0	0.0	0.0	0.0	0.0	0.0	0.0	0.0	0.0	0.0	0.0	0.0	0.0	0.0
Augite	0.0	0.0	0.0	0.0	0.0	0.0	0.5	0.0	0.0	0.0	0.0	0.0	0.0	0.0
Biotite	0.0	0.0	0.0	15.1	3.2	23.7	21.2	37.5	0.2	0.0	0.0	0.0	0.0	2.7
Carbonates	9.6	6.2	0.7	0.5	17.0	12.1	12.3	18.3	5.4	13.3	18.3	9.1	1.0	1.0
Chalcopyrite	0.0	0.0	0.0	0.0	0.0	0.0	0.0	0.0	0.0	0.0	0.0	0.0	0.0	0.0
Chlorite	13.3	19.5	29.4	24.7	38.5	19.5	28.4	1.5	18.8	10.1	2.5	1.5	0.7	0.2
Chloritoid	0.0	0.0	0.0	0.5	0.0	0.0	0.0	1.2	2.5	2.5	0.0	1.0	0.0	0.0
Epidote	0.0	0.0	0.0	0.0	0.0	0.0	0.2	0.0	0.0	0.0	0.0	0.0	0.0	0.0
Fuchsite	0.0	0.0	0.0	0.0	0.0	0.0	0.0	0.0	0.0	0.0	0.0	0.0	0.0	0.0
Grunerite	0.0	0.0	0.0	0.0	0.0	0.0	0.0	0.0	0.0	0.0	0.0	0.0	0.0	0.0
Hematite	0.0	0.0	0.0	0.0	0.0	0.0	0.0	0.0	0.0	0.0	0.0	0.0	0.0	0.0
Hornblende	0.0	0.0	0.0	0.0	0.0	0.0	0.5	0.0	0.0	0.0	0.0	0.0	0.0	0.0
Ilmenite	0.5	1.7	1.7	2.0	0.0	0.2	0.0	0.0	2.2	1.2	1.0	2.0	0.0	0.0
Magnetite	0.0	0.0	0.0	0.0	2.2	2.5	1.7	0.0	0.0	0.0	0.0	0.0	0.0	0.0
Orthopyroxene	0.0	0.0	0.0	0.0	0.0	0.0	0.2	0.0	0.0	0.0	0.0	0.0	0.0	0.0
Pyrite	2.0	1.5	0.0	0.2	0.0	0.5	0.2	5.9	0.0	0.5	11.1	4.2	0.0	3.0
Pyrrhotite	0.0	0.0	0.0	0.0	0.2	0.5	0.5	0.0	0.0	1.0	0.0	0.0	0.0	0.0
Rutile	0.0	0.0	0.0	0.0	0.0	0.2	0.0	1.0	0.0	0.0	0.0	0.0	0.0	0.2
White Mica	31.4	31.9	26.2	3.0	1.5	0.5	0.7	2.2	19.0	33.3	20.0	49.1	4.0	29.4
Titanite	0.5	0.0	0.5	0.0	0.0	0.0	0.0	0.2	0.0	0.0	0.0	0.0	0.0	0.0
Tourmaline	1.2	0.0	0.2	0.0	0.0	0.0	0.0	0.0	0.0	0.0	0.0	0.0	0.0	0.0
Zircon	0.0	0.2	0.0	0.0	0.0	0.0	0.0	0.0	0.0	0.0	0.0	0.0	0.0	0.0



<b>Mineral(s)</b>	<b>T164</b>	<b>T182</b>	<b>T184</b>	<b>T186</b>	<b>T187</b>	<b>T188</b>	<b>T192</b>	<b>T193</b>	<b>T194</b>	<b>T195</b>	<b>T196</b>	<b>T215</b>	<b>T239</b>	<b>T241</b>
Quartz	2.0	26.9	0.2	3.5	93.1	12.8	22.0	42.7	31.4	38.0	77.5	6.9	0.7	0.0
Potassium Feldspar	0.0	0.0	0.0	0.0	0.0	0.0	1.5	1.7	1.5	0.5	0.2	0.0	0.0	0.0
Plagioclase	0.5	3.2	1.2	1.5	0.0	0.0	49.4	36.5	28.9	23.2	2.2	82.2	39.0	27.7
Feldspar (undifferentiated)	3.7	0.0	5.9	3.0	0.0	0.0	0.0	0.0	0.0	0.0	0.0	0.0	0.0	1.0
Quartzofeldspathics (undifferentiated)	56.3	0.0	59.0	39.5	0.2	33.6	0.0	0.0	0.0	0.0	0.0	0.0	0.0	40.5
Total (sum of above)	62.5	30.1	66.4	47.4	93.3	46.4	72.8	81.0	61.7	61.7	80.0	89.1	39.8	69.1
Actinolite	0.0	4.0	0.0	0.0	0.0	0.0	0.0	0.0	0.0	0.0	0.0	0.0	0.0	0.0
Augite	0.0	0.2	0.0	0.0	0.0	0.0	0.2	0.0	0.0	0.0	0.0	0.0	0.0	0.0
Biotite	16.5	0.0	0.0	0.0	0.0	0.0	7.2	6.4	15.1	1.7	0.2	0.0	0.0	3.2
Carbonates	0.2	7.2	8.9	28.1	1.0	12.6	2.5	0.7	4.4	7.2	3.7	6.2	35.6	9.4
Chalcopyrite	0.0	0.0	0.0	0.0	0.0	0.0	0.0	0.0	0.0	0.0	0.0	0.0	0.0	0.0
Chlorite	1.7	35.8	13.6	5.7	0.2	0.2	8.9	2.5	2.0	0.2	0.2	1.0	20.5	12.3
Chloritoid	0.0	0.0	0.2	0.0	0.0	0.2	0.0	0.0	0.7	2.2	0.0	0.0	0.0	0.0
Epidote	1.0	16.0	0.0	0.0	0.0	0.0	2.7	0.2	0.5	0.2	0.2	0.0	0.0	0.5
Fuchsite	0.2	0.0	0.0	0.0	0.0	0.0	0.0	0.0	0.0	0.0	0.0	0.0	0.0	0.0
Grunerite	0.0	0.0	0.0	0.0	0.0	0.0	0.0	0.0	0.0	0.0	0.0	0.0	0.0	2.0
Hematite	0.0	0.0	0.0	0.0	0.0	0.0	0.0	0.0	0.0	0.0	0.0	2.5	0.0	0.0
Hornblende	0.0	2.5	0.0	0.0	0.0	0.0	0.0	0.0	0.0	0.0	0.0	0.0	0.0	0.0
Ilmenite	0.2	0.0	0.2	0.5	0.0	0.2	0.0	0.0	0.2	0.0	0.0	0.0	0.0	0.2
Magnetite	0.7	0.0	0.0	0.0	0.0	0.0	0.0	0.0	0.0	0.0	0.0	0.5	0.0	0.2
Orthopyroxene	0.0	0.2	0.0	0.0	0.0	0.0	0.2	0.0	0.0	0.0	0.0	0.0	0.0	0.0
Pyrite	0.0	0.0	0.0	0.2	0.5	3.2	0.2	0.0	0.0	3.2	3.0	0.0	0.0	0.0
Pyrrhotite	0.0	0.0	0.0	0.0	0.0	0.0	0.0	0.0	0.2	0.0	0.2	0.0	0.0	1.0
Rutile	0.0	0.0	0.5	1.2	0.0	1.5	0.2	0.0	0.0	0.0	0.0	0.0	1.0	0.5
White Mica	16.8	0.0	8.6	16.8	4.9	35.3	4.9	9.1	15.1	23.2	12.1	0.2	2.5	1.5
Titanite	0.0	4.0	1.0	0.0	0.0	0.0	0.0	0.0	0.0	0.0	0.0	0.2	0.5	0.0
Tourmaline	0.0	0.0	0.5	0.0	0.0	0.2	0.0	0.0	0.0	0.0	0.0	0.0	0.0	0.0
Zircon	0.0	0.0	0.0	0.0	0.0	0.0	0.0	0.0	0.0	0.2	0.2	0.2	0.2	0.0

## **Appendix F**

### **SEM-MLA mineral modal proportion data**

SEM-MLA data below is from the Bruneau Centre's SEM-MLA Research Lab (Memorial University). All values are in area percent. Methods are outlined in Section 3.5.

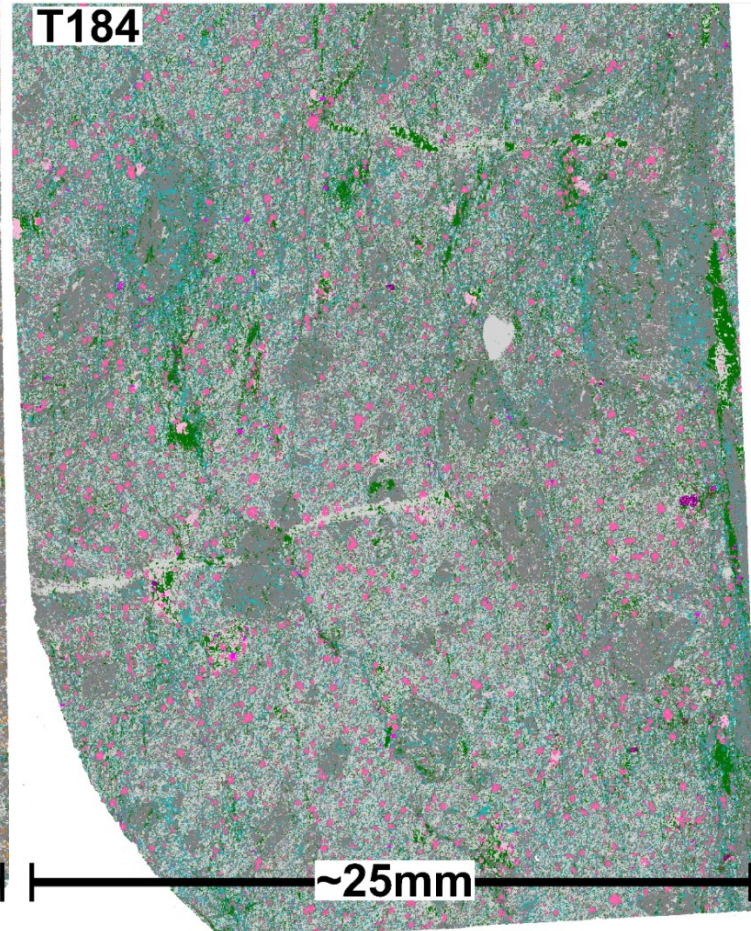
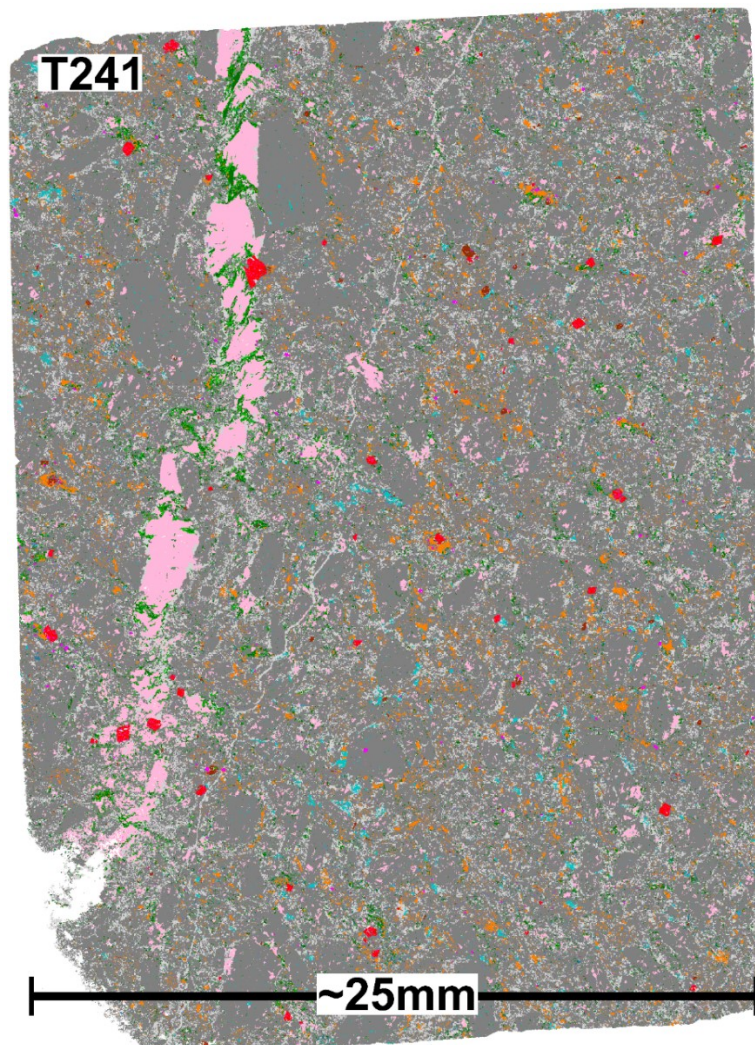
	<b>T184</b>	<b>T186</b>	<b>T186A</b>	<b>T188</b>	<b>T241</b>
<b>Ankerite</b>	4.13	8.42	7.68	7.40	0.09
<b>Apatite</b>	0.34	0.27	0.24	0.27	0.14
<b>Arsenopyrite</b>	0.00	0.00	0.00	0.00	0.00
<b>Biotite</b>	0.11	0.05	0.08	0.05	3.56
<b>Calcite</b>	0.58	1.87	0.84	0.27	5.80
<b>Chalcopyrite</b>	0.00	0.00	0.03	0.04	0.00
<b>Chlorite-Fe</b>	11.46	7.46	7.27	0.50	2.39
<b>Clinopyroxene (Fe-Mg)</b>	0.00	0.04	0.02	0.03	0.00
<b>Dolomite</b>	0.00	0.00	0.01	0.03	0.00
<b>Epidote</b>	0.28	0.85	0.61	0.37	1.25
<b>Galena</b>	0.00	0.00	0.00	0.00	0.00
<b>Garnet</b>	0.00	0.00	0.00	0.00	0.00
<b>Gold</b>	0.00	0.00	0.00	0.00	0.00
<b>Graphite</b>	0.00	0.00	0.00	0.00	0.01
<b>Grunerite</b>	0.00	0.00	0.00	0.00	0.30
<b>Hornblende</b>	0.01	0.09	0.07	0.02	0.21
<b>Illite</b>	1.65	1.41	1.31	0.25	0.54
<b>Ilmenite</b>	0.28	0.20	0.19	0.00	0.36
<b>Iron Oxide</b>	0.00	0.00	0.00	0.00	0.28
<b>Magnesite</b>	0.00	0.00	0.00	0.00	0.00
<b>Monazite-(Ce)</b>	0.00	0.00	0.00	0.00	0.00
<b>Muscovite</b>	7.26	9.12	7.46	29.94	0.93
<b>Orthoclase</b>	0.10	0.22	0.10	0.64	0.00
<b>Plagioclase</b>	43.73	33.23	37.33	3.45	69.81
<b>Pyrite</b>	0.00	0.05	0.77	2.26	0.00
<b>Pyrolusite</b>	0.00	0.00	0.00	0.00	0.00
<b>Pyrrhotite</b>	0.00	0.01	0.02	0.04	0.00
<b>Quartz</b>	29.84	36.48	35.76	54.28	14.15
<b>Rutile</b>	0.18	0.15	0.14	0.14	0.00
<b>Scheelite</b>	0.00	0.00	0.00	0.01	0.00
<b>Serpentine</b>	0.00	0.00	0.00	0.00	0.00
<b>Siderite</b>	0.00	0.00	0.00	0.00	0.13
<b>Sphalerite</b>	0.00	0.00	0.00	0.00	0.00
<b>Sylvanite</b>	0.00	0.00	0.00	0.00	0.00

	<b>T184</b>	<b>T186</b>	<b>T186A</b>	<b>T188</b>	<b>T241</b>
<b>Talc</b>	0.00	0.00	0.00	0.00	0.00
<b>Titanite</b>	0.01	0.01	0.01	0.00	0.00
<b>Tourmaline</b>	0.02	0.06	0.03	0.00	0.05
<b>Xenotime-(Y)</b>	0.00	0.00	0.00	0.00	0.00
<b>Zircon</b>	0.00	0.00	0.00	0.00	0.00
<b>Unknown</b>	0.00	0.00	0.00	0.00	0.00
<b>Low_Counts</b>	0.00	0.00	0.00	0.00	0.00
<b>No_XRay</b>	0.00	0.00	0.00	0.00	0.00
<b>Total</b>	100.00	100.00	100.00	100.00	100.00

## **Appendix G**

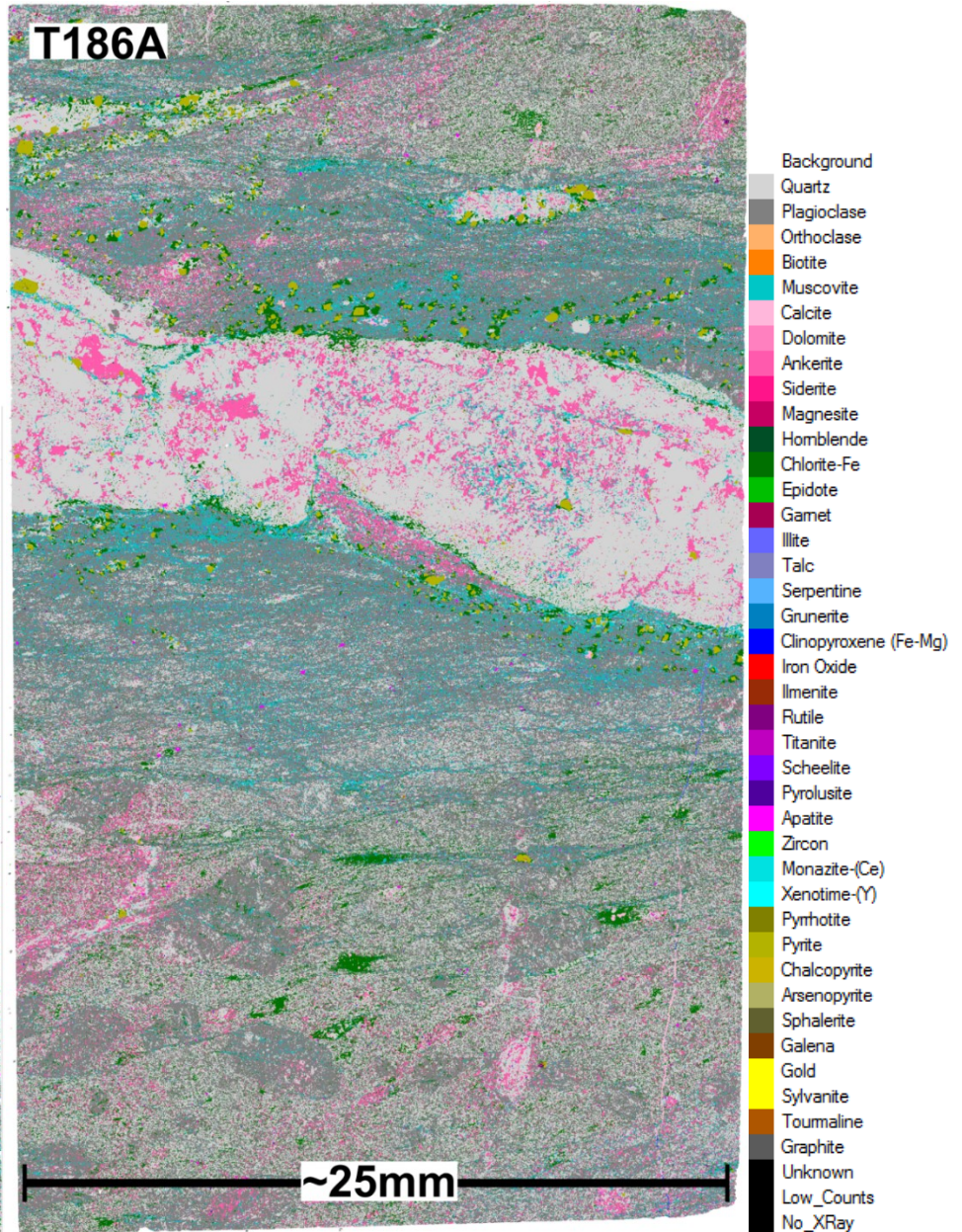
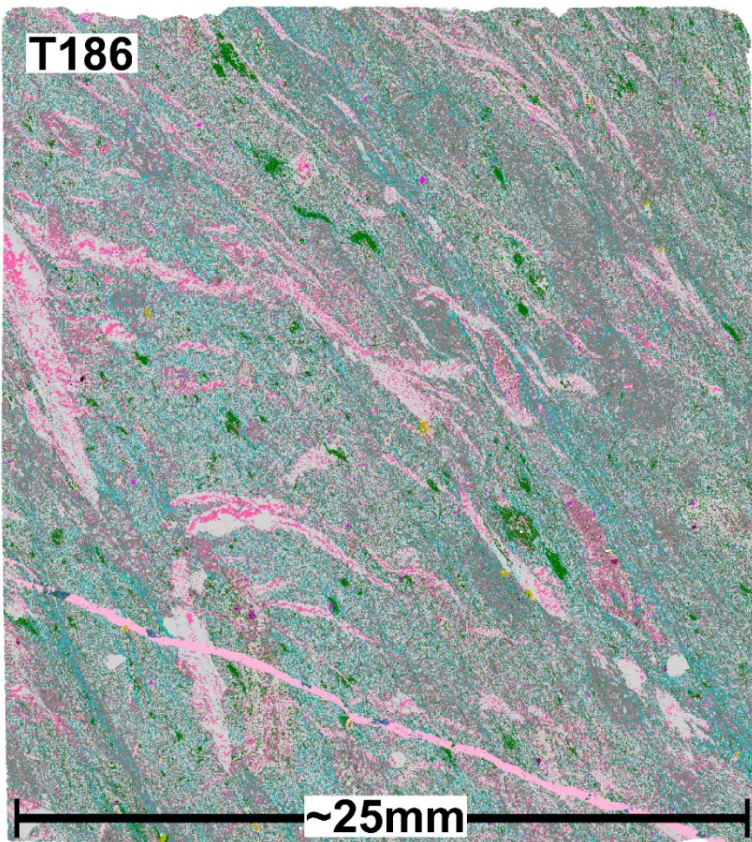
### **SEM-MLA thin section maps with false colours for minerals**

Thin section maps/images are from the Bruneau Centre's SEM-MLA Research Lab (Memorial University). These images were modified for this thesis by adding an approximate scale and sample numbers and are displayed below. Methods are outlined in Section 3.5.



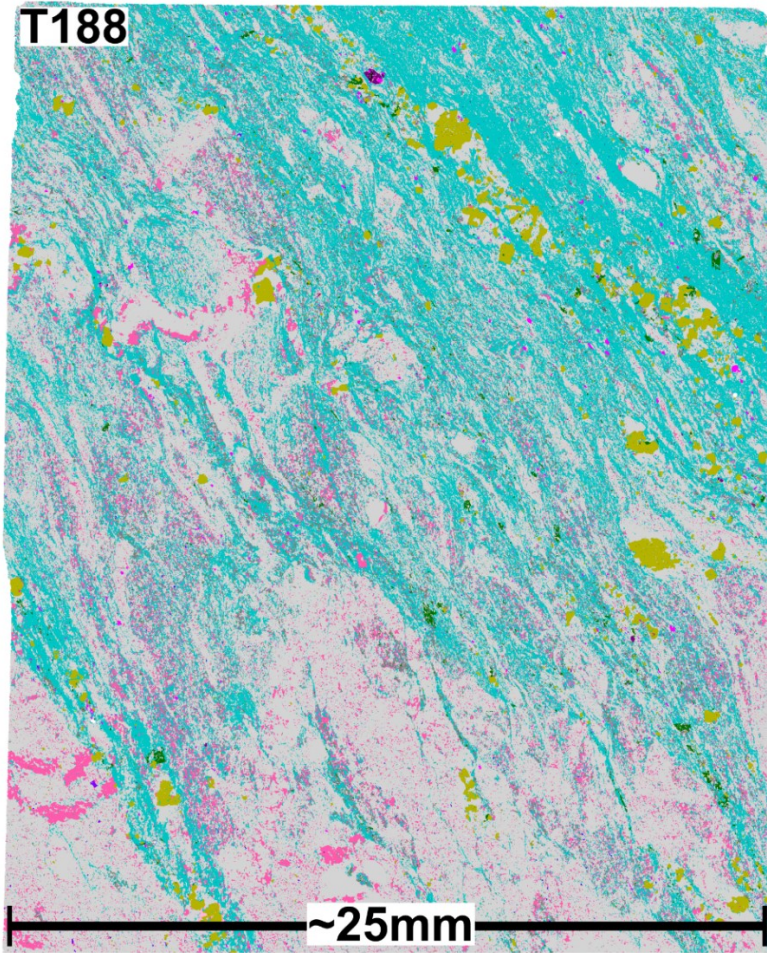
- Background
- Quartz
- Plagioclase
- Orthoclase
- Biotite
- Muscovite
- Calcite
- Dolomite
- Ankerite
- Siderite
- Magnesite
- Homblende
- Chlorite-Fe
- Epidote
- Gamet
- Illite
- Talc
- Serpentine
- Grunerite
- Clinopyroxene (Fe-Mg)
- Iron Oxide
- Ilmenite
- Rutile
- Titanite
- Scheelite
- Pyrolusite
- Apatite
- Zircon
- Monazite-(Ce)
- Xenotime-(Y)
- Pyrrhotite
- Pyrite
- Chalcopyrite
- Arsenopyrite
- Sphalerite
- Galena
- Gold
- Sylvanite
- Toumaline
- Graphite
- Unknown
- Low\_Counts
- No\_XRay







T188



- Background
- Quartz
- Plagioclase
- Orthoclase
- Biotite
- Muscovite
- Calcite
- Dolomite
- Ankerite
- Siderite
- Magnesite
- Hornblende
- Chlorite-Fe
- Epidote
- Garnet
- Illite
- Talc
- Serpentine
- Grunerite
- Clinopyroxene (Fe-Mg)
- Iron Oxide
- Ilmenite
- Rutile
- Titanite
- Scheelite
- Pyrolusite
- Apatite
- Zircon
- Monazite-(Ce)
- Xenotime-(Y)
- Pyrrhotite
- Pyrite
- Chalcopyrite
- Arsenopyrite
- Sphalerite
- Galena
- Gold
- Sylvanite
- Tourmaline
- Graphite
- Unknown
- Low\_Counts
- No\_XRay



## **Appendix H**

### **Electron microprobe data and mineral formulae**

Mineral chemical composition data in mass percent (determined via electron microprobe) is from Western University's Earth and Planetary Materials Analysis Lab. Other results in this appendix including mineral formulae and mineral endmember proportions are calculated based on this data. Not detected is abbreviated "nd". Methodology for electron microprobe analyses and other calculations pertaining to data in this appendix are summarized in Sections 3.6 and 4.3.

Biotite	Mass Percent											Total
	Al <sub>2</sub> O <sub>3</sub>	CaO	Cl	F	FeO	K <sub>2</sub> O	MgO	MnO	Na <sub>2</sub> O	SiO <sub>2</sub>	TiO <sub>2</sub>	
T139_bt_06	18.147	nd	0.177	0.12	21.73	9.292	8.352	0.074	0.44	34.77	1.752	94.765
T139_bt_07	18.388	nd	0.131	0.127	21.82	9.784	8.444	0.057	0.091	35.24	1.791	95.789
T139_bt_08	18.21	0.013	0.277	0.231	22.32	9.844	8.349	0.07	0.104	35.17	1.777	96.210
T139_bt_09	18.144	nd	0.252	0.407	21.86	9.347	8.299	0.079	0.389	34.88	1.753	95.184
T139_bt_10	18.085	nd	0.397	0.213	22.23	9.663	8.277	0.073	0.279	35.48	1.77	96.282
T139_bt_11	18.371	nd	0.198	0.241	21.86	9.618	8.701	0.077	0.175	35.55	1.758	96.408
T139_bt_35	18.222	nd	0.132	0.222	21.9	9.787	8.704	0.075	0.085	35.37	1.801	96.170
T139_bt_36	18.41	nd	0.06	0.326	22.08	9.556	8.776	0.055	0.094	34.9	1.74	95.844
T139_bt_37	17.734	nd	0.407	0.223	22.91	9.259	8.322	0.062	0.118	34.62	1.741	95.214
T139_bt_38	18.084	nd	0.231	0.295	22.3	9.8	8.575	0.06	0.085	35.39	1.777	96.411
T141_bt_01	18.241	nd	0.182	0.299	20.82	9.635	8.949	0.097	0.085	35.21	1.675	95.032
T141_bt_02	18.199	nd	0.252	0.082	21.87	9.594	8.633	0.075	0.086	34.94	1.988	95.622
T141_bt_03	17.647	nd	0.166	0.121	21.13	9.395	9.027	0.134	0.132	35.31	1.804	94.778
T141_bt_04	18.263	nd	0.221	0.015	21.41	9.745	9.008	0.11	0.1	35.77	1.749	96.335
T141_bt_05	18.13	nd	0.107	0.113	21.23	9.679	8.943	0.103	0.175	35.36	1.747	95.519
T141_bt_06	17.689	nd	0.213	0.191	21.47	9.669	9.152	0.113	0.094	35.46	1.659	95.586
T141_bt_07	17.768	0.035	0.434	0.301	21.89	9.587	8.596	0.09	0.169	35.2	1.892	95.744
T141_bt_25	18.133	nd	0.215	0.047	21.04	9.577	8.802	0.11	0.113	35.81	1.901	95.676
T141_bt_26	18.244	nd	0.22	0.077	21.2	9.691	8.961	0.096	0.103	35.33	1.772	95.614
T141_bt_27	17.869	nd	0.113	0.073	21.32	9.483	8.935	0.091	0.152	35.23	1.685	94.895
T192_bt_05	17.726	nd	0.031	0.366	21.13	9.782	9.058	0.093	0.104	35.21	1.789	95.130
T192_bt_06	17.466	nd	0.03	0.55	20.89	9.658	9.126	0.102	0.181	35.52	1.844	95.125
T192_bt_07	17.666	nd	0.037	0.236	21.18	9.833	9.138	0.116	0.104	35.39	1.833	95.420
T192_bt_08	17.623	nd	0.037	0.323	21.5	9.769	9.023	0.098	0.094	35.4	1.87	95.595
T192_bt_32	17.498	nd	0.029	0.267	21.29	9.672	8.934	0.116	0.077	35.57	1.868	95.201
T192_bt_33	17.504	nd	0.035	0.483	21.23	9.737	8.888	0.111	0.122	35.24	1.89	95.025
T192_bt_34	17.432	nd	0.036	0.319	21.33	9.867	8.992	0.123	0.067	35.4	1.853	95.275
T192_bt_35	17.842	nd	0.031	0.482	20.41	9.769	9.031	0.101	0.128	35.42	1.928	94.926

Biotite	Mass Percent											Total
	Al <sub>2</sub> O <sub>3</sub>	CaO	Cl	F	FeO	K <sub>2</sub> O	MgO	MnO	Na <sub>2</sub> O	SiO <sub>2</sub>	TiO <sub>2</sub>	
T195_bt_07	17.753	nd	0.044	0.994	13.13	9.798	14.98	0.08	0.156	37.31	1.279	95.099
T195_bt_11	17.959	0.021	0.036	1.115	13.23	9.808	14.58	0.067	0.19	37.67	1.335	95.531
T195_bt_12	17.896	nd	0.04	1.01	13.18	9.772	14.92	0.072	0.159	37.36	1.344	95.325
T195_bt_14	17.967	0.041	0.033	1.07	13.18	9.775	14.9	0.062	0.214	37.6	1.237	95.620
T195_bt_38	18.015	0.013	0.048	1.207	13.64	9.419	14.83	0.088	0.21	37.36	1.271	95.578
T195_bt_39	17.93	0.024	0.038	1.123	13.64	9.045	15.27	0.078	0.142	37.19	1.302	95.300

**Atoms per Formula Unit (22 oxygen basis)**

<b>Biotite</b>	<b>Al<sup>IV</sup></b>	<b>Al<sup>VI</sup></b>	<b>Ca</b>	<b>Cl</b>	<b>F</b>	<b>Fe<sup>2+</sup></b>	<b>K</b>	<b>Mg</b>	<b>Mn</b>	<b>Na</b>	<b>OH</b>	<b>Si</b>	<b>Ti</b>	<b>Total</b>	<b>Fe/(Fe+Mg)</b>
T139_bt_06	2.587	0.744	0.000	0.047	0.059	2.830	1.845	1.939	0.010	0.133	3.894	5.413	0.205	19.705	0.593
T139_bt_07	2.575	0.762	0.000	0.034	0.062	2.809	1.921	1.938	0.007	0.027	3.904	5.425	0.207	19.673	0.592
T139_bt_08	2.580	0.727	0.002	0.072	0.113	2.876	1.935	1.918	0.009	0.031	3.815	5.420	0.206	19.704	0.600
T139_bt_09	2.578	0.746	0.000	0.066	0.200	2.842	1.853	1.923	0.010	0.117	3.734	5.422	0.205	19.696	0.596
T139_bt_10	2.542	0.737	0.000	0.104	0.104	2.859	1.896	1.898	0.010	0.083	3.793	5.458	0.205	19.688	0.601
T139_bt_11	2.563	0.749	0.000	0.051	0.117	2.796	1.876	1.984	0.010	0.052	3.832	5.437	0.202	19.669	0.585
T139_bt_35	2.571	0.725	0.000	0.034	0.108	2.810	1.916	1.991	0.010	0.025	3.858	5.429	0.208	19.686	0.585
T139_bt_36	2.621	0.723	0.000	0.016	0.159	2.846	1.879	2.016	0.007	0.028	3.825	5.379	0.202	19.701	0.585
T139_bt_37	2.593	0.672	0.000	0.108	0.110	2.993	1.845	1.938	0.008	0.036	3.782	5.407	0.205	19.696	0.607
T139_bt_38	2.565	0.709	0.000	0.060	0.143	2.864	1.920	1.963	0.008	0.025	3.797	5.435	0.205	19.695	0.593
T141_bt_01	2.554	0.771	0.000	0.048	0.146	2.693	1.901	2.063	0.013	0.025	3.806	5.446	0.195	19.660	0.566
T141_bt_02	2.605	0.708	0.000	0.066	0.040	2.824	1.890	1.987	0.010	0.026	3.894	5.395	0.231	19.676	0.587
T141_bt_03	2.526	0.699	0.000	0.044	0.059	2.740	1.858	2.086	0.018	0.040	3.897	5.474	0.210	19.652	0.568
T141_bt_04	2.543	0.741	0.000	0.057	0.007	2.732	1.896	2.049	0.014	0.030	3.936	5.457	0.201	19.663	0.571
T141_bt_05	2.557	0.732	0.000	0.028	0.055	2.734	1.900	2.052	0.013	0.052	3.917	5.443	0.202	19.686	0.571
T141_bt_06	2.531	0.685	0.000	0.056	0.093	2.769	1.902	2.104	0.015	0.028	3.851	5.469	0.192	19.696	0.568
T141_bt_07	2.553	0.688	0.006	0.114	0.147	2.833	1.892	1.983	0.012	0.051	3.739	5.447	0.220	19.684	0.588
T141_bt_25	2.513	0.763	0.000	0.056	0.023	2.696	1.872	2.011	0.014	0.034	3.921	5.487	0.219	19.609	0.573
T141_bt_26	2.565	0.742	0.000	0.057	0.037	2.727	1.901	2.055	0.013	0.031	3.905	5.435	0.205	19.673	0.570
T141_bt_27	2.542	0.721	0.000	0.030	0.036	2.762	1.874	2.063	0.012	0.046	3.935	5.458	0.196	19.674	0.572
T192_bt_05	2.546	0.689	0.000	0.008	0.179	2.737	1.932	2.091	0.012	0.031	3.813	5.454	0.208	19.702	0.567
T192_bt_06	2.504	0.681	0.000	0.008	0.269	2.703	1.906	2.105	0.013	0.054	3.723	5.496	0.215	19.677	0.562
T192_bt_07	2.539	0.674	0.000	0.010	0.115	2.733	1.935	2.102	0.015	0.031	3.875	5.461	0.213	19.703	0.565
T192_bt_08	2.538	0.666	0.000	0.010	0.158	2.774	1.922	2.075	0.013	0.028	3.833	5.462	0.217	19.694	0.572
T192_bt_32	2.503	0.685	0.000	0.008	0.131	2.752	1.907	2.058	0.015	0.023	3.862	5.497	0.217	19.657	0.572
T192_bt_33	2.529	0.674	0.000	0.009	0.237	2.757	1.928	2.057	0.015	0.037	3.754	5.471	0.221	19.689	0.573
T192_bt_34	2.520	0.661	0.000	0.009	0.156	2.761	1.948	2.075	0.016	0.020	3.834	5.480	0.216	19.698	0.571
T192_bt_35	2.522	0.730	0.000	0.008	0.236	2.639	1.927	2.082	0.013	0.038	3.756	5.478	0.224	19.655	0.559

**Atoms per Formula Unit (22 oxygen basis)**

<b>Biotite</b>	<b>Al<sup>IV</sup></b>	<b>Al<sup>VI</sup></b>	<b>Ca</b>	<b>Cl</b>	<b>F</b>	<b>Fe<sup>2+</sup></b>	<b>K</b>	<b>Mg</b>	<b>Mn</b>	<b>Na</b>	<b>OH</b>	<b>Si</b>	<b>Ti</b>	<b>Total</b>	<b>Fe/(Fe+Mg)</b>
<b>T195_bt_07</b>	2.443	0.673	0.000	0.011	0.468	1.636	1.861	3.326	0.010	0.045	3.521	5.557	0.143	19.695	0.330
<b>T195_bt_11</b>	2.417	0.721	0.003	0.009	0.523	1.640	1.854	3.222	0.008	0.055	3.468	5.583	0.149	19.653	0.337
<b>T195_bt_12</b>	2.450	0.683	0.000	0.010	0.475	1.638	1.852	3.305	0.009	0.046	3.515	5.550	0.150	19.682	0.331
<b>T195_bt_14</b>	2.434	0.702	0.007	0.008	0.501	1.632	1.846	3.288	0.008	0.061	3.491	5.566	0.138	19.682	0.332
<b>T195_bt_38</b>	2.457	0.693	0.002	0.012	0.566	1.692	1.782	3.279	0.011	0.060	3.422	5.543	0.142	19.662	0.340
<b>T195_bt_39</b>	2.480	0.658	0.004	0.010	0.527	1.694	1.713	3.379	0.010	0.041	3.463	5.520	0.145	19.643	0.334

Chlorite	Mass Percent											
	Al <sub>2</sub> O <sub>3</sub>	CaO	Cl	F	FeO	K <sub>2</sub> O	MgO	MnO	Na <sub>2</sub> O	SiO <sub>2</sub>	TiO <sub>2</sub>	Total
T139_chl_12	22.908	nd	0.039	0.003	27.367	0.028	12.763	0.125	0.08	24.433	0.062	87.798
T139_chl_13	22.887	0.027	0.03	0.084	27.625	0.011	12.459	0.137	0.052	24.114	0.026	87.410
T139_chl_14	22.589	0.002	0.024	0.065	27.102	0.004	12.407	0.139	0.056	24.196	0.062	86.613
T139_chl_15	22.322	nd	0.035	nd	27.108	0.023	12.793	0.115	0.164	24.615	0.07	87.237
T139_chl_16	22.808	nd	0.02	nd	27.89	0.012	12.422	0.15	0.004	23.956	0.056	87.313
T139_chl_17	23.095	nd	0.022	nd	27.65	0.021	12.451	0.106	0.035	24.028	0.057	87.460
T139_chl_39	22.957	nd	0.047	nd	27.76	0.029	12.453	0.154	0.052	24.299	0.042	87.782
T139_chl_40	22.966	nd	0.012	0.072	27.09	0.017	12.569	0.147	0.048	24.228	0.057	87.173
T139_chl_41	23.819	nd	0.016	nd	27.481	0.03	12.243	0.126	0.026	23.96	0.055	87.752
T139_chl_42	23.068	nd	0.017	nd	26.418	0.093	13.002	0.128	0.01	24.944	0.046	87.722
T141_chl_08	23.164	0.001	0.018	0.085	26.777	0.014	13.019	0.203	0.011	24.261	0.049	87.562
T141_chl_09	22.979	nd	0.033	0.036	26.369	0.05	12.981	0.184	0.02	24.15	0.02	86.799
T141_chl_10	22.207	0.246	0.056	nd	25.189	0.043	13.457	0.179	0.086	25.358	0.088	86.896
T141_chl_11	23.045	0.044	0.041	0.029	25.683	0.113	12.924	0.187	0.104	24.102	0.049	86.300
T141_chl_28	23.084	0.002	0.018	0.032	25.98	0.035	13.162	0.175	0.021	24.373	0.053	86.917
T141_chl_29	22.733	nd	0.015	nd	26.106	0.033	13.493	0.193	0.006	24.596	0.059	87.231
T141_chl_30	23.138	nd	0.012	nd	26.129	0.058	13.165	0.179	0.019	24.146	0.071	86.914
T141_chl_31	22.48	0.015	0.023	0.03	25.414	0.046	13.872	0.207	0.076	25.015	0.058	87.218
T154_chl_06	23.425	0.001	0.069	0.103	31.556	0.046	8.625	0.189	0.1	22.668	0.053	86.776
T154_chl_07	23.512	nd	0.047	nd	31.894	0.042	8.459	0.175	0.098	22.696	0.033	86.945
T154_chl_08	23.666	0.017	0.068	0.006	30.566	0.131	8.391	0.154	0.184	23.03	0.059	86.254
T154_chl_09	23.723	0.098	0.027	0	32.083	0.017	8.365	0.199	0.025	22.785	0.029	87.345
T154_chl_30	23.148	0.005	0.034	nd	31.661	0.022	8.515	0.191	0.08	22.975	0.048	86.671
T154_chl_31	22.598	0.11	0.027	nd	30.934	0.023	8.419	0.184	0.057	23.061	0.058	85.465
T154_chl_32	23.231	0.321	0.025	nd	31.562	0.01	8.386	0.21	0.051	23.068	0.046	86.904
T157_chl_09	23.412	0.004	0.015	nd	25.67	0.011	13.153	0.145	0.002	24.187	0.06	86.656
T157_chl_10	23.433	nd	0.008	0.093	25.638	0.021	13.311	0.124	0.014	24.433	0.119	87.153
T157_chl_11	23.508	nd	0.007	0.07	25.639	0.012	12.907	0.124	0.02	23.984	0.079	86.319

Chlorite	Mass Percent											Total
	Al <sub>2</sub> O <sub>3</sub>	CaO	Cl	F	FeO	K <sub>2</sub> O	MgO	MnO	Na <sub>2</sub> O	SiO <sub>2</sub>	TiO <sub>2</sub>	
T157_chl_12	23.729	nd	0.013	0.111	25.69	0.031	12.754	0.137	0.016	24.263	0.054	86.748
T157_chl_32	23.997	nd	0.025	0.016	25.411	0.047	13.114	0.095	0.097	23.937	0.039	86.766
T157_chl_34	23.599	0.079	0.015	0.08	24.822	0.012	13.752	0.119	0.148	25.05	0.057	87.696
T157_chl_35	23.798	nd	0.013	0.004	24.868	0.005	13.566	0.113	0.005	24.392	0.024	86.783
T192_chl_09	22.067	nd	0.028	0.065	26.986	0.017	12.755	0.222	0.16	24.267	0.047	86.580
T192_chl_10	21.107	0.001	0.008	0.081	26.685	0.017	13.317	0.192	0.057	24.979	0.054	86.462
T192_chl_11	22.504	0.051	0.005	0.062	27.403	0.001	12.442	0.217	nd	24.008	0.071	86.737
T192_chl_12	22.145	nd	0.02	0.109	27.171	0.025	12.893	0.226	0.049	24.419	0.061	87.068
T192_chl_36	22.042	nd	0.012	0.082	26.775	0.009	12.641	0.204	0.049	24.111	0.059	85.947
T192_chl_37	21.219	nd	0.014	0.103	26.751	0.01	13.389	0.226	0.046	25.033	0.074	86.818
T192_chl_38	23.494	0.053	0.012	0.009	26.132	0.012	12.628	0.221	0.016	23.737	0.032	86.340
T195_chl_15	22.417	nd	0.01	0.132	17.464	0.053	19.884	0.159	0.009	26.393	0.039	86.502
T195_chl_16	22.486	0.038	0.013	0.142	17.437	0.017	19.878	0.129	0.026	26.387	0.035	86.525
T195_chl_17	22.655	nd	0.006	0.191	17.328	0.02	20.163	0.13	0.018	26.426	0.065	86.920
T195_chl_18	22.841	0.01	0.008	0.063	17.623	0.007	20.095	0.151	0.038	26.249	0.065	87.122
T195_chl_19	22.505	0.005	0.011	0.169	17.39	0.058	19.816	0.1	0.014	26.076	0.062	86.132
T195_chl_20	23.119	0.004	0.01	0.09	17.784	0.011	19.593	0.149	0.029	25.689	0.067	86.505
T195_chl_21	22.513	0.003	0.008	0.109	17.526	0.044	19.71	0.12	0.045	26.197	0.054	86.281
T195_chl_22	22.874	0.027	0.011	0.125	17.783	0.011	19.628	0.139	0.004	26.251	0.047	86.845
T195_chl_40	22.525	0.04	0.012	0.234	16.899	0.473	19.394	0.149	0.053	27.928	0.13	87.736
T195_chl_41	23.084	nd	0.003	0.196	17.251	0.001	19.829	0.128	nd	25.998	0.049	86.456
T195_chl_42	23.028	0.012	0.033	0.048	17.459	0.022	19.777	0.14	0.038	25.9	0.058	86.487

**Atoms per Formula Unit (28 oxygen basis)**

Chlorite	Al <sup>IV</sup>	Al <sup>VI</sup>	Ca	Cl	F	Fe <sup>2+</sup>	Fe <sup>3+</sup>	K	Mg	Mn	Na	OH	Si	Ti	Total	Total Fe
T139_chl_12	2.814	2.931	0.000	0.028	0.004	4.791	0.068	0.015	4.039	0.022	0.066	15.968	5.186	0.010	35.941	4.858
T139_chl_13	2.852	2.924	0.006	0.022	0.113	4.855	0.077	0.006	3.965	0.025	0.043	15.865	5.148	0.004	35.905	4.932
T139_chl_14	2.801	2.938	0.000	0.017	0.088	4.760	0.110	0.002	3.974	0.025	0.047	15.894	5.199	0.010	35.867	4.870
T139_chl_15	2.747	2.884	0.000	0.025	0.000	4.776	0.063	0.013	4.070	0.021	0.136	15.975	5.253	0.011	35.973	4.839
T139_chl_16	2.858	2.918	0.000	0.015	0.000	4.961	0.045	0.007	3.974	0.027	0.003	15.985	5.142	0.009	35.945	5.006
T139_chl_17	2.865	2.962	0.000	0.016	0.000	4.883	0.059	0.011	3.967	0.019	0.029	15.984	5.135	0.009	35.939	4.942
T139_chl_39	2.828	2.944	0.000	0.034	0.000	4.873	0.069	0.016	3.951	0.028	0.043	15.966	5.172	0.007	35.931	4.942
T139_chl_40	2.832	2.961	0.000	0.009	0.097	4.728	0.104	0.009	3.997	0.027	0.040	15.894	5.168	0.009	35.874	4.833
T139_chl_41	2.909	3.068	0.000	0.012	0.000	4.791	0.092	0.016	3.878	0.023	0.021	15.988	5.091	0.009	35.898	4.883
T139_chl_42	2.742	3.008	0.000	0.012	0.000	4.512	0.145	0.050	4.085	0.023	0.008	15.988	5.258	0.007	35.838	4.657
T141_chl_08	2.857	2.948	0.000	0.013	0.114	4.651	0.096	0.008	4.114	0.036	0.009	15.873	5.143	0.008	35.870	4.747
T141_chl_09	2.838	2.967	0.000	0.024	0.049	4.626	0.088	0.027	4.136	0.033	0.017	15.927	5.162	0.003	35.897	4.714
T141_chl_10	2.636	2.924	0.056	0.040	0.000	4.290	0.167	0.023	4.244	0.032	0.071	15.960	5.364	0.014	35.820	4.456
T141_chl_11	2.836	3.004	0.010	0.030	0.039	4.512	0.090	0.062	4.128	0.034	0.086	15.931	5.164	0.008	35.934	4.602
T141_chl_28	2.815	2.989	0.000	0.013	0.043	4.507	0.115	0.019	4.174	0.032	0.017	15.944	5.185	0.008	35.862	4.622
T141_chl_29	2.778	2.922	0.000	0.011	0.000	4.547	0.089	0.018	4.271	0.035	0.005	15.989	5.222	0.009	35.896	4.636
T141_chl_30	2.849	2.980	0.000	0.009	0.000	4.585	0.077	0.032	4.187	0.032	0.016	15.991	5.151	0.011	35.920	4.662
T141_chl_31	2.717	2.897	0.003	0.016	0.040	4.381	0.108	0.025	4.367	0.037	0.062	15.943	5.283	0.009	35.889	4.489
T154_chl_06	3.009	3.099	0.000	0.052	0.143	5.714	0.097	0.026	2.831	0.035	0.085	15.805	4.991	0.009	35.897	5.811
T154_chl_07	2.993	3.136	0.000	0.035	0.000	5.813	0.071	0.024	2.782	0.033	0.084	15.965	5.007	0.005	35.947	5.884
T154_chl_08	2.931	3.242	0.004	0.051	0.008	5.479	0.148	0.074	2.753	0.029	0.157	15.941	5.069	0.010	35.895	5.627
T154_chl_09	2.995	3.161	0.023	0.020	0.000	5.798	0.096	0.010	2.739	0.037	0.021	15.980	5.005	0.005	35.890	5.894
T154_chl_30	2.925	3.118	0.001	0.025	0.000	5.744	0.105	0.012	2.804	0.036	0.069	15.975	5.075	0.008	35.896	5.849
T154_chl_31	2.850	3.119	0.026	0.020	0.000	5.627	0.151	0.013	2.803	0.035	0.049	15.980	5.150	0.010	35.832	5.777
T154_chl_32	2.919	3.129	0.076	0.019	0.000	5.696	0.118	0.006	2.754	0.039	0.044	15.981	5.081	0.008	35.868	5.814
T157_chl_09	2.846	3.049	0.001	0.011	0.000	4.451	0.124	0.006	4.178	0.026	0.002	15.989	5.154	0.010	35.846	4.575
T157_chl_10	2.840	3.016	0.000	0.006	0.124	4.373	0.155	0.011	4.190	0.022	0.011	15.870	5.160	0.019	35.798	4.528
T157_chl_11	2.876	3.065	0.000	0.005	0.095	4.436	0.145	0.007	4.110	0.022	0.017	15.900	5.124	0.013	35.815	4.581



**Atoms per Formula Unit (28 oxygen basis)**

Chlorite	Al <sup>IV</sup>	Al <sup>VI</sup>	Ca	Cl	F	Fe <sup>2+</sup>	Fe <sup>3+</sup>	K	Mg	Mn	Na	OH	Si	Ti	Total	Total Fe
T157_chl_12	2.856	3.104	0.000	0.009	0.149	4.365	0.190	0.017	4.031	0.025	0.013	15.842	5.144	0.009	35.753	4.555
T157_chl_32	2.916	3.111	0.000	0.018	0.021	4.411	0.103	0.025	4.152	0.017	0.080	15.961	5.084	0.006	35.906	4.514
T157_chl_34	2.779	3.049	0.018	0.011	0.105	4.159	0.168	0.006	4.273	0.021	0.120	15.884	5.221	0.009	35.822	4.327
T157_chl_35	2.842	3.106	0.000	0.009	0.005	4.245	0.152	0.003	4.276	0.020	0.004	15.985	5.158	0.004	35.810	4.398
T192_chl_09	2.777	2.839	0.000	0.020	0.088	4.811	0.046	0.009	4.093	0.040	0.134	15.891	5.223	0.008	35.981	4.858
T192_chl_10	2.632	2.731	0.000	0.006	0.110	4.706	0.089	0.009	4.266	0.035	0.048	15.884	5.368	0.009	35.893	4.796
T192_chl_11	2.829	2.896	0.012	0.004	0.084	4.858	0.078	0.001	3.995	0.040	0.000	15.912	5.171	0.012	35.891	4.936
T192_chl_12	2.777	2.825	0.000	0.015	0.147	4.783	0.078	0.014	4.111	0.041	0.041	15.838	5.223	0.010	35.901	4.860
T192_chl_36	2.778	2.866	0.000	0.009	0.112	4.761	0.088	0.005	4.081	0.037	0.041	15.879	5.222	0.010	35.891	4.850
T192_chl_37	2.645	2.724	0.000	0.010	0.139	4.690	0.096	0.005	4.270	0.041	0.038	15.850	5.355	0.012	35.876	4.786
T192_chl_38	2.899	3.064	0.012	0.009	0.012	4.598	0.098	0.007	4.045	0.040	0.013	15.979	5.101	0.005	35.882	4.696
T195_chl_15	2.633	2.763	0.000	0.007	0.170	2.842	0.128	0.027	6.027	0.027	0.007	15.823	5.367	0.006	35.828	2.970
T195_chl_16	2.639	2.769	0.008	0.009	0.182	2.829	0.134	0.009	6.020	0.022	0.020	15.809	5.361	0.005	35.817	2.963
T195_chl_17	2.664	2.754	0.000	0.004	0.244	2.790	0.136	0.010	6.069	0.022	0.014	15.752	5.336	0.010	35.805	2.926
T195_chl_18	2.686	2.778	0.002	0.005	0.081	2.901	0.082	0.004	6.064	0.026	0.030	15.914	5.314	0.010	35.897	2.984
T195_chl_19	2.677	2.763	0.001	0.008	0.218	2.846	0.123	0.030	6.030	0.017	0.011	15.774	5.323	0.010	35.831	2.969
T195_chl_20	2.755	2.824	0.001	0.007	0.116	2.953	0.083	0.006	5.963	0.026	0.023	15.877	5.245	0.010	35.890	3.037
T195_chl_21	2.654	2.782	0.001	0.006	0.141	2.876	0.115	0.023	5.996	0.021	0.036	15.854	5.346	0.008	35.858	2.991
T195_chl_22	2.676	2.814	0.006	0.008	0.160	2.879	0.137	0.006	5.934	0.024	0.003	15.832	5.324	0.007	35.809	3.016
T195_chl_40	2.464	2.853	0.008	0.008	0.293	2.528	0.273	0.239	5.731	0.025	0.041	15.699	5.536	0.019	35.719	2.802
T195_chl_41	2.724	2.825	0.000	0.002	0.252	2.781	0.147	0.001	5.999	0.022	0.000	15.746	5.276	0.007	35.782	2.928
T195_chl_42	2.720	2.829	0.003	0.023	0.062	2.888	0.088	0.011	6.010	0.024	0.030	15.915	5.280	0.009	35.893	2.977

	Mass Percent											
White Mica	Al <sub>2</sub> O <sub>3</sub>	CaO	Cl	F	FeO	K <sub>2</sub> O	MgO	MnO	Na <sub>2</sub> O	SiO <sub>2</sub>	TiO <sub>2</sub>	Total
T139_wm_01	33.139	0.236	nd	0.079	3.01	10.23	0.999	0.009	1.121	47.385	0.145	96.320
T139_wm_02	33.803	0.047	0.01	0.094	3.188	10.393	1.012	0.003	0.97	48.032	0.287	97.797
T139_wm_03	33.862	0.062	0.007	nd	3.342	10.779	1.009	0.007	0.534	45.87	0.237	95.707
T139_wm_04	33.149	0.044	0.009	0.039	3.441	10.802	1.152	0.004	0.472	46.755	0.384	96.233
T139_wm_05	33.941	0	nd	0.082	3.231	10.906	1.149	0.01	0.456	46.666	0.377	96.783
T139_wm_33	33.806	0.044	0.002	nd	3.204	10.968	1.137	nd	0.431	46.418	0.175	96.185
T139_wm_34	33.719	nd	0.011	0.193	3.343	10.711	0.897	0.008	0.542	46.142	0.284	95.766
T154_wm_01	36.874	0.024	0.006	0.033	1.942	9.534	0.297	0.017	1.266	46.004	0.144	96.126
T154_wm_02	37.548	0.186	0.028	0.033	1.754	8.997	0.224	0.012	1.558	45.456	0.148	95.924
T154_wm_03	36.37	0.128	0.017	0.12	2.062	9.236	0.333	nd	1.306	45.393	0.17	95.081
T154_wm_04	38.26	0.684	0.01	0.011	1.643	8.35	0.202	0.002	1.619	44.665	0.168	95.607
T154_wm_05	36.522	0.025	0.011	0.117	2.086	9.661	0.319	nd	1.237	45.809	0.175	95.910
T154_wm_25	36.717	0.02	0.004	0.009	1.921	9.368	0.259	0.004	1.355	44.894	0.162	94.708
T154_wm_26	36.928	0.028	0.004	0.043	2.102	9.353	0.231	nd	1.316	44.985	0.184	95.155
T154_wm_27	36.722	0.019	0	0.211	2.169	9.644	0.322	0.008	1.178	45.577	0.181	95.942
T154_wm_28	36.93	0.037	0.006	nd	2.103	9.408	0.281	0.013	1.372	45.699	0.16	96.008
T154_wm_29	36.936	0.114	0.001	nd	1.876	9.266	0.263	nd	1.466	45.518	0.15	95.590
T157_wm_01	36.062	0.062	0.002	0.214	1.927	10.116	0.685	0.008	0.996	46.619	0.301	96.901
T157_wm_02	36.391	0.005	0.002	0.17	1.692	9.76	0.493	nd	1.163	45.577	0.296	95.477
T157_wm_03	36.147	nd	0.001	0.208	1.787	9.799	0.517	0.004	1.279	45.141	0.274	95.069
T157_wm_04	36.389	0.004	0.007	0.16	1.926	9.923	0.498	0.002	1.095	45.592	0.278	95.805
T157_wm_05	36.476	0.112	0.011	0.163	1.823	9.929	0.54	nd	1.043	46.534	0.309	96.869
T157_wm_06	36.355	0.011	0.005	0.065	1.805	9.735	0.541	0.001	1.222	46.042	0.308	96.062
T157_wm_07	36.775	0.035	nd	0.163	1.522	9.632	0.422	0.008	1.307	45.588	0.265	95.648
T157_wm_08	37.101	0.007	0.004	0.146	1.736	9.837	0.361	nd	1.235	45.542	0.257	96.164
T157_wm_27	36.968	0.028	0.003	0.111	1.442	9.519	0.465	0	1.339	45.936	0.304	96.068
T157_wm_28	36.076	0.01	0.001	0.175	1.498	9.766	0.728	nd	1.151	46.682	0.194	96.207

<b>T157_wm_29</b>	36.547	0.013	nd	0.159	1.884	9.898	0.558	0.014	1.158	46.067	0.343	96.574
<b>T157_wm_30</b>	36.352	0.138	0.002	0.213	1.989	9.922	0.615	0.008	1.136	46.338	0.272	96.895
<b>T157_wm_31</b>	36.914	0.028	nd	nd	1.652	9.707	0.42	nd	1.263	45.796	0.264	96.044
<b>T192_wm_01</b>	34.365	0.136	0.005	0.083	2.858	10.799	0.844	0.025	0.44	45.177	0.058	94.754
<b>T192_wm_02</b>	33.132	0.591	0.003	0.063	3.072	10.672	0.92	0.02	0.387	45.428	0.036	94.297
<b>T192_wm_03</b>	36.022	0.023	0	0.162	2.628	10.807	0.479	nd	0.545	45.174	0.076	95.848
<b>T192_wm_04</b>	34.908	0.043	nd	0.296	2.75	10.701	0.565	0.014	0.537	44.669	0.13	94.488
<b>T192_wm_29</b>	34.154	0.037	0.009	0.054	3.194	10.537	0.831	0	0.553	45.118	0.107	94.569
<b>T192_wm_30</b>	34.976	0.069	0.005	0.061	2.702	10.694	0.708	nd	0.516	45.637	0.105	95.446
<b>T192_wm_31</b>	34.366	0.003	nd	0.152	3.022	10.635	0.767	0.008	0.453	44.904	0.144	94.390
<b>T195_wm_01</b>	36.215	nd	0.001	0.152	1.267	10.72	0.885	nd	0.633	46.09	0.12	96.019
<b>T195_wm_02</b>	35.439	nd	0.002	0.181	1.652	10.797	1.098	0.017	0.586	46.149	0.42	96.264
<b>T195_wm_03</b>	35.007	0.005	0.004	0.045	1.597	10.816	1.176	nd	0.555	46.255	0.462	95.902
<b>T195_wm_04</b>	36.252	0.004	0.005	0.096	1.503	10.686	0.871	0.007	0.677	45.794	0.239	96.092
<b>T195_wm_06</b>	35.761	nd	0.002	0.125	1.573	10.831	0.963	nd	0.624	45.7	0.272	95.798
<b>T195_wm_23</b>	36.207	0.017	nd	0.015	1.455	10.705	0.829	nd	0.635	45.936	0.188	95.981
<b>T195_wm_24</b>	35.365	0.001	0.004	0.038	1.603	10.627	1.038	nd	0.607	45.921	0.959	96.146
<b>T195_wm_36</b>	35.899	0.01	0.003	0.074	1.587	10.712	0.904	0.015	0.576	45.858	0.181	95.787
<b>T195_wm_37</b>	35.362	0.011	0.01	0.188	1.552	10.659	1.051	0.019	0.667	45.671	0.393	95.502

White Mica	Atoms per Formula Unit (11 oxygen basis)										MMF Endmember Proportions (%)		
	Al	Ca	Fe <sup>2+</sup>	H	K	Mg	Mn	Na	Si	Ti	Muscovite	Mg-celadonite	Fe-celadonite
T139_wm_01	2.597	0.017	0.167	2	0.868	0.099	0.001	0.145	3.150	0.007	86.4	5.0	8.5
T139_wm_02	2.608	0.003	0.175	2	0.868	0.099	0.000	0.123	3.144	0.014	86.2	5.0	8.8
T139_wm_03	2.681	0.004	0.188	2	0.924	0.101	0.000	0.070	3.082	0.012	86.4	4.8	8.8
T139_wm_04	2.610	0.003	0.192	2	0.920	0.115	0.000	0.061	3.123	0.019	85.1	5.6	9.3
T139_wm_05	2.655	0.000	0.179	2	0.923	0.114	0.001	0.059	3.097	0.019	86.0	5.4	8.5
T139_wm_33	2.661	0.003	0.179	2	0.935	0.113	0.000	0.056	3.100	0.009	86.0	5.4	8.6
T139_wm_34	2.668	0.000	0.188	2	0.918	0.090	0.000	0.071	3.098	0.014	86.7	4.3	9.0
T154_wm_01	2.865	0.002	0.107	2	0.802	0.029	0.001	0.162	3.033	0.007	93.4	1.4	5.2
T154_wm_02	2.919	0.013	0.097	2	0.757	0.022	0.001	0.199	2.998	0.007	94.4	1.0	4.6
T154_wm_03	2.860	0.009	0.115	2	0.786	0.033	0.000	0.169	3.029	0.009	92.9	1.6	5.5
T154_wm_04	2.979	0.048	0.091	2	0.704	0.020	0.000	0.207	2.950	0.008	95.0	0.9	4.1
T154_wm_05	2.851	0.002	0.116	2	0.816	0.032	0.000	0.159	3.035	0.009	92.9	1.5	5.6
T154_wm_25	2.898	0.001	0.108	2	0.800	0.026	0.000	0.176	3.007	0.008	93.7	1.2	5.1
T154_wm_26	2.903	0.002	0.117	2	0.796	0.023	0.000	0.170	3.001	0.009	93.4	1.1	5.5
T154_wm_27	2.869	0.001	0.120	2	0.815	0.032	0.000	0.151	3.021	0.009	92.8	1.5	5.7
T154_wm_28	2.876	0.003	0.116	2	0.793	0.028	0.001	0.176	3.019	0.008	93.2	1.3	5.5
T154_wm_29	2.885	0.008	0.104	2	0.783	0.026	0.000	0.188	3.017	0.007	93.8	1.2	5.0
T157_wm_01	2.790	0.004	0.106	2	0.847	0.067	0.000	0.127	3.060	0.015	91.6	3.3	5.2
T157_wm_02	2.852	0.000	0.094	2	0.828	0.049	0.000	0.150	3.030	0.015	93.1	2.3	4.5
T157_wm_03	2.851	0.000	0.100	2	0.837	0.052	0.000	0.166	3.021	0.014	92.8	2.4	4.7
T157_wm_04	2.847	0.000	0.107	2	0.840	0.049	0.000	0.141	3.027	0.014	92.6	2.3	5.1
T157_wm_05	2.818	0.008	0.100	2	0.830	0.053	0.000	0.133	3.050	0.015	92.6	2.6	4.9
T157_wm_06	2.830	0.001	0.100	2	0.820	0.053	0.000	0.156	3.041	0.015	92.6	2.6	4.8
T157_wm_07	2.873	0.002	0.084	2	0.815	0.042	0.000	0.168	3.022	0.013	93.9	2.0	4.1
T157_wm_08	2.888	0.000	0.096	2	0.829	0.036	0.000	0.158	3.008	0.013	93.8	1.7	4.5
T157_wm_27	2.870	0.002	0.079	2	0.800	0.046	0.000	0.171	3.026	0.015	94.0	2.2	3.8
T157_wm_28	2.798	0.001	0.082	2	0.820	0.071	0.000	0.147	3.073	0.010	92.3	3.6	4.1
T157_wm_29	2.835	0.001	0.104	2	0.831	0.055	0.001	0.148	3.032	0.017	92.4	2.6	5.0

White Mica	Atoms per Formula Unit (11 oxygen basis)										MMF Endmember Proportions (%)		
	Al	Ca	Fe <sup>2+</sup>	H	K	Mg	Mn	Na	Si	Ti	Muscovite	Mg-celadonite	Fe-celadonite
T157_wm_30	2.813	0.010	0.109	2	0.831	0.060	0.000	0.145	3.043	0.013	91.9	2.9	5.2
T157_wm_31	2.871	0.002	0.091	2	0.817	0.041	0.000	0.162	3.022	0.013	93.7	2.0	4.4
T192_wm_01	2.745	0.010	0.162	2	0.934	0.085	0.001	0.058	3.061	0.003	88.4	4.0	7.6
T192_wm_02	2.664	0.043	0.175	2	0.929	0.094	0.001	0.051	3.099	0.002	87.0	4.5	8.5
T192_wm_03	2.839	0.002	0.147	2	0.922	0.048	0.000	0.071	3.021	0.004	91.0	2.2	6.8
T192_wm_04	2.797	0.003	0.156	2	0.928	0.057	0.001	0.071	3.037	0.007	90.0	2.7	7.3
T192_wm_29	2.734	0.003	0.181	2	0.913	0.084	0.000	0.073	3.064	0.005	87.6	3.9	8.5
T192_wm_30	2.765	0.005	0.152	2	0.915	0.071	0.000	0.067	3.061	0.005	89.4	3.4	7.2
T192_wm_31	2.756	0.000	0.172	2	0.923	0.078	0.000	0.060	3.055	0.007	88.3	3.6	8.0
T195_wm_01	2.825	0.000	0.070	2	0.905	0.087	0.000	0.081	3.050	0.006	92.3	4.2	3.4
T195_wm_02	2.767	0.000	0.092	2	0.912	0.108	0.001	0.075	3.057	0.021	90.4	5.2	4.4
T195_wm_03	2.740	0.000	0.089	2	0.916	0.116	0.000	0.071	3.072	0.023	90.0	5.6	4.3
T195_wm_04	2.830	0.000	0.083	2	0.903	0.086	0.000	0.087	3.033	0.012	92.0	4.1	4.0
T195_wm_06	2.805	0.000	0.088	2	0.920	0.096	0.000	0.081	3.041	0.014	91.3	4.5	4.2
T195_wm_23	2.826	0.001	0.081	2	0.905	0.082	0.000	0.082	3.043	0.009	92.2	3.9	3.9
T195_wm_24	2.761	0.000	0.089	2	0.898	0.103	0.000	0.078	3.042	0.048	90.9	4.9	4.2
T195_wm_36	2.811	0.001	0.088	2	0.908	0.090	0.001	0.074	3.047	0.009	91.5	4.3	4.2
T195_wm_37	2.782	0.001	0.087	2	0.908	0.105	0.001	0.086	3.049	0.020	90.9	5.0	4.1

Plagioclase	Mass Percent											Total
	Al <sub>2</sub> O <sub>3</sub>	CaO	Cl	F	FeO	K <sub>2</sub> O	MgO	MnO	Na <sub>2</sub> O	SiO <sub>2</sub>	TiO <sub>2</sub>	
T139_plag_23	26.025	7.147	0.001	nd	0.162	0.055	0.01	0.016	7.683	60.448	0.013	101.560
T139_plag_24	22.487	3.194	0.005	0.051	0.179	0.035	0.002	0.002	9.806	65.013	nd	100.751
T139_plag_25	26.04	7.241	0	0.002	0.251	0.053	0.005	0.013	7.501	59.729	nd	100.834
T139_plag_26	21.984	2.633	nd	nd	0.305	0.034	0.021	nd	10.224	65.667	nd	100.868
T139_plag_49	27.168	8.254	0.002	nd	0.386	0.208	0.001	0.013	6.667	57.792	nd	100.491
T139_plag_50	21.868	2.427	0.003	0.011	0.328	0.053	nd	0.01	10.371	65.828	0.04	100.934
T139_plag_51	25.045	6.08	0	nd	0.211	0.047	0.005	nd	8.253	61.029	0	100.670
T139_plag_52	23.771	4.589	0.001	0.098	0.192	0.05	nd	nd	9.145	63.417	0.017	101.239
T141_plag_17	24.723	5.967	0	0.079	0.235	0.052	0.014	nd	8.105	60.732	nd	99.874
T141_plag_18	24.917	6.064	0	nd	0.13	0.057	nd	nd	8.148	61.031	0.024	100.371
T141_plag_19	24.461	5.74	0.001	nd	0.159	0.067	nd	0.01	8.481	60.971	nd	99.890
T141_plag_20	24.392	5.737	0	nd	0.196	0.058	nd	nd	8.446	61.407	0.012	100.248
T141_plag_35	24.412	5.481	0.008	nd	0.103	0.349	0.003	0.016	8.276	61.279	nd	99.925
T141_plag_36	24.859	6.013	0.004	0.115	0.078	0.061	nd	nd	8.254	60.982	nd	100.317
T141_plag_37	24.282	5.589	0.002	0.054	0.132	0.07	nd	nd	8.53	61.438	0.007	100.081
T154_plag_16	24.934	6.285	0.001	0.018	0.048	0.039	0	0.009	8.033	60.865	0.008	100.232
T154_plag_17	26.589	7.663	0.006	nd	0.123	0.096	0.005	0.014	7.13	58.556	nd	100.181
T154_plag_18	27.631	7.612	0.006	0.087	0.118	0.106	0.002	nd	7.018	57.199	nd	99.741
T154_plag_19	25.052	6.538	0	0.036	0.138	0.043	nd	0.005	7.966	60.614	nd	100.377
T154_plag_20	25.765	7.321	0.005	0.018	0.138	0.036	0.004	0.005	7.324	59.134	0.01	99.751
T154_plag_35	25.887	7.309	0.004	nd	0.135	0.027	0.007	0.014	7.348	58.606	0.009	99.345
T154_plag_36	28.052	7.849	0.004	nd	0.068	0.047	nd	nd	6.709	56.667	0.015	99.410
T154_plag_37	25.812	7.352	nd	0.02	0.085	0.026	0.003	0.015	7.349	59.453	0.02	100.127
T154_plag_38	25.801	7.516	0.002	nd	0.06	0.026	nd	0.006	7.176	59.248	0.018	99.853
T154_plag_39	25.968	7.542	0	nd	0.334	0.032	0.008	0.001	7.267	59.178	nd	100.330
T154_plag_40	25.811	7.35	0.004	nd	0.119	0.054	nd	0.001	7.338	59.098	0.011	99.785
T157_plag_13	23.952	5.095	nd	0.089	0.051	0.051	nd	nd	8.717	62.19	nd	100.108
T157_plag_14	24.726	5.911	0.003	0.018	0.12	0.047	nd	0.013	8.285	61.1	0.001	100.216

<b>T157_plag_15</b>	23.257	4.391	0	nd	0.073	0.044	0	nd	9.179	63.26	0.001	100.205
<b>T157_plag_16</b>	23.118	4.118	nd	nd	0.039	0.039	nd	nd	9.367	63.881	0.008	100.570
<b>T157_plag_17</b>	25.471	6.89	0.002	0.033	0.05	0.044	nd	nd	7.661	60.105	0.004	100.246
<b>T157_plag_36</b>	23.468	4.407	0.005	0.061	0.278	0.036	0.002	0.008	9.185	63.124	0.012	100.559
<b>T157_plag_37</b>	23.789	4.855	nd	0.081	0.232	0.021	0.005	0.011	8.913	62.751	nd	100.624
<b>T157_plag_38</b>	25.272	6.559	0.002	nd	0.059	0.028	0.013	nd	7.959	61.145	nd	101.037
<b>T157_plag_39</b>	23.096	3.859	0.001	nd	0.067	0.027	nd	0.011	9.546	64.284	nd	100.891
<b>T192_plag_20</b>	22.959	4.066	0.001	0.024	0.029	0.057	0.004	0.014	9.294	63.421	0.002	99.861
<b>T192_plag_21</b>	19.875	1.142	0.018	0.021	0.041	0.105	0.002	0.022	11.215	67.207	nd	99.635
<b>T192_plag_22</b>	23.932	5.267	nd	0.114	0.019	0.044	nd	0.008	8.649	62.116	nd	100.101
<b>T192_plag_23</b>	19.791	0.52	nd	0.118	0.026	0.029	0.001	nd	11.418	67.904	nd	99.757
<b>T192_plag_24</b>	24.479	5.954	nd	0.07	0.021	0.047	0.007	0.004	8.185	61.014	0.003	99.755
<b>T192_plag_41</b>	23.393	4.564	0.004	nd	0.01	0.052	nd	nd	8.932	62.6	nd	99.554
<b>T192_plag_42</b>	22.161	3.269	0.003	0.047	nd	0.039	nd	0.005	9.668	64.155	nd	99.327
<b>T192_plag_43</b>	24.006	5.309	0.003	0.007	0.031	0.054	0.003	0.006	8.436	61.676	nd	99.527
<b>T192_plag_44</b>	22.053	3.097	0.001	0.061	0.029	0.054	nd	0.016	9.644	64.545	0.007	99.481
<b>T195_plag_24</b>	25.813	7.309	nd	0.005	0.05	0.055	0.004	0.015	7.41	59.748	nd	100.407
<b>T195_plag_25</b>	25.99	7.49	0.003	nd	0.036	0.06	0.003	nd	7.207	59.636	nd	100.424
<b>T195_plag_26</b>	25.313	6.857	0.03	0.004	0.036	0.061	0.006	nd	7.574	60.104	nd	99.977
<b>T195_plag_27</b>	24.717	5.939	0.003	0.008	0.091	0.046	0.024	0.002	8.023	61.331	nd	100.180
<b>T195_plag_28</b>	25.969	7.596	0.001	nd	0.027	0.054	nd	0.013	7.26	59.235	nd	100.155
<b>T195_plag_43</b>	26.166	7.676	nd	nd	0.039	0.059	nd	0.011	7.019	58.981	nd	99.951
<b>T195_plag_44</b>	22.363	3.131	nd	0.013	0.03	0.055	nd	nd	9.758	65.021	0.002	100.368
<b>T195_plag_45</b>	26.045	7.625	nd	nd	nd	0.053	nd	0.012	7.152	59.457	nd	100.344
<b>T195_plag_46</b>	27.787	9.392	nd	nd	0.108	0.174	0.114	0.001	6.064	56.85	0.01	100.500

Plagioclase	Atoms per Formula Unit (8 oxygen basis)										An-Ab-Or Endmember Proportions (%)		
	Al	Ca	Fe <sup>2+</sup>	Fe <sup>3+</sup>	K	Mg	Mn	Na	Si	Ti	Anorthite	Albite	Orthoclase
T139_plag_23	1.346	0.336	0.004	0.002	0.003	0.001	0.001	0.654	2.653	0.000	33.848	65.842	0.310
T139_plag_24	1.161	0.150	0.007	0.000	0.002	0.000	0.000	0.833	2.848	0.000	15.224	84.577	0.199
T139_plag_25	1.358	0.343	0.007	0.002	0.003	0.000	0.000	0.643	2.642	0.000	34.683	65.015	0.302
T139_plag_26	1.131	0.123	0.009	0.002	0.002	0.001	0.000	0.865	2.866	0.000	12.435	87.374	0.191
T139_plag_49	1.427	0.394	0.010	0.005	0.012	0.000	0.000	0.576	2.576	0.000	40.134	58.661	1.204
T139_plag_50	1.124	0.113	0.000	0.012	0.003	0.000	0.000	0.877	2.870	0.001	11.417	88.286	0.297
T139_plag_51	1.303	0.287	0.000	0.008	0.003	0.000	0.000	0.706	2.693	0.000	28.856	70.878	0.266
T139_plag_52	1.225	0.215	0.005	0.002	0.003	0.000	0.000	0.776	2.774	0.001	21.649	78.070	0.281
T141_plag_17	1.298	0.285	0.009	0.000	0.003	0.001	0.000	0.700	2.705	0.000	28.833	70.868	0.299
T141_plag_18	1.301	0.288	0.005	0.000	0.003	0.000	0.000	0.700	2.703	0.001	29.048	70.627	0.325
T141_plag_19	1.280	0.273	0.000	0.006	0.004	0.000	0.000	0.730	2.707	0.000	27.118	72.505	0.377
T141_plag_20	1.273	0.272	0.000	0.007	0.003	0.000	0.000	0.725	2.719	0.000	27.203	72.469	0.327
T141_plag_35	1.279	0.261	0.000	0.004	0.020	0.000	0.001	0.713	2.723	0.000	26.260	71.750	1.991
T141_plag_36	1.298	0.285	0.000	0.003	0.003	0.000	0.000	0.709	2.701	0.000	28.604	71.051	0.345
T141_plag_37	1.269	0.265	0.000	0.005	0.004	0.000	0.000	0.733	2.724	0.000	26.478	73.127	0.395
T154_plag_16	1.304	0.299	0.002	0.000	0.002	0.000	0.000	0.691	2.701	0.000	30.119	69.659	0.223
T154_plag_17	1.397	0.366	0.000	0.005	0.005	0.000	0.001	0.616	2.610	0.000	37.056	62.391	0.553
T154_plag_18	1.457	0.365	0.000	0.004	0.006	0.000	0.000	0.609	2.559	0.000	37.245	62.137	0.618
T154_plag_19	1.309	0.311	0.004	0.001	0.002	0.000	0.000	0.685	2.688	0.000	31.127	68.629	0.244
T154_plag_20	1.359	0.351	0.005	0.000	0.002	0.000	0.000	0.636	2.646	0.000	35.510	64.283	0.208
T154_plag_35	1.370	0.352	0.000	0.005	0.002	0.000	0.001	0.640	2.631	0.000	35.416	64.428	0.156
T154_plag_36	1.486	0.378	0.000	0.003	0.003	0.000	0.000	0.584	2.546	0.001	39.156	60.564	0.279
T154_plag_37	1.356	0.351	0.003	0.000	0.001	0.000	0.001	0.635	2.651	0.001	35.549	64.301	0.150
T154_plag_38	1.361	0.360	0.002	0.000	0.001	0.000	0.000	0.623	2.652	0.001	36.606	63.243	0.151
T154_plag_39	1.363	0.360	0.012	0.000	0.002	0.001	0.000	0.627	2.635	0.000	36.382	63.434	0.184
T154_plag_40	1.360	0.352	0.004	0.000	0.003	0.000	0.000	0.636	2.643	0.000	35.520	64.170	0.311
T157_plag_13	1.250	0.242	0.002	0.000	0.003	0.000	0.000	0.749	2.755	0.000	24.344	75.366	0.290
T157_plag_14	1.292	0.281	0.000	0.004	0.003	0.000	0.000	0.712	2.708	0.000	28.203	71.530	0.267



Plagioclase	Atoms per Formula Unit (8 oxygen basis)										An-Ab-Or Endmember Proportions (%)		
	Al	Ca	Fe <sup>2+</sup>	Fe <sup>3+</sup>	K	Mg	Mn	Na	Si	Ti	Anorthite	Albite	Orthoclase
T157_plag_15	1.210	0.208	0.003	0.000	0.002	0.000	0.000	0.785	2.792	0.000	20.857	78.895	0.249
T157_plag_16	1.197	0.194	0.001	0.000	0.002	0.000	0.000	0.798	2.807	0.000	19.503	80.277	0.220
T157_plag_17	1.335	0.328	0.002	0.000	0.002	0.000	0.000	0.660	2.672	0.000	33.116	66.632	0.252
T157_plag_36	1.217	0.208	0.000	0.010	0.002	0.000	0.000	0.784	2.778	0.000	20.915	78.881	0.203
T157_plag_37	1.235	0.229	0.009	0.000	0.001	0.000	0.000	0.761	2.764	0.000	23.110	76.771	0.119
T157_plag_38	1.312	0.310	0.002	0.000	0.002	0.001	0.000	0.680	2.694	0.000	31.241	68.600	0.159
T157_plag_39	1.191	0.181	0.002	0.000	0.002	0.000	0.000	0.810	2.813	0.000	18.233	81.615	0.152
T192_plag_20	1.198	0.193	0.001	0.000	0.003	0.000	0.001	0.798	2.807	0.000	19.406	80.270	0.324
T192_plag_21	1.029	0.054	0.000	0.002	0.006	0.000	0.001	0.955	2.953	0.000	5.297	94.124	0.580
T192_plag_22	1.250	0.250	0.001	0.000	0.002	0.000	0.000	0.743	2.753	0.000	25.117	74.634	0.250
T192_plag_23	1.023	0.024	0.001	0.000	0.002	0.000	0.000	0.971	2.979	0.000	2.451	97.386	0.163
T192_plag_24	1.286	0.284	0.001	0.000	0.003	0.000	0.000	0.707	2.719	0.000	28.596	71.135	0.269
T192_plag_41	1.226	0.217	0.000	0.000	0.003	0.000	0.000	0.770	2.783	0.000	21.954	77.748	0.298
T192_plag_42	1.160	0.156	0.000	0.000	0.002	0.000	0.000	0.833	2.849	0.000	15.709	84.068	0.223
T192_plag_43	1.262	0.254	0.001	0.000	0.003	0.000	0.000	0.729	2.751	0.000	25.724	73.965	0.312
T192_plag_44	1.153	0.147	0.001	0.000	0.003	0.000	0.001	0.830	2.864	0.000	15.025	84.663	0.312
T195_plag_24	1.352	0.348	0.002	0.000	0.003	0.000	0.001	0.639	2.655	0.000	35.168	64.517	0.315
T195_plag_25	1.363	0.357	0.001	0.000	0.003	0.000	0.000	0.622	2.653	0.000	36.354	63.299	0.347
T195_plag_26	1.331	0.328	0.001	0.000	0.003	0.000	0.000	0.655	2.681	0.000	33.230	66.418	0.352
T195_plag_27	1.294	0.283	0.003	0.000	0.003	0.002	0.000	0.691	2.725	0.000	28.954	70.779	0.267
T195_plag_28	1.364	0.363	0.001	0.000	0.003	0.000	0.000	0.628	2.641	0.000	36.523	63.167	0.309
T195_plag_43	1.380	0.368	0.001	0.000	0.003	0.000	0.000	0.609	2.639	0.000	37.540	62.116	0.344
T195_plag_44	1.159	0.147	0.001	0.000	0.003	0.000	0.000	0.832	2.858	0.000	15.014	84.672	0.314
T195_plag_45	1.367	0.364	0.000	0.000	0.003	0.000	0.000	0.618	2.648	0.000	36.961	62.733	0.306
T195_plag_46	1.463	0.450	0.004	0.000	0.010	0.008	0.000	0.525	2.540	0.000	45.654	53.339	1.007

Carbonates	Mass Percent												Total
	Al <sub>2</sub> O <sub>3</sub>	CaO	Cl	CO <sub>2</sub>	F	FeO	K <sub>2</sub> O	MgO	MnO	Na <sub>2</sub> O	SiO <sub>2</sub>	TiO <sub>2</sub>	
T139_carb_28	0.03	52.043	0.005	43.764	0.406	2.131	0.011	0.953	0.661	nd	0.05	nd	99.882
T139_carb_29	0.011	52.319	nd	44.067	0.035	2.027	nd	0.963	0.641	nd	0.015	nd	100.063
T139_carb_30	0.01	52.057	0.006	43.966	0.071	2.285	nd	1.014	0.678	nd	nd	nd	100.056
T139_carb_31	0.012	52.414	0.006	44.155	nd	2.141	0.002	0.945	0.668	nd	0.033	0.003	100.378
T139_carb_32	nd	52.177	0.004	43.51	0.53	2.122	nd	0.896	0.687	0.019	0.018	0.04	99.779
T139_carb_53	0.006	52.658	nd	43.732	nd	2.161	nd	0.967	0.662	nd	0.002	0.01	100.198
T139_carb_54	nd	52.381	0.002	43.759	0.224	2.099	nd	0.979	0.619	nd	0.003	0.004	99.975
T139_carb_55	0.009	52.084	0.003	43.894	0.042	2.133	0.005	1.025	0.697	0.019	0.075	0.014	99.982
T141_carb_21	0.035	53.243	0.001	43.093	0.224	1.809	0.002	0.793	0.736	0.013	0.045	0.006	99.905
T141_carb_22	0.008	52.98	0.002	44.556	nd	1.603	nd	0.709	0.648	0.019	0.004	nd	100.529
T141_carb_23	0.036	53.165	0.001	43.479	0.18	1.649	nd	0.746	0.715	0.002	0	0.03	99.927
T141_carb_24	0.018	52.911	0.004	43.959	nd	1.649	0.026	0.724	0.727	0.022	nd	0.016	100.055
T141_carb_38	0.031	52.272	0.004	44.599	nd	1.711	0.009	0.774	0.669	0.033	0.024	nd	100.125
T141_carb_39	0.037	52.791	nd	44.118	nd	1.614	0.002	0.834	0.707	0.005	0.012	nd	100.120
T141_carb_40	0.015	52.969	0.001	43.773	0.182	1.497	0.047	0.705	0.771	nd	0.033	0.028	99.944
T141_carb_41	0.016	52.568	nd	44.207	nd	1.682	0.02	0.765	0.807	0.029	0.028	0.01	100.132
T154_carb_21	nd	54.61	0.001	43.94	0.06	0.42	0.009	0.437	0.389	0.043	0.054	0.042	99.980
T154_carb_22	nd	56.737	0.004	42.577	0.181	0.153	0.006	0.116	0.153	0.022	0.06	0.007	99.939
T154_carb_23	0.027	52.121	nd	44.509	nd	2.063	0.017	0.497	0.777	nd	0.075	0.021	100.107
T154_carb_24	0.121	54.394	0.009	43.801	nd	0.706	0.024	0.438	0.438	0.03	0.143	0.027	100.129
T154_carb_41	0.006	55.602	0.001	43.492	0.007	0.233	0.001	0.257	0.347	0.041	0.045	nd	100.029
T154_carb_42	0.136	56.109	0.01	42.998	0.021	0.216	nd	0.168	0.165	nd	0.189	nd	100.001
T154_carb_43	0.055	55.585	0.002	43.614	nd	0.114	0.012	0.145	0.363	0.013	0.083	0.022	100.008
T154_carb_44	0.02	56.39	0.007	42.811	0.321	0.169	0.005	0.055	0.187	0.05	0.03	nd	99.908
T157_carb_18	nd	51.915	0.001	43.711	0.693	2.042	0.017	0.986	0.671	0.02	nd	0.003	99.767
T157_carb_19	0.007	51.906	nd	44.341	0.15	2.001	0.014	0.923	0.614	0.001	0.05	nd	99.944
T157_carb_20	0.031	51.581	0.004	44.976	nd	1.966	0.019	0.921	0.584	0.037	0.032	0	100.150
T157_carb_21	0.023	29.838	0	44.396	nd	11.534	0.029	12.741	1.45	0.027	0.183	0.021	100.242

Carbonates	Mass Percent												Total
	Al <sub>2</sub> O <sub>3</sub>	CaO	Cl	CO <sub>2</sub>	F	FeO	K <sub>2</sub> O	MgO	MnO	Na <sub>2</sub> O	SiO <sub>2</sub>	TiO <sub>2</sub>	
T157_carb_22	nd	52.452	nd	43.737	0.318	1.933	0.042	0.893	0.517	0.017	0.11	0.015	99.900
T157_carb_23	0.018	29.563	nd	44.192	nd	12.579	0.002	12.547	1.144	nd	0.02	nd	100.065
T157_carb_24	0.079	29.757	0.009	43.493	0.348	11.935	0.044	12.667	1.368	0.069	0.186	0.047	99.853
T157_carb_25	0.045	30.329	nd	43.581	nd	12.361	0.011	12.517	1.143	0.021	0.099	0.024	100.131
T157_carb_26	0.165	29.69	0.005	43.539	nd	12.383	0.005	12.477	1.335	0.104	0.373	0.036	100.111
T157_carb_40	0.01	52.427	0.008	43.765	0.084	2.042	nd	0.975	0.717	0.002	0.016	nd	100.009
T157_carb_41	0.009	52.283	nd	44.178	nd	1.969	0.002	0.956	0.617	0.031	0.062	nd	100.107
T157_carb_42	0.027	52.379	0.007	43.882	nd	1.991	nd	0.941	0.709	0.047	0.108	nd	100.089
T157_carb_43	0.014	52.231	nd	44.275	nd	2.125	0.005	0.918	0.563	0.01	0.052	nd	100.193
T157_carb_44	0.051	30.206	nd	44.177	nd	13.087	0.011	11.49	1.139	0.011	0.048	0.01	100.230
T192_carb_25	0.008	53.4	0.001	44.257	nd	1.182	0.007	0.466	0.662	0.034	0.061	0.028	100.106
T192_carb_26	0.001	53.078	0.009	44.39	0.186	1.18	0.006	0.492	0.605	0.022	0.061	nd	99.950
T192_carb_27	0.013	53.85	0.006	43.616	0.095	1.272	0.008	0.503	0.556	0.022	0.049	0.011	99.960
T192_carb_27	0.02	53.705	nd	43.557	0.357	1.261	0	0.525	0.64	nd	nd	nd	99.915
T192_carb_28	0.303	53.12	0.004	43.194	0.55	1.322	nd	0.449	0.602	0.01	0.494	nd	99.816
T192_carb_45	0.017	53.705	nd	43.937	0.093	1.118	nd	0.531	0.574	0.02	0.035	nd	99.991
T192_carb_46	nd	53.706	0.009	43.965	nd	1.162	0.003	0.571	0.584	0.024	0.062	0.001	100.085
T192_carb_47	0.013	53.351	nd	43.712	0.667	1.164	0.008	0.448	0.541	nd	0.089	0.021	99.733
T192_carb_48	0.032	55.284	nd	42.337	0.273	0.956	0.005	0.461	0.542	nd	0.113	0.002	99.890
T195_carb_29	nd	30.441	0.005	44.731	0.082	9.046	0.004	15.006	0.601	0.043	0.073	nd	99.996
T195_carb_30	0.002	30.65	nd	44.685	nd	9.264	0.006	14.839	0.482	0.013	0.16	nd	100.101
T195_carb_31	2.381	46.131	0.012	38.8	0.272	3.54	0.03	4.147	0.699	nd	3.965	0.048	99.908
T195_carb_32	2.963	44.055	0.022	38.264	nd	4.227	0.041	4.277	0.688	0.028	5.716	0.017	100.293
T195_carb_33	2.717	46.089	0.011	38.69	0.417	3.469	0.038	3.334	0.687	nd	4.606	nd	99.880
T195_carb_34	2.202	47.899	0.008	39.714	0.127	2.958	0.023	2.767	0.655	0.001	3.705	nd	100.004
T195_carb_35	1.486	52.279	0.006	41.028	0.266	0.406	0.203	0.443	0.777	0.176	2.925	0.005	99.887
T195_carb_47	0.685	52.859	0.002	42.914	0.228	0.415	0.137	0.656	0.742	0.026	1.207	0.129	99.904
T195_carb_49	0.04	53.298	0.003	43.41	0.057	1.237	0.173	1.182	0.598	nd	0.043	nd	100.016

**MSC Endmember Proportions (%)**

<b>Carbonates</b>	<b>Magnesite</b>	<b>Siderite</b>	<b>Calcite</b>
T139_carb_28	2.409	3.022	94.568
T139_carb_29	2.425	2.864	94.710
T139_carb_30	2.553	3.228	94.218
T139_carb_31	2.373	3.016	94.610
T139_carb_32	2.263	3.007	94.730
T139_carb_53	2.416	3.029	94.555
T139_carb_54	2.460	2.958	94.582
T139_carb_55	2.585	3.017	94.398
T141_carb_21	1.979	2.532	95.489
T141_carb_22	1.787	2.266	95.948
T141_carb_23	1.871	2.320	95.810
T141_carb_24	1.825	2.331	95.844
T141_carb_38	1.969	2.442	95.588
T141_carb_39	2.102	2.282	95.617
T141_carb_40	1.780	2.120	96.100
T141_carb_41	1.937	2.389	95.673
T154_carb_21	1.095	0.590	98.315
T154_carb_22	0.283	0.209	99.507
T154_carb_23	1.271	2.959	95.771
T154_carb_24	1.097	0.992	97.911
T154_carb_41	0.637	0.324	99.039
T154_carb_42	0.414	0.298	99.288
T154_carb_43	0.361	0.159	99.480
T154_carb_44	0.135	0.233	99.632
T157_carb_18	2.500	2.904	94.596
T157_carb_19	2.346	2.853	94.802
T157_carb_20	2.356	2.821	94.823
T157_carb_21	31.338	15.915	52.747

**MSC Endmember Proportions (%)**

<b>Carbonates</b>	<b>Magnesite</b>	<b>Siderite</b>	<b>Calcite</b>
T157_carb_22	2.251	2.733	95.016
T157_carb_23	30.714	17.274	52.012
T157_carb_24	31.085	16.431	52.484
T157_carb_25	30.344	16.811	52.845
T157_carb_26	30.609	17.042	52.349
T157_carb_40	2.450	2.878	94.672
T157_carb_41	2.412	2.787	94.801
T157_carb_42	2.370	2.813	94.817
T157_carb_43	2.315	3.007	94.678
T157_carb_44	28.341	18.109	53.550
T192_carb_25	1.179	1.678	97.142
T192_carb_26	1.252	1.684	97.064
T192_carb_27	1.260	1.788	96.952
T192_carb_27	1.318	1.776	96.906
T192_carb_28	1.140	1.884	96.976
T192_carb_45	1.336	1.578	97.087
T192_carb_46	1.434	1.637	96.929
T192_carb_47	1.136	1.655	97.209
T192_carb_48	1.132	1.317	97.551
T195_carb_29	35.763	12.094	52.143
T195_carb_30	35.276	12.355	52.369
T195_carb_31	10.555	5.055	84.390
T195_carb_32	11.164	6.190	82.647
T195_carb_33	8.681	5.067	86.252
T195_carb_34	7.122	4.271	88.607
T195_carb_35	1.158	0.596	98.246
T195_carb_47	1.687	0.599	97.714
T195_carb_49	2.942	1.727	95.331

## **Appendix I**

### **Electron microprobe configurations and standards**

Microprobe configurations and standards used during microprobe analysis for this thesis were provided by Marc Beauchamp at Western University's Earth and Planetary Materials Analysis Lab. Methodology for electron microprobe analysis is summarized in Section 3.6.

					Spectrometers				
Carbonates (15 kV accelerating voltage, 5 nA probe current, 25 µm spot size)					1	2	3	4	5
Element	Standard	Standard Details	L-Value	Back+ / Back-	TAP / LDE1	TAP / LDE2	PETJ / LIF	PETH / LIFH	PETL / LIFL
Si	Albite	Amelia Albite - Virginia, USA	77.793	3/6.5	TAP				
Al	Albite	Amelia Albite - Virginia, USA	90.953	3.5/6	TAP				
Ti	Rutile	Synthetic	88.221	3.5/4			PETJ		
Na	Albite	Amelia Albite - Virginia, USA	129.888	3.5/4		TAP			
Ca	Calcite	Smithsonian USNM 136321 - Unknown locality	107.739	2/3			PETJ		
K	Orthoclase	C.M. Taylor, MAD-10 corrected	119.874	2/2.5					PETL
Fe	Siderite	Smithsonian USNM R2460 - Ivigtut, Greenland	134.865	4/5				LIFH	
Mg	Dolomite	Smithsonian USNM 10057 - Oberdorf, Austria	107.842	3.5/5.5		TAP			
Mn	Siderite	Smithsonian USNM R2460 - Ivigtut, Greenland	146.364	4/4				LIFH	
F	Fluorite	Astimex, synthetic Harshaw Chemical Corp, USA	199.724	4.5/5		TAP			
Cl	Sodalite	Geller MicroAnalytical	151.442	2.5/3					PETL

					Spectrometers				
Plagioclase (15 kV accelerating voltage, 20 nA probe current, 5 µm spot size)					1	2	3	4	5
Element	Standard	Standard Details	L-Value	Back+ / Back-	TAP / LDE1	TAP / LDE2	PETJ / LIF	PETH / LIFH	PETL / LIFL
Si	Albite	Amelia Albite - Virginia, USA	77.793	3/6.5	TAP				
Al	Albite	Amelia Albite - Virginia, USA	90.953	3.5/6	TAP				
Ti	Rutile	Synthetic	88.221	3.5/4			PETJ		
Na	Albite	Amelia Albite - Virginia, USA	129.888	3.5/4		TAP			
Ca	Anorthite	Smithsonian USNM 137041, Great Sitkin Island, AL	107.724	2/3			PETJ		
K	Orthoclase	C.M. Taylor, MAD-10 corrected	119.874	2.5/2.5					PETL
Fe	Fayalite	Unknown provenance	134.874	4/5				LIFH	
Mg	Diopside	Smithsonian USNM 117733 - Natural Bridge, NY	107.874	3.5/5.5		TAP			
Mn	Rhodonite	Astimex, unknown locality	146.396	4/4				LIFH	
F	Fluorite	Astimex, synthetic Harshaw Chemical Corp, USA	199.724	4.5/5		TAP			
Cl	Sodalite	Geller MicroAnalytical	151.442	2.5/3					PETL

**White Mica, Biotite, Chlorite, and Epidote (15 kV accelerating voltage, 20 nA probe current, 10 µm spot size)**

**Spectrometers**

Element	Standard	Standard Details	L-Value	Back+ / Back-	Spectrometers				
					1	2	3	4	5
					TAP / LDE1	TAP / LDE2	PETJ / LIF	PETH / LIFH	PETL / LIFL
<b>Si</b>	Hornblende	Smithsonian USNM 143965 - Kakanui, New Zealand	77.793	3/6.5	TAP				
<b>Al</b>	Hornblende	Smithsonian USNM 143965 - Kakanui, New Zealand	90.963	3.5/6	TAP				
<b>Ti</b>	Rutile	Synthetic	88.221	3.5/4			PETJ		
<b>Na</b>	Albite	Amelia Albite - Virginia, USA	129.888	3.5/4		TAP			
<b>Ca</b>	Anorthite	Smithsonian USNM 137041 - Great Sitkin Island, AL	107.724	2/3			PETJ		
<b>K</b>	Orthoclase	C.M. Taylor, MAD-10 corrected	119.874	2.5/2.5					PETL
<b>Fe</b>	Fayalite	Unknown provenance	134.874	4/5				LIFH	
<b>Mg</b>	Diopside	Smithsonian USNM 117733 - Natural Bridge, NY	107.874	3.5/5.5		TAP			
<b>Mn</b>	Rhodonite	Astimex, unknown locality	146.396	4/4				LIFH	
<b>F</b>	Fluorite	Astimex, synthetic Harshaw Chemical Corp, USA	199.724	4.5/5		TAP			
<b>Cl</b>	Sodalite	Geller MicroAnalytical	151.442	2.5/3					PETL



**Appendix J**  
**Density measurements and QA/QC**

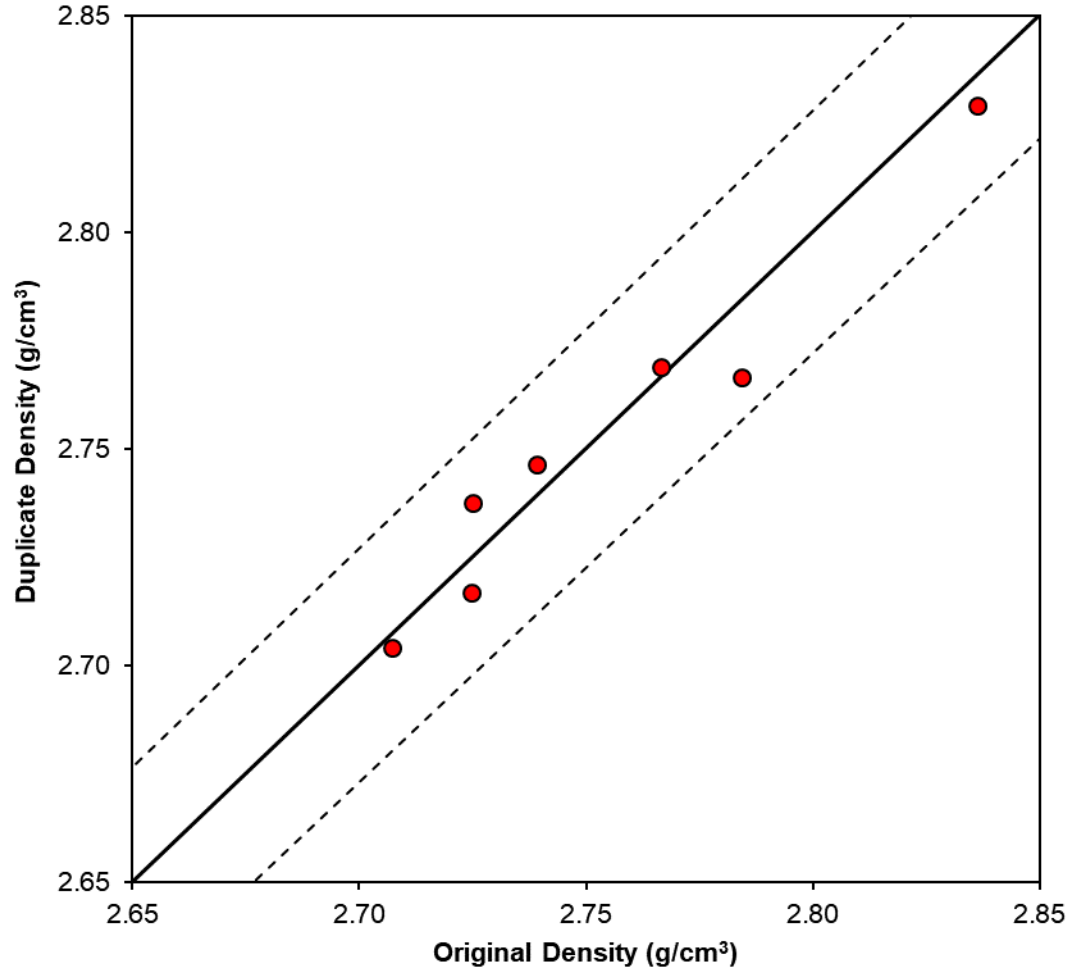
Methods are discussed in Section 3.7.

Sample ID	Density (g/cm <sup>3</sup> )		
	Original	Duplicate	Average
T6	2.754		
T8	2.766		
T11	2.709		
T56	2.797		
T58	2.754		
T59	2.725		
T65	2.743		
T66	2.802		
T71	2.748		
T72	2.831		
T73	2.811		
T81	2.787		
T105	2.772		
T113	2.772		
T114	2.767		
T115	2.720		
T116	2.741		
T139	2.836	2.829	2.833
T140	2.878		
T141	2.833		
T142	2.739	2.746	2.743
T154	2.760		
T156	2.771		
T157	2.795		
T158	2.878		
T162	2.714		
T164	2.722		
T182	3.020		

Sample ID	Density (g/cm <sup>3</sup> )		
	Original	Duplicate	Average
T184	2.725	2.738	2.731
T186	2.699		
T188	2.766	2.769	2.768
T192	2.725	2.717	2.721
T193	2.667		
T194	2.726		
T195	2.784	2.767	2.776
T213	2.803		
T215	2.621		
T216	2.787		
T218	2.754		
T228	2.806		
T239	2.785		
T240	2.772		
T241	2.707	2.704	2.706
T242	2.839		
T245	2.770		

Standards	Measured Density (g/cm <sup>3</sup> )						Ideal Density (g/cm <sup>3</sup> )	Average (g/cm <sup>3</sup> )	Std Dev (g/cm <sup>3</sup> )	Relative Standard Deviation (%)	Relative Difference (%)
Quartz Crystal 1	2.65	2.64	2.64	2.65	2.64	2.64	2.65	2.64	0.006	0.227	-0.246
Quartz Crystal 2	2.63	2.64	2.63	2.63	2.64	2.64	2.65	2.64	0.005	0.197	-0.470
Apatite	3.16	3.16	3.17	3.17	3.16	3.17	3.16-3.22	3.17	0.006	0.192	N/A

Duplicates (2% Precision Control Lines)



## **Appendix K**

### **Sulphur isotope data ( $^{32}\text{S}$ , $^{34}\text{S}$ ): Environmental Isotope Laboratory**

These results are from the Environmental Isotope Laboratory (University of Waterloo). Methods are outlined in Section 3.8.1.

Sample ID	Weight (mg)	Peak Area: Area (E-8)S		Total (%S)		$\delta^{34}\text{S}$ VCDT $\pm$ 0.3‰		Sulphur (%)
		Result 1	Result 2	Result 1	Result 2	Result 1	Result 2	
T16	3	2.10		0.77		1.75		0.77
T17	2.055	1.89		0.89		1.84		1.19
T20	3.143	3.23	4.03	1.13	1.43	1.85	1.54	1.17
T24	0.146	3.92	3.95	26.44	26.26	-0.15	-0.41	27
T27	3.009	1.82	2.06	0.59	0.72	2.96	2.10	0.77
T37	0.122	4.11	4.02	32.65	36.82	17.89	17.91	34.6
T56	1.226	3.05		2.41		2.06		2.27
T58	3.143	2.21		0.77		2.50		0.61
T71	0.348	5.51	5.02	15.37	14.23	1.99	1.87	13.9
T72	1.003	3.63	1.45	3.23	1.40	2.30	1.75	2.96
T73	3.002	4.70		1.72		2.15		1.58
T85	1.573	0.99	1.40	0.61	0.86	1.99	2.19	1.43
T86	3.099	7.36	6.42	2.61	2.34	2.30	2.39	2.08
T90	0.396	1.65	1.39	4.03	3.34	1.56	1.74	3.85
T98	3.029	1.08	0.66	0.39	0.21	1.51	2.73	0.83
T99	0.702	1.41	2.30	1.95	3.18	2.05	2.08	3.35
T100	1.981	2.59	4.25	1.47	2.36	1.88	1.83	1.63
T101	1.241	1.29		1.01		3.04		1.84
T105	1.265	1.46		1.12		0.46		2.09
T113	2.176	1.43		0.72		3.95		1.26

## **Appendix L**

### **Sulphur isotope data ( $^{32}\text{S}$ , $^{33}\text{S}$ , $^{34}\text{S}$ , $^{36}\text{S}$ ): Stable Isotope Laboratory**

These results are from the Stable Isotope Laboratory (University of Maryland).  $\delta^{33}\text{S}$ ,  $\delta^{34}\text{S}$ ,  $\delta^{36}\text{S}$ ,  $\Delta^{33}\text{S}$ ,  $\Delta^{36}\text{S}$  values are in ‰. Methods are summarized in Section 3.8.2.

Mass Spec Sequence	Sample ID	SF <sub>6</sub> Recovery	δ <sup>33</sup> S	δ <sup>34</sup> S	δ <sup>36</sup> S	Δ <sup>33</sup> S	Δ <sup>36</sup> S	Δ <sup>36</sup> S/Δ <sup>33</sup> S
SF16455b	IAEA-S1	100%	-0.04	-0.27	-1.30	0.095	-0.785	-8.3
SF16456	T100	101%	1.18	2.00	3.76	0.143	-0.048	-0.3
SF16457	T71	93%	1.45	2.92	5.53	-0.057	-0.023	0.4
SF16458	T142	99%	0.91	1.83	4.33	-0.033	0.846	-25.5
SF16459	T37	99%	9.50	19.60	38.36	-0.545	0.795	-1.5
SF16460	IAEA-S1	100%	-0.06	-0.29	-1.25	0.093	-0.695	-7.4
SF16461	T16	101%	1.79	1.92	3.54	0.806	-0.107	-0.1
SF16462	T24	100%	-0.79	-0.46	-0.13	-0.551	0.750	-1.4
SF16463	T199	94%	-1.20	-1.33	-1.81	-0.508	0.721	-1.4
SF16464	T73PYRR	97%	0.58	1.22	2.27	-0.046	-0.050	1.1
SF16465	IAEA-S1	100%	-0.08	-0.34	-1.24	0.095	-0.590	-6.2
SF16466	T73	100%	1.13	2.28	4.32	-0.045	-0.023	0.5
SF16467	T195 PYRR	97%	0.83	1.69	3.28	-0.045	0.055	-1.2
SF16468	T195	95%	1.41	2.83	5.37	-0.044	-0.018	0.4
SF16469	T127	95%	0.99	2.01	3.81	-0.047	-0.015	0.3
IAEA S1 analyzed with this dataset			-0.06	-0.30	-1.26	0.094	-0.690	-7.3



## **Appendix M**

### **LA-ICP-MS data**

Analyses were conducted at the Metal Isotope Geochemistry Laboratory at the University of Waterloo. The units for the values in the columns titled  $^{88}\text{Sr}$ ,  $^{232}\text{Th}$ , and  $^{238}\text{U}$  are in counts per second. Methods are described in Section 3.9.

Spot ID	<sup>88</sup> Sr	<sup>232</sup> Th	<sup>238</sup> U	~U (ppm)	~Th (ppm)	Th / U	<sup>206</sup> Pb/ <sup>238</sup> U		<sup>207</sup> Pb/ <sup>235</sup> U		<sup>207</sup> Pb/ <sup>206</sup> Pb		ρ	<sup>206</sup> Pb/ <sup>238</sup> U		<sup>207</sup> Pb/ <sup>235</sup> U		<sup>207</sup> Pb/ <sup>206</sup> Pb	
							Value	2 SE	Value	2 SE	Value	2 SE		Value	2 SE	Value	2 SE	Value	2 SE

**Least-altered Sample**

Un-1	108	33850	63790	59.84	29.26	0.489	0.533	0.011	14	0.3	0.1909	0.0028	0.757	2747	45	2745	20	2741	24
Un-2	101	12620	34170	31.53	10.43	0.331	0.544	0.014	14.27	0.38	0.1914	0.0043	0.632	2791	60	2756	26	2737	37
Un-3	71	8120	24360	22.23	6.43	0.289	0.54	0.015	14.27	0.41	0.1934	0.005	0.582	2771	62	2754	28	2749	41
Un-4	128	16620	52800	48	12.74	0.265	0.552	0.014	14.46	0.35	0.191	0.0039	0.662	2834	55	2773	24	2740	34
Un-5	102	13060	43700	39.8	9.78	0.246	0.556	0.013	14.67	0.34	0.1922	0.0037	0.658	2841	52	2785	22	2748	31
Un-6	157	40400	75900	69.9	29.92	0.428	0.551	0.014	14.55	0.36	0.1911	0.0036	0.718	2829	57	2776	24	2743	31
Un-7	110	29600	58600	65.8	26.48	0.402	0.56	0.016	14.72	0.34	0.1896	0.0038	0.718	2864	64	2788	23	2724	34
Un-8	63	11170	32700	39.6	10.96	0.277	0.54	0.013	14.23	0.35	0.1921	0.0042	0.597	2782	53	2759	23	2747	36
Un-9	139	27690	43950	57.7	30.22	0.524	0.535	0.013	14.08	0.33	0.1916	0.0037	0.673	2761	55	2746	23	2747	31
Un-10	106	22980	40500	57.7	28.13	0.488	0.551	0.013	14.23	0.33	0.1886	0.0037	0.648	2820	54	2756	23	2716	32
Un-11	58	14790	36800	57.3	20.53	0.358	0.555	0.013	14.35	0.35	0.1879	0.0039	0.624	2838	54	2763	24	2709	34
Un-12	95	15680	42500	71.7	24.69	0.344	0.537	0.013	14.22	0.36	0.1911	0.0039	0.661	2769	58	2755	24	2741	35
Un-13	85	25560	52500	112	59.8	0.534	0.546	0.014	14.07	0.33	0.189	0.0037	0.685	2798	59	2748	22	2720	32
Un-14	50	8750	25900	56	21.2	0.379	0.544	0.016	14.24	0.44	0.1916	0.0046	0.684	2786	66	2750	30	2740	41
Un-15	111	22100	51800	113	55.3	0.489	0.549	0.014	14.34	0.33	0.1914	0.0039	0.652	2812	58	2766	22	2740	33
Un-16	70	12850	34100	74.9	33.35	0.445	0.535	0.014	14.47	0.4	0.1978	0.0042	0.690	2762	60	2769	27	2792	34
Un-17	102	25490	50700	112.3	69	0.614	0.524	0.013	13.74	0.32	0.192	0.004	0.626	2709	57	2723	22	2744	34
Un-18	68	11880	32600	72.9	33.93	0.465	0.537	0.014	13.88	0.37	0.1894	0.0039	0.695	2762	60	2730	25	2731	33
Un-19	159	27440	87800	217.8	132.7	0.609	0.529	0.011	13.84	0.29	0.191	0.003	0.717	2730	48	2734	20	2745	26
Un-20	87	21610	67200	170.1	121.7	0.715	0.535	0.013	13.98	0.31	0.1909	0.0038	0.636	2756	55	2740	21	2740	33
Un-21	77	24100	44900	114.6	152	1.326	0.556	0.014	14.46	0.34	0.1901	0.0034	0.732	2840	56	2771	23	2731	29
Un-22	134	43200	87800	222	282	1.270	0.536	0.013	13.92	0.3	0.1895	0.0033	0.717	2760	54	2736	21	2727	28
Un-23	97	30100	60700	149.1	181.6	1.218	0.544	0.014	14.37	0.38	0.1928	0.0042	0.652	2798	58	2763	26	2750	35
Un-24	120	20200	47100	109.6	100.5	0.917	0.538	0.014	13.98	0.35	0.1893	0.0042	0.623	2764	59	2738	25	2724	36
Un-25	129	33570	73800	121.7	63.5	0.522	0.531	0.013	13.95	0.34	0.1907	0.0038	0.667	2739	55	2737	24	2734	33

Spot ID	<sup>88</sup> Sr	<sup>232</sup> Th	<sup>238</sup> U	~U (ppm)	~Th (ppm)	Th / U	<sup>206</sup> Pb/ <sup>238</sup> U		<sup>207</sup> Pb/ <sup>235</sup> U		<sup>207</sup> Pb/ <sup>206</sup> Pb		ρ	<sup>206</sup> Pb/ <sup>238</sup> U		<sup>207</sup> Pb/ <sup>235</sup> U		<sup>207</sup> Pb/ <sup>206</sup> Pb	
							Value	2 SE	Value	2 SE	Value	2 SE		Value	2 SE	Value	2 SE	Value	2 SE
Un-26	60	19100	59200	87.3	28.53	0.327	0.547	0.013	14.54	0.34	0.193	0.0037	0.669	2804	54	2777	23	2755	31
Un-27	57	8080	26160	34.9	9.9	0.284	0.545	0.015	14.29	0.37	0.1909	0.0044	0.629	2792	60	2761	25	2732	38
Un-28	48	12270	33900	40.8	12.66	0.310	0.545	0.016	14.38	0.39	0.1917	0.0042	0.702	2791	65	2763	26	2744	37
Un-29	61	20790	44300	49.09	18.68	0.381	0.531	0.011	13.85	0.25	0.1901	0.0034	0.582	2742	45	2738	18	2731	30
Un-30	57	14620	23770	24.62	11.86	0.482	0.53	0.012	13.68	0.32	0.1875	0.0034	0.690	2732	52	2722	23	2716	30
Un-31	71	13920	41900	39.5	9.92	0.251	0.527	0.012	13.79	0.3	0.19	0.0028	0.782	2723	49	2728	21	2734	24
Un-32	103	30590	58300	56.8	23.09	0.407	0.533	0.01	14.05	0.29	0.1912	0.0027	0.747	2754	41	2749	19	2745	23
Un-33	82	9970	36030	36.87	8.2	0.222	0.541	0.011	13.92	0.24	0.1872	0.0029	0.671	2783	45	2743	16	2709	26
Un-34	92	16950	49820	54.37	15.56	0.286	0.5284	0.0095	13.9	0.28	0.1907	0.0026	0.750	2730	40	2739	19	2744	23
Un-35	71	8420	24290	28.6	8.88	0.310	0.5317	0.0098	14.27	0.31	0.1953	0.0041	0.463	2755	44	2766	21	2771	34
Un-36	106	14320	36400	46.6	17.76	0.381	0.551	0.011	14.2	0.34	0.1881	0.0034	0.675	2831	46	2754	23	2714	30
Un-37	149	21140	49500	85.8	53.5	0.624	0.539	0.01	13.81	0.28	0.1867	0.003	0.661	2776	42	2730	20	2704	26
Un-38	97	18010	66900	124.2	55.8	0.449	0.547	0.011	14.3	0.28	0.191	0.0027	0.747	2806	46	2767	18	2743	23
Un-39	103	30400	59800	116.3	110.8	0.953	0.55	0.012	14.3	0.33	0.1903	0.0033	0.703	2819	51	2766	22	2734	28
Un-40	121	29200	73900	148.5	119.2	0.803	0.549	0.012	14.27	0.31	0.19	0.0032	0.701	2813	49	2766	20	2732	27
Un-41	103	10770	26400	53.5	45.8	0.856	0.551	0.014	14.48	0.4	0.1928	0.0041	0.681	2819	58	2772	27	2750	34
Un-42	142	29860	41300	82.3	121.7	1.479	0.544	0.013	14.11	0.36	0.1894	0.0041	0.618	2792	54	2747	24	2724	36
Un-43	96	25510	47100	70	51.4	0.734	0.546	0.013	14.24	0.31	0.1902	0.0035	0.677	2802	52	2758	21	2732	30
Un-44	80	12380	23080	31.58	21.44	0.679	0.542	0.012	14.23	0.39	0.1898	0.0041	0.638	2787	48	2756	25	2724	35
Un-45	92	38360	109800	139.8	58.5	0.418	0.555	0.012	14.47	0.32	0.1891	0.0034	0.662	2838	51	2773	22	2723	29
Un-46	167	24350	60300	72.3	33.6	0.465	0.549	0.011	14.23	0.29	0.1884	0.0033	0.624	2817	46	2761	19	2722	27
Un-47	94	17700	39500	45.4	22.69	0.500	0.562	0.013	14.86	0.35	0.1915	0.0037	0.658	2866	54	2797	23	2750	32

Spot ID	<sup>88</sup> Sr	<sup>232</sup> Th	<sup>238</sup> U	~U (ppm)	~Th (ppm)	Th / U	<sup>206</sup> Pb/ <sup>238</sup> U		<sup>207</sup> Pb/ <sup>235</sup> U		<sup>207</sup> Pb/ <sup>206</sup> Pb		ρ	<sup>206</sup> Pb/ <sup>238</sup> U		<sup>207</sup> Pb/ <sup>235</sup> U		<sup>207</sup> Pb/ <sup>206</sup> Pb	
							Value	2 SE	Value	2 SE	Value	2 SE		Value	2 SE	Value	2 SE	Value	2 SE

**Altered Sample - Proterozoic Ages**

Alt-1	142	120000	530500	989	412	0.417	0.2658	0.0051	3.342	0.059	0.0909	0.0015	0.602	1517	26	1488	14	1435	32
Alt-20	54	4750	591000	954	12.49	0.013	0.1954	0.0054	2.021	0.049	0.0752	0.0015	0.712	1152	28	1122	16	1054	40
Alt-22	203	5320	540000	822	11.85	0.014	0.1994	0.0046	2.053	0.045	0.0737	0.0013	0.694	1174	24	1129	15	1027	34
Alt-23	27	821	197100	308.9	1.77	0.006	0.1962	0.0037	2	0.045	0.0739	0.0016	0.463	1154	20	1111	15	1014	45
Alt-24	31	997	241000	391	2.08	0.005	0.2135	0.0044	2.196	0.052	0.0744	0.0012	0.743	1246	23	1175	17	1037	34
Alt-25	51	4970	530000	900	10.06	0.011	0.1944	0.004	2.013	0.04	0.0751	0.0013	0.634	1144	22	1117	14	1062	35
Alt-26	69	2530	189500	338	4.97	0.015	0.2055	0.0066	2.15	0.069	0.076	0.002	0.664	1201	35	1159	22	1067	56
Alt-34	421	27600	1026000	2100	48.2	0.023	0.2034	0.0051	2.078	0.047	0.0749	0.0015	0.652	1195	28	1137	16	1053	39
Alt-35	750	50300	506000	1010	87.1	0.086	0.2782	0.0086	3.57	0.12	0.0937	0.0018	0.826	1577	43	1530	27	1499	35
Alt-42	67	13100	160900	241	22.6	0.094	0.2168	0.0078	2.35	0.079	0.0791	0.0021	0.711	1260	41	1221	24	1151	50
Alt-47	1060	94100	368300	791	157	0.198	0.2111	0.0043	2.385	0.052	0.0819	0.0015	0.625	1233	23	1236	15	1227	35
Alt-48	51	17790	311400	758	31.32	0.041	0.1632	0.0036	1.623	0.039	0.0721	0.0013	0.697	974	20	975	15	975	38
Alt-51	257	81000	393000	767	159	0.207	0.1838	0.0065	2.295	0.093	0.0903	0.0018	0.871	1084	35	1197	28	1413	38
Alt-52	69	126800	92000	163.4	253.7	1.553	0.1996	0.0066	2.18	0.1	0.079	0.0021	0.821	1170	35	1162	32	1144	54

**Altered Sample - Archean Ages**

Alt-2	137	27290	64100	123.4	106.4	0.862	0.564	0.013	14.82	0.32	0.1898	0.0031	0.734	2874	54	2799	21	2731	26
Alt-3	110	26770	75900	149.7	120.7	0.806	0.548	0.013	14.5	0.32	0.1902	0.0028	0.796	2808	56	2779	21	2742	25
Alt-4a	265	29770	87300	171	126.9	0.742	0.559	0.014	14.75	0.35	0.1911	0.0032	0.766	2859	61	2796	22	2742	27
Alt-4b	275	39600	95600	188.3	182	0.967	0.544	0.013	14.34	0.33	0.192	0.004	0.606	2790	53	2763	23	2753	32
Alt-5	61	16070	60600	118.7	73	0.615	0.567	0.014	14.9	0.4	0.1908	0.0041	0.655	2894	58	2804	25	2737	36
Alt-6	133	43500	76200	148.4	191.1	1.288	0.533	0.013	14.13	0.37	0.192	0.0038	0.696	2751	56	2750	25	2749	33
Alt-7	109	19070	55500	107.7	80.1	0.744	0.548	0.015	14.59	0.39	0.1948	0.0043	0.667	2805	64	2777	25	2766	36
Alt-8	98	19280	47600	100.6	68	0.676	0.558	0.019	14.66	0.51	0.1904	0.0045	0.764	2840	78	2774	34	2735	42
Alt-9	126	21530	77500	169.5	74	0.437	0.556	0.016	14.42	0.38	0.1897	0.0039	0.725	2838	68	2766	26	2725	33
Alt-10	123	33830	65000	146.9	113.5	0.773	0.548	0.018	14.58	0.46	0.1939	0.0051	0.667	2801	75	2776	30	2755	45

Spot ID	<sup>88</sup> Sr	<sup>232</sup> Th	<sup>238</sup> U	~U (ppm)	~Th (ppm)	Th / U	<sup>206</sup> Pb/ <sup>238</sup> U		<sup>207</sup> Pb/ <sup>235</sup> U		<sup>207</sup> Pb/ <sup>206</sup> Pb		ρ	<sup>206</sup> Pb/ <sup>238</sup> U		<sup>207</sup> Pb/ <sup>235</sup> U		<sup>207</sup> Pb/ <sup>206</sup> Pb	
							Value	2 SE	Value	2 SE	Value	2 SE		Value	2 SE	Value	2 SE	Value	2 SE
Alt-11	205	20010	108500	252	65.6	0.260	0.565	0.019	14.88	0.47	0.1924	0.0046	0.733	2870	79	2795	30	2747	40
Alt-12	183	9260	26900	63.6	29.7	0.467	0.566	0.021	14.69	0.47	0.1917	0.0061	0.585	2882	85	2782	32	2723	52
Alt-14	38	9080	25710	61.1	28.6	0.468	0.543	0.022	14.66	0.55	0.1981	0.006	0.701	2771	93	2775	37	2778	51
Alt-15	51	10690	27020	57.5	31.48	0.547	0.57	0.021	15.02	0.54	0.1903	0.0051	0.729	2885	87	2800	34	2731	46
Alt-16	67	20370	68100	136.8	58.7	0.429	0.562	0.02	14.97	0.45	0.1909	0.0053	0.654	2868	84	2803	29	2733	49
Alt-17	82	14850	46800	88.7	41.9	0.472	0.577	0.02	15.28	0.44	0.1921	0.0044	0.754	2920	81	2827	27	2741	39
Alt-18	180	21370	68100	121.5	59	0.486	0.549	0.012	14.45	0.32	0.1904	0.0035	0.651	2814	50	2772	21	2734	29
Alt-19	95	20250	51200	86.7	54.6	0.630	0.55	0.011	14.51	0.27	0.1901	0.0034	0.573	2820	44	2778	18	2731	29
Alt-21	109	28940	46300	71.8	74	1.031	0.608	0.014	16.16	0.38	0.1906	0.0031	0.756	3053	58	2880	22	2741	27
Alt-27	56	18150	43500	81.5	34.83	0.427	0.582	0.013	15.38	0.39	0.1911	0.0036	0.695	2965	53	2835	23	2747	33
Alt-28	77	13550	43000	84.2	25.45	0.302	0.593	0.018	15.39	0.45	0.1882	0.004	0.746	3004	78	2825	29	2710	36
Alt-29	80	16510	55500	119.1	29.65	0.249	0.581	0.015	15.31	0.36	0.1911	0.004	0.644	2960	58	2833	21	2745	35
Alt-31	65	8140	23710	51	14.52	0.285	0.572	0.018	15.09	0.49	0.1946	0.0054	0.624	2900	73	2812	30	2754	47
Alt-32	401	14700	69300	148	26	0.176	0.597	0.017	15.56	0.48	0.1913	0.0049	0.630	3012	68	2834	31	2735	44
Alt-33	294	13640	27600	57.9	24.02	0.415	0.571	0.011	14.85	0.34	0.1907	0.0035	0.633	2911	47	2797	22	2739	30
Alt-36	45	16400	67000	129.3	28.03	0.217	0.583	0.017	15.2	0.41	0.192	0.0039	0.741	2946	69	2819	26	2744	33
Alt-37	73	16460	42300	78.9	27.69	0.351	0.582	0.019	15.12	0.47	0.1912	0.005	0.664	2941	77	2811	29	2734	44
Alt-38	117	21880	78900	127.5	32.61	0.256	0.586	0.016	15.09	0.38	0.188	0.004	0.674	2962	64	2813	24	2713	35
Alt-39	84	43190	108800	171.3	63.1	0.368	0.585	0.017	15.37	0.44	0.1918	0.0042	0.712	2957	71	2825	29	2749	39
Alt-40	111	29610	104600	161.2	43	0.267	0.581	0.017	15.14	0.39	0.191	0.0038	0.746	2938	69	2819	25	2745	34
Alt-41	2380	30400	87700	131.4	48.3	0.368	0.548	0.015	14.32	0.33	0.1901	0.0037	0.715	2825	64	2765	23	2733	33
Alt-43	80	12830	33400	50.2	23.72	0.473	0.572	0.014	15.14	0.37	0.1925	0.0043	0.583	2908	55	2814	24	2751	36
Alt-44	74	13870	38600	58.4	27.47	0.470	0.561	0.013	14.82	0.33	0.1911	0.0034	0.694	2864	54	2795	22	2740	30
Alt-45	89	23840	78700	120.6	49	0.406	0.561	0.011	14.7	0.3	0.1893	0.0032	0.644	2872	43	2795	18	2726	27
Alt-46	137	23150	76200	144.2	37.5	0.260	0.549	0.012	14.46	0.32	0.1901	0.0031	0.725	2815	48	2775	21	2733	27
Alt-49	86	36920	147800	394	69.1	0.175	0.575	0.012	15.05	0.33	0.1893	0.0028	0.762	2922	49	2817	20	2731	25
Alt-50	126	29660	113200	259	58.8	0.227	0.577	0.013	14.97	0.31	0.1883	0.0029	0.749	2929	52	2807	20	2719	26

Spot ID	<sup>88</sup> Sr	<sup>232</sup> Th	<sup>238</sup> U	~U (ppm)	~Th (ppm)	Th / U	<sup>206</sup> Pb/ <sup>238</sup> U		<sup>207</sup> Pb/ <sup>235</sup> U		<sup>207</sup> Pb/ <sup>206</sup> Pb		ρ	<sup>206</sup> Pb/ <sup>238</sup> U		<sup>207</sup> Pb/ <sup>235</sup> U		<sup>207</sup> Pb/ <sup>206</sup> Pb	
							Value	2 SE	Value	2 SE	Value	2 SE		Value	2 SE	Value	2 SE	Value	2 SE

**Standard DD91-1**

DD91-1_1	198	443400	692000	667	406.3	0.609	0.5207	0.0091	13.21	0.22	0.1842	0.0015	0.887	2698	39	2692	16	2688	13
DD91-1_2	189	85800	119700	124.7	70.3	0.564	0.5409	0.0093	13.73	0.24	0.1838	0.0022	0.762	2783	39	2727	17	2682	20
DD91-1_3	63	63200	87400	170.3	125.1	0.735	0.534	0.012	13.56	0.25	0.184	0.0028	0.740	2758	48	2714	18	2680	25
DD91-1_4	63	53590	97300	227.2	188.3	0.829	0.528	0.011	13.27	0.27	0.1842	0.0025	0.783	2728	45	2698	18	2684	23
DD91-1_5	100	239900	291300	283	176.8	0.625	0.538	0.013	13.68	0.29	0.1851	0.0032	0.717	2769	55	2720	21	2689	28
DD91-1_6	119	248000	365900	602	617	1.025	0.52	0.01	13.12	0.24	0.1836	0.0023	0.778	2692	45	2685	18	2682	21
DD91-1_7	114	90500	165100	185.1	111	0.600	0.539	0.013	13.74	0.29	0.1842	0.0031	0.731	2777	54	2725	20	2681	27
DD91-1_8	92	62600	85700	140.6	149.6	1.064	0.531	0.012	13.66	0.31	0.1844	0.0034	0.669	2739	50	2719	22	2681	30
DD91-1_9	72	86000	121300	247.3	314.9	1.273	0.523	0.011	13.22	0.26	0.1836	0.0028	0.721	2705	49	2689	19	2683	27
DD91-1_10	293	334000	397000	597	824	1.380	0.528	0.012	13.35	0.26	0.1817	0.0025	0.798	2726	49	2698	19	2661	23
DD91-1_11	461	273100	390000	699	448	0.641	0.545	0.013	13.64	0.3	0.1832	0.0029	0.764	2799	52	2717	21	2673	26

## **Appendix N**

### **Whole-rock geochemistry data including NRCan-provided reference materials**

Whole-rock geochemistry data from Activation Laboratories Ltd. Methods are outlined in Section 3.2. These results are from an open file report (Ciufu et al., 2019) with the exception of results pertaining to STPL standards which are also reported in this Appendix.

Analyte	SiO <sub>2</sub>	Al <sub>2</sub> O <sub>3</sub>	Fe <sub>2</sub> O <sub>3</sub>	MnO	MgO	CaO	Na <sub>2</sub> O	K <sub>2</sub> O	TiO <sub>2</sub>	P <sub>2</sub> O <sub>5</sub>	LOI	LOI2	Total	Total2
Units	%	%	%	%	%	%	%	%	%	%	%	%	%	%
DL	0.01	0.01	0.01	0.001	0.01	0.01	0.01	0.01	0.001	0.01			0.01	0.01
Method	FUS-ICP	FUS-ICP	FUS-ICP	FUS-ICP	FUS-ICP	FUS-ICP	FUS-ICP	FUS-ICP	FUS-ICP	FUS-ICP	FUS-ICP	FUS-ICP	FUS-ICP	FUS-ICP
T6	66.24	15.28	< 0.01	0.047	1.41	3.48	4.99	0.91	0.409	0.1	3.37	2.97	100.2	99.79
T8	63.77	15.24	0.72	0.114	2.85	4.39	3.33	1.11	0.649	0.26	2.86	2.31	100.7	100.2
T9	50.53	14.62	1.95	0.207	6.23	9.81	2.07	0.69	1.129	0.11	1.79	0.68	100.2	99.05
T11	63.01	15.26	0.64	0.105	2.14	4.29	4.92	0.46	0.561	0.19	2.69	2.15	99.6	99.06
T12	52.33	13.48	2.66	0.223	4.96	9.17	2.6	0.6	1.354	0.15	0.17	-1.11	100.4	99.08
T13	65.51	15.62	0.3	0.077	2.35	3.38	3.42	1.46	0.512	0.21	1.68	1.17	99.63	99.11
T14	46.75	12.66	2.2	0.21	4.82	10.11	2.02	0.09	1.217	0.1	2.94	1.85	94.03	92.93
T15	44.75	10.32	0.54	0.151	9.77	9.39	1.51	0.39	0.679	0.31	7.53	6.81	92.45	91.73
T16	37.89	12.42	1.22	0.205	6.36	13.62	3.39	0.63	0.772	0.61	9.32	8.6	93.55	92.83
T17	65.91	13.53	2.34	0.06	1.47	4.17	3.58	1.73	0.443	0.16	4.5	4.3	99.89	99.69
T19	48.37	13.03	1.04	0.146	6.15	8.35	1.49	0.59	0.899	0.1	7.02	5.88	98.52	97.37
T20	65.35	13.64	2.25	0.054	1.44	4	3.7	1.87	0.446	0.15	5.26	5.07	100.1	99.86
T21	56.32	18.24	3.05	0.36	1.69	0.59	1.55	2.21	0.771	0.22	3.24	1.99	100.7	99.45
T24	3.53	0.97	42.57	1.756	2.25	6.27	0.05	0.03	0.042	0.03	16.15	13.74	97.55	95.15
T27	63.63	15.4	1.18	0.165	1.16	2.67	3.03	2.28	0.516	0.22	3.42	2.86	99.21	98.65
T29	56.82	12.84	1.73	0.21	2.83	2.41	1.12	0.22	0.417	0.17	4.25	2.62	99.26	97.63
T31	56.55	21.27	2.42	0.403	0.58	1.23	1.16	0.58	0.724	0.22	3.18	2.12	98.77	97.71
T32	77.39	13.64	0.23	0.045	0.13	0.35	4.67	1.36	0.049	0.04	1.17	1	100.8	100.6
T37	8.07	0.55	45.1	0.793	0.4	1.93	0.07	0.02	0.016	0.03	26.4	24.68	100.5	98.77
T38	83.88	2.53	< 0.01	0.249	0.58	1	0.1	0.09	0.087	0.01	3.43	2.56	100.4	99.58
T39	47.67	12.11	1.43	0.52	5.3	7.08	2.85	0.04	1.022	0.08	5.84	4.62	96.08	94.85
T42	57.06	12.84	0.26	0.102	6.29	4.74	4.26	0.19	0.552	0.1	7.39	6.82	99.46	98.89
T43	64.26	15.24	0.1	0.094	2.14	2.67	4.41	1.47	0.478	0.23	3.32	2.78	99.85	99.3
T45	66.98	12.09	0.23	0.115	0.28	7.39	2.19	2.63	0.034	0.04	6.56	6.43	99.89	99.75
T50	39.9	11.14	< 0.01	0.163	10.03	10.4	1.2	0.4	0.685	0.33	15.53	16.46	99.01	99.94
T56	77.71	9.41	1.17	0.048	0.82	1.86	0.73	1.99	0.489	0.08	2.41	2.71	99.72	100



Analyte	SiO <sub>2</sub>	Al <sub>2</sub> O <sub>3</sub>	Fe <sub>2</sub> O <sub>3</sub>	MnO	MgO	CaO	Na <sub>2</sub> O	K <sub>2</sub> O	TiO <sub>2</sub>	P <sub>2</sub> O <sub>5</sub>	LOI	LOI2	Total	Total2
Units	%	%	%	%	%	%	%	%	%	%	%	%	%	%
DL	0.01	0.01	0.01	0.001	0.01	0.01	0.01	0.01	0.001	0.01			0.01	0.01
Method	FUS-ICP	FUS-ICP	FUS-ICP	FUS-ICP	FUS-ICP	FUS-ICP	FUS-ICP	FUS-ICP	FUS-ICP	FUS-ICP	FUS-ICP	FUS-ICP	FUS-ICP	FUS-ICP
T58	66.73	19.38	0.13	0.011	0.32	1.01	1.13	4.78	0.74	0.26	2.63	2.8	98.81	98.98
T59	64.26	15.94	0.87	0.073	0.41	8.45	3.28	1.04	0.599	0.25	3.15	3.35	100.3	100.5
T63	43.73	9.43	0.24	0.113	10.65	9.94	1.16	0.15	0.649	0.34	16.04	16.73	99.32	100
T65	64.04	15.57	1.37	0.067	2.02	3.81	4.24	1.03	0.503	0.19	1.63	2.04	98.56	98.98
T66	41.48	12.77	1.45	0.147	6.53	10.51	3.93	0.67	0.839	0.83	12.55	13.27	98.83	99.55
T71	58.78	8.09	12.87	0.038	0.31	1.13	0.43	2.24	0.272	0.05	10.7	11.22	100.1	100.7
T72	59.97	16.22	2.6	0.13	1.03	3.98	1.74	3.29	0.519	0.1	6.58	6.91	99.49	99.83
T73	61.29	14.01	3.02	0.154	1.63	5.16	2.31	1.78	0.465	0.11	3.91	4.39	98.62	99.1
T80	45.93	13.79	0.21	0.136	7.55	6.5	2.31	0.2	0.81	0.07	9.75	10.88	98.48	99.61
T81	40.85	9.66	0.68	0.23	9.72	11.27	1.43	0.08	0.636	0.32	17.29	18.04	99.62	100.4
T83	50.87	12.82	1.72	0.232	5.28	9.87	2.49	0.52	1.377	0.17	0.2	1.53	98.78	100.1
T85	64.18	14.65	1.17	0.104	0.76	5.37	3.72	1.28	0.435	0.11	4.41	4.74	99.51	99.85
T86	64.25	17.26	2.11	0.031	0.51	1.89	2.56	3.19	0.496	0.1	3.54	3.81	98.62	98.89
T87	41.94	12.38	2.18	0.24	4.57	9.85	1.81	1.22	1.075	0.09	12.62	13.69	98.54	99.6
T88	60.76	14.13	5.19	0.219	1.24	3.6	1.86	1.91	0.415	0.08	3.05	3.75	99.35	100.1
T89	44.08	11.9	0.54	0.203	5.32	10.09	1.56	0.12	1.017	0.1	11.46	12.7	98.72	99.97
T90	65.53	14.93	3.51	0.045	0.69	2.27	1.54	3.05	0.469	0.14	4.84	5.15	100.1	100.4
T94	64.5	18.3	0.77	0.029	1.27	1.84	4.06	2.17	0.544	0.1	2.83	3.17	99.74	100.1
T98	44.71	12.3	1.12	0.223	4.78	10.29	1.95	0.16	1.253	0.1	9.98	11.18	98.77	99.97
T99	55.78	10.72	3.14	0.142	3.24	8.17	3.04	0.33	0.821	0.1	7.56	8.15	98.93	99.53
T100	80.35	3.94	1.04	0.075	1.25	4.14	0.59	0.32	0.372	0.03	3.89	4.24	99.46	99.81
T101	47.22	11.71	2.15	0.2	4.4	9.56	2.28	0.02	1.161	0.09	9.38	10.44	98.74	99.8
T102	63.33	15.13	0.48	0.072	2.24	3.63	4.5	0.94	0.606	0.12	4.07	4.61	100.4	101
T104	96.64	0.4	< 0.01	0.015	0.06	0.99	0.03	0.09	0.007	< 0.01	0.85	0.9	99.38	99.42
T105	60.16	14.41	1.65	0.078	2.85	4.38	1.84	2.7	0.58	0.2	5.35	5.79	98.54	98.98
T106	48.83	13.73	1.71	0.184	5.13	9.21	1.3	0.3	1.519	0.14	3.7	5	98.65	99.95

Analyte	SiO <sub>2</sub>	Al <sub>2</sub> O <sub>3</sub>	Fe <sub>2</sub> O <sub>3</sub>	MnO	MgO	CaO	Na <sub>2</sub> O	K <sub>2</sub> O	TiO <sub>2</sub>	P <sub>2</sub> O <sub>5</sub>	LOI	LOI2	Total	Total2
Units	%	%	%	%	%	%	%	%	%	%	%	%	%	%
DL	0.01	0.01	0.01	0.001	0.01	0.01	0.01	0.01	0.001	0.01			0.01	0.01
Method	FUS-ICP	FUS-ICP	FUS-ICP	FUS-ICP	FUS-ICP	FUS-ICP	FUS-ICP	FUS-ICP	FUS-ICP	FUS-ICP	FUS-ICP	FUS-ICP	FUS-ICP	FUS-ICP
T113	62.1	14.19	1.62	0.092	2.61	5.35	2.09	2.31	0.555	0.19	5.62	6.01	100.6	101
T114	61.57	14.85	1.32	0.087	3.21	4.45	1.43	2.8	0.597	0.21	5.53	5.97	100.4	100.8
T115	60.27	14	0.84	0.096	2.84	5.5	2.19	2.16	0.553	0.21	6.01	6.45	99.03	99.46
T116	63.55	15.17	0.25	0.095	2.15	5.03	3	0.86	0.629	0.22	4.34	4.78	99.73	100.2
T117	65.89	15.19	0.79	0.049	1.42	4.09	3.77	1.06	0.465	0.09	2.14	2.52	98.74	99.12
T118	66.23	15.61	0.29	0.056	1.51	3.39	3.96	1.16	0.499	0.18	1.28	1.76	98.95	99.43
T134	55.56	20.91	0.64	0.055	0.21	1.15	7.66	7.95	0.305	0.06	1.87	1.63	98.7	98.47
T139	46.02	12.51	1.74	0.187	4.83	8.4	2.49	0.38	1.383	0.15	8.74	7.53	98.84	97.63
T140	46.94	13.3	2.89	0.194	4.67	7.74	2.04	1.12	1.475	0.13	7.75	6.57	99.93	98.76
T141	46.98	12.85	1.75	0.194	4.97	7.79	1.59	1.63	1.346	0.12	7.99	6.77	99.32	98.1
T142	47.85	12.45	1.98	0.178	4.18	8.6	2.26	2.01	1.147	0.1	8.46	7.49	98.9	97.93
T154	65.39	15.6	0.7	0.107	0.87	5.11	2.06	0.94	0.464	0.16	4.56	4.1	100.5	100.1
T156	58.56	16.2	1.42	0.125	1.27	5.72	3.29	1.48	0.522	0.15	6.44	5.9	100.5	99.98
T157	57.28	15.34	2.42	0.1	0.77	5.17	2.32	2.27	0.512	0.13	8.3	7.82	99.4	98.92
T158	64.61	12.6	2.43	0.081	0.62	3.92	1.42	1.94	0.426	0.14	7.08	6.66	99.38	98.97
T159	97.2	0.69	0.46	0.011	0.09	0.44	0.04	0.17	0.02	< 0.01	0.64	0.6	100.2	100.2
T162	70.78	14.71	0.42	0.038	0.59	2.81	3.32	2.19	0.294	0.09	2.87	2.63	100.6	100.3
T164	63.49	15.73	1.03	0.065	2.43	4.72	3.54	1.27	0.494	0.1	2.19	1.72	99.73	99.26
T165	57.44	17.5	0.9	0.113	0.2	7.65	8.82	0.16	0.283	0.04	4.31	4.18	98.64	98.51
T182	48.67	13.18	3.14	0.188	6.91	8.77	0.82	0.01	1.202	0.09	5.25	4.12	99.46	98.33
T183	63.27	14.19	0.41	0.287	2.34	4.84	2.5	1.11	0.519	0.15	5.86	5.41	99.94	99.49
T184	61.24	14.48	0.99	0.083	2.67	5.19	3.79	0.73	0.509	0.18	5.75	5.29	100.2	99.69
T186	59.28	14.09	0.13	0.082	2.54	5.59	3.19	1.24	0.51	0.18	6.83	6.29	99	98.46
T187	94.51	1.88	0.62	0.016	0.2	0.66	0.11	0.42	0.058	< 0.01	1.28	1.25	100.1	100.1
T188	62.77	11.66	1.43	0.095	2.04	4.48	0.72	2.78	0.418	0.16	8.82	8.5	98.6	98.27
T189	65.93	16.82	1.09	0.067	0.38	1.74	7.26	4.6	0.115	0.09	0.74	0.62	99.94	99.83

Analyte	SiO <sub>2</sub>	Al <sub>2</sub> O <sub>3</sub>	Fe <sub>2</sub> O <sub>3</sub>	MnO	MgO	CaO	Na <sub>2</sub> O	K <sub>2</sub> O	TiO <sub>2</sub>	P <sub>2</sub> O <sub>5</sub>	LOI	LOI2	Total	Total2
Units	%	%	%	%	%	%	%	%	%	%	%	%	%	%
DL	0.01	0.01	0.01	0.001	0.01	0.01	0.01	0.01	0.001	0.01			0.01	0.01
Method	FUS-ICP	FUS-ICP	FUS-ICP	FUS-ICP	FUS-ICP	FUS-ICP	FUS-ICP	FUS-ICP	FUS-ICP	FUS-ICP	FUS-ICP	FUS-ICP	FUS-ICP	FUS-ICP
T192	66.19	15.04	0.14	0.061	1.44	4.5	4.53	0.85	0.492	0.12	2.37	1.95	99.95	99.53
T193	71.52	13.86	0.57	0.033	0.74	2.65	4.74	1.09	0.229	0.05	1.74	1.55	99.11	98.92
T194	65.85	15.41	0.48	0.062	1.57	4.42	3.81	1.66	0.511	0.14	2.61	2.22	100.4	100
T195	65.18	15.53	0.93	0.054	1.46	3.49	2.08	2.78	0.519	0.12	4.67	4.33	100.2	99.83
T196	88.37	5.08	1.83	0.015	0.22	0.91	0.48	1.21	0.175	0.04	1.87	1.86	100.3	100.3
T200	46	16.56	2.19	0.166	9.92	9.26	1.8	0.03	0.62	0.06	4.11	3.12	100.5	99.51
T213	42.78	10.57	0.42	0.125	10.07	9.28	1.42	0.61	0.657	0.3	15.94	15.27	98.84	98.17
T215	65.46	16.68	0.76	0.035	0.52	2.3	8.92	0.05	0.202	0.08	2.15	2	98.59	98.45
T216	43.57	11.48	1.43	0.148	6.67	9.99	5.22	0.45	0.674	0.38	13.71	13.13	99.38	98.81
T218	59.98	15.88	0.81	0.087	1.79	4.78	3.42	1.04	0.449	0.06	8.09	7.67	100.5	100.1
T228	45.01	12.14	2.46	0.157	5.64	9.87	5.49	0.26	0.641	0.63	11.99	11.48	99.31	98.8
T239	41.44	9.01	0.23	0.161	9.3	12.73	1.37	0.22	0.575	0.26	18.21	17.63	99.27	98.69
T240	46.8	10.45	0.39	0.139	8.01	9.67	2.27	0.1	0.613	0.42	14.18	13.51	99.72	99.05
T241	68.19	16.05	0.4	0.058	1.18	2.23	5.79	0.65	0.435	0.07	1.03	0.62	100.2	99.8
T242	45.91	11.36	2.11	0.152	7.75	12.27	4.27	1.72	0.722	0.35	7.73	7.2	99.57	99.05
T245	44.09	12.75	0.65	0.16	7.03	11.44	2.52	0.22	0.773	0.75	11.36	10.57	99.53	98.75
STPL-BAS-023	46.46	15.97	1.5	0.165	8.55	11.01	1.84	0.04	0.83	0.06	3.45	2.52	99.11	98.18
STPL-BAS-025	46.84	15.8	1.92	0.165	8.82	10.98	1.82	0.05	0.829	0.05	3.34	2.47	99.29	98.42
STPL-BAS-026	46.74	15.96	2.45	0.162	8.76	10.95	1.83	0.05	0.803	0.07	3.5	2.68	99.37	98.55
STPL-BAS-027	46.74	16.17	2.33	0.166	8.64	11.32	1.83	0.04	0.831	0.06	3.8	3	99.82	99.02
STPL-BAS-029	45.62	16.37	3.25	0.167	8.62	11.14	1.79	0.05	0.89	0.07	3.9	4.66	99.42	100.2
STPL-BAS-030	45.46	17.07	3.43	0.17	8.67	11.29	1.79	0.06	0.891	0.06	3.86	4.62	100.2	100.9

Analyte	SiO <sub>2</sub>	Al <sub>2</sub> O <sub>3</sub>	Fe <sub>2</sub> O <sub>3</sub>	MnO	MgO	CaO	Na <sub>2</sub> O	K <sub>2</sub> O	TiO <sub>2</sub>	P <sub>2</sub> O <sub>5</sub>	LOI	LOI2	Total	Total2
Units	%	%	%	%	%	%	%	%	%	%	%	%	%	%
DL	0.01	0.01	0.01	0.001	0.01	0.01	0.01	0.01	0.001	0.01			0.01	0.01
Method	FUS-ICP	FUS-ICP	FUS-ICP	FUS-ICP	FUS-ICP	FUS-ICP	FUS-ICP	FUS-ICP	FUS-ICP	FUS-ICP	FUS-ICP	FUS-ICP	FUS-ICP	FUS-ICP
STPL-BAS-053	46.54	15.9	2.24	0.17	8.73	11.22	1.75	0.04	0.808	0.05	3.51	2.64	99.51	98.65
STPL-53-PML-025	76.18	12.19	0.39	0.034	0.55	1.41	3.45	2.12	0.195	0.04	2.13	2.22	99.59	99.68
STPL-PML-53-027	75.34	12.73	0.69	0.032	0.53	1.38	3.48	2.08	0.192	0.04	2.56	2.5	99.6	99.54
STPL-53-PML-036	75.41	12.99	0.09	0.034	0.56	1.4	3.39	2.1	0.196	0.04	2	1.86	99.54	99.41

Analyte	Fe <sub>2</sub> O <sub>3</sub> T	Ba	Be	Sc	Sr	V	Zr	FeO	B	Mass	C-Total	S-Total	CO <sub>2</sub>	Hg
Units	%	ppm	ppm	ppm	ppm	ppm	ppm	%	ppm	g	%	%	%	ppb
DL	0.01	2	1	1	2	5	1	0.1	0.5, 1		0.01	0.01	0.01	5
Method	FUS-ICP	FUS-ICP	FUS-ICP	FUS-ICP	FUS-ICP	FUS-ICP	FUS-ICP	TITR	PGNAA	PGNAA	CS	CS	CO <sub>2</sub>	1G
T6	3.98	239	< 1	7	262	61	132	3.6	15	1.1	0.6	0.08	2.02	< 5
T8	6.17	257	1	13	251	99	148	4.9	18	1.01	0.22	0.02	0.73	< 5
T9	12.96	188	< 1	36	184	294	92	9.9	1	1.07	0.06	0.1	0.19	< 5
T11	5.98	149	< 1	11	445	94	128	4.8	13	1.01	0.43	0.01	1.36	< 5
T12	15.33	200	< 1	41	158	351	120	11.4	< 0.5	1.1	0.06	0.04	0.18	< 5
T13	5.41	341	< 1	10	193	93	139	4.6	< 0.5	1.01	0.12	0.14	0.35	< 5
T14	13.1	18	< 1	33	191	285	77	9.8	< 0.5	1.04	2.01	0.15	6.84	< 5
T15	7.65	87	1	18	395	132	131	6.4	2	1.03	3.5	0.05	11.9	< 5
T16	8.34	148	2	32	899	197	213	6.4	9	1.02	4.1	0.77	14	< 5
T17	4.34	279	< 1	7	273	64	131	1.8	14	1.05	0.75	1.19	2.51	< 5
T19	12.38	40	< 1	37	168	278	58	10.2	9	1.09	2.1	0.21	7.1	< 5
T20	4.14	293	< 1	8	247	63	138	1.7	6	1.08	0.96	1.17	3.31	< 5
T21	15.5	1371	4	16	124	115	180	11.2	8	1.08	0.03	0.14	0.11	< 5
T24	66.47	13	< 1	1	48	18	11	21.5	3	1.07	2.84	27	9.75	< 5
T27	6.74	723	1	9	322	75	117	5	59	1.05	0.56	0.77	1.83	< 5
T29	17.97	72	< 1	11	88	88	112	14.6	29	1.03	0.49	0.26	1.62	< 5
T31	12.87	263	1	14	292	112	158	9.4	25	1.04	0.22	0.09	0.73	< 5
T32	1.9	473	1	2	90	9	48	1.5	22	1.01	0.08	0.03	0.21	< 5
T37	62.22	3	< 1	2	19	20	12	15.4	9	1.08	0.59	34.6	2.06	10
T38	8.5	39	< 1	4	30	46	11	7.8	176	1.09	0.37	1.97	1.12	< 5
T39	13.56	7	< 1	35	239	284	64	10.9	13	1.08	2.21	0.38	7.45	< 5
T42	5.93	123	< 1	12	417	96	83	5.1	3	1.08	1.86	0.14	6.29	< 5
T43	5.54	847	1	9	314	83	129	4.9	20	1.05	0.51	0.33	1.69	< 5
T45	1.56	874	1	1	158	5	40	1.2	11.5	1.06	1.62	0.03	5.68	< 5
T50	9.23	68	< 1	20	327	126	144	8.3	7.3	1.01	3.35	< 0.01	11.4	< 5
T56	4.17	177	< 1	7	128	75	79	2.7	35	1.05	0.08	2.27	0.39	< 5

Analyte	Fe <sub>2</sub> O <sub>3</sub> T	Ba	Be	Sc	Sr	V	Zr	FeO	B	Mass	C-Total	S-Total	CO <sub>2</sub>	Hg
Units	%	ppm	ppm	ppm	ppm	ppm	ppm	%	ppm	g	%	%	%	ppb
DL	0.01	2	1	1	2	5	1	0.1	0.5, 1		0.01	0.01	0.01	5
Method	FUS-ICP	FUS-ICP	FUS-ICP	FUS-ICP	FUS-ICP	FUS-ICP	FUS-ICP	TITR	PGNAA	PGNAA	CS	CS	CO <sub>2</sub>	1G
T58	1.8	441	1	11	124	111	144	1.5	41.6	1.03	< 0.01	0.61	0.1	< 5
T59	2.87	158	< 1	9	341	89	142	1.8	18.8	1.06	0.62	0.18	2.11	< 5
T63	7.13	21	1	21	631	129	124	6.2	7.5	1.06	3.72	0.03	12.7	< 5
T65	5.48	398	1	9	353	83	138	3.7	6.3	1.08	0.23	0.01	0.75	< 5
T66	8.56	1051	2	28	1071	229	218	6.4	13.2	1.07	3.24	0.13	10.9	< 5
T71	18.1	169	< 1	8	67	62	64	4.7	105	1.03	0.21	13.9	0.82	< 5
T72	5.93	285	1	10	193	90	114	3	19.4	1.07	0.91	2.96	3.11	< 5
T73	7.8	158	1	8	229	75	106	4.3	239	1.04	0.87	1.58	2.97	< 5
T80	11.44	11	< 1	38	225	261	47	10.1	0.9	1.07	1.73	0.05	5.9	< 5
T81	8.14	12	< 1	15	215	90	116	6.7	7.6	1.04	3.98	< 0.01	14.5	< 5
T83	14.96	192	< 1	43	154	349	107	11.9	< 0.5	1.12	0.13	0.13	0.41	< 5
T85	4.51	225	1	8	282	69	109	3	28.3	1.01	0.84	1.43	2.96	< 5
T86	4.78	384	1	10	236	84	116	2.4	125	1.05	0.18	2.08	0.69	< 5
T87	12.74	133	< 1	36	163	283	65	9.5	33.4	1.05	3.28	0.2	10.8	< 5
T88	12.08	200	< 1	9	168	76	110	6.2	35.3	1.03	0.53	0.41	1.81	< 5
T89	12.88	16	< 1	37	100	282	58	11.1	5.3	1.07	2.37	0.05	8.25	< 5
T90	6.63	285	1	10	196	79	97	2.8	29	1.05	0.44	3.85	1.55	< 5
T94	4.1	358	< 1	8	217	76	132	3	20.1	1.04	0.22	0.3	0.8	< 5
T98	13.02	44	< 1	37	149	312	73	10.7	7	1.07	2.24	0.83	7.69	< 5
T99	9.03	95	< 1	22	131	176	76	5.3	5.8	1.06	1.76	3.35	6.15	< 5
T100	4.49	80	< 1	11	56	97	23	3.1	5.2	1.02	0.91	1.63	3.08	< 5
T101	12.72	4	< 1	34	144	299	70	9.5	14.7	1.07	2.06	1.84	7.23	< 5
T102	5.81	179	< 1	12	171	104	112	4.8	19.4	1.07	0.67	0.11	2.36	< 5
T104	0.3	12	< 1	< 1	11	< 5	4	0.4	2	1.06	0.21	0.04	0.76	< 5
T105	5.99	271	1	11	141	89	130	3.9	34.8	1.04	0.84	2.09	2.95	< 5
T106	14.61	29	< 1	38	87	293	103	11.6	343	1.09	0.62	0.02	2.02	< 5

Analyte	Fe <sub>2</sub> O <sub>3</sub> T	Ba	Be	Sc	Sr	V	Zr	FeO	B	Mass	C-Total	S-Total	CO <sub>2</sub>	Hg
Units	%	ppm	ppm	ppm	ppm	ppm	ppm	%	ppm	g	%	%	%	ppb
DL	0.01	2	1	1	2	5	1	0.1	0.5, 1		0.01	0.01	0.01	5
Method	FUS-ICP	FUS-ICP	FUS-ICP	FUS-ICP	FUS-ICP	FUS-ICP	FUS-ICP	TITR	PGNAA	PGNAA	CS	CS	CO <sub>2</sub>	1G
T113	5.51	290	< 1	11	143	86	131	3.5	32.6	1.02	1.04	1.26	3.63	< 5
T114	5.66	377	< 1	12	110	93	138	3.9	18.5	1.02	0.83	0.43	2.91	< 5
T115	5.18	338	< 1	11	159	88	135	3.9	21.3	1.04	1.07	0.09	3.6	< 5
T116	4.7	181	< 1	11	380	87	147	4	15.6	1.06	0.78	< 0.01	2.66	< 5
T117	4.57	198	< 1	8	256	71	110	3.4	18.5	1.03	0.4	0.19	1.39	< 5
T118	5.07	236	< 1	9	242	80	138	4.3	12.7	1.07	0.11	0.13	0.36	< 5
T134	2.98	1732	1	< 1	1116	38	11	2.1	16	1.07	0.29	0.03	0.89	< 5
T139	13.75	43	< 1	36	162	331	89	10.8	20	1.03	1.86	0.38	6.15	< 5
T140	14.57	101	< 1	38	183	351	92	10.5	58	1.03	1.41	0.65	4.75	< 5
T141	13.87	134	< 1	36	190	330	92	10.9	128	1.01	1.46	1.22	4.75	< 5
T142	11.65	213	< 1	30	223	285	88	8.7	95	1.01	1.59	4.81	5.45	< 5
T154	5.26	249	< 1	9	354	75	139	4.1	15	1.04	0.7	0.02	2.32	< 5
T156	6.76	177	< 1	12	284	98	114	4.8	< 1	1.04	1.28	0.79	4.31	< 5
T157	7.2	207	< 1	11	267	89	113	4.3	17	1.07	1.14	4.48	3.77	< 5
T158	6.55	194	< 1	9	234	74	90	3.7	12	1	0.86	3.97	2.84	< 5
T159	0.9	17	< 1	< 1	8	7	5	0.4	23	1.02	0.09	0.18	0.29	< 5
T162	2.87	297	< 1	3	242	19	148	2.2	3	1.01	0.22	1.15	0.86	< 5
T164	5.7	228	< 1	10	301	87	122	4.2	13	1.07	0.2	0.02	0.8	< 5
T165	2.13	66	6	2	353	25	675	1.1	3	1.03	1.15	0.11	4	< 5
T182	14.37	4	< 1	43	192	345	69	10.1	< 1	1.03	0.42	0.21	1.43	< 5
T183	4.86	234	< 1	9	171	67	123	4	25	1.01	0.88	0.01	3.35	9
T184	5.55	162	< 1	11	263	84	136	4.1	25	1.02	1.14	0.18	4.03	< 5
T186	5.47	134	< 1	10	228	78	129	4.8	56	1	1.52	0.26	5.11	
T187	0.95	29	< 1	1	19	11	14	0.3	8	1.04	0.2	0.28	0.69	< 5
T188	4.65	174	< 1	9	117	70	110	2.9	62	1.01	1.69	2.14	5.88	< 5
T189	2.2	331	4	1	213	18	51	1	< 1	1.07	0.07	< 0.01	0.22	< 5

Analyte	Fe <sub>2</sub> O <sub>3</sub> T	Ba	Be	Sc	Sr	V	Zr	FeO	B	Mass	C-Total	S-Total	CO <sub>2</sub>	Hg
Units	%	ppm	ppm	ppm	ppm	ppm	ppm	%	ppm	g	%	%	%	ppb
DL	0.01	2	1	1	2	5	1	0.1	0.5, 1		0.01	0.01	0.01	5
Method	FUS-ICP	FUS-ICP	FUS-ICP	FUS-ICP	FUS-ICP	FUS-ICP	FUS-ICP	TITR	PGNAA	PGNAA	CS	CS	CO <sub>2</sub>	1G
T192	4.36	264	< 1	9	325	72	122	3.8	1	1.05	0.33	0.02	1.05	< 5
T193	2.46	222	< 1	4	159	32	44	1.7	< 1	1.06	0.25	0.15	0.87	< 5
T194	4.37	258	< 1	8	174	73	68	3.5	4	1.05	0.42	0.3	1.41	< 5
T195	4.27	336	< 1	8	228	73	76	3	15	1	0.59	1.68	1.89	< 5
T196	1.94	163	< 1	4	56	26	24	0.1	5	1.03	0.14	0.97	0.5	< 5
T200	11.97	13	< 1	17	172	127	23	8.8	4	1.03	< 0.01	< 0.01	< 0.01	< 5
T213	7.09	333	1	17	402	121	136	6	12	1.02	3.77	< 0.01	12.6	
T215	2.21	123	1	2	376	40	177	1.3	176	1.06	0.51	0.02	1.74	
T216	7.1	1015	2	15	1238	129	159	5.1	11	1.07	3.75	0.2	13	
T218	4.92	231	< 1	10	278	80	102	3.7	45	1.02	1.74	0.02	5.89	
T228	7.47	273	1	24	901	175	218	4.5	11	1.05	3.47	0.4	11.8	
T239	6.01	22	< 1	15	131	101	121	5.2	9	1.04	4.62	< 0.01	15.7	
T240	7.06	81	1	19	488	130	103	6	22	1.08	3.27	0.06	11.5	
T241	4.52	214	< 1	9	159	70	114	3.7	6	1.06	0.11	0.01	0.39	
T242	7.33	433	3	22	790	148	146	4.7	7	1.03	1.91	0.03	6.53	
T245	8.43	139	1	31	628	206	219	7	11	1.02	2.26	0.28	7.92	
STPL-BAS-023	10.73	16	< 1	38	114	259	31	8.3	< 1	1.07	0.05	0.09	0.14	
STPL-BAS-025	10.59	12	< 1	38	112	250	32	7.8			0.05	0.08	0.17	
STPL-BAS-026	10.56	12	< 1	36	111	243	31	7.3			0.07	0.08	0.2	
STPL-BAS-027	10.23	16	< 1	39	118	266	18	7.1	5	1.06	0.07	0.07	0.21	
STPL-BAS-029	10.81	16	< 1	38	115	252	31	6.8	13.9	1.07	0.02	0.07	0.21	< 5
STPL-BAS-030	10.88	16	< 1	39	118	255	33	6.7	6.1	1.09	0.04	0.07	0.17	< 5



Analyte	Fe <sub>2</sub> O <sub>3</sub> T	Ba	Be	Sc	Sr	V	Zr	FeO	B	Mass	C-Total	S-Total	CO <sub>2</sub>	Hg
Units	%	ppm	ppm	ppm	ppm	ppm	ppm	%	ppm	g	%	%	%	ppb
DL	0.01	2	1	1	2	5	1	0.1	0.5, 1		0.01	0.01	0.01	5
Method	FUS-ICP	FUS-ICP	FUS-ICP	FUS-ICP	FUS-ICP	FUS-ICP	FUS-ICP	TITR	PGNAA	PGNAA	CS	CS	CO2	1G
STPL-BAS-053	10.81	10	< 1	38	112	250	30	7.7	7	1.02	0.05	0.07	0.17	
STPL-53-PML-025	1.28	530	1	3	144	16	102	0.8	45.7	1.08	0.29	0.07	0.99	< 5
STPL-PML-53-027	1.25	515	1	3	144	11	110	0.5	37	1.02	0.3	0.06	0.95	
STPL-53-PML-036	1.43	523	1	3	143	13	108	1.2			0.31	0.07	0.97	

Analyte	As	Bi	Sb	Se	Te	Au	Au	Au	Pd	Pt	Ag	As	Bi	Ce	Co	Cr
Units	ppm	ppm	ppm	ppm	ppm	ppb	g/tonne	ppb	ppb	ppb	ppm	ppm	ppm	ppm	ppm	ppm
DL	0.1	0.02	0.02	0.1	0.02	5	0.03	1	0.5	0.5	0.5	5	0.1	0.05	1	20
Method	AR-MS	AR-MS	AR-MS	AR-MS	AR-MS	FA-AA	FA-GRA	FA-MS	FA-MS	FA-MS	FUS-MS	FUS-MS	FUS-MS	FUS-MS	FUS-MS	FUS-MS
T6	6.4	0.03	0.03	0.1	0.09			18	< 0.5	< 0.5	1.1	< 5	< 0.1	28.4	8	40
T8	4	0.05	< 0.02	< 0.1	0.05			11	< 0.5	< 0.5	0.9	< 5	< 0.1	55.2	15	100
T9	4.4	0.03	< 0.02	0.4	0.05			6	4.4	7.6	0.7	< 5	< 0.1	25.6	48	170
T11	3.7	< 0.02	0.06	< 0.1	< 0.02			6	< 0.5	0.5	0.8	< 5	< 0.1	53.6	16	50
T12	4.2	0.24	< 0.02	0.1	0.04			9	< 0.5	< 0.5	0.7	< 5	< 0.1	30.6	48	80
T13	3.7	< 0.02	< 0.02	< 0.1	0.03			30	< 0.5	< 0.5	0.7	< 5	< 0.1	63.8	10	60
T14	4.6	< 0.02	0.02	0.3	0.04			26	2.6	2.6	0.5	< 5	< 0.1	12.6	38	170
T15	6.2	0.03	< 0.02	0.1	0.05			11	2.6	1.4	1.7	5	< 0.1	97.4	35	750
T16	6.1	0.09	0.02	< 0.1	0.06			24	3.2	2.7	1.5	8	0.1	172	26	370
T17	24.4	0.15	0.05	0.5	0.13			928	< 0.5	< 0.5	0.6	15	< 0.1	45.5	10	40
T19	24.3	< 0.02	< 0.02	0.2	0.07			59	5.5	5.7	< 0.5	24	< 0.1	11.3	41	210
T20	35.8	0.06	< 0.02	0.3	0.13			418	< 0.5	< 0.5	0.6	31	< 0.1	45.6	10	40
T21	5.2	< 0.02	0.96	< 0.1	0.02			54	< 0.5	< 0.5	< 0.5	< 5	< 0.1	49	3	70
T24	4.1	0.06	0.02	0.6	0.13			60	0.8	< 0.5	< 0.5	< 5	< 0.1	4.11	< 1	< 20
T27	6.7	0.15	0.04	< 0.1	0.07			13	< 0.5	< 0.5	< 0.5	< 5	< 0.1	49.2	10	30
T29	4	0.03	< 0.02	< 0.1	0.05			8	< 0.5	< 0.5	< 0.5	< 5	< 0.1	33.3	26	70
T31	3	< 0.02	0.31	< 0.1	< 0.02			10	< 0.5	< 0.5	< 0.5	< 5	< 0.1	49.1	10	100
T32	3.3	< 0.02	< 0.02	< 0.1	< 0.02			9	< 0.5	< 0.5	< 0.5	< 5	< 0.1	24.6	< 1	< 20
T37	95.6	< 0.02	1.99	0.2	0.16			35	0.8	0.5	< 0.5	64	< 0.1	5.82	6	< 20
T38	12.2	< 0.02	0.21	0.1	< 0.02			14	< 0.5	< 0.5	< 0.5	7	< 0.1	2.27	3	70
T39	5.3	< 0.02	0.03	< 0.1	< 0.02			10	< 0.5	0.5	< 0.5	< 5	< 0.1	10.6	37	180
T42	4.6	0.03	< 0.02	0.2	< 0.02			12	0.5	0.7	< 0.5	< 5	< 0.1	26	26	280
T43	12.7	0.32	0.05	0.2	0.14			26	< 0.5	< 0.5	< 0.5	11	0.2	58.4	15	40
T45	4	< 0.02	< 0.02	< 0.1	0.06			3	< 0.5	< 0.5	< 0.5	< 5	< 0.1	25.5	< 1	< 20
T50	< 0.1	0.02	0.5	< 0.1	< 0.02			2	3.6	1.8	0.6	< 5	< 0.1	108	38	830
T56	42.3	0.05	0.1	< 0.1	0.92		45	> 30000	< 0.5	< 0.5	< 0.5	44	< 0.1	21.3	10	30

Analyte	As	Bi	Sb	Se	Te	Au	Au	Au	Pd	Pt	Ag	As	Bi	Ce	Co	Cr
Units	ppm	ppm	ppm	ppm	ppm	ppb	g/tonne	ppb	ppb	ppb	ppm	ppm	ppm	ppm	ppm	ppm
DL	0.1	0.02	0.02	0.1	0.02	5	0.03	1	0.5	0.5	0.5	5	0.1	0.05	1	20
Method	AR-MS	AR-MS	AR-MS	AR-MS	AR-MS	FA-AA	FA-GRA	FA-MS	FA-MS	FA-MS	FUS-MS	FUS-MS	FUS-MS	FUS-MS	FUS-MS	FUS-MS
T58	13.7	0.03	0.03	< 0.1	0.08			453	< 0.5	< 0.5	0.7	18	< 0.1	52.8	6	90
T59	6.8	< 0.02	0.07	< 0.1	0.03			130	< 0.5	< 0.5	0.6	8	< 0.1	46	9	80
T63	2.6	0.03	0.07	< 0.1	< 0.02			18	1.9	1.1	< 0.5	< 5	< 0.1	95.7	36	890
T65	< 0.1	< 0.02	0.44	< 0.1	< 0.02			12	< 0.5	< 0.5	0.7	< 5	< 0.1	52.7	15	50
T66	2	0.06	0.06	< 0.1	< 0.02			13	7	4.2	0.7	11	< 0.1	192	34	210
T71	414	0.46	0.18	1.8	1.73		40	> 30000	0.6	< 0.5	1	423	0.4	21.1	17	30
T72	102	0.31	0.07	< 0.1	0.19			833	< 0.5	< 0.5	< 0.5	108	0.8	44.5	23	40
T73	8.2	0.06	0.03	< 0.1	0.15			195	< 0.5	< 0.5	0.8	10	< 0.1	29.4	18	30
T80	0.2	< 0.02	0.54	< 0.1	< 0.02			10	7.6	5.9	< 0.5	< 5	< 0.1	8.13	45	300
T81	< 0.1	< 0.02	0.03	< 0.1	< 0.02			4	3	1.5	0.5	< 5	< 0.1	103	37	880
T83	0.7	0.11	0.09	< 0.1	< 0.02			3	< 0.5	1	0.6	< 5	0.1	30	48	90
T85	104	0.24	0.07	< 0.1	0.05			1490	< 0.5	< 0.5	0.5	104	0.2	30	12	20
T86	102	0.2	0.07	< 0.1	0.13			1650	< 0.5	< 0.5	0.6	112	0.2	27.5	21	20
T87	7.4	< 0.02	0.03	< 0.1	< 0.02			32	< 0.5	< 0.5	< 0.5	10	< 0.1	11.9	43	170
T88	1.1	< 0.02	0.04	< 0.1	0.02			70	< 0.5	< 0.5	< 0.5	< 5	< 0.1	28.2	16	< 20
T89	0.9	< 0.02	0.04	< 0.1	0.03			51	0.8	1.3	< 0.5	< 5	< 0.1	10.1	46	140
T90	139	0.14	0.18	0.8	2.82			6480	< 0.5	< 0.5	0.9	132	0.1	38	16	40
T94	34.7	0.04	< 0.02	< 0.1	0.11			240	< 0.5	< 0.5	0.6	41	< 0.1	26.6	14	< 20
T98	27.2	0.02	< 0.02	< 0.1	0.03			434	< 0.5	< 0.5	0.5	34	< 0.1	12.5	42	50
T99	323	0.46	0.19	< 0.1	0.34			2750	< 0.5	< 0.5	0.6	324	0.3	19.5	26	50
T100	175	0.19	0.15	< 0.1	0.45			24600	< 0.5	< 0.5	0.6	184	0.2	5.29	13	30
T101	171	0.15	0.03	< 0.1	0.15			624	< 0.5	< 0.5	< 0.5	194	0.1	10.9	44	50
T102	5.8	< 0.02	0.02	< 0.1	< 0.02			19	< 0.5	< 0.5	0.5	10	< 0.1	24.9	14	< 20
T104	16.6	0.02	0.05	< 0.1	0.88			10500	< 0.5	< 0.5	< 0.5	24	< 0.1	0.93	< 1	30
T105	277	0.36	0.08	< 0.1	0.34			2880	< 0.5	< 0.5	0.7	260	0.3	39.9	16	80
T106	< 0.1	< 0.02	0.41	< 0.1	< 0.02			1740	2	2.2	0.5	< 5	< 0.1	16.7	38	140

Analyte	As	Bi	Sb	Se	Te	Au	Au	Au	Pd	Pt	Ag	As	Bi	Ce	Co	Cr
Units	ppm	ppm	ppm	ppm	ppm	ppb	g/tonne	ppb	ppb	ppb	ppm	ppm	ppm	ppm	ppm	ppm
DL	0.1	0.02	0.02	0.1	0.02	5	0.03	1	0.5	0.5	0.5	5	0.1	0.05	1	20
Method	AR-MS	AR-MS	AR-MS	AR-MS	AR-MS	FA-AA	FA-GRA	FA-MS	FA-MS	FA-MS	FUS-MS	FUS-MS	FUS-MS	FUS-MS	FUS-MS	FUS-MS
T113	112	0.16	0.08	< 0.1	0.12			2210	< 0.5	< 0.5	0.6	109	0.2	39.5	14	70
T114	48.3	0.03	0.07	< 0.1	0.06			88	< 0.5	< 0.5	0.6	43	< 0.1	45.5	13	80
T115	10.7	< 0.02	< 0.02	< 0.1	< 0.02			22	< 0.5	< 0.5	0.5	15	< 0.1	43.7	14	70
T116	0.4	0.02	0.02	< 0.1	< 0.02			2	< 0.5	< 0.5	0.6	< 5	< 0.1	51.3	13	90
T117	< 0.1	0.08	< 0.02	< 0.1	0.02			22	< 0.5	< 0.5	< 0.5	< 5	< 0.1	26.8	10	20
T118	< 0.1	0.03	0.65	< 0.1	< 0.02			7	< 0.5	< 0.5	0.6	< 5	< 0.1	48.8	11	40
T134	< 0.1	0.05	< 0.02	< 0.1	0.02			1	< 0.5	< 0.5	< 0.5	< 5	< 0.1	34.4	3	< 20
T139	0.1	0.04	0.06	< 0.1	0.08			44	2.1	1.8	< 0.5	< 5	< 0.1	12.7	39	120
T140	4.1	0.04	0.04	< 0.1	0.11			453	1.9	1.6	< 0.5	< 5	< 0.1	12.5	38	110
T141	3.6	0.03	0.03	< 0.1	0.18			608	2	1.7	< 0.5	< 5	< 0.1	13.4	41	120
T142	130	0.35	0.07	1.2	0.47			6780	1.9	1.6	< 0.5	93	0.2	15	35	130
T154	< 0.1	< 0.02	0.09	< 0.1	< 0.02			5	< 0.5	< 0.5	< 0.5	< 5	< 0.1	44.4	11	30
T156	11	0.04	0.07	< 0.1	0.04			602	< 0.5	< 0.5	< 0.5	10	< 0.1	40.5	16	60
T157	127	0.11	0.09	0.6	0.34			2490	< 0.5	< 0.5	< 0.5	82	< 0.1	46.8	18	40
T158	140	0.09	0.12	0.5	0.26			1400	< 0.5	< 0.5	< 0.5	105	< 0.1	33.4	17	80
T159	3.8	0.04	0.02	< 0.1	3.75			2110	< 0.5	< 0.5	2.1	< 5	< 0.1	0.81	1	< 20
T162	54.2	0.12	0.05	< 0.1	0.2			606	< 0.5	< 0.5	0.8	49	< 0.1	29.9	4	30
T164	0.2	< 0.02	0.04	< 0.1	0.02			11	< 0.5	< 0.5	0.5	< 5	< 0.1	33.8	16	90
T165	< 0.1	1.9	0.11	< 0.1	0.23			2	< 0.5	< 0.5	2.3	< 5	1.4	107	4	< 20
T182	8.5	< 0.02	0.09	0.2	0.04			5	2	4.7	< 0.5	8	< 0.1	11.1	56	60
T183	< 0.1	< 0.02	0.04	< 0.1	< 0.02			1	< 0.5	< 0.5	< 0.5	< 5	< 0.1	39.6	10	60
T184	4.6	0.04	0.02	< 0.1	0.03			44	< 0.5	< 0.5	< 0.5	7	< 0.1	39.5	16	70
T186	16.2	0.3	0.08	< 0.1	0.03	125					< 0.5	18	< 0.1	47.2	15	70
T187	33.8	0.02	0.05	< 0.1	0.34			3480	< 0.5	< 0.5	< 0.5	29	< 0.1	5.38	2	100
T188	155	0.09	0.09	0.4	2.34			3830	2.2	< 0.5	1.3	114	< 0.1	37.1	13	90
T189	< 0.1	0.17	< 0.02	< 0.1	< 0.02			9	< 0.5	< 0.5	< 0.5	< 5	0.1	34.5	2	30

Analyte	As	Bi	Sb	Se	Te	Au	Au	Au	Pd	Pt	Ag	As	Bi	Ce	Co	Cr
Units	ppm	ppm	ppm	ppm	ppm	ppb	g/tonne	ppb	ppb	ppb	ppm	ppm	ppm	ppm	ppm	ppm
DL	0.1	0.02	0.02	0.1	0.02	5	0.03	1	0.5	0.5	0.5	5	0.1	0.05	1	20
Method	AR-MS	AR-MS	AR-MS	AR-MS	AR-MS	FA-AA	FA-GRA	FA-MS	FA-MS	FA-MS	FUS-MS	FUS-MS	FUS-MS	FUS-MS	FUS-MS	FUS-MS
T192	< 0.1	0.13	0.03	< 0.1	< 0.02			23	< 0.5	< 0.5	< 0.5	< 5	0.2	35.9	11	< 20
T193	< 0.1	0.17	0.06	< 0.1	0.06			52	< 0.5	< 0.5	< 0.5	< 5	< 0.1	37.8	5	80
T194	< 0.1	0.15	0.02	< 0.1	0.07			116	< 0.5	< 0.5	0.5	< 5	< 0.1	31.8	10	70
T195	73.5	0.96	0.06	0.1	0.62			1480	< 0.5	< 0.5	0.8	59	0.4	33.2	10	< 20
T196	55.2	1.57	0.09	0.2	1.76		50.5	> 30000	0.7	< 0.5	1	44	0.7	13.1	5	100
T200	16.7	< 0.02	0.04	< 0.1	0.02			8	1.3	1.4	< 0.5	14	< 0.1	5.31	64	270
T213	11.5	0.28	0.05	< 0.1	< 0.02	57					< 0.5	13	< 0.1	114	22	770
T215	1.9	0.29	0.05	< 0.1	< 0.02	6					0.6	< 5	< 0.1	72	4	30
T216	5.2	0.4	0.07	0.2	< 0.02	11					0.6	7	< 0.1	118	26	250
T218	< 0.1	0.24	0.06	< 0.1	< 0.02	11					< 0.5	< 5	< 0.1	22.8	14	30
T228	8.6	0.29	0.15	< 0.1	< 0.02	23					0.7	10	< 0.1	173	25	250
T239	1.6	0.22	0.04	0.1	< 0.02	< 5					< 0.5	< 5	< 0.1	99.9	34	800
T240	< 0.1	0.29	0.03	< 0.1	< 0.02	< 5					< 0.5	5	0.1	65.7	29	560
T241	< 0.1	0.21	0.05	< 0.1	< 0.02	< 5					< 0.5	< 5	< 0.1	29.7	10	< 20
T242	4.5	0.27	0.19	0.2	< 0.02	< 5					< 0.5	8	< 0.1	99.2	29	300
T245	8.1	0.32	0.03	< 0.1	0.11	81					0.7	11	< 0.1	192	33	260
STPL-BAS-023	1.5	< 0.02	0.29	< 0.1	0.02			7	13.9	9.9	< 0.5	< 5	< 0.1	5.49	49	310
STPL-BAS-025	4.9	< 0.02	0.21	0.2	0.05			9	10	8.2	< 0.5	< 5	< 0.1	6.24	49	330
STPL-BAS-026	5.1	< 0.02	0.29	0.3	0.05			8	10.2	8.5	< 0.5	< 5	< 0.1	5.6	47	310
STPL-BAS-027	1.5	< 0.02	0.36	< 0.1	0.03			6	13.6	9.6	< 0.5	< 5	< 0.1	5.63	49	310
STPL-BAS-029	2.2	< 0.02	0.26	< 0.1	< 0.02			6	11.2	8	0.6	< 5	< 0.1	5.58	49	340
STPL-BAS-030	2	< 0.02	0.26	< 0.1	0.1			3	10.6	7.4	< 0.5	6	< 0.1	5.44	46	310

Analyte	As	Bi	Sb	Se	Te	Au	Au	Au	Pd	Pt	Ag	As	Bi	Ce	Co	Cr
Units	ppm	ppm	ppm	ppm	ppm	ppb	g/tonne	ppb	ppb	ppb	ppm	ppm	ppm	ppm	ppm	ppm
DL	0.1	0.02	0.02	0.1	0.02	5	0.03	1	0.5	0.5	0.5	5	0.1	0.05	1	20
Method	AR-MS	AR-MS	AR-MS	AR-MS	AR-MS	FA-AA	FA-GRA	FA-MS	FA-MS	FA-MS	FUS-MS	FUS-MS	FUS-MS	FUS-MS	FUS-MS	FUS-MS
STPL-BAS-053	82	0.98	1.31	0.9	0.1	9					< 0.5	64	0.5	5.58	50	320
STPL-53-PML-025	40	0.09	0.08	< 0.1	0.04			12	< 0.5	< 0.5	< 0.5	35	< 0.1	72.8	< 1	40
STPL-PML-53-027	39.8	0.12	0.25	< 0.1	0.02			5	< 0.5	< 0.5	< 0.5	33	< 0.1	75.6	< 1	50
STPL-53-PML-036	40.6	0.11	0.15	< 0.1	< 0.02			6	< 0.5	< 0.5	< 0.5	37	< 0.1	76.9	1	50

Analyte	Cs	Cu	Dy	Er	Eu	Ga	Gd	Ge	Hf	Ho	In	La	Lu	Mo	Nb
Units	ppm	ppm	ppm	ppm	ppm	ppm	ppm	ppm	ppm	ppm	ppm	ppm	ppm	ppm	ppm
DL	0.1	10	0.01	0.01	0.005	1	0.01	0.5	0.1	0.01	0.1	0.05	0.002	2	0.2
Method	FUS-MS	FUS-MS	FUS-MS	FUS-MS	FUS-MS	FUS-MS	FUS-MS	FUS-MS	FUS-MS	FUS-MS	FUS-MS	FUS-MS	FUS-MS	FUS-MS	FUS-MS
T6	1.3	30	1.33	0.66	0.645	20	1.71	1	3.2	0.23	< 0.1	14.4	0.1	< 2	3
T8	0.8	60	2.68	1.42	1.34	20	3.49	1.4	3.6	0.54	< 0.1	24.5	0.22	< 2	5.5
T9	1	210	4.52	2.71	1.21	19	4.19	1.5	2.5	0.93	< 0.1	11.8	0.414	< 2	4.1
T11	0.5	90	2.42	1.29	1.11	20	3.08	1.1	3.2	0.44	< 0.1	26.9	0.203	< 2	3.7
T12	0.9	200	5.76	3.32	1.41	19	5.25	1.7	3.1	1.17	< 0.1	14.1	0.545	< 2	5
T13	2.1	40	2.29	1.2	1.25	21	3.35	0.9	3.4	0.42	< 0.1	30.7	0.171	< 2	3.9
T14	0.3	110	4.82	3.22	1.04	17	3.66	1.3	2.2	1.05	< 0.1	5.22	0.546	< 2	2.6
T15	0.7	30	2.49	1.24	1.45	14	4.02	1.1	3.6	0.43	< 0.1	45	0.207	< 2	5.2
T16	0.8	50	6.79	2.76	4.28	15	12.8	1.4	5.4	1.11	< 0.1	76.9	0.337	< 2	8.2
T17	3	10	1.9	0.93	0.959	18	2.42	0.9	3	0.36	< 0.1	21.2	0.143	< 2	3.8
T19	0.8	120	2.91	1.68	0.676	15	2.4	1.3	1.3	0.59	< 0.1	4.61	0.255	< 2	1.9
T20	2.2	20	1.75	0.91	0.912	19	2.41	1	3.1	0.34	< 0.1	21.7	0.137	< 2	4.1
T21	1.5	20	2.54	1.45	1.23	15	3.07	3.1	4.4	0.49	< 0.1	23.4	0.222	< 2	5.6
T24	< 0.1	20	0.55	0.39	0.493	2	0.52	< 0.5	0.3	0.12	< 0.1	2.36	0.074	< 2	< 0.2
T27	3.1	70	1.72	0.89	1.08	19	2.5	1.2	2.9	0.34	< 0.1	23.2	0.141	< 2	3.5
T29	0.5	30	2.02	1.14	0.853	19	2.32	1.1	2.8	0.39	< 0.1	16.1	0.187	< 2	3.9
T31	0.8	20	2.46	1.4	1.58	22	3.2	2.1	4.1	0.47	< 0.1	24.3	0.223	< 2	5.8
T32	1	< 10	1.91	0.99	0.332	20	2.06	1.3	1.9	0.37	< 0.1	13	0.136	< 2	4.5
T37	< 0.1	< 10	0.99	0.69	0.505	1	0.8	< 0.5	0.1	0.22	< 0.1	3.3	0.108	< 2	< 0.2
T38	0.6	< 10	0.49	0.3	0.187	4	0.42	1	0.2	0.1	< 0.1	1.03	0.042	< 2	< 0.2
T39	0.1	40	3.98	2.38	0.787	15	3.17	1.5	1.8	0.82	< 0.1	4	0.375	< 2	2.3
T42	0.3	20	1.69	0.92	0.831	16	2.19	0.9	2.1	0.35	< 0.1	11.9	0.128	< 2	1.7
T43	2.3	80	2	0.93	1.22	18	2.64	1.3	3.6	0.35	< 0.1	27.9	0.149	2	3.5
T45	0.9	10	1.97	1.02	0.839	17	2.3	1.1	1.9	0.37	< 0.1	11.7	0.137	< 2	4.3
T50	0.7	< 10	2.88	1.38	1.75	15	4.49	1.2	3.6	0.51	< 0.1	53.8	0.187	< 2	5.6
T56	1.9	10	1.52	0.88	0.595	12	1.65	2	1.7	0.3	< 0.1	9.82	0.136	3	2.1

Analyte	Cs	Cu	Dy	Er	Eu	Ga	Gd	Ge	Hf	Ho	In	La	Lu	Mo	Nb
Units	ppm	ppm	ppm	ppm	ppm	ppm	ppm	ppm	ppm	ppm	ppm	ppm	ppm	ppm	ppm
DL	0.1	10	0.01	0.01	0.005	1	0.01	0.5	0.1	0.01	0.1	0.05	0.002	2	0.2
Method	FUS-MS	FUS-MS	FUS-MS	FUS-MS	FUS-MS	FUS-MS	FUS-MS	FUS-MS	FUS-MS	FUS-MS	FUS-MS	FUS-MS	FUS-MS	FUS-MS	FUS-MS
T58	3.9	60	2.27	1.03	1.05	25	3.37	1.5	3.2	0.42	< 0.1	24	0.145	< 2	4.4
T59	0.9	40	2.31	1.08	1.08	21	3.12	1.2	2.8	0.41	< 0.1	20.4	0.129	< 2	4.5
T63	0.3	30	2.54	1.28	1.55	15	4.22	0.9	2.8	0.45	< 0.1	46	0.159	< 2	4.6
T65	2.7	70	2.17	1.21	1.07	19	3.04	0.9	3.3	0.4	< 0.1	25	0.169	< 2	3.6
T66	5.5	90	7.61	2.85	5.28	17	14.9	1.6	4.5	1.18	< 0.1	88.6	0.304	< 2	6.2
T71	1.5	50	1.47	0.81	0.473	13	1.66	1.5	1.5	0.29	< 0.1	10.1	0.137	3	1.5
T72	1.9	110	2.06	1.04	0.98	19	2.52	1.4	3.1	0.37	< 0.1	22.3	0.131	< 2	2.9
T73	1.2	50	1.69	0.92	0.696	21	2.13	1.2	2.7	0.33	< 0.1	14.4	0.151	2	2.9
T80	0.3	110	2.67	1.5	0.683	14	2.26	1.3	1.4	0.53	< 0.1	3.3	0.223	< 2	1.6
T81	0.2	< 10	2.67	1.27	1.99	13	4.26	1.1	2.9	0.43	< 0.1	49.7	0.169	< 2	4.6
T83	0.7	150	5.57	3.46	1.38	21	5.77	1.7	2.6	1.16	< 0.1	12.9	0.497	< 2	22.7
T85	1	50	1.65	1	0.676	21	2.05	1.1	2.6	0.33	< 0.1	15.1	0.143	3	2.9
T86	3.3	20	1.82	1	0.735	25	2.17	1.3	2.9	0.33	< 0.1	13.7	0.136	2	2.8
T87	1.1	80	4.06	2.43	0.78	18	3.23	1.3	1.7	0.83	< 0.1	4.99	0.388	< 2	2.5
T88	1.4	30	1.67	0.93	0.75	20	2.14	1.3	2.6	0.32	< 0.1	14.6	0.148	< 2	2.5
T89	0.4	180	3.81	2.41	0.803	17	3.18	1.3	1.5	0.81	< 0.1	3.69	0.394	< 2	2.2
T90	2.3	60	1.67	0.85	0.827	22	2.25	1.6	2.2	0.32	< 0.1	18.2	0.131	< 2	2.6
T94	2.8	< 10	1.13	0.6	0.601	26	1.72	1.1	3.1	0.22	< 0.1	12.5	0.102	< 2	2.6
T98	0.3	140	4.68	3.11	0.936	19	3.93	1.4	1.8	1.04	< 0.1	4.45	0.507	< 2	2.7
T99	0.4	110	3.25	1.99	0.598	16	2.89	1.5	1.8	0.68	< 0.1	8.52	0.267	< 2	2.6
T100	0.5	50	1.24	0.82	0.272	7	1.27	2.7	0.5	0.28	< 0.1	2.1	0.141	< 2	0.6
T101	0.1	80	4.07	2.63	0.709	18	3.19	1.5	1.8	0.86	< 0.1	3.89	0.411	< 2	2.5
T102	1.1	30	1.95	1.12	0.752	22	2.25	1.1	2.6	0.37	< 0.1	11.6	0.15	< 2	2.4
T104	0.1	10	0.09	0.06	0.023	< 1	0.12	2.8	< 0.1	0.02	< 0.1	0.2	0.01	< 2	< 0.2
T105	2.8	80	2.32	1.23	0.922	19	2.95	1.8	2.8	0.44	< 0.1	18.4	0.158	< 2	4.6
T106	0.8	20	6.52	3.93	1.07	19	5.29	1.3	3	1.3	< 0.1	6.41	0.629	< 2	3.6



Analyte	Cs	Cu	Dy	Er	Eu	Ga	Gd	Ge	Hf	Ho	In	La	Lu	Mo	Nb
Units	ppm	ppm	ppm	ppm	ppm	ppm	ppm	ppm	ppm	ppm	ppm	ppm	ppm	ppm	ppm
DL	0.1	10	0.01	0.01	0.005	1	0.01	0.5	0.1	0.01	0.1	0.05	0.002	2	0.2
Method	FUS-MS	FUS-MS	FUS-MS	FUS-MS	FUS-MS	FUS-MS	FUS-MS	FUS-MS	FUS-MS	FUS-MS	FUS-MS	FUS-MS	FUS-MS	FUS-MS	FUS-MS
T113	2.7	40	1.97	1.14	0.898	18	2.68	1.4	2.8	0.38	< 0.1	17.7	0.153	< 2	4.1
T114	3.6	90	2.34	1.23	1.09	21	3.15	1.3	2.9	0.42	< 0.1	20.3	0.155	< 2	4.9
T115	2.6	30	2.35	1.2	1.04	20	3.12	1.2	2.9	0.43	< 0.1	19.8	0.162	< 2	4.2
T116	1.2	< 10	2.32	1.15	1.13	21	3.44	1.1	3.3	0.42	< 0.1	23.3	0.159	< 2	5.5
T117	1.1	50	1.36	0.74	0.531	21	1.76	0.9	2.3	0.25	< 0.1	13.1	0.125	2	2.4
T118	1.8	30	2.14	1.19	1.19	18	3.01	0.9	3.3	0.4	< 0.1	23.3	0.168	< 2	3.5
T134	3.1	< 10	0.95	0.46	0.53	19	1.24	< 0.5	0.2	0.17	< 0.1	16.1	0.055	< 2	8.4
T139	1	60	5.46	3.55	1.19	19	4.31	1.3	2.4	1.17	< 0.1	4.63	0.582	< 2	2.7
T140	1.4	60	5.46	3.63	1.16	18	4.39	1.3	2.5	1.15	< 0.1	4.46	0.57	< 2	2.7
T141	2.3	60	5.83	3.7	1.21	18	4.42	1.2	2.5	1.21	< 0.1	4.87	0.599	< 2	2.6
T142	1.9	30	4.6	2.84	1	18	3.71	1.1	2.4	0.97	< 0.1	5.95	0.474	< 2	2.4
T154	1.5	< 10	1.92	0.98	0.984	20	2.59	1.3	3.4	0.35	< 0.1	21.4	0.141	< 2	3.6
T156	1.6	40	2.01	1.12	0.938	19	2.62	1	2.8	0.39	< 0.1	18.8	0.16	< 2	2.7
T157	2.4	20	2.65	1.28	1.32	20	3.26	1.1	3	0.47	< 0.1	21.8	0.175	< 2	2.7
T158	1.8	30	1.7	0.86	0.855	17	2.22	1.2	2.3	0.32	< 0.1	15.5	0.131	< 2	2.2
T159	0.1	< 10	0.18	0.08	0.051	1	0.15	1.8	0.1	0.03	< 0.1	0.35	0.008	< 2	< 0.2
T162	1.3	20	1.24	0.63	0.626	19	1.58	1.3	3.4	0.23	< 0.1	15.8	0.097	2	2.6
T164	1.9	20	1.76	0.92	0.902	20	2.25	1	3	0.33	< 0.1	16.7	0.143	< 2	2.8
T165	1.1	40	3.99	2.76	1.92	41	4.44	1.7	12.4	0.83	< 0.1	47.8	0.518	< 2	172
T182	0.2	190	4.35	2.72	1.04	16	3.53	1.6	1.9	0.88	< 0.1	4.11	0.43	< 2	2.9
T183	0.9	20	1.87	1.07	0.856	16	2.32	0.8	3.1	0.35	< 0.1	18.4	0.161	< 2	3.8
T184	0.9	40	2.14	1.16	0.943	18	2.63	1.1	3.3	0.4	< 0.1	18.3	0.176	< 2	4.5
T186	1.5	40	2.21	1.17	1.07	18	3.09	1	3.2	0.43	< 0.1	21.7	0.155	< 2	4.6
T187	0.4	< 10	0.24	0.12	0.126	3	0.31	3.2	0.3	0.05	< 0.1	2.51	0.019	6	0.4
T188	2.7	20	1.76	0.94	0.774	17	2.27	1.6	2.5	0.33	< 0.1	17.3	0.152	< 2	3.2
T189	2.9	< 10	0.72	0.41	0.429	24	1.1	0.8	1.2	0.14	< 0.1	18.1	0.076	< 2	12

Analyte	Cs	Cu	Dy	Er	Eu	Ga	Gd	Ge	Hf	Ho	In	La	Lu	Mo	Nb
Units	ppm	ppm	ppm	ppm	ppm	ppm	ppm	ppm	ppm	ppm	ppm	ppm	ppm	ppm	ppm
DL	0.1	10	0.01	0.01	0.005	1	0.01	0.5	0.1	0.01	0.1	0.05	0.002	2	0.2
Method	FUS-MS	FUS-MS	FUS-MS	FUS-MS	FUS-MS	FUS-MS	FUS-MS	FUS-MS	FUS-MS	FUS-MS	FUS-MS	FUS-MS	FUS-MS	FUS-MS	FUS-MS
T192	1	30	1.8	1	0.782	19	2.16	1	2.8	0.33	< 0.1	17.4	0.155	< 2	3.1
T193	0.7	60	1.36	0.74	0.417	19	1.75	1	2.1	0.25	< 0.1	18.9	0.125	< 2	2.2
T194	1.6	130	1.66	0.92	0.707	19	2	1.2	2.8	0.32	< 0.1	15.2	0.14	16	3.1
T195	1.4	170	1.65	0.98	0.734	20	2.02	1.5	3.2	0.32	< 0.1	15.8	0.161	17	4.6
T196	0.4	70	0.66	0.35	0.286	8	0.77	2.7	1	0.12	< 0.1	6.35	0.062	36	1
T200	0.1	50	2.12	1.38	0.59	16	1.68	1.2	0.9	0.44	< 0.1	2.12	0.229	< 2	1.2
T213	0.7	< 10	2.52	1.26	1.77	15	4.32	1.4	3.5	0.45	< 0.1	55.6	0.16	< 2	5.9
T215	0.2	10	1.68	0.96	0.972	20	2.39	0.7	4.3	0.31	< 0.1	40.1	0.163	< 2	13.7
T216	8.5	50	3.93	1.92	2.44	13	6.3	0.9	3.4	0.7	< 0.1	54.7	0.239	< 2	20.7
T218	1.1	30	1.47	0.84	0.645	18	1.72	1.1	2.7	0.28	< 0.1	10.9	0.119	< 2	2.7
T228	3.3	40	6.2	2.46	4.33	13	12.1	1.4	4.7	0.99	< 0.1	78.1	0.248	< 2	7.5
T239	0.4	< 10	2.56	1.26	1.32	13	3.72	1	3.1	0.46	< 0.1	49.4	0.151	< 2	5
T240	0.2	40	3.43	1.74	1.64	14	4.94	0.8	2.7	0.64	< 0.1	30.4	0.232	< 2	3.8
T241	1.1	< 10	1.6	0.9	0.655	19	1.99	0.8	3.1	0.31	< 0.1	15.4	0.128	< 2	2.9
T242	32.7	20	3.67	1.75	2.06	13	5.91	1.3	3.6	0.66	< 0.1	45.3	0.223	< 2	18.1
T245	0.8	40	7.29	2.8	4.67	14	14.3	1.1	5	1.15	< 0.1	87.2	0.287	< 2	6.5
STPL-BAS-023	0.2	120	2.32	1.4	0.643	16	1.92	1.7	0.9	0.48	< 0.1	2.06	0.231	< 2	1.4
STPL-BAS-025	0.2	130	2.35	1.49	0.656	16	2	1.5	1	0.5	< 0.1	2.47	0.221	< 2	1.5
STPL-BAS-026	0.2	110	2.33	1.44	0.662	15	1.85	1.4	0.9	0.47	< 0.1	1.96	0.213	< 2	1.5
STPL-BAS-027	0.2	130	2.34	1.49	0.653	16	2.01	1.5	0.9	0.51	< 0.1	2.08	0.226	< 2	1.4
STPL-BAS-029	0.3	120	2.42	1.43	0.643	17	2.04	1.7	0.8	0.5	< 0.1	1.8	0.23	< 2	1.4
STPL-BAS-030	0.2	120	2.24	1.45	0.622	17	2.08	1.4	0.7	0.47	< 0.1	1.72	0.214	< 2	1.3

Analyte	Cs	Cu	Dy	Er	Eu	Ga	Gd	Ge	Hf	Ho	In	La	Lu	Mo	Nb
Units	ppm	ppm	ppm	ppm	ppm	ppm	ppm	ppm	ppm	ppm	ppm	ppm	ppm	ppm	ppm
DL	0.1	10	0.01	0.01	0.005	1	0.01	0.5	0.1	0.01	0.1	0.05	0.002	2	0.2
Method	FUS-MS	FUS-MS	FUS-MS	FUS-MS	FUS-MS	FUS-MS	FUS-MS	FUS-MS	FUS-MS	FUS-MS	FUS-MS	FUS-MS	FUS-MS	FUS-MS	FUS-MS
STPL-BAS-053	0.2	120	2.32	1.38	0.605	15	1.83	1.4	0.9	0.48	< 0.1	1.93	0.219	< 2	1.5
STPL-53-PML-025	1.8	10	2.35	1.57	0.672	11	2.42	1.3	2.3	0.5	< 0.1	41.1	0.33	< 2	7.4
STPL-PML-53-027	2	20	2.41	1.66	0.699	12	2.59	1.4	2.7	0.5	< 0.1	42.2	0.329	< 2	8.5
STPL-53-PML-036	2.2	10	2.6	1.67	0.732	12	2.63	1.5	2.6	0.55	< 0.1	43.4	0.354	< 2	9

Analyte	Nd	Ni	Pb	Pr	Rb	Sb	Sm	Sn	Ta	Tb	Th	Tl	Tm	U	W
Units	ppm	ppm	ppm	ppm	ppm	ppm	ppm	ppm	ppm	ppm	ppm	ppm	ppm	ppm	ppm
DL	0.05	20	5	0.01	1	0.2	0.01	1	0.01	0.01	0.05	0.05	0.005	0.01	0.5
Method	FUS-MS	FUS-MS	FUS-MS	FUS-MS	FUS-MS	FUS-MS	FUS-MS	FUS-MS	FUS-MS	FUS-MS	FUS-MS	FUS-MS	FUS-MS	FUS-MS	FUS-MS
T6	11.7	< 20	< 5	3.14	25	< 0.2	2.11	< 1	0.25	0.24	2	0.2	0.094	0.42	1.8
T8	24.9	70	< 5	6.64	29	< 0.2	4.6	< 1	0.44	0.5	2.85	0.14	0.205	0.69	1.7
T9	13.8	90	5	3.24	20	< 0.2	3.63	1	0.31	0.72	1.83	0.1	0.419	0.51	< 0.5
T11	23.6	40	< 5	6.23	15	< 0.2	4	< 1	0.31	0.42	3.28	0.1	0.178	0.72	0.7
T12	17.2	50	< 5	3.96	19	< 0.2	4.44	1	0.32	0.91	1.87	0.16	0.512	0.47	< 0.5
T13	26.7	30	< 5	7.31	30	< 0.2	4.43	< 1	0.35	0.41	3.98	0.12	0.17	0.92	1
T14	9.11	90	< 5	1.87	2	< 0.2	2.84	< 1	0.12	0.73	0.43	< 0.05	0.49	0.12	0.5
T15	39.6	280	< 5	11.1	12	0.4	5.94	1	0.27	0.46	6.15	< 0.05	0.173	1.01	10.9
T16	88.7	140	6	21.8	21	0.8	16.7	2	0.35	1.54	9.8	< 0.05	0.368	2.86	15.8
T17	19.4	< 20	< 5	5.23	39	< 0.2	3.45	< 1	0.25	0.33	2.35	0.11	0.135	0.63	10.2
T19	7.28	80	< 5	1.54	12	0.7	2.1	< 1	0.16	0.47	0.44	< 0.05	0.247	0.13	6.8
T20	19.4	< 20	< 5	5.14	41	< 0.2	3.29	< 1	0.34	0.31	2.31	0.13	0.131	0.6	4.1
T21	20.6	< 20	< 5	5.42	41	0.6	3.57	4	0.55	0.43	2.6	1.07	0.221	0.47	3
T24	2.03	< 20	< 5	0.5	< 1	< 0.2	0.43	< 1	< 0.01	0.09	0.16	0.11	0.066	0.22	< 0.5
T27	21.3	30	< 5	5.74	57	< 0.2	3.4	< 1	0.27	0.32	2.98	0.29	0.13	0.59	3.5
T29	14.6	90	6	3.87	5	< 0.2	2.54	< 1	0.28	0.35	2.07	< 0.05	0.183	0.55	< 0.5
T31	20.5	30	< 5	5.43	12	0.6	3.52	< 1	0.58	0.44	3.22	< 0.05	0.215	0.82	< 0.5
T32	9.35	< 20	< 5	2.63	28	< 0.2	2.24	1	0.66	0.36	2.14	< 0.05	0.14	0.82	< 0.5
T37	2.69	< 20	< 5	0.66	< 1	0.9	0.6	< 1	< 0.01	0.13	0.17	< 0.05	0.108	0.23	< 0.5
T38	1.31	20	< 5	0.3	3	< 0.2	0.34	< 1	< 0.01	0.08	0.08	< 0.05	0.048	0.05	< 0.5
T39	7.88	80	< 5	1.59	< 1	< 0.2	2.48	< 1	0.12	0.55	0.34	< 0.05	0.357	0.11	5.2
T42	12.9	230	< 5	3.27	5	0.5	2.44	< 1	0.11	0.3	1.32	< 0.05	0.142	0.46	1.9
T43	25.1	40	< 5	6.66	39	< 0.2	3.9	< 1	0.28	0.36	3.64	0.13	0.136	0.86	8.1
T45	10.9	< 20	< 5	2.97	61	< 0.2	2.51	1	0.54	0.36	2.14	0.34	0.149	0.92	0.6
T50	44.1	250	< 5	12.1	9	0.6	6.86	< 1	0.29	0.55	6.96	0.07	0.184	1.16	4.6
T56	10	< 20	< 5	2.57	41	< 0.2	1.68	< 1	0.23	0.27	1.15	0.22	0.124	0.27	148

Analyte	Nd	Ni	Pb	Pr	Rb	Sb	Sm	Sn	Ta	Tb	Th	Tl	Tm	U	W
Units	ppm	ppm	ppm	ppm	ppm	ppm	ppm	ppm	ppm	ppm	ppm	ppm	ppm	ppm	ppm
DL	0.05	20	5	0.01	1	0.2	0.01	1	0.01	0.01	0.05	0.05	0.005	0.01	0.5
Method	FUS-MS	FUS-MS	FUS-MS	FUS-MS	FUS-MS	FUS-MS	FUS-MS	FUS-MS	FUS-MS	FUS-MS	FUS-MS	FUS-MS	FUS-MS	FUS-MS	FUS-MS
T58	23.4	20	6	6.11	97	< 0.2	4.23	< 1	0.43	0.45	2.93	0.24	0.145	0.54	565
T59	19.9	40	9	5.23	22	< 0.2	3.77	< 1	0.4	0.43	2.45	< 0.05	0.148	0.53	17.5
T63	37.4	270	5	10.4	4	0.6	5.94	< 1	0.26	0.52	5.6	< 0.05	0.169	1.06	5.1
T65	24.1	30	6	6.1	28	< 0.2	4.08	< 1	0.32	0.41	3.17	0.11	0.171	1.04	< 0.5
T66	97.8	50	9	23.8	22	0.4	19.1	1	0.24	1.69	9.27	< 0.05	0.341	2.57	10.5
T71	9.21	50	7	2.38	46	0.2	1.67	< 1	0.16	0.24	1.43	< 0.05	0.122	0.42	66.5
T72	19.4	40	< 5	5.08	67	< 0.2	3.41	< 1	0.33	0.36	3.05	0.17	0.145	0.75	13.8
T73	12	30	7	3.18	39	< 0.2	2.37	< 1	0.29	0.3	2.5	< 0.05	0.136	0.64	6.4
T80	5.67	100	< 5	1.17	4	0.3	1.71	< 1	0.11	0.44	0.31	0.14	0.223	0.09	0.6
T81	40.1	430	< 5	11.5	3	0.4	6.28	< 1	0.3	0.54	6.44	< 0.05	0.177	1.04	16.2
T83	16.4	50	5	3.82	17	< 0.2	4.82	< 1	8.46	0.92	3.72	< 0.05	0.513	0.82	5
T85	12.4	20	< 5	3.23	27	< 0.2	2.43	< 1	0.34	0.31	2.68	< 0.05	0.155	0.73	5.9
T86	11.3	30	9	3.01	70	0.2	2.25	< 1	0.32	0.3	3.08	< 0.05	0.151	0.86	212
T87	8.15	80	< 5	1.69	27	< 0.2	2.39	< 1	0.15	0.61	0.35	< 0.05	0.367	0.11	8.3
T88	11.4	30	< 5	3.05	41	< 0.2	2.25	< 1	0.28	0.31	2.53	< 0.05	0.142	0.7	7
T89	7.13	70	< 5	1.51	5	< 0.2	2.41	< 1	0.15	0.58	0.34	< 0.05	0.377	0.09	6.1
T90	16.1	30	< 5	4.4	62	< 0.2	2.81	< 1	0.28	0.31	2.41	< 0.05	0.126	0.61	422
T94	11.5	< 20	< 5	3.03	52	< 0.2	2.01	< 1	0.24	0.21	2.15	< 0.05	0.088	0.6	13.6
T98	9.23	60	< 5	1.84	4	< 0.2	2.87	< 1	0.2	0.7	0.36	< 0.05	0.495	0.12	13.3
T99	9.72	40	< 5	2.44	7	0.6	2.54	< 1	0.2	0.49	0.9	< 0.05	0.299	0.99	27.4
T100	3.31	20	< 5	0.74	8	0.2	0.94	< 1	0.06	0.2	0.15	< 0.05	0.132	0.07	11.2
T101	7.84	60	< 5	1.6	< 1	0.3	2.46	< 1	0.17	0.62	0.35	< 0.05	0.409	0.13	16
T102	11.3	20	< 5	2.81	21	< 0.2	2.16	< 1	0.19	0.33	1.48	< 0.05	0.164	0.39	4.1
T104	0.49	< 20	< 5	0.1	2	< 0.2	0.06	< 1	< 0.01	0.02	< 0.05	< 0.05	0.009	0.05	0.8
T105	17.9	60	< 5	4.6	55	< 0.2	3.29	< 1	0.39	0.41	2.3	< 0.05	0.176	0.59	12.6
T106	12.4	60	< 5	2.5	4	< 0.2	3.92	< 1	0.23	0.99	0.58	< 0.05	0.595	0.18	8

Analyte	Nd	Ni	Pb	Pr	Rb	Sb	Sm	Sn	Ta	Tb	Th	Tl	Tm	U	W
Units	ppm	ppm	ppm	ppm	ppm	ppm	ppm	ppm	ppm	ppm	ppm	ppm	ppm	ppm	ppm
DL	0.05	20	5	0.01	1	0.2	0.01	1	0.01	0.01	0.05	0.05	0.005	0.01	0.5
Method	FUS-MS	FUS-MS	FUS-MS	FUS-MS	FUS-MS	FUS-MS	FUS-MS	FUS-MS	FUS-MS	FUS-MS	FUS-MS	FUS-MS	FUS-MS	FUS-MS	FUS-MS
T113	17.7	60	< 5	4.61	46	0.2	3.23	< 1	0.31	0.35	2.18	< 0.05	0.169	0.51	13
T114	20.9	60	< 5	5.28	59	0.3	3.74	< 1	0.41	0.44	2.35	< 0.05	0.171	0.61	13.4
T115	19.4	60	6	5.23	45	< 0.2	3.56	< 1	0.37	0.42	2.19	< 0.05	0.185	0.57	6.7
T116	22.8	50	< 5	5.86	21	0.2	4.02	< 1	0.43	0.46	2.62	< 0.05	0.159	0.34	4.5
T117	11.2	< 20	< 5	3.01	26	< 0.2	2.04	< 1	0.2	0.26	1.67	< 0.05	0.11	0.46	4.6
T118	22.3	20	< 5	5.77	28	0.3	3.92	< 1	0.33	0.42	3.14	0.08	0.172	0.6	1.5
T134	13.6	< 20	< 5	3.83	193	< 0.2	2.06	< 1	0.65	0.17	1.08	0.95	0.059	0.28	2.8
T139	10.1	80	< 5	1.98	9	< 0.2	3.43	< 1	0.16	0.81	0.36	0.29	0.533	0.09	11.3
T140	10.3	70	< 5	1.93	19	< 0.2	3.55	< 1	0.15	0.83	0.34	0.24	0.545	0.09	17.2
T141	10.6	80	< 5	2.08	32	< 0.2	3.63	< 1	0.16	0.85	0.38	0.21	0.553	0.1	15.6
T142	10	70	< 5	2.08	37	< 0.2	3.05	< 1	0.17	0.69	0.49	0.19	0.443	0.13	30
T154	19.4	30	< 5	5.1	20	< 0.2	3.36	< 1	0.35	0.36	2.96	0.11	0.141	0.61	1.4
T156	19.2	30	< 5	4.81	30	< 0.2	3.51	< 1	0.25	0.38	2.39	0.14	0.16	0.55	13.2
T157	22.2	40	< 5	5.6	45	< 0.2	4.21	< 1	0.24	0.49	2.28	0.17	0.173	0.47	12.9
T158	16.1	40	< 5	3.99	37	< 0.2	2.94	< 1	0.17	0.31	1.92	0.14	0.126	0.41	22.2
T159	0.45	< 20	< 5	0.1	3	< 0.2	0.14	< 1	0.02	0.03	0.06	< 0.05	0.01	0.02	686
T162	11.8	< 20	< 5	3.18	39	< 0.2	2.22	< 1	0.28	0.23	2.11	0.13	0.091	0.54	17.9
T164	14.7	60	< 5	3.85	32	< 0.2	2.95	< 1	0.28	0.31	2.16	0.12	0.127	0.47	6.8
T165	41.3	< 20	51	12.1	10	< 0.2	6.49	2	7.9	0.66	16.6	0.09	0.468	21.7	4.4
T182	8.8	60	< 5	1.65	< 1	< 0.2	2.91	< 1	0.16	0.65	0.29	< 0.05	0.403	0.08	2.1
T183	17.3	40	< 5	4.48	25	< 0.2	3.2	< 1	0.39	0.34	2.6	0.09	0.155	0.61	0.8
T184	17.8	60	< 5	4.53	15	< 0.2	3.24	< 1	0.37	0.38	2.27	< 0.05	0.165	0.56	3.5
T186	20.2	60	11	5.41	25	< 0.2	3.81	< 1	0.42	0.41	2.52	0.09	0.162	0.56	6.8
T187	2.32	< 20	< 5	0.6	8	< 0.2	0.41	< 1	0.05	0.04	0.24	< 0.05	0.016	0.05	9.2
T188	17.2	50	< 5	4.29	51	< 0.2	3.14	< 1	0.31	0.32	1.86	0.11	0.14	0.48	282
T189	12.9	< 20	6	3.63	170	< 0.2	1.84	< 1	0.63	0.14	6.55	0.66	0.064	1.18	2.6

Analyte	Nd	Ni	Pb	Pr	Rb	Sb	Sm	Sn	Ta	Tb	Th	Tl	Tm	U	W
Units	ppm	ppm	ppm	ppm	ppm	ppm	ppm	ppm	ppm	ppm	ppm	ppm	ppm	ppm	ppm
DL	0.05	20	5	0.01	1	0.2	0.01	1	0.01	0.01	0.05	0.05	0.005	0.01	0.5
Method	FUS-MS	FUS-MS	FUS-MS	FUS-MS	FUS-MS	FUS-MS	FUS-MS	FUS-MS	FUS-MS	FUS-MS	FUS-MS	FUS-MS	FUS-MS	FUS-MS	FUS-MS
T192	15.3	< 20	< 5	4	18	< 0.2	2.83	< 1	0.27	0.32	2.29	0.11	0.15	0.51	2.9
T193	14.5	< 20	< 5	4.1	20	< 0.2	2.56	< 1	0.33	0.24	4.19	0.08	0.11	1.17	3
T194	13.8	< 20	< 5	3.63	40	< 0.2	2.64	< 1	0.29	0.3	2.15	0.12	0.133	0.6	9.7
T195	14	< 20	< 5	3.8	48	< 0.2	2.61	< 1	0.36	0.3	2.35	0.1	0.145	0.72	43.3
T196	5.7	< 20	< 5	1.49	19	< 0.2	0.99	< 1	0.09	0.11	0.84	< 0.05	0.054	0.17	1550
T200	3.97	270	< 5	0.78	< 1	< 0.2	1.35	< 1	0.08	0.33	0.44	< 0.05	0.213	0.12	4.1
T213	41.6	320	< 5	12.2	16	0.3	6.36	< 1	0.33	0.51	7.4	< 0.05	0.167	1.17	21.3
T215	23.5	< 20	< 5	7	< 1	0.2	3.32	< 1	0.75	0.3	23.9	< 0.05	0.136	4.5	1.5
T216	53.1	100	8	14	18	0.4	8.93	< 1	0.89	0.77	11.1	< 0.05	0.248	2.45	1.9
T218	9.99	40	< 5	2.57	27	0.3	2.08	< 1	0.27	0.25	2.11	< 0.05	0.123	0.41	< 0.5
T228	83.5	40	7	20.8	13	0.7	16.3	< 1	0.32	1.35	10.1	< 0.05	0.313	3.05	7.2
T239	35.9	540	< 5	10.5	6	0.3	5.13	< 1	0.3	0.49	7.14	< 0.05	0.172	1.1	5.1
T240	31.5	130	< 5	7.87	2	0.5	6.4	< 1	0.28	0.65	4.81	< 0.05	0.244	1.37	< 0.5
T241	12	< 20	< 5	3.23	15	< 0.2	2.28	< 1	0.32	0.28	2.99	< 0.05	0.134	0.68	0.7
T242	46	110	8	11.9	104	0.4	8	< 1	0.76	0.72	10.8	0.4	0.238	2.4	0.8
T245	93.9	60	< 5	23.6	8	< 0.2	19.1	< 1	0.3	1.58	9.56	< 0.05	0.343	2.45	64.3
STPL-BAS-023	4.59	190	< 5	0.85	< 1	0.8	1.52	< 1	0.09	0.35	0.11	0.08	0.21	0.03	1.1
STPL-BAS-025	4.71	190	< 5	0.98	< 1	0.6	1.56	< 1	0.08	0.36	0.12	< 0.05	0.213	0.03	< 0.5
STPL-BAS-026	4.72	180	< 5	0.86	< 1	0.5	1.54	< 1	0.08	0.37	0.12	< 0.05	0.211	0.03	< 0.5
STPL-BAS-027	4.36	190	< 5	0.88	< 1	0.7	1.54	< 1	0.09	0.37	0.12	< 0.05	0.221	0.03	11.4
STPL-BAS-029	4.53	190	< 5	0.83	2	0.8	1.36	< 1	0.1	0.37	0.11	< 0.05	0.219	0.04	1.9
STPL-BAS-030	4.41	170	< 5	0.82	2	0.6	1.41	< 1	0.11	0.35	0.1	< 0.05	0.217	0.24	3.8

Analyte	Nd	Ni	Pb	Pr	Rb	Sb	Sm	Sn	Ta	Tb	Th	Tl	Tm	U	W
Units	ppm	ppm	ppm	ppm	ppm	ppm	ppm	ppm	ppm	ppm	ppm	ppm	ppm	ppm	ppm
DL	0.05	20	5	0.01	1	0.2	0.01	1	0.01	0.01	0.05	0.05	0.005	0.01	0.5
Method	FUS-MS	FUS-MS	FUS-MS	FUS-MS	FUS-MS	FUS-MS	FUS-MS	FUS-MS	FUS-MS	FUS-MS	FUS-MS	FUS-MS	FUS-MS	FUS-MS	FUS-MS
STPL-BAS-053	4.68	190	< 5	0.85	< 1	1.6	1.34	< 1	0.13	0.34	0.12	< 0.05	0.211	< 0.01	0.6
STPL-53-PML-025	23.4	< 20	8	7.23	61	< 0.2	3.51	< 1	0.76	0.39	10.5	0.11	0.257	2.37	1.8
STPL-PML-53-027	24.1	< 20	8	7.29	68	< 0.2	3.68	< 1	0.9	0.41	10.1	0.11	0.275	2.35	1.9
STPL-53-PML-036	24.2	< 20	8	7.6	69	< 0.2	3.69	< 1	0.89	0.41	10.3	0.1	0.296	2.5	0.8



Analyte	Y	Yb	Zn	Ag	Cd	Co	Cr	Cu	In	Li	Mn	Mo	Ni	Pb	Zn
Units	ppm	ppm	ppm	ppm	ppm	ppm	ppm	ppm	ppm	ppm	ppm	ppm	ppm	ppm	ppm
DL	0.5	0.01	30	1	0.2	0.5	1	0.5	0.2	1	2	1	1	2	0.5
Method	FUS-MS	FUS-MS	FUS-MS	TD-MS	TD-MS	TD-MS	TD-MS	TD-MS	TD-MS	TD-MS	TD-MS	TD-MS	TD-MS	TD-MS	TD-MS
T6	6.8	0.59		2	< 0.2	9	23	39.8	< 0.2	41	331	< 1	14	3	48.6
T8	14.4	1.41		< 1	< 0.2	15.8	56	63.4	< 0.2	38	809	< 1	61	2	62.5
T9	25.1	2.66		< 1	< 0.2	50.5	96	211	< 0.2	15	1520	< 1	82	5	115
T11	12.8	1.22		< 1	< 0.2	16.7	37	88.3	< 0.2	14	762	< 1	32	4	76.5
T12	31.1	3.4		< 1	0.9	50.6	57	203	0.2	4	1650	2	45	5	144
T13	11.2	1.11		< 1	< 0.2	10.1	37	40	< 0.2	36	583	1	20	5	116
T14	28.7	3.5		< 1	< 0.2	38.9	102	117	< 0.2	35	1430	< 1	71	2	101
T15	13	1.13		< 1	< 0.2	36.5	576	23.7	< 0.2	86	1050	< 1	272	2	87.5
T16	34.2	2.13		< 1	< 0.2	27.8	268	40.2	< 0.2	41	1410	< 1	56	6	54.2
T17	9.2	0.86		< 1	< 0.2	10.3	31	18.7	< 0.2	26	405	< 1	14	6	46.5
T19	16	1.6		< 1	< 0.2	43.2	162	134	< 0.2	70	1020	< 1	81	2	132
T20	9.3	0.89		< 1	< 0.2	11.4	20	23.3	< 0.2	24	359	< 1	14	4	32.5
T21	14.7	1.5		< 1	< 0.2	3.4	61	20.2	< 0.2	27	2490	< 1	17	11	82.6
T24	6.3	0.46		< 1	< 0.2	1.5	13	99.4	< 0.2	1	> 10000	2	51	6	22.8
T27	9.6	0.91		< 1	< 0.2	11	25	81.7	< 0.2	21	1080	1	26	4	30.2
T29	11.5	1.21		< 1	< 0.2	29.1	68	38.7	< 0.2	35	1470	1	93	7	148
T31	13.5	1.41		< 1	< 0.2	11.1	78	35.6	< 0.2	15	2720	< 1	38	3	61.9
T32	11.1	0.91		< 1	< 0.2	1	12	8.4	< 0.2	5	293	1	3	4	39.1
T37	8	0.68		< 1	< 0.2	39.6	15	73.9	< 0.2	< 1	5480	6	83	6	43.7
T38	2.9	0.3		< 1	0.8	4.1	55	16.3	< 0.2	8	1710	< 1	26	3	170
T39	22.5	2.57		< 1	< 0.2	41.1	122	47	< 0.2	55	3680	< 1	78	< 2	100
T42	8.8	0.85		< 1	< 0.2	27.3	144	24.9	< 0.2	52	722	< 1	223	2	84.1
T43	10	0.94		< 1	< 0.2	16.4	32	90.6	< 0.2	36	648	2	31	3	56.6
T45	11.3	0.96		< 1	< 0.2	1.5	14	14.4	< 0.2	11	779	< 1	2	3	8.6
T50	14.2	1.19	140	< 1	< 0.2	40.3	579	7.4	< 0.2	80	1260	1	295	3	140
T56	8.2	0.82		5	< 0.2	11.7	42	13.1	< 0.2	16	347	2	11	4	34.8
T58	10.3	0.96		< 1	< 0.2	7	80	71.6	< 0.2	20	93	< 1	22	3	14.3

Analyte	Y	Yb	Zn	Ag	Cd	Co	Cr	Cu	In	Li	Mn	Mo	Ni	Pb	Zn
Units	ppm	ppm	ppm	ppm	ppm	ppm	ppm	ppm	ppm	ppm	ppm	ppm	ppm	ppm	ppm
DL	0.5	0.01	30	1	0.2	0.5	1	0.5	0.2	1	2	1	1	2	0.5
Method	FUS-MS	FUS-MS	FUS-MS	TD-MS	TD-MS	TD-MS	TD-MS	TD-MS	TD-MS	TD-MS	TD-MS	TD-MS	TD-MS	TD-MS	TD-MS
T59	12.1	0.86		< 1	< 0.2	11.5	62	25.1	< 0.2	14	585	< 1	40	6	27.5
T63	12.9	1.08		< 1	< 0.2	40.6	410	29.3	< 0.2	70	896	< 1	283	5	91.9
T65	11.6	1.16	80	< 1	< 0.2	14.8	32	72.4	< 0.2	31	461	2	29	6	69.5
T66	34.1	2.03		< 1	< 0.2	34.5	179	74.9	< 0.2	48	1070	< 1	46	8	103
T71	7.9	0.9		4	< 0.2	17.3	31	59	< 0.2	16	322	3	42	7	35.9
T72	9.9	0.88		2	< 0.2	25	34	113	< 0.2	22	927	1	41	6	38.2
T73	9.3	0.97		< 1	< 0.2	19.1	23	55.1	< 0.2	26	1100	1	22	6	143
T80	13.1	1.48	80	< 1	< 0.2	47.7	228	120	< 0.2	65	995	< 1	116	2	80.7
T81	12.6	1.08		< 1	< 0.2	41.1	413	3.8	< 0.2	47	1760	< 1	437	3	97.5
T83	32.1	3.34		< 1	< 0.2	49.6	66	155	< 0.2	7	1750	< 1	44	6	138
T85	9.6	0.98		< 1	< 0.2	13.6	20	42.7	< 0.2	20	754	3	14	5	28.9
T86	9.6	0.93		< 1	< 0.2	23.2	24	17.9	< 0.2	38	224	3	26	5	20.2
T87	23.6	2.52		< 1	< 0.2	48.2	112	85.1	< 0.2	27	1770	< 1	75	2	134
T88	8.9	0.97		< 1	< 0.2	17.9	21	34.8	< 0.2	28	1640	< 1	25	3	161
T89	22.7	2.59		< 1	< 0.2	47.6	121	182	< 0.2	49	1580	1	62	< 2	118
T90	8.9	0.86		4	< 0.2	16.9	28	67.1	< 0.2	17	328	1	30	5	33.5
T94	5.9	0.64		< 1	< 0.2	15.2	16	2.3	< 0.2	21	222	< 1	13	2	33.8
T98	27.4	3.34		< 1	< 0.2	44	43	140	< 0.2	56	1690	< 1	46	< 2	111
T99	18.4	1.87		< 1	< 0.2	29.3	39	112	< 0.2	41	1030	1	39	4	81.3
T100	8.1	0.95		4	< 0.2	14.2	37	50.1	< 0.2	18	568	< 1	15	3	31.7
T101	24	2.74		< 1	< 0.2	45.8	44	76.7	< 0.2	60	1460	< 1	44	2	111
T102	11	1.01		< 1	< 0.2	15.2	17	28.9	< 0.2	30	558	< 1	20	< 2	54.8
T104	0.6	0.06		3	< 0.2	0.5	39	12.9	< 0.2	< 1	134	1	2	< 2	< 0.5
T105	12.1	1.06		1	< 0.2	18.3	85	84.6	< 0.2	47	624	2	65	4	81.8
T106	36.5	4.05	160	< 1	< 0.2	38.7	91	15.5	< 0.2	41	1240	< 1	52	< 2	137
T113	10.4	1.06		< 1	< 0.2	16.6	80	47.4	< 0.2	31	712	1	62	3	67.2
T114	12.1	1.07		< 1	< 0.2	14.9	67	99.4	< 0.2	35	675	< 1	63	< 2	75

Analyte	Y	Yb	Zn	Ag	Cd	Co	Cr	Cu	In	Li	Mn	Mo	Ni	Pb	Zn
Units	ppm	ppm	ppm	ppm	ppm	ppm	ppm	ppm	ppm	ppm	ppm	ppm	ppm	ppm	ppm
DL	0.5	0.01	30	1	0.2	0.5	1	0.5	0.2	1	2	1	1	2	0.5
Method	FUS-MS	FUS-MS	FUS-MS	TD-MS	TD-MS	TD-MS	TD-MS	TD-MS	TD-MS	TD-MS	TD-MS	TD-MS	TD-MS	TD-MS	TD-MS
T115	12.9	1.13		< 1	< 0.2	17.8	59	27.2	< 0.2	30	751	< 1	60	4	62.5
T116	11.7	1.08		< 1	< 0.2	14.9	68	0.8	< 0.2	38	732	< 1	52	2	49.7
T117	7.7	0.78		< 1	< 0.2	11.1	20	54.9	< 0.2	22	366	2	11	3	37.2
T118	11.9	1.08	60	< 1	< 0.2	10.6	26	31.7	< 0.2	33	393	< 1	23	4	62.5
T134	5	0.36	40	< 1	< 0.2	3.3	4	< 0.5	< 0.2	49	405	< 1	< 1	3	17.5
T139	32.4	3.6	130	< 1	< 0.2	37.5	89	62.4	< 0.2	41	1570	< 1	71	2	142
T140	32.3	3.52	130	< 1	< 0.2	37.9	85	59.3	< 0.2	48	1560	< 1	63	3	136
T141	33.5	3.72	140	< 1	< 0.2	41.1	94	71.9	< 0.2	56	1550	< 1	77	3	143
T142	25.9	2.98	70	< 1	< 0.2	35.3	80	28.2	< 0.2	70	1430	1	72	4	66.7
T154	10	0.9	80	< 1	< 0.2	11.6	31	7.6	< 0.2	81	924	< 1	24	3	67
T156	10.7	1.02	80	< 1	< 0.2	15.9	55	53.8	< 0.2	24	955	< 1	36	4	79.3
T157	13.8	1.11	40	< 1	< 0.2	18.4	31	27	< 0.2	24	748	3	39	4	33.1
T158	8.8	0.83	30	< 1	< 0.2	16.4	54	24.9	< 0.2	43	635	< 1	35	3	26.2
T159	1	0.06	< 30	5	< 0.2	1.1	9	5.4	< 0.2	3	97	< 1	3	< 2	11.8
T162	6.4	0.62	110	< 1	0.3	4.1	23	17.1	< 0.2	32	297	2	2	7	138
T164	9.2	0.91	70	< 1	< 0.2	15.7	63	16.7	< 0.2	46	580	< 1	60	4	76.2
T165	24.6	3.34	< 30	1	< 0.2	5.2	6	46.1	< 0.2	10	958	< 1	2	35	16.5
T182	24	2.73	80	< 1	< 0.2	58.6	44	208	< 0.2	11	1580	< 1	59	< 2	84.3
T183	10.3	1	560	< 1	1.8	9.8	54	18.5	< 0.2	16	2340	2	32	4	692
T184	11.6	1.14	70	< 1	< 0.2	15.7	62	41.5	< 0.2	38	695	< 1	55	4	71.4
T186	11.9	1.06	100	< 1	< 0.2	14.8	59	36.5	< 0.2	31	564	< 1	54	14	88.5
T187	1.2	0.11	< 30	< 1	< 0.2	1.9	76	5.6	< 0.2	3	146	6	10	< 2	18.6
T188	9.5	0.93	30	3	< 0.2	13.3	54	27.6	< 0.2	15	687	< 1	47	6	25.8
T189	4.1	0.46	50	< 1	< 0.2	2	20	4.7	< 0.2	24	495	2	4	7	53.7
T192	9.4	0.96	60	< 1	< 0.2	10.6	14	34.4	< 0.2	17	488	< 1	13	3	62.4
T193	8	0.75	30	< 1	< 0.2	5	53	67.5	< 0.2	10	246	< 1	6	3	29.1
T194	8.9	0.87	70	< 1	< 0.2	9.6	55	142	< 0.2	18	492	15	14	3	62.2

Analyte	Y	Yb	Zn	Ag	Cd	Co	Cr	Cu	In	Li	Mn	Mo	Ni	Pb	Zn
Units	ppm	ppm	ppm	ppm	ppm	ppm	ppm	ppm	ppm	ppm	ppm	ppm	ppm	ppm	ppm
DL	0.5	0.01	30	1	0.2	0.5	1	0.5	0.2	1	2	1	1	2	0.5
Method	FUS-MS	FUS-MS	FUS-MS	TD-MS	TD-MS	TD-MS	TD-MS	TD-MS	TD-MS	TD-MS	TD-MS	TD-MS	TD-MS	TD-MS	TD-MS
T195	9.3	0.97	80	1	< 0.2	9.3	19	204	< 0.2	17	417	18	12	4	63.5
T196	3.5	0.38	30	5	< 0.2	4.7	81	74.5	< 0.2	5	115	35	8	2	34.5
T200	12.5	1.46	100	< 1	< 0.2	62.5	259	45.6	< 0.2	10	1360	< 1	268	< 2	99
T213	12.7	1.08	160	< 1	< 0.2	22.2	522	3.8	< 0.2	84	915	1	298	3	165
T215	9.6	1	< 30	< 1	< 0.2	3.9	17	12.4	< 0.2	4	229	1	10	4	9.9
T216	20.4	1.66	80	< 1	< 0.2	25.2	127	45.4	< 0.2	30	1050	1	92	8	60.9
T218	8.2	0.79	40	< 1	< 0.2	13.5	21	31.9	< 0.2	20	589	< 1	35	4	35.7
T228	29.5	1.79	100	< 1	< 0.2	25	122	34.3	< 0.2	30	1070	< 1	40	7	92.2
T239	13.2	1	70	< 1	< 0.2	32.5	343	3	< 0.2	39	1120	< 1	472	3	60.1
T240	17.3	1.57	100	< 1	< 0.2	30.8	282	45.2	< 0.2	33	979	< 1	119	5	66.4
T241	8.8	0.84	50	< 1	< 0.2	10.1	19	3.5	< 0.2	25	402	< 1	17	< 2	47.7
T242	18.9	1.52	70	< 1	< 0.2	28	242	23.5	< 0.2	63	1070	< 1	99	9	59.1
T245	32.8	2.02	100	< 1	< 0.2	32.9	127	45.3	< 0.2	56	1080	< 1	45	4	87
STPL-BAS-023	13.2	1.47	90	< 1	< 0.2	47.3	162	124	< 0.2	14	1400	< 1	175	< 2	59.3
STPL-BAS-025	13.1	1.5		< 1	< 0.2	53.7	153	126	< 0.2	14	1220	< 1	183	< 2	68.2
STPL-BAS-026	12.7	1.37		< 1	< 0.2	51.5	220	125	< 0.2	13	1180	< 1	179	< 2	73.4
STPL-BAS-027	13.5	1.42	80	< 1	< 0.2	48.8	197	126	< 0.2	14	1350	< 1	167	< 2	64.7
STPL-BAS-029	13.2	1.51		< 1	< 0.2	52.3	178	129	< 0.2	14	1310	< 1	179	< 2	67.5
STPL-BAS-030	12.7	1.39		< 1	< 0.2	50.1	251	127	< 0.2	13	1270	< 1	173	< 2	65.7
STPL-BAS-053	13.1	1.4	120	< 1	< 0.2	48.5	168	114	< 0.2	14	1210	< 1	173	5	52.6
STPL-53-PML-025	14.4	1.88		< 1	< 0.2	1.1	36	9.5	< 0.2	10	245	< 1	2	10	78.4

Analyte	Y	Yb	Zn	Ag	Cd	Co	Cr	Cu	In	Li	Mn	Mo	Ni	Pb	Zn
Units	ppm	ppm	ppm	ppm	ppm	ppm	ppm	ppm	ppm	ppm	ppm	ppm	ppm	ppm	ppm
DL	0.5	0.01	30	1	0.2	0.5	1	0.5	0.2	1	2	1	1	2	0.5
Method	FUS-MS	FUS-MS	FUS-MS	TD-MS	TD-MS	TD-MS	TD-MS	TD-MS	TD-MS	TD-MS	TD-MS	TD-MS	TD-MS	TD-MS	TD-MS
STPL-PML-53-027	16	2.03	40	< 1	< 0.2	1.1	35	22	< 0.2	12	258	< 1	2	8	27.7
STPL-53-PML-036	15.8	2.15		< 1	< 0.2	1.3	21	12.5	< 0.2	11	241	< 1	2	8	26

## **Appendix O**

### **Whole-rock geochemistry QA/QC data (Lab-provided reference materials, duplicates, and method blanks)**

Whole-rock geochemistry QA/QC from Activation Laboratories Ltd. Methods are summarized in Section 3.2. These results are from an open file report (Ciufu et al., 2019).

Analyte	SiO <sub>2</sub>	Al <sub>2</sub> O <sub>3</sub>	Fe <sub>2</sub> O <sub>3</sub>	MnO	MgO	CaO	Na <sub>2</sub> O	K <sub>2</sub> O	TiO <sub>2</sub>	P <sub>2</sub> O <sub>5</sub>	LOI	LOI2
Units	%	%	%	%	%	%	%	%	%	%	%	%
Detection Limit	0.01	0.01	0.01	0.001	0.01	0.01	0.01	0.01	0.001	0.01		
Method	FUS-ICP	FUS-ICP	FUS-ICP	FUS-ICP	FUS-ICP	FUS-ICP	FUS-ICP	FUS-ICP	FUS-ICP	FUS-ICP	FUS-ICP	FUS-ICP
GXR-1 Meas	-	-	-	-	-	-	-	-	-	-	-	-
GXR-1 Cert	-	-	-	-	-	-	-	-	-	-	-	-
NIST 694 Meas	11.64	2	-	0.013	0.37	43.22	0.9	0.56	0.12	30.18	-	-
NIST 694 Cert	11.2	1.8	-	0.0116	0.33	43.6	0.86	0.51	0.11	30.2	-	-
DNC-1 Meas	47.4	18.88	-	0.147	10.33	11.43	1.92	0.22	0.495	0.07	-	-
DNC-1 Cert	47.15	18.34	-	0.15	10.13	11.49	1.89	0.234	0.48	0.07	-	-
GBW 07113 Meas	71.65	12.8	-	0.14	0.14	0.6	2.46	5.4	0.27	0.05	-	-
GBW 07113 Cert	72.8	13	-	0.14	0.16	0.59	2.57	5.43	0.3	0.05	-	-
GBW 07113 Meas	71.65	12.8	-	0.14	0.14	0.6	2.46	5.4	0.27	0.05	-	-
GBW 07113 Cert	72.8	13	-	0.14	0.16	0.59	2.57	5.43	0.3	0.05	-	-
GBW 07113 Meas	73.81	12.87	-	0.14	0.17	0.6	2.46	5.47	0.28	0.03	-	-
GBW 07113 Cert	72.8	13	-	0.14	0.16	0.59	2.57	5.43	0.3	0.05	-	-
GXR-4 Meas	-	-	-	-	-	-	-	-	-	-	-	-
GXR-4 Cert	-	-	-	-	-	-	-	-	-	-	-	-
GXR-6 Meas	-	-	-	-	-	-	-	-	-	-	-	-
GXR-6 Cert	-	-	-	-	-	-	-	-	-	-	-	-
LKSD-3 Meas	-	-	-	-	-	-	-	-	-	-	-	-
LKSD-3 Cert	-	-	-	-	-	-	-	-	-	-	-	-
TDB-1 Meas	-	-	-	-	-	-	-	-	-	-	-	-
TDB-1 Cert	-	-	-	-	-	-	-	-	-	-	-	-
SY-2 Meas	-	-	-	-	-	-	-	-	-	-	-	-
SY-2 Cert	-	-	-	-	-	-	-	-	-	-	-	-
SY-3 Meas	-	-	-	-	-	-	-	-	-	-	-	-
SY-3 Cert	-	-	-	-	-	-	-	-	-	-	-	-
BaSO4 Meas	-	-	-	-	-	-	-	-	-	-	-	-
BaSO4 Cert	-	-	-	-	-	-	-	-	-	-	-	-
BaSO4 Meas	-	-	-	-	-	-	-	-	-	-	-	-
BaSO4 Cert	-	-	-	-	-	-	-	-	-	-	-	-
BaSO4 Meas	-	-	-	-	-	-	-	-	-	-	-	-
BaSO4 Cert	-	-	-	-	-	-	-	-	-	-	-	-
W-2a Meas	53.02	15.53	-	0.166	6.61	11.01	2.18	0.62	1.123	0.17	-	-
W-2a Cert	52.4	15.4	-	0.163	6.37	10.9	2.14	0.626	1.06	0.13	-	-
SY-4 Meas	50.17	21.39	-	0.104	0.54	7.82	7.14	1.69	0.294	0.13	-	-
SY-4 Cert	49.9	20.69	-	0.108	0.54	8.05	7.1	1.66	0.287	0.131	-	-
CTA-AC-1 Meas	-	-	-	-	-	-	-	-	-	-	-	-
CTA-AC-1 Cert	-	-	-	-	-	-	-	-	-	-	-	-
BIR-1a Meas	48.29	15.68	-	0.172	9.78	13.51	1.81	0.02	0.966	0.01	-	-

Analyte	SiO <sub>2</sub>	Al <sub>2</sub> O <sub>3</sub>	Fe <sub>2</sub> O <sub>3</sub>	MnO	MgO	CaO	Na <sub>2</sub> O	K <sub>2</sub> O	TiO <sub>2</sub>	P <sub>2</sub> O <sub>5</sub>	LOI	LOI2
Units	%	%	%	%	%	%	%	%	%	%	%	%
Detection Limit	0.01	0.01	0.01	0.001	0.01	0.01	0.01	0.01	0.001	0.01		
Method	FUS-ICP	FUS-ICP	FUS-ICP	FUS-ICP	FUS-ICP	FUS-ICP	FUS-ICP	FUS-ICP	FUS-ICP	FUS-ICP	FUS-ICP	FUS-ICP
BIR-1a Cert	47.96	15.5	-	0.175	9.7	13.3	1.82	0.03	0.96	0.021	-	-
BIR-1a Meas	-	-	-	-	-	-	-	-	-	-	-	-
BIR-1a Cert	-	-	-	-	-	-	-	-	-	-	-	-
NCS DC86312 Meas	-	-	-	-	-	-	-	-	-	-	-	-
NCS DC86312 Cert	-	-	-	-	-	-	-	-	-	-	-	-
JGb-2 Meas	-	-	-	-	-	-	-	-	-	-	-	-
JGb-2 Cert	-	-	-	-	-	-	-	-	-	-	-	-
JGb-2 Meas	-	-	-	-	-	-	-	-	-	-	-	-
JGb-2 Cert	-	-	-	-	-	-	-	-	-	-	-	-
JGb-2 Meas	-	-	-	-	-	-	-	-	-	-	-	-
JGb-2 Cert	-	-	-	-	-	-	-	-	-	-	-	-
JGb-2 Meas	-	-	-	-	-	-	-	-	-	-	-	-
JGb-2 Cert	-	-	-	-	-	-	-	-	-	-	-	-
JGb-2 Meas	-	-	-	-	-	-	-	-	-	-	-	-
JGb-2 Cert	-	-	-	-	-	-	-	-	-	-	-	-
JGb-2 Meas	-	-	-	-	-	-	-	-	-	-	-	-
JGb-2 Cert	-	-	-	-	-	-	-	-	-	-	-	-
SCH-1 Meas	8.25	1.04	-	1.015	0.03	-	0.03	0.02	0.049	0.14	-	-
SCH-1 Cert	8.09	0.962	-	1.003	0.033	-	0.026	0.031	0.052	0.124	-	-
NCS DC70009 (GBW07241) Meas	-	-	-	-	-	-	-	-	-	-	-	-
NCS DC70009 (GBW07241) Cert	-	-	-	-	-	-	-	-	-	-	-	-
SGR-1b Meas	-	-	-	-	-	-	-	-	-	-	-	-
SGR-1b Cert	-	-	-	-	-	-	-	-	-	-	-	-
SGR-1b Meas	-	-	-	-	-	-	-	-	-	-	-	-
SGR-1b Cert	-	-	-	-	-	-	-	-	-	-	-	-
SGR-1b Meas	-	-	-	-	-	-	-	-	-	-	-	-
SGR-1b Cert	-	-	-	-	-	-	-	-	-	-	-	-
OREAS 100a (Fusion) Meas	-	-	-	-	-	-	-	-	-	-	-	-
OREAS 100a (Fusion) Cert	-	-	-	-	-	-	-	-	-	-	-	-
OREAS 101a (Fusion) Meas	-	-	-	-	-	-	-	-	-	-	-	-
OREAS 101a (Fusion) Cert	-	-	-	-	-	-	-	-	-	-	-	-
OREAS 101b (Fusion) Meas	-	-	-	-	-	-	-	-	-	-	-	-
OREAS 101b (Fusion) Cert	-	-	-	-	-	-	-	-	-	-	-	-
OREAS 98 (S by LECO) Meas	-	-	-	-	-	-	-	-	-	-	-	-
OREAS 98 (S by LECO) Cert	-	-	-	-	-	-	-	-	-	-	-	-
OREAS 132b (S by LECO) Meas	-	-	-	-	-	-	-	-	-	-	-	-
OREAS 132b (S by LECO) Cert	-	-	-	-	-	-	-	-	-	-	-	-
JR-1 Meas	-	-	-	-	-	-	-	-	-	-	-	-
JR-1 Cert	-	-	-	-	-	-	-	-	-	-	-	-



Analyte	SiO <sub>2</sub>	Al <sub>2</sub> O <sub>3</sub>	Fe <sub>2</sub> O <sub>3</sub>	MnO	MgO	CaO	Na <sub>2</sub> O	K <sub>2</sub> O	TiO <sub>2</sub>	P <sub>2</sub> O <sub>5</sub>	LOI	LOI2
Units	%	%	%	%	%	%	%	%	%	%	%	%
Detection Limit	0.01	0.01	0.01	0.001	0.01	0.01	0.01	0.01	0.001	0.01		
Method	FUS-ICP	FUS-ICP	FUS-ICP	FUS-ICP	FUS-ICP	FUS-ICP	FUS-ICP	FUS-ICP	FUS-ICP	FUS-ICP	FUS-ICP	FUS-ICP
NCS DC86318 Meas	-	-	-	-	-	-	-	-	-	-	-	-
NCS DC86318 Cert	-	-	-	-	-	-	-	-	-	-	-	-
USZ 25-2006 Meas	-	-	-	-	-	-	-	-	-	-	-	-
USZ 25-2006 Cert	-	-	-	-	-	-	-	-	-	-	-	-
USZ 25-2006 Meas	-	-	-	-	-	-	-	-	-	-	-	-
USZ 25-2006 Cert	-	-	-	-	-	-	-	-	-	-	-	-
GS309-4 Meas	-	-	-	-	-	-	-	-	-	-	-	-
GS309-4 Cert	-	-	-	-	-	-	-	-	-	-	-	-
GS311-4 Meas	-	-	-	-	-	-	-	-	-	-	-	-
GS311-4 Cert	-	-	-	-	-	-	-	-	-	-	-	-
GS311-4 Meas	-	-	-	-	-	-	-	-	-	-	-	-
GS311-4 Cert	-	-	-	-	-	-	-	-	-	-	-	-
GS311-4 Meas	-	-	-	-	-	-	-	-	-	-	-	-
GS311-4 Cert	-	-	-	-	-	-	-	-	-	-	-	-
GS311-4 Meas	-	-	-	-	-	-	-	-	-	-	-	-
GS311-4 Cert	-	-	-	-	-	-	-	-	-	-	-	-
GS900-5 Meas	-	-	-	-	-	-	-	-	-	-	-	-
GS900-5 Cert	-	-	-	-	-	-	-	-	-	-	-	-
GS900-5 Meas	-	-	-	-	-	-	-	-	-	-	-	-
GS900-5 Cert	-	-	-	-	-	-	-	-	-	-	-	-
GS900-5 Meas	-	-	-	-	-	-	-	-	-	-	-	-
GS900-5 Cert	-	-	-	-	-	-	-	-	-	-	-	-
OREAS 45d (Aqua Regia) Meas	-	-	-	-	-	-	-	-	-	-	-	-
OREAS 45d (Aqua Regia) Cert	-	-	-	-	-	-	-	-	-	-	-	-
CDN-PGMS-24 Meas	-	-	-	-	-	-	-	-	-	-	-	-
CDN-PGMS-24 Cert	-	-	-	-	-	-	-	-	-	-	-	-
CDN-PGMS-24 Meas	-	-	-	-	-	-	-	-	-	-	-	-
CDN-PGMS-24 Cert	-	-	-	-	-	-	-	-	-	-	-	-
CDN-PGMS-24 Meas	-	-	-	-	-	-	-	-	-	-	-	-
CDN-PGMS-24 Cert	-	-	-	-	-	-	-	-	-	-	-	-
CaCO3 Meas	-	-	-	-	-	-	-	-	-	-	-	-
CaCO3 Cert	-	-	-	-	-	-	-	-	-	-	-	-
CaCO3 Meas	-	-	-	-	-	-	-	-	-	-	-	-
CaCO3 Cert	-	-	-	-	-	-	-	-	-	-	-	-
SdAR-M2 (U.S.G.S.) Meas	-	-	-	-	-	-	-	-	-	-	-	-
SdAR-M2 (U.S.G.S.) Cert	-	-	-	-	-	-	-	-	-	-	-	-
GXR-1 Meas	-	-	-	-	-	-	-	-	-	-	-	-

Analyte	SiO <sub>2</sub>	Al <sub>2</sub> O <sub>3</sub>	Fe <sub>2</sub> O <sub>3</sub>	MnO	MgO	CaO	Na <sub>2</sub> O	K <sub>2</sub> O	TiO <sub>2</sub>	P <sub>2</sub> O <sub>5</sub>	LOI	LOI2
Units	%	%	%	%	%	%	%	%	%	%	%	%
Detection Limit	0.01	0.01	0.01	0.001	0.01	0.01	0.01	0.01	0.001	0.01		
Method	FUS-ICP	FUS-ICP	FUS-ICP	FUS-ICP	FUS-ICP	FUS-ICP	FUS-ICP	FUS-ICP	FUS-ICP	FUS-ICP	FUS-ICP	FUS-ICP
GXR-1 Cert	-	-	-	-	-	-	-	-	-	-	-	-
GXR-1 Meas	-	-	-	-	-	-	-	-	-	-	-	-
GXR-1 Cert	-	-	-	-	-	-	-	-	-	-	-	-
GXR-1 Meas	-	-	-	-	-	-	-	-	-	-	-	-
GXR-1 Cert	-	-	-	-	-	-	-	-	-	-	-	-
GXR-1 Meas	-	-	-	-	-	-	-	-	-	-	-	-
GXR-1 Cert	-	-	-	-	-	-	-	-	-	-	-	-
NIST 694 Meas	11.03	1.94	-	0.01	0.34	43.16	0.87	0.55	0.12	30.21	-	-
NIST 694 Cert	11.2	1.8	-	0.0116	0.33	43.6	0.86	0.51	0.11	30.2	-	-
DNC-1 Meas	46.89	18	-	0.15	9.89	11.32	1.91	0.22	0.47	0.07	-	-
DNC-1 Cert	47.15	18.34	-	0.15	10.13	11.49	1.89	0.234	0.48	0.07	-	-
GBW 07113 Meas	72.6	12.8	-	0.14	0.14	0.59	2.51	5.45	0.28	0.03	-	-
GBW 07113 Cert	72.8	13	-	0.14	0.16	0.59	2.57	5.43	0.3	0.05	-	-
GXR-4 Meas	-	-	-	-	-	-	-	-	-	-	-	-
GXR-4 Cert	-	-	-	-	-	-	-	-	-	-	-	-
GXR-4 Meas	-	-	-	-	-	-	-	-	-	-	-	-
GXR-4 Cert	-	-	-	-	-	-	-	-	-	-	-	-
GXR-4 Meas	-	-	-	-	-	-	-	-	-	-	-	-
GXR-4 Cert	-	-	-	-	-	-	-	-	-	-	-	-
GXR-4 Meas	-	-	-	-	-	-	-	-	-	-	-	-
GXR-4 Cert	-	-	-	-	-	-	-	-	-	-	-	-
SDC-1 Meas	-	-	-	-	-	-	-	-	-	-	-	-
SDC-1 Cert	-	-	-	-	-	-	-	-	-	-	-	-
SDC-1 Meas	-	-	-	-	-	-	-	-	-	-	-	-
SDC-1 Cert	-	-	-	-	-	-	-	-	-	-	-	-
SDC-1 Meas	-	-	-	-	-	-	-	-	-	-	-	-
SDC-1 Cert	-	-	-	-	-	-	-	-	-	-	-	-
SDC-1 Meas	-	-	-	-	-	-	-	-	-	-	-	-
SDC-1 Cert	-	-	-	-	-	-	-	-	-	-	-	-
GXR-6 Meas	-	-	-	-	-	-	-	-	-	-	-	-
GXR-6 Cert	-	-	-	-	-	-	-	-	-	-	-	-
GXR-6 Meas	-	-	-	-	-	-	-	-	-	-	-	-
GXR-6 Cert	-	-	-	-	-	-	-	-	-	-	-	-
GXR-6 Meas	-	-	-	-	-	-	-	-	-	-	-	-
GXR-6 Cert	-	-	-	-	-	-	-	-	-	-	-	-
GXR-6 Meas	-	-	-	-	-	-	-	-	-	-	-	-
GXR-6 Cert	-	-	-	-	-	-	-	-	-	-	-	-

Analyte	SiO <sub>2</sub>	Al <sub>2</sub> O <sub>3</sub>	Fe <sub>2</sub> O <sub>3</sub>	MnO	MgO	CaO	Na <sub>2</sub> O	K <sub>2</sub> O	TiO <sub>2</sub>	P <sub>2</sub> O <sub>5</sub>	LOI	LOI2
Units	%	%	%	%	%	%	%	%	%	%	%	%
Detection Limit	0.01	0.01	0.01	0.001	0.01	0.01	0.01	0.01	0.001	0.01		
Method	FUS-ICP	FUS-ICP	FUS-ICP	FUS-ICP	FUS-ICP	FUS-ICP	FUS-ICP	FUS-ICP	FUS-ICP	FUS-ICP	FUS-ICP	FUS-ICP
LKSD-3 Meas	-	-	-	-	-	-	-	-	-	-	-	-
LKSD-3 Cert	-	-	-	-	-	-	-	-	-	-	-	-
TDB-1 Meas	-	-	-	-	-	-	-	-	-	-	-	-
TDB-1 Cert	-	-	-	-	-	-	-	-	-	-	-	-
SY-2 Meas	-	-	-	-	-	-	-	-	-	-	-	-
SY-2 Cert	-	-	-	-	-	-	-	-	-	-	-	-
SY-3 Meas	-	-	-	-	-	-	-	-	-	-	-	-
SY-3 Cert	-	-	-	-	-	-	-	-	-	-	-	-
BaSO4 Meas	-	-	-	-	-	-	-	-	-	-	-	-
BaSO4 Cert	-	-	-	-	-	-	-	-	-	-	-	-
BaSO4 Meas	-	-	-	-	-	-	-	-	-	-	-	-
BaSO4 Cert	-	-	-	-	-	-	-	-	-	-	-	-
W-2a Meas	52.53	15.76	-	0.17	6.35	10.92	2.2	0.61	1.1	0.14	-	-
W-2a Cert	52.4	15.4	-	0.163	6.37	10.9	2.14	0.626	1.06	0.13	-	-
SY-4 Meas	50.24	20.62	-	0.11	0.51	8.05	6.94	1.65	0.29	0.13	-	-
SY-4 Cert	49.9	20.69	-	0.108	0.54	8.05	7.1	1.66	0.287	0.131	-	-
CTA-AC-1 Meas	-	-	-	-	-	-	-	-	-	-	-	-
CTA-AC-1 Cert	-	-	-	-	-	-	-	-	-	-	-	-
BIR-1a Meas	48.54	15.48	-	0.17	9.48	13.54	1.84	0.02	0.97	0.03	-	-
BIR-1a Cert	47.96	15.5	-	0.175	9.7	13.3	1.82	0.03	0.96	0.021	-	-
Calcium Carbonate Meas	-	-	-	-	-	-	-	-	-	-	-	-
Calcium Carbonate Cert	-	-	-	-	-	-	-	-	-	-	-	-
NCS DC86312 Meas	-	-	-	-	-	-	-	-	-	-	-	-
NCS DC86312 Cert	-	-	-	-	-	-	-	-	-	-	-	-
JGb-2 Meas	-	-	-	-	-	-	-	-	-	-	-	-
JGb-2 Cert	-	-	-	-	-	-	-	-	-	-	-	-
JGb-2 Meas	-	-	-	-	-	-	-	-	-	-	-	-
JGb-2 Cert	-	-	-	-	-	-	-	-	-	-	-	-
JGb-2 Meas	-	-	-	-	-	-	-	-	-	-	-	-
JGb-2 Cert	-	-	-	-	-	-	-	-	-	-	-	-
NCS DC70009 (GBW07241) Meas	-	-	-	-	-	-	-	-	-	-	-	-
NCS DC70009 (GBW07241) Cert	-	-	-	-	-	-	-	-	-	-	-	-
SGR-1b Meas	-	-	-	-	-	-	-	-	-	-	-	-
SGR-1b Cert	-	-	-	-	-	-	-	-	-	-	-	-
SGR-1b Meas	-	-	-	-	-	-	-	-	-	-	-	-
SGR-1b Cert	-	-	-	-	-	-	-	-	-	-	-	-
OREAS 100a (Fusion) Meas	-	-	-	-	-	-	-	-	-	-	-	-

Analyte	SiO <sub>2</sub>	Al <sub>2</sub> O <sub>3</sub>	Fe <sub>2</sub> O <sub>3</sub>	MnO	MgO	CaO	Na <sub>2</sub> O	K <sub>2</sub> O	TiO <sub>2</sub>	P <sub>2</sub> O <sub>5</sub>	LOI	LOI2
Units	%	%	%	%	%	%	%	%	%	%	%	%
Detection Limit	0.01	0.01	0.01	0.001	0.01	0.01	0.01	0.01	0.001	0.01		
Method	FUS-ICP	FUS-ICP	FUS-ICP	FUS-ICP	FUS-ICP	FUS-ICP	FUS-ICP	FUS-ICP	FUS-ICP	FUS-ICP	FUS-ICP	FUS-ICP
OREAS 100a (Fusion) Cert	-	-	-	-	-	-	-	-	-	-	-	-
OREAS 101a (Fusion) Meas	-	-	-	-	-	-	-	-	-	-	-	-
OREAS 101a (Fusion) Cert	-	-	-	-	-	-	-	-	-	-	-	-
OREAS 101b (Fusion) Meas	-	-	-	-	-	-	-	-	-	-	-	-
OREAS 101b (Fusion) Cert	-	-	-	-	-	-	-	-	-	-	-	-
JR-1 Meas	-	-	-	-	-	-	-	-	-	-	-	-
JR-1 Cert	-	-	-	-	-	-	-	-	-	-	-	-
NCS DC86318 Meas	-	-	-	-	-	-	-	-	-	-	-	-
NCS DC86318 Cert	-	-	-	-	-	-	-	-	-	-	-	-
USZ 25-2006 Meas	-	-	-	-	-	-	-	-	-	-	-	-
USZ 25-2006 Cert	-	-	-	-	-	-	-	-	-	-	-	-
USZ 25-2006 Meas	-	-	-	-	-	-	-	-	-	-	-	-
USZ 25-2006 Cert	-	-	-	-	-	-	-	-	-	-	-	-
DNC-1a Meas	-	-	-	-	-	-	-	-	-	-	-	-
DNC-1a Cert	-	-	-	-	-	-	-	-	-	-	-	-
DNC-1a Meas	-	-	-	-	-	-	-	-	-	-	-	-
DNC-1a Cert	-	-	-	-	-	-	-	-	-	-	-	-
DNC-1a Meas	-	-	-	-	-	-	-	-	-	-	-	-
DNC-1a Cert	-	-	-	-	-	-	-	-	-	-	-	-
DNC-1a Meas	-	-	-	-	-	-	-	-	-	-	-	-
DNC-1a Cert	-	-	-	-	-	-	-	-	-	-	-	-
GS311-4 Meas	-	-	-	-	-	-	-	-	-	-	-	-
GS311-4 Cert	-	-	-	-	-	-	-	-	-	-	-	-
GS311-4 Meas	-	-	-	-	-	-	-	-	-	-	-	-
GS311-4 Cert	-	-	-	-	-	-	-	-	-	-	-	-
GS900-5 Meas	-	-	-	-	-	-	-	-	-	-	-	-
GS900-5 Cert	-	-	-	-	-	-	-	-	-	-	-	-
GS900-5 Meas	-	-	-	-	-	-	-	-	-	-	-	-
GS900-5 Cert	-	-	-	-	-	-	-	-	-	-	-	-
OREAS 45d (Aqua Regia) Meas	-	-	-	-	-	-	-	-	-	-	-	-
OREAS 45d (Aqua Regia) Cert	-	-	-	-	-	-	-	-	-	-	-	-
OREAS 45d (Aqua Regia) Meas	-	-	-	-	-	-	-	-	-	-	-	-
OREAS 45d (Aqua Regia) Cert	-	-	-	-	-	-	-	-	-	-	-	-
OREAS 45d (Aqua Regia) Meas	-	-	-	-	-	-	-	-	-	-	-	-
OREAS 45d (Aqua Regia) Cert	-	-	-	-	-	-	-	-	-	-	-	-
SBC-1 Meas	-	-	-	-	-	-	-	-	-	-	-	-
SBC-1 Cert	-	-	-	-	-	-	-	-	-	-	-	-

Analyte	SiO <sub>2</sub>	Al <sub>2</sub> O <sub>3</sub>	Fe <sub>2</sub> O <sub>3</sub>	MnO	MgO	CaO	Na <sub>2</sub> O	K <sub>2</sub> O	TiO <sub>2</sub>	P <sub>2</sub> O <sub>5</sub>	LOI	LOI2
Units	%	%	%	%	%	%	%	%	%	%	%	%
Detection Limit	0.01	0.01	0.01	0.001	0.01	0.01	0.01	0.01	0.001	0.01		
Method	FUS-ICP	FUS-ICP	FUS-ICP	FUS-ICP	FUS-ICP	FUS-ICP	FUS-ICP	FUS-ICP	FUS-ICP	FUS-ICP	FUS-ICP	FUS-ICP
SBC-1 Meas	-	-	-	-	-	-	-	-	-	-	-	-
SBC-1 Cert	-	-	-	-	-	-	-	-	-	-	-	-
SBC-1 Meas	-	-	-	-	-	-	-	-	-	-	-	-
SBC-1 Cert	-	-	-	-	-	-	-	-	-	-	-	-
SBC-1 Meas	-	-	-	-	-	-	-	-	-	-	-	-
SBC-1 Cert	-	-	-	-	-	-	-	-	-	-	-	-
OREAS 45d (4-Acid) Meas	-	-	-	-	-	-	-	-	-	-	-	-
OREAS 45d (4-Acid) Cert	-	-	-	-	-	-	-	-	-	-	-	-
OREAS 45d (4-Acid) Meas	-	-	-	-	-	-	-	-	-	-	-	-
OREAS 45d (4-Acid) Cert	-	-	-	-	-	-	-	-	-	-	-	-
OREAS 45d (4-Acid) Meas	-	-	-	-	-	-	-	-	-	-	-	-
OREAS 45d (4-Acid) Cert	-	-	-	-	-	-	-	-	-	-	-	-
OREAS 45d (4-Acid) Meas	-	-	-	-	-	-	-	-	-	-	-	-
OREAS 45d (4-Acid) Cert	-	-	-	-	-	-	-	-	-	-	-	-
OxK110 Meas	-	-	-	-	-	-	-	-	-	-	-	-
OxK110 Cert	-	-	-	-	-	-	-	-	-	-	-	-
CDN-PGMS-24 Meas	-	-	-	-	-	-	-	-	-	-	-	-
CDN-PGMS-24 Cert	-	-	-	-	-	-	-	-	-	-	-	-
CDN-PGMS-24 Meas	-	-	-	-	-	-	-	-	-	-	-	-
CDN-PGMS-24 Cert	-	-	-	-	-	-	-	-	-	-	-	-
OXN117 Meas	-	-	-	-	-	-	-	-	-	-	-	-
OXN117 Cert	-	-	-	-	-	-	-	-	-	-	-	-
CaCO3 Meas	-	-	-	-	-	-	-	-	-	-	-	-
CaCO3 Cert	-	-	-	-	-	-	-	-	-	-	-	-
SdAR-M2 (U.S.G.S.) Meas	-	-	-	-	-	-	-	-	-	-	-	-
SdAR-M2 (U.S.G.S.) Cert	-	-	-	-	-	-	-	-	-	-	-	-
SdAR-M2 (U.S.G.S.) Meas	-	-	-	-	-	-	-	-	-	-	-	-
SdAR-M2 (U.S.G.S.) Cert	-	-	-	-	-	-	-	-	-	-	-	-
SdAR-M2 (U.S.G.S.) Meas	-	-	-	-	-	-	-	-	-	-	-	-
SdAR-M2 (U.S.G.S.) Cert	-	-	-	-	-	-	-	-	-	-	-	-
SdAR-M2 (U.S.G.S.) Meas	-	-	-	-	-	-	-	-	-	-	-	-
SdAR-M2 (U.S.G.S.) Cert	-	-	-	-	-	-	-	-	-	-	-	-
GXR-1 Meas	-	-	-	-	-	-	-	-	-	-	-	-
GXR-1 Cert	-	-	-	-	-	-	-	-	-	-	-	-
GXR-1 Meas	-	-	-	-	-	-	-	-	-	-	-	-
GXR-1 Cert	-	-	-	-	-	-	-	-	-	-	-	-
NIST 694 Meas	11.17	1.87	-	0.01	0.33	42.67	0.85	0.55	0.11	30.2	-	-

Analyte	SiO <sub>2</sub>	Al <sub>2</sub> O <sub>3</sub>	Fe <sub>2</sub> O <sub>3</sub>	MnO	MgO	CaO	Na <sub>2</sub> O	K <sub>2</sub> O	TiO <sub>2</sub>	P <sub>2</sub> O <sub>5</sub>	LOI	LOI2
Units	%	%	%	%	%	%	%	%	%	%	%	%
Detection Limit	0.01	0.01	0.01	0.001	0.01	0.01	0.01	0.01	0.001	0.01		
Method	FUS-ICP	FUS-ICP	FUS-ICP	FUS-ICP	FUS-ICP	FUS-ICP	FUS-ICP	FUS-ICP	FUS-ICP	FUS-ICP	FUS-ICP	FUS-ICP
NIST 694 Cert	11.2	1.8	-	0.0116	0.33	43.6	0.86	0.51	0.11	30.2	-	-
DNC-1 Meas	47.7	18.69	-	0.15	10.06	11.53	1.94	0.22	0.48	0.07	-	-
DNC-1 Cert	47.15	18.34	-	0.15	10.13	11.49	1.89	0.234	0.48	0.07	-	-
GBW 07113 Meas	71.48	12.87	-	0.14	0.14	0.59	2.51	5.43	0.28	0.04	-	-
GBW 07113 Cert	72.8	13	-	0.14	0.16	0.59	2.57	5.43	0.3	0.05	-	-
GXR-4 Meas	-	-	-	-	-	-	-	-	-	-	-	-
GXR-4 Cert	-	-	-	-	-	-	-	-	-	-	-	-
GXR-4 Meas	-	-	-	-	-	-	-	-	-	-	-	-
GXR-4 Cert	-	-	-	-	-	-	-	-	-	-	-	-
SDC-1 Meas	-	-	-	-	-	-	-	-	-	-	-	-
SDC-1 Cert	-	-	-	-	-	-	-	-	-	-	-	-
GXR-6 Meas	-	-	-	-	-	-	-	-	-	-	-	-
GXR-6 Cert	-	-	-	-	-	-	-	-	-	-	-	-
GXR-6 Meas	-	-	-	-	-	-	-	-	-	-	-	-
GXR-6 Cert	-	-	-	-	-	-	-	-	-	-	-	-
LKSD-3 Meas	-	-	-	-	-	-	-	-	-	-	-	-
LKSD-3 Cert	-	-	-	-	-	-	-	-	-	-	-	-
TDB-1 Meas	-	-	-	-	-	-	-	-	-	-	-	-
TDB-1 Cert	-	-	-	-	-	-	-	-	-	-	-	-
SY-2 Meas	-	-	-	-	-	-	-	-	-	-	-	-
SY-2 Cert	-	-	-	-	-	-	-	-	-	-	-	-
SY-3 Meas	-	-	-	-	-	-	-	-	-	-	-	-
SY-3 Cert	-	-	-	-	-	-	-	-	-	-	-	-
BaSO4 Meas	-	-	-	-	-	-	-	-	-	-	-	-
BaSO4 Cert	-	-	-	-	-	-	-	-	-	-	-	-
BaSO4 Meas	-	-	-	-	-	-	-	-	-	-	-	-
BaSO4 Cert	-	-	-	-	-	-	-	-	-	-	-	-
BaSO4 Meas	-	-	-	-	-	-	-	-	-	-	-	-
BaSO4 Cert	-	-	-	-	-	-	-	-	-	-	-	-
W-2a Meas	53.24	15.58	-	0.17	6.33	11.12	2.25	0.61	1.08	0.14	-	-
W-2a Cert	52.4	15.4	-	0.163	6.37	10.9	2.14	0.626	1.06	0.13	-	-
DTS-2b Meas	-	-	-	-	-	-	-	-	-	-	-	-
DTS-2b Cert	-	-	-	-	-	-	-	-	-	-	-	-
SY-4 Meas	50.12	21.14	-	0.11	0.5	8.08	6.87	1.65	0.3	0.13	-	-
SY-4 Cert	49.9	20.69	-	0.108	0.54	8.05	7.1	1.66	0.287	0.131	-	-
CTA-AC-1 Meas	-	-	-	-	-	-	-	-	-	-	-	-
CTA-AC-1 Cert	-	-	-	-	-	-	-	-	-	-	-	-

Analyte	SiO <sub>2</sub>	Al <sub>2</sub> O <sub>3</sub>	Fe <sub>2</sub> O <sub>3</sub>	MnO	MgO	CaO	Na <sub>2</sub> O	K <sub>2</sub> O	TiO <sub>2</sub>	P <sub>2</sub> O <sub>5</sub>	LOI	LOI2
Units	%	%	%	%	%	%	%	%	%	%	%	%
Detection Limit	0.01	0.01	0.01	0.001	0.01	0.01	0.01	0.01	0.001	0.01		
Method	FUS-ICP	FUS-ICP	FUS-ICP	FUS-ICP	FUS-ICP	FUS-ICP	FUS-ICP	FUS-ICP	FUS-ICP	FUS-ICP	FUS-ICP	FUS-ICP
BIR-1a Meas	47.43	15.62	-	0.17	9.47	13.58	1.83	0.02	0.96	0.03	-	-
BIR-1a Cert	47.96	15.5	-	0.175	9.7	13.3	1.82	0.03	0.96	0.021	-	-
NCS DC86312 Meas	-	-	-	-	-	-	-	-	-	-	-	-
NCS DC86312 Cert	-	-	-	-	-	-	-	-	-	-	-	-
JGb-2 Meas	-	-	-	-	-	-	-	-	-	-	-	-
JGb-2 Cert	-	-	-	-	-	-	-	-	-	-	-	-
NCS DC70009 (GBW07241) Meas	-	-	-	-	-	-	-	-	-	-	-	-
NCS DC70009 (GBW07241) Cert	-	-	-	-	-	-	-	-	-	-	-	-
SGR-1b Meas	-	-	-	-	-	-	-	-	-	-	-	-
SGR-1b Cert	-	-	-	-	-	-	-	-	-	-	-	-
SGR-1b Meas	-	-	-	-	-	-	-	-	-	-	-	-
SGR-1b Cert	-	-	-	-	-	-	-	-	-	-	-	-
SGR-1b Meas	-	-	-	-	-	-	-	-	-	-	-	-
SGR-1b Cert	-	-	-	-	-	-	-	-	-	-	-	-
OREAS 100a (Fusion) Meas	-	-	-	-	-	-	-	-	-	-	-	-
OREAS 100a (Fusion) Cert	-	-	-	-	-	-	-	-	-	-	-	-
OREAS 101a (Fusion) Meas	-	-	-	-	-	-	-	-	-	-	-	-
OREAS 101a (Fusion) Cert	-	-	-	-	-	-	-	-	-	-	-	-
OREAS 101b (Fusion) Meas	-	-	-	-	-	-	-	-	-	-	-	-
OREAS 101b (Fusion) Cert	-	-	-	-	-	-	-	-	-	-	-	-
OREAS 98 (S by LECO) Meas	-	-	-	-	-	-	-	-	-	-	-	-
OREAS 98 (S by LECO) Cert	-	-	-	-	-	-	-	-	-	-	-	-
OREAS 132b (S by LECO) Meas	-	-	-	-	-	-	-	-	-	-	-	-
OREAS 132b (S by LECO) Cert	-	-	-	-	-	-	-	-	-	-	-	-
JR-1 Meas	-	-	-	-	-	-	-	-	-	-	-	-
JR-1 Cert	-	-	-	-	-	-	-	-	-	-	-	-
NCS DC86318 Meas	-	-	-	-	-	-	-	-	-	-	-	-
NCS DC86318 Cert	-	-	-	-	-	-	-	-	-	-	-	-
USZ 25-2006 Meas	-	-	-	-	-	-	-	-	-	-	-	-
USZ 25-2006 Cert	-	-	-	-	-	-	-	-	-	-	-	-
DNC-1a Meas	-	-	-	-	-	-	-	-	-	-	-	-
DNC-1a Cert	-	-	-	-	-	-	-	-	-	-	-	-
PK2 Meas	-	-	-	-	-	-	-	-	-	-	-	-
PK2 Cert	-	-	-	-	-	-	-	-	-	-	-	-
GS309-4 Meas	-	-	-	-	-	-	-	-	-	-	-	-
GS309-4 Cert	-	-	-	-	-	-	-	-	-	-	-	-
GS311-4 Meas	-	-	-	-	-	-	-	-	-	-	-	-

Analyte	SiO <sub>2</sub>	Al <sub>2</sub> O <sub>3</sub>	Fe <sub>2</sub> O <sub>3</sub>	MnO	MgO	CaO	Na <sub>2</sub> O	K <sub>2</sub> O	TiO <sub>2</sub>	P <sub>2</sub> O <sub>5</sub>	LOI	LOI2
Units	%	%	%	%	%	%	%	%	%	%	%	%
Detection Limit	0.01	0.01	0.01	0.001	0.01	0.01	0.01	0.01	0.001	0.01		
Method	FUS-ICP	FUS-ICP	FUS-ICP	FUS-ICP	FUS-ICP	FUS-ICP	FUS-ICP	FUS-ICP	FUS-ICP	FUS-ICP	FUS-ICP	FUS-ICP
GS311-4 Cert	-	-	-	-	-	-	-	-	-	-	-	-
GS311-4 Meas	-	-	-	-	-	-	-	-	-	-	-	-
GS311-4 Cert	-	-	-	-	-	-	-	-	-	-	-	-
GS311-4 Meas	-	-	-	-	-	-	-	-	-	-	-	-
GS311-4 Cert	-	-	-	-	-	-	-	-	-	-	-	-
GS900-5 Meas	-	-	-	-	-	-	-	-	-	-	-	-
GS900-5 Cert	-	-	-	-	-	-	-	-	-	-	-	-
GS900-5 Meas	-	-	-	-	-	-	-	-	-	-	-	-
GS900-5 Cert	-	-	-	-	-	-	-	-	-	-	-	-
GS900-5 Meas	-	-	-	-	-	-	-	-	-	-	-	-
GS900-5 Cert	-	-	-	-	-	-	-	-	-	-	-	-
OREAS 45d (Aqua Regia) Meas	-	-	-	-	-	-	-	-	-	-	-	-
OREAS 45d (Aqua Regia) Cert	-	-	-	-	-	-	-	-	-	-	-	-
SBC-1 Meas	-	-	-	-	-	-	-	-	-	-	-	-
SBC-1 Cert	-	-	-	-	-	-	-	-	-	-	-	-
OREAS 45d (4-Acid) Meas	-	-	-	-	-	-	-	-	-	-	-	-
OREAS 45d (4-Acid) Cert	-	-	-	-	-	-	-	-	-	-	-	-
CaCO3 Meas	-	-	-	-	-	-	-	-	-	-	-	-
CaCO3 Cert	-	-	-	-	-	-	-	-	-	-	-	-
SdAR-M2 (U.S.G.S.) Meas	-	-	-	-	-	-	-	-	-	-	-	-
SdAR-M2 (U.S.G.S.) Cert	-	-	-	-	-	-	-	-	-	-	-	-
SdAR-M2 (U.S.G.S.) Meas	-	-	-	-	-	-	-	-	-	-	-	-
SdAR-M2 (U.S.G.S.) Cert	-	-	-	-	-	-	-	-	-	-	-	-
GXR-1 Meas	-	-	-	-	-	-	-	-	-	-	-	-
GXR-1 Cert	-	-	-	-	-	-	-	-	-	-	-	-
GXR-1 Meas	-	-	-	-	-	-	-	-	-	-	-	-
GXR-1 Cert	-	-	-	-	-	-	-	-	-	-	-	-
NIST 694 Meas	11.09	1.84	-	0.01	0.34	42.63	0.85	0.54	0.12	30.2	-	-
NIST 694 Cert	11.2	1.8	-	0.0116	0.33	43.6	0.86	0.51	0.11	30.2	-	-
DNC-1 Meas	47.26	17.65	-	0.14	10.2	11.46	1.92	0.22	0.46	0.09	-	-
DNC-1 Cert	47.15	18.34	-	0.15	10.13	11.49	1.89	0.234	0.48	0.07	-	-
GBW 07113 Meas	71.07	13.41	-	0.14	0.15	0.62	2.5	5.43	0.28	0.04	-	-
GBW 07113 Cert	72.8	13	-	0.14	0.16	0.59	2.57	5.43	0.3	0.05	-	-
GXR-4 Meas	-	-	-	-	-	-	-	-	-	-	-	-
GXR-4 Cert	-	-	-	-	-	-	-	-	-	-	-	-
GXR-4 Meas	-	-	-	-	-	-	-	-	-	-	-	-
GXR-4 Cert	-	-	-	-	-	-	-	-	-	-	-	-



Analyte	SiO <sub>2</sub>	Al <sub>2</sub> O <sub>3</sub>	Fe <sub>2</sub> O <sub>3</sub>	MnO	MgO	CaO	Na <sub>2</sub> O	K <sub>2</sub> O	TiO <sub>2</sub>	P <sub>2</sub> O <sub>5</sub>	LOI	LOI2
Units	%	%	%	%	%	%	%	%	%	%	%	%
Detection Limit	0.01	0.01	0.01	0.001	0.01	0.01	0.01	0.01	0.001	0.01		
Method	FUS-ICP	FUS-ICP	FUS-ICP	FUS-ICP	FUS-ICP	FUS-ICP	FUS-ICP	FUS-ICP	FUS-ICP	FUS-ICP	FUS-ICP	FUS-ICP
SDC-1 Meas	-	-	-	-	-	-	-	-	-	-	-	-
SDC-1 Cert	-	-	-	-	-	-	-	-	-	-	-	-
SDC-1 Meas	-	-	-	-	-	-	-	-	-	-	-	-
SDC-1 Cert	-	-	-	-	-	-	-	-	-	-	-	-
GXR-6 Meas	-	-	-	-	-	-	-	-	-	-	-	-
GXR-6 Cert	-	-	-	-	-	-	-	-	-	-	-	-
GXR-6 Meas	-	-	-	-	-	-	-	-	-	-	-	-
GXR-6 Cert	-	-	-	-	-	-	-	-	-	-	-	-
LKSD-3 Meas	-	-	-	-	-	-	-	-	-	-	-	-
LKSD-3 Cert	-	-	-	-	-	-	-	-	-	-	-	-
TDB-1 Meas	-	-	-	-	-	-	-	-	-	-	-	-
TDB-1 Cert	-	-	-	-	-	-	-	-	-	-	-	-
SY-2 Meas	-	-	-	-	-	-	-	-	-	-	-	-
SY-2 Cert	-	-	-	-	-	-	-	-	-	-	-	-
SY-3 Meas	-	-	-	-	-	-	-	-	-	-	-	-
SY-3 Cert	-	-	-	-	-	-	-	-	-	-	-	-
BaSO4 Meas	-	-	-	-	-	-	-	-	-	-	-	-
BaSO4 Cert	-	-	-	-	-	-	-	-	-	-	-	-
BaSO4 Meas	-	-	-	-	-	-	-	-	-	-	-	-
BaSO4 Cert	-	-	-	-	-	-	-	-	-	-	-	-
W-2a Meas	53.2	15.84	-	0.17	6.56	11.18	2.21	0.61	1.11	0.14	-	-
W-2a Cert	52.4	15.4	-	0.163	6.37	10.9	2.14	0.626	1.06	0.13	-	-
SY-4 Meas	50.58	20.02	-	0.11	0.5	8.18	6.98	1.66	0.28	0.13	-	-
SY-4 Cert	49.9	20.69	-	0.108	0.54	8.05	7.1	1.66	0.287	0.131	-	-
CTA-AC-1 Meas	-	-	-	-	-	-	-	-	-	-	-	-
CTA-AC-1 Cert	-	-	-	-	-	-	-	-	-	-	-	-
BIR-1a Meas	47.69	15.73	-	0.17	9.73	13.46	1.76	0.02	0.97	0.04	-	-
BIR-1a Cert	47.96	15.5	-	0.175	9.7	13.3	1.82	0.03	0.96	0.021	-	-
BIR-1a Meas	-	-	-	-	-	-	-	-	-	-	-	-
BIR-1a Cert	-	-	-	-	-	-	-	-	-	-	-	-
NCS DC86312 Meas	-	-	-	-	-	-	-	-	-	-	-	-
NCS DC86312 Cert	-	-	-	-	-	-	-	-	-	-	-	-
JGb-2 Meas	-	-	-	-	-	-	-	-	-	-	-	-
JGb-2 Cert	-	-	-	-	-	-	-	-	-	-	-	-
JGb-2 Meas	-	-	-	-	-	-	-	-	-	-	-	-
JGb-2 Cert	-	-	-	-	-	-	-	-	-	-	-	-
JGb-2 Meas	-	-	-	-	-	-	-	-	-	-	-	-

Analyte	SiO <sub>2</sub>	Al <sub>2</sub> O <sub>3</sub>	Fe <sub>2</sub> O <sub>3</sub>	MnO	MgO	CaO	Na <sub>2</sub> O	K <sub>2</sub> O	TiO <sub>2</sub>	P <sub>2</sub> O <sub>5</sub>	LOI	LOI2
Units	%	%	%	%	%	%	%	%	%	%	%	%
Detection Limit	0.01	0.01	0.01	0.001	0.01	0.01	0.01	0.01	0.001	0.01		
Method	FUS-ICP	FUS-ICP	FUS-ICP	FUS-ICP	FUS-ICP	FUS-ICP	FUS-ICP	FUS-ICP	FUS-ICP	FUS-ICP	FUS-ICP	FUS-ICP
JGb-2 Cert	-	-	-	-	-	-	-	-	-	-	-	-
JGb-2 Meas	-	-	-	-	-	-	-	-	-	-	-	-
JGb-2 Cert	-	-	-	-	-	-	-	-	-	-	-	-
NCS DC70009 (GBW07241) Meas	-	-	-	-	-	-	-	-	-	-	-	-
NCS DC70009 (GBW07241) Cert	-	-	-	-	-	-	-	-	-	-	-	-
SGR-1b Meas	-	-	-	-	-	-	-	-	-	-	-	-
SGR-1b Cert	-	-	-	-	-	-	-	-	-	-	-	-
SGR-1b Meas	-	-	-	-	-	-	-	-	-	-	-	-
SGR-1b Cert	-	-	-	-	-	-	-	-	-	-	-	-
OREAS 100a (Fusion) Meas	-	-	-	-	-	-	-	-	-	-	-	-
OREAS 100a (Fusion) Cert	-	-	-	-	-	-	-	-	-	-	-	-
OREAS 101a (Fusion) Meas	-	-	-	-	-	-	-	-	-	-	-	-
OREAS 101a (Fusion) Cert	-	-	-	-	-	-	-	-	-	-	-	-
OREAS 101b (Fusion) Meas	-	-	-	-	-	-	-	-	-	-	-	-
OREAS 101b (Fusion) Cert	-	-	-	-	-	-	-	-	-	-	-	-
JR-1 Meas	-	-	-	-	-	-	-	-	-	-	-	-
JR-1 Cert	-	-	-	-	-	-	-	-	-	-	-	-
NCS DC86318 Meas	-	-	-	-	-	-	-	-	-	-	-	-
NCS DC86318 Cert	-	-	-	-	-	-	-	-	-	-	-	-
USZ 25-2006 Meas	-	-	-	-	-	-	-	-	-	-	-	-
USZ 25-2006 Cert	-	-	-	-	-	-	-	-	-	-	-	-
USZ 25-2006 Meas	-	-	-	-	-	-	-	-	-	-	-	-
USZ 25-2006 Cert	-	-	-	-	-	-	-	-	-	-	-	-
DNC-1a Meas	-	-	-	-	-	-	-	-	-	-	-	-
DNC-1a Cert	-	-	-	-	-	-	-	-	-	-	-	-
DNC-1a Meas	-	-	-	-	-	-	-	-	-	-	-	-
DNC-1a Cert	-	-	-	-	-	-	-	-	-	-	-	-
PK2 Meas	-	-	-	-	-	-	-	-	-	-	-	-
PK2 Cert	-	-	-	-	-	-	-	-	-	-	-	-
GS311-4 Meas	-	-	-	-	-	-	-	-	-	-	-	-
GS311-4 Cert	-	-	-	-	-	-	-	-	-	-	-	-
GS311-4 Meas	-	-	-	-	-	-	-	-	-	-	-	-
GS311-4 Cert	-	-	-	-	-	-	-	-	-	-	-	-
GS900-5 Meas	-	-	-	-	-	-	-	-	-	-	-	-
GS900-5 Cert	-	-	-	-	-	-	-	-	-	-	-	-
GS900-5 Meas	-	-	-	-	-	-	-	-	-	-	-	-
GS900-5 Cert	-	-	-	-	-	-	-	-	-	-	-	-

Analyte	SiO <sub>2</sub>	Al <sub>2</sub> O <sub>3</sub>	Fe <sub>2</sub> O <sub>3</sub>	MnO	MgO	CaO	Na <sub>2</sub> O	K <sub>2</sub> O	TiO <sub>2</sub>	P <sub>2</sub> O <sub>5</sub>	LOI	LOI2
Units	%	%	%	%	%	%	%	%	%	%	%	%
Detection Limit	0.01	0.01	0.01	0.001	0.01	0.01	0.01	0.01	0.001	0.01		
Method	FUS-ICP	FUS-ICP	FUS-ICP	FUS-ICP	FUS-ICP	FUS-ICP	FUS-ICP	FUS-ICP	FUS-ICP	FUS-ICP	FUS-ICP	FUS-ICP
OREAS 45d (Aqua Regia) Meas	-	-	-	-	-	-	-	-	-	-	-	-
OREAS 45d (Aqua Regia) Cert	-	-	-	-	-	-	-	-	-	-	-	-
SBC-1 Meas	-	-	-	-	-	-	-	-	-	-	-	-
SBC-1 Cert	-	-	-	-	-	-	-	-	-	-	-	-
SBC-1 Meas	-	-	-	-	-	-	-	-	-	-	-	-
SBC-1 Cert	-	-	-	-	-	-	-	-	-	-	-	-
OREAS 45d (4-Acid) Meas	-	-	-	-	-	-	-	-	-	-	-	-
OREAS 45d (4-Acid) Cert	-	-	-	-	-	-	-	-	-	-	-	-
OxK110 Meas	-	-	-	-	-	-	-	-	-	-	-	-
OxK110 Cert	-	-	-	-	-	-	-	-	-	-	-	-
OXN117 Meas	-	-	-	-	-	-	-	-	-	-	-	-
OXN117 Cert	-	-	-	-	-	-	-	-	-	-	-	-
CaCO3 Meas	-	-	-	-	-	-	-	-	-	-	-	-
CaCO3 Cert	-	-	-	-	-	-	-	-	-	-	-	-
CaCO3 Meas	-	-	-	-	-	-	-	-	-	-	-	-
CaCO3 Cert	-	-	-	-	-	-	-	-	-	-	-	-
SdAR-M2 (U.S.G.S.) Meas	-	-	-	-	-	-	-	-	-	-	-	-
SdAR-M2 (U.S.G.S.) Cert	-	-	-	-	-	-	-	-	-	-	-	-
GXR-1 Meas	-	-	-	-	-	-	-	-	-	-	-	-
GXR-1 Cert	-	-	-	-	-	-	-	-	-	-	-	-
GXR-1 Meas	-	-	-	-	-	-	-	-	-	-	-	-
GXR-1 Cert	-	-	-	-	-	-	-	-	-	-	-	-
NIST 694 Meas	11.39	1.88	-	0.01	0.34	42.94	0.88	0.55	0.11	30.28	-	-
NIST 694 Cert	11.2	1.8	-	0.0116	0.33	43.6	0.86	0.51	0.11	30.2	-	-
DNC-1 Meas	47.33	18.66	-	0.15	10.08	11.46	1.94	0.22	0.48	0.05	-	-
DNC-1 Cert	47.15	18.34	-	0.15	10.13	11.49	1.89	0.234	0.48	0.07	-	-
GBW 07113 Meas	-	-	-	-	-	-	-	-	-	-	-	-
GBW 07113 Cert	-	-	-	-	-	-	-	-	-	-	-	-
GXR-4 Meas	-	-	-	-	-	-	-	-	-	-	-	-
GXR-4 Cert	-	-	-	-	-	-	-	-	-	-	-	-
GXR-4 Meas	-	-	-	-	-	-	-	-	-	-	-	-
GXR-4 Cert	-	-	-	-	-	-	-	-	-	-	-	-
GXR-4 Meas	-	-	-	-	-	-	-	-	-	-	-	-
GXR-4 Cert	-	-	-	-	-	-	-	-	-	-	-	-
SDC-1 Meas	-	-	-	-	-	-	-	-	-	-	-	-
SDC-1 Cert	-	-	-	-	-	-	-	-	-	-	-	-
SDC-1 Meas	-	-	-	-	-	-	-	-	-	-	-	-

Analyte	SiO <sub>2</sub>	Al <sub>2</sub> O <sub>3</sub>	Fe <sub>2</sub> O <sub>3</sub>	MnO	MgO	CaO	Na <sub>2</sub> O	K <sub>2</sub> O	TiO <sub>2</sub>	P <sub>2</sub> O <sub>5</sub>	LOI	LOI2
Units	%	%	%	%	%	%	%	%	%	%	%	%
Detection Limit	0.01	0.01	0.01	0.001	0.01	0.01	0.01	0.01	0.001	0.01		
Method	FUS-ICP	FUS-ICP	FUS-ICP	FUS-ICP	FUS-ICP	FUS-ICP	FUS-ICP	FUS-ICP	FUS-ICP	FUS-ICP	FUS-ICP	FUS-ICP
SDC-1 Cert	-	-	-	-	-	-	-	-	-	-	-	-
GXR-6 Meas	-	-	-	-	-	-	-	-	-	-	-	-
GXR-6 Cert	-	-	-	-	-	-	-	-	-	-	-	-
GXR-6 Meas	-	-	-	-	-	-	-	-	-	-	-	-
GXR-6 Cert	-	-	-	-	-	-	-	-	-	-	-	-
GXR-6 Meas	-	-	-	-	-	-	-	-	-	-	-	-
GXR-6 Cert	-	-	-	-	-	-	-	-	-	-	-	-
LKSD-3 Meas	-	-	-	-	-	-	-	-	-	-	-	-
LKSD-3 Cert	-	-	-	-	-	-	-	-	-	-	-	-
TDB-1 Meas	-	-	-	-	-	-	-	-	-	-	-	-
TDB-1 Cert	-	-	-	-	-	-	-	-	-	-	-	-
SY-2 Meas	-	-	-	-	-	-	-	-	-	-	-	-
SY-2 Cert	-	-	-	-	-	-	-	-	-	-	-	-
SY-3 Meas	-	-	-	-	-	-	-	-	-	-	-	-
SY-3 Cert	-	-	-	-	-	-	-	-	-	-	-	-
BaSO4 Meas	-	-	-	-	-	-	-	-	-	-	-	-
BaSO4 Cert	-	-	-	-	-	-	-	-	-	-	-	-
W-2a Meas	52.41	15.45	-	0.17	6.35	11.11	2.21	0.61	1.07	0.13	-	-
W-2a Cert	52.4	15.4	-	0.163	6.37	10.9	2.14	0.626	1.06	0.14	-	-
SY-4 Meas	50.5	20.18	-	0.11	0.5	8.1	6.89	1.66	0.28	0.12	-	-
SY-4 Cert	49.9	20.69	-	0.108	0.54	8.05	7.1	1.66	0.287	0.131	-	-
CTA-AC-1 Meas	-	-	-	-	-	-	-	-	-	-	-	-
CTA-AC-1 Cert	-	-	-	-	-	-	-	-	-	-	-	-
BIR-1a Meas	48.2	15.59	-	0.17	9.52	13.4	1.84	0.02	0.93	0.02	-	-
BIR-1a Cert	47.96	15.5	-	0.175	9.7	13.3	1.82	0.03	0.96	0.021	-	-
NCS DC86312 Meas	-	-	-	-	-	-	-	-	-	-	-	-
NCS DC86312 Cert	-	-	-	-	-	-	-	-	-	-	-	-
JGb-2 Meas	-	-	-	-	-	-	-	-	-	-	-	-
JGb-2 Cert	-	-	-	-	-	-	-	-	-	-	-	-
JGb-2 Meas	-	-	-	-	-	-	-	-	-	-	-	-
JGb-2 Cert	-	-	-	-	-	-	-	-	-	-	-	-
JGb-2 Meas	-	-	-	-	-	-	-	-	-	-	-	-
JGb-2 Cert	-	-	-	-	-	-	-	-	-	-	-	-
NCS DC70009 (GBW07241) Meas	-	-	-	-	-	-	-	-	-	-	-	-
NCS DC70009 (GBW07241) Cert	-	-	-	-	-	-	-	-	-	-	-	-
SGR-1b Meas	-	-	-	-	-	-	-	-	-	-	-	-
SGR-1b Cert	-	-	-	-	-	-	-	-	-	-	-	-

Analyte	SiO <sub>2</sub>	Al <sub>2</sub> O <sub>3</sub>	Fe <sub>2</sub> O <sub>3</sub>	MnO	MgO	CaO	Na <sub>2</sub> O	K <sub>2</sub> O	TiO <sub>2</sub>	P <sub>2</sub> O <sub>5</sub>	LOI	LOI2
Units	%	%	%	%	%	%	%	%	%	%	%	%
Detection Limit	0.01	0.01	0.01	0.001	0.01	0.01	0.01	0.01	0.001	0.01		
Method	FUS-ICP	FUS-ICP	FUS-ICP	FUS-ICP	FUS-ICP	FUS-ICP	FUS-ICP	FUS-ICP	FUS-ICP	FUS-ICP	FUS-ICP	FUS-ICP
OREAS 100a (Fusion) Meas	-	-	-	-	-	-	-	-	-	-	-	-
OREAS 100a (Fusion) Cert	-	-	-	-	-	-	-	-	-	-	-	-
OREAS 101a (Fusion) Meas	-	-	-	-	-	-	-	-	-	-	-	-
OREAS 101a (Fusion) Cert	-	-	-	-	-	-	-	-	-	-	-	-
OREAS 101b (Fusion) Meas	-	-	-	-	-	-	-	-	-	-	-	-
OREAS 101b (Fusion) Cert	-	-	-	-	-	-	-	-	-	-	-	-
JR-1 Meas	-	-	-	-	-	-	-	-	-	-	-	-
JR-1 Cert	-	-	-	-	-	-	-	-	-	-	-	-
NCS DC86318 Meas	-	-	-	-	-	-	-	-	-	-	-	-
NCS DC86318 Cert	-	-	-	-	-	-	-	-	-	-	-	-
USZ 25-2006 Meas	-	-	-	-	-	-	-	-	-	-	-	-
USZ 25-2006 Cert	-	-	-	-	-	-	-	-	-	-	-	-
USZ 25-2006 Meas	-	-	-	-	-	-	-	-	-	-	-	-
USZ 25-2006 Cert	-	-	-	-	-	-	-	-	-	-	-	-
DNC-1a Meas	-	-	-	-	-	-	-	-	-	-	-	-
DNC-1a Cert	-	-	-	-	-	-	-	-	-	-	-	-
DNC-1a Meas	-	-	-	-	-	-	-	-	-	-	-	-
DNC-1a Cert	-	-	-	-	-	-	-	-	-	-	-	-
GS311-4 Meas	-	-	-	-	-	-	-	-	-	-	-	-
GS311-4 Cert	-	-	-	-	-	-	-	-	-	-	-	-
GS900-5 Meas	-	-	-	-	-	-	-	-	-	-	-	-
GS900-5 Cert	-	-	-	-	-	-	-	-	-	-	-	-
OREAS 45d (Aqua Regia) Meas	-	-	-	-	-	-	-	-	-	-	-	-
OREAS 45d (Aqua Regia) Cert	-	-	-	-	-	-	-	-	-	-	-	-
SBC-1 Meas	-	-	-	-	-	-	-	-	-	-	-	-
SBC-1 Cert	-	-	-	-	-	-	-	-	-	-	-	-
SBC-1 Meas	-	-	-	-	-	-	-	-	-	-	-	-
SBC-1 Cert	-	-	-	-	-	-	-	-	-	-	-	-
OREAS 45d (4-Acid) Meas	-	-	-	-	-	-	-	-	-	-	-	-
OREAS 45d (4-Acid) Cert	-	-	-	-	-	-	-	-	-	-	-	-
OREAS 45d (4-Acid) Meas	-	-	-	-	-	-	-	-	-	-	-	-
OREAS 45d (4-Acid) Cert	-	-	-	-	-	-	-	-	-	-	-	-
CaCO3 Meas	-	-	-	-	-	-	-	-	-	-	-	-
CaCO3 Cert	-	-	-	-	-	-	-	-	-	-	-	-
CaCO3 Meas	-	-	-	-	-	-	-	-	-	-	-	-
CaCO3 Cert	-	-	-	-	-	-	-	-	-	-	-	-
SdAR-M2 (U.S.G.S.) Meas	-	-	-	-	-	-	-	-	-	-	-	-

Analyte	SiO <sub>2</sub>	Al <sub>2</sub> O <sub>3</sub>	Fe <sub>2</sub> O <sub>3</sub>	MnO	MgO	CaO	Na <sub>2</sub> O	K <sub>2</sub> O	TiO <sub>2</sub>	P <sub>2</sub> O <sub>5</sub>	LOI	LOI2
Units	%	%	%	%	%	%	%	%	%	%	%	%
Detection Limit	0.01	0.01	0.01	0.001	0.01	0.01	0.01	0.01	0.001	0.01		
Method	FUS-ICP	FUS-ICP	FUS-ICP	FUS-ICP	FUS-ICP	FUS-ICP	FUS-ICP	FUS-ICP	FUS-ICP	FUS-ICP	FUS-ICP	FUS-ICP
SdAR-M2 (U.S.G.S.) Cert	-	-	-	-	-	-	-	-	-	-	-	-
SdAR-M2 (U.S.G.S.) Meas	-	-	-	-	-	-	-	-	-	-	-	-
SdAR-M2 (U.S.G.S.) Cert	-	-	-	-	-	-	-	-	-	-	-	-
SdAR-M2 (U.S.G.S.) Meas	-	-	-	-	-	-	-	-	-	-	-	-
SdAR-M2 (U.S.G.S.) Cert	-	-	-	-	-	-	-	-	-	-	-	-
OREAS 214 Meas	-	-	-	-	-	-	-	-	-	-	-	-
OREAS 214 Cert	-	-	-	-	-	-	-	-	-	-	-	-
OREAS 218 Meas	-	-	-	-	-	-	-	-	-	-	-	-
OREAS 218 Cert	-	-	-	-	-	-	-	-	-	-	-	-
OREAS 218 Meas	-	-	-	-	-	-	-	-	-	-	-	-
OREAS 218 Cert	-	-	-	-	-	-	-	-	-	-	-	-
T9 Geochem Orig	-	-	-	-	-	-	-	-	-	-	-	-
T9 Geochem Dup	-	-	-	-	-	-	-	-	-	-	-	-
T14 Geochem Orig	-	-	-	-	-	-	-	-	-	-	-	-
T14 Geochem Dup	-	-	-	-	-	-	-	-	-	-	-	-
T17 Geochem Orig	-	-	-	-	-	-	-	-	-	-	-	-
T17 Geochem Dup	-	-	-	-	-	-	-	-	-	-	-	-
STPL-BAS-025 Orig	-	-	-	-	-	-	-	-	-	-	-	-
STPL-BAS-025 Dup	-	-	-	-	-	-	-	-	-	-	-	-
T24 Geochem Orig	3.6	0.99	42.95	1.769	2.29	6.34	0.05	0.04	0.042	0.03	16.15	13.74
T24 Geochem Dup	3.47	0.95	42.18	1.742	2.22	6.21	0.05	0.03	0.041	0.03	16.15	13.74
T27 Geochem Orig	-	-	-	-	-	-	-	-	-	-	-	-
T27 Geochem Dup	-	-	-	-	-	-	-	-	-	-	-	-
T31 Geochem Orig	-	-	-	-	-	-	-	-	-	-	-	-
T31 Geochem Dup	-	-	-	-	-	-	-	-	-	-	-	-
T37 Geochem Orig	-	-	-	-	-	-	-	-	-	-	-	-
T37 Geochem Dup	-	-	-	-	-	-	-	-	-	-	-	-
T42 Geochem Orig	-	-	-	-	-	-	-	-	-	-	-	-
T42 Geochem Dup	-	-	-	-	-	-	-	-	-	-	-	-
T45 Geochem Orig	-	-	-	-	-	-	-	-	-	-	-	-
T45 Geochem Dup	-	-	-	-	-	-	-	-	-	-	-	-
STPL-53-PML-036 Orig	-	-	-	-	-	-	-	-	-	-	-	-
STPL-53-PML-036 Dup	-	-	-	-	-	-	-	-	-	-	-	-
STPL-BAS-025 Orig	-	-	-	-	-	-	-	-	-	-	-	-
STPL-BAS-025 Dup	-	-	-	-	-	-	-	-	-	-	-	-
T42 Geochem Orig	-	-	-	-	-	-	-	-	-	-	-	-
T42 Geochem Dup	-	-	-	-	-	-	-	-	-	-	-	-

Analyte	SiO <sub>2</sub>	Al <sub>2</sub> O <sub>3</sub>	Fe <sub>2</sub> O <sub>3</sub>	MnO	MgO	CaO	Na <sub>2</sub> O	K <sub>2</sub> O	TiO <sub>2</sub>	P <sub>2</sub> O <sub>5</sub>	LOI	LOI2
Units	%	%	%	%	%	%	%	%	%	%	%	%
Detection Limit	0.01	0.01	0.01	0.001	0.01	0.01	0.01	0.01	0.001	0.01		
Method	FUS-ICP	FUS-ICP	FUS-ICP	FUS-ICP	FUS-ICP	FUS-ICP	FUS-ICP	FUS-ICP	FUS-ICP	FUS-ICP	FUS-ICP	FUS-ICP
T45 Geochem Orig	-	-	-	-	-	-	-	-	-	-	-	-
T45 Geochem Dup	-	-	-	-	-	-	-	-	-	-	-	-
T59 Orig	-	-	-	-	-	-	-	-	-	-	-	-
T59 Dup	-	-	-	-	-	-	-	-	-	-	-	-
T72 Orig	-	-	-	-	-	-	-	-	-	-	-	-
T72 Dup	-	-	-	-	-	-	-	-	-	-	-	-
T73 Orig	-	-	-	-	-	-	-	-	-	-	-	-
T73 Dup	-	-	-	-	-	-	-	-	-	-	-	-
STPL-BAS-029 Orig	-	-	-	-	-	-	-	-	-	-	-	-
STPL-BAS-029 Dup	-	-	-	-	-	-	-	-	-	-	-	-
T81 Orig	-	-	-	-	-	-	-	-	-	-	-	-
T81 Dup	-	-	-	-	-	-	-	-	-	-	-	-
T86 Orig	-	-	-	-	-	-	-	-	-	-	-	-
T86 Dup	-	-	-	-	-	-	-	-	-	-	-	-
T88 Orig	60.41	14.1	5.11	0.215	1.23	3.57	1.86	1.9	0.415	0.08	3.05	3.75
T88 Dup	61.11	14.16	5.26	0.222	1.25	3.63	1.86	1.92	0.415	0.08	3.05	3.75
T89 Orig	-	-	-	-	-	-	-	-	-	-	-	-
T89 Dup	-	-	-	-	-	-	-	-	-	-	-	-
T94 Orig	-	-	-	-	-	-	-	-	-	-	-	-
T94 Dup	-	-	-	-	-	-	-	-	-	-	-	-
T98 Orig	-	-	-	-	-	-	-	-	-	-	-	-
T98 Dup	-	-	-	-	-	-	-	-	-	-	-	-
T99 Orig	-	-	-	-	-	-	-	-	-	-	-	-
T99 Dup	-	-	-	-	-	-	-	-	-	-	-	-
T101 Orig	-	-	-	-	-	-	-	-	-	-	-	-
T101 Dup	-	-	-	-	-	-	-	-	-	-	-	-
T102 Orig	-	-	-	-	-	-	-	-	-	-	-	-
T102 Dup	-	-	-	-	-	-	-	-	-	-	-	-
T114 Orig	-	-	-	-	-	-	-	-	-	-	-	-
T114 Dup	-	-	-	-	-	-	-	-	-	-	-	-
T116 Orig	-	-	-	-	-	-	-	-	-	-	-	-
T116 Dup	-	-	-	-	-	-	-	-	-	-	-	-
T117 Orig	65.89	15.19	0.79	0.049	1.42	4.09	3.77	1.06	0.465	0.09	2.14	2.52
T117 Split PREP DUP	67	15.72	0.67	0.049	1.42	4.11	3.78	1.05	0.459	0.13	2.19	2.57
STPL-53-PML-025 Orig	76.18	12.19	0.39	0.034	0.55	1.41	3.45	2.12	0.195	0.04	2.13	2.22
STPL-53-PML-025 Dup	-	-	-	-	-	-	-	-	-	-	-	-
T65 Orig	-	-	-	-	-	-	-	-	-	-	-	-

Analyte	SiO <sub>2</sub>	Al <sub>2</sub> O <sub>3</sub>	Fe <sub>2</sub> O <sub>3</sub>	MnO	MgO	CaO	Na <sub>2</sub> O	K <sub>2</sub> O	TiO <sub>2</sub>	P <sub>2</sub> O <sub>5</sub>	LOI	LOI2
Units	%	%	%	%	%	%	%	%	%	%	%	%
Detection Limit	0.01	0.01	0.01	0.001	0.01	0.01	0.01	0.01	0.001	0.01		
Method	FUS-ICP	FUS-ICP	FUS-ICP	FUS-ICP	FUS-ICP	FUS-ICP	FUS-ICP	FUS-ICP	FUS-ICP	FUS-ICP	FUS-ICP	FUS-ICP
T65 Dup	-	-	-	-	-	-	-	-	-	-	-	-
T106 Orig	-	-	-	-	-	-	-	-	-	-	-	-
T106 Dup	-	-	-	-	-	-	-	-	-	-	-	-
T118 Orig	66.25	15.36	0.27	0.055	1.51	3.4	3.97	1.16	0.497	0.18	1.28	1.76
T118 Dup	66.21	15.85	0.31	0.056	1.51	3.38	3.95	1.16	0.502	0.17	1.28	1.76
T141 Orig	-	-	-	-	-	-	-	-	-	-	-	-
T141 Dup	-	-	-	-	-	-	-	-	-	-	-	-
STPL-BAS-023 Orig	-	-	-	-	-	-	-	-	-	-	-	-
STPL-BAS-023 Dup	-	-	-	-	-	-	-	-	-	-	-	-
T154 Orig	-	-	-	-	-	-	-	-	-	-	-	-
T154 Dup	-	-	-	-	-	-	-	-	-	-	-	-
T157 Orig	-	-	-	-	-	-	-	-	-	-	-	-
T157 Dup	-	-	-	-	-	-	-	-	-	-	-	-
T158 Orig	-	-	-	-	-	-	-	-	-	-	-	-
T158 Dup	-	-	-	-	-	-	-	-	-	-	-	-
STPL-PML-53-027 Orig	75.59	13.08	0.71	0.032	0.53	1.39	3.48	2.09	0.198	0.04	2.56	2.5
STPL-PML-53-027 Dup	75.08	12.38	0.67	0.032	0.53	1.38	3.47	2.08	0.186	0.04	2.56	2.5
T182 Orig	-	-	-	-	-	-	-	-	-	-	-	-
T182 Dup	-	-	-	-	-	-	-	-	-	-	-	-
T183 Orig	-	-	-	-	-	-	-	-	-	-	-	-
T183 Dup	-	-	-	-	-	-	-	-	-	-	-	-
T187 Orig	-	-	-	-	-	-	-	-	-	-	-	-
T187 Dup	-	-	-	-	-	-	-	-	-	-	-	-
T188 Orig	-	-	-	-	-	-	-	-	-	-	-	-
T188 Dup	-	-	-	-	-	-	-	-	-	-	-	-
T189 Orig	-	-	-	-	-	-	-	-	-	-	-	-
T189 Dup	-	-	-	-	-	-	-	-	-	-	-	-
T200 Orig	45.99	16.3	2.18	0.165	10.1	9.28	1.81	0.03	0.629	0.06	4.11	3.12
T200 Dup	46.02	16.82	2.2	0.166	9.74	9.24	1.79	0.03	0.612	0.05	4.11	3.12
T218 Orig	-	-	-	-	-	-	-	-	-	-	-	-
T218 Dup	-	-	-	-	-	-	-	-	-	-	-	-
T239 Orig	-	-	-	-	-	-	-	-	-	-	-	-
T239 Dup	-	-	-	-	-	-	-	-	-	-	-	-
T240 Orig	-	-	-	-	-	-	-	-	-	-	-	-
T240 Dup	-	-	-	-	-	-	-	-	-	-	-	-
T242 Orig	-	-	-	-	-	-	-	-	-	-	-	-
T242 Dup	-	-	-	-	-	-	-	-	-	-	-	-









Analyte	Total	Total2	Fe <sub>2</sub> O <sub>3</sub> T	Ba	Be	Sc	Sr	V	Zr	FeO	B	Mass
Units	%	%	%	ppm	ppm	ppm	ppm	ppm	ppm	%	ppm	g
Detection Limit	0.01	0.01	0.01	2	1	1	2	5	1	0.1	0.5-1	
Method	FUS-ICP	FUS-ICP	FUS-ICP	FUS-ICP	FUS-ICP	FUS-ICP	FUS-ICP	FUS-ICP	FUS-ICP	TITR	PGNAA	PGNAA
GXR-1 Meas	-	-	-	-	-	-	-	-	-	-	-	-
GXR-1 Cert	-	-	-	-	-	-	-	-	-	-	-	-
NIST 694 Meas	-	-	0.76	-	-	-	-	1600	-	-	-	-
NIST 694 Cert	-	-	0.79	-	-	-	-	1740	-	-	-	-
DNC-1 Meas	-	-	10.03	107	-	32	140	154	36	-	-	-
DNC-1 Cert	-	-	9.97	118	-	31	144	148	38	-	-	-
GBW 07113 Meas	-	-	3.13	499	4	5	41	7	381	1.9	-	-
GBW 07113 Cert	-	-	3.21	506	4	5	43	5	403	1.86	-	-
GBW 07113 Meas	-	-	3.13	499	4	5	41	7	381	-	-	-
GBW 07113 Cert	-	-	3.21	506	4	5	43	5	403	-	-	-
GBW 07113 Meas	-	-	3.24	509	4	5	38	6	380	-	-	-
GBW 07113 Cert	-	-	3.21	506	4	5	43	5	403	-	-	-
GXR-4 Meas	-	-	-	-	-	-	-	-	-	-	-	-
GXR-4 Cert	-	-	-	-	-	-	-	-	-	-	-	-
GXR-6 Meas	-	-	-	-	-	-	-	-	-	-	-	-
GXR-6 Cert	-	-	-	-	-	-	-	-	-	-	-	-
LKSD-3 Meas	-	-	-	-	-	-	-	-	-	-	-	-
LKSD-3 Cert	-	-	-	-	-	-	-	-	-	-	-	-
TDB-1 Meas	-	-	-	-	-	-	-	-	-	-	-	-
TDB-1 Cert	-	-	-	-	-	-	-	-	-	-	-	-
SY-2 Meas	-	-	-	-	-	-	-	-	-	-	92	-
SY-2 Cert	-	-	-	-	-	-	-	-	-	-	88	-
SY-3 Meas	-	-	-	-	-	-	-	-	-	-	102	-
SY-3 Cert	-	-	-	-	-	-	-	-	-	-	107	-
BaSO4 Meas	-	-	-	-	-	-	-	-	-	-	-	-
BaSO4 Cert	-	-	-	-	-	-	-	-	-	-	-	-
BaSO4 Meas	-	-	-	-	-	-	-	-	-	-	-	-
BaSO4 Cert	-	-	-	-	-	-	-	-	-	-	-	-
BaSO4 Meas	-	-	-	-	-	-	-	-	-	-	-	-
BaSO4 Cert	-	-	-	-	-	-	-	-	-	-	-	-
W-2a Meas	-	-	10.83	178	<1	36	193	275	89	-	-	-
W-2a Cert	-	-	10.7	182	1.3	36	190	262	94	-	-	-
SY-4 Meas	-	-	6.07	354	3	1	1250	8	543	3	-	-
SY-4 Cert	-	-	6.21	340	2.6	1.1	1191	8	517	2.86	-	-
CTA-AC-1 Meas	-	-	-	-	-	-	-	-	-	-	-	-
CTA-AC-1 Cert	-	-	-	-	-	-	-	-	-	-	-	-
BIR-1a Meas	-	-	11.45	9	<1	44	105	326	17	8.1	-	-

Analyte	Total	Total2	Fe <sub>2</sub> O <sub>3</sub> T	Ba	Be	Sc	Sr	V	Zr	FeO	B	Mass
Units	%	%	%	ppm	ppm	ppm	ppm	ppm	ppm	%	ppm	g
Detection Limit	0.01	0.01	0.01	2	1	1	2	5	1	0.1	0.5-1	
Method	FUS-ICP	FUS-ICP	FUS-ICP	FUS-ICP	FUS-ICP	FUS-ICP	FUS-ICP	FUS-ICP	FUS-ICP	TITR	PGNAA	PGNAA
BIR-1a Cert	-	-	11.3	6	0.58	44	110	310	18	8.34	-	-
BIR-1a Meas	-	-	-	-	-	-	-	-	-	8.3	-	-
BIR-1a Cert	-	-	-	-	-	-	-	-	-	8.34	-	-
NCS DC86312 Meas	-	-	-	-	-	-	-	-	-	-	-	-
NCS DC86312 Cert	-	-	-	-	-	-	-	-	-	-	-	-
JGb-2 Meas	-	-	-	-	-	-	-	-	-	5.1	-	-
JGb-2 Cert	-	-	-	-	-	-	-	-	-	5.41	-	-
JGb-2 Meas	-	-	-	-	-	-	-	-	-	5.2	-	-
JGb-2 Cert	-	-	-	-	-	-	-	-	-	5.41	-	-
JGb-2 Meas	-	-	-	-	-	-	-	-	-	5.3	-	-
JGb-2 Cert	-	-	-	-	-	-	-	-	-	5.41	-	-
JGb-2 Meas	-	-	-	-	-	-	-	-	-	5.2	-	-
JGb-2 Cert	-	-	-	-	-	-	-	-	-	5.41	-	-
JGb-2 Meas	-	-	-	-	-	-	-	-	-	5.2	-	-
JGb-2 Cert	-	-	-	-	-	-	-	-	-	5.41	-	-
JGb-2 Meas	-	-	-	-	-	-	-	-	-	5.2	-	-
JGb-2 Cert	-	-	-	-	-	-	-	-	-	5.41	-	-
SCH-1 Meas	-	-	89.78	-	-	-	-	-	-	-	-	-
SCH-1 Cert	-	-	86.84	-	-	-	-	-	-	-	-	-
NCS DC70009 (GBW07241) Meas	-	-	-	-	-	-	-	-	-	-	-	-
NCS DC70009 (GBW07241) Cert	-	-	-	-	-	-	-	-	-	-	-	-
SGR-1b Meas	-	-	-	-	-	-	-	-	-	-	-	-
SGR-1b Cert	-	-	-	-	-	-	-	-	-	-	-	-
SGR-1b Meas	-	-	-	-	-	-	-	-	-	-	-	-
SGR-1b Cert	-	-	-	-	-	-	-	-	-	-	-	-
SGR-1b Meas	-	-	-	-	-	-	-	-	-	-	-	-
SGR-1b Cert	-	-	-	-	-	-	-	-	-	-	-	-
OREAS 100a (Fusion) Meas	-	-	-	-	-	-	-	-	-	-	-	-
OREAS 100a (Fusion) Cert	-	-	-	-	-	-	-	-	-	-	-	-
OREAS 101a (Fusion) Meas	-	-	-	-	-	-	-	-	-	-	-	-
OREAS 101a (Fusion) Cert	-	-	-	-	-	-	-	-	-	-	-	-
OREAS 101b (Fusion) Meas	-	-	-	-	-	-	-	-	-	-	-	-
OREAS 101b (Fusion) Cert	-	-	-	-	-	-	-	-	-	-	-	-
OREAS 98 (S by LECO) Meas	-	-	-	-	-	-	-	-	-	-	-	-
OREAS 98 (S by LECO) Cert	-	-	-	-	-	-	-	-	-	-	-	-
OREAS 132b (S by LECO) Meas	-	-	-	-	-	-	-	-	-	-	-	-
OREAS 132b (S by LECO) Cert	-	-	-	-	-	-	-	-	-	-	-	-
JR-1 Meas	-	-	-	-	-	-	-	-	-	-	-	-
JR-1 Cert	-	-	-	-	-	-	-	-	-	-	-	-

Analyte	Total	Total2	Fe <sub>2</sub> O <sub>3</sub> T	Ba	Be	Sc	Sr	V	Zr	FeO	B	Mass
Units	%	%	%	ppm	ppm	ppm	ppm	ppm	ppm	%	ppm	g
Detection Limit	0.01	0.01	0.01	2	1	1	2	5	1	0.1	0.5-1	
Method	FUS-ICP	FUS-ICP	FUS-ICP	FUS-ICP	FUS-ICP	FUS-ICP	FUS-ICP	FUS-ICP	FUS-ICP	TITR	PGNAA	PGNAA
NCS DC86318 Meas	-	-	-	-	-	-	-	-	-	-	-	-
NCS DC86318 Cert	-	-	-	-	-	-	-	-	-	-	-	-
USZ 25-2006 Meas	-	-	-	-	-	-	-	-	-	-	-	-
USZ 25-2006 Cert	-	-	-	-	-	-	-	-	-	-	-	-
USZ 25-2006 Meas	-	-	-	-	-	-	-	-	-	-	-	-
USZ 25-2006 Cert	-	-	-	-	-	-	-	-	-	-	-	-
GS309-4 Meas	-	-	-	-	-	-	-	-	-	-	-	-
GS309-4 Cert	-	-	-	-	-	-	-	-	-	-	-	-
GS311-4 Meas	-	-	-	-	-	-	-	-	-	-	-	-
GS311-4 Cert	-	-	-	-	-	-	-	-	-	-	-	-
GS311-4 Meas	-	-	-	-	-	-	-	-	-	-	-	-
GS311-4 Cert	-	-	-	-	-	-	-	-	-	-	-	-
GS311-4 Meas	-	-	-	-	-	-	-	-	-	-	-	-
GS311-4 Cert	-	-	-	-	-	-	-	-	-	-	-	-
GS311-4 Meas	-	-	-	-	-	-	-	-	-	-	-	-
GS311-4 Cert	-	-	-	-	-	-	-	-	-	-	-	-
GS900-5 Meas	-	-	-	-	-	-	-	-	-	-	-	-
GS900-5 Cert	-	-	-	-	-	-	-	-	-	-	-	-
GS900-5 Meas	-	-	-	-	-	-	-	-	-	-	-	-
GS900-5 Cert	-	-	-	-	-	-	-	-	-	-	-	-
GS900-5 Meas	-	-	-	-	-	-	-	-	-	-	-	-
GS900-5 Cert	-	-	-	-	-	-	-	-	-	-	-	-
OREAS 45d (Aqua Regia) Meas	-	-	-	-	-	-	-	-	-	-	-	-
OREAS 45d (Aqua Regia) Cert	-	-	-	-	-	-	-	-	-	-	-	-
CDN-PGMS-24 Meas	-	-	-	-	-	-	-	-	-	-	-	-
CDN-PGMS-24 Cert	-	-	-	-	-	-	-	-	-	-	-	-
CDN-PGMS-24 Meas	-	-	-	-	-	-	-	-	-	-	-	-
CDN-PGMS-24 Cert	-	-	-	-	-	-	-	-	-	-	-	-
CDN-PGMS-24 Meas	-	-	-	-	-	-	-	-	-	-	-	-
CDN-PGMS-24 Cert	-	-	-	-	-	-	-	-	-	-	-	-
CaCO3 Meas	-	-	-	-	-	-	-	-	-	-	-	-
CaCO3 Cert	-	-	-	-	-	-	-	-	-	-	-	-
CaCO3 Meas	-	-	-	-	-	-	-	-	-	-	-	-
CaCO3 Cert	-	-	-	-	-	-	-	-	-	-	-	-
SdAR-M2 (U.S.G.S.) Meas	-	-	-	-	-	-	-	-	-	-	-	-
SdAR-M2 (U.S.G.S.) Cert	-	-	-	-	-	-	-	-	-	-	-	-
GXR-1 Meas	-	-	-	-	-	-	-	-	-	-	-	-

Analyte	Total	Total2	Fe <sub>2</sub> O <sub>3</sub> T	Ba	Be	Sc	Sr	V	Zr	FeO	B	Mass
Units	%	%	%	ppm	ppm	ppm	ppm	ppm	ppm	%	ppm	g
Detection Limit	0.01	0.01	0.01	2	1	1	2	5	1	0.1	0.5-1	PGNAA
Method	FUS-ICP	FUS-ICP	FUS-ICP	FUS-ICP	FUS-ICP	FUS-ICP	FUS-ICP	FUS-ICP	FUS-ICP	TITR	PGNAA	PGNAA
GXR-1 Cert	-	-	-	-	-	-	-	-	-	-	-	-
GXR-1 Meas	-	-	-	-	-	-	-	-	-	-	-	-
GXR-1 Cert	-	-	-	-	-	-	-	-	-	-	-	-
GXR-1 Meas	-	-	-	-	-	-	-	-	-	-	-	-
GXR-1 Cert	-	-	-	-	-	-	-	-	-	-	-	-
GXR-1 Meas	-	-	-	-	-	-	-	-	-	-	-	-
GXR-1 Cert	-	-	-	-	-	-	-	-	-	-	-	-
NIST 694 Meas	-	-	0.76	-	-	-	-	1617	-	-	-	-
NIST 694 Cert	-	-	0.79	-	-	-	-	1740	-	-	-	-
DNC-1 Meas	-	-	9.33	107	-	31	144	151	35	-	-	-
DNC-1 Cert	-	-	9.97	118	-	31	144	148	38	-	-	-
GBW 07113 Meas	-	-	3.12	505	4	5	40	6	388	1.9	-	-
GBW 07113 Cert	-	-	3.21	506	4	5	43	5	403	1.86	-	-
GXR-4 Meas	-	-	-	-	-	-	-	-	-	-	-	-
GXR-4 Cert	-	-	-	-	-	-	-	-	-	-	-	-
GXR-4 Meas	-	-	-	-	-	-	-	-	-	-	-	-
GXR-4 Cert	-	-	-	-	-	-	-	-	-	-	-	-
GXR-4 Meas	-	-	-	-	-	-	-	-	-	-	-	-
GXR-4 Cert	-	-	-	-	-	-	-	-	-	-	-	-
GXR-4 Meas	-	-	-	-	-	-	-	-	-	-	-	-
GXR-4 Cert	-	-	-	-	-	-	-	-	-	-	-	-
GXR-4 Meas	-	-	-	-	-	-	-	-	-	-	-	-
GXR-4 Cert	-	-	-	-	-	-	-	-	-	-	-	-
SDC-1 Meas	-	-	-	-	-	-	-	-	-	-	-	-
SDC-1 Cert	-	-	-	-	-	-	-	-	-	-	-	-
SDC-1 Meas	-	-	-	-	-	-	-	-	-	-	-	-
SDC-1 Cert	-	-	-	-	-	-	-	-	-	-	-	-
SDC-1 Meas	-	-	-	-	-	-	-	-	-	-	-	-
SDC-1 Cert	-	-	-	-	-	-	-	-	-	-	-	-
SDC-1 Meas	-	-	-	-	-	-	-	-	-	-	-	-
SDC-1 Cert	-	-	-	-	-	-	-	-	-	-	-	-
GXR-6 Meas	-	-	-	-	-	-	-	-	-	-	-	-
GXR-6 Cert	-	-	-	-	-	-	-	-	-	-	-	-
GXR-6 Meas	-	-	-	-	-	-	-	-	-	-	-	-
GXR-6 Cert	-	-	-	-	-	-	-	-	-	-	-	-
GXR-6 Meas	-	-	-	-	-	-	-	-	-	-	-	-
GXR-6 Cert	-	-	-	-	-	-	-	-	-	-	-	-
GXR-6 Meas	-	-	-	-	-	-	-	-	-	-	-	-
GXR-6 Cert	-	-	-	-	-	-	-	-	-	-	-	-

Analyte	Total	Total2	Fe <sub>2</sub> O <sub>3</sub> T	Ba	Be	Sc	Sr	V	Zr	FeO	B	Mass
Units	%	%	%	ppm	ppm	ppm	ppm	ppm	ppm	%	ppm	g
Detection Limit	0.01	0.01	0.01	2	1	1	2	5	1	0.1	0.5-1	
Method	FUS-ICP	FUS-ICP	FUS-ICP	FUS-ICP	FUS-ICP	FUS-ICP	FUS-ICP	FUS-ICP	FUS-ICP	TITR	PGNAA	PGNAA
LKSD-3 Meas	-	-	-	-	-	-	-	-	-	-	-	-
LKSD-3 Cert	-	-	-	-	-	-	-	-	-	-	-	-
TDB-1 Meas	-	-	-	-	-	-	-	-	-	-	-	-
TDB-1 Cert	-	-	-	-	-	-	-	-	-	-	-	-
SY-2 Meas	-	-	-	-	-	-	-	-	-	-	82.7	-
SY-2 Cert	-	-	-	-	-	-	-	-	-	-	88	-
SY-3 Meas	-	-	-	-	-	-	-	-	-	-	111	-
SY-3 Cert	-	-	-	-	-	-	-	-	-	-	107	-
BaSO4 Meas	-	-	-	-	-	-	-	-	-	-	-	-
BaSO4 Cert	-	-	-	-	-	-	-	-	-	-	-	-
BaSO4 Meas	-	-	-	-	-	-	-	-	-	-	-	-
BaSO4 Cert	-	-	-	-	-	-	-	-	-	-	-	-
W-2a Meas	-	-	10.61	174	<1	35	197	268	93	-	-	-
W-2a Cert	-	-	10.7	182	1.3	36	190	262	94	-	-	-
SY-4 Meas	-	-	6.19	344	3	<1	1192	9	542	2.9	-	-
SY-4 Cert	-	-	6.21	340	2.6	1.1	1191	8	517	2.86	-	-
CTA-AC-1 Meas	-	-	-	-	-	-	-	-	-	-	-	-
CTA-AC-1 Cert	-	-	-	-	-	-	-	-	-	-	-	-
BIR-1a Meas	-	-	11.1	8	<1	44	111	328	15	8.4	-	-
BIR-1a Cert	-	-	11.3	6	0.58	44	110	310	18	8.34	-	-
Calcium Carbonate Meas	-	-	-	-	-	-	-	-	-	-	-	-
Calcium Carbonate Cert	-	-	-	-	-	-	-	-	-	-	-	-
NCS DC86312 Meas	-	-	-	-	-	-	-	-	-	-	-	-
NCS DC86312 Cert	-	-	-	-	-	-	-	-	-	-	-	-
JGb-2 Meas	-	-	-	-	-	-	-	-	-	5.2	-	-
JGb-2 Cert	-	-	-	-	-	-	-	-	-	5.41	-	-
JGb-2 Meas	-	-	-	-	-	-	-	-	-	5.3	-	-
JGb-2 Cert	-	-	-	-	-	-	-	-	-	5.41	-	-
JGb-2 Meas	-	-	-	-	-	-	-	-	-	5.2	-	-
JGb-2 Cert	-	-	-	-	-	-	-	-	-	5.41	-	-
NCS DC70009 (GBW07241) Meas	-	-	-	-	-	-	-	-	-	-	-	-
NCS DC70009 (GBW07241) Cert	-	-	-	-	-	-	-	-	-	-	-	-
SGR-1b Meas	-	-	-	-	-	-	-	-	-	-	-	-
SGR-1b Cert	-	-	-	-	-	-	-	-	-	-	-	-
SGR-1b Meas	-	-	-	-	-	-	-	-	-	-	-	-
SGR-1b Cert	-	-	-	-	-	-	-	-	-	-	-	-
OREAS 100a (Fusion) Meas	-	-	-	-	-	-	-	-	-	-	-	-



Analyte	Total	Total2	Fe <sub>2</sub> O <sub>3</sub> T	Ba	Be	Sc	Sr	V	Zr	FeO	B	Mass
Units	%	%	%	ppm	ppm	ppm	ppm	ppm	ppm	%	ppm	g
Detection Limit	0.01	0.01	0.01	2	1	1	2	5	1	0.1	0.5-1	
Method	FUS-ICP	FUS-ICP	FUS-ICP	FUS-ICP	FUS-ICP	FUS-ICP	FUS-ICP	FUS-ICP	FUS-ICP	TITR	PGNAA	PGNAA
OREAS 100a (Fusion) Cert	-	-	-	-	-	-	-	-	-	-	-	-
OREAS 101a (Fusion) Meas	-	-	-	-	-	-	-	-	-	-	-	-
OREAS 101a (Fusion) Cert	-	-	-	-	-	-	-	-	-	-	-	-
OREAS 101b (Fusion) Meas	-	-	-	-	-	-	-	-	-	-	-	-
OREAS 101b (Fusion) Cert	-	-	-	-	-	-	-	-	-	-	-	-
JR-1 Meas	-	-	-	-	-	-	-	-	-	-	-	-
JR-1 Cert	-	-	-	-	-	-	-	-	-	-	-	-
NCS DC86318 Meas	-	-	-	-	-	-	-	-	-	-	-	-
NCS DC86318 Cert	-	-	-	-	-	-	-	-	-	-	-	-
USZ 25-2006 Meas	-	-	-	-	-	-	-	-	-	-	-	-
USZ 25-2006 Cert	-	-	-	-	-	-	-	-	-	-	-	-
USZ 25-2006 Meas	-	-	-	-	-	-	-	-	-	-	-	-
USZ 25-2006 Cert	-	-	-	-	-	-	-	-	-	-	-	-
DNC-1a Meas	-	-	-	-	-	-	-	-	-	-	-	-
DNC-1a Cert	-	-	-	-	-	-	-	-	-	-	-	-
DNC-1a Meas	-	-	-	-	-	-	-	-	-	-	-	-
DNC-1a Cert	-	-	-	-	-	-	-	-	-	-	-	-
DNC-1a Meas	-	-	-	-	-	-	-	-	-	-	-	-
DNC-1a Cert	-	-	-	-	-	-	-	-	-	-	-	-
DNC-1a Meas	-	-	-	-	-	-	-	-	-	-	-	-
DNC-1a Cert	-	-	-	-	-	-	-	-	-	-	-	-
GS311-4 Meas	-	-	-	-	-	-	-	-	-	-	-	-
GS311-4 Cert	-	-	-	-	-	-	-	-	-	-	-	-
GS311-4 Meas	-	-	-	-	-	-	-	-	-	-	-	-
GS311-4 Cert	-	-	-	-	-	-	-	-	-	-	-	-
GS900-5 Meas	-	-	-	-	-	-	-	-	-	-	-	-
GS900-5 Cert	-	-	-	-	-	-	-	-	-	-	-	-
GS900-5 Meas	-	-	-	-	-	-	-	-	-	-	-	-
GS900-5 Cert	-	-	-	-	-	-	-	-	-	-	-	-
OREAS 45d (Aqua Regia) Meas	-	-	-	-	-	-	-	-	-	-	-	-
OREAS 45d (Aqua Regia) Cert	-	-	-	-	-	-	-	-	-	-	-	-
OREAS 45d (Aqua Regia) Meas	-	-	-	-	-	-	-	-	-	-	-	-
OREAS 45d (Aqua Regia) Cert	-	-	-	-	-	-	-	-	-	-	-	-
OREAS 45d (Aqua Regia) Meas	-	-	-	-	-	-	-	-	-	-	-	-
OREAS 45d (Aqua Regia) Cert	-	-	-	-	-	-	-	-	-	-	-	-
SBC-1 Meas	-	-	-	-	-	-	-	-	-	-	-	-
SBC-1 Cert	-	-	-	-	-	-	-	-	-	-	-	-

Analyte	Total	Total2	Fe <sub>2</sub> O <sub>3</sub> T	Ba	Be	Sc	Sr	V	Zr	FeO	B	Mass
Units	%	%	%	ppm	ppm	ppm	ppm	ppm	ppm	%	ppm	g
Detection Limit	0.01	0.01	0.01	2	1	1	2	5	1	0.1	0.5-1	
Method	FUS-ICP	FUS-ICP	FUS-ICP	FUS-ICP	FUS-ICP	FUS-ICP	FUS-ICP	FUS-ICP	FUS-ICP	TITR	PGNAA	PGNAA
SBC-1 Meas	-	-	-	-	-	-	-	-	-	-	-	-
SBC-1 Cert	-	-	-	-	-	-	-	-	-	-	-	-
SBC-1 Meas	-	-	-	-	-	-	-	-	-	-	-	-
SBC-1 Cert	-	-	-	-	-	-	-	-	-	-	-	-
SBC-1 Meas	-	-	-	-	-	-	-	-	-	-	-	-
SBC-1 Cert	-	-	-	-	-	-	-	-	-	-	-	-
OREAS 45d (4-Acid) Meas	-	-	-	-	-	-	-	-	-	-	-	-
OREAS 45d (4-Acid) Cert	-	-	-	-	-	-	-	-	-	-	-	-
OREAS 45d (4-Acid) Meas	-	-	-	-	-	-	-	-	-	-	-	-
OREAS 45d (4-Acid) Cert	-	-	-	-	-	-	-	-	-	-	-	-
OREAS 45d (4-Acid) Meas	-	-	-	-	-	-	-	-	-	-	-	-
OREAS 45d (4-Acid) Cert	-	-	-	-	-	-	-	-	-	-	-	-
OREAS 45d (4-Acid) Meas	-	-	-	-	-	-	-	-	-	-	-	-
OREAS 45d (4-Acid) Cert	-	-	-	-	-	-	-	-	-	-	-	-
OxK110 Meas	-	-	-	-	-	-	-	-	-	-	-	-
OxK110 Cert	-	-	-	-	-	-	-	-	-	-	-	-
CDN-PGMS-24 Meas	-	-	-	-	-	-	-	-	-	-	-	-
CDN-PGMS-24 Cert	-	-	-	-	-	-	-	-	-	-	-	-
CDN-PGMS-24 Meas	-	-	-	-	-	-	-	-	-	-	-	-
CDN-PGMS-24 Cert	-	-	-	-	-	-	-	-	-	-	-	-
OXN117 Meas	-	-	-	-	-	-	-	-	-	-	-	-
OXN117 Cert	-	-	-	-	-	-	-	-	-	-	-	-
CaCO3 Meas	-	-	-	-	-	-	-	-	-	-	-	-
CaCO3 Cert	-	-	-	-	-	-	-	-	-	-	-	-
SdAR-M2 (U.S.G.S.) Meas	-	-	-	-	-	-	-	-	-	-	-	-
SdAR-M2 (U.S.G.S.) Cert	-	-	-	-	-	-	-	-	-	-	-	-
SdAR-M2 (U.S.G.S.) Meas	-	-	-	-	-	-	-	-	-	-	-	-
SdAR-M2 (U.S.G.S.) Cert	-	-	-	-	-	-	-	-	-	-	-	-
SdAR-M2 (U.S.G.S.) Meas	-	-	-	-	-	-	-	-	-	-	-	-
SdAR-M2 (U.S.G.S.) Cert	-	-	-	-	-	-	-	-	-	-	-	-
SdAR-M2 (U.S.G.S.) Meas	-	-	-	-	-	-	-	-	-	-	-	-
SdAR-M2 (U.S.G.S.) Cert	-	-	-	-	-	-	-	-	-	-	-	-
GXR-1 Meas	-	-	-	-	-	-	-	-	-	-	-	-
GXR-1 Cert	-	-	-	-	-	-	-	-	-	-	-	-
GXR-1 Meas	-	-	-	-	-	-	-	-	-	-	-	-
GXR-1 Cert	-	-	-	-	-	-	-	-	-	-	-	-
NIST 694 Meas	-	-	0.73	-	-	-	-	1610	-	-	-	-

Analyte	Total	Total2	Fe <sub>2</sub> O <sub>3</sub> T	Ba	Be	Sc	Sr	V	Zr	FeO	B	Mass
Units	%	%	%	ppm	ppm	ppm	ppm	ppm	ppm	%	ppm	g
Detection Limit	0.01	0.01	0.01	2	1	1	2	5	1	0.1	0.5-1	
Method	FUS-ICP	FUS-ICP	FUS-ICP	FUS-ICP	FUS-ICP	FUS-ICP	FUS-ICP	FUS-ICP	FUS-ICP	TITR	PGNAA	PGNAA
NIST 694 Cert	-	-	0.79	-	-	-	-	1740	-	-	-	-
DNC-1 Meas	-	-	9.78	111	-	31	145	152	39	-	-	-
DNC-1 Cert	-	-	9.97	118	-	31	144	148	38	-	-	-
GBW 07113 Meas	-	-	3.19	502	4	5	39	5	396	-	-	-
GBW 07113 Cert	-	-	3.21	506	4	5	43	5	403	-	-	-
GXR-4 Meas	-	-	-	-	-	-	-	-	-	-	-	-
GXR-4 Cert	-	-	-	-	-	-	-	-	-	-	-	-
GXR-4 Meas	-	-	-	-	-	-	-	-	-	-	-	-
GXR-4 Cert	-	-	-	-	-	-	-	-	-	-	-	-
SDC-1 Meas	-	-	-	-	-	-	-	-	-	-	-	-
SDC-1 Cert	-	-	-	-	-	-	-	-	-	-	-	-
GXR-6 Meas	-	-	-	-	-	-	-	-	-	-	-	-
GXR-6 Cert	-	-	-	-	-	-	-	-	-	-	-	-
GXR-6 Meas	-	-	-	-	-	-	-	-	-	-	-	-
GXR-6 Cert	-	-	-	-	-	-	-	-	-	-	-	-
LKSD-3 Meas	-	-	-	-	-	-	-	-	-	-	-	-
LKSD-3 Cert	-	-	-	-	-	-	-	-	-	-	-	-
TDB-1 Meas	-	-	-	-	-	-	-	-	-	-	-	-
TDB-1 Cert	-	-	-	-	-	-	-	-	-	-	-	-
SY-2 Meas	-	-	-	-	-	-	-	-	-	-	87.8	-
SY-2 Cert	-	-	-	-	-	-	-	-	-	-	88	-
SY-3 Meas	-	-	-	-	-	-	-	-	-	-	116	-
SY-3 Cert	-	-	-	-	-	-	-	-	-	-	107	-
BaSO4 Meas	-	-	-	-	-	-	-	-	-	-	-	-
BaSO4 Cert	-	-	-	-	-	-	-	-	-	-	-	-
BaSO4 Meas	-	-	-	-	-	-	-	-	-	-	-	-
BaSO4 Cert	-	-	-	-	-	-	-	-	-	-	-	-
BaSO4 Meas	-	-	-	-	-	-	-	-	-	-	-	-
BaSO4 Cert	-	-	-	-	-	-	-	-	-	-	-	-
W-2a Meas	-	-	10.73	174	<1	36	193	270	90	-	-	-
W-2a Cert	-	-	10.7	182	1.3	36	190	262	94	-	-	-
DTS-2b Meas	-	-	-	-	-	-	-	-	-	-	-	-
DTS-2b Cert	-	-	-	-	-	-	-	-	-	-	-	-
SY-4 Meas	-	-	6.21	347	3	<1	1225	7	530	-	-	-
SY-4 Cert	-	-	6.21	340	2.6	1.1	1191	8	517	-	-	-
CTA-AC-1 Meas	-	-	-	-	-	-	-	-	-	-	-	-
CTA-AC-1 Cert	-	-	-	-	-	-	-	-	-	-	-	-

Analyte	Total	Total2	Fe <sub>2</sub> O <sub>3</sub> T	Ba	Be	Sc	Sr	V	Zr	FeO	B	Mass
Units	%	%	%	ppm	ppm	ppm	ppm	ppm	ppm	%	ppm	g
Detection Limit	0.01	0.01	0.01	2	1	1	2	5	1	0.1	0.5-1	
Method	FUS-ICP	FUS-ICP	FUS-ICP	FUS-ICP	FUS-ICP	FUS-ICP	FUS-ICP	FUS-ICP	FUS-ICP	TITR	PGNAA	PGNAA
BIR-1a Meas	-	-	11.09	6	<1	43	104	329	13	-	-	-
BIR-1a Cert	-	-	11.3	6	0.58	44	110	310	18	-	-	-
NCS DC86312 Meas	-	-	-	-	-	-	-	-	-	-	-	-
NCS DC86312 Cert	-	-	-	-	-	-	-	-	-	-	-	-
JGb-2 Meas	-	-	-	-	-	-	-	-	-	5.3	-	-
JGb-2 Cert	-	-	-	-	-	-	-	-	-	5.41	-	-
NCS DC70009 (GBW07241) Meas	-	-	-	-	-	-	-	-	-	-	-	-
NCS DC70009 (GBW07241) Cert	-	-	-	-	-	-	-	-	-	-	-	-
SGR-1b Meas	-	-	-	-	-	-	-	-	-	-	-	-
SGR-1b Cert	-	-	-	-	-	-	-	-	-	-	-	-
SGR-1b Meas	-	-	-	-	-	-	-	-	-	-	-	-
SGR-1b Cert	-	-	-	-	-	-	-	-	-	-	-	-
SGR-1b Meas	-	-	-	-	-	-	-	-	-	-	-	-
SGR-1b Cert	-	-	-	-	-	-	-	-	-	-	-	-
OREAS 100a (Fusion) Meas	-	-	-	-	-	-	-	-	-	-	-	-
OREAS 100a (Fusion) Cert	-	-	-	-	-	-	-	-	-	-	-	-
OREAS 101a (Fusion) Meas	-	-	-	-	-	-	-	-	-	-	-	-
OREAS 101a (Fusion) Cert	-	-	-	-	-	-	-	-	-	-	-	-
OREAS 101b (Fusion) Meas	-	-	-	-	-	-	-	-	-	-	-	-
OREAS 101b (Fusion) Cert	-	-	-	-	-	-	-	-	-	-	-	-
OREAS 98 (S by LECO) Meas	-	-	-	-	-	-	-	-	-	-	-	-
OREAS 98 (S by LECO) Cert	-	-	-	-	-	-	-	-	-	-	-	-
OREAS 132b (S by LECO) Meas	-	-	-	-	-	-	-	-	-	-	-	-
OREAS 132b (S by LECO) Cert	-	-	-	-	-	-	-	-	-	-	-	-
JR-1 Meas	-	-	-	-	-	-	-	-	-	-	-	-
JR-1 Cert	-	-	-	-	-	-	-	-	-	-	-	-
NCS DC86318 Meas	-	-	-	-	-	-	-	-	-	-	-	-
NCS DC86318 Cert	-	-	-	-	-	-	-	-	-	-	-	-
USZ 25-2006 Meas	-	-	-	-	-	-	-	-	-	-	-	-
USZ 25-2006 Cert	-	-	-	-	-	-	-	-	-	-	-	-
DNC-1a Meas	-	-	-	-	-	-	-	-	-	-	-	-
DNC-1a Cert	-	-	-	-	-	-	-	-	-	-	-	-
PK2 Meas	-	-	-	-	-	-	-	-	-	-	-	-
PK2 Cert	-	-	-	-	-	-	-	-	-	-	-	-
GS309-4 Meas	-	-	-	-	-	-	-	-	-	-	-	-
GS309-4 Cert	-	-	-	-	-	-	-	-	-	-	-	-
GS311-4 Meas	-	-	-	-	-	-	-	-	-	-	-	-

Analyte	Total	Total2	Fe <sub>2</sub> O <sub>3</sub> T	Ba	Be	Sc	Sr	V	Zr	FeO	B	Mass
Units	%	%	%	ppm	ppm	ppm	ppm	ppm	ppm	%	ppm	g
Detection Limit	0.01	0.01	0.01	2	1	1	2	5	1	0.1	0.5-1	
Method	FUS-ICP	FUS-ICP	FUS-ICP	FUS-ICP	FUS-ICP	FUS-ICP	FUS-ICP	FUS-ICP	FUS-ICP	TITR	PGNAA	PGNAA
GS311-4 Cert	-	-	-	-	-	-	-	-	-	-	-	-
GS311-4 Meas	-	-	-	-	-	-	-	-	-	-	-	-
GS311-4 Cert	-	-	-	-	-	-	-	-	-	-	-	-
GS311-4 Meas	-	-	-	-	-	-	-	-	-	-	-	-
GS311-4 Cert	-	-	-	-	-	-	-	-	-	-	-	-
GS900-5 Meas	-	-	-	-	-	-	-	-	-	-	-	-
GS900-5 Cert	-	-	-	-	-	-	-	-	-	-	-	-
GS900-5 Meas	-	-	-	-	-	-	-	-	-	-	-	-
GS900-5 Cert	-	-	-	-	-	-	-	-	-	-	-	-
GS900-5 Meas	-	-	-	-	-	-	-	-	-	-	-	-
GS900-5 Cert	-	-	-	-	-	-	-	-	-	-	-	-
OREAS 45d (Aqua Regia) Meas	-	-	-	-	-	-	-	-	-	-	-	-
OREAS 45d (Aqua Regia) Cert	-	-	-	-	-	-	-	-	-	-	-	-
SBC-1 Meas	-	-	-	-	-	-	-	-	-	-	-	-
SBC-1 Cert	-	-	-	-	-	-	-	-	-	-	-	-
OREAS 45d (4-Acid) Meas	-	-	-	-	-	-	-	-	-	-	-	-
OREAS 45d (4-Acid) Cert	-	-	-	-	-	-	-	-	-	-	-	-
CaCO3 Meas	-	-	-	-	-	-	-	-	-	-	-	-
CaCO3 Cert	-	-	-	-	-	-	-	-	-	-	-	-
SdAR-M2 (U.S.G.S.) Meas	-	-	-	-	-	-	-	-	-	-	-	-
SdAR-M2 (U.S.G.S.) Cert	-	-	-	-	-	-	-	-	-	-	-	-
SdAR-M2 (U.S.G.S.) Meas	-	-	-	-	-	-	-	-	-	-	-	-
SdAR-M2 (U.S.G.S.) Cert	-	-	-	-	-	-	-	-	-	-	-	-
GXR-1 Meas	-	-	-	-	-	-	-	-	-	-	-	-
GXR-1 Cert	-	-	-	-	-	-	-	-	-	-	-	-
GXR-1 Meas	-	-	-	-	-	-	-	-	-	-	-	-
GXR-1 Cert	-	-	-	-	-	-	-	-	-	-	-	-
NIST 694 Meas	-	-	0.75	-	-	-	-	1668	-	-	-	-
NIST 694 Cert	-	-	0.79	-	-	-	-	1740	-	-	-	-
DNC-1 Meas	-	-	9.59	108	-	31	137	157	37	-	-	-
DNC-1 Cert	-	-	9.97	118	-	31	144	148	38	-	-	-
GBW 07113 Meas	-	-	3.31	499	4	6	44	<5	392	1.9	-	-
GBW 07113 Cert	-	-	3.21	506	4	5	43	5	403	1.86	-	-
GXR-4 Meas	-	-	-	-	-	-	-	-	-	-	-	-
GXR-4 Cert	-	-	-	-	-	-	-	-	-	-	-	-
GXR-4 Meas	-	-	-	-	-	-	-	-	-	-	-	-
GXR-4 Cert	-	-	-	-	-	-	-	-	-	-	-	-

Analyte	Total	Total2	Fe <sub>2</sub> O <sub>3</sub> T	Ba	Be	Sc	Sr	V	Zr	FeO	B	Mass
Units	%	%	%	ppm	ppm	ppm	ppm	ppm	ppm	%	ppm	g
Detection Limit	0.01	0.01	0.01	2	1	1	2	5	1	0.1	0.5-1	
Method	FUS-ICP	FUS-ICP	FUS-ICP	FUS-ICP	FUS-ICP	FUS-ICP	FUS-ICP	FUS-ICP	FUS-ICP	TITR	PGNAA	PGNAA
SDC-1 Meas	-	-	-	-	-	-	-	-	-	-	-	-
SDC-1 Cert	-	-	-	-	-	-	-	-	-	-	-	-
SDC-1 Meas	-	-	-	-	-	-	-	-	-	-	-	-
SDC-1 Cert	-	-	-	-	-	-	-	-	-	-	-	-
GXR-6 Meas	-	-	-	-	-	-	-	-	-	-	-	-
GXR-6 Cert	-	-	-	-	-	-	-	-	-	-	-	-
GXR-6 Meas	-	-	-	-	-	-	-	-	-	-	-	-
GXR-6 Cert	-	-	-	-	-	-	-	-	-	-	-	-
LKSD-3 Meas	-	-	-	-	-	-	-	-	-	-	-	-
LKSD-3 Cert	-	-	-	-	-	-	-	-	-	-	-	-
TDB-1 Meas	-	-	-	-	-	-	-	-	-	-	-	-
TDB-1 Cert	-	-	-	-	-	-	-	-	-	-	-	-
SY-2 Meas	-	-	-	-	-	-	-	-	-	-	89	-
SY-2 Cert	-	-	-	-	-	-	-	-	-	-	88	-
SY-3 Meas	-	-	-	-	-	-	-	-	-	-	109	-
SY-3 Cert	-	-	-	-	-	-	-	-	-	-	107	-
BaSO4 Meas	-	-	-	-	-	-	-	-	-	-	-	-
BaSO4 Cert	-	-	-	-	-	-	-	-	-	-	-	-
BaSO4 Meas	-	-	-	-	-	-	-	-	-	-	-	-
BaSO4 Cert	-	-	-	-	-	-	-	-	-	-	-	-
W-2a Meas	-	-	11.11	174	<1	35	199	279	92	-	-	-
W-2a Cert	-	-	10.7	182	1.3	36	190	262	94	-	-	-
SY-4 Meas	-	-	6.13	347	3	1	1179	6	537	2.9	-	-
SY-4 Cert	-	-	6.21	340	2.6	1.1	1191	8	517	2.86	-	-
CTA-AC-1 Meas	-	-	-	-	-	-	-	-	-	-	-	-
CTA-AC-1 Cert	-	-	-	-	-	-	-	-	-	-	-	-
BIR-1a Meas	-	-	11.34	8	<1	43	108	334	14	8.1	-	-
BIR-1a Cert	-	-	11.3	6	0.58	44	110	310	18	8.34	-	-
BIR-1a Meas	-	-	-	-	-	-	-	-	-	8.3	-	-
BIR-1a Cert	-	-	-	-	-	-	-	-	-	8.34	-	-
NCS DC86312 Meas	-	-	-	-	-	-	-	-	-	-	-	-
NCS DC86312 Cert	-	-	-	-	-	-	-	-	-	-	-	-
JGb-2 Meas	-	-	-	-	-	-	-	-	-	5.2	-	-
JGb-2 Cert	-	-	-	-	-	-	-	-	-	5.41	-	-
JGb-2 Meas	-	-	-	-	-	-	-	-	-	5.3	-	-
JGb-2 Cert	-	-	-	-	-	-	-	-	-	5.41	-	-
JGb-2 Meas	-	-	-	-	-	-	-	-	-	5.3	-	-

Analyte	Total	Total2	Fe <sub>2</sub> O <sub>3</sub> T	Ba	Be	Sc	Sr	V	Zr	FeO	B	Mass
Units	%	%	%	ppm	ppm	ppm	ppm	ppm	ppm	%	ppm	g
Detection Limit	0.01	0.01	0.01	2	1	1	2	5	1	0.1	0.5-1	
Method	FUS-ICP	FUS-ICP	FUS-ICP	FUS-ICP	FUS-ICP	FUS-ICP	FUS-ICP	FUS-ICP	FUS-ICP	TITR	PGNAA	PGNAA
JGb-2 Cert	-	-	-	-	-	-	-	-	-	5.41	-	-
JGb-2 Meas	-	-	-	-	-	-	-	-	-	5.2	-	-
JGb-2 Cert	-	-	-	-	-	-	-	-	-	5.41	-	-
NCS DC70009 (GBW07241) Meas	-	-	-	-	-	-	-	-	-	-	-	-
NCS DC70009 (GBW07241) Cert	-	-	-	-	-	-	-	-	-	-	-	-
SGR-1b Meas	-	-	-	-	-	-	-	-	-	-	-	-
SGR-1b Cert	-	-	-	-	-	-	-	-	-	-	-	-
SGR-1b Meas	-	-	-	-	-	-	-	-	-	-	-	-
SGR-1b Cert	-	-	-	-	-	-	-	-	-	-	-	-
OREAS 100a (Fusion) Meas	-	-	-	-	-	-	-	-	-	-	-	-
OREAS 100a (Fusion) Cert	-	-	-	-	-	-	-	-	-	-	-	-
OREAS 101a (Fusion) Meas	-	-	-	-	-	-	-	-	-	-	-	-
OREAS 101a (Fusion) Cert	-	-	-	-	-	-	-	-	-	-	-	-
OREAS 101b (Fusion) Meas	-	-	-	-	-	-	-	-	-	-	-	-
OREAS 101b (Fusion) Cert	-	-	-	-	-	-	-	-	-	-	-	-
JR-1 Meas	-	-	-	-	-	-	-	-	-	-	-	-
JR-1 Cert	-	-	-	-	-	-	-	-	-	-	-	-
NCS DC86318 Meas	-	-	-	-	-	-	-	-	-	-	-	-
NCS DC86318 Cert	-	-	-	-	-	-	-	-	-	-	-	-
USZ 25-2006 Meas	-	-	-	-	-	-	-	-	-	-	-	-
USZ 25-2006 Cert	-	-	-	-	-	-	-	-	-	-	-	-
USZ 25-2006 Meas	-	-	-	-	-	-	-	-	-	-	-	-
USZ 25-2006 Cert	-	-	-	-	-	-	-	-	-	-	-	-
DNC-1a Meas	-	-	-	-	-	-	-	-	-	-	-	-
DNC-1a Cert	-	-	-	-	-	-	-	-	-	-	-	-
DNC-1a Meas	-	-	-	-	-	-	-	-	-	-	-	-
DNC-1a Cert	-	-	-	-	-	-	-	-	-	-	-	-
PK2 Meas	-	-	-	-	-	-	-	-	-	-	-	-
PK2 Cert	-	-	-	-	-	-	-	-	-	-	-	-
GS311-4 Meas	-	-	-	-	-	-	-	-	-	-	-	-
GS311-4 Cert	-	-	-	-	-	-	-	-	-	-	-	-
GS311-4 Meas	-	-	-	-	-	-	-	-	-	-	-	-
GS311-4 Cert	-	-	-	-	-	-	-	-	-	-	-	-
GS900-5 Meas	-	-	-	-	-	-	-	-	-	-	-	-
GS900-5 Cert	-	-	-	-	-	-	-	-	-	-	-	-
GS900-5 Meas	-	-	-	-	-	-	-	-	-	-	-	-
GS900-5 Cert	-	-	-	-	-	-	-	-	-	-	-	-

Analyte	Total	Total2	Fe <sub>2</sub> O <sub>3</sub> T	Ba	Be	Sc	Sr	V	Zr	FeO	B	Mass
Units	%	%	%	ppm	ppm	ppm	ppm	ppm	ppm	%	ppm	g
Detection Limit	0.01	0.01	0.01	2	1	1	2	5	1	0.1	0.5-1	
Method	FUS-ICP	FUS-ICP	FUS-ICP	FUS-ICP	FUS-ICP	FUS-ICP	FUS-ICP	FUS-ICP	FUS-ICP	TITR	PGNAA	PGNAA
OREAS 45d (Aqua Regia) Meas	-	-	-	-	-	-	-	-	-	-	-	-
OREAS 45d (Aqua Regia) Cert	-	-	-	-	-	-	-	-	-	-	-	-
SBC-1 Meas	-	-	-	-	-	-	-	-	-	-	-	-
SBC-1 Cert	-	-	-	-	-	-	-	-	-	-	-	-
SBC-1 Meas	-	-	-	-	-	-	-	-	-	-	-	-
SBC-1 Cert	-	-	-	-	-	-	-	-	-	-	-	-
OREAS 45d (4-Acid) Meas	-	-	-	-	-	-	-	-	-	-	-	-
OREAS 45d (4-Acid) Cert	-	-	-	-	-	-	-	-	-	-	-	-
OxK110 Meas	-	-	-	-	-	-	-	-	-	-	-	-
OxK110 Cert	-	-	-	-	-	-	-	-	-	-	-	-
OXN117 Meas	-	-	-	-	-	-	-	-	-	-	-	-
OXN117 Cert	-	-	-	-	-	-	-	-	-	-	-	-
CaCO3 Meas	-	-	-	-	-	-	-	-	-	-	-	-
CaCO3 Cert	-	-	-	-	-	-	-	-	-	-	-	-
CaCO3 Meas	-	-	-	-	-	-	-	-	-	-	-	-
CaCO3 Cert	-	-	-	-	-	-	-	-	-	-	-	-
SdAR-M2 (U.S.G.S.) Meas	-	-	-	-	-	-	-	-	-	-	-	-
SdAR-M2 (U.S.G.S.) Cert	-	-	-	-	-	-	-	-	-	-	-	-
GXR-1 Meas	-	-	-	-	-	-	-	-	-	-	-	-
GXR-1 Cert	-	-	-	-	-	-	-	-	-	-	-	-
GXR-1 Meas	-	-	-	-	-	-	-	-	-	-	-	-
GXR-1 Cert	-	-	-	-	-	-	-	-	-	-	-	-
NIST 694 Meas	-	-	0.76	-	-	-	-	1598	-	-	-	-
NIST 694 Cert	-	-	0.79	-	-	-	-	1740	-	-	-	-
DNC-1 Meas	-	-	9.76	108	-	31	144	148	36	-	-	-
DNC-1 Cert	-	-	9.97	118	-	31	144	148	38	-	-	-
GBW 07113 Meas	-	-	-	-	-	-	-	-	-	1.8	-	-
GBW 07113 Cert	-	-	-	-	-	-	-	-	-	1.86	-	-
GXR-4 Meas	-	-	-	-	-	-	-	-	-	-	-	-
GXR-4 Cert	-	-	-	-	-	-	-	-	-	-	-	-
GXR-4 Meas	-	-	-	-	-	-	-	-	-	-	-	-
GXR-4 Cert	-	-	-	-	-	-	-	-	-	-	-	-
GXR-4 Meas	-	-	-	-	-	-	-	-	-	-	-	-
GXR-4 Cert	-	-	-	-	-	-	-	-	-	-	-	-
SDC-1 Meas	-	-	-	-	-	-	-	-	-	-	-	-
SDC-1 Cert	-	-	-	-	-	-	-	-	-	-	-	-
SDC-1 Meas	-	-	-	-	-	-	-	-	-	-	-	-



Analyte	Total	Total2	Fe <sub>2</sub> O <sub>3</sub> T	Ba	Be	Sc	Sr	V	Zr	FeO	B	Mass
Units	%	%	%	ppm	ppm	ppm	ppm	ppm	ppm	%	ppm	g
Detection Limit	0.01	0.01	0.01	2	1	1	2	5	1	0.1	0.5-1	
Method	FUS-ICP	FUS-ICP	FUS-ICP	FUS-ICP	FUS-ICP	FUS-ICP	FUS-ICP	FUS-ICP	FUS-ICP	TITR	PGNAA	PGNAA
SDC-1 Cert	-	-	-	-	-	-	-	-	-	-	-	-
GXR-6 Meas	-	-	-	-	-	-	-	-	-	-	-	-
GXR-6 Cert	-	-	-	-	-	-	-	-	-	-	-	-
GXR-6 Meas	-	-	-	-	-	-	-	-	-	-	-	-
GXR-6 Cert	-	-	-	-	-	-	-	-	-	-	-	-
GXR-6 Meas	-	-	-	-	-	-	-	-	-	-	-	-
GXR-6 Cert	-	-	-	-	-	-	-	-	-	-	-	-
LKSD-3 Meas	-	-	-	-	-	-	-	-	-	-	-	-
LKSD-3 Cert	-	-	-	-	-	-	-	-	-	-	-	-
TDB-1 Meas	-	-	-	-	-	-	-	-	-	-	-	-
TDB-1 Cert	-	-	-	-	-	-	-	-	-	-	-	-
SY-2 Meas	-	-	-	-	-	-	-	-	-	-	85	-
SY-2 Cert	-	-	-	-	-	-	-	-	-	-	88	-
SY-3 Meas	-	-	-	-	-	-	-	-	-	-	111	-
SY-3 Cert	-	-	-	-	-	-	-	-	-	-	107	-
BaSO4 Meas	-	-	-	-	-	-	-	-	-	-	-	-
BaSO4 Cert	-	-	-	-	-	-	-	-	-	-	-	-
W-2a Meas	-	-	10.64	171	<1	35	203	264	88	-	-	-
W-2a Cert	-	-	10.7	182	1.3	36	190	262	94	-	-	-
SY-4 Meas	-	-	6.09	347	3	<1	1183	7	538	2.8	-	-
SY-4 Cert	-	-	6.21	340	2.6	1.1	1191	8	517	2.86	-	-
CTA-AC-1 Meas	-	-	-	-	-	-	-	-	-	-	-	-
CTA-AC-1 Cert	-	-	-	-	-	-	-	-	-	-	-	-
BIR-1a Meas	-	-	10.95	6	<1	43	107	321	15	8.5	-	-
BIR-1a Cert	-	-	11.3	6	0.58	44	110	310	18	8.34	-	-
NCS DC86312 Meas	-	-	-	-	-	-	-	-	-	-	-	-
NCS DC86312 Cert	-	-	-	-	-	-	-	-	-	-	-	-
JGb-2 Meas	-	-	-	-	-	-	-	-	-	5.2	-	-
JGb-2 Cert	-	-	-	-	-	-	-	-	-	5.41	-	-
JGb-2 Meas	-	-	-	-	-	-	-	-	-	5.2	-	-
JGb-2 Cert	-	-	-	-	-	-	-	-	-	5.41	-	-
JGb-2 Meas	-	-	-	-	-	-	-	-	-	5.2	-	-
JGb-2 Cert	-	-	-	-	-	-	-	-	-	5.41	-	-
NCS DC70009 (GBW07241) Meas	-	-	-	-	-	-	-	-	-	-	-	-
NCS DC70009 (GBW07241) Cert	-	-	-	-	-	-	-	-	-	-	-	-
SGR-1b Meas	-	-	-	-	-	-	-	-	-	-	-	-
SGR-1b Cert	-	-	-	-	-	-	-	-	-	-	-	-

Analyte	Total	Total2	Fe <sub>2</sub> O <sub>3</sub> T	Ba	Be	Sc	Sr	V	Zr	FeO	B	Mass
Units	%	%	%	ppm	ppm	ppm	ppm	ppm	ppm	%	ppm	g
Detection Limit	0.01	0.01	0.01	2	1	1	2	5	1	0.1	0.5-1	
Method	FUS-ICP	FUS-ICP	FUS-ICP	FUS-ICP	FUS-ICP	FUS-ICP	FUS-ICP	FUS-ICP	FUS-ICP	TITR	PGNAA	PGNAA
OREAS 100a (Fusion) Meas	-	-	-	-	-	-	-	-	-	-	-	-
OREAS 100a (Fusion) Cert	-	-	-	-	-	-	-	-	-	-	-	-
OREAS 101a (Fusion) Meas	-	-	-	-	-	-	-	-	-	-	-	-
OREAS 101a (Fusion) Cert	-	-	-	-	-	-	-	-	-	-	-	-
OREAS 101b (Fusion) Meas	-	-	-	-	-	-	-	-	-	-	-	-
OREAS 101b (Fusion) Cert	-	-	-	-	-	-	-	-	-	-	-	-
JR-1 Meas	-	-	-	-	-	-	-	-	-	-	-	-
JR-1 Cert	-	-	-	-	-	-	-	-	-	-	-	-
NCS DC86318 Meas	-	-	-	-	-	-	-	-	-	-	-	-
NCS DC86318 Cert	-	-	-	-	-	-	-	-	-	-	-	-
USZ 25-2006 Meas	-	-	-	-	-	-	-	-	-	-	-	-
USZ 25-2006 Cert	-	-	-	-	-	-	-	-	-	-	-	-
USZ 25-2006 Meas	-	-	-	-	-	-	-	-	-	-	-	-
USZ 25-2006 Cert	-	-	-	-	-	-	-	-	-	-	-	-
DNC-1a Meas	-	-	-	-	-	-	-	-	-	-	-	-
DNC-1a Cert	-	-	-	-	-	-	-	-	-	-	-	-
DNC-1a Meas	-	-	-	-	-	-	-	-	-	-	-	-
DNC-1a Cert	-	-	-	-	-	-	-	-	-	-	-	-
GS311-4 Meas	-	-	-	-	-	-	-	-	-	-	-	-
GS311-4 Cert	-	-	-	-	-	-	-	-	-	-	-	-
GS900-5 Meas	-	-	-	-	-	-	-	-	-	-	-	-
GS900-5 Cert	-	-	-	-	-	-	-	-	-	-	-	-
OREAS 45d (Aqua Regia) Meas	-	-	-	-	-	-	-	-	-	-	-	-
OREAS 45d (Aqua Regia) Cert	-	-	-	-	-	-	-	-	-	-	-	-
SBC-1 Meas	-	-	-	-	-	-	-	-	-	-	-	-
SBC-1 Cert	-	-	-	-	-	-	-	-	-	-	-	-
SBC-1 Meas	-	-	-	-	-	-	-	-	-	-	-	-
SBC-1 Cert	-	-	-	-	-	-	-	-	-	-	-	-
OREAS 45d (4-Acid) Meas	-	-	-	-	-	-	-	-	-	-	-	-
OREAS 45d (4-Acid) Cert	-	-	-	-	-	-	-	-	-	-	-	-
OREAS 45d (4-Acid) Meas	-	-	-	-	-	-	-	-	-	-	-	-
OREAS 45d (4-Acid) Cert	-	-	-	-	-	-	-	-	-	-	-	-
CaCO3 Meas	-	-	-	-	-	-	-	-	-	-	-	-
CaCO3 Cert	-	-	-	-	-	-	-	-	-	-	-	-
CaCO3 Meas	-	-	-	-	-	-	-	-	-	-	-	-
CaCO3 Cert	-	-	-	-	-	-	-	-	-	-	-	-
SdAR-M2 (U.S.G.S.) Meas	-	-	-	-	-	-	-	-	-	-	-	-

Analyte	Total	Total2	Fe <sub>2</sub> O <sub>3</sub> T	Ba	Be	Sc	Sr	V	Zr	FeO	B	Mass
Units	%	%	%	ppm	ppm	ppm	ppm	ppm	ppm	%	ppm	g
Detection Limit	0.01	0.01	0.01	2	1	1	2	5	1	0.1	0.5-1	
Method	FUS-ICP	FUS-ICP	FUS-ICP	FUS-ICP	FUS-ICP	FUS-ICP	FUS-ICP	FUS-ICP	FUS-ICP	TITR	PGNAA	PGNAA
SdAR-M2 (U.S.G.S.) Cert	-	-	-	-	-	-	-	-	-	-	-	-
SdAR-M2 (U.S.G.S.) Meas	-	-	-	-	-	-	-	-	-	-	-	-
SdAR-M2 (U.S.G.S.) Cert	-	-	-	-	-	-	-	-	-	-	-	-
SdAR-M2 (U.S.G.S.) Meas	-	-	-	-	-	-	-	-	-	-	-	-
SdAR-M2 (U.S.G.S.) Cert	-	-	-	-	-	-	-	-	-	-	-	-
OREAS 214 Meas	-	-	-	-	-	-	-	-	-	-	-	-
OREAS 214 Cert	-	-	-	-	-	-	-	-	-	-	-	-
OREAS 218 Meas	-	-	-	-	-	-	-	-	-	-	-	-
OREAS 218 Cert	-	-	-	-	-	-	-	-	-	-	-	-
OREAS 218 Meas	-	-	-	-	-	-	-	-	-	-	-	-
OREAS 218 Cert	-	-	-	-	-	-	-	-	-	-	-	-
T9 Geochem Orig	-	-	-	-	-	-	-	-	-	-	-	-
T9 Geochem Dup	-	-	-	-	-	-	-	-	-	-	-	-
T14 Geochem Orig	-	-	-	-	-	-	-	-	-	9.8	-	-
T14 Geochem Dup	-	-	-	-	-	-	-	-	-	9.8	-	-
T17 Geochem Orig	-	-	-	-	-	-	-	-	-	-	-	-
T17 Geochem Dup	-	-	-	-	-	-	-	-	-	-	-	-
STPL-BAS-025 Orig	-	-	-	-	-	-	-	-	-	-	-	-
STPL-BAS-025 Dup	-	-	-	-	-	-	-	-	-	-	-	-
T24 Geochem Orig	98.14	95.73	66.86	13	<1	2	48	20	10	-	-	-
T24 Geochem Dup	96.96	94.56	66.08	12	<1	1	47	16	12	-	-	-
T27 Geochem Orig	-	-	-	-	-	-	-	-	-	-	-	-
T27 Geochem Dup	-	-	-	-	-	-	-	-	-	-	-	-
T31 Geochem Orig	-	-	-	-	-	-	-	-	-	9.3	-	-
T31 Geochem Dup	-	-	-	-	-	-	-	-	-	9.5	-	-
T37 Geochem Orig	-	-	-	-	-	-	-	-	-	-	-	-
T37 Geochem Dup	-	-	-	-	-	-	-	-	-	-	-	-
T42 Geochem Orig	-	-	-	-	-	-	-	-	-	4.7	-	-
T42 Geochem Dup	-	-	-	-	-	-	-	-	-	5.5	-	-
T45 Geochem Orig	-	-	-	-	-	-	-	-	-	-	10	1.05
T45 Geochem Dup	-	-	-	-	-	-	-	-	-	-	13	1.06
STPL-53-PML-036 Orig	-	-	-	-	-	-	-	-	-	1.1	-	-
STPL-53-PML-036 Dup	-	-	-	-	-	-	-	-	-	1.3	-	-
STPL-BAS-025 Orig	-	-	-	-	-	-	-	-	-	-	-	-
STPL-BAS-025 Dup	-	-	-	-	-	-	-	-	-	-	-	-
T42 Geochem Orig	-	-	-	-	-	-	-	-	-	-	-	-
T42 Geochem Dup	-	-	-	-	-	-	-	-	-	-	-	-

Analyte	Total	Total2	Fe <sub>2</sub> O <sub>3</sub> T	Ba	Be	Sc	Sr	V	Zr	FeO	B	Mass
Units	%	%	%	ppm	ppm	ppm	ppm	ppm	ppm	%	ppm	g
Detection Limit	0.01	0.01	0.01	2	1	1	2	5	1	0.1	0.5-1	
Method	FUS-ICP	FUS-ICP	FUS-ICP	FUS-ICP	FUS-ICP	FUS-ICP	FUS-ICP	FUS-ICP	FUS-ICP	TITR	PGNAA	PGNAA
T45 Geochem Orig	-	-	-	-	-	-	-	-	-	-	-	-
T45 Geochem Dup	-	-	-	-	-	-	-	-	-	-	-	-
T59 Orig	-	-	-	-	-	-	-	-	-	-	-	-
T59 Dup	-	-	-	-	-	-	-	-	-	-	-	-
T72 Orig	-	-	-	-	-	-	-	-	-	3	-	-
T72 Dup	-	-	-	-	-	-	-	-	-	3	-	-
T73 Orig	-	-	-	-	-	-	-	-	-	-	-	-
T73 Dup	-	-	-	-	-	-	-	-	-	-	-	-
STPL-BAS-029 Orig	-	-	-	-	-	-	-	-	-	-	-	-
STPL-BAS-029 Dup	-	-	-	-	-	-	-	-	-	-	-	-
T81 Orig	-	-	-	-	-	-	-	-	-	-	-	-
T81 Dup	-	-	-	-	-	-	-	-	-	-	-	-
T86 Orig	-	-	-	-	-	-	-	-	-	-	-	-
T86 Dup	-	-	-	-	-	-	-	-	-	-	-	-
T88 Orig	98.84	99.54	12.01	199	<1	9	168	76	110	-	-	-
T88 Dup	99.87	100.6	12.15	201	<1	9	168	77	110	-	-	-
T89 Orig	-	-	-	-	-	-	-	-	-	-	-	-
T89 Dup	-	-	-	-	-	-	-	-	-	-	-	-
T94 Orig	-	-	-	-	-	-	-	-	-	2.9	-	-
T94 Dup	-	-	-	-	-	-	-	-	-	3	-	-
T98 Orig	-	-	-	-	-	-	-	-	-	-	-	-
T98 Dup	-	-	-	-	-	-	-	-	-	-	-	-
T99 Orig	-	-	-	-	-	-	-	-	-	-	-	-
T99 Dup	-	-	-	-	-	-	-	-	-	-	-	-
T101 Orig	-	-	-	-	-	-	-	-	-	-	-	-
T101 Dup	-	-	-	-	-	-	-	-	-	-	-	-
T102 Orig	-	-	-	-	-	-	-	-	-	-	-	-
T102 Dup	-	-	-	-	-	-	-	-	-	-	-	-
T114 Orig	-	-	-	-	-	-	-	-	-	3.9	-	-
T114 Dup	-	-	-	-	-	-	-	-	-	4	-	-
T116 Orig	-	-	-	-	-	-	-	-	-	-	-	-
T116 Dup	-	-	-	-	-	-	-	-	-	-	-	-
T117 Orig	98.74	99.12	4.57	198	<1	8	256	71	110	3.4	18.5	1.03
T117 Split PREP DUP	100.4	100.8	4.45	197	<1	8	259	70	114	3.4	20.3	1.09
STPL-53-PML-025 Orig	99.59	99.68	1.28	530	1	3	144	16	102	-	-	-
STPL-53-PML-025 Dup	-	-	-	-	-	-	-	-	-	-	-	-
T65 Orig	-	-	-	-	-	-	-	-	-	-	-	-

Analyte	Total	Total2	Fe <sub>2</sub> O <sub>3</sub> T	Ba	Be	Sc	Sr	V	Zr	FeO	B	Mass
Units	%	%	%	ppm	ppm	ppm	ppm	ppm	ppm	%	ppm	g
Detection Limit	0.01	0.01	0.01	2	1	1	2	5	1	0.1	0.5-1	PGNAA
Method	FUS-ICP	FUS-ICP	FUS-ICP	FUS-ICP	FUS-ICP	FUS-ICP	FUS-ICP	FUS-ICP	FUS-ICP	TITR	PGNAA	PGNAA
T65 Dup	-	-	-	-	-	-	-	-	-	-	-	-
T106 Orig	-	-	-	-	-	-	-	-	-	11.6	-	-
T106 Dup	-	-	-	-	-	-	-	-	-	11.5	-	-
T118 Orig	98.73	99.21	5.05	237	<1	9	243	80	137	-	-	-
T118 Dup	99.17	99.65	5.09	236	<1	9	241	80	139	-	-	-
T141 Orig	-	-	-	-	-	-	-	-	-	10.8	-	-
T141 Dup	-	-	-	-	-	-	-	-	-	10.9	-	-
STPL-BAS-023 Orig	-	-	-	-	-	-	-	-	-	-	-	-
STPL-BAS-023 Dup	-	-	-	-	-	-	-	-	-	-	-	-
T154 Orig	-	-	-	-	-	-	-	-	-	-	-	-
T154 Dup	-	-	-	-	-	-	-	-	-	-	-	-
T157 Orig	-	-	-	-	-	-	-	-	-	-	-	-
T157 Dup	-	-	-	-	-	-	-	-	-	-	-	-
T158 Orig	-	-	-	-	-	-	-	-	-	-	-	-
T158 Dup	-	-	-	-	-	-	-	-	-	-	-	-
STPL-PML-53-027 Orig	100.3	100.2	1.27	515	1	3	146	11	110	-	-	-
STPL-PML-53-027 Dup	98.95	98.89	1.23	515	1	3	143	12	109	-	-	-
T182 Orig	-	-	-	-	-	-	-	-	-	10.1	-	-
T182 Dup	-	-	-	-	-	-	-	-	-	10.1	-	-
T183 Orig	-	-	-	-	-	-	-	-	-	-	-	-
T183 Dup	-	-	-	-	-	-	-	-	-	-	-	-
T187 Orig	-	-	-	-	-	-	-	-	-	-	-	-
T187 Dup	-	-	-	-	-	-	-	-	-	-	-	-
T188 Orig	-	-	-	-	-	-	-	-	-	-	-	-
T188 Dup	-	-	-	-	-	-	-	-	-	-	-	-
T189 Orig	-	-	-	-	-	-	-	-	-	-	-	-
T189 Dup	-	-	-	-	-	-	-	-	-	-	-	-
T200 Orig	100.4	99.45	11.97	13	<1	17	171	128	23	8.8	-	-
T200 Dup	100.6	99.58	11.98	13	<1	17	173	126	22	8.8	-	-
T218 Orig	-	-	-	-	-	-	-	-	-	-	-	-
T218 Dup	-	-	-	-	-	-	-	-	-	-	-	-
T239 Orig	-	-	-	-	-	-	-	-	-	-	-	-
T239 Dup	-	-	-	-	-	-	-	-	-	-	-	-
T240 Orig	-	-	-	-	-	-	-	-	-	6	-	-
T240 Dup	-	-	-	-	-	-	-	-	-	6	-	-
T242 Orig	-	-	-	-	-	-	-	-	-	-	-	-
T242 Dup	-	-	-	-	-	-	-	-	-	-	-	-

Analyte	Total	Total2	Fe <sub>2</sub> O <sub>3</sub> T	Ba	Be	Sc	Sr	V	Zr	FeO	B	Mass
Units	%	%	%	ppm	ppm	ppm	ppm	ppm	ppm	%	ppm	g
Detection Limit	0.01	0.01	0.01	2	1	1	2	5	1	0.1	0.5-1	PGNAA
Method	FUS-ICP	FUS-ICP	FUS-ICP	FUS-ICP	FUS-ICP	FUS-ICP	FUS-ICP	FUS-ICP	FUS-ICP	TITR	PGNAA	PGNAA
STPL-BAS-053 Orig	-	-	-	-	-	-	-	-	-	-	-	-
STPL-BAS-053 Dup	-	-	-	-	-	-	-	-	-	-	-	-
Method Blank	-	-	-	-	-	-	-	-	-	-	-	-
Method Blank	-	-	-	-	-	-	-	-	-	<0.1	-	-
Method Blank	-	-	-	-	-	-	-	-	-	<0.1	-	-
Method Blank	-	-	-	-	-	-	-	-	-	<0.1	-	-
Method Blank	-	-	-	-	-	-	-	-	-	0.1	-	-
Method Blank	-	-	-	-	-	-	-	-	-	<0.1	-	-
Method Blank	-	-	-	-	-	-	-	-	-	<0.1	-	-
Method Blank	-	-	-	-	-	-	-	-	-	-	-	-
Method Blank	-	-	-	-	-	-	-	-	-	-	-	-
Method Blank	-	-	-	-	-	-	-	-	-	-	-	-
Method Blank	-	-	-	-	-	-	-	-	-	-	-	-
Method Blank	-	-	-	-	-	-	-	-	-	-	-	-
Method Blank	-	-	-	-	-	-	-	-	-	-	-	-
Method Blank	-	-	-	-	-	-	-	-	-	-	-	-
Method Blank	-	-	-	-	-	-	-	-	-	-	-	-
Method Blank	-	-	-	-	-	-	-	-	-	-	-	-
Method Blank	-	-	-	-	-	-	-	-	-	-	-	-
Method Blank	-	-	-	-	-	-	-	-	-	-	-	-
Method Blank	-	-	-	-	-	-	-	-	-	-	-	-
Method Blank	-	-	-	-	-	-	-	-	-	-	-	-
Method Blank	-	-	-	-	-	-	-	-	-	-	-	-
Method Blank	-	-	-	-	-	-	-	-	-	-	-	-
Method Blank	-	-	-	-	-	-	-	-	-	-	-	-
Method Blank	-	-	-	-	-	-	-	-	-	-	-	-
Method Blank	-	-	-	-	-	-	-	-	-	-	-	-
Method Blank	-	-	-	-	-	-	-	-	-	-	-	-
Method Blank	-	-	-	-	-	-	-	-	-	-	-	-
Method Blank	-	-	-	-	-	-	-	-	-	-	-	-
Method Blank	-	-	-	-	-	-	-	-	-	-	-	-
Method Blank	-	-	-	-	-	-	-	-	-	-	-	-
Method Blank	-	-	-	-	-	-	-	-	-	-	-	-
Method Blank	-	-	-	-	-	-	-	-	-	-	-	-
Method Blank	-	-	-	-	-	-	-	-	-	-	-	-
Method Blank	-	-	-	-	-	-	-	-	-	-	-	-
Method Blank	-	-	-	-	-	-	-	-	-	<0.1	-	-
Method Blank	-	-	-	-	-	-	-	-	-	<0.1	-	-
Method Blank	-	-	-	-	-	-	-	-	-	<0.1	-	-
Method Blank	-	-	-	-	-	-	-	-	-	<0.1	-	-
Method Blank	-	-	-	-	-	-	-	-	-	<0.1	-	-

Analyte	Total	Total2	Fe <sub>2</sub> O <sub>3</sub> T	Ba	Be	Sc	Sr	V	Zr	FeO	B	Mass
Units	%	%	%	ppm	ppm	ppm	ppm	ppm	ppm	%	ppm	g
Detection Limit	0.01	0.01	0.01	2	1	1	2	5	1	0.1	0.5-1	PGNAA
Method	FUS-ICP	FUS-ICP	FUS-ICP	FUS-ICP	FUS-ICP	FUS-ICP	FUS-ICP	FUS-ICP	FUS-ICP	TITR	PGNAA	PGNAA
Method Blank	-	-	-	-	-	-	-	-	-	-	-	-
Method Blank	-	-	-	-	-	-	-	-	-	-	<0.5	1
Method Blank	-	-	-	-	-	-	-	-	-	-	-	-
Method Blank	-	-	-	-	-	-	-	-	-	-	-	-
Method Blank	-	-	-	-	-	-	-	-	-	-	-	-
Method Blank	-	-	-	-	-	-	-	-	-	-	-	-
Method Blank	-	-	-	-	-	-	-	-	-	-	-	-
Method Blank	-	-	-	-	-	-	-	-	-	-	-	-
Method Blank	-	-	-	-	-	-	-	-	-	-	-	-
Method Blank	-	-	-	-	-	-	-	-	-	-	-	-
Method Blank	-	-	-	-	-	-	-	-	-	-	-	-
Method Blank	-	-	-	-	-	-	-	-	-	<0.1	-	-
Method Blank	-	<0.01	<0.01	<2	<1	<1	<2	<5	<1	-	-	-
Method Blank	-	-	-	-	-	-	-	-	-	-	-	-
Method Blank	-	-	-	-	-	-	-	-	-	-	-	-
Method Blank	-	-	-	-	-	-	-	-	-	-	<0.5	-
Method Blank	-	-	-	-	-	-	-	-	-	-	-	-
Method Blank	-	-	-	-	-	-	-	-	-	-	-	-
Method Blank	-	-	-	-	-	-	-	-	-	-	-	-
Method Blank	-	-	-	-	-	-	-	-	-	-	-	-
Method Blank	-	-	-	-	-	-	-	-	-	-	-	-
Method Blank	-	-	-	-	-	-	-	-	-	-	-	-
Method Blank	-	-	-	-	-	-	-	-	-	-	-	-
Method Blank	-	-	-	-	-	-	-	-	-	-	-	-
Method Blank	-	-	-	-	-	-	-	-	-	<0.1	-	-
Method Blank	-	-	-	-	-	-	-	-	-	<0.1	-	-
Method Blank	-	-	-	-	-	-	-	-	-	<0.1	-	-
Method Blank	-	-	-	-	-	-	-	-	-	<0.1	-	-
Method Blank	-	-	-	-	-	-	-	-	-	<0.1	-	-
Method Blank	-	<0.01	<0.01	<2	<1	<1	<2	<5	1	-	-	-
Method Blank	-	-	-	-	-	-	-	-	-	-	-	-
Method Blank	-	-	-	-	-	-	-	-	-	-	-	-
Method Blank	-	-	-	-	-	-	-	-	-	-	-	-
Method Blank	-	-	-	-	-	-	-	-	-	-	-	-
Method Blank	-	-	-	-	-	-	-	-	-	-	-	-
Method Blank	-	-	-	-	-	-	-	-	-	-	-	-
Method Blank	-	-	-	-	-	-	-	-	-	-	-	-
Method Blank	-	-	-	-	-	-	-	-	-	-	-	-
Method Blank	-	-	-	-	-	-	-	-	-	-	-	-
Method Blank	-	-	-	-	-	-	-	-	-	-	-	-

Analyte	Total	Total2	Fe <sub>2</sub> O <sub>3</sub> T	Ba	Be	Sc	Sr	V	Zr	FeO	B	Mass
Units	%	%	%	ppm	ppm	ppm	ppm	ppm	ppm	%	ppm	g
Detection Limit	0.01	0.01	0.01	2	1	1	2	5	1	0.1	0.5-1	PGNAA
Method	FUS-ICP	FUS-ICP	FUS-ICP	FUS-ICP	FUS-ICP	FUS-ICP	FUS-ICP	FUS-ICP	FUS-ICP	TITR	PGNAA	PGNAA
Method Blank	-	-	-	-	-	-	-	-	-	-	-	-
Method Blank	-	-	-	-	-	-	-	-	-	-	-	-
Method Blank	-	-	-	-	-	-	-	-	-	-	-	-
Method Blank	-	-	-	-	-	-	-	-	-	-	-	-
Method Blank	-	-	0.02	<2	<1	<1	<2	<5	2	-	-	-
Method Blank	-	-	-	-	-	-	-	-	-	-	-	-
Method Blank	-	-	-	-	-	-	-	-	-	-	-	-
Method Blank	-	-	-	-	-	-	-	-	-	-	-	-
Method Blank	-	-	-	-	-	-	-	-	-	-	-	-
Method Blank	-	-	-	-	-	-	-	-	-	-	-	-
Method Blank	-	-	-	-	-	-	-	-	-	-	-	-
Method Blank	-	-	-	-	-	-	-	-	-	-	-	-
Method Blank	-	-	-	-	-	-	-	-	-	<0.1	-	-
Method Blank	-	-	-	-	-	-	-	-	-	<0.1	-	-
Method Blank	-	-	-	-	-	-	-	-	-	<0.1	-	-
Method Blank	-	-	-	-	-	-	-	-	-	<0.1	-	-
Method Blank	-	-	-	-	-	-	-	-	-	<0.1	-	-
Method Blank	-	-	-	-	-	-	-	-	-	-	-	-
Method Blank	-	-	-	-	-	-	-	-	-	-	-	-
Method Blank	-	-	-	-	-	-	-	-	-	-	-	-
Method Blank	-	-	-	-	-	-	-	-	-	-	-	-
Method Blank	-	-	-	-	-	-	-	-	-	-	-	-
Method Blank	-	-	-	-	-	-	-	-	-	-	-	-
Method Blank	-	-	-	-	-	-	-	-	-	-	-	-
Method Blank	-	-	-	-	-	-	-	-	-	-	<1	1



Analyte	C-Total	S-Total	CO <sub>2</sub>	Hg	As	Bi	Sb	Se	Te	Au	Au	Au	Pd	Pt
Units	%	%	%	ppb	ppm	ppm	ppm	ppm	ppm	ppb	g/tonne	ppb	ppb	ppb
Detection Limit	0.01	0.01	0.01	5	0.1	0.02	0.02	0.1	0.02	5	0.03	1	0.5	0.5
Method	CS	CS	CO2	1G	AR-MS	AR-MS	AR-MS	AR-MS	AR-MS	FA-AA	FA-GRA	FA-MS	FA-MS	FA-MS
GXR-1 Meas	-	-	-	4090	370	1500	81	13.6	13.9	-	-	-	-	-
GXR-1 Cert	-	-	-	3900	427	1380	122	16.6	13	-	-	-	-	-
NIST 694 Meas	-	-	-	-	-	-	-	-	-	-	-	-	-	-
NIST 694 Cert	-	-	-	-	-	-	-	-	-	-	-	-	-	-
DNC-1 Meas	-	-	-	-	-	-	-	-	-	-	-	-	-	-
DNC-1 Cert	-	-	-	-	-	-	-	-	-	-	-	-	-	-
GBW 07113 Meas	-	-	-	-	-	-	-	-	-	-	-	-	-	-
GBW 07113 Cert	-	-	-	-	-	-	-	-	-	-	-	-	-	-
GBW 07113 Meas	-	-	-	-	-	-	-	-	-	-	-	-	-	-
GBW 07113 Cert	-	-	-	-	-	-	-	-	-	-	-	-	-	-
GBW 07113 Meas	-	-	-	-	-	-	-	-	-	-	-	-	-	-
GBW 07113 Cert	-	-	-	-	-	-	-	-	-	-	-	-	-	-
GXR-4 Meas	-	-	-	103	92.4	17.9	3.09	4.7	0.95	-	-	-	-	-
GXR-4 Cert	-	-	-	110	98	19	4.8	5.6	0.97	-	-	-	-	-
GXR-6 Meas	-	-	-	74	229	0.17	1.97	0.3	0.05	-	-	-	-	-
GXR-6 Cert	-	-	-	68	330	0.29	3.6	0.94	0.018	-	-	-	-	-
LKSD-3 Meas	-	-	-	-	-	-	-	-	-	-	-	-	-	-
LKSD-3 Cert	-	-	-	-	-	-	-	-	-	-	-	-	-	-
TDB-1 Meas	-	-	-	-	-	-	-	-	-	-	-	-	-	-
TDB-1 Cert	-	-	-	-	-	-	-	-	-	-	-	-	-	-
SY-2 Meas	-	-	-	-	-	-	-	-	-	-	-	-	-	-
SY-2 Cert	-	-	-	-	-	-	-	-	-	-	-	-	-	-
SY-3 Meas	-	-	-	-	-	-	-	-	-	-	-	-	-	-
SY-3 Cert	-	-	-	-	-	-	-	-	-	-	-	-	-	-
BaSO4 Meas	-	14.1	-	-	-	-	-	-	-	-	-	-	-	-
BaSO4 Cert	-	14	-	-	-	-	-	-	-	-	-	-	-	-
BaSO4 Meas	-	14.2	-	-	-	-	-	-	-	-	-	-	-	-
BaSO4 Cert	-	14	-	-	-	-	-	-	-	-	-	-	-	-
BaSO4 Meas	-	14.5	-	-	-	-	-	-	-	-	-	-	-	-
BaSO4 Cert	-	14	-	-	-	-	-	-	-	-	-	-	-	-
W-2a Meas	-	-	-	-	-	-	-	-	-	-	-	-	-	-
W-2a Cert	-	-	-	-	-	-	-	-	-	-	-	-	-	-
SY-4 Meas	-	-	-	-	-	-	-	-	-	-	-	-	-	-
SY-4 Cert	-	-	-	-	-	-	-	-	-	-	-	-	-	-
CTA-AC-1 Meas	-	-	-	-	-	-	-	-	-	-	-	-	-	-
CTA-AC-1 Cert	-	-	-	-	-	-	-	-	-	-	-	-	-	-
BIR-1a Meas	-	-	-	-	-	-	-	-	-	-	-	-	-	-

Analyte	C-Total	S-Total	CO <sub>2</sub>	Hg	As	Bi	Sb	Se	Te	Au	Au	Au	Pd	Pt
Units	%	%	%	ppb	ppm	ppm	ppm	ppm	ppm	ppb	g/tonne	ppb	ppb	ppb
Detection Limit	0.01	0.01	0.01	5	0.1	0.02	0.02	0.1	0.02	5	0.03	1	0.5	0.5
Method	CS	CS	CO2	1G	AR-MS	AR-MS	AR-MS	AR-MS	AR-MS	FA-AA	FA-GRA	FA-MS	FA-MS	FA-MS
BIR-1a Cert	-	-	-	-	-	-	-	-	-	-	-	-	-	-
BIR-1a Meas	-	-	-	-	-	-	-	-	-	-	-	-	-	-
BIR-1a Cert	-	-	-	-	-	-	-	-	-	-	-	-	-	-
NCS DC86312 Meas	-	-	-	-	-	-	-	-	-	-	-	-	-	-
NCS DC86312 Cert	-	-	-	-	-	-	-	-	-	-	-	-	-	-
JGb-2 Meas	-	-	-	-	-	-	-	-	-	-	-	-	-	-
JGb-2 Cert	-	-	-	-	-	-	-	-	-	-	-	-	-	-
JGb-2 Meas	-	-	-	-	-	-	-	-	-	-	-	-	-	-
JGb-2 Cert	-	-	-	-	-	-	-	-	-	-	-	-	-	-
JGb-2 Meas	-	-	-	-	-	-	-	-	-	-	-	-	-	-
JGb-2 Cert	-	-	-	-	-	-	-	-	-	-	-	-	-	-
JGb-2 Meas	-	-	-	-	-	-	-	-	-	-	-	-	-	-
JGb-2 Cert	-	-	-	-	-	-	-	-	-	-	-	-	-	-
JGb-2 Meas	-	-	-	-	-	-	-	-	-	-	-	-	-	-
JGb-2 Cert	-	-	-	-	-	-	-	-	-	-	-	-	-	-
JGb-2 Meas	-	-	-	-	-	-	-	-	-	-	-	-	-	-
JGb-2 Cert	-	-	-	-	-	-	-	-	-	-	-	-	-	-
SCH-1 Meas	-	-	-	-	-	-	-	-	-	-	-	-	-	-
SCH-1 Cert	-	-	-	-	-	-	-	-	-	-	-	-	-	-
NCS DC70009 (GBW07241) Meas	-	-	-	-	-	-	-	-	-	-	-	-	-	-
NCS DC70009 (GBW07241) Cert	-	-	-	-	-	-	-	-	-	-	-	-	-	-
SGR-1b Meas	27.9	1.48	-	-	-	-	-	-	-	-	-	-	-	-
SGR-1b Cert	28	1.53	-	-	-	-	-	-	-	-	-	-	-	-
SGR-1b Meas	27.3	1.58	-	-	-	-	-	-	-	-	-	-	-	-
SGR-1b Cert	28	1.53	-	-	-	-	-	-	-	-	-	-	-	-
SGR-1b Meas	27.6	1.64	-	-	-	-	-	-	-	-	-	-	-	-
SGR-1b Cert	28	1.53	-	-	-	-	-	-	-	-	-	-	-	-
OREAS 100a (Fusion) Meas	-	-	-	-	-	-	-	-	-	-	-	-	-	-
OREAS 100a (Fusion) Cert	-	-	-	-	-	-	-	-	-	-	-	-	-	-
OREAS 101a (Fusion) Meas	-	-	-	-	-	-	-	-	-	-	-	-	-	-
OREAS 101a (Fusion) Cert	-	-	-	-	-	-	-	-	-	-	-	-	-	-
OREAS 101b (Fusion) Meas	-	-	-	-	-	-	-	-	-	-	-	-	-	-
OREAS 101b (Fusion) Cert	-	-	-	-	-	-	-	-	-	-	-	-	-	-
OREAS 98 (S by LECO) Meas	-	16.6	-	-	-	-	-	-	-	-	-	-	-	-
OREAS 98 (S by LECO) Cert	-	16	-	-	-	-	-	-	-	-	-	-	-	-
OREAS 132b (S by LECO) Meas	-	8.52	-	-	-	-	-	-	-	-	-	-	-	-
OREAS 132b (S by LECO) Cert	-	8.23	-	-	-	-	-	-	-	-	-	-	-	-
JR-1 Meas	-	-	-	-	-	-	-	-	-	-	-	-	-	-
JR-1 Cert	-	-	-	-	-	-	-	-	-	-	-	-	-	-

Analyte	C-Total	S-Total	CO <sub>2</sub>	Hg	As	Bi	Sb	Se	Te	Au	Au	Au	Pd	Pt
Units	%	%	%	ppb	ppm	ppm	ppm	ppm	ppm	ppb	g/tonne	ppb	ppb	ppb
Detection Limit	0.01	0.01	0.01	5	0.1	0.02	0.02	0.1	0.02	5	0.03	1	0.5	0.5
Method	CS	CS	CO2	1G	AR-MS	AR-MS	AR-MS	AR-MS	AR-MS	FA-AA	FA-GRA	FA-MS	FA-MS	FA-MS
NCS DC86318 Meas	-	-	-	-	-	-	-	-	-	-	-	-	-	-
NCS DC86318 Cert	-	-	-	-	-	-	-	-	-	-	-	-	-	-
USZ 25-2006 Meas	-	-	1.07	-	-	-	-	-	-	-	-	-	-	-
USZ 25-2006 Cert	-	-	1.04	-	-	-	-	-	-	-	-	-	-	-
USZ 25-2006 Meas	-	-	1.1	-	-	-	-	-	-	-	-	-	-	-
USZ 25-2006 Cert	-	-	1.04	-	-	-	-	-	-	-	-	-	-	-
GS309-4 Meas	0.15	31.5	-	-	-	-	-	-	-	-	-	-	-	-
GS309-4 Cert	0.22	34.12	-	-	-	-	-	-	-	-	-	-	-	-
GS311-4 Meas	1.1	0.59	-	-	-	-	-	-	-	-	-	-	-	-
GS311-4 Cert	1.11	0.54	-	-	-	-	-	-	-	-	-	-	-	-
GS311-4 Meas	1.1	0.55	-	-	-	-	-	-	-	-	-	-	-	-
GS311-4 Cert	1.11	0.54	-	-	-	-	-	-	-	-	-	-	-	-
GS311-4 Meas	1.14	0.55	-	-	-	-	-	-	-	-	-	-	-	-
GS311-4 Cert	1.11	0.54	-	-	-	-	-	-	-	-	-	-	-	-
GS900-5 Meas	0.64	0.35	-	-	-	-	-	-	-	-	-	-	-	-
GS900-5 Cert	0.65	0.34	-	-	-	-	-	-	-	-	-	-	-	-
GS900-5 Meas	0.65	0.35	-	-	-	-	-	-	-	-	-	-	-	-
GS900-5 Cert	0.65	0.34	-	-	-	-	-	-	-	-	-	-	-	-
GS900-5 Meas	0.65	0.37	-	-	-	-	-	-	-	-	-	-	-	-
GS900-5 Cert	0.65	0.34	-	-	-	-	-	-	-	-	-	-	-	-
OREAS 45d (Aqua Regia) Meas	-	-	-	-	7.2	0.27	-	-	-	-	-	-	-	-
OREAS 45d (Aqua Regia) Cert	-	-	-	-	6.5	0.3	-	-	-	-	-	-	-	-
CDN-PGMS-24 Meas	-	-	-	-	-	-	-	-	-	-	-	687	5130	1170
CDN-PGMS-24 Cert	-	-	-	-	-	-	-	-	-	-	-	806	4880	1090
CDN-PGMS-24 Meas	-	-	-	-	-	-	-	-	-	-	-	889	4850	1100
CDN-PGMS-24 Cert	-	-	-	-	-	-	-	-	-	-	-	806	4880	1090
CDN-PGMS-24 Meas	-	-	-	-	-	-	-	-	-	-	-	809	4910	1120
CDN-PGMS-24 Cert	-	-	-	-	-	-	-	-	-	-	-	806	4880	1090
CDN-PGMS-24 Meas	-	-	-	-	-	-	-	-	-	-	-	790	4620	1150
CDN-PGMS-24 Cert	-	-	-	-	-	-	-	-	-	-	-	806	4880	1090
CaCO3 Meas	-	-	43.5	-	-	-	-	-	-	-	-	-	-	-
CaCO3 Cert	-	-	44.1	-	-	-	-	-	-	-	-	-	-	-
CaCO3 Meas	-	-	43.6	-	-	-	-	-	-	-	-	-	-	-
CaCO3 Cert	-	-	44.1	-	-	-	-	-	-	-	-	-	-	-
SdAR-M2 (U.S.G.S.) Meas	-	-	-	1420	-	1.05	-	-	-	-	-	-	-	-
SdAR-M2 (U.S.G.S.) Cert	-	-	-	1440	-	1.05	-	-	-	-	-	-	-	-
GXR-1 Meas	-	-	-	3970	363	1490	71.9	9.6	12.4	-	-	-	-	-

Analyte	C-Total	S-Total	CO <sub>2</sub>	Hg	As	Bi	Sb	Se	Te	Au	Au	Au	Pd	Pt
Units	%	%	%	ppb	ppm	ppm	ppm	ppm	ppm	ppb	g/tonne	ppb	ppb	ppb
Detection Limit	0.01	0.01	0.01	5	0.1	0.02	0.02	0.1	0.02	5	0.03	1	0.5	0.5
Method	CS	CS	CO <sub>2</sub>	1G	AR-MS	AR-MS	AR-MS	AR-MS	AR-MS	FA-AA	FA-GRA	FA-MS	FA-MS	FA-MS
GXR-1 Cert	-	-	-	3900	427	1380	122	16.6	13	-	-	-	-	-
GXR-1 Meas	-	-	-	-	389	1460	83.6	17.3	13.1	-	-	-	-	-
GXR-1 Cert	-	-	-	-	427	1380	122	16.6	13	-	-	-	-	-
GXR-1 Meas	-	-	-	-	363	1490	71.9	9.6	12.4	-	-	-	-	-
GXR-1 Cert	-	-	-	-	427	1380	122	16.6	13	-	-	-	-	-
GXR-1 Meas	-	-	-	-	-	-	-	-	-	-	-	-	-	-
GXR-1 Cert	-	-	-	-	-	-	-	-	-	-	-	-	-	-
NIST 694 Meas	-	-	-	-	-	-	-	-	-	-	-	-	-	-
NIST 694 Cert	-	-	-	-	-	-	-	-	-	-	-	-	-	-
DNC-1 Meas	-	-	-	-	-	-	-	-	-	-	-	-	-	-
DNC-1 Cert	-	-	-	-	-	-	-	-	-	-	-	-	-	-
GBW 07113 Meas	-	-	-	-	-	-	-	-	-	-	-	-	-	-
GBW 07113 Cert	-	-	-	-	-	-	-	-	-	-	-	-	-	-
GXR-4 Meas	-	-	-	102	87.1	16.5	2.82	2.8	0.94	-	-	-	-	-
GXR-4 Cert	-	-	-	110	98	19	4.8	5.6	0.97	-	-	-	-	-
GXR-4 Meas	-	-	-	-	91.2	16	2.88	4.5	0.95	-	-	-	-	-
GXR-4 Cert	-	-	-	-	98	19	4.8	5.6	0.97	-	-	-	-	-
GXR-4 Meas	-	-	-	-	87.1	16.5	2.82	2.8	0.94	-	-	-	-	-
GXR-4 Cert	-	-	-	-	98	19	4.8	5.6	0.97	-	-	-	-	-
GXR-4 Meas	-	-	-	-	-	-	-	-	-	-	-	-	-	-
GXR-4 Cert	-	-	-	-	-	-	-	-	-	-	-	-	-	-
SDC-1 Meas	-	-	-	-	-	-	-	-	-	-	-	-	-	-
SDC-1 Cert	-	-	-	-	-	-	-	-	-	-	-	-	-	-
SDC-1 Meas	-	-	-	-	-	-	-	-	-	-	-	-	-	-
SDC-1 Cert	-	-	-	-	-	-	-	-	-	-	-	-	-	-
SDC-1 Meas	-	-	-	-	-	-	-	-	-	-	-	-	-	-
SDC-1 Cert	-	-	-	-	-	-	-	-	-	-	-	-	-	-
SDC-1 Meas	-	-	-	-	-	-	-	-	-	-	-	-	-	-
SDC-1 Cert	-	-	-	-	-	-	-	-	-	-	-	-	-	-
GXR-6 Meas	-	-	-	64	198	0.15	1.6	<0.1	0.13	-	-	-	-	-
GXR-6 Cert	-	-	-	68	330	0.29	3.6	0.94	0.018	-	-	-	-	-
GXR-6 Meas	-	-	-	-	171	0.14	1.35	<0.1	0.03	-	-	-	-	-
GXR-6 Cert	-	-	-	-	330	0.29	3.6	0.94	0.018	-	-	-	-	-
GXR-6 Meas	-	-	-	-	198	0.15	1.6	<0.1	0.13	-	-	-	-	-
GXR-6 Cert	-	-	-	-	330	0.29	3.6	0.94	0.018	-	-	-	-	-
GXR-6 Meas	-	-	-	-	-	-	-	-	-	-	-	-	-	-
GXR-6 Cert	-	-	-	-	-	-	-	-	-	-	-	-	-	-

Analyte	C-Total	S-Total	CO <sub>2</sub>	Hg	As	Bi	Sb	Se	Te	Au	Au	Au	Pd	Pt
Units	%	%	%	ppb	ppm	ppm	ppm	ppm	ppm	ppb	g/tonne	ppb	ppb	ppb
Detection Limit	0.01	0.01	0.01	5	0.1	0.02	0.02	0.1	0.02	5	0.03	1	0.5	0.5
Method	CS	CS	CO2	1G	AR-MS	AR-MS	AR-MS	AR-MS	AR-MS	FA-AA	FA-GRA	FA-MS	FA-MS	FA-MS
LKSD-3 Meas	-	-	-	-	-	-	-	-	-	-	-	-	-	-
LKSD-3 Cert	-	-	-	-	-	-	-	-	-	-	-	-	-	-
TDB-1 Meas	-	-	-	-	-	-	-	-	-	-	-	-	-	-
TDB-1 Cert	-	-	-	-	-	-	-	-	-	-	-	-	-	-
SY-2 Meas	-	-	-	-	-	-	-	-	-	-	-	-	-	-
SY-2 Cert	-	-	-	-	-	-	-	-	-	-	-	-	-	-
SY-3 Meas	-	-	-	-	-	-	-	-	-	-	-	-	-	-
SY-3 Cert	-	-	-	-	-	-	-	-	-	-	-	-	-	-
BaSO4 Meas	-	13.9	-	-	-	-	-	-	-	-	-	-	-	-
BaSO4 Cert	-	14	-	-	-	-	-	-	-	-	-	-	-	-
BaSO4 Meas	-	13.9	-	-	-	-	-	-	-	-	-	-	-	-
BaSO4 Cert	-	14	-	-	-	-	-	-	-	-	-	-	-	-
W-2a Meas	-	-	-	-	-	-	-	-	-	-	-	-	-	-
W-2a Cert	-	-	-	-	-	-	-	-	-	-	-	-	-	-
SY-4 Meas	-	-	-	-	-	-	-	-	-	-	-	-	-	-
SY-4 Cert	-	-	-	-	-	-	-	-	-	-	-	-	-	-
CTA-AC-1 Meas	-	-	-	-	-	-	-	-	-	-	-	-	-	-
CTA-AC-1 Cert	-	-	-	-	-	-	-	-	-	-	-	-	-	-
BIR-1a Meas	-	-	-	-	-	-	-	-	-	-	-	-	-	-
BIR-1a Cert	-	-	-	-	-	-	-	-	-	-	-	-	-	-
Calcium Carbonate Meas	-	-	43.6	-	-	-	-	-	-	-	-	-	-	-
Calcium Carbonate Cert	-	-	44.05	-	-	-	-	-	-	-	-	-	-	-
NCS DC86312 Meas	-	-	-	-	-	-	-	-	-	-	-	-	-	-
NCS DC86312 Cert	-	-	-	-	-	-	-	-	-	-	-	-	-	-
JGb-2 Meas	-	-	-	-	-	-	-	-	-	-	-	-	-	-
JGb-2 Cert	-	-	-	-	-	-	-	-	-	-	-	-	-	-
JGb-2 Meas	-	-	-	-	-	-	-	-	-	-	-	-	-	-
JGb-2 Cert	-	-	-	-	-	-	-	-	-	-	-	-	-	-
JGb-2 Meas	-	-	-	-	-	-	-	-	-	-	-	-	-	-
JGb-2 Cert	-	-	-	-	-	-	-	-	-	-	-	-	-	-
NCS DC70009 (GBW07241) Meas	-	-	-	-	-	-	-	-	-	-	-	-	-	-
NCS DC70009 (GBW07241) Cert	-	-	-	-	-	-	-	-	-	-	-	-	-	-
SGR-1b Meas	28.1	1.56	-	-	-	-	-	-	-	-	-	-	-	-
SGR-1b Cert	28	1.53	-	-	-	-	-	-	-	-	-	-	-	-
SGR-1b Meas	27.9	1.56	-	-	-	-	-	-	-	-	-	-	-	-
SGR-1b Cert	28	1.53	-	-	-	-	-	-	-	-	-	-	-	-
OREAS 100a (Fusion) Meas	-	-	-	-	-	-	-	-	-	-	-	-	-	-

Analyte	C-Total	S-Total	CO <sub>2</sub>	Hg	As	Bi	Sb	Se	Te	Au	Au	Au	Pd	Pt
Units	%	%	%	ppb	ppm	ppm	ppm	ppm	ppm	ppb	g/tonne	ppb	ppb	ppb
Detection Limit	0.01	0.01	0.01	5	0.1	0.02	0.02	0.1	0.02	5	0.03	1	0.5	0.5
Method	CS	CS	CO2	1G	AR-MS	AR-MS	AR-MS	AR-MS	AR-MS	FA-AA	FA-GRA	FA-MS	FA-MS	FA-MS
OREAS 100a (Fusion) Cert	-	-	-	-	-	-	-	-	-	-	-	-	-	-
OREAS 101a (Fusion) Meas	-	-	-	-	-	-	-	-	-	-	-	-	-	-
OREAS 101a (Fusion) Cert	-	-	-	-	-	-	-	-	-	-	-	-	-	-
OREAS 101b (Fusion) Meas	-	-	-	-	-	-	-	-	-	-	-	-	-	-
OREAS 101b (Fusion) Cert	-	-	-	-	-	-	-	-	-	-	-	-	-	-
JR-1 Meas	-	-	-	-	-	-	-	-	-	-	-	-	-	-
JR-1 Cert	-	-	-	-	-	-	-	-	-	-	-	-	-	-
NCS DC86318 Meas	-	-	-	-	-	-	-	-	-	-	-	-	-	-
NCS DC86318 Cert	-	-	-	-	-	-	-	-	-	-	-	-	-	-
USZ 25-2006 Meas	-	-	1.08	-	-	-	-	-	-	-	-	-	-	-
USZ 25-2006 Cert	-	-	1.04	-	-	-	-	-	-	-	-	-	-	-
USZ 25-2006 Meas	-	-	1.06	-	-	-	-	-	-	-	-	-	-	-
USZ 25-2006 Cert	-	-	1.04	-	-	-	-	-	-	-	-	-	-	-
DNC-1a Meas	-	-	-	-	-	-	-	-	-	-	-	-	-	-
DNC-1a Cert	-	-	-	-	-	-	-	-	-	-	-	-	-	-
DNC-1a Meas	-	-	-	-	-	-	-	-	-	-	-	-	-	-
DNC-1a Cert	-	-	-	-	-	-	-	-	-	-	-	-	-	-
DNC-1a Meas	-	-	-	-	-	-	-	-	-	-	-	-	-	-
DNC-1a Cert	-	-	-	-	-	-	-	-	-	-	-	-	-	-
DNC-1a Meas	-	-	-	-	-	-	-	-	-	-	-	-	-	-
DNC-1a Cert	-	-	-	-	-	-	-	-	-	-	-	-	-	-
DNC-1a Meas	-	-	-	-	-	-	-	-	-	-	-	-	-	-
DNC-1a Cert	-	-	-	-	-	-	-	-	-	-	-	-	-	-
GS311-4 Meas	1.11	0.53	-	-	-	-	-	-	-	-	-	-	-	-
GS311-4 Cert	1.11	0.54	-	-	-	-	-	-	-	-	-	-	-	-
GS311-4 Meas	1.09	0.53	-	-	-	-	-	-	-	-	-	-	-	-
GS311-4 Cert	1.11	0.54	-	-	-	-	-	-	-	-	-	-	-	-
GS900-5 Meas	0.61	0.32	-	-	-	-	-	-	-	-	-	-	-	-
GS900-5 Cert	0.65	0.34	-	-	-	-	-	-	-	-	-	-	-	-
GS900-5 Meas	0.62	0.32	-	-	-	-	-	-	-	-	-	-	-	-
GS900-5 Cert	0.65	0.34	-	-	-	-	-	-	-	-	-	-	-	-
OREAS 45d (Aqua Regia) Meas	-	-	-	-	3.6	0.37	-	-	-	-	-	-	-	-
OREAS 45d (Aqua Regia) Cert	-	-	-	-	6.5	0.3	-	-	-	-	-	-	-	-
OREAS 45d (Aqua Regia) Meas	-	-	-	-	3.3	0.23	-	-	-	-	-	-	-	-
OREAS 45d (Aqua Regia) Cert	-	-	-	-	6.5	0.3	-	-	-	-	-	-	-	-
OREAS 45d (Aqua Regia) Meas	-	-	-	-	3.6	0.37	-	-	-	-	-	-	-	-
OREAS 45d (Aqua Regia) Cert	-	-	-	-	6.5	0.3	-	-	-	-	-	-	-	-
SBC-1 Meas	-	-	-	-	-	-	-	-	-	-	-	-	-	-
SBC-1 Cert	-	-	-	-	-	-	-	-	-	-	-	-	-	-

Analyte	C-Total	S-Total	CO <sub>2</sub>	Hg	As	Bi	Sb	Se	Te	Au	Au	Au	Pd	Pt
Units	%	%	%	ppb	ppm	ppm	ppm	ppm	ppm	ppb	g/tonne	ppb	ppb	ppb
Detection Limit	0.01	0.01	0.01	5	0.1	0.02	0.02	0.1	0.02	5	0.03	1	0.5	0.5
Method	CS	CS	CO2	1G	AR-MS	AR-MS	AR-MS	AR-MS	AR-MS	FA-AA	FA-GRA	FA-MS	FA-MS	FA-MS
SBC-1 Meas	-	-	-	-	-	-	-	-	-	-	-	-	-	-
SBC-1 Cert	-	-	-	-	-	-	-	-	-	-	-	-	-	-
SBC-1 Meas	-	-	-	-	-	-	-	-	-	-	-	-	-	-
SBC-1 Cert	-	-	-	-	-	-	-	-	-	-	-	-	-	-
SBC-1 Meas	-	-	-	-	-	-	-	-	-	-	-	-	-	-
SBC-1 Cert	-	-	-	-	-	-	-	-	-	-	-	-	-	-
OREAS 45d (4-Acid) Meas	-	-	-	-	-	-	-	-	-	-	-	-	-	-
OREAS 45d (4-Acid) Cert	-	-	-	-	-	-	-	-	-	-	-	-	-	-
OREAS 45d (4-Acid) Meas	-	-	-	-	-	-	-	-	-	-	-	-	-	-
OREAS 45d (4-Acid) Cert	-	-	-	-	-	-	-	-	-	-	-	-	-	-
OREAS 45d (4-Acid) Meas	-	-	-	-	-	-	-	-	-	-	-	-	-	-
OREAS 45d (4-Acid) Cert	-	-	-	-	-	-	-	-	-	-	-	-	-	-
OREAS 45d (4-Acid) Meas	-	-	-	-	-	-	-	-	-	-	-	-	-	-
OREAS 45d (4-Acid) Cert	-	-	-	-	-	-	-	-	-	-	-	-	-	-
OxK110 Meas	-	-	-	-	-	-	-	-	-	-	3.52	-	-	-
OxK110 Cert	-	-	-	-	-	-	-	-	-	-	3.602	-	-	-
CDN-PGMS-24 Meas	-	-	-	-	-	-	-	-	-	-	-	818	4580	1010
CDN-PGMS-24 Cert	-	-	-	-	-	-	-	-	-	-	-	806	4880	1090
CDN-PGMS-24 Meas	-	-	-	-	-	-	-	-	-	-	-	785	4690	1100
CDN-PGMS-24 Cert	-	-	-	-	-	-	-	-	-	-	-	806	4880	1090
OXN117 Meas	-	-	-	-	-	-	-	-	-	-	7.46	-	-	-
OXN117 Cert	-	-	-	-	-	-	-	-	-	-	7.679	-	-	-
CaCO3 Meas	-	-	43.4	-	-	-	-	-	-	-	-	-	-	-
CaCO3 Cert	-	-	44.1	-	-	-	-	-	-	-	-	-	-	-
SdAR-M2 (U.S.G.S.) Meas	-	-	-	1400	-	0.91	-	-	-	-	-	-	-	-
SdAR-M2 (U.S.G.S.) Cert	-	-	-	1440	-	1.05	-	-	-	-	-	-	-	-
SdAR-M2 (U.S.G.S.) Meas	-	-	-	-	-	0.94	-	-	-	-	-	-	-	-
SdAR-M2 (U.S.G.S.) Cert	-	-	-	-	-	1.05	-	-	-	-	-	-	-	-
SdAR-M2 (U.S.G.S.) Meas	-	-	-	-	-	0.91	-	-	-	-	-	-	-	-
SdAR-M2 (U.S.G.S.) Cert	-	-	-	-	-	1.05	-	-	-	-	-	-	-	-
SdAR-M2 (U.S.G.S.) Meas	-	-	-	-	-	-	-	-	-	-	-	-	-	-
SdAR-M2 (U.S.G.S.) Cert	-	-	-	-	-	-	-	-	-	-	-	-	-	-
GXR-1 Meas	-	-	-	3790	396	1510	71.8	14.7	14.2	-	-	-	-	-
GXR-1 Cert	-	-	-	3900	427	1380	122	16.6	13	-	-	-	-	-
GXR-1 Meas	-	-	-	3790	-	-	-	-	-	-	-	-	-	-
GXR-1 Cert	-	-	-	3900	-	-	-	-	-	-	-	-	-	-
NIST 694 Meas	-	-	-	-	-	-	-	-	-	-	-	-	-	-

Analyte	C-Total	S-Total	CO <sub>2</sub>	Hg	As	Bi	Sb	Se	Te	Au	Au	Au	Pd	Pt
Units	%	%	%	ppb	ppm	ppm	ppm	ppm	ppm	ppb	g/tonne	ppb	ppb	ppb
Detection Limit	0.01	0.01	0.01	5	0.1	0.02	0.02	0.1	0.02	5	0.03	1	0.5	0.5
Method	CS	CS	CO2	1G	AR-MS	AR-MS	AR-MS	AR-MS	AR-MS	FA-AA	FA-GRA	FA-MS	FA-MS	FA-MS
NIST 694 Cert	-	-	-	-	-	-	-	-	-	-	-	-	-	-
DNC-1 Meas	-	-	-	-	-	-	-	-	-	-	-	-	-	-
DNC-1 Cert	-	-	-	-	-	-	-	-	-	-	-	-	-	-
GBW 07113 Meas	-	-	-	-	-	-	-	-	-	-	-	-	-	-
GBW 07113 Cert	-	-	-	-	-	-	-	-	-	-	-	-	-	-
GXR-4 Meas	-	-	-	113	-	-	-	-	-	-	-	-	-	-
GXR-4 Cert	-	-	-	110	-	-	-	-	-	-	-	-	-	-
GXR-4 Meas	-	-	-	113	-	-	-	-	-	-	-	-	-	-
GXR-4 Cert	-	-	-	110	-	-	-	-	-	-	-	-	-	-
SDC-1 Meas	-	-	-	-	-	-	-	-	-	-	-	-	-	-
SDC-1 Cert	-	-	-	-	-	-	-	-	-	-	-	-	-	-
GXR-6 Meas	-	-	-	72	242	0.12	1.75	0.1	0.07	-	-	-	-	-
GXR-6 Cert	-	-	-	68	330	0.29	3.6	0.94	0.018	-	-	-	-	-
GXR-6 Meas	-	-	-	72	-	-	-	-	-	-	-	-	-	-
GXR-6 Cert	-	-	-	68	-	-	-	-	-	-	-	-	-	-
LKSD-3 Meas	-	-	-	-	-	-	-	-	-	-	-	-	-	-
LKSD-3 Cert	-	-	-	-	-	-	-	-	-	-	-	-	-	-
TDB-1 Meas	-	-	-	-	-	-	-	-	-	-	-	-	-	-
TDB-1 Cert	-	-	-	-	-	-	-	-	-	-	-	-	-	-
SY-2 Meas	-	-	-	-	-	-	-	-	-	-	-	-	-	-
SY-2 Cert	-	-	-	-	-	-	-	-	-	-	-	-	-	-
SY-3 Meas	-	-	-	-	-	-	-	-	-	-	-	-	-	-
SY-3 Cert	-	-	-	-	-	-	-	-	-	-	-	-	-	-
BaSO4 Meas	-	14.2	-	-	-	-	-	-	-	-	-	-	-	-
BaSO4 Cert	-	14	-	-	-	-	-	-	-	-	-	-	-	-
BaSO4 Meas	-	14.3	-	-	-	-	-	-	-	-	-	-	-	-
BaSO4 Cert	-	14	-	-	-	-	-	-	-	-	-	-	-	-
BaSO4 Meas	-	14.3	-	-	-	-	-	-	-	-	-	-	-	-
BaSO4 Cert	-	14	-	-	-	-	-	-	-	-	-	-	-	-
W-2a Meas	-	-	-	-	-	-	-	-	-	-	-	-	-	-
W-2a Cert	-	-	-	-	-	-	-	-	-	-	-	-	-	-
DTS-2b Meas	-	-	-	-	-	-	-	-	-	-	-	-	-	-
DTS-2b Cert	-	-	-	-	-	-	-	-	-	-	-	-	-	-
SY-4 Meas	-	-	-	-	-	-	-	-	-	-	-	-	-	-
SY-4 Cert	-	-	-	-	-	-	-	-	-	-	-	-	-	-
CTA-AC-1 Meas	-	-	-	-	-	-	-	-	-	-	-	-	-	-
CTA-AC-1 Cert	-	-	-	-	-	-	-	-	-	-	-	-	-	-



Analyte	C-Total	S-Total	CO <sub>2</sub>	Hg	As	Bi	Sb	Se	Te	Au	Au	Au	Pd	Pt
Units	%	%	%	ppb	ppm	ppm	ppm	ppm	ppm	ppb	g/tonne	ppb	ppb	ppb
Detection Limit	0.01	0.01	0.01	5	0.1	0.02	0.02	0.1	0.02	5	0.03	1	0.5	0.5
Method	CS	CS	CO2	1G	AR-MS	AR-MS	AR-MS	AR-MS	AR-MS	FA-AA	FA-GRA	FA-MS	FA-MS	FA-MS
BIR-1a Meas	-	-	-	-	-	-	-	-	-	-	-	-	-	-
BIR-1a Cert	-	-	-	-	-	-	-	-	-	-	-	-	-	-
NCS DC86312 Meas	-	-	-	-	-	-	-	-	-	-	-	-	-	-
NCS DC86312 Cert	-	-	-	-	-	-	-	-	-	-	-	-	-	-
JGb-2 Meas	-	-	-	-	-	-	-	-	-	-	-	-	-	-
JGb-2 Cert	-	-	-	-	-	-	-	-	-	-	-	-	-	-
NCS DC70009 (GBW07241) Meas	-	-	-	-	-	-	-	-	-	-	-	-	-	-
NCS DC70009 (GBW07241) Cert	-	-	-	-	-	-	-	-	-	-	-	-	-	-
SGR-1b Meas	27.9	1.55	-	-	-	-	-	-	-	-	-	-	-	-
SGR-1b Cert	28	1.53	-	-	-	-	-	-	-	-	-	-	-	-
SGR-1b Meas	28	1.56	-	-	-	-	-	-	-	-	-	-	-	-
SGR-1b Cert	28	1.53	-	-	-	-	-	-	-	-	-	-	-	-
SGR-1b Meas	27.6	1.54	-	-	-	-	-	-	-	-	-	-	-	-
SGR-1b Cert	28	1.53	-	-	-	-	-	-	-	-	-	-	-	-
OREAS 100a (Fusion) Meas	-	-	-	-	-	-	-	-	-	-	-	-	-	-
OREAS 100a (Fusion) Cert	-	-	-	-	-	-	-	-	-	-	-	-	-	-
OREAS 101a (Fusion) Meas	-	-	-	-	-	-	-	-	-	-	-	-	-	-
OREAS 101a (Fusion) Cert	-	-	-	-	-	-	-	-	-	-	-	-	-	-
OREAS 101b (Fusion) Meas	-	-	-	-	-	-	-	-	-	-	-	-	-	-
OREAS 101b (Fusion) Cert	-	-	-	-	-	-	-	-	-	-	-	-	-	-
OREAS 98 (S by LECO) Meas	-	16.5	-	-	-	-	-	-	-	-	-	-	-	-
OREAS 98 (S by LECO) Cert	-	16	-	-	-	-	-	-	-	-	-	-	-	-
OREAS 132b (S by LECO) Meas	-	8.52	-	-	-	-	-	-	-	-	-	-	-	-
OREAS 132b (S by LECO) Cert	-	8.23	-	-	-	-	-	-	-	-	-	-	-	-
JR-1 Meas	-	-	-	-	-	-	-	-	-	-	-	-	-	-
JR-1 Cert	-	-	-	-	-	-	-	-	-	-	-	-	-	-
NCS DC86318 Meas	-	-	-	-	-	-	-	-	-	-	-	-	-	-
NCS DC86318 Cert	-	-	-	-	-	-	-	-	-	-	-	-	-	-
USZ 25-2006 Meas	-	-	1.1	-	-	-	-	-	-	-	-	-	-	-
USZ 25-2006 Cert	-	-	1.04	-	-	-	-	-	-	-	-	-	-	-
DNC-1a Meas	-	-	-	-	-	-	-	-	-	-	-	-	-	-
DNC-1a Cert	-	-	-	-	-	-	-	-	-	-	-	-	-	-
PK2 Meas	-	-	-	-	-	-	-	-	-	-	-	4930	6270	4780
PK2 Cert	-	-	-	-	-	-	-	-	-	-	-	4790	5918	4749
GS309-4 Meas	0.18	33.1	-	-	-	-	-	-	-	-	-	-	-	-
GS309-4 Cert	0.22	34.12	-	-	-	-	-	-	-	-	-	-	-	-
GS311-4 Meas	1.07	0.53	-	-	-	-	-	-	-	-	-	-	-	-

Analyte	C-Total	S-Total	CO <sub>2</sub>	Hg	As	Bi	Sb	Se	Te	Au	Au	Au	Pd	Pt
Units	%	%	%	ppb	ppm	ppm	ppm	ppm	ppm	ppb	g/tonne	ppb	ppb	ppb
Detection Limit	0.01	0.01	0.01	5	0.1	0.02	0.02	0.1	0.02	5	0.03	1	0.5	0.5
Method	CS	CS	CO2	1G	AR-MS	AR-MS	AR-MS	AR-MS	AR-MS	FA-AA	FA-GRA	FA-MS	FA-MS	FA-MS
GS311-4 Cert	1.11	0.54	-	-	-	-	-	-	-	-	-	-	-	-
GS311-4 Meas	1.09	0.56	-	-	-	-	-	-	-	-	-	-	-	-
GS311-4 Cert	1.11	0.54	-	-	-	-	-	-	-	-	-	-	-	-
GS311-4 Meas	1.09	0.55	-	-	-	-	-	-	-	-	-	-	-	-
GS311-4 Cert	1.11	0.54	-	-	-	-	-	-	-	-	-	-	-	-
GS900-5 Meas	0.62	0.34	-	-	-	-	-	-	-	-	-	-	-	-
GS900-5 Cert	0.65	0.34	-	-	-	-	-	-	-	-	-	-	-	-
GS900-5 Meas	0.63	0.35	-	-	-	-	-	-	-	-	-	-	-	-
GS900-5 Cert	0.65	0.34	-	-	-	-	-	-	-	-	-	-	-	-
GS900-5 Meas	0.62	0.34	-	-	-	-	-	-	-	-	-	-	-	-
GS900-5 Cert	0.65	0.34	-	-	-	-	-	-	-	-	-	-	-	-
OREAS 45d (Aqua Regia) Meas	-	-	-	-	4.6	0.2	-	-	-	-	-	-	-	-
OREAS 45d (Aqua Regia) Cert	-	-	-	-	6.5	0.3	-	-	-	-	-	-	-	-
SBC-1 Meas	-	-	-	-	-	-	-	-	-	-	-	-	-	-
SBC-1 Cert	-	-	-	-	-	-	-	-	-	-	-	-	-	-
OREAS 45d (4-Acid) Meas	-	-	-	-	-	-	-	-	-	-	-	-	-	-
OREAS 45d (4-Acid) Cert	-	-	-	-	-	-	-	-	-	-	-	-	-	-
CaCO3 Meas	-	-	43.6	-	-	-	-	-	-	-	-	-	-	-
CaCO3 Cert	-	-	44.1	-	-	-	-	-	-	-	-	-	-	-
SdAR-M2 (U.S.G.S.) Meas	-	-	-	1310	-	0.74	-	-	-	-	-	-	-	-
SdAR-M2 (U.S.G.S.) Cert	-	-	-	1440	-	1.05	-	-	-	-	-	-	-	-
SdAR-M2 (U.S.G.S.) Meas	-	-	-	1310	-	-	-	-	-	-	-	-	-	-
SdAR-M2 (U.S.G.S.) Cert	-	-	-	1440	-	-	-	-	-	-	-	-	-	-
GXR-1 Meas	-	-	-	3900	382	1280	73.4	13.8	14	-	-	-	-	-
GXR-1 Cert	-	-	-	3900	427	1380	122	16.6	13	-	-	-	-	-
GXR-1 Meas	-	-	-	-	-	-	-	-	-	-	-	-	-	-
GXR-1 Cert	-	-	-	-	-	-	-	-	-	-	-	-	-	-
NIST 694 Meas	-	-	-	-	-	-	-	-	-	-	-	-	-	-
NIST 694 Cert	-	-	-	-	-	-	-	-	-	-	-	-	-	-
DNC-1 Meas	-	-	-	-	-	-	-	-	-	-	-	-	-	-
DNC-1 Cert	-	-	-	-	-	-	-	-	-	-	-	-	-	-
GBW 07113 Meas	-	-	-	-	-	-	-	-	-	-	-	-	-	-
GBW 07113 Cert	-	-	-	-	-	-	-	-	-	-	-	-	-	-
GXR-4 Meas	-	-	-	109	100	20.1	2.53	5.1	0.92	-	-	-	-	-
GXR-4 Cert	-	-	-	110	98	19	4.8	5.6	0.97	-	-	-	-	-
GXR-4 Meas	-	-	-	-	-	-	-	-	-	-	-	-	-	-
GXR-4 Cert	-	-	-	-	-	-	-	-	-	-	-	-	-	-

Analyte	C-Total	S-Total	CO <sub>2</sub>	Hg	As	Bi	Sb	Se	Te	Au	Au	Au	Pd	Pt
Units	%	%	%	ppb	ppm	ppm	ppm	ppm	ppm	ppb	g/tonne	ppb	ppb	ppb
Detection Limit	0.01	0.01	0.01	5	0.1	0.02	0.02	0.1	0.02	5	0.03	1	0.5	0.5
Method	CS	CS	CO2	1G	AR-MS	AR-MS	AR-MS	AR-MS	AR-MS	FA-AA	FA-GRA	FA-MS	FA-MS	FA-MS
SDC-1 Meas	-	-	-	-	-	-	-	-	-	-	-	-	-	-
SDC-1 Cert	-	-	-	-	-	-	-	-	-	-	-	-	-	-
SDC-1 Meas	-	-	-	-	-	-	-	-	-	-	-	-	-	-
SDC-1 Cert	-	-	-	-	-	-	-	-	-	-	-	-	-	-
GXR-6 Meas	-	-	-	73	237	0.18	0.7	<0.1	<0.02	-	-	-	-	-
GXR-6 Cert	-	-	-	68	330	0.29	3.6	0.94	0.018	-	-	-	-	-
GXR-6 Meas	-	-	-	-	-	-	-	-	-	-	-	-	-	-
GXR-6 Cert	-	-	-	-	-	-	-	-	-	-	-	-	-	-
LKSD-3 Meas	-	-	-	-	-	-	-	-	-	-	-	-	-	-
LKSD-3 Cert	-	-	-	-	-	-	-	-	-	-	-	-	-	-
TDB-1 Meas	-	-	-	-	-	-	-	-	-	-	-	-	-	-
TDB-1 Cert	-	-	-	-	-	-	-	-	-	-	-	-	-	-
SY-2 Meas	-	-	-	-	-	-	-	-	-	-	-	-	-	-
SY-2 Cert	-	-	-	-	-	-	-	-	-	-	-	-	-	-
SY-3 Meas	-	-	-	-	-	-	-	-	-	-	-	-	-	-
SY-3 Cert	-	-	-	-	-	-	-	-	-	-	-	-	-	-
BaSO4 Meas	-	14.2	-	-	-	-	-	-	-	-	-	-	-	-
BaSO4 Cert	-	14	-	-	-	-	-	-	-	-	-	-	-	-
BaSO4 Meas	-	14.3	-	-	-	-	-	-	-	-	-	-	-	-
BaSO4 Cert	-	14	-	-	-	-	-	-	-	-	-	-	-	-
W-2a Meas	-	-	-	-	-	-	-	-	-	-	-	-	-	-
W-2a Cert	-	-	-	-	-	-	-	-	-	-	-	-	-	-
SY-4 Meas	-	-	-	-	-	-	-	-	-	-	-	-	-	-
SY-4 Cert	-	-	-	-	-	-	-	-	-	-	-	-	-	-
CTA-AC-1 Meas	-	-	-	-	-	-	-	-	-	-	-	-	-	-
CTA-AC-1 Cert	-	-	-	-	-	-	-	-	-	-	-	-	-	-
BIR-1a Meas	-	-	-	-	-	-	-	-	-	-	-	-	-	-
BIR-1a Cert	-	-	-	-	-	-	-	-	-	-	-	-	-	-
BIR-1a Meas	-	-	-	-	-	-	-	-	-	-	-	-	-	-
BIR-1a Cert	-	-	-	-	-	-	-	-	-	-	-	-	-	-
NCS DC86312 Meas	-	-	-	-	-	-	-	-	-	-	-	-	-	-
NCS DC86312 Cert	-	-	-	-	-	-	-	-	-	-	-	-	-	-
JGb-2 Meas	-	-	-	-	-	-	-	-	-	-	-	-	-	-
JGb-2 Cert	-	-	-	-	-	-	-	-	-	-	-	-	-	-
JGb-2 Meas	-	-	-	-	-	-	-	-	-	-	-	-	-	-
JGb-2 Cert	-	-	-	-	-	-	-	-	-	-	-	-	-	-
JGb-2 Meas	-	-	-	-	-	-	-	-	-	-	-	-	-	-

Analyte	C-Total	S-Total	CO <sub>2</sub>	Hg	As	Bi	Sb	Se	Te	Au	Au	Au	Pd	Pt
Units	%	%	%	ppb	ppm	ppm	ppm	ppm	ppm	ppb	g/tonne	ppb	ppb	ppb
Detection Limit	0.01	0.01	0.01	5	0.1	0.02	0.02	0.1	0.02	5	0.03	1	0.5	0.5
Method	CS	CS	CO2	1G	AR-MS	AR-MS	AR-MS	AR-MS	AR-MS	FA-AA	FA-GRA	FA-MS	FA-MS	FA-MS
JGb-2 Cert	-	-	-	-	-	-	-	-	-	-	-	-	-	-
JGb-2 Meas	-	-	-	-	-	-	-	-	-	-	-	-	-	-
JGb-2 Cert	-	-	-	-	-	-	-	-	-	-	-	-	-	-
NCS DC70009 (GBW07241) Meas	-	-	-	-	-	-	-	-	-	-	-	-	-	-
NCS DC70009 (GBW07241) Cert	-	-	-	-	-	-	-	-	-	-	-	-	-	-
SGR-1b Meas	28.4	1.53	-	-	-	-	-	-	-	-	-	-	-	-
SGR-1b Cert	28	1.53	-	-	-	-	-	-	-	-	-	-	-	-
SGR-1b Meas	28.4	1.56	-	-	-	-	-	-	-	-	-	-	-	-
SGR-1b Cert	28	1.53	-	-	-	-	-	-	-	-	-	-	-	-
OREAS 100a (Fusion) Meas	-	-	-	-	-	-	-	-	-	-	-	-	-	-
OREAS 100a (Fusion) Cert	-	-	-	-	-	-	-	-	-	-	-	-	-	-
OREAS 101a (Fusion) Meas	-	-	-	-	-	-	-	-	-	-	-	-	-	-
OREAS 101a (Fusion) Cert	-	-	-	-	-	-	-	-	-	-	-	-	-	-
OREAS 101b (Fusion) Meas	-	-	-	-	-	-	-	-	-	-	-	-	-	-
OREAS 101b (Fusion) Cert	-	-	-	-	-	-	-	-	-	-	-	-	-	-
JR-1 Meas	-	-	-	-	-	-	-	-	-	-	-	-	-	-
JR-1 Cert	-	-	-	-	-	-	-	-	-	-	-	-	-	-
NCS DC86318 Meas	-	-	-	-	-	-	-	-	-	-	-	-	-	-
NCS DC86318 Cert	-	-	-	-	-	-	-	-	-	-	-	-	-	-
USZ 25-2006 Meas	-	-	1.03	-	-	-	-	-	-	-	-	-	-	-
USZ 25-2006 Cert	-	-	1.04	-	-	-	-	-	-	-	-	-	-	-
USZ 25-2006 Meas	-	-	1.04	-	-	-	-	-	-	-	-	-	-	-
USZ 25-2006 Cert	-	-	1.04	-	-	-	-	-	-	-	-	-	-	-
DNC-1a Meas	-	-	-	-	-	-	-	-	-	-	-	-	-	-
DNC-1a Cert	-	-	-	-	-	-	-	-	-	-	-	-	-	-
DNC-1a Meas	-	-	-	-	-	-	-	-	-	-	-	-	-	-
DNC-1a Cert	-	-	-	-	-	-	-	-	-	-	-	-	-	-
PK2 Meas	-	-	-	-	-	-	-	-	-	-	-	5090	6210	4940
PK2 Cert	-	-	-	-	-	-	-	-	-	-	-	4790	5918	4749
GS311-4 Meas	1.11	0.57	-	-	-	-	-	-	-	-	-	-	-	-
GS311-4 Cert	1.11	0.54	-	-	-	-	-	-	-	-	-	-	-	-
GS311-4 Meas	1.1	0.57	-	-	-	-	-	-	-	-	-	-	-	-
GS311-4 Cert	1.11	0.54	-	-	-	-	-	-	-	-	-	-	-	-
GS900-5 Meas	0.63	0.37	-	-	-	-	-	-	-	-	-	-	-	-
GS900-5 Cert	0.65	0.34	-	-	-	-	-	-	-	-	-	-	-	-
GS900-5 Meas	0.59	0.35	-	-	-	-	-	-	-	-	-	-	-	-
GS900-5 Cert	0.65	0.34	-	-	-	-	-	-	-	-	-	-	-	-

Analyte	C-Total	S-Total	CO <sub>2</sub>	Hg	As	Bi	Sb	Se	Te	Au	Au	Au	Pd	Pt
Units	%	%	%	ppb	ppm	ppm	ppm	ppm	ppm	ppb	g/tonne	ppb	ppb	ppb
Detection Limit	0.01	0.01	0.01	5	0.1	0.02	0.02	0.1	0.02	5	0.03	1	0.5	0.5
Method	CS	CS	CO2	1G	AR-MS	AR-MS	AR-MS	AR-MS	AR-MS	FA-AA	FA-GRA	FA-MS	FA-MS	FA-MS
OREAS 45d (Aqua Regia) Meas	-	-	-	-	3.9	0.28	-	-	-	-	-	-	-	-
OREAS 45d (Aqua Regia) Cert	-	-	-	-	6.5	0.3	-	-	-	-	-	-	-	-
SBC-1 Meas	-	-	-	-	-	-	-	-	-	-	-	-	-	-
SBC-1 Cert	-	-	-	-	-	-	-	-	-	-	-	-	-	-
SBC-1 Meas	-	-	-	-	-	-	-	-	-	-	-	-	-	-
SBC-1 Cert	-	-	-	-	-	-	-	-	-	-	-	-	-	-
OREAS 45d (4-Acid) Meas	-	-	-	-	-	-	-	-	-	-	-	-	-	-
OREAS 45d (4-Acid) Cert	-	-	-	-	-	-	-	-	-	-	-	-	-	-
OxK110 Meas	-	-	-	-	-	-	-	-	-	-	3.61	-	-	-
OxK110 Cert	-	-	-	-	-	-	-	-	-	-	3.602	-	-	-
OXN117 Meas	-	-	-	-	-	-	-	-	-	-	7.47	-	-	-
OXN117 Cert	-	-	-	-	-	-	-	-	-	-	7.679	-	-	-
CaCO3 Meas	-	-	43.6	-	-	-	-	-	-	-	-	-	-	-
CaCO3 Cert	-	-	44.1	-	-	-	-	-	-	-	-	-	-	-
CaCO3 Meas	-	-	43.3	-	-	-	-	-	-	-	-	-	-	-
CaCO3 Cert	-	-	44.1	-	-	-	-	-	-	-	-	-	-	-
SdAR-M2 (U.S.G.S.) Meas	-	-	-	1370	-	1.09	-	-	-	-	-	-	-	-
SdAR-M2 (U.S.G.S.) Cert	-	-	-	1440	-	1.05	-	-	-	-	-	-	-	-
GXR-1 Meas	-	-	-	-	388	1620	68.3	14.8	14	-	-	-	-	-
GXR-1 Cert	-	-	-	-	427	1380	122	16.6	13	-	-	-	-	-
GXR-1 Meas	-	-	-	-	353	1370	70.8	14	13.4	-	-	-	-	-
GXR-1 Cert	-	-	-	-	427	1380	122	16.6	13	-	-	-	-	-
NIST 694 Meas	-	-	-	-	-	-	-	-	-	-	-	-	-	-
NIST 694 Cert	-	-	-	-	-	-	-	-	-	-	-	-	-	-
DNC-1 Meas	-	-	-	-	-	-	-	-	-	-	-	-	-	-
DNC-1 Cert	-	-	-	-	-	-	-	-	-	-	-	-	-	-
GBW 07113 Meas	-	-	-	-	-	-	-	-	-	-	-	-	-	-
GBW 07113 Cert	-	-	-	-	-	-	-	-	-	-	-	-	-	-
GXR-4 Meas	-	-	-	-	93	21.1	2.08	5.7	0.76	-	-	-	-	-
GXR-4 Cert	-	-	-	-	98	19	4.8	5.6	0.97	-	-	-	-	-
GXR-4 Meas	-	-	-	-	88.2	18.7	3.01	5.1	0.86	-	-	-	-	-
GXR-4 Cert	-	-	-	-	98	19	4.8	5.6	0.97	-	-	-	-	-
GXR-4 Meas	-	-	-	-	117	19.7	2.89	5.3	0.73	-	-	-	-	-
GXR-4 Cert	-	-	-	-	98	19	4.8	5.6	0.97	-	-	-	-	-
SDC-1 Meas	-	-	-	-	-	-	-	-	-	-	-	-	-	-
SDC-1 Cert	-	-	-	-	-	-	-	-	-	-	-	-	-	-
SDC-1 Meas	-	-	-	-	-	-	-	-	-	-	-	-	-	-

Analyte	C-Total	S-Total	CO <sub>2</sub>	Hg	As	Bi	Sb	Se	Te	Au	Au	Au	Pd	Pt
Units	%	%	%	ppb	ppm	ppm	ppm	ppm	ppm	ppb	g/tonne	ppb	ppb	ppb
Detection Limit	0.01	0.01	0.01	5	0.1	0.02	0.02	0.1	0.02	5	0.03	1	0.5	0.5
Method	CS	CS	CO2	1G	AR-MS	AR-MS	AR-MS	AR-MS	AR-MS	FA-AA	FA-GRA	FA-MS	FA-MS	FA-MS
SDC-1 Cert	-	-	-	-	-	-	-	-	-	-	-	-	-	-
GXR-6 Meas	-	-	-	-	221	0.2	0.69	0.2	0.03	-	-	-	-	-
GXR-6 Cert	-	-	-	-	330	0.29	3.6	0.94	0.018	-	-	-	-	-
GXR-6 Meas	-	-	-	-	202	0.17	1.63	0.4	0.06	-	-	-	-	-
GXR-6 Cert	-	-	-	-	330	0.29	3.6	0.94	0.018	-	-	-	-	-
GXR-6 Meas	-	-	-	-	257	0.23	1.03	0.1	<0.02	-	-	-	-	-
GXR-6 Cert	-	-	-	-	330	0.29	3.6	0.94	0.018	-	-	-	-	-
LKSD-3 Meas	-	-	-	-	-	-	-	-	-	-	-	-	-	-
LKSD-3 Cert	-	-	-	-	-	-	-	-	-	-	-	-	-	-
TDB-1 Meas	-	-	-	-	-	-	-	-	-	-	-	-	-	-
TDB-1 Cert	-	-	-	-	-	-	-	-	-	-	-	-	-	-
SY-2 Meas	-	-	-	-	-	-	-	-	-	-	-	-	-	-
SY-2 Cert	-	-	-	-	-	-	-	-	-	-	-	-	-	-
SY-3 Meas	-	-	-	-	-	-	-	-	-	-	-	-	-	-
SY-3 Cert	-	-	-	-	-	-	-	-	-	-	-	-	-	-
BaSO4 Meas	-	14.4	-	-	-	-	-	-	-	-	-	-	-	-
BaSO4 Cert	-	14	-	-	-	-	-	-	-	-	-	-	-	-
W-2a Meas	-	-	-	-	-	-	-	-	-	-	-	-	-	-
W-2a Cert	-	-	-	-	-	-	-	-	-	-	-	-	-	-
SY-4 Meas	-	-	-	-	-	-	-	-	-	-	-	-	-	-
SY-4 Cert	-	-	-	-	-	-	-	-	-	-	-	-	-	-
CTA-AC-1 Meas	-	-	-	-	-	-	-	-	-	-	-	-	-	-
CTA-AC-1 Cert	-	-	-	-	-	-	-	-	-	-	-	-	-	-
BIR-1a Meas	-	-	-	-	-	-	-	-	-	-	-	-	-	-
BIR-1a Cert	-	-	-	-	-	-	-	-	-	-	-	-	-	-
NCS DC86312 Meas	-	-	-	-	-	-	-	-	-	-	-	-	-	-
NCS DC86312 Cert	-	-	-	-	-	-	-	-	-	-	-	-	-	-
JGb-2 Meas	-	-	-	-	-	-	-	-	-	-	-	-	-	-
JGb-2 Cert	-	-	-	-	-	-	-	-	-	-	-	-	-	-
JGb-2 Meas	-	-	-	-	-	-	-	-	-	-	-	-	-	-
JGb-2 Cert	-	-	-	-	-	-	-	-	-	-	-	-	-	-
JGb-2 Meas	-	-	-	-	-	-	-	-	-	-	-	-	-	-
JGb-2 Cert	-	-	-	-	-	-	-	-	-	-	-	-	-	-
NCS DC70009 (GBW07241) Meas	-	-	-	-	-	-	-	-	-	-	-	-	-	-
NCS DC70009 (GBW07241) Cert	-	-	-	-	-	-	-	-	-	-	-	-	-	-
SGR-1b Meas	27.7	1.5	-	-	-	-	-	-	-	-	-	-	-	-
SGR-1b Cert	28	1.53	-	-	-	-	-	-	-	-	-	-	-	-

Analyte	C-Total	S-Total	CO <sub>2</sub>	Hg	As	Bi	Sb	Se	Te	Au	Au	Au	Pd	Pt
Units	%	%	%	ppb	ppm	ppm	ppm	ppm	ppm	ppb	g/tonne	ppb	ppb	ppb
Detection Limit	0.01	0.01	0.01	5	0.1	0.02	0.02	0.1	0.02	5	0.03	1	0.5	0.5
Method	CS	CS	CO <sub>2</sub>	1G	AR-MS	AR-MS	AR-MS	AR-MS	AR-MS	FA-AA	FA-GRA	FA-MS	FA-MS	FA-MS
OREAS 100a (Fusion) Meas	-	-	-	-	-	-	-	-	-	-	-	-	-	-
OREAS 100a (Fusion) Cert	-	-	-	-	-	-	-	-	-	-	-	-	-	-
OREAS 101a (Fusion) Meas	-	-	-	-	-	-	-	-	-	-	-	-	-	-
OREAS 101a (Fusion) Cert	-	-	-	-	-	-	-	-	-	-	-	-	-	-
OREAS 101b (Fusion) Meas	-	-	-	-	-	-	-	-	-	-	-	-	-	-
OREAS 101b (Fusion) Cert	-	-	-	-	-	-	-	-	-	-	-	-	-	-
JR-1 Meas	-	-	-	-	-	-	-	-	-	-	-	-	-	-
JR-1 Cert	-	-	-	-	-	-	-	-	-	-	-	-	-	-
NCS DC86318 Meas	-	-	-	-	-	-	-	-	-	-	-	-	-	-
NCS DC86318 Cert	-	-	-	-	-	-	-	-	-	-	-	-	-	-
USZ 25-2006 Meas	-	-	1.07	-	-	-	-	-	-	-	-	-	-	-
USZ 25-2006 Cert	-	-	1.04	-	-	-	-	-	-	-	-	-	-	-
USZ 25-2006 Meas	-	-	1.09	-	-	-	-	-	-	-	-	-	-	-
USZ 25-2006 Cert	-	-	1.04	-	-	-	-	-	-	-	-	-	-	-
DNC-1a Meas	-	-	-	-	-	-	-	-	-	-	-	-	-	-
DNC-1a Cert	-	-	-	-	-	-	-	-	-	-	-	-	-	-
DNC-1a Meas	-	-	-	-	-	-	-	-	-	-	-	-	-	-
DNC-1a Cert	-	-	-	-	-	-	-	-	-	-	-	-	-	-
GS311-4 Meas	1.12	0.53	-	-	-	-	-	-	-	-	-	-	-	-
GS311-4 Cert	1.11	0.54	-	-	-	-	-	-	-	-	-	-	-	-
GS900-5 Meas	0.63	0.33	-	-	-	-	-	-	-	-	-	-	-	-
GS900-5 Cert	0.65	0.34	-	-	-	-	-	-	-	-	-	-	-	-
OREAS 45d (Aqua Regia) Meas	-	-	-	-	4.7	0.35	-	-	-	-	-	-	-	-
OREAS 45d (Aqua Regia) Cert	-	-	-	-	6.5	0.3	-	-	-	-	-	-	-	-
SBC-1 Meas	-	-	-	-	-	-	-	-	-	-	-	-	-	-
SBC-1 Cert	-	-	-	-	-	-	-	-	-	-	-	-	-	-
SBC-1 Meas	-	-	-	-	-	-	-	-	-	-	-	-	-	-
SBC-1 Cert	-	-	-	-	-	-	-	-	-	-	-	-	-	-
OREAS 45d (4-Acid) Meas	-	-	-	-	-	-	-	-	-	-	-	-	-	-
OREAS 45d (4-Acid) Cert	-	-	-	-	-	-	-	-	-	-	-	-	-	-
OREAS 45d (4-Acid) Meas	-	-	-	-	-	-	-	-	-	-	-	-	-	-
OREAS 45d (4-Acid) Cert	-	-	-	-	-	-	-	-	-	-	-	-	-	-
CaCO <sub>3</sub> Meas	-	-	43.6	-	-	-	-	-	-	-	-	-	-	-
CaCO <sub>3</sub> Cert	-	-	44.1	-	-	-	-	-	-	-	-	-	-	-
CaCO <sub>3</sub> Meas	-	-	43.3	-	-	-	-	-	-	-	-	-	-	-
CaCO <sub>3</sub> Cert	-	-	44.1	-	-	-	-	-	-	-	-	-	-	-
SdAR-M2 (U.S.G.S.) Meas	-	-	-	-	-	1.25	-	-	-	-	-	-	-	-

Analyte	C-Total	S-Total	CO <sub>2</sub>	Hg	As	Bi	Sb	Se	Te	Au	Au	Au	Pd	Pt
Units	%	%	%	ppb	ppm	ppm	ppm	ppm	ppm	ppb	g/tonne	ppb	ppb	ppb
Detection Limit	0.01	0.01	0.01	5	0.1	0.02	0.02	0.1	0.02	5	0.03	1	0.5	0.5
Method	CS	CS	CO2	1G	AR-MS	AR-MS	AR-MS	AR-MS	AR-MS	FA-AA	FA-GRA	FA-MS	FA-MS	FA-MS
SdAR-M2 (U.S.G.S.) Cert	-	-	-	-	-	1.05	-	-	-	-	-	-	-	-
SdAR-M2 (U.S.G.S.) Meas	-	-	-	-	-	1.07	-	-	-	-	-	-	-	-
SdAR-M2 (U.S.G.S.) Cert	-	-	-	-	-	1.05	-	-	-	-	-	-	-	-
SdAR-M2 (U.S.G.S.) Meas	-	-	-	-	-	1.15	-	-	-	-	-	-	-	-
SdAR-M2 (U.S.G.S.) Cert	-	-	-	-	-	1.05	-	-	-	-	-	-	-	-
OREAS 214 Meas	-	-	-	-	-	-	-	-	-	3050	-	-	-	-
OREAS 214 Cert	-	-	-	-	-	-	-	-	-	3030	-	-	-	-
OREAS 218 Meas	-	-	-	-	-	-	-	-	-	551	-	-	-	-
OREAS 218 Cert	-	-	-	-	-	-	-	-	-	531	-	-	-	-
OREAS 218 Meas	-	-	-	-	-	-	-	-	-	544	-	-	-	-
OREAS 218 Cert	-	-	-	-	-	-	-	-	-	531	-	-	-	-
T9 Geochem Orig	-	-	-	<5	4.3	0.03	0.02	0.4	0.04	-	-	7	4.5	7.6
T9 Geochem Dup	-	-	-	<5	4.5	0.03	<0.02	0.4	0.06	-	-	4	4.4	7.5
T14 Geochem Orig	-	-	-	-	-	-	-	-	-	-	-	-	-	-
T14 Geochem Dup	-	-	-	-	-	-	-	-	-	-	-	-	-	-
T17 Geochem Orig	0.75	1.2	-	-	-	-	-	-	-	-	-	-	-	-
T17 Geochem Dup	0.76	1.18	-	-	-	-	-	-	-	-	-	-	-	-
STPL-BAS-025 Orig	-	-	0.18	-	-	-	-	-	-	-	-	-	-	-
STPL-BAS-025 Dup	-	-	0.16	-	-	-	-	-	-	-	-	-	-	-
T24 Geochem Orig	-	-	-	-	-	-	-	-	-	-	-	-	-	-
T24 Geochem Dup	-	-	-	-	-	-	-	-	-	-	-	-	-	-
T27 Geochem Orig	-	-	-	<5	6.9	0.17	0.04	0.2	0.09	-	-	-	-	-
T27 Geochem Dup	-	-	-	<5	6.6	0.12	0.04	<0.1	0.04	-	-	-	-	-
T31 Geochem Orig	-	-	-	-	-	-	-	-	-	-	-	7	<0.5	<0.5
T31 Geochem Dup	-	-	-	-	-	-	-	-	-	-	-	13	<0.5	<0.5
T37 Geochem Orig	0.58	33.6	-	-	-	-	-	-	-	-	-	-	-	-
T37 Geochem Dup	0.6	35.6	-	-	-	-	-	-	-	-	-	-	-	-
T42 Geochem Orig	-	-	-	-	-	-	-	-	-	-	-	-	-	-
T42 Geochem Dup	-	-	-	-	-	-	-	-	-	-	-	-	-	-
T45 Geochem Orig	-	-	-	-	-	-	-	-	-	-	-	2	<0.5	<0.5
T45 Geochem Dup	-	-	-	-	-	-	-	-	-	-	-	5	<0.5	<0.5
STPL-53-PML-036 Orig	-	-	0.97	-	-	-	-	-	-	-	-	-	-	-
STPL-53-PML-036 Dup	-	-	0.97	-	-	-	-	-	-	-	-	-	-	-
STPL-BAS-025 Orig	-	-	-	-	-	-	-	-	-	-	-	-	-	-
STPL-BAS-025 Dup	-	-	-	-	-	-	-	-	-	-	-	-	-	-
T42 Geochem Orig	-	-	-	-	-	-	-	-	-	-	-	-	-	-
T42 Geochem Dup	-	-	-	-	-	-	-	-	-	-	-	-	-	-



Analyte	C-Total	S-Total	CO <sub>2</sub>	Hg	As	Bi	Sb	Se	Te	Au	Au	Au	Pd	Pt
Units	%	%	%	ppb	ppm	ppm	ppm	ppm	ppm	ppb	g/tonne	ppb	ppb	ppb
Detection Limit	0.01	0.01	0.01	5	0.1	0.02	0.02	0.1	0.02	5	0.03	1	0.5	0.5
Method	CS	CS	CO2	1G	AR-MS	AR-MS	AR-MS	AR-MS	AR-MS	FA-AA	FA-GRA	FA-MS	FA-MS	FA-MS
T45 Geochem Orig	-	-	-	-	-	-	-	-	-	-	-	-	-	-
T45 Geochem Dup	-	-	-	-	-	-	-	-	-	-	-	-	-	-
T59 Orig	-	-	-	-	-	-	-	-	-	-	-	133	<0.5	<0.5
T59 Dup	-	-	-	-	-	-	-	-	-	-	-	128	<0.5	<0.5
T72 Orig	-	-	-	-	-	-	-	-	-	-	-	-	-	-
T72 Dup	-	-	-	-	-	-	-	-	-	-	-	-	-	-
T73 Orig	-	-	-	<5	-	-	-	-	-	-	-	-	-	-
T73 Dup	-	-	-	<5	-	-	-	-	-	-	-	-	-	-
STPL-BAS-029 Orig	-	-	-	<5	-	-	-	-	-	-	-	-	-	-
STPL-BAS-029 Dup	-	-	-	<5	-	-	-	-	-	-	-	-	-	-
T81 Orig	4.26	<0.01	14.4	-	-	-	-	-	-	-	-	-	-	-
T81 Dup	3.69	<0.01	14.5	-	-	-	-	-	-	-	-	-	-	-
T86 Orig	-	-	-	-	-	-	-	-	-	-	-	1630	<0.5	<0.5
T86 Dup	-	-	-	-	-	-	-	-	-	-	-	1670	<0.5	<0.5
T88 Orig	-	-	-	-	-	-	-	-	-	-	-	-	-	-
T88 Dup	-	-	-	-	-	-	-	-	-	-	-	-	-	-
T89 Orig	-	-	-	<5	-	-	-	-	-	-	-	-	-	-
T89 Dup	-	-	-	<5	-	-	-	-	-	-	-	-	-	-
T94 Orig	-	-	-	-	-	-	-	-	-	-	-	-	-	-
T94 Dup	-	-	-	-	-	-	-	-	-	-	-	-	-	-
T98 Orig	-	-	7.68	-	-	-	-	-	-	-	-	-	-	-
T98 Dup	-	-	7.69	-	-	-	-	-	-	-	-	-	-	-
T99 Orig	1.76	3.44	-	-	-	-	-	-	-	-	-	-	-	-
T99 Dup	1.76	3.27	-	-	-	-	-	-	-	-	-	-	-	-
T101 Orig	-	-	-	-	-	-	-	-	-	-	-	-	-	-
T101 Dup	-	-	-	-	-	-	-	-	-	-	-	-	-	-
T102 Orig	-	-	-	<5	-	-	-	-	-	-	-	17	<0.5	<0.5
T102 Dup	-	-	-	<5	-	-	-	-	-	-	-	21	<0.5	<0.5
T114 Orig	-	-	-	-	-	-	-	-	-	-	-	-	-	-
T114 Dup	-	-	-	-	-	-	-	-	-	-	-	-	-	-
T116 Orig	-	-	2.66	-	-	-	-	-	-	-	-	2	<0.5	<0.5
T116 Dup	-	-	2.65	-	-	-	-	-	-	-	-	2	<0.5	<0.5
T117 Orig	0.4	0.19	1.39	-	-	-	-	-	-	-	-	22	<0.5	<0.5
T117 Split PREP DUP	0.4	0.18	1.38	-	2.3	0.07	0.03	<0.1	0.04	-	-	23	<0.5	<0.5
STPL-53-PML-025 Orig	-	-	-	-	-	-	-	-	-	-	-	-	-	-
STPL-53-PML-025 Dup	-	-	-	-	-	-	-	-	-	-	-	-	-	-
T65 Orig	-	-	-	-	-	-	-	-	-	-	-	12	<0.5	<0.5

Analyte	C-Total	S-Total	CO <sub>2</sub>	Hg	As	Bi	Sb	Se	Te	Au	Au	Au	Pd	Pt
Units	%	%	%	ppb	ppm	ppm	ppm	ppm	ppm	ppb	g/tonne	ppb	ppb	ppb
Detection Limit	0.01	0.01	0.01	5	0.1	0.02	0.02	0.1	0.02	5	0.03	1	0.5	0.5
Method	CS	CS	CO2	1G	AR-MS	AR-MS	AR-MS	AR-MS	AR-MS	FA-AA	FA-GRA	FA-MS	FA-MS	FA-MS
T65 Dup	-	-	-	-	-	-	-	-	-	-	-	12	<0.5	<0.5
T106 Orig	-	-	-	-	-	-	-	-	-	-	-	-	-	-
T106 Dup	-	-	-	-	-	-	-	-	-	-	-	-	-	-
T118 Orig	-	-	-	-	-	-	-	-	-	-	-	-	-	-
T118 Dup	-	-	-	-	-	-	-	-	-	-	-	-	-	-
T141 Orig	-	-	-	-	-	-	-	-	-	-	-	-	-	-
T141 Dup	-	-	-	-	-	-	-	-	-	-	-	-	-	-
STPL-BAS-023 Orig	-	-	-	-	1.4	<0.02	0.28	<0.1	0.02	-	-	-	-	-
STPL-BAS-023 Dup	-	-	-	-	1.6	<0.02	0.3	<0.1	0.03	-	-	-	-	-
T154 Orig	-	-	-	<5	<0.1	0.02	0.09	<0.1	0.02	-	-	-	-	-
T154 Dup	-	-	-	<5	<0.1	<0.02	0.1	<0.1	<0.02	-	-	-	-	-
T157 Orig	1.14	4.5	-	-	-	-	-	-	-	-	-	-	-	-
T157 Dup	1.14	4.47	-	-	-	-	-	-	-	-	-	-	-	-
T158 Orig	-	-	2.8	-	-	-	-	-	-	-	-	1360	<0.5	<0.5
T158 Dup	-	-	2.88	-	-	-	-	-	-	-	-	1430	<0.5	<0.5
STPL-PML-53-027 Orig	-	-	-	-	-	-	-	-	-	-	-	-	-	-
STPL-PML-53-027 Dup	-	-	-	-	-	-	-	-	-	-	-	-	-	-
T182 Orig	-	-	-	-	-	-	-	-	-	-	-	-	-	-
T182 Dup	-	-	-	-	-	-	-	-	-	-	-	-	-	-
T183 Orig	-	-	-	-	-	-	-	-	-	-	-	-	-	-
T183 Dup	-	-	-	-	-	-	-	-	-	-	-	-	-	-
T187 Orig	0.2	0.27	-	-	-	-	-	-	-	-	-	-	-	-
T187 Dup	0.21	0.28	-	-	-	-	-	-	-	-	-	-	-	-
T188 Orig	-	-	5.87	-	-	-	-	-	-	-	-	-	-	-
T188 Dup	-	-	5.88	-	-	-	-	-	-	-	-	-	-	-
T189 Orig	-	-	-	-	-	-	-	-	-	-	-	9	<0.5	<0.5
T189 Dup	-	-	-	-	-	-	-	-	-	-	-	8	<0.5	<0.5
T200 Orig	<0.01	<0.01	-	-	-	-	-	-	-	-	-	-	-	-
T200 Dup	<0.01	<0.01	-	-	-	-	-	-	-	-	-	-	-	-
T218 Orig	-	-	-	-	<0.1	0.24	0.05	0.1	<0.02	-	-	-	-	-
T218 Dup	-	-	-	-	<0.1	0.24	0.07	<0.1	<0.02	-	-	-	-	-
T239 Orig	-	-	-	-	-	-	-	-	-	<5	-	-	-	-
T239 Dup	-	-	-	-	-	-	-	-	-	<5	-	-	-	-
T240 Orig	-	-	-	-	-	-	-	-	-	-	-	-	-	-
T240 Dup	-	-	-	-	-	-	-	-	-	-	-	-	-	-
T242 Orig	1.88	0.03	6.55	-	-	-	-	-	-	-	-	-	-	-
T242 Dup	1.93	0.03	6.52	-	-	-	-	-	-	-	-	-	-	-



Analyte Units Detection Limit Method	C-Total % 0.01 CS	S-Total % 0.01 CS	CO <sub>2</sub> % 0.01 CO2	Hg ppb 5 1G	As ppm 0.1 AR-MS	Bi ppm 0.02 AR-MS	Sb ppm 0.02 AR-MS	Se ppm 0.1 AR-MS	Te ppm 0.02 AR-MS	Au ppb 5 FA-AA	Au g/tonne 0.03 FA-GRA	Au ppb 1 FA-MS	Pd ppb 0.5 FA-MS	Pt ppb 0.5 FA-MS
Method Blank	-	-	-	-	<0.1	<0.02	0.05	<0.1	<0.02	-	-	-	-	-
Method Blank	-	-	-	-	-	-	-	-	-	-	-	-	-	-
Method Blank	-	-	-	-	-	-	-	-	-	-	<0.03	-	-	-
Method Blank	-	-	-	-	-	-	-	-	-	-	-	-	-	-
Method Blank	-	-	-	-	-	-	-	-	-	-	-	-	-	-
Method Blank	-	-	-	-	-	-	-	-	-	-	-	-	-	-
Method Blank	-	-	-	-	-	-	-	-	-	-	-	<1	<0.5	<0.5
Method Blank	-	-	-	-	<0.1	0.03	0.03	<0.1	0.03	-	-	-	-	-
Method Blank	-	-	-	<5	-	-	-	-	-	-	-	-	-	-
Method Blank	-	-	-	<5	-	-	-	-	-	-	-	-	-	-
Method Blank	-	-	-	-	-	-	-	-	-	-	-	-	-	-
Method Blank	-	-	-	-	-	-	-	-	-	-	-	-	-	-
Method Blank	-	-	-	-	-	-	-	-	-	-	-	-	-	-
Method Blank	-	-	<0.01	-	-	-	-	-	-	-	-	-	-	-
Method Blank	-	-	-	<5	-	-	-	-	-	-	-	-	-	-
Method Blank	-	-	-	-	-	-	-	-	-	-	-	-	-	-
Method Blank	-	-	-	-	-	-	-	-	-	-	-	-	-	-
Method Blank	-	-	-	-	-	-	-	-	-	-	-	-	-	-
Method Blank	-	-	-	-	-	-	-	-	-	-	-	-	-	-
Method Blank	-	-	-	-	-	-	-	-	-	-	-	-	-	-
Method Blank	-	-	-	-	-	-	-	-	-	-	-	-	-	-
Method Blank	-	-	-	-	-	-	-	-	-	-	-	-	-	-
Method Blank	-	-	<0.01	-	-	-	-	-	-	-	-	-	-	-
Method Blank	-	-	<0.01	-	-	-	-	-	-	-	-	-	-	-
Method Blank	-	-	-	-	-	-	-	-	-	-	-	-	-	-
Method Blank	-	-	-	-	-	-	-	-	-	-	-	-	-	-
Method Blank	-	-	-	-	-	-	-	-	-	-	-	-	-	-
Method Blank	-	-	-	-	-	-	-	-	-	-	-	-	-	-
Method Blank	-	-	-	-	-	-	-	-	-	-	-	-	-	-
Method Blank	-	-	-	-	<0.1	<0.02	<0.02	<0.1	<0.02	-	-	-	-	-
Method Blank	-	-	-	-	-	-	-	-	-	-	-	<1	<0.5	<0.5
Method Blank	-	-	-	-	-	-	-	-	-	-	-	<1	<0.5	<0.5
Method Blank	-	-	-	-	-	-	-	-	-	-	-	-	-	-
Method Blank	-	-	-	<5	-	-	-	-	-	-	-	-	-	-
Method Blank	-	-	-	-	-	-	-	-	-	-	<0.03	-	-	-
Method Blank	-	-	-	-	-	-	-	-	-	-	-	-	-	-

Analyte	C-Total	S-Total	CO <sub>2</sub>	Hg	As	Bi	Sb	Se	Te	Au	Au	Au	Pd	Pt
Units	%	%	%	ppb	ppm	ppm	ppm	ppm	ppm	ppb	g/tonne	ppb	ppb	ppb
Detection Limit	0.01	0.01	0.01	5	0.1	0.02	0.02	0.1	0.02	5	0.03	1	0.5	0.5
Method	CS	CS	CO2	1G	AR-MS	AR-MS	AR-MS	AR-MS	AR-MS	FA-AA	FA-GRA	FA-MS	FA-MS	FA-MS
Method Blank	-	-	-	-	-	-	-	-	-	-	-	-	-	-
Method Blank	-	-	-	-	-	-	-	-	-	-	-	-	-	-
Method Blank	-	-	-	-	-	-	-	-	-	-	-	-	-	-
Method Blank	-	-	-	-	-	-	-	-	-	-	-	-	-	-
Method Blank	-	-	-	-	-	-	-	-	-	-	-	-	-	-
Method Blank	-	-	-	-	-	-	-	-	-	-	-	-	-	-
Method Blank	-	-	<0.01	-	-	-	-	-	-	-	-	-	-	-
Method Blank	-	-	-	-	<0.1	<0.02	<0.02	<0.1	<0.02	-	-	-	-	-
Method Blank	-	-	-	-	<0.1	<0.02	<0.02	<0.1	<0.02	-	-	-	-	-
Method Blank	-	-	-	-	<0.1	<0.02	<0.02	<0.1	<0.02	-	-	-	-	-
Method Blank	-	-	-	-	<0.1	0.09	<0.02	0.1	<0.02	-	-	-	-	-
Method Blank	-	-	-	-	<0.1	0.09	<0.02	<0.1	<0.02	-	-	-	-	-
Method Blank	-	-	-	-	-	-	-	-	-	-	-	-	-	-
Method Blank	-	-	-	-	-	-	-	-	-	-	-	-	-	-
Method Blank	-	-	-	-	-	-	-	-	-	-	-	-	-	-
Method Blank	-	-	-	-	-	-	-	-	-	-	-	-	-	-
Method Blank	-	-	-	-	-	-	-	-	-	-	-	-	-	-
Method Blank	-	-	-	-	-	-	-	-	-	<5	-	-	-	-
Method Blank	-	-	-	-	-	-	-	-	-	<5	-	-	-	-
Method Blank	-	-	-	-	-	-	-	-	-	<5	-	-	-	-
Method Blank	-	-	-	-	-	-	-	-	-	<5	-	-	-	-
Method Blank	-	-	<0.01	-	-	-	-	-	-	-	-	-	-	-
Method Blank	-	-	-	-	-	-	-	-	-	-	-	-	-	-
Method Blank	-	-	-	-	-	-	-	-	-	-	-	-	-	-

Analyte	Ag	As	Bi	Ce	Co	Cr	Cs	Cu	Dy	Er	Eu	Ga
Units	ppm	ppm	ppm	ppm	ppm	ppm	ppm	ppm	ppm	ppm	ppm	ppm
Detection Limit	0.5	5	0.1	0.05	1	20	0.1	10	0.01	0.01	0.005	1
Method	FUS-MS	FUS-MS	FUS-MS	FUS-MS	FUS-MS	FUS-MS	FUS-MS	FUS-MS	FUS-MS	FUS-MS	FUS-MS	FUS-MS
GXR-1 Meas	-	-	-	-	-	-	-	-	-	-	-	-
GXR-1 Cert	-	-	-	-	-	-	-	-	-	-	-	-
NIST 694 Meas	-	-	-	-	-	-	-	-	-	-	-	-
NIST 694 Cert	-	-	-	-	-	-	-	-	-	-	-	-
DNC-1 Meas	-	-	-	-	57	280	-	100	-	-	0.65	15
DNC-1 Cert	-	-	-	-	57	270	-	100	-	-	0.59	15
GBW 07113 Meas	-	-	-	-	-	-	-	-	-	-	-	-
GBW 07113 Cert	-	-	-	-	-	-	-	-	-	-	-	-
GBW 07113 Meas	-	-	-	-	-	-	-	-	-	-	-	-
GBW 07113 Cert	-	-	-	-	-	-	-	-	-	-	-	-
GBW 07113 Meas	-	-	-	-	-	-	-	-	-	-	-	-
GBW 07113 Cert	-	-	-	-	-	-	-	-	-	-	-	-
GXR-4 Meas	-	-	-	-	-	-	-	-	-	-	-	-
GXR-4 Cert	-	-	-	-	-	-	-	-	-	-	-	-
GXR-6 Meas	-	-	-	-	-	-	-	-	-	-	-	-
GXR-6 Cert	-	-	-	-	-	-	-	-	-	-	-	-
LKSD-3 Meas	2.7	29	-	95.2	30	90	2.3	30	5.3	-	1.5	-
LKSD-3 Cert	2.7	27	-	90	30	87	2.3	35	4.9	-	1.5	-
TDB-1 Meas	-	-	-	39.7	-	270	-	340	-	-	2.1	-
TDB-1 Cert	-	-	-	41	-	251	-	323	-	-	2.1	-
SY-2 Meas	-	-	-	-	-	-	-	-	-	-	-	-
SY-2 Cert	-	-	-	-	-	-	-	-	-	-	-	-
SY-3 Meas	-	-	-	-	-	-	-	-	-	-	-	-
SY-3 Cert	-	-	-	-	-	-	-	-	-	-	-	-
BaSO4 Meas	-	-	-	-	-	-	-	-	-	-	-	-
BaSO4 Cert	-	-	-	-	-	-	-	-	-	-	-	-
BaSO4 Meas	-	-	-	-	-	-	-	-	-	-	-	-
BaSO4 Cert	-	-	-	-	-	-	-	-	-	-	-	-
BaSO4 Meas	-	-	-	-	-	-	-	-	-	-	-	-
BaSO4 Cert	-	-	-	-	-	-	-	-	-	-	-	-
W-2a Meas	-	<5	<0.1	23.7	43	100	-	110	3.9	2.3	-	18
W-2a Cert	-	1.2	0.03	23	43	92	-	110	3.6	2.5	-	17
SY-4 Meas	-	-	-	-	-	-	-	-	-	-	-	-
SY-4 Cert	-	-	-	-	-	-	-	-	-	-	-	-
CTA-AC-1 Meas	-	-	-	>3000	3	-	-	-	-	-	50.5	-
CTA-AC-1 Cert	-	-	-	3326	2.72	-	-	-	-	-	46.7	-
BIR-1a Meas	-	-	-	2.2	50	380	-	120	-	-	0.59	16

Analyte	Ag	As	Bi	Ce	Co	Cr	Cs	Cu	Dy	Er	Eu	Ga
Units	ppm	ppm	ppm	ppm	ppm	ppm	ppm	ppm	ppm	ppm	ppm	ppm
Detection Limit	0.5	5	0.1	0.05	1	20	0.1	10	0.01	0.01	0.005	1
Method	FUS-MS	FUS-MS	FUS-MS	FUS-MS	FUS-MS	FUS-MS	FUS-MS	FUS-MS	FUS-MS	FUS-MS	FUS-MS	FUS-MS
BIR-1a Cert	-	-	-	1.9	52	370	-	125	-	-	0.55	16
BIR-1a Meas	-	-	-	-	-	-	-	-	-	-	-	-
BIR-1a Cert	-	-	-	-	-	-	-	-	-	-	-	-
NCS DC86312 Meas	-	-	-	192	-	-	-	-	183	98.9	-	-
NCS DC86312 Cert	-	-	-	190	-	-	-	-	183	96.2	-	-
JGb-2 Meas	-	-	-	-	-	-	-	-	-	-	-	-
JGb-2 Cert	-	-	-	-	-	-	-	-	-	-	-	-
JGb-2 Meas	-	-	-	-	-	-	-	-	-	-	-	-
JGb-2 Cert	-	-	-	-	-	-	-	-	-	-	-	-
JGb-2 Meas	-	-	-	-	-	-	-	-	-	-	-	-
JGb-2 Cert	-	-	-	-	-	-	-	-	-	-	-	-
JGb-2 Meas	-	-	-	-	-	-	-	-	-	-	-	-
JGb-2 Cert	-	-	-	-	-	-	-	-	-	-	-	-
JGb-2 Meas	-	-	-	-	-	-	-	-	-	-	-	-
JGb-2 Cert	-	-	-	-	-	-	-	-	-	-	-	-
JGb-2 Meas	-	-	-	-	-	-	-	-	-	-	-	-
JGb-2 Cert	-	-	-	-	-	-	-	-	-	-	-	-
SCH-1 Meas	-	-	-	-	-	-	-	-	-	-	-	-
SCH-1 Cert	-	-	-	-	-	-	-	-	-	-	-	-
NCS DC70009 (GBW07241) Meas	-	72	-	63.1	-	-	43.6	1000	22.4	13.4	0.14	17
NCS DC70009 (GBW07241) Cert	-	69.9	-	60.3	-	-	41	960	20.7	13.4	0.16	16.5
SGR-1b Meas	-	-	-	-	-	-	-	-	-	-	-	-
SGR-1b Cert	-	-	-	-	-	-	-	-	-	-	-	-
SGR-1b Meas	-	-	-	-	-	-	-	-	-	-	-	-
SGR-1b Cert	-	-	-	-	-	-	-	-	-	-	-	-
SGR-1b Meas	-	-	-	-	-	-	-	-	-	-	-	-
SGR-1b Cert	-	-	-	-	-	-	-	-	-	-	-	-
OREAS 100a (Fusion) Meas	-	-	-	500	17	-	-	180	24.4	14.9	3.97	-
OREAS 100a (Fusion) Cert	-	-	-	463	18.1	-	-	169	23.2	14.9	3.71	-
OREAS 101a (Fusion) Meas	-	-	-	1460	47	-	-	430	34.1	21.1	8.73	-
OREAS 101a (Fusion) Cert	-	-	-	1396	48.8	-	-	434	33.3	19.5	8.06	-
OREAS 101b (Fusion) Meas	-	-	-	1360	46	-	-	420	32.8	20.3	8.2	-
OREAS 101b (Fusion) Cert	-	-	-	1331	47	-	-	416	32.1	18.7	7.77	-
OREAS 98 (S by LECO) Meas	-	-	-	-	-	-	-	-	-	-	-	-
OREAS 98 (S by LECO) Cert	-	-	-	-	-	-	-	-	-	-	-	-
OREAS 132b (S by LECO) Meas	-	-	-	-	-	-	-	-	-	-	-	-
OREAS 132b (S by LECO) Cert	-	-	-	-	-	-	-	-	-	-	-	-
JR-1 Meas	-	19	0.5	49.9	-	<20	20.8	-	5.9	-	0.3	16
JR-1 Cert	-	16.3	0.56	47.2	-	2.83	20.8	-	5.69	-	0.3	16.1

Analyte	Ag	As	Bi	Ce	Co	Cr	Cs	Cu	Dy	Er	Eu	Ga
Units	ppm	ppm	ppm	ppm	ppm	ppm	ppm	ppm	ppm	ppm	ppm	ppm
Detection Limit	0.5	5	0.1	0.05	1	20	0.1	10	0.01	0.01	0.005	1
Method	FUS-MS	FUS-MS	FUS-MS	FUS-MS	FUS-MS	FUS-MS	FUS-MS	FUS-MS	FUS-MS	FUS-MS	FUS-MS	FUS-MS
NCS DC86318 Meas	-	-	-	425	-	-	11.5	-	>1000	>1000	19.5	-
NCS DC86318 Cert	-	-	-	430	-	-	10.28	-	3220	1750	18.91	-
USZ 25-2006 Meas	-	-	-	-	-	-	-	-	-	-	-	-
USZ 25-2006 Cert	-	-	-	-	-	-	-	-	-	-	-	-
USZ 25-2006 Meas	-	-	-	-	-	-	-	-	-	-	-	-
USZ 25-2006 Cert	-	-	-	-	-	-	-	-	-	-	-	-
GS309-4 Meas	-	-	-	-	-	-	-	-	-	-	-	-
GS309-4 Cert	-	-	-	-	-	-	-	-	-	-	-	-
GS311-4 Meas	-	-	-	-	-	-	-	-	-	-	-	-
GS311-4 Cert	-	-	-	-	-	-	-	-	-	-	-	-
GS311-4 Meas	-	-	-	-	-	-	-	-	-	-	-	-
GS311-4 Cert	-	-	-	-	-	-	-	-	-	-	-	-
GS311-4 Meas	-	-	-	-	-	-	-	-	-	-	-	-
GS311-4 Cert	-	-	-	-	-	-	-	-	-	-	-	-
GS311-4 Meas	-	-	-	-	-	-	-	-	-	-	-	-
GS311-4 Cert	-	-	-	-	-	-	-	-	-	-	-	-
GS900-5 Meas	-	-	-	-	-	-	-	-	-	-	-	-
GS900-5 Cert	-	-	-	-	-	-	-	-	-	-	-	-
GS900-5 Meas	-	-	-	-	-	-	-	-	-	-	-	-
GS900-5 Cert	-	-	-	-	-	-	-	-	-	-	-	-
GS900-5 Meas	-	-	-	-	-	-	-	-	-	-	-	-
GS900-5 Cert	-	-	-	-	-	-	-	-	-	-	-	-
OREAS 45d (Aqua Regia) Meas	-	-	-	-	-	-	-	-	-	-	-	-
OREAS 45d (Aqua Regia) Cert	-	-	-	-	-	-	-	-	-	-	-	-
CDN-PGMS-24 Meas	-	-	-	-	-	-	-	-	-	-	-	-
CDN-PGMS-24 Cert	-	-	-	-	-	-	-	-	-	-	-	-
CDN-PGMS-24 Meas	-	-	-	-	-	-	-	-	-	-	-	-
CDN-PGMS-24 Cert	-	-	-	-	-	-	-	-	-	-	-	-
CDN-PGMS-24 Meas	-	-	-	-	-	-	-	-	-	-	-	-
CDN-PGMS-24 Cert	-	-	-	-	-	-	-	-	-	-	-	-
CaCO3 Meas	-	-	-	-	-	-	-	-	-	-	-	-
CaCO3 Cert	-	-	-	-	-	-	-	-	-	-	-	-
CaCO3 Meas	-	-	-	-	-	-	-	-	-	-	-	-
CaCO3 Cert	-	-	-	-	-	-	-	-	-	-	-	-
SdAR-M2 (U.S.G.S.) Meas	-	-	-	-	-	-	-	-	-	-	-	-
SdAR-M2 (U.S.G.S.) Cert	-	-	-	-	-	-	-	-	-	-	-	-
GXR-1 Meas	-	-	-	-	-	-	-	-	-	-	-	-



Analyte	Ag	As	Bi	Ce	Co	Cr	Cs	Cu	Dy	Er	Eu	Ga
Units	ppm	ppm	ppm	ppm	ppm	ppm	ppm	ppm	ppm	ppm	ppm	ppm
Detection Limit	0.5	5	0.1	0.05	1	20	0.1	10	0.01	0.01	0.005	1
Method	FUS-MS	FUS-MS	FUS-MS	FUS-MS	FUS-MS	FUS-MS	FUS-MS	FUS-MS	FUS-MS	FUS-MS	FUS-MS	FUS-MS
GXR-1 Cert	-	-	-	-	-	-	-	-	-	-	-	-
GXR-1 Meas	-	-	-	-	-	-	-	-	-	-	-	-
GXR-1 Cert	-	-	-	-	-	-	-	-	-	-	-	-
GXR-1 Meas	-	-	-	-	-	-	-	-	-	-	-	-
GXR-1 Cert	-	-	-	-	-	-	-	-	-	-	-	-
GXR-1 Meas	-	-	-	-	-	-	-	-	-	-	-	-
GXR-1 Cert	-	-	-	-	-	-	-	-	-	-	-	-
NIST 694 Meas	-	-	-	-	-	-	-	-	-	-	-	-
NIST 694 Cert	-	-	-	-	-	-	-	-	-	-	-	-
DNC-1 Meas	-	-	-	-	56	280	-	90	-	-	0.58	-
DNC-1 Cert	-	-	-	-	57	270	-	100	-	-	0.59	-
GBW 07113 Meas	-	-	-	-	-	-	-	-	-	-	-	-
GBW 07113 Cert	-	-	-	-	-	-	-	-	-	-	-	-
GXR-4 Meas	-	-	-	-	-	-	-	-	-	-	-	-
GXR-4 Cert	-	-	-	-	-	-	-	-	-	-	-	-
GXR-4 Meas	-	-	-	-	-	-	-	-	-	-	-	-
GXR-4 Cert	-	-	-	-	-	-	-	-	-	-	-	-
GXR-4 Meas	-	-	-	-	-	-	-	-	-	-	-	-
GXR-4 Cert	-	-	-	-	-	-	-	-	-	-	-	-
GXR-4 Meas	-	-	-	-	-	-	-	-	-	-	-	-
GXR-4 Cert	-	-	-	-	-	-	-	-	-	-	-	-
GXR-4 Meas	-	-	-	-	-	-	-	-	-	-	-	-
GXR-4 Cert	-	-	-	-	-	-	-	-	-	-	-	-
SDC-1 Meas	-	-	-	-	-	-	-	-	-	-	-	-
SDC-1 Cert	-	-	-	-	-	-	-	-	-	-	-	-
SDC-1 Meas	-	-	-	-	-	-	-	-	-	-	-	-
SDC-1 Cert	-	-	-	-	-	-	-	-	-	-	-	-
SDC-1 Meas	-	-	-	-	-	-	-	-	-	-	-	-
SDC-1 Cert	-	-	-	-	-	-	-	-	-	-	-	-
SDC-1 Meas	-	-	-	-	-	-	-	-	-	-	-	-
SDC-1 Cert	-	-	-	-	-	-	-	-	-	-	-	-
GXR-6 Meas	-	-	-	-	-	-	-	-	-	-	-	-
GXR-6 Cert	-	-	-	-	-	-	-	-	-	-	-	-
GXR-6 Meas	-	-	-	-	-	-	-	-	-	-	-	-
GXR-6 Cert	-	-	-	-	-	-	-	-	-	-	-	-
GXR-6 Meas	-	-	-	-	-	-	-	-	-	-	-	-
GXR-6 Cert	-	-	-	-	-	-	-	-	-	-	-	-
GXR-6 Meas	-	-	-	-	-	-	-	-	-	-	-	-
GXR-6 Cert	-	-	-	-	-	-	-	-	-	-	-	-

Analyte	Ag	As	Bi	Ce	Co	Cr	Cs	Cu	Dy	Er	Eu	Ga
Units	ppm	ppm	ppm	ppm	ppm	ppm	ppm	ppm	ppm	ppm	ppm	ppm
Detection Limit	0.5	5	0.1	0.05	1	20	0.1	10	0.01	0.01	0.005	1
Method	FUS-MS	FUS-MS	FUS-MS	FUS-MS	FUS-MS	FUS-MS	FUS-MS	FUS-MS	FUS-MS	FUS-MS	FUS-MS	FUS-MS
LKSD-3 Meas	2.5	28	-	87.3	27	80	2.5	30	4.7	-	1.4	-
LKSD-3 Cert	2.7	27	-	90	30	87	2.3	35	4.9	-	1.5	-
TDB-1 Meas	-	-	-	39.9	-	250	-	350	-	-	2.1	-
TDB-1 Cert	-	-	-	41	-	251	-	323	-	-	2.1	-
SY-2 Meas	-	-	-	-	-	-	-	-	-	-	-	-
SY-2 Cert	-	-	-	-	-	-	-	-	-	-	-	-
SY-3 Meas	-	-	-	-	-	-	-	-	-	-	-	-
SY-3 Cert	-	-	-	-	-	-	-	-	-	-	-	-
BaSO4 Meas	-	-	-	-	-	-	-	-	-	-	-	-
BaSO4 Cert	-	-	-	-	-	-	-	-	-	-	-	-
BaSO4 Meas	-	-	-	-	-	-	-	-	-	-	-	-
BaSO4 Cert	-	-	-	-	-	-	-	-	-	-	-	-
W-2a Meas	-	<5	<0.1	24.3	43	90	-	110	-	-	-	18
W-2a Cert	-	1.2	0.03	23	43	92	-	110	-	-	-	17
SY-4 Meas	-	-	-	-	-	-	-	-	-	-	-	-
SY-4 Cert	-	-	-	-	-	-	-	-	-	-	-	-
CTA-AC-1 Meas	-	-	-	>3000	-	-	-	60	-	-	44.6	-
CTA-AC-1 Cert	-	-	-	3326	-	-	-	54	-	-	46.7	-
BIR-1a Meas	-	-	-	1.9	48	400	-	120	-	-	0.55	15
BIR-1a Cert	-	-	-	1.9	52	370	-	125	-	-	0.55	16
Calcium Carbonate Meas	-	-	-	-	-	-	-	-	-	-	-	-
Calcium Carbonate Cert	-	-	-	-	-	-	-	-	-	-	-	-
NCS DC86312 Meas	-	-	-	172	-	-	-	-	181	97.2	-	-
NCS DC86312 Cert	-	-	-	190	-	-	-	-	183	96.2	-	-
JGb-2 Meas	-	-	-	-	-	-	-	-	-	-	-	-
JGb-2 Cert	-	-	-	-	-	-	-	-	-	-	-	-
JGb-2 Meas	-	-	-	-	-	-	-	-	-	-	-	-
JGb-2 Cert	-	-	-	-	-	-	-	-	-	-	-	-
JGb-2 Meas	-	-	-	-	-	-	-	-	-	-	-	-
JGb-2 Cert	-	-	-	-	-	-	-	-	-	-	-	-
NCS DC70009 (GBW07241) Meas	-	68	-	55.9	4	30	37.8	880	20.3	12.6	-	16
NCS DC70009 (GBW07241) Cert	-	69.9	-	60.3	3.7	30	41	960	20.7	13.4	-	16.5
SGR-1b Meas	-	-	-	-	-	-	-	-	-	-	-	-
SGR-1b Cert	-	-	-	-	-	-	-	-	-	-	-	-
SGR-1b Meas	-	-	-	-	-	-	-	-	-	-	-	-
SGR-1b Cert	-	-	-	-	-	-	-	-	-	-	-	-
OREAS 100a (Fusion) Meas	-	-	-	446	17	-	-	160	22.3	14.7	3.5	-

Analyte	Ag	As	Bi	Ce	Co	Cr	Cs	Cu	Dy	Er	Eu	Ga
Units	ppm	ppm	ppm	ppm	ppm	ppm	ppm	ppm	ppm	ppm	ppm	ppm
Detection Limit	0.5	5	0.1	0.05	1	20	0.1	10	0.01	0.01	0.005	1
Method	FUS-MS	FUS-MS	FUS-MS	FUS-MS	FUS-MS	FUS-MS	FUS-MS	FUS-MS	FUS-MS	FUS-MS	FUS-MS	FUS-MS
OREAS 100a (Fusion) Cert	-	-	-	463	18.1	-	-	169	23.2	14.9	3.71	-
OREAS 101a (Fusion) Meas	-	-	-	1370	47	-	-	430	30.9	19.2	7.79	-
OREAS 101a (Fusion) Cert	-	-	-	1396	48.8	-	-	434	33.3	19.5	8.06	-
OREAS 101b (Fusion) Meas	-	-	-	1380	45	-	-	420	32.1	19.3	8.1	-
OREAS 101b (Fusion) Cert	-	-	-	1331	47	-	-	416	32.1	18.7	7.77	-
JR-1 Meas	-	15	0.6	44.9	-	-	20.6	<10	6	-	0.27	15
JR-1 Cert	-	16.3	0.56	47.2	-	-	20.8	2.68	5.69	-	0.3	16.1
NCS DC86318 Meas	-	-	-	416	-	-	11	-	>1000	>1000	19.4	-
NCS DC86318 Cert	-	-	-	430	-	-	10.28	-	3220	1750	18.91	-
USZ 25-2006 Meas	-	-	-	-	-	-	-	-	-	-	-	-
USZ 25-2006 Cert	-	-	-	-	-	-	-	-	-	-	-	-
USZ 25-2006 Meas	-	-	-	-	-	-	-	-	-	-	-	-
USZ 25-2006 Cert	-	-	-	-	-	-	-	-	-	-	-	-
DNC-1a Meas	-	-	-	-	-	-	-	-	-	-	-	-
DNC-1a Cert	-	-	-	-	-	-	-	-	-	-	-	-
DNC-1a Meas	-	-	-	-	-	-	-	-	-	-	-	-
DNC-1a Cert	-	-	-	-	-	-	-	-	-	-	-	-
DNC-1a Meas	-	-	-	-	-	-	-	-	-	-	-	-
DNC-1a Cert	-	-	-	-	-	-	-	-	-	-	-	-
DNC-1a Meas	-	-	-	-	-	-	-	-	-	-	-	-
DNC-1a Cert	-	-	-	-	-	-	-	-	-	-	-	-
DNC-1a Meas	-	-	-	-	-	-	-	-	-	-	-	-
DNC-1a Cert	-	-	-	-	-	-	-	-	-	-	-	-
GS311-4 Meas	-	-	-	-	-	-	-	-	-	-	-	-
GS311-4 Cert	-	-	-	-	-	-	-	-	-	-	-	-
GS311-4 Meas	-	-	-	-	-	-	-	-	-	-	-	-
GS311-4 Cert	-	-	-	-	-	-	-	-	-	-	-	-
GS900-5 Meas	-	-	-	-	-	-	-	-	-	-	-	-
GS900-5 Cert	-	-	-	-	-	-	-	-	-	-	-	-
GS900-5 Meas	-	-	-	-	-	-	-	-	-	-	-	-
GS900-5 Cert	-	-	-	-	-	-	-	-	-	-	-	-
OREAS 45d (Aqua Regia) Meas	-	-	-	-	-	-	-	-	-	-	-	-
OREAS 45d (Aqua Regia) Cert	-	-	-	-	-	-	-	-	-	-	-	-
OREAS 45d (Aqua Regia) Meas	-	-	-	-	-	-	-	-	-	-	-	-
OREAS 45d (Aqua Regia) Cert	-	-	-	-	-	-	-	-	-	-	-	-
OREAS 45d (Aqua Regia) Meas	-	-	-	-	-	-	-	-	-	-	-	-
OREAS 45d (Aqua Regia) Cert	-	-	-	-	-	-	-	-	-	-	-	-
SBC-1 Meas	-	-	-	-	-	-	-	-	-	-	-	-
SBC-1 Cert	-	-	-	-	-	-	-	-	-	-	-	-

Analyte	Ag	As	Bi	Ce	Co	Cr	Cs	Cu	Dy	Er	Eu	Ga
Units	ppm	ppm	ppm	ppm	ppm	ppm	ppm	ppm	ppm	ppm	ppm	ppm
Detection Limit	0.5	5	0.1	0.05	1	20	0.1	10	0.01	0.01	0.005	1
Method	FUS-MS	FUS-MS	FUS-MS	FUS-MS	FUS-MS	FUS-MS	FUS-MS	FUS-MS	FUS-MS	FUS-MS	FUS-MS	FUS-MS
SBC-1 Meas	-	-	-	-	-	-	-	-	-	-	-	-
SBC-1 Cert	-	-	-	-	-	-	-	-	-	-	-	-
SBC-1 Meas	-	-	-	-	-	-	-	-	-	-	-	-
SBC-1 Cert	-	-	-	-	-	-	-	-	-	-	-	-
SBC-1 Meas	-	-	-	-	-	-	-	-	-	-	-	-
SBC-1 Cert	-	-	-	-	-	-	-	-	-	-	-	-
OREAS 45d (4-Acid) Meas	-	-	-	-	-	-	-	-	-	-	-	-
OREAS 45d (4-Acid) Cert	-	-	-	-	-	-	-	-	-	-	-	-
OREAS 45d (4-Acid) Meas	-	-	-	-	-	-	-	-	-	-	-	-
OREAS 45d (4-Acid) Cert	-	-	-	-	-	-	-	-	-	-	-	-
OREAS 45d (4-Acid) Meas	-	-	-	-	-	-	-	-	-	-	-	-
OREAS 45d (4-Acid) Cert	-	-	-	-	-	-	-	-	-	-	-	-
OREAS 45d (4-Acid) Meas	-	-	-	-	-	-	-	-	-	-	-	-
OREAS 45d (4-Acid) Cert	-	-	-	-	-	-	-	-	-	-	-	-
OxK110 Meas	-	-	-	-	-	-	-	-	-	-	-	-
OxK110 Cert	-	-	-	-	-	-	-	-	-	-	-	-
CDN-PGMS-24 Meas	-	-	-	-	-	-	-	-	-	-	-	-
CDN-PGMS-24 Cert	-	-	-	-	-	-	-	-	-	-	-	-
CDN-PGMS-24 Meas	-	-	-	-	-	-	-	-	-	-	-	-
CDN-PGMS-24 Cert	-	-	-	-	-	-	-	-	-	-	-	-
OXN117 Meas	-	-	-	-	-	-	-	-	-	-	-	-
OXN117 Cert	-	-	-	-	-	-	-	-	-	-	-	-
CaCO3 Meas	-	-	-	-	-	-	-	-	-	-	-	-
CaCO3 Cert	-	-	-	-	-	-	-	-	-	-	-	-
SdAR-M2 (U.S.G.S.) Meas	-	-	-	-	-	-	-	-	-	-	-	-
SdAR-M2 (U.S.G.S.) Cert	-	-	-	-	-	-	-	-	-	-	-	-
SdAR-M2 (U.S.G.S.) Meas	-	-	-	-	-	-	-	-	-	-	-	-
SdAR-M2 (U.S.G.S.) Cert	-	-	-	-	-	-	-	-	-	-	-	-
SdAR-M2 (U.S.G.S.) Meas	-	-	-	-	-	-	-	-	-	-	-	-
SdAR-M2 (U.S.G.S.) Cert	-	-	-	-	-	-	-	-	-	-	-	-
SdAR-M2 (U.S.G.S.) Meas	-	-	-	-	-	-	-	-	-	-	-	-
SdAR-M2 (U.S.G.S.) Cert	-	-	-	-	-	-	-	-	-	-	-	-
GXR-1 Meas	-	-	-	-	-	-	-	-	-	-	-	-
GXR-1 Cert	-	-	-	-	-	-	-	-	-	-	-	-
GXR-1 Meas	-	-	-	-	-	-	-	-	-	-	-	-
GXR-1 Cert	-	-	-	-	-	-	-	-	-	-	-	-
NIST 694 Meas	-	-	-	-	-	-	-	-	-	-	-	-

Analyte	Ag	As	Bi	Ce	Co	Cr	Cs	Cu	Dy	Er	Eu	Ga
Units	ppm	ppm	ppm	ppm	ppm	ppm	ppm	ppm	ppm	ppm	ppm	ppm
Detection Limit	0.5	5	0.1	0.05	1	20	0.1	10	0.01	0.01	0.005	1
Method	FUS-MS	FUS-MS	FUS-MS	FUS-MS	FUS-MS	FUS-MS	FUS-MS	FUS-MS	FUS-MS	FUS-MS	FUS-MS	FUS-MS
NIST 694 Cert	-	-	-	-	-	-	-	-	-	-	-	-
DNC-1 Meas	-	-	-	-	54	280	-	100	-	-	0.56	-
DNC-1 Cert	-	-	-	-	57	270	-	100	-	-	0.59	-
GBW 07113 Meas	-	-	-	-	-	-	-	-	-	-	-	-
GBW 07113 Cert	-	-	-	-	-	-	-	-	-	-	-	-
GXR-4 Meas	-	-	-	-	-	-	-	-	-	-	-	-
GXR-4 Cert	-	-	-	-	-	-	-	-	-	-	-	-
GXR-4 Meas	-	-	-	-	-	-	-	-	-	-	-	-
GXR-4 Cert	-	-	-	-	-	-	-	-	-	-	-	-
SDC-1 Meas	-	-	-	-	-	-	-	-	-	-	-	-
SDC-1 Cert	-	-	-	-	-	-	-	-	-	-	-	-
GXR-6 Meas	-	-	-	-	-	-	-	-	-	-	-	-
GXR-6 Cert	-	-	-	-	-	-	-	-	-	-	-	-
GXR-6 Meas	-	-	-	-	-	-	-	-	-	-	-	-
GXR-6 Cert	-	-	-	-	-	-	-	-	-	-	-	-
LKSD-3 Meas	2.6	25	-	88.6	30	80	2.5	30	4.5	-	-	-
LKSD-3 Cert	2.7	27	-	90	30	87	2.3	35	4.9	-	-	-
TDB-1 Meas	-	-	-	39.7	-	250	-	320	-	-	2	-
TDB-1 Cert	-	-	-	41	-	251	-	323	-	-	2.1	-
SY-2 Meas	-	-	-	-	-	-	-	-	-	-	-	-
SY-2 Cert	-	-	-	-	-	-	-	-	-	-	-	-
SY-3 Meas	-	-	-	-	-	-	-	-	-	-	-	-
SY-3 Cert	-	-	-	-	-	-	-	-	-	-	-	-
BaSO4 Meas	-	-	-	-	-	-	-	-	-	-	-	-
BaSO4 Cert	-	-	-	-	-	-	-	-	-	-	-	-
BaSO4 Meas	-	-	-	-	-	-	-	-	-	-	-	-
BaSO4 Cert	-	-	-	-	-	-	-	-	-	-	-	-
BaSO4 Meas	-	-	-	-	-	-	-	-	-	-	-	-
BaSO4 Cert	-	-	-	-	-	-	-	-	-	-	-	-
W-2a Meas	-	-	<0.1	23.3	43	90	1	110	3.9	2.5	-	17
W-2a Cert	-	-	0.03	23	43	92	0.99	110	3.6	2.5	-	17
DTS-2b Meas	-	-	-	-	131	>10000	-	-	-	-	-	-
DTS-2b Cert	-	-	-	-	120	15500	-	-	-	-	-	-
SY-4 Meas	-	-	-	-	-	-	-	-	-	-	-	-
SY-4 Cert	-	-	-	-	-	-	-	-	-	-	-	-
CTA-AC-1 Meas	-	-	-	>3000	-	-	-	60	-	-	44.9	-
CTA-AC-1 Cert	-	-	-	3326	-	-	-	54	-	-	46.7	-

Analyte	Ag	As	Bi	Ce	Co	Cr	Cs	Cu	Dy	Er	Eu	Ga
Units	ppm	ppm	ppm	ppm	ppm	ppm	ppm	ppm	ppm	ppm	ppm	ppm
Detection Limit	0.5	5	0.1	0.05	1	20	0.1	10	0.01	0.01	0.005	1
Method	FUS-MS	FUS-MS	FUS-MS	FUS-MS	FUS-MS	FUS-MS	FUS-MS	FUS-MS	FUS-MS	FUS-MS	FUS-MS	FUS-MS
BIR-1a Meas	-	-	-	2	51	380	-	130	3.6	-	0.52	15
BIR-1a Cert	-	-	-	1.9	52	370	-	125	4	-	0.55	16
NCS DC86312 Meas	-	-	-	181	-	-	-	-	179	95.1	-	-
NCS DC86312 Cert	-	-	-	190	-	-	-	-	183	96.2	-	-
JGb-2 Meas	-	-	-	-	-	-	-	-	-	-	-	-
JGb-2 Cert	-	-	-	-	-	-	-	-	-	-	-	-
NCS DC70009 (GBW07241) Meas	1.6	68	-	59.1	4	-	37.2	960	19.5	12.6	-	16
NCS DC70009 (GBW07241) Cert	1.8	69.9	-	60.3	3.7	-	41	960	20.7	13.4	-	16.5
SGR-1b Meas	-	-	-	-	-	-	-	-	-	-	-	-
SGR-1b Cert	-	-	-	-	-	-	-	-	-	-	-	-
SGR-1b Meas	-	-	-	-	-	-	-	-	-	-	-	-
SGR-1b Cert	-	-	-	-	-	-	-	-	-	-	-	-
SGR-1b Meas	-	-	-	-	-	-	-	-	-	-	-	-
SGR-1b Cert	-	-	-	-	-	-	-	-	-	-	-	-
OREAS 100a (Fusion) Meas	-	-	-	466	17	-	-	160	22.9	14.7	3.38	-
OREAS 100a (Fusion) Cert	-	-	-	463	18.1	-	-	169	23.2	14.9	3.71	-
OREAS 101a (Fusion) Meas	-	-	-	1310	51	-	-	460	32.3	-	7.98	-
OREAS 101a (Fusion) Cert	-	-	-	1396	48.8	-	-	434	33.3	-	8.06	-
OREAS 101b (Fusion) Meas	-	-	-	1380	45	-	-	410	32.3	19	8.12	-
OREAS 101b (Fusion) Cert	-	-	-	1331	47	-	-	416	32.1	18.7	7.77	-
OREAS 98 (S by LECO) Meas	-	-	-	-	-	-	-	-	-	-	-	-
OREAS 98 (S by LECO) Cert	-	-	-	-	-	-	-	-	-	-	-	-
OREAS 132b (S by LECO) Meas	-	-	-	-	-	-	-	-	-	-	-	-
OREAS 132b (S by LECO) Cert	-	-	-	-	-	-	-	-	-	-	-	-
JR-1 Meas	-	17	0.4	48.3	-	-	19.8	-	6.04	3.72	0.27	17
JR-1 Cert	-	16.3	0.56	47.2	-	-	20.8	-	5.69	3.61	0.3	16.1
NCS DC86318 Meas	-	-	-	411	-	-	11.2	-	>1000	>1000	18.5	-
NCS DC86318 Cert	-	-	-	430	-	-	10.28	-	3220	1750	18.91	-
USZ 25-2006 Meas	-	-	-	-	-	-	-	-	-	-	-	-
USZ 25-2006 Cert	-	-	-	-	-	-	-	-	-	-	-	-
DNC-1a Meas	-	-	-	-	-	-	-	-	-	-	-	-
DNC-1a Cert	-	-	-	-	-	-	-	-	-	-	-	-
PK2 Meas	-	-	-	-	-	-	-	-	-	-	-	-
PK2 Cert	-	-	-	-	-	-	-	-	-	-	-	-
GS309-4 Meas	-	-	-	-	-	-	-	-	-	-	-	-
GS309-4 Cert	-	-	-	-	-	-	-	-	-	-	-	-
GS311-4 Meas	-	-	-	-	-	-	-	-	-	-	-	-

Analyte	Ag	As	Bi	Ce	Co	Cr	Cs	Cu	Dy	Er	Eu	Ga
Units	ppm	ppm	ppm	ppm	ppm	ppm	ppm	ppm	ppm	ppm	ppm	ppm
Detection Limit	0.5	5	0.1	0.05	1	20	0.1	10	0.01	0.01	0.005	1
Method	FUS-MS	FUS-MS	FUS-MS	FUS-MS	FUS-MS	FUS-MS	FUS-MS	FUS-MS	FUS-MS	FUS-MS	FUS-MS	FUS-MS
GS311-4 Cert	-	-	-	-	-	-	-	-	-	-	-	-
GS311-4 Meas	-	-	-	-	-	-	-	-	-	-	-	-
GS311-4 Cert	-	-	-	-	-	-	-	-	-	-	-	-
GS311-4 Meas	-	-	-	-	-	-	-	-	-	-	-	-
GS311-4 Cert	-	-	-	-	-	-	-	-	-	-	-	-
GS900-5 Meas	-	-	-	-	-	-	-	-	-	-	-	-
GS900-5 Cert	-	-	-	-	-	-	-	-	-	-	-	-
GS900-5 Meas	-	-	-	-	-	-	-	-	-	-	-	-
GS900-5 Cert	-	-	-	-	-	-	-	-	-	-	-	-
GS900-5 Meas	-	-	-	-	-	-	-	-	-	-	-	-
GS900-5 Cert	-	-	-	-	-	-	-	-	-	-	-	-
OREAS 45d (Aqua Regia) Meas	-	-	-	-	-	-	-	-	-	-	-	-
OREAS 45d (Aqua Regia) Cert	-	-	-	-	-	-	-	-	-	-	-	-
SBC-1 Meas	-	-	-	-	-	-	-	-	-	-	-	-
SBC-1 Cert	-	-	-	-	-	-	-	-	-	-	-	-
OREAS 45d (4-Acid) Meas	-	-	-	-	-	-	-	-	-	-	-	-
OREAS 45d (4-Acid) Cert	-	-	-	-	-	-	-	-	-	-	-	-
CaCO3 Meas	-	-	-	-	-	-	-	-	-	-	-	-
CaCO3 Cert	-	-	-	-	-	-	-	-	-	-	-	-
SdAR-M2 (U.S.G.S.) Meas	-	-	-	-	-	-	-	-	-	-	-	-
SdAR-M2 (U.S.G.S.) Cert	-	-	-	-	-	-	-	-	-	-	-	-
SdAR-M2 (U.S.G.S.) Meas	-	-	-	-	-	-	-	-	-	-	-	-
SdAR-M2 (U.S.G.S.) Cert	-	-	-	-	-	-	-	-	-	-	-	-
GXR-1 Meas	-	-	-	-	-	-	-	-	-	-	-	-
GXR-1 Cert	-	-	-	-	-	-	-	-	-	-	-	-
GXR-1 Meas	-	-	-	-	-	-	-	-	-	-	-	-
GXR-1 Cert	-	-	-	-	-	-	-	-	-	-	-	-
NIST 694 Meas	-	-	-	-	-	-	-	-	-	-	-	-
NIST 694 Cert	-	-	-	-	-	-	-	-	-	-	-	-
DNC-1 Meas	-	-	-	-	52	280	-	100	-	-	0.55	14
DNC-1 Cert	-	-	-	-	57	270	-	100	-	-	0.59	15
GBW 07113 Meas	-	-	-	-	-	-	-	-	-	-	-	-
GBW 07113 Cert	-	-	-	-	-	-	-	-	-	-	-	-
GXR-4 Meas	-	-	-	-	-	-	-	-	-	-	-	-
GXR-4 Cert	-	-	-	-	-	-	-	-	-	-	-	-
GXR-4 Meas	-	-	-	-	-	-	-	-	-	-	-	-
GXR-4 Cert	-	-	-	-	-	-	-	-	-	-	-	-

Analyte	Ag	As	Bi	Ce	Co	Cr	Cs	Cu	Dy	Er	Eu	Ga
Units	ppm	ppm	ppm	ppm	ppm	ppm	ppm	ppm	ppm	ppm	ppm	ppm
Detection Limit	0.5	5	0.1	0.05	1	20	0.1	10	0.01	0.01	0.005	1
Method	FUS-MS	FUS-MS	FUS-MS	FUS-MS	FUS-MS	FUS-MS	FUS-MS	FUS-MS	FUS-MS	FUS-MS	FUS-MS	FUS-MS
SDC-1 Meas	-	-	-	-	-	-	-	-	-	-	-	-
SDC-1 Cert	-	-	-	-	-	-	-	-	-	-	-	-
SDC-1 Meas	-	-	-	-	-	-	-	-	-	-	-	-
SDC-1 Cert	-	-	-	-	-	-	-	-	-	-	-	-
GXR-6 Meas	-	-	-	-	-	-	-	-	-	-	-	-
GXR-6 Cert	-	-	-	-	-	-	-	-	-	-	-	-
GXR-6 Meas	-	-	-	-	-	-	-	-	-	-	-	-
GXR-6 Cert	-	-	-	-	-	-	-	-	-	-	-	-
LKSD-3 Meas	2.7	30	-	92.4	28	80	2.3	40	5	-	1.5	-
LKSD-3 Cert	2.7	27	-	90	30	87	2.3	35	4.9	-	1.5	-
TDB-1 Meas	-	-	-	40.2	-	250	-	350	-	-	2.1	-
TDB-1 Cert	-	-	-	41	-	251	-	323	-	-	2.1	-
SY-2 Meas	-	-	-	-	-	-	-	-	-	-	-	-
SY-2 Cert	-	-	-	-	-	-	-	-	-	-	-	-
SY-3 Meas	-	-	-	-	-	-	-	-	-	-	-	-
SY-3 Cert	-	-	-	-	-	-	-	-	-	-	-	-
BaSO4 Meas	-	-	-	-	-	-	-	-	-	-	-	-
BaSO4 Cert	-	-	-	-	-	-	-	-	-	-	-	-
BaSO4 Meas	-	-	-	-	-	-	-	-	-	-	-	-
BaSO4 Cert	-	-	-	-	-	-	-	-	-	-	-	-
W-2a Meas	-	<5	<0.1	24.3	44	100	-	110	-	2.3	-	19
W-2a Cert	-	1.2	0.03	23	43	92	-	110	-	2.5	-	17
SY-4 Meas	-	-	-	-	-	-	-	-	-	-	-	-
SY-4 Cert	-	-	-	-	-	-	-	-	-	-	-	-
CTA-AC-1 Meas	-	-	-	>3000	-	-	-	60	-	-	44.4	-
CTA-AC-1 Cert	-	-	-	3326	-	-	-	54	-	-	46.7	-
BIR-1a Meas	-	-	-	1.8	48	390	-	130	3.7	-	0.5	16
BIR-1a Cert	-	-	-	1.9	52	370	-	125	4	-	0.55	16
BIR-1a Meas	-	-	-	-	-	-	-	-	-	-	-	-
BIR-1a Cert	-	-	-	-	-	-	-	-	-	-	-	-
NCS DC86312 Meas	-	-	-	173	-	-	-	-	180	94.5	-	-
NCS DC86312 Cert	-	-	-	190	-	-	-	-	183	96.2	-	-
JGb-2 Meas	-	-	-	-	-	-	-	-	-	-	-	-
JGb-2 Cert	-	-	-	-	-	-	-	-	-	-	-	-
JGb-2 Meas	-	-	-	-	-	-	-	-	-	-	-	-
JGb-2 Cert	-	-	-	-	-	-	-	-	-	-	-	-
JGb-2 Meas	-	-	-	-	-	-	-	-	-	-	-	-



Analyte	Ag	As	Bi	Ce	Co	Cr	Cs	Cu	Dy	Er	Eu	Ga
Units	ppm	ppm	ppm	ppm	ppm	ppm	ppm	ppm	ppm	ppm	ppm	ppm
Detection Limit	0.5	5	0.1	0.05	1	20	0.1	10	0.01	0.01	0.005	1
Method	FUS-MS	FUS-MS	FUS-MS	FUS-MS	FUS-MS	FUS-MS	FUS-MS	FUS-MS	FUS-MS	FUS-MS	FUS-MS	FUS-MS
JGb-2 Cert	-	-	-	-	-	-	-	-	-	-	-	-
JGb-2 Meas	-	-	-	-	-	-	-	-	-	-	-	-
JGb-2 Cert	-	-	-	-	-	-	-	-	-	-	-	-
NCS DC70009 (GBW07241) Meas	-	71	-	60.1	-	-	38.1	960	22	13.5	-	17
NCS DC70009 (GBW07241) Cert	-	69.9	-	60.3	-	-	41	960	20.7	13.4	-	16.5
SGR-1b Meas	-	-	-	-	-	-	-	-	-	-	-	-
SGR-1b Cert	-	-	-	-	-	-	-	-	-	-	-	-
SGR-1b Meas	-	-	-	-	-	-	-	-	-	-	-	-
SGR-1b Cert	-	-	-	-	-	-	-	-	-	-	-	-
OREAS 100a (Fusion) Meas	-	-	-	497	17	-	-	180	24	15.3	3.66	-
OREAS 100a (Fusion) Cert	-	-	-	463	18.1	-	-	169	23.2	14.9	3.71	-
OREAS 101a (Fusion) Meas	-	-	-	1340	46	-	-	420	30.4	18.3	7.57	-
OREAS 101a (Fusion) Cert	-	-	-	1396	48.8	-	-	430	33.3	19.5	8.06	-
OREAS 101b (Fusion) Meas	-	-	-	1430	45	-	-	430	32.4	19.3	8.29	-
OREAS 101b (Fusion) Cert	-	-	-	1331	47	-	-	420	32.1	18.7	7.77	-
JR-1 Meas	-	17	0.6	44.4	-	-	20.3	<10	-	-	0.27	16
JR-1 Cert	-	16.3	0.56	47.2	-	-	20.8	2.68	-	-	0.3	16.1
NCS DC86318 Meas	-	-	-	421	-	-	10.9	-	>1000	>1000	19.3	-
NCS DC86318 Cert	-	-	-	430	-	-	10.28	-	3220	1750	18.91	-
USZ 25-2006 Meas	-	-	-	-	-	-	-	-	-	-	-	-
USZ 25-2006 Cert	-	-	-	-	-	-	-	-	-	-	-	-
USZ 25-2006 Meas	-	-	-	-	-	-	-	-	-	-	-	-
USZ 25-2006 Cert	-	-	-	-	-	-	-	-	-	-	-	-
DNC-1a Meas	-	-	-	-	-	-	-	-	-	-	-	-
DNC-1a Cert	-	-	-	-	-	-	-	-	-	-	-	-
DNC-1a Meas	-	-	-	-	-	-	-	-	-	-	-	-
DNC-1a Cert	-	-	-	-	-	-	-	-	-	-	-	-
PK2 Meas	-	-	-	-	-	-	-	-	-	-	-	-
PK2 Cert	-	-	-	-	-	-	-	-	-	-	-	-
GS311-4 Meas	-	-	-	-	-	-	-	-	-	-	-	-
GS311-4 Cert	-	-	-	-	-	-	-	-	-	-	-	-
GS311-4 Meas	-	-	-	-	-	-	-	-	-	-	-	-
GS311-4 Cert	-	-	-	-	-	-	-	-	-	-	-	-
GS900-5 Meas	-	-	-	-	-	-	-	-	-	-	-	-
GS900-5 Cert	-	-	-	-	-	-	-	-	-	-	-	-
GS900-5 Meas	-	-	-	-	-	-	-	-	-	-	-	-
GS900-5 Cert	-	-	-	-	-	-	-	-	-	-	-	-

Analyte	Ag	As	Bi	Ce	Co	Cr	Cs	Cu	Dy	Er	Eu	Ga
Units	ppm	ppm	ppm	ppm	ppm	ppm	ppm	ppm	ppm	ppm	ppm	ppm
Detection Limit	0.5	5	0.1	0.05	1	20	0.1	10	0.01	0.01	0.005	1
Method	FUS-MS	FUS-MS	FUS-MS	FUS-MS	FUS-MS	FUS-MS	FUS-MS	FUS-MS	FUS-MS	FUS-MS	FUS-MS	FUS-MS
OREAS 45d (Aqua Regia) Meas	-	-	-	-	-	-	-	-	-	-	-	-
OREAS 45d (Aqua Regia) Cert	-	-	-	-	-	-	-	-	-	-	-	-
SBC-1 Meas	-	-	-	-	-	-	-	-	-	-	-	-
SBC-1 Cert	-	-	-	-	-	-	-	-	-	-	-	-
SBC-1 Meas	-	-	-	-	-	-	-	-	-	-	-	-
SBC-1 Cert	-	-	-	-	-	-	-	-	-	-	-	-
OREAS 45d (4-Acid) Meas	-	-	-	-	-	-	-	-	-	-	-	-
OREAS 45d (4-Acid) Cert	-	-	-	-	-	-	-	-	-	-	-	-
OxK110 Meas	-	-	-	-	-	-	-	-	-	-	-	-
OxK110 Cert	-	-	-	-	-	-	-	-	-	-	-	-
OXN117 Meas	-	-	-	-	-	-	-	-	-	-	-	-
OXN117 Cert	-	-	-	-	-	-	-	-	-	-	-	-
CaCO3 Meas	-	-	-	-	-	-	-	-	-	-	-	-
CaCO3 Cert	-	-	-	-	-	-	-	-	-	-	-	-
CaCO3 Meas	-	-	-	-	-	-	-	-	-	-	-	-
CaCO3 Cert	-	-	-	-	-	-	-	-	-	-	-	-
SdAR-M2 (U.S.G.S.) Meas	-	-	-	-	-	-	-	-	-	-	-	-
SdAR-M2 (U.S.G.S.) Cert	-	-	-	-	-	-	-	-	-	-	-	-
GXR-1 Meas	-	-	-	-	-	-	-	-	-	-	-	-
GXR-1 Cert	-	-	-	-	-	-	-	-	-	-	-	-
GXR-1 Meas	-	-	-	-	-	-	-	-	-	-	-	-
GXR-1 Cert	-	-	-	-	-	-	-	-	-	-	-	-
NIST 694 Meas	-	-	-	-	-	-	-	-	-	-	-	-
NIST 694 Cert	-	-	-	-	-	-	-	-	-	-	-	-
DNC-1 Meas	-	-	-	-	54	280	-	100	-	-	0.62	-
DNC-1 Cert	-	-	-	-	57	270	-	100	-	-	0.59	-
GBW 07113 Meas	-	-	-	-	-	-	-	-	-	-	-	-
GBW 07113 Cert	-	-	-	-	-	-	-	-	-	-	-	-
GXR-4 Meas	-	-	-	-	-	-	-	-	-	-	-	-
GXR-4 Cert	-	-	-	-	-	-	-	-	-	-	-	-
GXR-4 Meas	-	-	-	-	-	-	-	-	-	-	-	-
GXR-4 Cert	-	-	-	-	-	-	-	-	-	-	-	-
GXR-4 Meas	-	-	-	-	-	-	-	-	-	-	-	-
GXR-4 Cert	-	-	-	-	-	-	-	-	-	-	-	-
SDC-1 Meas	-	-	-	-	-	-	-	-	-	-	-	-
SDC-1 Cert	-	-	-	-	-	-	-	-	-	-	-	-
SDC-1 Meas	-	-	-	-	-	-	-	-	-	-	-	-

Analyte	Ag	As	Bi	Ce	Co	Cr	Cs	Cu	Dy	Er	Eu	Ga
Units	ppm	ppm	ppm	ppm	ppm	ppm	ppm	ppm	ppm	ppm	ppm	ppm
Detection Limit	0.5	5	0.1	0.05	1	20	0.1	10	0.01	0.01	0.005	1
Method	FUS-MS	FUS-MS	FUS-MS	FUS-MS	FUS-MS	FUS-MS	FUS-MS	FUS-MS	FUS-MS	FUS-MS	FUS-MS	FUS-MS
SDC-1 Cert	-	-	-	-	-	-	-	-	-	-	-	-
GXR-6 Meas	-	-	-	-	-	-	-	-	-	-	-	-
GXR-6 Cert	-	-	-	-	-	-	-	-	-	-	-	-
GXR-6 Meas	-	-	-	-	-	-	-	-	-	-	-	-
GXR-6 Cert	-	-	-	-	-	-	-	-	-	-	-	-
GXR-6 Meas	-	-	-	-	-	-	-	-	-	-	-	-
GXR-6 Cert	-	-	-	-	-	-	-	-	-	-	-	-
LKSD-3 Meas	-	28	-	89	28	90	2.1	30	4.9	-	1.5	-
LKSD-3 Cert	-	27	-	90	30	87	2.3	35	4.9	-	1.5	-
TDB-1 Meas	-	-	-	40.2	-	250	-	340	-	-	2.1	-
TDB-1 Cert	-	-	-	41	-	251	-	323	-	-	2.1	-
SY-2 Meas	-	-	-	-	-	-	-	-	-	-	-	-
SY-2 Cert	-	-	-	-	-	-	-	-	-	-	-	-
SY-3 Meas	-	-	-	-	-	-	-	-	-	-	-	-
SY-3 Cert	-	-	-	-	-	-	-	-	-	-	-	-
BaSO4 Meas	-	-	-	-	-	-	-	-	-	-	-	-
BaSO4 Cert	-	-	-	-	-	-	-	-	-	-	-	-
W-2a Meas	-	-	<0.1	24	44	90	-	110	3.9	-	1.2	18
W-2a Cert	-	-	0.03	23	43	92	-	110	3.6	-	1	17
SY-4 Meas	-	-	-	-	-	-	-	-	-	-	-	-
SY-4 Cert	-	-	-	-	-	-	-	-	-	-	-	-
CTA-AC-1 Meas	-	-	-	>3000	-	-	-	50	-	-	45.1	-
CTA-AC-1 Cert	-	-	-	3326	-	-	-	54	-	-	46.7	-
BIR-1a Meas	-	-	-	1.8	49	390	-	120	-	-	0.55	15
BIR-1a Cert	-	-	-	1.9	52	370	-	125	-	-	0.55	16
NCS DC86312 Meas	-	-	-	177	-	-	-	-	190	97.8	-	-
NCS DC86312 Cert	-	-	-	190	-	-	-	-	183	96.2	-	-
JGb-2 Meas	-	-	-	-	-	-	-	-	-	-	-	-
JGb-2 Cert	-	-	-	-	-	-	-	-	-	-	-	-
JGb-2 Meas	-	-	-	-	-	-	-	-	-	-	-	-
JGb-2 Cert	-	-	-	-	-	-	-	-	-	-	-	-
JGb-2 Meas	-	-	-	-	-	-	-	-	-	-	-	-
JGb-2 Cert	-	-	-	-	-	-	-	-	-	-	-	-
NCS DC70009 (GBW07241) Meas	2	68	-	60	4	40	39.4	950	21.7	13.2	-	16
NCS DC70009 (GBW07241) Cert	1.8	69.9	-	60.3	3.7	30	41	960	20.7	13.4	-	16.5
SGR-1b Meas	-	-	-	-	-	-	-	-	-	-	-	-
SGR-1b Cert	-	-	-	-	-	-	-	-	-	-	-	-

Analyte	Ag	As	Bi	Ce	Co	Cr	Cs	Cu	Dy	Er	Eu	Ga
Units	ppm	ppm	ppm	ppm	ppm	ppm	ppm	ppm	ppm	ppm	ppm	ppm
Detection Limit	0.5	5	0.1	0.05	1	20	0.1	10	0.01	0.01	0.005	1
Method	FUS-MS	FUS-MS	FUS-MS	FUS-MS	FUS-MS	FUS-MS	FUS-MS	FUS-MS	FUS-MS	FUS-MS	FUS-MS	FUS-MS
OREAS 100a (Fusion) Meas	-	-	-	477	18	-	-	170	23.5	14.8	3.64	-
OREAS 100a (Fusion) Cert	-	-	-	463	18.1	-	-	169	23.2	14.9	3.71	-
OREAS 101a (Fusion) Meas	-	-	-	1430	44	-	-	440	32.5	19.3	8.31	-
OREAS 101a (Fusion) Cert	-	-	-	1396	48.8	-	-	430	33.3	19.5	8.06	-
OREAS 101b (Fusion) Meas	-	-	-	1440	46	-	-	420	32.3	19.2	8.35	-
OREAS 101b (Fusion) Cert	-	-	-	1331	47	-	-	420	32.1	18.7	7.77	-
JR-1 Meas	-	15	0.5	47.2	-	<20	18.8	<10	5.41	3.84	0.28	16
JR-1 Cert	-	16.3	0.56	47.2	-	2.83	20.8	2.68	5.69	3.61	0.3	16.1
NCS DC86318 Meas	-	-	-	417	-	-	11	-	>1000	>1000	19.3	-
NCS DC86318 Cert	-	-	-	430	-	-	10.28	-	3220	1750	18.91	-
USZ 25-2006 Meas	-	-	-	-	-	-	-	-	-	-	-	-
USZ 25-2006 Cert	-	-	-	-	-	-	-	-	-	-	-	-
USZ 25-2006 Meas	-	-	-	-	-	-	-	-	-	-	-	-
USZ 25-2006 Cert	-	-	-	-	-	-	-	-	-	-	-	-
DNC-1a Meas	-	-	-	-	-	-	-	-	-	-	-	-
DNC-1a Cert	-	-	-	-	-	-	-	-	-	-	-	-
DNC-1a Meas	-	-	-	-	-	-	-	-	-	-	-	-
DNC-1a Cert	-	-	-	-	-	-	-	-	-	-	-	-
GS311-4 Meas	-	-	-	-	-	-	-	-	-	-	-	-
GS311-4 Cert	-	-	-	-	-	-	-	-	-	-	-	-
GS900-5 Meas	-	-	-	-	-	-	-	-	-	-	-	-
GS900-5 Cert	-	-	-	-	-	-	-	-	-	-	-	-
OREAS 45d (Aqua Regia) Meas	-	-	-	-	-	-	-	-	-	-	-	-
OREAS 45d (Aqua Regia) Cert	-	-	-	-	-	-	-	-	-	-	-	-
SBC-1 Meas	-	-	-	-	-	-	-	-	-	-	-	-
SBC-1 Cert	-	-	-	-	-	-	-	-	-	-	-	-
SBC-1 Meas	-	-	-	-	-	-	-	-	-	-	-	-
SBC-1 Cert	-	-	-	-	-	-	-	-	-	-	-	-
OREAS 45d (4-Acid) Meas	-	-	-	-	-	-	-	-	-	-	-	-
OREAS 45d (4-Acid) Cert	-	-	-	-	-	-	-	-	-	-	-	-
OREAS 45d (4-Acid) Meas	-	-	-	-	-	-	-	-	-	-	-	-
OREAS 45d (4-Acid) Cert	-	-	-	-	-	-	-	-	-	-	-	-
CaCO3 Meas	-	-	-	-	-	-	-	-	-	-	-	-
CaCO3 Cert	-	-	-	-	-	-	-	-	-	-	-	-
CaCO3 Meas	-	-	-	-	-	-	-	-	-	-	-	-
CaCO3 Cert	-	-	-	-	-	-	-	-	-	-	-	-
SdAR-M2 (U.S.G.S.) Meas	-	-	-	-	-	-	-	-	-	-	-	-

Analyte	Ag	As	Bi	Ce	Co	Cr	Cs	Cu	Dy	Er	Eu	Ga
Units	ppm	ppm	ppm	ppm	ppm	ppm	ppm	ppm	ppm	ppm	ppm	ppm
Detection Limit	0.5	5	0.1	0.05	1	20	0.1	10	0.01	0.01	0.005	1
Method	FUS-MS	FUS-MS	FUS-MS	FUS-MS	FUS-MS	FUS-MS	FUS-MS	FUS-MS	FUS-MS	FUS-MS	FUS-MS	FUS-MS
SdAR-M2 (U.S.G.S.) Cert	-	-	-	-	-	-	-	-	-	-	-	-
SdAR-M2 (U.S.G.S.) Meas	-	-	-	-	-	-	-	-	-	-	-	-
SdAR-M2 (U.S.G.S.) Cert	-	-	-	-	-	-	-	-	-	-	-	-
SdAR-M2 (U.S.G.S.) Meas	-	-	-	-	-	-	-	-	-	-	-	-
SdAR-M2 (U.S.G.S.) Cert	-	-	-	-	-	-	-	-	-	-	-	-
OREAS 214 Meas	-	-	-	-	-	-	-	-	-	-	-	-
OREAS 214 Cert	-	-	-	-	-	-	-	-	-	-	-	-
OREAS 218 Meas	-	-	-	-	-	-	-	-	-	-	-	-
OREAS 218 Cert	-	-	-	-	-	-	-	-	-	-	-	-
OREAS 218 Meas	-	-	-	-	-	-	-	-	-	-	-	-
OREAS 218 Cert	-	-	-	-	-	-	-	-	-	-	-	-
T9 Geochem Orig	-	-	-	-	-	-	-	-	-	-	-	-
T9 Geochem Dup	-	-	-	-	-	-	-	-	-	-	-	-
T14 Geochem Orig	-	-	-	-	-	-	-	-	-	-	-	-
T14 Geochem Dup	-	-	-	-	-	-	-	-	-	-	-	-
T17 Geochem Orig	-	-	-	-	-	-	-	-	-	-	-	-
T17 Geochem Dup	-	-	-	-	-	-	-	-	-	-	-	-
STPL-BAS-025 Orig	-	-	-	-	-	-	-	-	-	-	-	-
STPL-BAS-025 Dup	-	-	-	-	-	-	-	-	-	-	-	-
T24 Geochem Orig	<0.5	<5	<0.1	4.18	<1	<20	<0.1	10	0.56	0.39	0.514	2
T24 Geochem Dup	<0.5	<5	<0.1	4.03	<1	<20	<0.1	20	0.54	0.39	0.471	2
T27 Geochem Orig	-	-	-	-	-	-	-	-	-	-	-	-
T27 Geochem Dup	-	-	-	-	-	-	-	-	-	-	-	-
T31 Geochem Orig	-	-	-	-	-	-	-	-	-	-	-	-
T31 Geochem Dup	-	-	-	-	-	-	-	-	-	-	-	-
T37 Geochem Orig	-	-	-	-	-	-	-	-	-	-	-	-
T37 Geochem Dup	-	-	-	-	-	-	-	-	-	-	-	-
T42 Geochem Orig	-	-	-	-	-	-	-	-	-	-	-	-
T42 Geochem Dup	-	-	-	-	-	-	-	-	-	-	-	-
T45 Geochem Orig	-	-	-	-	-	-	-	-	-	-	-	-
T45 Geochem Dup	-	-	-	-	-	-	-	-	-	-	-	-
STPL-53-PML-036 Orig	-	-	-	-	-	-	-	-	-	-	-	-
STPL-53-PML-036 Dup	-	-	-	-	-	-	-	-	-	-	-	-
STPL-BAS-025 Orig	-	-	-	-	-	-	-	-	-	-	-	-
STPL-BAS-025 Dup	-	-	-	-	-	-	-	-	-	-	-	-
T42 Geochem Orig	-	-	-	-	-	-	-	-	-	-	-	-
T42 Geochem Dup	-	-	-	-	-	-	-	-	-	-	-	-

Analyte	Ag	As	Bi	Ce	Co	Cr	Cs	Cu	Dy	Er	Eu	Ga
Units	ppm	ppm	ppm	ppm	ppm	ppm	ppm	ppm	ppm	ppm	ppm	ppm
Detection Limit	0.5	5	0.1	0.05	1	20	0.1	10	0.01	0.01	0.005	1
Method	FUS-MS	FUS-MS	FUS-MS	FUS-MS	FUS-MS	FUS-MS	FUS-MS	FUS-MS	FUS-MS	FUS-MS	FUS-MS	FUS-MS
T45 Geochem Orig	-	-	-	-	-	-	-	-	-	-	-	-
T45 Geochem Dup	-	-	-	-	-	-	-	-	-	-	-	-
T59 Orig	-	-	-	-	-	-	-	-	-	-	-	-
T59 Dup	-	-	-	-	-	-	-	-	-	-	-	-
T72 Orig	-	-	-	-	-	-	-	-	-	-	-	-
T72 Dup	-	-	-	-	-	-	-	-	-	-	-	-
T73 Orig	-	-	-	-	-	-	-	-	-	-	-	-
T73 Dup	-	-	-	-	-	-	-	-	-	-	-	-
STPL-BAS-029 Orig	-	-	-	-	-	-	-	-	-	-	-	-
STPL-BAS-029 Dup	-	-	-	-	-	-	-	-	-	-	-	-
T81 Orig	-	-	-	-	-	-	-	-	-	-	-	-
T81 Dup	-	-	-	-	-	-	-	-	-	-	-	-
T86 Orig	-	-	-	-	-	-	-	-	-	-	-	-
T86 Dup	-	-	-	-	-	-	-	-	-	-	-	-
T88 Orig	<0.5	<5	<0.1	28.4	16	<20	1.4	30	1.72	0.91	0.763	20
T88 Dup	<0.5	<5	<0.1	28	16	<20	1.4	30	1.63	0.95	0.738	20
T89 Orig	-	-	-	-	-	-	-	-	-	-	-	-
T89 Dup	-	-	-	-	-	-	-	-	-	-	-	-
T94 Orig	-	-	-	-	-	-	-	-	-	-	-	-
T94 Dup	-	-	-	-	-	-	-	-	-	-	-	-
T98 Orig	-	-	-	-	-	-	-	-	-	-	-	-
T98 Dup	-	-	-	-	-	-	-	-	-	-	-	-
T99 Orig	-	-	-	-	-	-	-	-	-	-	-	-
T99 Dup	-	-	-	-	-	-	-	-	-	-	-	-
T101 Orig	-	-	-	-	-	-	-	-	-	-	-	-
T101 Dup	-	-	-	-	-	-	-	-	-	-	-	-
T102 Orig	-	-	-	-	-	-	-	-	-	-	-	-
T102 Dup	-	-	-	-	-	-	-	-	-	-	-	-
T114 Orig	-	-	-	-	-	-	-	-	-	-	-	-
T114 Dup	-	-	-	-	-	-	-	-	-	-	-	-
T116 Orig	-	-	-	-	-	-	-	-	-	-	-	-
T116 Dup	-	-	-	-	-	-	-	-	-	-	-	-
T117 Orig	<0.5	<5	<0.1	26.8	10	20	1.1	50	1.36	0.74	0.531	21
T117 Split PREP DUP	<0.5	<5	<0.1	25.8	11	<20	1	50	1.37	0.76	0.59	22
STPL-53-PML-025 Orig	<0.5	31	<0.1	74.6	<1	50	1.9	10	2.49	1.61	0.698	11
STPL-53-PML-025 Dup	<0.5	39	<0.1	71.1	<1	40	1.8	10	2.2	1.53	0.646	10
T65 Orig	-	-	-	-	-	-	-	-	-	-	-	-

Analyte	Ag	As	Bi	Ce	Co	Cr	Cs	Cu	Dy	Er	Eu	Ga
Units	ppm	ppm	ppm	ppm	ppm	ppm	ppm	ppm	ppm	ppm	ppm	ppm
Detection Limit	0.5	5	0.1	0.05	1	20	0.1	10	0.01	0.01	0.005	1
Method	FUS-MS	FUS-MS	FUS-MS	FUS-MS	FUS-MS	FUS-MS	FUS-MS	FUS-MS	FUS-MS	FUS-MS	FUS-MS	FUS-MS
T65 Dup	-	-	-	-	-	-	-	-	-	-	-	-
T106 Orig	-	-	-	-	-	-	-	-	-	-	-	-
T106 Dup	-	-	-	-	-	-	-	-	-	-	-	-
T118 Orig	0.6	<5	<0.1	47.7	10	40	1.8	30	2.05	1.14	1.14	18
T118 Dup	0.7	<5	<0.1	49.9	11	40	1.9	30	2.23	1.25	1.23	18
T141 Orig	-	-	-	-	-	-	-	-	-	-	-	-
T141 Dup	-	-	-	-	-	-	-	-	-	-	-	-
STPL-BAS-023 Orig	-	-	-	-	-	-	-	-	-	-	-	-
STPL-BAS-023 Dup	-	-	-	-	-	-	-	-	-	-	-	-
T154 Orig	-	-	-	-	-	-	-	-	-	-	-	-
T154 Dup	-	-	-	-	-	-	-	-	-	-	-	-
T157 Orig	-	-	-	-	-	-	-	-	-	-	-	-
T157 Dup	-	-	-	-	-	-	-	-	-	-	-	-
T158 Orig	-	-	-	-	-	-	-	-	-	-	-	-
T158 Dup	-	-	-	-	-	-	-	-	-	-	-	-
STPL-PML-53-027 Orig	<0.5	34	<0.1	74.7	<1	50	2	20	2.36	1.64	0.701	12
STPL-PML-53-027 Dup	<0.5	31	<0.1	76.4	<1	50	2	20	2.47	1.68	0.698	12
T182 Orig	-	-	-	-	-	-	-	-	-	-	-	-
T182 Dup	-	-	-	-	-	-	-	-	-	-	-	-
T183 Orig	-	-	-	-	-	-	-	-	-	-	-	-
T183 Dup	-	-	-	-	-	-	-	-	-	-	-	-
T187 Orig	-	-	-	-	-	-	-	-	-	-	-	-
T187 Dup	-	-	-	-	-	-	-	-	-	-	-	-
T188 Orig	-	-	-	-	-	-	-	-	-	-	-	-
T188 Dup	-	-	-	-	-	-	-	-	-	-	-	-
T189 Orig	-	-	-	-	-	-	-	-	-	-	-	-
T189 Dup	-	-	-	-	-	-	-	-	-	-	-	-
T200 Orig	<0.5	14	<0.1	5.31	65	270	0.1	50	2.17	1.42	0.587	16
T200 Dup	<0.5	14	<0.1	5.31	63	260	0.1	50	2.06	1.35	0.593	15
T218 Orig	-	-	-	-	-	-	-	-	-	-	-	-
T218 Dup	-	-	-	-	-	-	-	-	-	-	-	-
T239 Orig	-	-	-	-	-	-	-	-	-	-	-	-
T239 Dup	-	-	-	-	-	-	-	-	-	-	-	-
T240 Orig	-	-	-	-	-	-	-	-	-	-	-	-
T240 Dup	-	-	-	-	-	-	-	-	-	-	-	-
T242 Orig	-	-	-	-	-	-	-	-	-	-	-	-
T242 Dup	-	-	-	-	-	-	-	-	-	-	-	-









Analyte	Gd	Ge	Hf	Ho	In	La	Lu	Mo	Nb	Nd	Ni	Pb
Units	ppm	ppm	ppm	ppm	ppm	ppm	ppm	ppm	ppm	ppm	ppm	ppm
Detection Limit	0.01	0.5	0.1	0.01	0.1	0.05	0.002	2	0.2	0.05	20	5
Method	FUS-MS	FUS-MS	FUS-MS	FUS-MS	FUS-MS	FUS-MS	FUS-MS	FUS-MS	FUS-MS	FUS-MS	FUS-MS	FUS-MS
GXR-1 Meas	-	-	-	-	-	-	-	-	-	-	-	-
GXR-1 Cert	-	-	-	-	-	-	-	-	-	-	-	-
NIST 694 Meas	-	-	-	-	-	-	-	-	-	-	-	-
NIST 694 Cert	-	-	-	-	-	-	-	-	-	-	-	-
DNC-1 Meas	-	-	-	-	-	3.8	-	-	-	5.3	250	7
DNC-1 Cert	-	-	-	-	-	3.6	-	-	-	5.2	247	6.3
GBW 07113 Meas	-	-	-	-	-	-	-	-	-	-	-	-
GBW 07113 Cert	-	-	-	-	-	-	-	-	-	-	-	-
GBW 07113 Meas	-	-	-	-	-	-	-	-	-	-	-	-
GBW 07113 Cert	-	-	-	-	-	-	-	-	-	-	-	-
GBW 07113 Meas	-	-	-	-	-	-	-	-	-	-	-	-
GBW 07113 Cert	-	-	-	-	-	-	-	-	-	-	-	-
GXR-4 Meas	-	-	-	-	-	-	-	-	-	-	-	-
GXR-4 Cert	-	-	-	-	-	-	-	-	-	-	-	-
GXR-6 Meas	-	-	-	-	-	-	-	-	-	-	-	-
GXR-6 Cert	-	-	-	-	-	-	-	-	-	-	-	-
LKSD-3 Meas	-	-	4.6	-	-	50.4	0.44	<2	-	46.4	50	-
LKSD-3 Cert	-	-	4.8	-	-	52	0.4	2	-	44	47	-
TDB-1 Meas	-	-	-	-	-	16.7	-	-	-	25	90	-
TDB-1 Cert	-	-	-	-	-	17	-	-	-	23	92	-
SY-2 Meas	-	-	-	-	-	-	-	-	-	-	-	-
SY-2 Cert	-	-	-	-	-	-	-	-	-	-	-	-
SY-3 Meas	-	-	-	-	-	-	-	-	-	-	-	-
SY-3 Cert	-	-	-	-	-	-	-	-	-	-	-	-
BaSO4 Meas	-	-	-	-	-	-	-	-	-	-	-	-
BaSO4 Cert	-	-	-	-	-	-	-	-	-	-	-	-
BaSO4 Meas	-	-	-	-	-	-	-	-	-	-	-	-
BaSO4 Cert	-	-	-	-	-	-	-	-	-	-	-	-
BaSO4 Meas	-	-	-	-	-	-	-	-	-	-	-	-
BaSO4 Cert	-	-	-	-	-	-	-	-	-	-	-	-
W-2a Meas	-	1.3	-	0.79	-	10.8	0.31	<2	7.4	13.2	70	-
W-2a Cert	-	1	-	0.76	-	10	0.33	0.6	7.9	13	70	-
SY-4 Meas	-	-	-	-	-	-	-	-	-	-	-	-
SY-4 Cert	-	-	-	-	-	-	-	-	-	-	-	-
CTA-AC-1 Meas	125	-	-	-	-	>2000	1.14	-	-	1170	-	-
CTA-AC-1 Cert	124	-	-	-	-	2176	1.08	-	-	1087	-	-
BIR-1a Meas	2	-	0.6	-	-	0.7	0.28	-	-	2.6	180	<5

Analyte	Gd	Ge	Hf	Ho	In	La	Lu	Mo	Nb	Nd	Ni	Pb
Units	ppm	ppm	ppm	ppm	ppm	ppm	ppm	ppm	ppm	ppm	ppm	ppm
Detection Limit	0.01	0.5	0.1	0.01	0.1	0.05	0.002	2	0.2	0.05	20	5
Method	FUS-MS	FUS-MS	FUS-MS	FUS-MS	FUS-MS	FUS-MS	FUS-MS	FUS-MS	FUS-MS	FUS-MS	FUS-MS	FUS-MS
BIR-1a Cert	2	-	0.6	-	-	0.63	0.3	-	-	2.5	170	3
BIR-1a Meas	-	-	-	-	-	-	-	-	-	-	-	-
BIR-1a Cert	-	-	-	-	-	-	-	-	-	-	-	-
NCS DC86312 Meas	231	-	-	38.1	-	>2000	12.5	-	-	1740	-	-
NCS DC86312 Cert	225	-	-	36	-	2360	11.96	-	-	1600	-	-
JGb-2 Meas	-	-	-	-	-	-	-	-	-	-	-	-
JGb-2 Cert	-	-	-	-	-	-	-	-	-	-	-	-
JGb-2 Meas	-	-	-	-	-	-	-	-	-	-	-	-
JGb-2 Cert	-	-	-	-	-	-	-	-	-	-	-	-
JGb-2 Meas	-	-	-	-	-	-	-	-	-	-	-	-
JGb-2 Cert	-	-	-	-	-	-	-	-	-	-	-	-
JGb-2 Meas	-	-	-	-	-	-	-	-	-	-	-	-
JGb-2 Cert	-	-	-	-	-	-	-	-	-	-	-	-
JGb-2 Meas	-	-	-	-	-	-	-	-	-	-	-	-
JGb-2 Cert	-	-	-	-	-	-	-	-	-	-	-	-
JGb-2 Meas	-	-	-	-	-	-	-	-	-	-	-	-
JGb-2 Cert	-	-	-	-	-	-	-	-	-	-	-	-
SCH-1 Meas	-	-	-	-	-	-	-	-	-	-	-	-
SCH-1 Cert	-	-	-	-	-	-	-	-	-	-	-	-
NCS DC70009 (GBW07241) Meas	15.7	11.3	-	4.6	2	24.7	2.53	-	-	34.4	-	-
NCS DC70009 (GBW07241) Cert	14.8	11.2	-	4.5	1.3	23.7	2.4	-	-	32.9	-	-
SGR-1b Meas	-	-	-	-	-	-	-	-	-	-	-	-
SGR-1b Cert	-	-	-	-	-	-	-	-	-	-	-	-
SGR-1b Meas	-	-	-	-	-	-	-	-	-	-	-	-
SGR-1b Cert	-	-	-	-	-	-	-	-	-	-	-	-
SGR-1b Meas	-	-	-	-	-	-	-	-	-	-	-	-
SGR-1b Cert	-	-	-	-	-	-	-	-	-	-	-	-
OREAS 100a (Fusion) Meas	22.2	-	-	5.2	-	265	2.41	25	-	161	-	-
OREAS 100a (Fusion) Cert	23.6	-	-	4.81	-	260	2.26	24.1	-	152	-	-
OREAS 101a (Fusion) Meas	-	-	-	6.88	-	812	2.79	21	-	428	-	-
OREAS 101a (Fusion) Cert	-	-	-	6.46	-	816	2.66	21.9	-	403	-	-
OREAS 101b (Fusion) Meas	-	-	-	6.54	-	788	2.64	20	-	400	-	-
OREAS 101b (Fusion) Cert	-	-	-	6.34	-	789	2.58	20.9	-	378	-	-
OREAS 98 (S by LECO) Meas	-	-	-	-	-	-	-	-	-	-	-	-
OREAS 98 (S by LECO) Cert	-	-	-	-	-	-	-	-	-	-	-	-
OREAS 132b (S by LECO) Meas	-	-	-	-	-	-	-	-	-	-	-	-
OREAS 132b (S by LECO) Cert	-	-	-	-	-	-	-	-	-	-	-	-
JR-1 Meas	5	2.1	4.4	-	<0.1	20.2	0.77	3	16.2	24.9	<20	20
JR-1 Cert	5.06	1.88	4.51	-	0.028	19.7	0.71	3.25	15.2	23.3	1.67	19.3

Analyte	Gd	Ge	Hf	Ho	In	La	Lu	Mo	Nb	Nd	Ni	Pb
Units	ppm	ppm	ppm	ppm	ppm	ppm	ppm	ppm	ppm	ppm	ppm	ppm
Detection Limit	0.01	0.5	0.1	0.01	0.1	0.05	0.002	2	0.2	0.05	20	5
Method	FUS-MS	FUS-MS	FUS-MS	FUS-MS	FUS-MS	FUS-MS	FUS-MS	FUS-MS	FUS-MS	FUS-MS	FUS-MS	FUS-MS
NCS DC86318 Meas	>1000	-	-	601	-	1950	246	-	-	>2000	-	-
NCS DC86318 Cert	2095	-	-	560	-	1960	260	-	-	3430	-	-
USZ 25-2006 Meas	-	-	-	-	-	-	-	-	-	-	-	-
USZ 25-2006 Cert	-	-	-	-	-	-	-	-	-	-	-	-
USZ 25-2006 Meas	-	-	-	-	-	-	-	-	-	-	-	-
USZ 25-2006 Cert	-	-	-	-	-	-	-	-	-	-	-	-
GS309-4 Meas	-	-	-	-	-	-	-	-	-	-	-	-
GS309-4 Cert	-	-	-	-	-	-	-	-	-	-	-	-
GS311-4 Meas	-	-	-	-	-	-	-	-	-	-	-	-
GS311-4 Cert	-	-	-	-	-	-	-	-	-	-	-	-
GS311-4 Meas	-	-	-	-	-	-	-	-	-	-	-	-
GS311-4 Cert	-	-	-	-	-	-	-	-	-	-	-	-
GS311-4 Meas	-	-	-	-	-	-	-	-	-	-	-	-
GS311-4 Cert	-	-	-	-	-	-	-	-	-	-	-	-
GS311-4 Meas	-	-	-	-	-	-	-	-	-	-	-	-
GS311-4 Cert	-	-	-	-	-	-	-	-	-	-	-	-
GS900-5 Meas	-	-	-	-	-	-	-	-	-	-	-	-
GS900-5 Cert	-	-	-	-	-	-	-	-	-	-	-	-
GS900-5 Meas	-	-	-	-	-	-	-	-	-	-	-	-
GS900-5 Cert	-	-	-	-	-	-	-	-	-	-	-	-
GS900-5 Meas	-	-	-	-	-	-	-	-	-	-	-	-
GS900-5 Cert	-	-	-	-	-	-	-	-	-	-	-	-
OREAS 45d (Aqua Regia) Meas	-	-	-	-	-	-	-	-	-	-	-	-
OREAS 45d (Aqua Regia) Cert	-	-	-	-	-	-	-	-	-	-	-	-
CDN-PGMS-24 Meas	-	-	-	-	-	-	-	-	-	-	-	-
CDN-PGMS-24 Cert	-	-	-	-	-	-	-	-	-	-	-	-
CDN-PGMS-24 Meas	-	-	-	-	-	-	-	-	-	-	-	-
CDN-PGMS-24 Cert	-	-	-	-	-	-	-	-	-	-	-	-
CDN-PGMS-24 Meas	-	-	-	-	-	-	-	-	-	-	-	-
CDN-PGMS-24 Cert	-	-	-	-	-	-	-	-	-	-	-	-
CaCO3 Meas	-	-	-	-	-	-	-	-	-	-	-	-
CaCO3 Cert	-	-	-	-	-	-	-	-	-	-	-	-
CaCO3 Meas	-	-	-	-	-	-	-	-	-	-	-	-
CaCO3 Cert	-	-	-	-	-	-	-	-	-	-	-	-
SdAR-M2 (U.S.G.S.) Meas	-	-	-	-	-	-	-	-	-	-	-	-
SdAR-M2 (U.S.G.S.) Cert	-	-	-	-	-	-	-	-	-	-	-	-
GXR-1 Meas	-	-	-	-	-	-	-	-	-	-	-	-

Analyte	Gd	Ge	Hf	Ho	In	La	Lu	Mo	Nb	Nd	Ni	Pb
Units	ppm	ppm	ppm	ppm	ppm	ppm	ppm	ppm	ppm	ppm	ppm	ppm
Detection Limit	0.01	0.5	0.1	0.01	0.1	0.05	0.002	2	0.2	0.05	20	5
Method	FUS-MS	FUS-MS	FUS-MS	FUS-MS	FUS-MS	FUS-MS	FUS-MS	FUS-MS	FUS-MS	FUS-MS	FUS-MS	FUS-MS
GXR-1 Cert	-	-	-	-	-	-	-	-	-	-	-	-
GXR-1 Meas	-	-	-	-	-	-	-	-	-	-	-	-
GXR-1 Cert	-	-	-	-	-	-	-	-	-	-	-	-
GXR-1 Meas	-	-	-	-	-	-	-	-	-	-	-	-
GXR-1 Cert	-	-	-	-	-	-	-	-	-	-	-	-
GXR-1 Meas	-	-	-	-	-	-	-	-	-	-	-	-
GXR-1 Cert	-	-	-	-	-	-	-	-	-	-	-	-
NIST 694 Meas	-	-	-	-	-	-	-	-	-	-	-	-
NIST 694 Cert	-	-	-	-	-	-	-	-	-	-	-	-
DNC-1 Meas	-	-	-	-	-	3.6	-	-	-	4.7	260	-
DNC-1 Cert	-	-	-	-	-	3.6	-	-	-	5.2	247	-
GBW 07113 Meas	-	-	-	-	-	-	-	-	-	-	-	-
GBW 07113 Cert	-	-	-	-	-	-	-	-	-	-	-	-
GXR-4 Meas	-	-	-	-	-	-	-	-	-	-	-	-
GXR-4 Cert	-	-	-	-	-	-	-	-	-	-	-	-
GXR-4 Meas	-	-	-	-	-	-	-	-	-	-	-	-
GXR-4 Cert	-	-	-	-	-	-	-	-	-	-	-	-
GXR-4 Meas	-	-	-	-	-	-	-	-	-	-	-	-
GXR-4 Cert	-	-	-	-	-	-	-	-	-	-	-	-
GXR-4 Meas	-	-	-	-	-	-	-	-	-	-	-	-
GXR-4 Cert	-	-	-	-	-	-	-	-	-	-	-	-
GXR-4 Meas	-	-	-	-	-	-	-	-	-	-	-	-
GXR-4 Cert	-	-	-	-	-	-	-	-	-	-	-	-
SDC-1 Meas	-	-	-	-	-	-	-	-	-	-	-	-
SDC-1 Cert	-	-	-	-	-	-	-	-	-	-	-	-
SDC-1 Meas	-	-	-	-	-	-	-	-	-	-	-	-
SDC-1 Cert	-	-	-	-	-	-	-	-	-	-	-	-
SDC-1 Meas	-	-	-	-	-	-	-	-	-	-	-	-
SDC-1 Cert	-	-	-	-	-	-	-	-	-	-	-	-
SDC-1 Meas	-	-	-	-	-	-	-	-	-	-	-	-
SDC-1 Cert	-	-	-	-	-	-	-	-	-	-	-	-
GXR-6 Meas	-	-	-	-	-	-	-	-	-	-	-	-
GXR-6 Cert	-	-	-	-	-	-	-	-	-	-	-	-
GXR-6 Meas	-	-	-	-	-	-	-	-	-	-	-	-
GXR-6 Cert	-	-	-	-	-	-	-	-	-	-	-	-
GXR-6 Meas	-	-	-	-	-	-	-	-	-	-	-	-
GXR-6 Cert	-	-	-	-	-	-	-	-	-	-	-	-
GXR-6 Meas	-	-	-	-	-	-	-	-	-	-	-	-
GXR-6 Cert	-	-	-	-	-	-	-	-	-	-	-	-

Analyte	Gd	Ge	Hf	Ho	In	La	Lu	Mo	Nb	Nd	Ni	Pb
Units	ppm	ppm	ppm	ppm	ppm	ppm	ppm	ppm	ppm	ppm	ppm	ppm
Detection Limit	0.01	0.5	0.1	0.01	0.1	0.05	0.002	2	0.2	0.05	20	5
Method	FUS-MS	FUS-MS	FUS-MS	FUS-MS	FUS-MS	FUS-MS	FUS-MS	FUS-MS	FUS-MS	FUS-MS	FUS-MS	FUS-MS
LKSD-3 Meas	-	-	4.4	-	-	-	0.39	<2	-	41.1	50	-
LKSD-3 Cert	-	-	4.8	-	-	-	0.4	2	-	44	47	-
TDB-1 Meas	-	-	-	-	-	16.9	-	-	-	24.5	100	-
TDB-1 Cert	-	-	-	-	-	17	-	-	-	23	92	-
SY-2 Meas	-	-	-	-	-	-	-	-	-	-	-	-
SY-2 Cert	-	-	-	-	-	-	-	-	-	-	-	-
SY-3 Meas	-	-	-	-	-	-	-	-	-	-	-	-
SY-3 Cert	-	-	-	-	-	-	-	-	-	-	-	-
BaSO4 Meas	-	-	-	-	-	-	-	-	-	-	-	-
BaSO4 Cert	-	-	-	-	-	-	-	-	-	-	-	-
BaSO4 Meas	-	-	-	-	-	-	-	-	-	-	-	-
BaSO4 Cert	-	-	-	-	-	-	-	-	-	-	-	-
W-2a Meas	-	1.6	-	0.8	-	10.1	0.31	<2	-	13.2	80	-
W-2a Cert	-	1	-	0.76	-	10	0.33	0.6	-	13	70	-
SY-4 Meas	-	-	-	-	-	-	-	-	-	-	-	-
SY-4 Cert	-	-	-	-	-	-	-	-	-	-	-	-
CTA-AC-1 Meas	126	-	-	-	-	>2000	1.1	-	-	1090	-	-
CTA-AC-1 Cert	124	-	-	-	-	2176	1.08	-	-	1087	-	-
BIR-1a Meas	1.9	-	0.6	-	-	0.6	-	-	-	2.3	180	<5
BIR-1a Cert	2	-	0.6	-	-	0.63	-	-	-	2.5	170	3
Calcium Carbonate Meas	-	-	-	-	-	-	-	-	-	-	-	-
Calcium Carbonate Cert	-	-	-	-	-	-	-	-	-	-	-	-
NCS DC86312 Meas	234	-	-	34.3	-	>2000	12	-	-	1510	-	-
NCS DC86312 Cert	225	-	-	36	-	2360	11.96	-	-	1600	-	-
JGb-2 Meas	-	-	-	-	-	-	-	-	-	-	-	-
JGb-2 Cert	-	-	-	-	-	-	-	-	-	-	-	-
JGb-2 Meas	-	-	-	-	-	-	-	-	-	-	-	-
JGb-2 Cert	-	-	-	-	-	-	-	-	-	-	-	-
JGb-2 Meas	-	-	-	-	-	-	-	-	-	-	-	-
JGb-2 Cert	-	-	-	-	-	-	-	-	-	-	-	-
NCS DC70009 (GBW07241) Meas	14.3	11.3	-	4.2	1	22.2	2.17	-	-	29.9	<20	-
NCS DC70009 (GBW07241) Cert	14.8	11.2	-	4.5	1.3	23.7	2.4	-	-	32.9	2.8	-
SGR-1b Meas	-	-	-	-	-	-	-	-	-	-	-	-
SGR-1b Cert	-	-	-	-	-	-	-	-	-	-	-	-
SGR-1b Meas	-	-	-	-	-	-	-	-	-	-	-	-
SGR-1b Cert	-	-	-	-	-	-	-	-	-	-	-	-
OREAS 100a (Fusion) Meas	22.4	-	-	4.7	-	248	2.08	23	-	144	-	-

Analyte	Gd	Ge	Hf	Ho	In	La	Lu	Mo	Nb	Nd	Ni	Pb
Units	ppm	ppm	ppm	ppm	ppm	ppm	ppm	ppm	ppm	ppm	ppm	ppm
Detection Limit	0.01	0.5	0.1	0.01	0.1	0.05	0.002	2	0.2	0.05	20	5
Method	FUS-MS	FUS-MS	FUS-MS	FUS-MS	FUS-MS	FUS-MS	FUS-MS	FUS-MS	FUS-MS	FUS-MS	FUS-MS	FUS-MS
OREAS 100a (Fusion) Cert	23.6	-	-	4.81	-	260	2.26	24.1	-	152	-	-
OREAS 101a (Fusion) Meas	41.9	-	-	6.16	-	797	2.5	21	-	377	-	-
OREAS 101a (Fusion) Cert	43.4	-	-	6.46	-	816	2.66	21.9	-	403	-	-
OREAS 101b (Fusion) Meas	-	-	-	6.4	-	800	2.69	20	-	382	-	-
OREAS 101b (Fusion) Cert	-	-	-	6.34	-	789	2.58	20.9	-	378	-	-
JR-1 Meas	5.5	2	4.4	-	<0.1	19	0.7	3	15.1	21.9	<20	18
JR-1 Cert	5.06	1.88	4.51	-	0.028	19.7	0.71	3.25	15.2	23.3	1.67	19.3
NCS DC86318 Meas	>1000	-	-	599	-	2000	257	-	-	>2000	-	-
NCS DC86318 Cert	2095	-	-	560	-	1960	260	-	-	3430	-	-
USZ 25-2006 Meas	-	-	-	-	-	-	-	-	-	-	-	-
USZ 25-2006 Cert	-	-	-	-	-	-	-	-	-	-	-	-
USZ 25-2006 Meas	-	-	-	-	-	-	-	-	-	-	-	-
USZ 25-2006 Cert	-	-	-	-	-	-	-	-	-	-	-	-
DNC-1a Meas	-	-	-	-	-	-	-	-	-	-	-	-
DNC-1a Cert	-	-	-	-	-	-	-	-	-	-	-	-
DNC-1a Meas	-	-	-	-	-	-	-	-	-	-	-	-
DNC-1a Cert	-	-	-	-	-	-	-	-	-	-	-	-
DNC-1a Meas	-	-	-	-	-	-	-	-	-	-	-	-
DNC-1a Cert	-	-	-	-	-	-	-	-	-	-	-	-
DNC-1a Meas	-	-	-	-	-	-	-	-	-	-	-	-
DNC-1a Cert	-	-	-	-	-	-	-	-	-	-	-	-
DNC-1a Meas	-	-	-	-	-	-	-	-	-	-	-	-
DNC-1a Cert	-	-	-	-	-	-	-	-	-	-	-	-
GS311-4 Meas	-	-	-	-	-	-	-	-	-	-	-	-
GS311-4 Cert	-	-	-	-	-	-	-	-	-	-	-	-
GS311-4 Meas	-	-	-	-	-	-	-	-	-	-	-	-
GS311-4 Cert	-	-	-	-	-	-	-	-	-	-	-	-
GS900-5 Meas	-	-	-	-	-	-	-	-	-	-	-	-
GS900-5 Cert	-	-	-	-	-	-	-	-	-	-	-	-
GS900-5 Meas	-	-	-	-	-	-	-	-	-	-	-	-
GS900-5 Cert	-	-	-	-	-	-	-	-	-	-	-	-
OREAS 45d (Aqua Regia) Meas	-	-	-	-	-	-	-	-	-	-	-	-
OREAS 45d (Aqua Regia) Cert	-	-	-	-	-	-	-	-	-	-	-	-
OREAS 45d (Aqua Regia) Meas	-	-	-	-	-	-	-	-	-	-	-	-
OREAS 45d (Aqua Regia) Cert	-	-	-	-	-	-	-	-	-	-	-	-
OREAS 45d (Aqua Regia) Meas	-	-	-	-	-	-	-	-	-	-	-	-
OREAS 45d (Aqua Regia) Cert	-	-	-	-	-	-	-	-	-	-	-	-
SBC-1 Meas	-	-	-	-	-	-	-	-	-	-	-	-
SBC-1 Cert	-	-	-	-	-	-	-	-	-	-	-	-



Analyte	Gd	Ge	Hf	Ho	In	La	Lu	Mo	Nb	Nd	Ni	Pb
Units	ppm	ppm	ppm	ppm	ppm	ppm	ppm	ppm	ppm	ppm	ppm	ppm
Detection Limit	0.01	0.5	0.1	0.01	0.1	0.05	0.002	2	0.2	0.05	20	5
Method	FUS-MS	FUS-MS	FUS-MS	FUS-MS	FUS-MS	FUS-MS	FUS-MS	FUS-MS	FUS-MS	FUS-MS	FUS-MS	FUS-MS
SBC-1 Meas	-	-	-	-	-	-	-	-	-	-	-	-
SBC-1 Cert	-	-	-	-	-	-	-	-	-	-	-	-
SBC-1 Meas	-	-	-	-	-	-	-	-	-	-	-	-
SBC-1 Cert	-	-	-	-	-	-	-	-	-	-	-	-
SBC-1 Meas	-	-	-	-	-	-	-	-	-	-	-	-
SBC-1 Cert	-	-	-	-	-	-	-	-	-	-	-	-
OREAS 45d (4-Acid) Meas	-	-	-	-	-	-	-	-	-	-	-	-
OREAS 45d (4-Acid) Cert	-	-	-	-	-	-	-	-	-	-	-	-
OREAS 45d (4-Acid) Meas	-	-	-	-	-	-	-	-	-	-	-	-
OREAS 45d (4-Acid) Cert	-	-	-	-	-	-	-	-	-	-	-	-
OREAS 45d (4-Acid) Meas	-	-	-	-	-	-	-	-	-	-	-	-
OREAS 45d (4-Acid) Cert	-	-	-	-	-	-	-	-	-	-	-	-
OREAS 45d (4-Acid) Meas	-	-	-	-	-	-	-	-	-	-	-	-
OREAS 45d (4-Acid) Cert	-	-	-	-	-	-	-	-	-	-	-	-
OxK110 Meas	-	-	-	-	-	-	-	-	-	-	-	-
OxK110 Cert	-	-	-	-	-	-	-	-	-	-	-	-
CDN-PGMS-24 Meas	-	-	-	-	-	-	-	-	-	-	-	-
CDN-PGMS-24 Cert	-	-	-	-	-	-	-	-	-	-	-	-
CDN-PGMS-24 Meas	-	-	-	-	-	-	-	-	-	-	-	-
CDN-PGMS-24 Cert	-	-	-	-	-	-	-	-	-	-	-	-
OXN117 Meas	-	-	-	-	-	-	-	-	-	-	-	-
OXN117 Cert	-	-	-	-	-	-	-	-	-	-	-	-
CaCO3 Meas	-	-	-	-	-	-	-	-	-	-	-	-
CaCO3 Cert	-	-	-	-	-	-	-	-	-	-	-	-
SdAR-M2 (U.S.G.S.) Meas	-	-	-	-	-	-	-	-	-	-	-	-
SdAR-M2 (U.S.G.S.) Cert	-	-	-	-	-	-	-	-	-	-	-	-
SdAR-M2 (U.S.G.S.) Meas	-	-	-	-	-	-	-	-	-	-	-	-
SdAR-M2 (U.S.G.S.) Cert	-	-	-	-	-	-	-	-	-	-	-	-
SdAR-M2 (U.S.G.S.) Meas	-	-	-	-	-	-	-	-	-	-	-	-
SdAR-M2 (U.S.G.S.) Cert	-	-	-	-	-	-	-	-	-	-	-	-
SdAR-M2 (U.S.G.S.) Meas	-	-	-	-	-	-	-	-	-	-	-	-
SdAR-M2 (U.S.G.S.) Cert	-	-	-	-	-	-	-	-	-	-	-	-
GXR-1 Meas	-	-	-	-	-	-	-	-	-	-	-	-
GXR-1 Cert	-	-	-	-	-	-	-	-	-	-	-	-
GXR-1 Meas	-	-	-	-	-	-	-	-	-	-	-	-
GXR-1 Cert	-	-	-	-	-	-	-	-	-	-	-	-
NIST 694 Meas	-	-	-	-	-	-	-	-	-	-	-	-

Analyte	Gd	Ge	Hf	Ho	In	La	Lu	Mo	Nb	Nd	Ni	Pb
Units	ppm	ppm	ppm	ppm	ppm	ppm	ppm	ppm	ppm	ppm	ppm	ppm
Detection Limit	0.01	0.5	0.1	0.01	0.1	0.05	0.002	2	0.2	0.05	20	5
Method	FUS-MS	FUS-MS	FUS-MS	FUS-MS	FUS-MS	FUS-MS	FUS-MS	FUS-MS	FUS-MS	FUS-MS	FUS-MS	FUS-MS
NIST 694 Cert	-	-	-	-	-	-	-	-	-	-	-	-
DNC-1 Meas	-	-	-	-	-	3.4	-	-	-	4.8	250	-
DNC-1 Cert	-	-	-	-	-	3.6	-	-	-	5.2	247	-
GBW 07113 Meas	-	-	-	-	-	-	-	-	-	-	-	-
GBW 07113 Cert	-	-	-	-	-	-	-	-	-	-	-	-
GXR-4 Meas	-	-	-	-	-	-	-	-	-	-	-	-
GXR-4 Cert	-	-	-	-	-	-	-	-	-	-	-	-
GXR-4 Meas	-	-	-	-	-	-	-	-	-	-	-	-
GXR-4 Cert	-	-	-	-	-	-	-	-	-	-	-	-
SDC-1 Meas	-	-	-	-	-	-	-	-	-	-	-	-
SDC-1 Cert	-	-	-	-	-	-	-	-	-	-	-	-
GXR-6 Meas	-	-	-	-	-	-	-	-	-	-	-	-
GXR-6 Cert	-	-	-	-	-	-	-	-	-	-	-	-
GXR-6 Meas	-	-	-	-	-	-	-	-	-	-	-	-
GXR-6 Cert	-	-	-	-	-	-	-	-	-	-	-	-
LKSD-3 Meas	-	-	4.5	-	-	53.2	0.37	<2	-	39.9	50	-
LKSD-3 Cert	-	-	4.8	-	-	52	0.4	2	-	44	47	-
TDB-1 Meas	-	-	-	-	-	17.1	-	-	-	23.8	90	-
TDB-1 Cert	-	-	-	-	-	17	-	-	-	23	92	-
SY-2 Meas	-	-	-	-	-	-	-	-	-	-	-	-
SY-2 Cert	-	-	-	-	-	-	-	-	-	-	-	-
SY-3 Meas	-	-	-	-	-	-	-	-	-	-	-	-
SY-3 Cert	-	-	-	-	-	-	-	-	-	-	-	-
BaSO4 Meas	-	-	-	-	-	-	-	-	-	-	-	-
BaSO4 Cert	-	-	-	-	-	-	-	-	-	-	-	-
BaSO4 Meas	-	-	-	-	-	-	-	-	-	-	-	-
BaSO4 Cert	-	-	-	-	-	-	-	-	-	-	-	-
BaSO4 Meas	-	-	-	-	-	-	-	-	-	-	-	-
BaSO4 Cert	-	-	-	-	-	-	-	-	-	-	-	-
W-2a Meas	-	1.6	2.5	0.78	-	10.8	0.32	<2	7.9	12.7	70	-
W-2a Cert	-	1	2.6	0.76	-	10	0.33	0.6	7.9	13	70	-
DTS-2b Meas	-	-	-	-	-	-	-	-	-	-	3380	-
DTS-2b Cert	-	-	-	-	-	-	-	-	-	-	3780	-
SY-4 Meas	-	-	-	-	-	-	-	-	-	-	-	-
SY-4 Cert	-	-	-	-	-	-	-	-	-	-	-	-
CTA-AC-1 Meas	115	-	1.2	-	-	>2000	1.02	-	-	1100	-	-
CTA-AC-1 Cert	124	-	1.13	-	-	2176	1.08	-	-	1087	-	-

Analyte	Gd	Ge	Hf	Ho	In	La	Lu	Mo	Nb	Nd	Ni	Pb
Units	ppm	ppm	ppm	ppm	ppm	ppm	ppm	ppm	ppm	ppm	ppm	ppm
Detection Limit	0.01	0.5	0.1	0.01	0.1	0.05	0.002	2	0.2	0.05	20	5
Method	FUS-MS	FUS-MS	FUS-MS	FUS-MS	FUS-MS	FUS-MS	FUS-MS	FUS-MS	FUS-MS	FUS-MS	FUS-MS	FUS-MS
BIR-1a Meas	1.9	-	0.6	-	-	0.7	-	-	-	2.5	170	-
BIR-1a Cert	2	-	0.6	-	-	0.63	-	-	-	2.5	170	-
NCS DC86312 Meas	219	-	-	32.9	-	>2000	11.7	-	-	1560	-	-
NCS DC86312 Cert	225	-	-	36	-	2360	11.96	-	-	1600	-	-
JGb-2 Meas	-	-	-	-	-	-	-	-	-	-	-	-
JGb-2 Cert	-	-	-	-	-	-	-	-	-	-	-	-
NCS DC70009 (GBW07241) Meas	14.4	11.2	-	-	1	23.2	-	-	-	-	-	-
NCS DC70009 (GBW07241) Cert	14.8	11.2	-	-	1.3	23.7	-	-	-	-	-	-
SGR-1b Meas	-	-	-	-	-	-	-	-	-	-	-	-
SGR-1b Cert	-	-	-	-	-	-	-	-	-	-	-	-
SGR-1b Meas	-	-	-	-	-	-	-	-	-	-	-	-
SGR-1b Cert	-	-	-	-	-	-	-	-	-	-	-	-
SGR-1b Meas	-	-	-	-	-	-	-	-	-	-	-	-
SGR-1b Cert	-	-	-	-	-	-	-	-	-	-	-	-
OREAS 100a (Fusion) Meas	-	-	-	4.69	-	247	2.3	23	-	145	-	-
OREAS 100a (Fusion) Cert	-	-	-	4.81	-	260	2.26	24.1	-	152	-	-
OREAS 101a (Fusion) Meas	41.4	-	-	-	-	797	2.6	21	-	391	-	-
OREAS 101a (Fusion) Cert	43.4	-	-	-	-	816	2.66	21.9	-	403	-	-
OREAS 101b (Fusion) Meas	-	-	-	6.33	-	802	2.75	20	-	382	-	-
OREAS 101b (Fusion) Cert	-	-	-	6.34	-	789	2.58	20.9	-	378	-	-
OREAS 98 (S by LECO) Meas	-	-	-	-	-	-	-	-	-	-	-	-
OREAS 98 (S by LECO) Cert	-	-	-	-	-	-	-	-	-	-	-	-
OREAS 132b (S by LECO) Meas	-	-	-	-	-	-	-	-	-	-	-	-
OREAS 132b (S by LECO) Cert	-	-	-	-	-	-	-	-	-	-	-	-
JR-1 Meas	-	2	4.3	1.21	<0.1	20.3	0.72	3	14.3	24.1	<20	20
JR-1 Cert	-	1.88	4.51	1.11	0.028	19.7	0.71	3.25	15.2	23.3	1.67	19.3
NCS DC86318 Meas	>1000	-	-	574	-	1910	247	-	-	>2000	-	-
NCS DC86318 Cert	2095	-	-	560	-	1960	260	-	-	3430	-	-
USZ 25-2006 Meas	-	-	-	-	-	-	-	-	-	-	-	-
USZ 25-2006 Cert	-	-	-	-	-	-	-	-	-	-	-	-
DNC-1a Meas	-	-	-	-	-	-	-	-	-	-	-	-
DNC-1a Cert	-	-	-	-	-	-	-	-	-	-	-	-
PK2 Meas	-	-	-	-	-	-	-	-	-	-	-	-
PK2 Cert	-	-	-	-	-	-	-	-	-	-	-	-
GS309-4 Meas	-	-	-	-	-	-	-	-	-	-	-	-
GS309-4 Cert	-	-	-	-	-	-	-	-	-	-	-	-
GS311-4 Meas	-	-	-	-	-	-	-	-	-	-	-	-

Analyte	Gd	Ge	Hf	Ho	In	La	Lu	Mo	Nb	Nd	Ni	Pb
Units	ppm	ppm	ppm	ppm	ppm	ppm	ppm	ppm	ppm	ppm	ppm	ppm
Detection Limit	0.01	0.5	0.1	0.01	0.1	0.05	0.002	2	0.2	0.05	20	5
Method	FUS-MS	FUS-MS	FUS-MS	FUS-MS	FUS-MS	FUS-MS	FUS-MS	FUS-MS	FUS-MS	FUS-MS	FUS-MS	FUS-MS
GS311-4 Cert	-	-	-	-	-	-	-	-	-	-	-	-
GS311-4 Meas	-	-	-	-	-	-	-	-	-	-	-	-
GS311-4 Cert	-	-	-	-	-	-	-	-	-	-	-	-
GS311-4 Meas	-	-	-	-	-	-	-	-	-	-	-	-
GS311-4 Cert	-	-	-	-	-	-	-	-	-	-	-	-
GS900-5 Meas	-	-	-	-	-	-	-	-	-	-	-	-
GS900-5 Cert	-	-	-	-	-	-	-	-	-	-	-	-
GS900-5 Meas	-	-	-	-	-	-	-	-	-	-	-	-
GS900-5 Cert	-	-	-	-	-	-	-	-	-	-	-	-
GS900-5 Meas	-	-	-	-	-	-	-	-	-	-	-	-
GS900-5 Cert	-	-	-	-	-	-	-	-	-	-	-	-
GS900-5 Meas	-	-	-	-	-	-	-	-	-	-	-	-
GS900-5 Cert	-	-	-	-	-	-	-	-	-	-	-	-
OREAS 45d (Aqua Regia) Meas	-	-	-	-	-	-	-	-	-	-	-	-
OREAS 45d (Aqua Regia) Cert	-	-	-	-	-	-	-	-	-	-	-	-
SBC-1 Meas	-	-	-	-	-	-	-	-	-	-	-	-
SBC-1 Cert	-	-	-	-	-	-	-	-	-	-	-	-
OREAS 45d (4-Acid) Meas	-	-	-	-	-	-	-	-	-	-	-	-
OREAS 45d (4-Acid) Cert	-	-	-	-	-	-	-	-	-	-	-	-
CaCO3 Meas	-	-	-	-	-	-	-	-	-	-	-	-
CaCO3 Cert	-	-	-	-	-	-	-	-	-	-	-	-
SdAR-M2 (U.S.G.S.) Meas	-	-	-	-	-	-	-	-	-	-	-	-
SdAR-M2 (U.S.G.S.) Cert	-	-	-	-	-	-	-	-	-	-	-	-
SdAR-M2 (U.S.G.S.) Meas	-	-	-	-	-	-	-	-	-	-	-	-
SdAR-M2 (U.S.G.S.) Cert	-	-	-	-	-	-	-	-	-	-	-	-
GXR-1 Meas	-	-	-	-	-	-	-	-	-	-	-	-
GXR-1 Cert	-	-	-	-	-	-	-	-	-	-	-	-
GXR-1 Meas	-	-	-	-	-	-	-	-	-	-	-	-
GXR-1 Cert	-	-	-	-	-	-	-	-	-	-	-	-
NIST 694 Meas	-	-	-	-	-	-	-	-	-	-	-	-
NIST 694 Cert	-	-	-	-	-	-	-	-	-	-	-	-
DNC-1 Meas	-	-	-	-	-	3.5	-	-	-	-	260	-
DNC-1 Cert	-	-	-	-	-	3.6	-	-	-	-	247	-
GBW 07113 Meas	-	-	-	-	-	-	-	-	-	-	-	-
GBW 07113 Cert	-	-	-	-	-	-	-	-	-	-	-	-
GXR-4 Meas	-	-	-	-	-	-	-	-	-	-	-	-
GXR-4 Cert	-	-	-	-	-	-	-	-	-	-	-	-
GXR-4 Meas	-	-	-	-	-	-	-	-	-	-	-	-
GXR-4 Cert	-	-	-	-	-	-	-	-	-	-	-	-

Analyte	Gd	Ge	Hf	Ho	In	La	Lu	Mo	Nb	Nd	Ni	Pb
Units	ppm	ppm	ppm	ppm	ppm	ppm	ppm	ppm	ppm	ppm	ppm	ppm
Detection Limit	0.01	0.5	0.1	0.01	0.1	0.05	0.002	2	0.2	0.05	20	5
Method	FUS-MS	FUS-MS	FUS-MS	FUS-MS	FUS-MS	FUS-MS	FUS-MS	FUS-MS	FUS-MS	FUS-MS	FUS-MS	FUS-MS
SDC-1 Meas	-	-	-	-	-	-	-	-	-	-	-	-
SDC-1 Cert	-	-	-	-	-	-	-	-	-	-	-	-
SDC-1 Meas	-	-	-	-	-	-	-	-	-	-	-	-
SDC-1 Cert	-	-	-	-	-	-	-	-	-	-	-	-
GXR-6 Meas	-	-	-	-	-	-	-	-	-	-	-	-
GXR-6 Cert	-	-	-	-	-	-	-	-	-	-	-	-
GXR-6 Meas	-	-	-	-	-	-	-	-	-	-	-	-
GXR-6 Cert	-	-	-	-	-	-	-	-	-	-	-	-
LKSD-3 Meas	-	-	4.5	-	-	49.7	0.42	<2	-	46.4	50	-
LKSD-3 Cert	-	-	4.8	-	-	52	0.4	2	-	44	47	-
TDB-1 Meas	-	-	-	-	-	17	-	-	-	24.3	90	-
TDB-1 Cert	-	-	-	-	-	17	-	-	-	23	92	-
SY-2 Meas	-	-	-	-	-	-	-	-	-	-	-	-
SY-2 Cert	-	-	-	-	-	-	-	-	-	-	-	-
SY-3 Meas	-	-	-	-	-	-	-	-	-	-	-	-
SY-3 Cert	-	-	-	-	-	-	-	-	-	-	-	-
BaSO4 Meas	-	-	-	-	-	-	-	-	-	-	-	-
BaSO4 Cert	-	-	-	-	-	-	-	-	-	-	-	-
BaSO4 Meas	-	-	-	-	-	-	-	-	-	-	-	-
BaSO4 Cert	-	-	-	-	-	-	-	-	-	-	-	-
W-2a Meas	-	1.7	2.3	0.79	-	10.1	0.33	<2	7.5	13.1	80	9
W-2a Cert	-	1	2.6	0.76	-	10	0.33	0.6	7.9	13	70	9.3
SY-4 Meas	-	-	-	-	-	-	-	-	-	-	-	-
SY-4 Cert	-	-	-	-	-	-	-	-	-	-	-	-
CTA-AC-1 Meas	122	-	1.9	-	-	>2000	1.11	-	-	1120	-	-
CTA-AC-1 Cert	124	-	1.13	-	-	2176	1.08	-	-	1087	-	-
BIR-1a Meas	1.9	-	0.6	-	-	0.6	-	-	-	2.4	170	-
BIR-1a Cert	2	-	0.6	-	-	0.63	-	-	-	2.5	170	-
BIR-1a Meas	-	-	-	-	-	-	-	-	-	-	-	-
BIR-1a Cert	-	-	-	-	-	-	-	-	-	-	-	-
NCS DC86312 Meas	224	-	-	33.2	-	>2000	11.7	-	-	1570	-	-
NCS DC86312 Cert	225	-	-	36	-	2360	11.96	-	-	1600	-	-
JGb-2 Meas	-	-	-	-	-	-	-	-	-	-	-	-
JGb-2 Cert	-	-	-	-	-	-	-	-	-	-	-	-
JGb-2 Meas	-	-	-	-	-	-	-	-	-	-	-	-
JGb-2 Cert	-	-	-	-	-	-	-	-	-	-	-	-
JGb-2 Meas	-	-	-	-	-	-	-	-	-	-	-	-

Analyte	Gd	Ge	Hf	Ho	In	La	Lu	Mo	Nb	Nd	Ni	Pb
Units	ppm	ppm	ppm	ppm	ppm	ppm	ppm	ppm	ppm	ppm	ppm	ppm
Detection Limit	0.01	0.5	0.1	0.01	0.1	0.05	0.002	2	0.2	0.05	20	5
Method	FUS-MS	FUS-MS	FUS-MS	FUS-MS	FUS-MS	FUS-MS	FUS-MS	FUS-MS	FUS-MS	FUS-MS	FUS-MS	FUS-MS
JGb-2 Cert	-	-	-	-	-	-	-	-	-	-	-	-
JGb-2 Meas	-	-	-	-	-	-	-	-	-	-	-	-
JGb-2 Cert	-	-	-	-	-	-	-	-	-	-	-	-
NCS DC70009 (GBW07241) Meas	15.1	10.8	-	4.3	1	24.4	2.32	-	-	32.6	-	-
NCS DC70009 (GBW07241) Cert	14.8	11.2	-	4.5	1.3	23.7	2.4	-	-	32.9	-	-
SGR-1b Meas	-	-	-	-	-	-	-	-	-	-	-	-
SGR-1b Cert	-	-	-	-	-	-	-	-	-	-	-	-
SGR-1b Meas	-	-	-	-	-	-	-	-	-	-	-	-
SGR-1b Cert	-	-	-	-	-	-	-	-	-	-	-	-
OREAS 100a (Fusion) Meas	22.8	-	-	4.82	-	272	2.22	23	-	155	-	-
OREAS 100a (Fusion) Cert	23.6	-	-	4.81	-	260	2.26	24.1	-	152	-	-
OREAS 101a (Fusion) Meas	39.9	-	-	5.97	-	803	-	22	-	374	-	-
OREAS 101a (Fusion) Cert	43.4	-	-	6.46	-	816	-	21.9	-	403	-	-
OREAS 101b (Fusion) Meas	-	-	-	6.42	-	833	2.71	20	-	389	-	-
OREAS 101b (Fusion) Cert	-	-	-	6.34	-	789	2.58	21	-	378	-	-
JR-1 Meas	5.3	-	4.2	1.21	<0.1	19.4	0.69	3	15.8	23.1	<20	18
JR-1 Cert	5.06	-	4.51	1.11	0.028	19.7	0.71	3.25	15.2	23.3	1.67	19.3
NCS DC86318 Meas	>1000	-	-	602	-	>2000	256	-	-	>2000	-	-
NCS DC86318 Cert	2095	-	-	560	-	1960	260	-	-	3430	-	-
USZ 25-2006 Meas	-	-	-	-	-	-	-	-	-	-	-	-
USZ 25-2006 Cert	-	-	-	-	-	-	-	-	-	-	-	-
USZ 25-2006 Meas	-	-	-	-	-	-	-	-	-	-	-	-
USZ 25-2006 Cert	-	-	-	-	-	-	-	-	-	-	-	-
DNC-1a Meas	-	-	-	-	-	-	-	-	-	-	-	-
DNC-1a Cert	-	-	-	-	-	-	-	-	-	-	-	-
DNC-1a Meas	-	-	-	-	-	-	-	-	-	-	-	-
DNC-1a Cert	-	-	-	-	-	-	-	-	-	-	-	-
PK2 Meas	-	-	-	-	-	-	-	-	-	-	-	-
PK2 Cert	-	-	-	-	-	-	-	-	-	-	-	-
GS311-4 Meas	-	-	-	-	-	-	-	-	-	-	-	-
GS311-4 Cert	-	-	-	-	-	-	-	-	-	-	-	-
GS311-4 Meas	-	-	-	-	-	-	-	-	-	-	-	-
GS311-4 Cert	-	-	-	-	-	-	-	-	-	-	-	-
GS900-5 Meas	-	-	-	-	-	-	-	-	-	-	-	-
GS900-5 Cert	-	-	-	-	-	-	-	-	-	-	-	-
GS900-5 Meas	-	-	-	-	-	-	-	-	-	-	-	-
GS900-5 Cert	-	-	-	-	-	-	-	-	-	-	-	-

Analyte	Gd	Ge	Hf	Ho	In	La	Lu	Mo	Nb	Nd	Ni	Pb
Units	ppm	ppm	ppm	ppm	ppm	ppm	ppm	ppm	ppm	ppm	ppm	ppm
Detection Limit	0.01	0.5	0.1	0.01	0.1	0.05	0.002	2	0.2	0.05	20	5
Method	FUS-MS	FUS-MS	FUS-MS	FUS-MS	FUS-MS	FUS-MS	FUS-MS	FUS-MS	FUS-MS	FUS-MS	FUS-MS	FUS-MS
OREAS 45d (Aqua Regia) Meas	-	-	-	-	-	-	-	-	-	-	-	-
OREAS 45d (Aqua Regia) Cert	-	-	-	-	-	-	-	-	-	-	-	-
SBC-1 Meas	-	-	-	-	-	-	-	-	-	-	-	-
SBC-1 Cert	-	-	-	-	-	-	-	-	-	-	-	-
SBC-1 Meas	-	-	-	-	-	-	-	-	-	-	-	-
SBC-1 Cert	-	-	-	-	-	-	-	-	-	-	-	-
OREAS 45d (4-Acid) Meas	-	-	-	-	-	-	-	-	-	-	-	-
OREAS 45d (4-Acid) Cert	-	-	-	-	-	-	-	-	-	-	-	-
OxK110 Meas	-	-	-	-	-	-	-	-	-	-	-	-
OxK110 Cert	-	-	-	-	-	-	-	-	-	-	-	-
OXN117 Meas	-	-	-	-	-	-	-	-	-	-	-	-
OXN117 Cert	-	-	-	-	-	-	-	-	-	-	-	-
CaCO3 Meas	-	-	-	-	-	-	-	-	-	-	-	-
CaCO3 Cert	-	-	-	-	-	-	-	-	-	-	-	-
CaCO3 Meas	-	-	-	-	-	-	-	-	-	-	-	-
CaCO3 Cert	-	-	-	-	-	-	-	-	-	-	-	-
SdAR-M2 (U.S.G.S.) Meas	-	-	-	-	-	-	-	-	-	-	-	-
SdAR-M2 (U.S.G.S.) Cert	-	-	-	-	-	-	-	-	-	-	-	-
GXR-1 Meas	-	-	-	-	-	-	-	-	-	-	-	-
GXR-1 Cert	-	-	-	-	-	-	-	-	-	-	-	-
GXR-1 Meas	-	-	-	-	-	-	-	-	-	-	-	-
GXR-1 Cert	-	-	-	-	-	-	-	-	-	-	-	-
NIST 694 Meas	-	-	-	-	-	-	-	-	-	-	-	-
NIST 694 Cert	-	-	-	-	-	-	-	-	-	-	-	-
DNC-1 Meas	-	-	-	-	-	3.8	-	-	-	4.8	250	6
DNC-1 Cert	-	-	-	-	-	3.6	-	-	-	5.2	247	6.3
GBW 07113 Meas	-	-	-	-	-	-	-	-	-	-	-	-
GBW 07113 Cert	-	-	-	-	-	-	-	-	-	-	-	-
GXR-4 Meas	-	-	-	-	-	-	-	-	-	-	-	-
GXR-4 Cert	-	-	-	-	-	-	-	-	-	-	-	-
GXR-4 Meas	-	-	-	-	-	-	-	-	-	-	-	-
GXR-4 Cert	-	-	-	-	-	-	-	-	-	-	-	-
GXR-4 Meas	-	-	-	-	-	-	-	-	-	-	-	-
GXR-4 Cert	-	-	-	-	-	-	-	-	-	-	-	-
SDC-1 Meas	-	-	-	-	-	-	-	-	-	-	-	-
SDC-1 Cert	-	-	-	-	-	-	-	-	-	-	-	-
SDC-1 Meas	-	-	-	-	-	-	-	-	-	-	-	-

Analyte	Gd	Ge	Hf	Ho	In	La	Lu	Mo	Nb	Nd	Ni	Pb
Units	ppm	ppm	ppm	ppm	ppm	ppm	ppm	ppm	ppm	ppm	ppm	ppm
Detection Limit	0.01	0.5	0.1	0.01	0.1	0.05	0.002	2	0.2	0.05	20	5
Method	FUS-MS	FUS-MS	FUS-MS	FUS-MS	FUS-MS	FUS-MS	FUS-MS	FUS-MS	FUS-MS	FUS-MS	FUS-MS	FUS-MS
SDC-1 Cert	-	-	-	-	-	-	-	-	-	-	-	-
GXR-6 Meas	-	-	-	-	-	-	-	-	-	-	-	-
GXR-6 Cert	-	-	-	-	-	-	-	-	-	-	-	-
GXR-6 Meas	-	-	-	-	-	-	-	-	-	-	-	-
GXR-6 Cert	-	-	-	-	-	-	-	-	-	-	-	-
GXR-6 Meas	-	-	-	-	-	-	-	-	-	-	-	-
GXR-6 Cert	-	-	-	-	-	-	-	-	-	-	-	-
LKSD-3 Meas	-	-	4.5	-	-	50.2	0.4	<2	-	43.4	50	-
LKSD-3 Cert	-	-	4.8	-	-	52	0.4	2	-	44	47	-
TDB-1 Meas	-	-	-	-	-	17	-	-	-	24.3	90	-
TDB-1 Cert	-	-	-	-	-	17	-	-	-	23	92	-
SY-2 Meas	-	-	-	-	-	-	-	-	-	-	-	-
SY-2 Cert	-	-	-	-	-	-	-	-	-	-	-	-
SY-3 Meas	-	-	-	-	-	-	-	-	-	-	-	-
SY-3 Cert	-	-	-	-	-	-	-	-	-	-	-	-
BaSO4 Meas	-	-	-	-	-	-	-	-	-	-	-	-
BaSO4 Cert	-	-	-	-	-	-	-	-	-	-	-	-
W-2a Meas	-	1.7	2.5	0.79	-	10.6	0.32	<2	7.8	13.1	70	-
W-2a Cert	-	1	2.6	0.76	-	10	0.33	0.6	7.9	13	70	-
SY-4 Meas	-	-	-	-	-	-	-	-	-	-	-	-
SY-4 Cert	-	-	-	-	-	-	-	-	-	-	-	-
CTA-AC-1 Meas	119	-	1.2	-	-	>2000	1.02	-	-	1130	-	-
CTA-AC-1 Cert	124	-	1.13	-	-	2176	1.08	-	-	1087	-	-
BIR-1a Meas	1.9	-	0.6	-	-	0.6	-	-	0.6	2.4	170	<5
BIR-1a Cert	2	-	0.6	-	-	0.63	-	-	0.6	2.5	170	3
NCS DC86312 Meas	231	-	-	34.1	-	>2000	11.8	-	-	1580	-	-
NCS DC86312 Cert	225	-	-	36	-	2360	11.96	-	-	1600	-	-
JGb-2 Meas	-	-	-	-	-	-	-	-	-	-	-	-
JGb-2 Cert	-	-	-	-	-	-	-	-	-	-	-	-
JGb-2 Meas	-	-	-	-	-	-	-	-	-	-	-	-
JGb-2 Cert	-	-	-	-	-	-	-	-	-	-	-	-
JGb-2 Meas	-	-	-	-	-	-	-	-	-	-	-	-
JGb-2 Cert	-	-	-	-	-	-	-	-	-	-	-	-
NCS DC70009 (GBW07241) Meas	15	10.2	-	4.2	1	24.2	2.31	-	-	33	-	-
NCS DC70009 (GBW07241) Cert	14.8	11.2	-	4.5	1.3	23.7	2.4	-	-	32.9	-	-
SGR-1b Meas	-	-	-	-	-	-	-	-	-	-	-	-
SGR-1b Cert	-	-	-	-	-	-	-	-	-	-	-	-



Analyte	Gd	Ge	Hf	Ho	In	La	Lu	Mo	Nb	Nd	Ni	Pb
Units	ppm	ppm	ppm	ppm	ppm	ppm	ppm	ppm	ppm	ppm	ppm	ppm
Detection Limit	0.01	0.5	0.1	0.01	0.1	0.05	0.002	2	0.2	0.05	20	5
Method	FUS-MS	FUS-MS	FUS-MS	FUS-MS	FUS-MS	FUS-MS	FUS-MS	FUS-MS	FUS-MS	FUS-MS	FUS-MS	FUS-MS
OREAS 100a (Fusion) Meas	22.2	-	-	4.7	-	269	2.12	23	-	152	-	-
OREAS 100a (Fusion) Cert	23.6	-	-	4.81	-	260	2.26	24.1	-	152	-	-
OREAS 101a (Fusion) Meas	43.7	-	-	6.29	-	833	2.49	21	-	391	-	-
OREAS 101a (Fusion) Cert	43.4	-	-	6.46	-	816	2.66	21.9	-	403	-	-
OREAS 101b (Fusion) Meas	-	-	-	6.43	-	829	2.63	20	-	389	-	-
OREAS 101b (Fusion) Cert	-	-	-	6.34	-	789	2.58	21	-	378	-	-
JR-1 Meas	5.5	-	4.4	1.15	<0.1	20.3	0.7	3	15	23.4	<20	19
JR-1 Cert	5.06	-	4.51	1.11	0.028	19.7	0.71	3.25	15.2	23.3	1.67	19.3
NCS DC86318 Meas	>1000	-	-	596	-	2000	247	-	-	>2000	-	-
NCS DC86318 Cert	2095	-	-	560	-	1960	260	-	-	3430	-	-
USZ 25-2006 Meas	-	-	-	-	-	-	-	-	-	-	-	-
USZ 25-2006 Cert	-	-	-	-	-	-	-	-	-	-	-	-
USZ 25-2006 Meas	-	-	-	-	-	-	-	-	-	-	-	-
USZ 25-2006 Cert	-	-	-	-	-	-	-	-	-	-	-	-
DNC-1a Meas	-	-	-	-	-	-	-	-	-	-	-	-
DNC-1a Cert	-	-	-	-	-	-	-	-	-	-	-	-
DNC-1a Meas	-	-	-	-	-	-	-	-	-	-	-	-
DNC-1a Cert	-	-	-	-	-	-	-	-	-	-	-	-
GS311-4 Meas	-	-	-	-	-	-	-	-	-	-	-	-
GS311-4 Cert	-	-	-	-	-	-	-	-	-	-	-	-
GS900-5 Meas	-	-	-	-	-	-	-	-	-	-	-	-
GS900-5 Cert	-	-	-	-	-	-	-	-	-	-	-	-
OREAS 45d (Aqua Regia) Meas	-	-	-	-	-	-	-	-	-	-	-	-
OREAS 45d (Aqua Regia) Cert	-	-	-	-	-	-	-	-	-	-	-	-
SBC-1 Meas	-	-	-	-	-	-	-	-	-	-	-	-
SBC-1 Cert	-	-	-	-	-	-	-	-	-	-	-	-
SBC-1 Meas	-	-	-	-	-	-	-	-	-	-	-	-
SBC-1 Cert	-	-	-	-	-	-	-	-	-	-	-	-
OREAS 45d (4-Acid) Meas	-	-	-	-	-	-	-	-	-	-	-	-
OREAS 45d (4-Acid) Cert	-	-	-	-	-	-	-	-	-	-	-	-
OREAS 45d (4-Acid) Meas	-	-	-	-	-	-	-	-	-	-	-	-
OREAS 45d (4-Acid) Cert	-	-	-	-	-	-	-	-	-	-	-	-
CaCO3 Meas	-	-	-	-	-	-	-	-	-	-	-	-
CaCO3 Cert	-	-	-	-	-	-	-	-	-	-	-	-
CaCO3 Meas	-	-	-	-	-	-	-	-	-	-	-	-
CaCO3 Cert	-	-	-	-	-	-	-	-	-	-	-	-
SdAR-M2 (U.S.G.S.) Meas	-	-	-	-	-	-	-	-	-	-	-	-

Analyte	Gd	Ge	Hf	Ho	In	La	Lu	Mo	Nb	Nd	Ni	Pb
Units	ppm	ppm	ppm	ppm	ppm	ppm	ppm	ppm	ppm	ppm	ppm	ppm
Detection Limit	0.01	0.5	0.1	0.01	0.1	0.05	0.002	2	0.2	0.05	20	5
Method	FUS-MS	FUS-MS	FUS-MS	FUS-MS	FUS-MS	FUS-MS	FUS-MS	FUS-MS	FUS-MS	FUS-MS	FUS-MS	FUS-MS
SdAR-M2 (U.S.G.S.) Cert	-	-	-	-	-	-	-	-	-	-	-	-
SdAR-M2 (U.S.G.S.) Meas	-	-	-	-	-	-	-	-	-	-	-	-
SdAR-M2 (U.S.G.S.) Cert	-	-	-	-	-	-	-	-	-	-	-	-
SdAR-M2 (U.S.G.S.) Meas	-	-	-	-	-	-	-	-	-	-	-	-
SdAR-M2 (U.S.G.S.) Cert	-	-	-	-	-	-	-	-	-	-	-	-
OREAS 214 Meas	-	-	-	-	-	-	-	-	-	-	-	-
OREAS 214 Cert	-	-	-	-	-	-	-	-	-	-	-	-
OREAS 218 Meas	-	-	-	-	-	-	-	-	-	-	-	-
OREAS 218 Cert	-	-	-	-	-	-	-	-	-	-	-	-
OREAS 218 Meas	-	-	-	-	-	-	-	-	-	-	-	-
OREAS 218 Cert	-	-	-	-	-	-	-	-	-	-	-	-
T9 Geochem Orig	-	-	-	-	-	-	-	-	-	-	-	-
T9 Geochem Dup	-	-	-	-	-	-	-	-	-	-	-	-
T14 Geochem Orig	-	-	-	-	-	-	-	-	-	-	-	-
T14 Geochem Dup	-	-	-	-	-	-	-	-	-	-	-	-
T17 Geochem Orig	-	-	-	-	-	-	-	-	-	-	-	-
T17 Geochem Dup	-	-	-	-	-	-	-	-	-	-	-	-
STPL-BAS-025 Orig	-	-	-	-	-	-	-	-	-	-	-	-
STPL-BAS-025 Dup	-	-	-	-	-	-	-	-	-	-	-	-
T24 Geochem Orig	0.51	<0.5	0.4	0.12	<0.1	2.37	0.077	<2	0.2	2.17	<20	<5
T24 Geochem Dup	0.54	<0.5	0.2	0.12	<0.1	2.36	0.071	<2	<0.2	1.89	<20	<5
T27 Geochem Orig	-	-	-	-	-	-	-	-	-	-	-	-
T27 Geochem Dup	-	-	-	-	-	-	-	-	-	-	-	-
T31 Geochem Orig	-	-	-	-	-	-	-	-	-	-	-	-
T31 Geochem Dup	-	-	-	-	-	-	-	-	-	-	-	-
T37 Geochem Orig	-	-	-	-	-	-	-	-	-	-	-	-
T37 Geochem Dup	-	-	-	-	-	-	-	-	-	-	-	-
T42 Geochem Orig	-	-	-	-	-	-	-	-	-	-	-	-
T42 Geochem Dup	-	-	-	-	-	-	-	-	-	-	-	-
T45 Geochem Orig	-	-	-	-	-	-	-	-	-	-	-	-
T45 Geochem Dup	-	-	-	-	-	-	-	-	-	-	-	-
STPL-53-PML-036 Orig	-	-	-	-	-	-	-	-	-	-	-	-
STPL-53-PML-036 Dup	-	-	-	-	-	-	-	-	-	-	-	-
STPL-BAS-025 Orig	-	-	-	-	-	-	-	-	-	-	-	-
STPL-BAS-025 Dup	-	-	-	-	-	-	-	-	-	-	-	-
T42 Geochem Orig	-	-	-	-	-	-	-	-	-	-	-	-
T42 Geochem Dup	-	-	-	-	-	-	-	-	-	-	-	-

Analyte	Gd	Ge	Hf	Ho	In	La	Lu	Mo	Nb	Nd	Ni	Pb
Units	ppm	ppm	ppm	ppm	ppm	ppm	ppm	ppm	ppm	ppm	ppm	ppm
Detection Limit	0.01	0.5	0.1	0.01	0.1	0.05	0.002	2	0.2	0.05	20	5
Method	FUS-MS	FUS-MS	FUS-MS	FUS-MS	FUS-MS	FUS-MS	FUS-MS	FUS-MS	FUS-MS	FUS-MS	FUS-MS	FUS-MS
T45 Geochem Orig	-	-	-	-	-	-	-	-	-	-	-	-
T45 Geochem Dup	-	-	-	-	-	-	-	-	-	-	-	-
T59 Orig	-	-	-	-	-	-	-	-	-	-	-	-
T59 Dup	-	-	-	-	-	-	-	-	-	-	-	-
T72 Orig	-	-	-	-	-	-	-	-	-	-	-	-
T72 Dup	-	-	-	-	-	-	-	-	-	-	-	-
T73 Orig	-	-	-	-	-	-	-	-	-	-	-	-
T73 Dup	-	-	-	-	-	-	-	-	-	-	-	-
STPL-BAS-029 Orig	-	-	-	-	-	-	-	-	-	-	-	-
STPL-BAS-029 Dup	-	-	-	-	-	-	-	-	-	-	-	-
T81 Orig	-	-	-	-	-	-	-	-	-	-	-	-
T81 Dup	-	-	-	-	-	-	-	-	-	-	-	-
T86 Orig	-	-	-	-	-	-	-	-	-	-	-	-
T86 Dup	-	-	-	-	-	-	-	-	-	-	-	-
T88 Orig	2.16	1.3	2.6	0.33	<0.1	14.8	0.14	<2	2.5	11.4	30	7
T88 Dup	2.12	1.3	2.6	0.32	<0.1	14.5	0.157	<2	2.6	11.5	30	<5
T89 Orig	-	-	-	-	-	-	-	-	-	-	-	-
T89 Dup	-	-	-	-	-	-	-	-	-	-	-	-
T94 Orig	-	-	-	-	-	-	-	-	-	-	-	-
T94 Dup	-	-	-	-	-	-	-	-	-	-	-	-
T98 Orig	-	-	-	-	-	-	-	-	-	-	-	-
T98 Dup	-	-	-	-	-	-	-	-	-	-	-	-
T99 Orig	-	-	-	-	-	-	-	-	-	-	-	-
T99 Dup	-	-	-	-	-	-	-	-	-	-	-	-
T101 Orig	-	-	-	-	-	-	-	-	-	-	-	-
T101 Dup	-	-	-	-	-	-	-	-	-	-	-	-
T102 Orig	-	-	-	-	-	-	-	-	-	-	-	-
T102 Dup	-	-	-	-	-	-	-	-	-	-	-	-
T114 Orig	-	-	-	-	-	-	-	-	-	-	-	-
T114 Dup	-	-	-	-	-	-	-	-	-	-	-	-
T116 Orig	-	-	-	-	-	-	-	-	-	-	-	-
T116 Dup	-	-	-	-	-	-	-	-	-	-	-	-
T117 Orig	1.76	0.9	2.3	0.25	<0.1	13.1	0.125	2	2.4	11.2	<20	<5
T117 Split PREP DUP	1.88	0.9	2.7	0.25	<0.1	12.6	0.129	2	2.4	10.7	<20	<5
STPL-53-PML-025 Orig	2.48	1.3	2.6	0.53	<0.1	42.8	0.345	<2	7.5	24.8	<20	8
STPL-53-PML-025 Dup	2.37	1.2	2.1	0.46	<0.1	39.5	0.315	<2	7.3	22.1	<20	7
T65 Orig	-	-	-	-	-	-	-	-	-	-	-	-

Analyte	Gd	Ge	Hf	Ho	In	La	Lu	Mo	Nb	Nd	Ni	Pb
Units	ppm	ppm	ppm	ppm	ppm	ppm	ppm	ppm	ppm	ppm	ppm	ppm
Detection Limit	0.01	0.5	0.1	0.01	0.1	0.05	0.002	2	0.2	0.05	20	5
Method	FUS-MS	FUS-MS	FUS-MS	FUS-MS	FUS-MS	FUS-MS	FUS-MS	FUS-MS	FUS-MS	FUS-MS	FUS-MS	FUS-MS
T65 Dup	-	-	-	-	-	-	-	-	-	-	-	-
T106 Orig	-	-	-	-	-	-	-	-	-	-	-	-
T106 Dup	-	-	-	-	-	-	-	-	-	-	-	-
T118 Orig	2.86	0.9	3.2	0.39	<0.1	22.6	0.158	<2	3.4	21.3	20	<5
T118 Dup	3.17	1	3.4	0.42	<0.1	23.9	0.178	<2	3.5	23.2	20	<5
T141 Orig	-	-	-	-	-	-	-	-	-	-	-	-
T141 Dup	-	-	-	-	-	-	-	-	-	-	-	-
STPL-BAS-023 Orig	-	-	-	-	-	-	-	-	-	-	-	-
STPL-BAS-023 Dup	-	-	-	-	-	-	-	-	-	-	-	-
T154 Orig	-	-	-	-	-	-	-	-	-	-	-	-
T154 Dup	-	-	-	-	-	-	-	-	-	-	-	-
T157 Orig	-	-	-	-	-	-	-	-	-	-	-	-
T157 Dup	-	-	-	-	-	-	-	-	-	-	-	-
T158 Orig	-	-	-	-	-	-	-	-	-	-	-	-
T158 Dup	-	-	-	-	-	-	-	-	-	-	-	-
STPL-PML-53-027 Orig	2.62	1.4	2.6	0.5	<0.1	42.2	0.323	<2	8.6	24.2	<20	8
STPL-PML-53-027 Dup	2.57	1.4	2.7	0.51	<0.1	42.2	0.334	<2	8.3	24	<20	8
T182 Orig	-	-	-	-	-	-	-	-	-	-	-	-
T182 Dup	-	-	-	-	-	-	-	-	-	-	-	-
T183 Orig	-	-	-	-	-	-	-	-	-	-	-	-
T183 Dup	-	-	-	-	-	-	-	-	-	-	-	-
T187 Orig	-	-	-	-	-	-	-	-	-	-	-	-
T187 Dup	-	-	-	-	-	-	-	-	-	-	-	-
T188 Orig	-	-	-	-	-	-	-	-	-	-	-	-
T188 Dup	-	-	-	-	-	-	-	-	-	-	-	-
T189 Orig	-	-	-	-	-	-	-	-	-	-	-	-
T189 Dup	-	-	-	-	-	-	-	-	-	-	-	-
T200 Orig	1.74	1.2	1	0.46	<0.1	2.09	0.235	<2	1.2	3.99	280	<5
T200 Dup	1.62	1.2	0.9	0.43	<0.1	2.15	0.222	<2	1.1	3.95	270	<5
T218 Orig	-	-	-	-	-	-	-	-	-	-	-	-
T218 Dup	-	-	-	-	-	-	-	-	-	-	-	-
T239 Orig	-	-	-	-	-	-	-	-	-	-	-	-
T239 Dup	-	-	-	-	-	-	-	-	-	-	-	-
T240 Orig	-	-	-	-	-	-	-	-	-	-	-	-
T240 Dup	-	-	-	-	-	-	-	-	-	-	-	-
T242 Orig	-	-	-	-	-	-	-	-	-	-	-	-
T242 Dup	-	-	-	-	-	-	-	-	-	-	-	-







Analyte	Pr	Rb	Sb	Sm	Sn	Ta	Tb	Th	Tl	Tm	U	W
Units	ppm	ppm	ppm	ppm	ppm	ppm	ppm	ppm	ppm	ppm	ppm	ppm
Detection Limit	0.01	1	0.2	0.01	1	0.01	0.01	0.05	0.05	0.005	0.01	0.5
Method	FUS-MS	FUS-MS	FUS-MS	FUS-MS	FUS-MS	FUS-MS	FUS-MS	FUS-MS	FUS-MS	FUS-MS	FUS-MS	FUS-MS
GXR-1 Meas	-	-	-	-	-	-	-	-	-	-	-	-
GXR-1 Cert	-	-	-	-	-	-	-	-	-	-	-	-
NIST 694 Meas	-	-	-	-	-	-	-	-	-	-	-	-
NIST 694 Cert	-	-	-	-	-	-	-	-	-	-	-	-
DNC-1 Meas	-	-	1	-	-	-	-	-	-	-	-	-
DNC-1 Cert	-	-	0.96	-	-	-	-	-	-	-	-	-
GBW 07113 Meas	-	-	-	-	-	-	-	-	-	-	-	-
GBW 07113 Cert	-	-	-	-	-	-	-	-	-	-	-	-
GBW 07113 Meas	-	-	-	-	-	-	-	-	-	-	-	-
GBW 07113 Cert	-	-	-	-	-	-	-	-	-	-	-	-
GBW 07113 Meas	-	-	-	-	-	-	-	-	-	-	-	-
GBW 07113 Cert	-	-	-	-	-	-	-	-	-	-	-	-
GXR-4 Meas	-	-	-	-	-	-	-	-	-	-	-	-
GXR-4 Cert	-	-	-	-	-	-	-	-	-	-	-	-
GXR-6 Meas	-	-	-	-	-	-	-	-	-	-	-	-
GXR-6 Cert	-	-	-	-	-	-	-	-	-	-	-	-
LKSD-3 Meas	-	76	1.2	8.2	2	0.71	-	11.8	-	-	4.7	<0.5
LKSD-3 Cert	-	78	1.3	8	3	0.7	-	11.4	-	-	4.6	2
TDB-1 Meas	-	-	-	-	-	-	-	-	-	-	-	-
TDB-1 Cert	-	-	-	-	-	-	-	-	-	-	-	-
SY-2 Meas	-	-	-	-	-	-	-	-	-	-	-	-
SY-2 Cert	-	-	-	-	-	-	-	-	-	-	-	-
SY-3 Meas	-	-	-	-	-	-	-	-	-	-	-	-
SY-3 Cert	-	-	-	-	-	-	-	-	-	-	-	-
BaSO4 Meas	-	-	-	-	-	-	-	-	-	-	-	-
BaSO4 Cert	-	-	-	-	-	-	-	-	-	-	-	-
BaSO4 Meas	-	-	-	-	-	-	-	-	-	-	-	-
BaSO4 Cert	-	-	-	-	-	-	-	-	-	-	-	-
BaSO4 Meas	-	-	-	-	-	-	-	-	-	-	-	-
BaSO4 Cert	-	-	-	-	-	-	-	-	-	-	-	-
W-2a Meas	-	19	-	3.3	-	-	0.59	2.2	0.05	-	0.52	<0.5
W-2a Cert	-	21	-	3.3	-	-	0.63	2.4	0.2	-	0.53	0.3
SY-4 Meas	-	-	-	-	-	-	-	-	-	-	-	-
SY-4 Cert	-	-	-	-	-	-	-	-	-	-	-	-
CTA-AC-1 Meas	-	-	-	164	-	2.45	14.7	-	-	-	4.6	-
CTA-AC-1 Cert	-	-	-	162	-	2.65	13.9	-	-	-	4.4	-
BIR-1a Meas	-	-	-	1.2	-	-	-	-	-	-	-	-



Analyte	Pr	Rb	Sb	Sm	Sn	Ta	Tb	Th	Tl	Tm	U	W
Units	ppm	ppm	ppm	ppm	ppm	ppm	ppm	ppm	ppm	ppm	ppm	ppm
Detection Limit	0.01	1	0.2	0.01	1	0.01	0.01	0.05	0.05	0.005	0.01	0.5
Method	FUS-MS	FUS-MS	FUS-MS	FUS-MS	FUS-MS	FUS-MS	FUS-MS	FUS-MS	FUS-MS	FUS-MS	FUS-MS	FUS-MS
BIR-1a Cert	-	-	-	1.1	-	-	-	-	-	-	-	-
BIR-1a Meas	-	-	-	-	-	-	-	-	-	-	-	-
BIR-1a Cert	-	-	-	-	-	-	-	-	-	-	-	-
NCS DC86312 Meas	-	-	-	-	-	-	33.7	25.8	-	15.1	-	-
NCS DC86312 Cert	-	-	-	-	-	-	34.6	23.6	-	15.1	-	-
JGb-2 Meas	-	-	-	-	-	-	-	-	-	-	-	-
JGb-2 Cert	-	-	-	-	-	-	-	-	-	-	-	-
JGb-2 Meas	-	-	-	-	-	-	-	-	-	-	-	-
JGb-2 Cert	-	-	-	-	-	-	-	-	-	-	-	-
JGb-2 Meas	-	-	-	-	-	-	-	-	-	-	-	-
JGb-2 Cert	-	-	-	-	-	-	-	-	-	-	-	-
JGb-2 Meas	-	-	-	-	-	-	-	-	-	-	-	-
JGb-2 Cert	-	-	-	-	-	-	-	-	-	-	-	-
JGb-2 Meas	-	-	-	-	-	-	-	-	-	-	-	-
JGb-2 Cert	-	-	-	-	-	-	-	-	-	-	-	-
JGb-2 Meas	-	-	-	-	-	-	-	-	-	-	-	-
JGb-2 Cert	-	-	-	-	-	-	-	-	-	-	-	-
SCH-1 Meas	-	-	-	-	-	-	-	-	-	-	-	-
SCH-1 Cert	-	-	-	-	-	-	-	-	-	-	-	-
NCS DC70009 (GBW07241) Meas	8	541	-	13.1	>1000	-	3.2	28.5	-	2.2	-	2100
NCS DC70009 (GBW07241) Cert	7.9	500	-	12.5	1701	-	3.3	28.3	-	2.2	-	2200
SGR-1b Meas	-	-	-	-	-	-	-	-	-	-	-	-
SGR-1b Cert	-	-	-	-	-	-	-	-	-	-	-	-
SGR-1b Meas	-	-	-	-	-	-	-	-	-	-	-	-
SGR-1b Cert	-	-	-	-	-	-	-	-	-	-	-	-
SGR-1b Meas	-	-	-	-	-	-	-	-	-	-	-	-
SGR-1b Cert	-	-	-	-	-	-	-	-	-	-	-	-
OREAS 100a (Fusion) Meas	49.3	-	-	23.4	-	-	3.69	52.9	-	2.45	148	-
OREAS 100a (Fusion) Cert	47.1	-	-	23.6	-	-	3.8	51.6	-	2.31	135	-
OREAS 101a (Fusion) Meas	138	-	-	53.4	-	-	-	36	-	3	457	-
OREAS 101a (Fusion) Cert	134	-	-	48.8	-	-	-	36.6	-	2.9	422	-
OREAS 101b (Fusion) Meas	129	-	-	50	-	-	5	38.1	-	2.89	418	-
OREAS 101b (Fusion) Cert	127	-	-	48	-	-	5.37	37.1	-	2.66	396	-
OREAS 98 (S by LECO) Meas	-	-	-	-	-	-	-	-	-	-	-	-
OREAS 98 (S by LECO) Cert	-	-	-	-	-	-	-	-	-	-	-	-
OREAS 132b (S by LECO) Meas	-	-	-	-	-	-	-	-	-	-	-	-
OREAS 132b (S by LECO) Cert	-	-	-	-	-	-	-	-	-	-	-	-
JR-1 Meas	5.9	265	1.2	5.9	3	1.81	0.99	26.4	1.5	0.7	9.6	1.8
JR-1 Cert	5.58	257	1.19	6.03	2.86	1.86	1.01	26.7	1.56	0.67	8.88	1.59

Analyte	Pr	Rb	Sb	Sm	Sn	Ta	Tb	Th	Tl	Tm	U	W
Units	ppm	ppm	ppm	ppm	ppm	ppm	ppm	ppm	ppm	ppm	ppm	ppm
Detection Limit	0.01	1	0.2	0.01	1	0.01	0.01	0.05	0.05	0.005	0.01	0.5
Method	FUS-MS	FUS-MS	FUS-MS	FUS-MS	FUS-MS	FUS-MS	FUS-MS	FUS-MS	FUS-MS	FUS-MS	FUS-MS	FUS-MS
NCS DC86318 Meas	727	377	-	>1000	-	-	479	69.3	-	277	-	-
NCS DC86318 Cert	740	369.42	-	1720	-	-	470	67	-	270	-	-
USZ 25-2006 Meas	-	-	-	-	-	-	-	-	-	-	-	-
USZ 25-2006 Cert	-	-	-	-	-	-	-	-	-	-	-	-
USZ 25-2006 Meas	-	-	-	-	-	-	-	-	-	-	-	-
USZ 25-2006 Cert	-	-	-	-	-	-	-	-	-	-	-	-
GS309-4 Meas	-	-	-	-	-	-	-	-	-	-	-	-
GS309-4 Cert	-	-	-	-	-	-	-	-	-	-	-	-
GS311-4 Meas	-	-	-	-	-	-	-	-	-	-	-	-
GS311-4 Cert	-	-	-	-	-	-	-	-	-	-	-	-
GS311-4 Meas	-	-	-	-	-	-	-	-	-	-	-	-
GS311-4 Cert	-	-	-	-	-	-	-	-	-	-	-	-
GS311-4 Meas	-	-	-	-	-	-	-	-	-	-	-	-
GS311-4 Cert	-	-	-	-	-	-	-	-	-	-	-	-
GS311-4 Meas	-	-	-	-	-	-	-	-	-	-	-	-
GS311-4 Cert	-	-	-	-	-	-	-	-	-	-	-	-
GS900-5 Meas	-	-	-	-	-	-	-	-	-	-	-	-
GS900-5 Cert	-	-	-	-	-	-	-	-	-	-	-	-
GS900-5 Meas	-	-	-	-	-	-	-	-	-	-	-	-
GS900-5 Cert	-	-	-	-	-	-	-	-	-	-	-	-
GS900-5 Meas	-	-	-	-	-	-	-	-	-	-	-	-
GS900-5 Cert	-	-	-	-	-	-	-	-	-	-	-	-
OREAS 45d (Aqua Regia) Meas	-	-	-	-	-	-	-	-	-	-	-	-
OREAS 45d (Aqua Regia) Cert	-	-	-	-	-	-	-	-	-	-	-	-
CDN-PGMS-24 Meas	-	-	-	-	-	-	-	-	-	-	-	-
CDN-PGMS-24 Cert	-	-	-	-	-	-	-	-	-	-	-	-
CDN-PGMS-24 Meas	-	-	-	-	-	-	-	-	-	-	-	-
CDN-PGMS-24 Cert	-	-	-	-	-	-	-	-	-	-	-	-
CDN-PGMS-24 Meas	-	-	-	-	-	-	-	-	-	-	-	-
CDN-PGMS-24 Cert	-	-	-	-	-	-	-	-	-	-	-	-
CaCO3 Meas	-	-	-	-	-	-	-	-	-	-	-	-
CaCO3 Cert	-	-	-	-	-	-	-	-	-	-	-	-
CaCO3 Meas	-	-	-	-	-	-	-	-	-	-	-	-
CaCO3 Cert	-	-	-	-	-	-	-	-	-	-	-	-
SdAR-M2 (U.S.G.S.) Meas	-	-	-	-	-	-	-	-	-	-	-	-
SdAR-M2 (U.S.G.S.) Cert	-	-	-	-	-	-	-	-	-	-	-	-
GXR-1 Meas	-	-	-	-	-	-	-	-	-	-	-	-

Analyte	Pr	Rb	Sb	Sm	Sn	Ta	Tb	Th	Tl	Tm	U	W
Units	ppm	ppm	ppm	ppm	ppm	ppm	ppm	ppm	ppm	ppm	ppm	ppm
Detection Limit	0.01	1	0.2	0.01	1	0.01	0.01	0.05	0.05	0.005	0.01	0.5
Method	FUS-MS	FUS-MS	FUS-MS	FUS-MS	FUS-MS	FUS-MS	FUS-MS	FUS-MS	FUS-MS	FUS-MS	FUS-MS	FUS-MS
GXR-1 Cert	-	-	-	-	-	-	-	-	-	-	-	-
GXR-1 Meas	-	-	-	-	-	-	-	-	-	-	-	-
GXR-1 Cert	-	-	-	-	-	-	-	-	-	-	-	-
GXR-1 Meas	-	-	-	-	-	-	-	-	-	-	-	-
GXR-1 Cert	-	-	-	-	-	-	-	-	-	-	-	-
GXR-1 Meas	-	-	-	-	-	-	-	-	-	-	-	-
GXR-1 Cert	-	-	-	-	-	-	-	-	-	-	-	-
NIST 694 Meas	-	-	-	-	-	-	-	-	-	-	-	-
NIST 694 Cert	-	-	-	-	-	-	-	-	-	-	-	-
DNC-1 Meas	-	-	-	-	-	-	-	-	-	-	-	-
DNC-1 Cert	-	-	-	-	-	-	-	-	-	-	-	-
GBW 07113 Meas	-	-	-	-	-	-	-	-	-	-	-	-
GBW 07113 Cert	-	-	-	-	-	-	-	-	-	-	-	-
GXR-4 Meas	-	-	-	-	-	-	-	-	-	-	-	-
GXR-4 Cert	-	-	-	-	-	-	-	-	-	-	-	-
GXR-4 Meas	-	-	-	-	-	-	-	-	-	-	-	-
GXR-4 Cert	-	-	-	-	-	-	-	-	-	-	-	-
GXR-4 Meas	-	-	-	-	-	-	-	-	-	-	-	-
GXR-4 Cert	-	-	-	-	-	-	-	-	-	-	-	-
GXR-4 Meas	-	-	-	-	-	-	-	-	-	-	-	-
GXR-4 Cert	-	-	-	-	-	-	-	-	-	-	-	-
SDC-1 Meas	-	-	-	-	-	-	-	-	-	-	-	-
SDC-1 Cert	-	-	-	-	-	-	-	-	-	-	-	-
SDC-1 Meas	-	-	-	-	-	-	-	-	-	-	-	-
SDC-1 Cert	-	-	-	-	-	-	-	-	-	-	-	-
SDC-1 Meas	-	-	-	-	-	-	-	-	-	-	-	-
SDC-1 Cert	-	-	-	-	-	-	-	-	-	-	-	-
SDC-1 Meas	-	-	-	-	-	-	-	-	-	-	-	-
SDC-1 Cert	-	-	-	-	-	-	-	-	-	-	-	-
GXR-6 Meas	-	-	-	-	-	-	-	-	-	-	-	-
GXR-6 Cert	-	-	-	-	-	-	-	-	-	-	-	-
GXR-6 Meas	-	-	-	-	-	-	-	-	-	-	-	-
GXR-6 Cert	-	-	-	-	-	-	-	-	-	-	-	-
GXR-6 Meas	-	-	-	-	-	-	-	-	-	-	-	-
GXR-6 Cert	-	-	-	-	-	-	-	-	-	-	-	-
GXR-6 Meas	-	-	-	-	-	-	-	-	-	-	-	-
GXR-6 Cert	-	-	-	-	-	-	-	-	-	-	-	-

Analyte	Pr	Rb	Sb	Sm	Sn	Ta	Tb	Th	Tl	Tm	U	W
Units	ppm	ppm	ppm	ppm	ppm	ppm	ppm	ppm	ppm	ppm	ppm	ppm
Detection Limit	0.01	1	0.2	0.01	1	0.01	0.01	0.05	0.05	0.005	0.01	0.5
Method	FUS-MS	FUS-MS	FUS-MS	FUS-MS	FUS-MS	FUS-MS	FUS-MS	FUS-MS	FUS-MS	FUS-MS	FUS-MS	FUS-MS
LKSD-3 Meas	-	75	1.2	7.7	2	0.73	1	-	-	-	4.2	-
LKSD-3 Cert	-	78	1.3	8	3	0.7	1	-	-	-	4.6	-
TDB-1 Meas	-	21	-	-	-	-	-	-	-	-	-	-
TDB-1 Cert	-	23	-	-	-	-	-	-	-	-	-	-
SY-2 Meas	-	-	-	-	-	-	-	-	-	-	-	-
SY-2 Cert	-	-	-	-	-	-	-	-	-	-	-	-
SY-3 Meas	-	-	-	-	-	-	-	-	-	-	-	-
SY-3 Cert	-	-	-	-	-	-	-	-	-	-	-	-
BaSO4 Meas	-	-	-	-	-	-	-	-	-	-	-	-
BaSO4 Cert	-	-	-	-	-	-	-	-	-	-	-	-
BaSO4 Meas	-	-	-	-	-	-	-	-	-	-	-	-
BaSO4 Cert	-	-	-	-	-	-	-	-	-	-	-	-
W-2a Meas	-	20	-	3.4	-	0.47	0.64	2.4	0.06	-	0.53	<0.5
W-2a Cert	-	21	-	3.3	-	0.5	0.63	2.4	0.2	-	0.53	0.3
SY-4 Meas	-	-	-	-	-	-	-	-	-	-	-	-
SY-4 Cert	-	-	-	-	-	-	-	-	-	-	-	-
CTA-AC-1 Meas	-	-	-	158	-	2.45	13.5	22.5	-	-	4	-
CTA-AC-1 Cert	-	-	-	162	-	2.65	13.9	21.8	-	-	4.4	-
BIR-1a Meas	-	-	-	1.1	-	-	-	-	-	-	-	-
BIR-1a Cert	-	-	-	1.1	-	-	-	-	-	-	-	-
Calcium Carbonate Meas	-	-	-	-	-	-	-	-	-	-	-	-
Calcium Carbonate Cert	-	-	-	-	-	-	-	-	-	-	-	-
NCS DC86312 Meas	-	-	-	-	-	-	37.5	24.3	-	13.2	-	-
NCS DC86312 Cert	-	-	-	-	-	-	34.6	23.6	-	15.1	-	-
JGb-2 Meas	-	-	-	-	-	-	-	-	-	-	-	-
JGb-2 Cert	-	-	-	-	-	-	-	-	-	-	-	-
JGb-2 Meas	-	-	-	-	-	-	-	-	-	-	-	-
JGb-2 Cert	-	-	-	-	-	-	-	-	-	-	-	-
JGb-2 Meas	-	-	-	-	-	-	-	-	-	-	-	-
JGb-2 Cert	-	-	-	-	-	-	-	-	-	-	-	-
NCS DC70009 (GBW07241) Meas	7.3	452	3	11.7	>1000	-	3.5	27.6	1.79	2.1	-	2120
NCS DC70009 (GBW07241) Cert	7.9	500	3.1	12.5	1701	-	3.3	28.3	1.8	2.2	-	2200
SGR-1b Meas	-	-	-	-	-	-	-	-	-	-	-	-
SGR-1b Cert	-	-	-	-	-	-	-	-	-	-	-	-
SGR-1b Meas	-	-	-	-	-	-	-	-	-	-	-	-
SGR-1b Cert	-	-	-	-	-	-	-	-	-	-	-	-
OREAS 100a (Fusion) Meas	44	-	-	23	-	-	4	48.7	-	2.2	132	-

Analyte	Pr	Rb	Sb	Sm	Sn	Ta	Tb	Th	Tl	Tm	U	W
Units	ppm	ppm	ppm	ppm	ppm	ppm	ppm	ppm	ppm	ppm	ppm	ppm
Detection Limit	0.01	1	0.2	0.01	1	0.01	0.01	0.05	0.05	0.005	0.01	0.5
Method	FUS-MS	FUS-MS	FUS-MS	FUS-MS	FUS-MS	FUS-MS	FUS-MS	FUS-MS	FUS-MS	FUS-MS	FUS-MS	FUS-MS
OREAS 100a (Fusion) Cert	47.1	-	-	23.6	-	-	3.8	51.6	-	2.31	135	-
OREAS 101a (Fusion) Meas	123	-	-	47.6	-	-	5.96	34	-	2.7	402	-
OREAS 101a (Fusion) Cert	134	-	-	48.8	-	-	5.92	36.6	-	2.9	422	-
OREAS 101b (Fusion) Meas	126	-	-	49	-	-	5.39	38	-	2.76	405	-
OREAS 101b (Fusion) Cert	127	-	-	48	-	-	5.37	37.1	-	2.66	396	-
JR-1 Meas	5.6	252	-	5.46	3	2.01	1.09	25.4	1.5	0.62	8.6	1.7
JR-1 Cert	5.58	257	-	6.03	2.86	1.86	1.01	26.7	1.56	0.67	8.88	1.59
NCS DC86318 Meas	738	383	-	>1000	-	-	504	70.3	-	269	-	-
NCS DC86318 Cert	740	369.42	-	1720	-	-	470	67	-	270	-	-
USZ 25-2006 Meas	-	-	-	-	-	-	-	-	-	-	-	-
USZ 25-2006 Cert	-	-	-	-	-	-	-	-	-	-	-	-
USZ 25-2006 Meas	-	-	-	-	-	-	-	-	-	-	-	-
USZ 25-2006 Cert	-	-	-	-	-	-	-	-	-	-	-	-
DNC-1a Meas	-	-	-	-	-	-	-	-	-	-	-	-
DNC-1a Cert	-	-	-	-	-	-	-	-	-	-	-	-
DNC-1a Meas	-	-	-	-	-	-	-	-	-	-	-	-
DNC-1a Cert	-	-	-	-	-	-	-	-	-	-	-	-
DNC-1a Meas	-	-	-	-	-	-	-	-	-	-	-	-
DNC-1a Cert	-	-	-	-	-	-	-	-	-	-	-	-
DNC-1a Meas	-	-	-	-	-	-	-	-	-	-	-	-
DNC-1a Cert	-	-	-	-	-	-	-	-	-	-	-	-
DNC-1a Meas	-	-	-	-	-	-	-	-	-	-	-	-
DNC-1a Cert	-	-	-	-	-	-	-	-	-	-	-	-
GS311-4 Meas	-	-	-	-	-	-	-	-	-	-	-	-
GS311-4 Cert	-	-	-	-	-	-	-	-	-	-	-	-
GS311-4 Meas	-	-	-	-	-	-	-	-	-	-	-	-
GS311-4 Cert	-	-	-	-	-	-	-	-	-	-	-	-
GS900-5 Meas	-	-	-	-	-	-	-	-	-	-	-	-
GS900-5 Cert	-	-	-	-	-	-	-	-	-	-	-	-
GS900-5 Meas	-	-	-	-	-	-	-	-	-	-	-	-
GS900-5 Cert	-	-	-	-	-	-	-	-	-	-	-	-
OREAS 45d (Aqua Regia) Meas	-	-	-	-	-	-	-	-	-	-	-	-
OREAS 45d (Aqua Regia) Cert	-	-	-	-	-	-	-	-	-	-	-	-
OREAS 45d (Aqua Regia) Meas	-	-	-	-	-	-	-	-	-	-	-	-
OREAS 45d (Aqua Regia) Cert	-	-	-	-	-	-	-	-	-	-	-	-
OREAS 45d (Aqua Regia) Meas	-	-	-	-	-	-	-	-	-	-	-	-
OREAS 45d (Aqua Regia) Cert	-	-	-	-	-	-	-	-	-	-	-	-
SBC-1 Meas	-	-	-	-	-	-	-	-	-	-	-	-
SBC-1 Cert	-	-	-	-	-	-	-	-	-	-	-	-

Analyte	Pr	Rb	Sb	Sm	Sn	Ta	Tb	Th	Tl	Tm	U	W
Units	ppm	ppm	ppm	ppm	ppm	ppm	ppm	ppm	ppm	ppm	ppm	ppm
Detection Limit	0.01	1	0.2	0.01	1	0.01	0.01	0.05	0.05	0.005	0.01	0.5
Method	FUS-MS	FUS-MS	FUS-MS	FUS-MS	FUS-MS	FUS-MS	FUS-MS	FUS-MS	FUS-MS	FUS-MS	FUS-MS	FUS-MS
SBC-1 Meas	-	-	-	-	-	-	-	-	-	-	-	-
SBC-1 Cert	-	-	-	-	-	-	-	-	-	-	-	-
SBC-1 Meas	-	-	-	-	-	-	-	-	-	-	-	-
SBC-1 Cert	-	-	-	-	-	-	-	-	-	-	-	-
SBC-1 Meas	-	-	-	-	-	-	-	-	-	-	-	-
SBC-1 Cert	-	-	-	-	-	-	-	-	-	-	-	-
OREAS 45d (4-Acid) Meas	-	-	-	-	-	-	-	-	-	-	-	-
OREAS 45d (4-Acid) Cert	-	-	-	-	-	-	-	-	-	-	-	-
OREAS 45d (4-Acid) Meas	-	-	-	-	-	-	-	-	-	-	-	-
OREAS 45d (4-Acid) Cert	-	-	-	-	-	-	-	-	-	-	-	-
OREAS 45d (4-Acid) Meas	-	-	-	-	-	-	-	-	-	-	-	-
OREAS 45d (4-Acid) Cert	-	-	-	-	-	-	-	-	-	-	-	-
OREAS 45d (4-Acid) Meas	-	-	-	-	-	-	-	-	-	-	-	-
OREAS 45d (4-Acid) Cert	-	-	-	-	-	-	-	-	-	-	-	-
OxK110 Meas	-	-	-	-	-	-	-	-	-	-	-	-
OxK110 Cert	-	-	-	-	-	-	-	-	-	-	-	-
CDN-PGMS-24 Meas	-	-	-	-	-	-	-	-	-	-	-	-
CDN-PGMS-24 Cert	-	-	-	-	-	-	-	-	-	-	-	-
CDN-PGMS-24 Meas	-	-	-	-	-	-	-	-	-	-	-	-
CDN-PGMS-24 Cert	-	-	-	-	-	-	-	-	-	-	-	-
OXN117 Meas	-	-	-	-	-	-	-	-	-	-	-	-
OXN117 Cert	-	-	-	-	-	-	-	-	-	-	-	-
CaCO3 Meas	-	-	-	-	-	-	-	-	-	-	-	-
CaCO3 Cert	-	-	-	-	-	-	-	-	-	-	-	-
SdAR-M2 (U.S.G.S.) Meas	-	-	-	-	-	-	-	-	-	-	-	-
SdAR-M2 (U.S.G.S.) Cert	-	-	-	-	-	-	-	-	-	-	-	-
SdAR-M2 (U.S.G.S.) Meas	-	-	-	-	-	-	-	-	-	-	-	-
SdAR-M2 (U.S.G.S.) Cert	-	-	-	-	-	-	-	-	-	-	-	-
SdAR-M2 (U.S.G.S.) Meas	-	-	-	-	-	-	-	-	-	-	-	-
SdAR-M2 (U.S.G.S.) Cert	-	-	-	-	-	-	-	-	-	-	-	-
SdAR-M2 (U.S.G.S.) Meas	-	-	-	-	-	-	-	-	-	-	-	-
SdAR-M2 (U.S.G.S.) Cert	-	-	-	-	-	-	-	-	-	-	-	-
GXR-1 Meas	-	-	-	-	-	-	-	-	-	-	-	-
GXR-1 Cert	-	-	-	-	-	-	-	-	-	-	-	-
GXR-1 Meas	-	-	-	-	-	-	-	-	-	-	-	-
GXR-1 Cert	-	-	-	-	-	-	-	-	-	-	-	-
NIST 694 Meas	-	-	-	-	-	-	-	-	-	-	-	-

Analyte	Pr	Rb	Sb	Sm	Sn	Ta	Tb	Th	Tl	Tm	U	W
Units	ppm	ppm	ppm	ppm	ppm	ppm	ppm	ppm	ppm	ppm	ppm	ppm
Detection Limit	0.01	1	0.2	0.01	1	0.01	0.01	0.05	0.05	0.005	0.01	0.5
Method	FUS-MS	FUS-MS	FUS-MS	FUS-MS	FUS-MS	FUS-MS	FUS-MS	FUS-MS	FUS-MS	FUS-MS	FUS-MS	FUS-MS
NIST 694 Cert	-	-	-	-	-	-	-	-	-	-	-	-
DNC-1 Meas	-	4	0.9	-	-	-	-	-	-	-	-	-
DNC-1 Cert	-	5	0.96	-	-	-	-	-	-	-	-	-
GBW 07113 Meas	-	-	-	-	-	-	-	-	-	-	-	-
GBW 07113 Cert	-	-	-	-	-	-	-	-	-	-	-	-
GXR-4 Meas	-	-	-	-	-	-	-	-	-	-	-	-
GXR-4 Cert	-	-	-	-	-	-	-	-	-	-	-	-
GXR-4 Meas	-	-	-	-	-	-	-	-	-	-	-	-
GXR-4 Cert	-	-	-	-	-	-	-	-	-	-	-	-
SDC-1 Meas	-	-	-	-	-	-	-	-	-	-	-	-
SDC-1 Cert	-	-	-	-	-	-	-	-	-	-	-	-
GXR-6 Meas	-	-	-	-	-	-	-	-	-	-	-	-
GXR-6 Cert	-	-	-	-	-	-	-	-	-	-	-	-
GXR-6 Meas	-	-	-	-	-	-	-	-	-	-	-	-
GXR-6 Cert	-	-	-	-	-	-	-	-	-	-	-	-
LKSD-3 Meas	-	75	-	7.8	3	0.75	0.9	10.7	-	-	4.7	-
LKSD-3 Cert	-	78	-	8	3	0.7	1	11.4	-	-	4.6	-
TDB-1 Meas	-	-	-	-	-	-	-	2.8	-	-	-	-
TDB-1 Cert	-	-	-	-	-	-	-	2.7	-	-	-	-
SY-2 Meas	-	-	-	-	-	-	-	-	-	-	-	-
SY-2 Cert	-	-	-	-	-	-	-	-	-	-	-	-
SY-3 Meas	-	-	-	-	-	-	-	-	-	-	-	-
SY-3 Cert	-	-	-	-	-	-	-	-	-	-	-	-
BaSO4 Meas	-	-	-	-	-	-	-	-	-	-	-	-
BaSO4 Cert	-	-	-	-	-	-	-	-	-	-	-	-
BaSO4 Meas	-	-	-	-	-	-	-	-	-	-	-	-
BaSO4 Cert	-	-	-	-	-	-	-	-	-	-	-	-
BaSO4 Meas	-	-	-	-	-	-	-	-	-	-	-	-
BaSO4 Cert	-	-	-	-	-	-	-	-	-	-	-	-
W-2a Meas	-	20	-	3.3	-	0.52	0.59	2.3	<0.05	0.37	0.48	<0.5
W-2a Cert	-	21	-	3.3	-	0.5	0.63	2.4	0.2	0.38	0.53	0.3
DTS-2b Meas	-	-	-	-	-	-	-	-	-	-	-	-
DTS-2b Cert	-	-	-	-	-	-	-	-	-	-	-	-
SY-4 Meas	-	-	-	-	-	-	-	-	-	-	-	-
SY-4 Cert	-	-	-	-	-	-	-	-	-	-	-	-
CTA-AC-1 Meas	-	-	-	155	-	2.7	13.7	20	-	-	4.5	-
CTA-AC-1 Cert	-	-	-	162	-	2.65	13.9	21.8	-	-	4.4	-

Analyte	Pr	Rb	Sb	Sm	Sn	Ta	Tb	Th	Tl	Tm	U	W
Units	ppm	ppm	ppm	ppm	ppm	ppm	ppm	ppm	ppm	ppm	ppm	ppm
Detection Limit	0.01	1	0.2	0.01	1	0.01	0.01	0.05	0.05	0.005	0.01	0.5
Method	FUS-MS	FUS-MS	FUS-MS	FUS-MS	FUS-MS	FUS-MS	FUS-MS	FUS-MS	FUS-MS	FUS-MS	FUS-MS	FUS-MS
BIR-1a Meas	-	-	-	1.1	-	-	-	-	-	-	-	-
BIR-1a Cert	-	-	-	1.1	-	-	-	-	-	-	-	-
NCS DC86312 Meas	-	-	-	-	-	-	32.9	22.2	-	14.5	-	-
NCS DC86312 Cert	-	-	-	-	-	-	34.6	23.6	-	15.1	-	-
JGb-2 Meas	-	-	-	-	-	-	-	-	-	-	-	-
JGb-2 Cert	-	-	-	-	-	-	-	-	-	-	-	-
NCS DC70009 (GBW07241) Meas	-	487	3	11.6	>1000	-	3.1	26.7	1.75	2	-	2180
NCS DC70009 (GBW07241) Cert	-	500	3.1	12.5	1701	-	3.3	28.3	1.8	2.2	-	2200
SGR-1b Meas	-	-	-	-	-	-	-	-	-	-	-	-
SGR-1b Cert	-	-	-	-	-	-	-	-	-	-	-	-
SGR-1b Meas	-	-	-	-	-	-	-	-	-	-	-	-
SGR-1b Cert	-	-	-	-	-	-	-	-	-	-	-	-
SGR-1b Meas	-	-	-	-	-	-	-	-	-	-	-	-
SGR-1b Cert	-	-	-	-	-	-	-	-	-	-	-	-
OREAS 100a (Fusion) Meas	43.6	-	-	21.6	-	-	3.96	50.5	-	2.15	129	-
OREAS 100a (Fusion) Cert	47.1	-	-	23.6	-	-	3.8	51.6	-	2.31	135	-
OREAS 101a (Fusion) Meas	126	-	-	44.9	-	-	6.29	35.5	-	2.8	420	-
OREAS 101a (Fusion) Cert	134	-	-	48.8	-	-	5.92	36.6	-	2.9	422	-
OREAS 101b (Fusion) Meas	127	-	-	50	-	-	-	34.4	-	2.75	385	-
OREAS 101b (Fusion) Cert	127	-	-	48	-	-	-	37.1	-	2.66	396	-
OREAS 98 (S by LECO) Meas	-	-	-	-	-	-	-	-	-	-	-	-
OREAS 98 (S by LECO) Cert	-	-	-	-	-	-	-	-	-	-	-	-
OREAS 132b (S by LECO) Meas	-	-	-	-	-	-	-	-	-	-	-	-
OREAS 132b (S by LECO) Cert	-	-	-	-	-	-	-	-	-	-	-	-
JR-1 Meas	6	250	-	5.68	3	1.97	0.91	25.4	1.5	0.64	8.4	2
JR-1 Cert	5.58	257	-	6.03	2.86	1.86	1.01	26.7	1.56	0.67	8.88	1.59
NCS DC86318 Meas	707	366	-	>1000	-	-	468	63.8	-	259	-	-
NCS DC86318 Cert	740	369.42	-	1720	-	-	470	67	-	270	-	-
USZ 25-2006 Meas	-	-	-	-	-	-	-	-	-	-	-	-
USZ 25-2006 Cert	-	-	-	-	-	-	-	-	-	-	-	-
DNC-1a Meas	-	-	-	-	-	-	-	-	-	-	-	-
DNC-1a Cert	-	-	-	-	-	-	-	-	-	-	-	-
PK2 Meas	-	-	-	-	-	-	-	-	-	-	-	-
PK2 Cert	-	-	-	-	-	-	-	-	-	-	-	-
GS309-4 Meas	-	-	-	-	-	-	-	-	-	-	-	-
GS309-4 Cert	-	-	-	-	-	-	-	-	-	-	-	-
GS311-4 Meas	-	-	-	-	-	-	-	-	-	-	-	-



Analyte	Pr	Rb	Sb	Sm	Sn	Ta	Tb	Th	Tl	Tm	U	W
Units	ppm	ppm	ppm	ppm	ppm	ppm	ppm	ppm	ppm	ppm	ppm	ppm
Detection Limit	0.01	1	0.2	0.01	1	0.01	0.01	0.05	0.05	0.005	0.01	0.5
Method	FUS-MS	FUS-MS	FUS-MS	FUS-MS	FUS-MS	FUS-MS	FUS-MS	FUS-MS	FUS-MS	FUS-MS	FUS-MS	FUS-MS
GS311-4 Cert	-	-	-	-	-	-	-	-	-	-	-	-
GS311-4 Meas	-	-	-	-	-	-	-	-	-	-	-	-
GS311-4 Cert	-	-	-	-	-	-	-	-	-	-	-	-
GS311-4 Meas	-	-	-	-	-	-	-	-	-	-	-	-
GS311-4 Cert	-	-	-	-	-	-	-	-	-	-	-	-
GS900-5 Meas	-	-	-	-	-	-	-	-	-	-	-	-
GS900-5 Cert	-	-	-	-	-	-	-	-	-	-	-	-
GS900-5 Meas	-	-	-	-	-	-	-	-	-	-	-	-
GS900-5 Cert	-	-	-	-	-	-	-	-	-	-	-	-
GS900-5 Meas	-	-	-	-	-	-	-	-	-	-	-	-
GS900-5 Cert	-	-	-	-	-	-	-	-	-	-	-	-
OREAS 45d (Aqua Regia) Meas	-	-	-	-	-	-	-	-	-	-	-	-
OREAS 45d (Aqua Regia) Cert	-	-	-	-	-	-	-	-	-	-	-	-
SBC-1 Meas	-	-	-	-	-	-	-	-	-	-	-	-
SBC-1 Cert	-	-	-	-	-	-	-	-	-	-	-	-
OREAS 45d (4-Acid) Meas	-	-	-	-	-	-	-	-	-	-	-	-
OREAS 45d (4-Acid) Cert	-	-	-	-	-	-	-	-	-	-	-	-
CaCO3 Meas	-	-	-	-	-	-	-	-	-	-	-	-
CaCO3 Cert	-	-	-	-	-	-	-	-	-	-	-	-
SdAR-M2 (U.S.G.S.) Meas	-	-	-	-	-	-	-	-	-	-	-	-
SdAR-M2 (U.S.G.S.) Cert	-	-	-	-	-	-	-	-	-	-	-	-
SdAR-M2 (U.S.G.S.) Meas	-	-	-	-	-	-	-	-	-	-	-	-
SdAR-M2 (U.S.G.S.) Cert	-	-	-	-	-	-	-	-	-	-	-	-
GXR-1 Meas	-	-	-	-	-	-	-	-	-	-	-	-
GXR-1 Cert	-	-	-	-	-	-	-	-	-	-	-	-
GXR-1 Meas	-	-	-	-	-	-	-	-	-	-	-	-
GXR-1 Cert	-	-	-	-	-	-	-	-	-	-	-	-
NIST 694 Meas	-	-	-	-	-	-	-	-	-	-	-	-
NIST 694 Cert	-	-	-	-	-	-	-	-	-	-	-	-
DNC-1 Meas	-	-	0.9	-	-	-	-	-	-	-	-	-
DNC-1 Cert	-	-	0.96	-	-	-	-	-	-	-	-	-
GBW 07113 Meas	-	-	-	-	-	-	-	-	-	-	-	-
GBW 07113 Cert	-	-	-	-	-	-	-	-	-	-	-	-
GXR-4 Meas	-	-	-	-	-	-	-	-	-	-	-	-
GXR-4 Cert	-	-	-	-	-	-	-	-	-	-	-	-
GXR-4 Meas	-	-	-	-	-	-	-	-	-	-	-	-
GXR-4 Cert	-	-	-	-	-	-	-	-	-	-	-	-

Analyte	Pr	Rb	Sb	Sm	Sn	Ta	Tb	Th	Tl	Tm	U	W
Units	ppm	ppm	ppm	ppm	ppm	ppm	ppm	ppm	ppm	ppm	ppm	ppm
Detection Limit	0.01	1	0.2	0.01	1	0.01	0.01	0.05	0.05	0.005	0.01	0.5
Method	FUS-MS	FUS-MS	FUS-MS	FUS-MS	FUS-MS	FUS-MS	FUS-MS	FUS-MS	FUS-MS	FUS-MS	FUS-MS	FUS-MS
SDC-1 Meas	-	-	-	-	-	-	-	-	-	-	-	-
SDC-1 Cert	-	-	-	-	-	-	-	-	-	-	-	-
SDC-1 Meas	-	-	-	-	-	-	-	-	-	-	-	-
SDC-1 Cert	-	-	-	-	-	-	-	-	-	-	-	-
GXR-6 Meas	-	-	-	-	-	-	-	-	-	-	-	-
GXR-6 Cert	-	-	-	-	-	-	-	-	-	-	-	-
GXR-6 Meas	-	-	-	-	-	-	-	-	-	-	-	-
GXR-6 Cert	-	-	-	-	-	-	-	-	-	-	-	-
LKSD-3 Meas	-	78	-	8	2	0.76	1	10.7	-	-	4.3	-
LKSD-3 Cert	-	78	-	8	3	0.7	1	11.4	-	-	4.6	-
TDB-1 Meas	-	24	-	-	-	-	-	2.7	-	-	-	-
TDB-1 Cert	-	23	-	-	-	-	-	2.7	-	-	-	-
SY-2 Meas	-	-	-	-	-	-	-	-	-	-	-	-
SY-2 Cert	-	-	-	-	-	-	-	-	-	-	-	-
SY-3 Meas	-	-	-	-	-	-	-	-	-	-	-	-
SY-3 Cert	-	-	-	-	-	-	-	-	-	-	-	-
BaSO4 Meas	-	-	-	-	-	-	-	-	-	-	-	-
BaSO4 Cert	-	-	-	-	-	-	-	-	-	-	-	-
BaSO4 Meas	-	-	-	-	-	-	-	-	-	-	-	-
BaSO4 Cert	-	-	-	-	-	-	-	-	-	-	-	-
W-2a Meas	-	20	0.8	3.4	-	0.53	0.65	2.3	<0.05	-	0.53	1.8
W-2a Cert	-	21	0.79	3.3	-	0.5	0.63	2.4	0.2	-	0.53	0.3
SY-4 Meas	-	-	-	-	-	-	-	-	-	-	-	-
SY-4 Cert	-	-	-	-	-	-	-	-	-	-	-	-
CTA-AC-1 Meas	-	-	-	158	-	2.73	-	22.1	-	-	4.3	-
CTA-AC-1 Cert	-	-	-	162	-	2.65	-	21.8	-	-	4.4	-
BIR-1a Meas	-	-	-	1	-	-	-	-	-	-	-	-
BIR-1a Cert	-	-	-	1.1	-	-	-	-	-	-	-	-
BIR-1a Meas	-	-	-	-	-	-	-	-	-	-	-	-
BIR-1a Cert	-	-	-	-	-	-	-	-	-	-	-	-
NCS DC86312 Meas	-	-	-	-	-	-	34	24.2	-	13.8	-	-
NCS DC86312 Cert	-	-	-	-	-	-	34.6	23.6	-	15.1	-	-
JGb-2 Meas	-	-	-	-	-	-	-	-	-	-	-	-
JGb-2 Cert	-	-	-	-	-	-	-	-	-	-	-	-
JGb-2 Meas	-	-	-	-	-	-	-	-	-	-	-	-
JGb-2 Cert	-	-	-	-	-	-	-	-	-	-	-	-
JGb-2 Meas	-	-	-	-	-	-	-	-	-	-	-	-

Analyte	Pr	Rb	Sb	Sm	Sn	Ta	Tb	Th	Tl	Tm	U	W
Units	ppm	ppm	ppm	ppm	ppm	ppm	ppm	ppm	ppm	ppm	ppm	ppm
Detection Limit	0.01	1	0.2	0.01	1	0.01	0.01	0.05	0.05	0.005	0.01	0.5
Method	FUS-MS	FUS-MS	FUS-MS	FUS-MS	FUS-MS	FUS-MS	FUS-MS	FUS-MS	FUS-MS	FUS-MS	FUS-MS	FUS-MS
JGb-2 Cert	-	-	-	-	-	-	-	-	-	-	-	-
JGb-2 Meas	-	-	-	-	-	-	-	-	-	-	-	-
JGb-2 Cert	-	-	-	-	-	-	-	-	-	-	-	-
NCS DC70009 (GBW07241) Meas	8	512	3.3	12.4	>1000	-	3.4	30.3	-	2.2	-	2230
NCS DC70009 (GBW07241) Cert	7.9	500	3.1	12.5	1700	-	3.3	28.3	-	2.2	-	2200
SGR-1b Meas	-	-	-	-	-	-	-	-	-	-	-	-
SGR-1b Cert	-	-	-	-	-	-	-	-	-	-	-	-
SGR-1b Meas	-	-	-	-	-	-	-	-	-	-	-	-
SGR-1b Cert	-	-	-	-	-	-	-	-	-	-	-	-
OREAS 100a (Fusion) Meas	47	-	-	24.5	-	-	3.9	51.3	-	2.25	136	-
OREAS 100a (Fusion) Cert	47.1	-	-	23.6	-	-	3.8	51.6	-	2.31	135	-
OREAS 101a (Fusion) Meas	130	-	-	46.2	-	-	5.8	33	-	2.6	388	-
OREAS 101a (Fusion) Cert	134	-	-	48.8	-	-	5.92	36.6	-	2.9	422	-
OREAS 101b (Fusion) Meas	128	-	-	51	-	-	5.36	37.5	-	2.81	411	-
OREAS 101b (Fusion) Cert	127	-	-	48	-	-	5.37	37.1	-	2.66	396	-
JR-1 Meas	5.6	252	1.1	5.54	3	1.98	1	25.4	1.58	0.64	8.4	-
JR-1 Cert	5.58	257	1.19	6.03	2.86	1.86	1.01	26.7	1.56	0.67	8.88	-
NCS DC86318 Meas	736	385	-	>1000	-	-	512	66.6	-	272	-	-
NCS DC86318 Cert	740	369.42	-	1720	-	-	470	67	-	270	-	-
USZ 25-2006 Meas	-	-	-	-	-	-	-	-	-	-	-	-
USZ 25-2006 Cert	-	-	-	-	-	-	-	-	-	-	-	-
USZ 25-2006 Meas	-	-	-	-	-	-	-	-	-	-	-	-
USZ 25-2006 Cert	-	-	-	-	-	-	-	-	-	-	-	-
DNC-1a Meas	-	-	-	-	-	-	-	-	-	-	-	-
DNC-1a Cert	-	-	-	-	-	-	-	-	-	-	-	-
DNC-1a Meas	-	-	-	-	-	-	-	-	-	-	-	-
DNC-1a Cert	-	-	-	-	-	-	-	-	-	-	-	-
PK2 Meas	-	-	-	-	-	-	-	-	-	-	-	-
PK2 Cert	-	-	-	-	-	-	-	-	-	-	-	-
GS311-4 Meas	-	-	-	-	-	-	-	-	-	-	-	-
GS311-4 Cert	-	-	-	-	-	-	-	-	-	-	-	-
GS311-4 Meas	-	-	-	-	-	-	-	-	-	-	-	-
GS311-4 Cert	-	-	-	-	-	-	-	-	-	-	-	-
GS900-5 Meas	-	-	-	-	-	-	-	-	-	-	-	-
GS900-5 Cert	-	-	-	-	-	-	-	-	-	-	-	-
GS900-5 Meas	-	-	-	-	-	-	-	-	-	-	-	-
GS900-5 Cert	-	-	-	-	-	-	-	-	-	-	-	-

Analyte	Pr	Rb	Sb	Sm	Sn	Ta	Tb	Th	Tl	Tm	U	W
Units	ppm	ppm	ppm	ppm	ppm	ppm	ppm	ppm	ppm	ppm	ppm	ppm
Detection Limit	0.01	1	0.2	0.01	1	0.01	0.01	0.05	0.05	0.005	0.01	0.5
Method	FUS-MS	FUS-MS	FUS-MS	FUS-MS	FUS-MS	FUS-MS	FUS-MS	FUS-MS	FUS-MS	FUS-MS	FUS-MS	FUS-MS
OREAS 45d (Aqua Regia) Meas	-	-	-	-	-	-	-	-	-	-	-	-
OREAS 45d (Aqua Regia) Cert	-	-	-	-	-	-	-	-	-	-	-	-
SBC-1 Meas	-	-	-	-	-	-	-	-	-	-	-	-
SBC-1 Cert	-	-	-	-	-	-	-	-	-	-	-	-
SBC-1 Meas	-	-	-	-	-	-	-	-	-	-	-	-
SBC-1 Cert	-	-	-	-	-	-	-	-	-	-	-	-
OREAS 45d (4-Acid) Meas	-	-	-	-	-	-	-	-	-	-	-	-
OREAS 45d (4-Acid) Cert	-	-	-	-	-	-	-	-	-	-	-	-
OxK110 Meas	-	-	-	-	-	-	-	-	-	-	-	-
OxK110 Cert	-	-	-	-	-	-	-	-	-	-	-	-
OXN117 Meas	-	-	-	-	-	-	-	-	-	-	-	-
OXN117 Cert	-	-	-	-	-	-	-	-	-	-	-	-
CaCO3 Meas	-	-	-	-	-	-	-	-	-	-	-	-
CaCO3 Cert	-	-	-	-	-	-	-	-	-	-	-	-
CaCO3 Meas	-	-	-	-	-	-	-	-	-	-	-	-
CaCO3 Cert	-	-	-	-	-	-	-	-	-	-	-	-
SdAR-M2 (U.S.G.S.) Meas	-	-	-	-	-	-	-	-	-	-	-	-
SdAR-M2 (U.S.G.S.) Cert	-	-	-	-	-	-	-	-	-	-	-	-
GXR-1 Meas	-	-	-	-	-	-	-	-	-	-	-	-
GXR-1 Cert	-	-	-	-	-	-	-	-	-	-	-	-
GXR-1 Meas	-	-	-	-	-	-	-	-	-	-	-	-
GXR-1 Cert	-	-	-	-	-	-	-	-	-	-	-	-
NIST 694 Meas	-	-	-	-	-	-	-	-	-	-	-	-
NIST 694 Cert	-	-	-	-	-	-	-	-	-	-	-	-
DNC-1 Meas	-	-	0.9	-	-	-	-	-	-	-	-	-
DNC-1 Cert	-	-	0.96	-	-	-	-	-	-	-	-	-
GBW 07113 Meas	-	-	-	-	-	-	-	-	-	-	-	-
GBW 07113 Cert	-	-	-	-	-	-	-	-	-	-	-	-
GXR-4 Meas	-	-	-	-	-	-	-	-	-	-	-	-
GXR-4 Cert	-	-	-	-	-	-	-	-	-	-	-	-
GXR-4 Meas	-	-	-	-	-	-	-	-	-	-	-	-
GXR-4 Cert	-	-	-	-	-	-	-	-	-	-	-	-
GXR-4 Meas	-	-	-	-	-	-	-	-	-	-	-	-
GXR-4 Cert	-	-	-	-	-	-	-	-	-	-	-	-
SDC-1 Meas	-	-	-	-	-	-	-	-	-	-	-	-
SDC-1 Cert	-	-	-	-	-	-	-	-	-	-	-	-
SDC-1 Meas	-	-	-	-	-	-	-	-	-	-	-	-

Analyte	Pr	Rb	Sb	Sm	Sn	Ta	Tb	Th	Tl	Tm	U	W
Units	ppm	ppm	ppm	ppm	ppm	ppm	ppm	ppm	ppm	ppm	ppm	ppm
Detection Limit	0.01	1	0.2	0.01	1	0.01	0.01	0.05	0.05	0.005	0.01	0.5
Method	FUS-MS	FUS-MS	FUS-MS	FUS-MS	FUS-MS	FUS-MS	FUS-MS	FUS-MS	FUS-MS	FUS-MS	FUS-MS	FUS-MS
SDC-1 Cert	-	-	-	-	-	-	-	-	-	-	-	-
GXR-6 Meas	-	-	-	-	-	-	-	-	-	-	-	-
GXR-6 Cert	-	-	-	-	-	-	-	-	-	-	-	-
GXR-6 Meas	-	-	-	-	-	-	-	-	-	-	-	-
GXR-6 Cert	-	-	-	-	-	-	-	-	-	-	-	-
GXR-6 Meas	-	-	-	-	-	-	-	-	-	-	-	-
GXR-6 Cert	-	-	-	-	-	-	-	-	-	-	-	-
LKSD-3 Meas	-	73	1.5	7.8	2	0.77	-	10.9	-	-	4.6	-
LKSD-3 Cert	-	78	1.3	8	3	0.7	-	11.4	-	-	4.6	-
TDB-1 Meas	-	22	-	-	-	-	-	2.7	-	-	-	-
TDB-1 Cert	-	23	-	-	-	-	-	2.7	-	-	-	-
SY-2 Meas	-	-	-	-	-	-	-	-	-	-	-	-
SY-2 Cert	-	-	-	-	-	-	-	-	-	-	-	-
SY-3 Meas	-	-	-	-	-	-	-	-	-	-	-	-
SY-3 Cert	-	-	-	-	-	-	-	-	-	-	-	-
BaSO4 Meas	-	-	-	-	-	-	-	-	-	-	-	-
BaSO4 Cert	-	-	-	-	-	-	-	-	-	-	-	-
W-2a Meas	-	19	-	3.4	-	0.44	0.65	2.3	<0.05	-	0.57	<0.5
W-2a Cert	-	21	-	3.3	-	0.5	0.63	2.4	0.2	-	0.53	0.3
SY-4 Meas	-	-	-	-	-	-	-	-	-	-	-	-
SY-4 Cert	-	-	-	-	-	-	-	-	-	-	-	-
CTA-AC-1 Meas	-	-	-	160	-	2.66	13	23.3	-	-	4.2	-
CTA-AC-1 Cert	-	-	-	162	-	2.65	13.9	21.8	-	-	4.4	-
BIR-1a Meas	-	-	-	1.1	-	-	-	-	-	-	-	-
BIR-1a Cert	-	-	-	1.1	-	-	-	-	-	-	-	-
NCS DC86312 Meas	-	-	-	-	-	-	31.5	-	-	13.2	-	-
NCS DC86312 Cert	-	-	-	-	-	-	34.6	-	-	15.1	-	-
JGb-2 Meas	-	-	-	-	-	-	-	-	-	-	-	-
JGb-2 Cert	-	-	-	-	-	-	-	-	-	-	-	-
JGb-2 Meas	-	-	-	-	-	-	-	-	-	-	-	-
JGb-2 Cert	-	-	-	-	-	-	-	-	-	-	-	-
JGb-2 Meas	-	-	-	-	-	-	-	-	-	-	-	-
JGb-2 Cert	-	-	-	-	-	-	-	-	-	-	-	-
NCS DC70009 (GBW07241) Meas	7.9	507	3.2	12.4	>1000	-	3.2	30.6	1.73	2.2	-	2270
NCS DC70009 (GBW07241) Cert	7.9	500	3.1	12.5	1700	-	3.3	28.3	1.8	2.2	-	2200
SGR-1b Meas	-	-	-	-	-	-	-	-	-	-	-	-
SGR-1b Cert	-	-	-	-	-	-	-	-	-	-	-	-

Analyte	Pr	Rb	Sb	Sm	Sn	Ta	Tb	Th	Tl	Tm	U	W
Units	ppm	ppm	ppm	ppm	ppm	ppm	ppm	ppm	ppm	ppm	ppm	ppm
Detection Limit	0.01	1	0.2	0.01	1	0.01	0.01	0.05	0.05	0.005	0.01	0.5
Method	FUS-MS	FUS-MS	FUS-MS	FUS-MS	FUS-MS	FUS-MS	FUS-MS	FUS-MS	FUS-MS	FUS-MS	FUS-MS	FUS-MS
OREAS 100a (Fusion) Meas	46.9	-	-	23.5	-	-	3.61	52.7	-	2.24	134	-
OREAS 100a (Fusion) Cert	47.1	-	-	23.6	-	-	3.8	51.6	-	2.31	135	-
OREAS 101a (Fusion) Meas	128	-	-	49.1	-	-	5.96	36.2	-	2.7	444	-
OREAS 101a (Fusion) Cert	134	-	-	48.8	-	-	5.92	36.6	-	2.9	422	-
OREAS 101b (Fusion) Meas	129	-	-	50	-	-	5.3	39.3	-	2.79	-	-
OREAS 101b (Fusion) Cert	127	-	-	48	-	-	5.37	37.1	-	2.66	-	-
JR-1 Meas	6	245	-	5.67	2	-	1.03	27.1	-	0.67	9.11	1.4
JR-1 Cert	5.58	257	-	6.03	2.86	-	1.01	26.7	-	0.67	8.88	1.59
NCS DC86318 Meas	735	380	-	>1000	-	-	481	71.2	-	265	-	-
NCS DC86318 Cert	740	369.42	-	1720	-	-	470	67	-	270	-	-
USZ 25-2006 Meas	-	-	-	-	-	-	-	-	-	-	-	-
USZ 25-2006 Cert	-	-	-	-	-	-	-	-	-	-	-	-
USZ 25-2006 Meas	-	-	-	-	-	-	-	-	-	-	-	-
USZ 25-2006 Cert	-	-	-	-	-	-	-	-	-	-	-	-
DNC-1a Meas	-	-	-	-	-	-	-	-	-	-	-	-
DNC-1a Cert	-	-	-	-	-	-	-	-	-	-	-	-
DNC-1a Meas	-	-	-	-	-	-	-	-	-	-	-	-
DNC-1a Cert	-	-	-	-	-	-	-	-	-	-	-	-
GS311-4 Meas	-	-	-	-	-	-	-	-	-	-	-	-
GS311-4 Cert	-	-	-	-	-	-	-	-	-	-	-	-
GS900-5 Meas	-	-	-	-	-	-	-	-	-	-	-	-
GS900-5 Cert	-	-	-	-	-	-	-	-	-	-	-	-
OREAS 45d (Aqua Regia) Meas	-	-	-	-	-	-	-	-	-	-	-	-
OREAS 45d (Aqua Regia) Cert	-	-	-	-	-	-	-	-	-	-	-	-
SBC-1 Meas	-	-	-	-	-	-	-	-	-	-	-	-
SBC-1 Cert	-	-	-	-	-	-	-	-	-	-	-	-
SBC-1 Meas	-	-	-	-	-	-	-	-	-	-	-	-
SBC-1 Cert	-	-	-	-	-	-	-	-	-	-	-	-
OREAS 45d (4-Acid) Meas	-	-	-	-	-	-	-	-	-	-	-	-
OREAS 45d (4-Acid) Cert	-	-	-	-	-	-	-	-	-	-	-	-
OREAS 45d (4-Acid) Meas	-	-	-	-	-	-	-	-	-	-	-	-
OREAS 45d (4-Acid) Cert	-	-	-	-	-	-	-	-	-	-	-	-
CaCO3 Meas	-	-	-	-	-	-	-	-	-	-	-	-
CaCO3 Cert	-	-	-	-	-	-	-	-	-	-	-	-
CaCO3 Meas	-	-	-	-	-	-	-	-	-	-	-	-
CaCO3 Cert	-	-	-	-	-	-	-	-	-	-	-	-
SdAR-M2 (U.S.G.S.) Meas	-	-	-	-	-	-	-	-	-	-	-	-

Analyte	Pr	Rb	Sb	Sm	Sn	Ta	Tb	Th	Tl	Tm	U	W
Units	ppm	ppm	ppm	ppm	ppm	ppm	ppm	ppm	ppm	ppm	ppm	ppm
Detection Limit	0.01	1	0.2	0.01	1	0.01	0.01	0.05	0.05	0.005	0.01	0.5
Method	FUS-MS	FUS-MS	FUS-MS	FUS-MS	FUS-MS	FUS-MS	FUS-MS	FUS-MS	FUS-MS	FUS-MS	FUS-MS	FUS-MS
SdAR-M2 (U.S.G.S.) Cert	-	-	-	-	-	-	-	-	-	-	-	-
SdAR-M2 (U.S.G.S.) Meas	-	-	-	-	-	-	-	-	-	-	-	-
SdAR-M2 (U.S.G.S.) Cert	-	-	-	-	-	-	-	-	-	-	-	-
SdAR-M2 (U.S.G.S.) Meas	-	-	-	-	-	-	-	-	-	-	-	-
SdAR-M2 (U.S.G.S.) Cert	-	-	-	-	-	-	-	-	-	-	-	-
OREAS 214 Meas	-	-	-	-	-	-	-	-	-	-	-	-
OREAS 214 Cert	-	-	-	-	-	-	-	-	-	-	-	-
OREAS 218 Meas	-	-	-	-	-	-	-	-	-	-	-	-
OREAS 218 Cert	-	-	-	-	-	-	-	-	-	-	-	-
OREAS 218 Meas	-	-	-	-	-	-	-	-	-	-	-	-
OREAS 218 Cert	-	-	-	-	-	-	-	-	-	-	-	-
T9 Geochem Orig	-	-	-	-	-	-	-	-	-	-	-	-
T9 Geochem Dup	-	-	-	-	-	-	-	-	-	-	-	-
T14 Geochem Orig	-	-	-	-	-	-	-	-	-	-	-	-
T14 Geochem Dup	-	-	-	-	-	-	-	-	-	-	-	-
T17 Geochem Orig	-	-	-	-	-	-	-	-	-	-	-	-
T17 Geochem Dup	-	-	-	-	-	-	-	-	-	-	-	-
STPL-BAS-025 Orig	-	-	-	-	-	-	-	-	-	-	-	-
STPL-BAS-025 Dup	-	-	-	-	-	-	-	-	-	-	-	-
T24 Geochem Orig	0.54	<1	<0.2	0.44	<1	<0.01	0.09	0.16	0.15	0.067	0.23	<0.5
T24 Geochem Dup	0.47	<1	<0.2	0.42	<1	<0.01	0.09	0.16	0.07	0.065	0.22	11.7
T27 Geochem Orig	-	-	-	-	-	-	-	-	-	-	-	-
T27 Geochem Dup	-	-	-	-	-	-	-	-	-	-	-	-
T31 Geochem Orig	-	-	-	-	-	-	-	-	-	-	-	-
T31 Geochem Dup	-	-	-	-	-	-	-	-	-	-	-	-
T37 Geochem Orig	-	-	-	-	-	-	-	-	-	-	-	-
T37 Geochem Dup	-	-	-	-	-	-	-	-	-	-	-	-
T42 Geochem Orig	-	-	-	-	-	-	-	-	-	-	-	-
T42 Geochem Dup	-	-	-	-	-	-	-	-	-	-	-	-
T45 Geochem Orig	-	-	-	-	-	-	-	-	-	-	-	-
T45 Geochem Dup	-	-	-	-	-	-	-	-	-	-	-	-
STPL-53-PML-036 Orig	-	-	-	-	-	-	-	-	-	-	-	-
STPL-53-PML-036 Dup	-	-	-	-	-	-	-	-	-	-	-	-
STPL-BAS-025 Orig	-	-	-	-	-	-	-	-	-	-	-	-
STPL-BAS-025 Dup	-	-	-	-	-	-	-	-	-	-	-	-
T42 Geochem Orig	-	-	-	-	-	-	-	-	-	-	-	-
T42 Geochem Dup	-	-	-	-	-	-	-	-	-	-	-	-

Analyte	Pr	Rb	Sb	Sm	Sn	Ta	Tb	Th	Tl	Tm	U	W
Units	ppm	ppm	ppm	ppm	ppm	ppm	ppm	ppm	ppm	ppm	ppm	ppm
Detection Limit	0.01	1	0.2	0.01	1	0.01	0.01	0.05	0.05	0.005	0.01	0.5
Method	FUS-MS	FUS-MS	FUS-MS	FUS-MS	FUS-MS	FUS-MS	FUS-MS	FUS-MS	FUS-MS	FUS-MS	FUS-MS	FUS-MS
T45 Geochem Orig	-	-	-	-	-	-	-	-	-	-	-	-
T45 Geochem Dup	-	-	-	-	-	-	-	-	-	-	-	-
T59 Orig	-	-	-	-	-	-	-	-	-	-	-	-
T59 Dup	-	-	-	-	-	-	-	-	-	-	-	-
T72 Orig	-	-	-	-	-	-	-	-	-	-	-	-
T72 Dup	-	-	-	-	-	-	-	-	-	-	-	-
T73 Orig	-	-	-	-	-	-	-	-	-	-	-	-
T73 Dup	-	-	-	-	-	-	-	-	-	-	-	-
STPL-BAS-029 Orig	-	-	-	-	-	-	-	-	-	-	-	-
STPL-BAS-029 Dup	-	-	-	-	-	-	-	-	-	-	-	-
T81 Orig	-	-	-	-	-	-	-	-	-	-	-	-
T81 Dup	-	-	-	-	-	-	-	-	-	-	-	-
T86 Orig	-	-	-	-	-	-	-	-	-	-	-	-
T86 Dup	-	-	-	-	-	-	-	-	-	-	-	-
T88 Orig	3.06	41	0.2	2.15	<1	0.29	0.31	2.56	<0.05	0.137	0.7	9
T88 Dup	3.05	41	<0.2	2.35	<1	0.28	0.3	2.49	<0.05	0.148	0.7	5
T89 Orig	-	-	-	-	-	-	-	-	-	-	-	-
T89 Dup	-	-	-	-	-	-	-	-	-	-	-	-
T94 Orig	-	-	-	-	-	-	-	-	-	-	-	-
T94 Dup	-	-	-	-	-	-	-	-	-	-	-	-
T98 Orig	-	-	-	-	-	-	-	-	-	-	-	-
T98 Dup	-	-	-	-	-	-	-	-	-	-	-	-
T99 Orig	-	-	-	-	-	-	-	-	-	-	-	-
T99 Dup	-	-	-	-	-	-	-	-	-	-	-	-
T101 Orig	-	-	-	-	-	-	-	-	-	-	-	-
T101 Dup	-	-	-	-	-	-	-	-	-	-	-	-
T102 Orig	-	-	-	-	-	-	-	-	-	-	-	-
T102 Dup	-	-	-	-	-	-	-	-	-	-	-	-
T114 Orig	-	-	-	-	-	-	-	-	-	-	-	-
T114 Dup	-	-	-	-	-	-	-	-	-	-	-	-
T116 Orig	-	-	-	-	-	-	-	-	-	-	-	-
T116 Dup	-	-	-	-	-	-	-	-	-	-	-	-
T117 Orig	3.01	26	<0.2	2.04	<1	0.2	0.26	1.67	<0.05	0.11	0.46	4.6
T117 Split PREP DUP	2.87	27	<0.2	2.18	<1	0.19	0.25	1.77	<0.05	0.112	0.46	2.9
STPL-53-PML-025 Orig	7.42	63	<0.2	3.48	<1	0.82	0.4	11	0.12	0.26	2.48	2.2
STPL-53-PML-025 Dup	7.03	58	<0.2	3.54	<1	0.7	0.38	9.89	0.09	0.253	2.25	1.4
T65 Orig	-	-	-	-	-	-	-	-	-	-	-	-



Analyte	Pr	Rb	Sb	Sm	Sn	Ta	Tb	Th	Tl	Tm	U	W
Units	ppm	ppm	ppm	ppm	ppm	ppm	ppm	ppm	ppm	ppm	ppm	ppm
Detection Limit	0.01	1	0.2	0.01	1	0.01	0.01	0.05	0.05	0.005	0.01	0.5
Method	FUS-MS	FUS-MS	FUS-MS	FUS-MS	FUS-MS	FUS-MS	FUS-MS	FUS-MS	FUS-MS	FUS-MS	FUS-MS	FUS-MS
T65 Dup	-	-	-	-	-	-	-	-	-	-	-	-
T106 Orig	-	-	-	-	-	-	-	-	-	-	-	-
T106 Dup	-	-	-	-	-	-	-	-	-	-	-	-
T118 Orig	5.69	27	0.3	3.86	<1	0.32	0.41	3.03	0.07	0.163	0.59	1.5
T118 Dup	5.84	29	0.3	3.98	<1	0.34	0.43	3.25	0.08	0.182	0.61	1.4
T141 Orig	-	-	-	-	-	-	-	-	-	-	-	-
T141 Dup	-	-	-	-	-	-	-	-	-	-	-	-
STPL-BAS-023 Orig	-	-	-	-	-	-	-	-	-	-	-	-
STPL-BAS-023 Dup	-	-	-	-	-	-	-	-	-	-	-	-
T154 Orig	-	-	-	-	-	-	-	-	-	-	-	-
T154 Dup	-	-	-	-	-	-	-	-	-	-	-	-
T157 Orig	-	-	-	-	-	-	-	-	-	-	-	-
T157 Dup	-	-	-	-	-	-	-	-	-	-	-	-
T158 Orig	-	-	-	-	-	-	-	-	-	-	-	-
T158 Dup	-	-	-	-	-	-	-	-	-	-	-	-
STPL-PML-53-027 Orig	7.22	68	0.3	3.75	<1	0.93	0.4	9.93	0.12	0.265	2.31	1.3
STPL-PML-53-027 Dup	7.36	68	<0.2	3.61	<1	0.87	0.41	10.2	0.11	0.285	2.38	2.4
T182 Orig	-	-	-	-	-	-	-	-	-	-	-	-
T182 Dup	-	-	-	-	-	-	-	-	-	-	-	-
T183 Orig	-	-	-	-	-	-	-	-	-	-	-	-
T183 Dup	-	-	-	-	-	-	-	-	-	-	-	-
T187 Orig	-	-	-	-	-	-	-	-	-	-	-	-
T187 Dup	-	-	-	-	-	-	-	-	-	-	-	-
T188 Orig	-	-	-	-	-	-	-	-	-	-	-	-
T188 Dup	-	-	-	-	-	-	-	-	-	-	-	-
T189 Orig	-	-	-	-	-	-	-	-	-	-	-	-
T189 Dup	-	-	-	-	-	-	-	-	-	-	-	-
T200 Orig	0.79	<1	<0.2	1.34	<1	0.09	0.34	0.44	<0.05	0.217	0.12	5
T200 Dup	0.77	<1	<0.2	1.35	<1	0.07	0.32	0.45	<0.05	0.209	0.12	3.1
T218 Orig	-	-	-	-	-	-	-	-	-	-	-	-
T218 Dup	-	-	-	-	-	-	-	-	-	-	-	-
T239 Orig	-	-	-	-	-	-	-	-	-	-	-	-
T239 Dup	-	-	-	-	-	-	-	-	-	-	-	-
T240 Orig	-	-	-	-	-	-	-	-	-	-	-	-
T240 Dup	-	-	-	-	-	-	-	-	-	-	-	-
T242 Orig	-	-	-	-	-	-	-	-	-	-	-	-
T242 Dup	-	-	-	-	-	-	-	-	-	-	-	-







Analyte	Y	Yb	Zn	Ag	Cd	Co	Cr	Cu	In	Li	Mn	Mo	Ni	Pb	Zn
Units	ppm	ppm	ppm	ppm	ppm	ppm	ppm	ppm	ppm	ppm	ppm	ppm	ppm	ppm	ppm
Detection Limit	0.5	0.01	30	1	0.2	0.5	1	0.5	0.2	1	2	1	1	2	0.5
Method	FUS-MS	FUS-MS	FUS-MS	TD-MS	TD-MS	TD-MS	TD-MS	TD-MS	TD-MS	TD-MS	TD-MS	TD-MS	TD-MS	TD-MS	TD-MS
GXR-1 Meas	-	-	-	-	-	-	-	-	-	-	-	-	-	-	-
GXR-1 Cert	-	-	-	-	-	-	-	-	-	-	-	-	-	-	-
NIST 694 Meas	-	-	-	-	-	-	-	-	-	-	-	-	-	-	-
NIST 694 Cert	-	-	-	-	-	-	-	-	-	-	-	-	-	-	-
DNC-1 Meas	17.1	2.2	-	-	-	-	-	-	-	-	-	-	-	-	-
DNC-1 Cert	18	2	-	-	-	-	-	-	-	-	-	-	-	-	-
GBW 07113 Meas	-	-	-	-	-	-	-	-	-	-	-	-	-	-	-
GBW 07113 Cert	-	-	-	-	-	-	-	-	-	-	-	-	-	-	-
GBW 07113 Meas	-	-	-	-	-	-	-	-	-	-	-	-	-	-	-
GBW 07113 Cert	-	-	-	-	-	-	-	-	-	-	-	-	-	-	-
GBW 07113 Meas	-	-	-	-	-	-	-	-	-	-	-	-	-	-	-
GBW 07113 Cert	-	-	-	-	-	-	-	-	-	-	-	-	-	-	-
GXR-4 Meas	-	-	-	-	-	-	-	-	-	-	-	-	-	-	-
GXR-4 Cert	-	-	-	-	-	-	-	-	-	-	-	-	-	-	-
GXR-6 Meas	-	-	-	-	-	-	-	-	-	-	-	-	-	-	-
GXR-6 Cert	-	-	-	-	-	-	-	-	-	-	-	-	-	-	-
LKSD-3 Meas	28.8	3	-	-	-	-	-	-	-	-	-	-	-	-	-
LKSD-3 Cert	30	2.7	-	-	-	-	-	-	-	-	-	-	-	-	-
TDB-1 Meas	33.8	3.4	-	-	-	-	-	-	-	-	-	-	-	-	-
TDB-1 Cert	36	3.4	-	-	-	-	-	-	-	-	-	-	-	-	-
SY-2 Meas	-	-	-	-	-	-	-	-	-	-	-	-	-	-	-
SY-2 Cert	-	-	-	-	-	-	-	-	-	-	-	-	-	-	-
SY-3 Meas	-	-	-	-	-	-	-	-	-	-	-	-	-	-	-
SY-3 Cert	-	-	-	-	-	-	-	-	-	-	-	-	-	-	-
BaSO4 Meas	-	-	-	-	-	-	-	-	-	-	-	-	-	-	-
BaSO4 Cert	-	-	-	-	-	-	-	-	-	-	-	-	-	-	-
BaSO4 Meas	-	-	-	-	-	-	-	-	-	-	-	-	-	-	-
BaSO4 Cert	-	-	-	-	-	-	-	-	-	-	-	-	-	-	-
BaSO4 Meas	-	-	-	-	-	-	-	-	-	-	-	-	-	-	-
BaSO4 Cert	-	-	-	-	-	-	-	-	-	-	-	-	-	-	-
W-2a Meas	23	2.1	-	-	-	-	-	-	-	-	-	-	-	-	-
W-2a Cert	24	2.1	-	-	-	-	-	-	-	-	-	-	-	-	-
SY-4 Meas	-	-	-	-	-	-	-	-	-	-	-	-	-	-	-
SY-4 Cert	-	-	-	-	-	-	-	-	-	-	-	-	-	-	-
CTA-AC-1 Meas	-	12.2	-	-	-	-	-	-	-	-	-	-	-	-	-
CTA-AC-1 Cert	-	11.4	-	-	-	-	-	-	-	-	-	-	-	-	-
BIR-1a Meas	15.5	1.8	-	-	-	-	-	-	-	-	-	-	-	-	-

Analyte	Y	Yb	Zn	Ag	Cd	Co	Cr	Cu	In	Li	Mn	Mo	Ni	Pb	Zn
Units	ppm	ppm	ppm	ppm	ppm	ppm	ppm	ppm	ppm	ppm	ppm	ppm	ppm	ppm	ppm
Detection Limit	0.5	0.01	30	1	0.2	0.5	1	0.5	0.2	1	2	1	1	2	0.5
Method	FUS-MS	FUS-MS	FUS-MS	TD-MS	TD-MS	TD-MS	TD-MS	TD-MS	TD-MS	TD-MS	TD-MS	TD-MS	TD-MS	TD-MS	TD-MS
BIR-1a Cert	16	1.7	-	-	-	-	-	-	-	-	-	-	-	-	-
BIR-1a Meas	-	-	-	-	-	-	-	-	-	-	-	-	-	-	-
BIR-1a Cert	-	-	-	-	-	-	-	-	-	-	-	-	-	-	-
NCS DC86312 Meas	1010	94.4	-	-	-	-	-	-	-	-	-	-	-	-	-
NCS DC86312 Cert	976	87.79	-	-	-	-	-	-	-	-	-	-	-	-	-
JGb-2 Meas	-	-	-	-	-	-	-	-	-	-	-	-	-	-	-
JGb-2 Cert	-	-	-	-	-	-	-	-	-	-	-	-	-	-	-
JGb-2 Meas	-	-	-	-	-	-	-	-	-	-	-	-	-	-	-
JGb-2 Cert	-	-	-	-	-	-	-	-	-	-	-	-	-	-	-
JGb-2 Meas	-	-	-	-	-	-	-	-	-	-	-	-	-	-	-
JGb-2 Cert	-	-	-	-	-	-	-	-	-	-	-	-	-	-	-
JGb-2 Meas	-	-	-	-	-	-	-	-	-	-	-	-	-	-	-
JGb-2 Cert	-	-	-	-	-	-	-	-	-	-	-	-	-	-	-
JGb-2 Meas	-	-	-	-	-	-	-	-	-	-	-	-	-	-	-
JGb-2 Cert	-	-	-	-	-	-	-	-	-	-	-	-	-	-	-
JGb-2 Meas	-	-	-	-	-	-	-	-	-	-	-	-	-	-	-
JGb-2 Cert	-	-	-	-	-	-	-	-	-	-	-	-	-	-	-
SCH-1 Meas	-	-	-	-	-	-	-	-	-	-	-	-	-	-	-
SCH-1 Cert	-	-	-	-	-	-	-	-	-	-	-	-	-	-	-
NCS DC70009 (GBW07241) Meas	-	15.8	-	-	-	-	-	-	-	-	-	-	-	-	-
NCS DC70009 (GBW07241) Cert	-	14.9	-	-	-	-	-	-	-	-	-	-	-	-	-
SGR-1b Meas	-	-	-	-	-	-	-	-	-	-	-	-	-	-	-
SGR-1b Cert	-	-	-	-	-	-	-	-	-	-	-	-	-	-	-
SGR-1b Meas	-	-	-	-	-	-	-	-	-	-	-	-	-	-	-
SGR-1b Cert	-	-	-	-	-	-	-	-	-	-	-	-	-	-	-
SGR-1b Meas	-	-	-	-	-	-	-	-	-	-	-	-	-	-	-
SGR-1b Cert	-	-	-	-	-	-	-	-	-	-	-	-	-	-	-
OREAS 100a (Fusion) Meas	140	15	-	-	-	-	-	-	-	-	-	-	-	-	-
OREAS 100a (Fusion) Cert	142	14.9	-	-	-	-	-	-	-	-	-	-	-	-	-
OREAS 101a (Fusion) Meas	181	17.8	-	-	-	-	-	-	-	-	-	-	-	-	-
OREAS 101a (Fusion) Cert	183	17.5	-	-	-	-	-	-	-	-	-	-	-	-	-
OREAS 101b (Fusion) Meas	174	18.7	-	-	-	-	-	-	-	-	-	-	-	-	-
OREAS 101b (Fusion) Cert	178	17.6	-	-	-	-	-	-	-	-	-	-	-	-	-
OREAS 98 (S by LECO) Meas	-	-	-	-	-	-	-	-	-	-	-	-	-	-	-
OREAS 98 (S by LECO) Cert	-	-	-	-	-	-	-	-	-	-	-	-	-	-	-
OREAS 132b (S by LECO) Meas	-	-	-	-	-	-	-	-	-	-	-	-	-	-	-
OREAS 132b (S by LECO) Cert	-	-	-	-	-	-	-	-	-	-	-	-	-	-	-
JR-1 Meas	41.8	4.82	-	-	-	-	-	-	-	-	-	-	-	-	-
JR-1 Cert	45.1	4.55	-	-	-	-	-	-	-	-	-	-	-	-	-

Analyte	Y	Yb	Zn	Ag	Cd	Co	Cr	Cu	In	Li	Mn	Mo	Ni	Pb	Zn
Units	ppm	ppm	ppm	ppm	ppm	ppm	ppm	ppm	ppm	ppm	ppm	ppm	ppm	ppm	ppm
Detection Limit	0.5	0.01	30	1	0.2	0.5	1	0.5	0.2	1	2	1	1	2	0.5
Method	FUS-MS	FUS-MS	FUS-MS	TD-MS	TD-MS	TD-MS	TD-MS	TD-MS	TD-MS	TD-MS	TD-MS	TD-MS	TD-MS	TD-MS	TD-MS
NCS DC86318 Meas	>10000	>1000	-	-	-	-	-	-	-	-	-	-	-	-	-
NCS DC86318 Cert	17008	1840	-	-	-	-	-	-	-	-	-	-	-	-	-
USZ 25-2006 Meas	-	-	-	-	-	-	-	-	-	-	-	-	-	-	-
USZ 25-2006 Cert	-	-	-	-	-	-	-	-	-	-	-	-	-	-	-
USZ 25-2006 Meas	-	-	-	-	-	-	-	-	-	-	-	-	-	-	-
USZ 25-2006 Cert	-	-	-	-	-	-	-	-	-	-	-	-	-	-	-
GS309-4 Meas	-	-	-	-	-	-	-	-	-	-	-	-	-	-	-
GS309-4 Cert	-	-	-	-	-	-	-	-	-	-	-	-	-	-	-
GS311-4 Meas	-	-	-	-	-	-	-	-	-	-	-	-	-	-	-
GS311-4 Cert	-	-	-	-	-	-	-	-	-	-	-	-	-	-	-
GS311-4 Meas	-	-	-	-	-	-	-	-	-	-	-	-	-	-	-
GS311-4 Cert	-	-	-	-	-	-	-	-	-	-	-	-	-	-	-
GS311-4 Meas	-	-	-	-	-	-	-	-	-	-	-	-	-	-	-
GS311-4 Cert	-	-	-	-	-	-	-	-	-	-	-	-	-	-	-
GS311-4 Meas	-	-	-	-	-	-	-	-	-	-	-	-	-	-	-
GS311-4 Cert	-	-	-	-	-	-	-	-	-	-	-	-	-	-	-
GS900-5 Meas	-	-	-	-	-	-	-	-	-	-	-	-	-	-	-
GS900-5 Cert	-	-	-	-	-	-	-	-	-	-	-	-	-	-	-
GS900-5 Meas	-	-	-	-	-	-	-	-	-	-	-	-	-	-	-
GS900-5 Cert	-	-	-	-	-	-	-	-	-	-	-	-	-	-	-
GS900-5 Meas	-	-	-	-	-	-	-	-	-	-	-	-	-	-	-
GS900-5 Cert	-	-	-	-	-	-	-	-	-	-	-	-	-	-	-
OREAS 45d (Aqua Regia) Meas	-	-	-	-	-	-	-	-	-	-	-	-	-	-	-
OREAS 45d (Aqua Regia) Cert	-	-	-	-	-	-	-	-	-	-	-	-	-	-	-
CDN-PGMS-24 Meas	-	-	-	-	-	-	-	-	-	-	-	-	-	-	-
CDN-PGMS-24 Cert	-	-	-	-	-	-	-	-	-	-	-	-	-	-	-
CDN-PGMS-24 Meas	-	-	-	-	-	-	-	-	-	-	-	-	-	-	-
CDN-PGMS-24 Cert	-	-	-	-	-	-	-	-	-	-	-	-	-	-	-
CDN-PGMS-24 Meas	-	-	-	-	-	-	-	-	-	-	-	-	-	-	-
CDN-PGMS-24 Cert	-	-	-	-	-	-	-	-	-	-	-	-	-	-	-
CDN-PGMS-24 Meas	-	-	-	-	-	-	-	-	-	-	-	-	-	-	-
CDN-PGMS-24 Cert	-	-	-	-	-	-	-	-	-	-	-	-	-	-	-
CaCO3 Meas	-	-	-	-	-	-	-	-	-	-	-	-	-	-	-
CaCO3 Cert	-	-	-	-	-	-	-	-	-	-	-	-	-	-	-
CaCO3 Meas	-	-	-	-	-	-	-	-	-	-	-	-	-	-	-
CaCO3 Cert	-	-	-	-	-	-	-	-	-	-	-	-	-	-	-
SdAR-M2 (U.S.G.S.) Meas	-	-	-	-	-	-	-	-	-	-	-	-	-	-	-
SdAR-M2 (U.S.G.S.) Cert	-	-	-	-	-	-	-	-	-	-	-	-	-	-	-
GXR-1 Meas	-	-	-	30	2.1	7.3	13	918	0.8	7	792	17	37	625	753

Analyte	Y	Yb	Zn	Ag	Cd	Co	Cr	Cu	In	Li	Mn	Mo	Ni	Pb	Zn
Units	ppm	ppm	ppm	ppm	ppm	ppm	ppm	ppm	ppm	ppm	ppm	ppm	ppm	ppm	ppm
Detection Limit	0.5	0.01	30	1	0.2	0.5	1	0.5	0.2	1	2	1	1	2	0.5
Method	FUS-MS	FUS-MS	FUS-MS	TD-MS	TD-MS	TD-MS	TD-MS	TD-MS	TD-MS	TD-MS	TD-MS	TD-MS	TD-MS	TD-MS	TD-MS
GXR-1 Cert	-	-	-	31	3.3	8.2	12	1110	0.77	8.2	852	18	41	730	760
GXR-1 Meas	-	-	-	31	2.1	7.7	17	960	0.8	7	791	19	37	663	757
GXR-1 Cert	-	-	-	31	3.3	8.2	12	1110	0.77	8.2	852	18	41	730	760
GXR-1 Meas	-	-	-	32	2.2	8.1	14	1140	0.9	8	799	16	40	716	771
GXR-1 Cert	-	-	-	31	3.3	8.2	12	1110	0.77	8.2	852	18	41	730	760
GXR-1 Meas	-	-	-	32	2.3	8.4	22	1160	0.8	8	880	15	43	727	802
GXR-1 Cert	-	-	-	31	3.3	8.2	12	1110	0.77	8.2	852	18	41	730	760
NIST 694 Meas	-	-	-	-	-	-	-	-	-	-	-	-	-	-	-
NIST 694 Cert	-	-	-	-	-	-	-	-	-	-	-	-	-	-	-
DNC-1 Meas	16.8	2	-	-	-	-	-	-	-	-	-	-	-	-	-
DNC-1 Cert	18	2	-	-	-	-	-	-	-	-	-	-	-	-	-
GBW 07113 Meas	-	-	-	-	-	-	-	-	-	-	-	-	-	-	-
GBW 07113 Cert	-	-	-	-	-	-	-	-	-	-	-	-	-	-	-
GXR-4 Meas	-	-	-	3	<0.2	13.9	67	5370	0.2	10	144	292	39	51	73.7
GXR-4 Cert	-	-	-	4	0.86	14.6	64	6520	0.27	11.1	155	310	42	52	73
GXR-4 Meas	-	-	-	3	<0.2	14.2	40	5600	0.2	11	150	310	40	53	77.2
GXR-4 Cert	-	-	-	4	0.86	14.6	64	6520	0.27	11.1	155	310	42	52	73
GXR-4 Meas	-	-	-	3	<0.2	14.6	41	5350	0.2	11	153	278	40	51	66.5
GXR-4 Cert	-	-	-	4	0.86	14.6	64	6520	0.27	11.1	155	310	42	52	73
GXR-4 Meas	-	-	-	3	<0.2	14.2	52	5750	0.2	11	164	272	40	52	70.4
GXR-4 Cert	-	-	-	4	0.86	14.6	64	6520	0.27	11.1	155	310	42	52	73
SDC-1 Meas	-	-	-	-	-	18.1	66	31.6	-	34	829	-	35	26	109
SDC-1 Cert	-	-	-	-	-	18	64	30	-	34	880	-	38	25	103
SDC-1 Meas	-	-	-	-	-	18.8	56	34.3	-	32	888	-	36	27	118
SDC-1 Cert	-	-	-	-	-	18	64	30	-	34	880	-	38	25	103
SDC-1 Meas	-	-	-	-	-	17.2	112	28.4	-	34	730	-	32	25	103
SDC-1 Cert	-	-	-	-	-	18	64	30	-	34	880	-	38	25	103
SDC-1 Meas	-	-	-	-	-	17.9	49	33.3	-	36	787	-	33	27	117
SDC-1 Cert	-	-	-	-	-	18	64	30	-	34	880	-	38	25	103
GXR-6 Meas	-	-	-	<1	<0.2	13.1	86	69.7	<0.2	36	991	2	23	95	131
GXR-6 Cert	-	-	-	1.3	1	13.8	96	66	0.26	32	1010	2.4	27	101	118
GXR-6 Meas	-	-	-	<1	<0.2	13.4	52	73.7	<0.2	36	1020	1	25	102	139
GXR-6 Cert	-	-	-	1.3	1	13.8	96	66	0.26	32	1010	2.4	27	101	118
GXR-6 Meas	-	-	-	<1	<0.2	13.3	51	65.8	<0.2	40	900	1	24	101	126
GXR-6 Cert	-	-	-	1.3	1	13.8	96	66	0.26	32	1010	2.4	27	101	118
GXR-6 Meas	-	-	-	<1	<0.2	12.9	56	66	<0.2	37	902	2	23	101	124
GXR-6 Cert	-	-	-	1.3	1	13.8	96	66	0.26	32	1010	2.4	27	101	118



Analyte	Y	Yb	Zn	Ag	Cd	Co	Cr	Cu	In	Li	Mn	Mo	Ni	Pb	Zn
Units	ppm	ppm	ppm	ppm	ppm	ppm	ppm	ppm	ppm	ppm	ppm	ppm	ppm	ppm	ppm
Detection Limit	0.5	0.01	30	1	0.2	0.5	1	0.5	0.2	1	2	1	1	2	0.5
Method	FUS-MS	FUS-MS	FUS-MS	TD-MS	TD-MS	TD-MS	TD-MS	TD-MS	TD-MS	TD-MS	TD-MS	TD-MS	TD-MS	TD-MS	TD-MS
LKSD-3 Meas	29.9	2.7	-	-	-	-	-	-	-	-	-	-	-	-	-
LKSD-3 Cert	30	2.7	-	-	-	-	-	-	-	-	-	-	-	-	-
TDB-1 Meas	35.9	3.4	-	-	-	-	-	-	-	-	-	-	-	-	-
TDB-1 Cert	36	3.4	-	-	-	-	-	-	-	-	-	-	-	-	-
SY-2 Meas	-	-	-	-	-	-	-	-	-	-	-	-	-	-	-
SY-2 Cert	-	-	-	-	-	-	-	-	-	-	-	-	-	-	-
SY-3 Meas	-	-	-	-	-	-	-	-	-	-	-	-	-	-	-
SY-3 Cert	-	-	-	-	-	-	-	-	-	-	-	-	-	-	-
BaSO4 Meas	-	-	-	-	-	-	-	-	-	-	-	-	-	-	-
BaSO4 Cert	-	-	-	-	-	-	-	-	-	-	-	-	-	-	-
BaSO4 Meas	-	-	-	-	-	-	-	-	-	-	-	-	-	-	-
BaSO4 Cert	-	-	-	-	-	-	-	-	-	-	-	-	-	-	-
W-2a Meas	21.6	2.1	-	-	-	-	-	-	-	-	-	-	-	-	-
W-2a Cert	24	2.1	-	-	-	-	-	-	-	-	-	-	-	-	-
SY-4 Meas	-	-	-	-	-	-	-	-	-	-	-	-	-	-	-
SY-4 Cert	-	-	-	-	-	-	-	-	-	-	-	-	-	-	-
CTA-AC-1 Meas	282	10.4	-	-	-	-	-	-	-	-	-	-	-	-	-
CTA-AC-1 Cert	272	11.4	-	-	-	-	-	-	-	-	-	-	-	-	-
BIR-1a Meas	15.9	1.7	-	-	-	-	-	-	-	-	-	-	-	-	-
BIR-1a Cert	16	1.7	-	-	-	-	-	-	-	-	-	-	-	-	-
Calcium Carbonate Meas	-	-	-	-	-	-	-	-	-	-	-	-	-	-	-
Calcium Carbonate Cert	-	-	-	-	-	-	-	-	-	-	-	-	-	-	-
NCS DC86312 Meas	912	82.3	-	-	-	-	-	-	-	-	-	-	-	-	-
NCS DC86312 Cert	976	87.79	-	-	-	-	-	-	-	-	-	-	-	-	-
JGb-2 Meas	-	-	-	-	-	-	-	-	-	-	-	-	-	-	-
JGb-2 Cert	-	-	-	-	-	-	-	-	-	-	-	-	-	-	-
JGb-2 Meas	-	-	-	-	-	-	-	-	-	-	-	-	-	-	-
JGb-2 Cert	-	-	-	-	-	-	-	-	-	-	-	-	-	-	-
JGb-2 Meas	-	-	-	-	-	-	-	-	-	-	-	-	-	-	-
JGb-2 Cert	-	-	-	-	-	-	-	-	-	-	-	-	-	-	-
NCS DC70009 (GBW07241) Meas	126	15.2	-	-	-	-	-	-	-	-	-	-	-	-	-
NCS DC70009 (GBW07241) Cert	128	14.9	-	-	-	-	-	-	-	-	-	-	-	-	-
SGR-1b Meas	-	-	-	-	-	-	-	-	-	-	-	-	-	-	-
SGR-1b Cert	-	-	-	-	-	-	-	-	-	-	-	-	-	-	-
SGR-1b Meas	-	-	-	-	-	-	-	-	-	-	-	-	-	-	-
SGR-1b Cert	-	-	-	-	-	-	-	-	-	-	-	-	-	-	-
OREAS 100a (Fusion) Meas	140	14.5	-	-	-	-	-	-	-	-	-	-	-	-	-

Analyte	Y	Yb	Zn	Ag	Cd	Co	Cr	Cu	In	Li	Mn	Mo	Ni	Pb	Zn
Units	ppm	ppm	ppm	ppm	ppm	ppm	ppm	ppm	ppm	ppm	ppm	ppm	ppm	ppm	ppm
Detection Limit	0.5	0.01	30	1	0.2	0.5	1	0.5	0.2	1	2	1	1	2	0.5
Method	FUS-MS	FUS-MS	FUS-MS	TD-MS	TD-MS	TD-MS	TD-MS	TD-MS	TD-MS	TD-MS	TD-MS	TD-MS	TD-MS	TD-MS	TD-MS
OREAS 100a (Fusion) Cert	142	14.9	-	-	-	-	-	-	-	-	-	-	-	-	-
OREAS 101a (Fusion) Meas	180	17.5	-	-	-	-	-	-	-	-	-	-	-	-	-
OREAS 101a (Fusion) Cert	183	17.5	-	-	-	-	-	-	-	-	-	-	-	-	-
OREAS 101b (Fusion) Meas	179	18.1	-	-	-	-	-	-	-	-	-	-	-	-	-
OREAS 101b (Fusion) Cert	178	17.6	-	-	-	-	-	-	-	-	-	-	-	-	-
JR-1 Meas	42.6	4.58	-	-	-	-	-	-	-	-	-	-	-	-	-
JR-1 Cert	45.1	4.55	-	-	-	-	-	-	-	-	-	-	-	-	-
NCS DC86318 Meas	-	>1000	-	-	-	-	-	-	-	-	-	-	-	-	-
NCS DC86318 Cert	-	1840	-	-	-	-	-	-	-	-	-	-	-	-	-
USZ 25-2006 Meas	-	-	-	-	-	-	-	-	-	-	-	-	-	-	-
USZ 25-2006 Cert	-	-	-	-	-	-	-	-	-	-	-	-	-	-	-
USZ 25-2006 Meas	-	-	-	-	-	-	-	-	-	-	-	-	-	-	-
USZ 25-2006 Cert	-	-	-	-	-	-	-	-	-	-	-	-	-	-	-
DNC-1a Meas	-	-	-	-	-	59.4	229	107	-	5	-	-	260	6	68.6
DNC-1a Cert	-	-	-	-	-	57	270	100	-	5.2	-	-	247	6.3	70
DNC-1a Meas	-	-	-	-	-	60	181	107	-	5	-	-	272	7	72
DNC-1a Cert	-	-	-	-	-	57	270	100	-	5.2	-	-	247	6.3	70
DNC-1a Meas	-	-	-	-	-	55.5	125	97.3	-	5	-	-	250	6	62.9
DNC-1a Cert	-	-	-	-	-	57	270	100	-	5.2	-	-	247	6.3	70
DNC-1a Meas	-	-	-	-	-	42.1	146	58.3	-	5	-	-	193	6	67.1
DNC-1a Cert	-	-	-	-	-	57	270	100	-	5.2	-	-	247	6.3	70
GS311-4 Meas	-	-	-	-	-	-	-	-	-	-	-	-	-	-	-
GS311-4 Cert	-	-	-	-	-	-	-	-	-	-	-	-	-	-	-
GS311-4 Meas	-	-	-	-	-	-	-	-	-	-	-	-	-	-	-
GS311-4 Cert	-	-	-	-	-	-	-	-	-	-	-	-	-	-	-
GS900-5 Meas	-	-	-	-	-	-	-	-	-	-	-	-	-	-	-
GS900-5 Cert	-	-	-	-	-	-	-	-	-	-	-	-	-	-	-
GS900-5 Meas	-	-	-	-	-	-	-	-	-	-	-	-	-	-	-
GS900-5 Cert	-	-	-	-	-	-	-	-	-	-	-	-	-	-	-
OREAS 45d (Aqua Regia) Meas	-	-	-	-	-	-	-	-	-	-	-	-	-	-	-
OREAS 45d (Aqua Regia) Cert	-	-	-	-	-	-	-	-	-	-	-	-	-	-	-
OREAS 45d (Aqua Regia) Meas	-	-	-	-	-	-	-	-	-	-	-	-	-	-	-
OREAS 45d (Aqua Regia) Cert	-	-	-	-	-	-	-	-	-	-	-	-	-	-	-
OREAS 45d (Aqua Regia) Meas	-	-	-	-	-	-	-	-	-	-	-	-	-	-	-
OREAS 45d (Aqua Regia) Cert	-	-	-	-	-	-	-	-	-	-	-	-	-	-	-
SBC-1 Meas	-	-	-	-	0.3	23.2	107	32.9	-	163	-	2	86	37	217
SBC-1 Cert	-	-	-	-	0.4	22.7	109	31	-	163	-	2.4	82.8	35	186

Analyte	Y	Yb	Zn	Ag	Cd	Co	Cr	Cu	In	Li	Mn	Mo	Ni	Pb	Zn
Units	ppm	ppm	ppm	ppm	ppm	ppm	ppm	ppm	ppm	ppm	ppm	ppm	ppm	ppm	ppm
Detection Limit	0.5	0.01	30	1	0.2	0.5	1	0.5	0.2	1	2	1	1	2	0.5
Method	FUS-MS	FUS-MS	FUS-MS	TD-MS	TD-MS	TD-MS	TD-MS	TD-MS	TD-MS	TD-MS	TD-MS	TD-MS	TD-MS	TD-MS	TD-MS
SBC-1 Meas	-	-	-	-	0.3	23.9	74	35.1	-	148	-	2	89	39	222
SBC-1 Cert	-	-	-	-	0.4	22.7	109	31	-	163	-	2.4	82.8	35	186
SBC-1 Meas	-	-	-	-	0.3	22.7	81	30.2	-	167	-	2	84	36	195
SBC-1 Cert	-	-	-	-	0.4	22.7	109	31	-	163	-	2.4	82.8	35	186
SBC-1 Meas	-	-	-	-	0.4	23.4	88	33.6	-	160	-	3	86	39	211
SBC-1 Cert	-	-	-	-	0.4	22.7	109	31	-	163	-	2.4	82.8	35	186
OREAS 45d (4-Acid) Meas	-	-	-	-	-	30.6	471	378	<0.2	20	465	1	233	23	43.9
OREAS 45d (4-Acid) Cert	-	-	-	-	-	29.5	549	371	0.096	21.5	490	2.5	231	21.8	45.7
OREAS 45d (4-Acid) Meas	-	-	-	-	-	30.9	433	379	<0.2	21	465	2	229	25	43.4
OREAS 45d (4-Acid) Cert	-	-	-	-	-	29.5	549	371	0.096	21.5	490	2.5	231	21.8	45.7
OREAS 45d (4-Acid) Meas	-	-	-	-	-	30	453	375	<0.2	20	468	2	228	22	44.1
OREAS 45d (4-Acid) Cert	-	-	-	-	-	29.5	549	371	0.096	21.5	490	2.5	231	21.8	45.7
OREAS 45d (4-Acid) Meas	-	-	-	-	-	32.4	506	404	<0.2	21	474	2	248	24	45.4
OREAS 45d (4-Acid) Cert	-	-	-	-	-	29.5	549	371	0.096	21.5	490	2.5	231	21.8	45.7
OxK110 Meas	-	-	-	-	-	-	-	-	-	-	-	-	-	-	-
OxK110 Cert	-	-	-	-	-	-	-	-	-	-	-	-	-	-	-
CDN-PGMS-24 Meas	-	-	-	-	-	-	-	-	-	-	-	-	-	-	-
CDN-PGMS-24 Cert	-	-	-	-	-	-	-	-	-	-	-	-	-	-	-
CDN-PGMS-24 Meas	-	-	-	-	-	-	-	-	-	-	-	-	-	-	-
CDN-PGMS-24 Cert	-	-	-	-	-	-	-	-	-	-	-	-	-	-	-
OXN117 Meas	-	-	-	-	-	-	-	-	-	-	-	-	-	-	-
OXN117 Cert	-	-	-	-	-	-	-	-	-	-	-	-	-	-	-
CaCO3 Meas	-	-	-	-	-	-	-	-	-	-	-	-	-	-	-
CaCO3 Cert	-	-	-	-	-	-	-	-	-	-	-	-	-	-	-
SdAR-M2 (U.S.G.S.) Meas	-	-	-	-	4.4	13.6	60	251	-	17	-	11	49	644	810
SdAR-M2 (U.S.G.S.) Cert	-	-	-	-	5.1	12.4	49.6	236	-	17.9	-	13.3	48.8	808	760
SdAR-M2 (U.S.G.S.) Meas	-	-	-	-	4.5	13.6	38	257	-	16	-	13	50	668	824
SdAR-M2 (U.S.G.S.) Cert	-	-	-	-	5.1	12.4	49.6	236	-	17.9	-	13.3	48.8	808	760
SdAR-M2 (U.S.G.S.) Meas	-	-	-	-	4.9	14	36	253	-	18	-	12	49	729	836
SdAR-M2 (U.S.G.S.) Cert	-	-	-	-	5.1	12.4	49.6	236	-	17.9	-	13.3	48.8	808	760
SdAR-M2 (U.S.G.S.) Meas	-	-	-	-	5.2	13.7	35	258	-	18	-	10	53	745	829
SdAR-M2 (U.S.G.S.) Cert	-	-	-	-	5.1	12.4	49.6	236	-	17.9	-	13.3	48.8	808	760
GXR-1 Meas	-	-	-	32	2.3	7.2	28	994	0.8	13	728	18	38	662	658
GXR-1 Cert	-	-	-	31	3.3	8.2	12	1110	0.77	8.2	852	18	41	730	760
GXR-1 Meas	-	-	-	-	-	-	-	-	-	-	-	-	-	-	-
GXR-1 Cert	-	-	-	-	-	-	-	-	-	-	-	-	-	-	-
NIST 694 Meas	-	-	-	-	-	-	-	-	-	-	-	-	-	-	-

Analyte	Y	Yb	Zn	Ag	Cd	Co	Cr	Cu	In	Li	Mn	Mo	Ni	Pb	Zn
Units	ppm	ppm	ppm	ppm	ppm	ppm	ppm	ppm	ppm	ppm	ppm	ppm	ppm	ppm	ppm
Detection Limit	0.5	0.01	30	1	0.2	0.5	1	0.5	0.2	1	2	1	1	2	0.5
Method	FUS-MS	FUS-MS	FUS-MS	TD-MS	TD-MS	TD-MS	TD-MS	TD-MS	TD-MS	TD-MS	TD-MS	TD-MS	TD-MS	TD-MS	TD-MS
NIST 694 Cert	-	-	-	-	-	-	-	-	-	-	-	-	-	-	-
DNC-1 Meas	18.8	1.8	60	-	-	-	-	-	-	-	-	-	-	-	-
DNC-1 Cert	18	2	70	-	-	-	-	-	-	-	-	-	-	-	-
GBW 07113 Meas	-	-	-	-	-	-	-	-	-	-	-	-	-	-	-
GBW 07113 Cert	-	-	-	-	-	-	-	-	-	-	-	-	-	-	-
GXR-4 Meas	-	-	-	3	0.3	13.4	36	5860	0.2	11	142	324	39	51	63.7
GXR-4 Cert	-	-	-	4	0.86	14.6	64	6520	0.27	11.1	155	310	42	52	73
GXR-4 Meas	-	-	-	-	-	-	-	-	-	-	-	-	-	-	-
GXR-4 Cert	-	-	-	-	-	-	-	-	-	-	-	-	-	-	-
SDC-1 Meas	-	-	-	-	-	17.7	39	33	-	37	759	-	34	25	99.7
SDC-1 Cert	-	-	-	-	-	18	64	30	-	34	880	-	38	25	103
GXR-6 Meas	-	-	-	-	-	-	-	-	-	-	-	-	-	-	-
GXR-6 Cert	-	-	-	-	-	-	-	-	-	-	-	-	-	-	-
GXR-6 Meas	-	-	-	-	-	-	-	-	-	-	-	-	-	-	-
GXR-6 Cert	-	-	-	-	-	-	-	-	-	-	-	-	-	-	-
LKSD-3 Meas	29.7	2.6	160	-	-	-	-	-	-	-	-	-	-	-	-
LKSD-3 Cert	30	2.7	152	-	-	-	-	-	-	-	-	-	-	-	-
TDB-1 Meas	34.1	3.3	150	-	-	-	-	-	-	-	-	-	-	-	-
TDB-1 Cert	36	3.4	155	-	-	-	-	-	-	-	-	-	-	-	-
SY-2 Meas	-	-	-	-	-	-	-	-	-	-	-	-	-	-	-
SY-2 Cert	-	-	-	-	-	-	-	-	-	-	-	-	-	-	-
SY-3 Meas	-	-	-	-	-	-	-	-	-	-	-	-	-	-	-
SY-3 Cert	-	-	-	-	-	-	-	-	-	-	-	-	-	-	-
BaSO4 Meas	-	-	-	-	-	-	-	-	-	-	-	-	-	-	-
BaSO4 Cert	-	-	-	-	-	-	-	-	-	-	-	-	-	-	-
BaSO4 Meas	-	-	-	-	-	-	-	-	-	-	-	-	-	-	-
BaSO4 Cert	-	-	-	-	-	-	-	-	-	-	-	-	-	-	-
BaSO4 Meas	-	-	-	-	-	-	-	-	-	-	-	-	-	-	-
BaSO4 Cert	-	-	-	-	-	-	-	-	-	-	-	-	-	-	-
W-2a Meas	21.2	2.1	80	-	-	-	-	-	-	-	-	-	-	-	-
W-2a Cert	24	2.1	80	-	-	-	-	-	-	-	-	-	-	-	-
DTS-2b Meas	-	-	-	-	-	-	-	-	-	-	-	-	-	-	-
DTS-2b Cert	-	-	-	-	-	-	-	-	-	-	-	-	-	-	-
SY-4 Meas	-	-	-	-	-	-	-	-	-	-	-	-	-	-	-
SY-4 Cert	-	-	-	-	-	-	-	-	-	-	-	-	-	-	-
CTA-AC-1 Meas	286	-	40	-	-	-	-	-	-	-	-	-	-	-	-
CTA-AC-1 Cert	272	-	38	-	-	-	-	-	-	-	-	-	-	-	-

Analyte	Y	Yb	Zn	Ag	Cd	Co	Cr	Cu	In	Li	Mn	Mo	Ni	Pb	Zn
Units	ppm	ppm	ppm	ppm	ppm	ppm	ppm	ppm	ppm	ppm	ppm	ppm	ppm	ppm	ppm
Detection Limit	0.5	0.01	30	1	0.2	0.5	1	0.5	0.2	1	2	1	1	2	0.5
Method	FUS-MS	FUS-MS	FUS-MS	TD-MS	TD-MS	TD-MS	TD-MS	TD-MS	TD-MS	TD-MS	TD-MS	TD-MS	TD-MS	TD-MS	TD-MS
BIR-1a Meas	16.7	1.7	70	-	-	-	-	-	-	-	-	-	-	-	-
BIR-1a Cert	16	1.7	70	-	-	-	-	-	-	-	-	-	-	-	-
NCS DC86312 Meas	896	84.4	-	-	-	-	-	-	-	-	-	-	-	-	-
NCS DC86312 Cert	976	87.79	-	-	-	-	-	-	-	-	-	-	-	-	-
JGb-2 Meas	-	-	-	-	-	-	-	-	-	-	-	-	-	-	-
JGb-2 Cert	-	-	-	-	-	-	-	-	-	-	-	-	-	-	-
NCS DC70009 (GBW07241) Meas	128	15	90	-	-	-	-	-	-	-	-	-	-	-	-
NCS DC70009 (GBW07241) Cert	128	14.9	100	-	-	-	-	-	-	-	-	-	-	-	-
SGR-1b Meas	-	-	-	-	-	-	-	-	-	-	-	-	-	-	-
SGR-1b Cert	-	-	-	-	-	-	-	-	-	-	-	-	-	-	-
SGR-1b Meas	-	-	-	-	-	-	-	-	-	-	-	-	-	-	-
SGR-1b Cert	-	-	-	-	-	-	-	-	-	-	-	-	-	-	-
SGR-1b Meas	-	-	-	-	-	-	-	-	-	-	-	-	-	-	-
SGR-1b Cert	-	-	-	-	-	-	-	-	-	-	-	-	-	-	-
OREAS 100a (Fusion) Meas	135	14	-	-	-	-	-	-	-	-	-	-	-	-	-
OREAS 100a (Fusion) Cert	142	14.9	-	-	-	-	-	-	-	-	-	-	-	-	-
OREAS 101a (Fusion) Meas	178	16.6	-	-	-	-	-	-	-	-	-	-	-	-	-
OREAS 101a (Fusion) Cert	183	17.5	-	-	-	-	-	-	-	-	-	-	-	-	-
OREAS 101b (Fusion) Meas	178	18	-	-	-	-	-	-	-	-	-	-	-	-	-
OREAS 101b (Fusion) Cert	178	17.6	-	-	-	-	-	-	-	-	-	-	-	-	-
OREAS 98 (S by LECO) Meas	-	-	-	-	-	-	-	-	-	-	-	-	-	-	-
OREAS 98 (S by LECO) Cert	-	-	-	-	-	-	-	-	-	-	-	-	-	-	-
OREAS 132b (S by LECO) Meas	-	-	-	-	-	-	-	-	-	-	-	-	-	-	-
OREAS 132b (S by LECO) Cert	-	-	-	-	-	-	-	-	-	-	-	-	-	-	-
JR-1 Meas	43	4.87	30	-	-	-	-	-	-	-	-	-	-	-	-
JR-1 Cert	45.1	4.55	30.6	-	-	-	-	-	-	-	-	-	-	-	-
NCS DC86318 Meas	>10000	>1000	-	-	-	-	-	-	-	-	-	-	-	-	-
NCS DC86318 Cert	17008	1840	-	-	-	-	-	-	-	-	-	-	-	-	-
USZ 25-2006 Meas	-	-	-	-	-	-	-	-	-	-	-	-	-	-	-
USZ 25-2006 Cert	-	-	-	-	-	-	-	-	-	-	-	-	-	-	-
DNC-1a Meas	-	-	-	-	-	60.4	168	105	-	6	-	-	284	6	67.5
DNC-1a Cert	-	-	-	-	-	57	270	100	-	5.2	-	-	247	6.3	70
PK2 Meas	-	-	-	-	-	-	-	-	-	-	-	-	-	-	-
PK2 Cert	-	-	-	-	-	-	-	-	-	-	-	-	-	-	-
GS309-4 Meas	-	-	-	-	-	-	-	-	-	-	-	-	-	-	-
GS309-4 Cert	-	-	-	-	-	-	-	-	-	-	-	-	-	-	-
GS311-4 Meas	-	-	-	-	-	-	-	-	-	-	-	-	-	-	-

Analyte	Y	Yb	Zn	Ag	Cd	Co	Cr	Cu	In	Li	Mn	Mo	Ni	Pb	Zn
Units	ppm	ppm	ppm	ppm	ppm	ppm	ppm	ppm	ppm	ppm	ppm	ppm	ppm	ppm	ppm
Detection Limit	0.5	0.01	30	1	0.2	0.5	1	0.5	0.2	1	2	1	1	2	0.5
Method	FUS-MS	FUS-MS	FUS-MS	TD-MS	TD-MS	TD-MS	TD-MS	TD-MS	TD-MS	TD-MS	TD-MS	TD-MS	TD-MS	TD-MS	TD-MS
GS311-4 Cert	-	-	-	-	-	-	-	-	-	-	-	-	-	-	-
GS311-4 Meas	-	-	-	-	-	-	-	-	-	-	-	-	-	-	-
GS311-4 Cert	-	-	-	-	-	-	-	-	-	-	-	-	-	-	-
GS311-4 Meas	-	-	-	-	-	-	-	-	-	-	-	-	-	-	-
GS311-4 Cert	-	-	-	-	-	-	-	-	-	-	-	-	-	-	-
GS900-5 Meas	-	-	-	-	-	-	-	-	-	-	-	-	-	-	-
GS900-5 Cert	-	-	-	-	-	-	-	-	-	-	-	-	-	-	-
GS900-5 Meas	-	-	-	-	-	-	-	-	-	-	-	-	-	-	-
GS900-5 Cert	-	-	-	-	-	-	-	-	-	-	-	-	-	-	-
GS900-5 Meas	-	-	-	-	-	-	-	-	-	-	-	-	-	-	-
GS900-5 Cert	-	-	-	-	-	-	-	-	-	-	-	-	-	-	-
OREAS 45d (Aqua Regia) Meas	-	-	-	-	-	-	-	-	-	-	-	-	-	-	-
OREAS 45d (Aqua Regia) Cert	-	-	-	-	-	-	-	-	-	-	-	-	-	-	-
SBC-1 Meas	-	-	-	-	0.4	22.6	62	31.5	-	182	-	2	88	36	183
SBC-1 Cert	-	-	-	-	0.4	22.7	109	31	-	163	-	2.4	82.8	35	186
OREAS 45d (4-Acid) Meas	-	-	-	-	-	29.8	392	368	<0.2	24	441	2	240	23	42.9
OREAS 45d (4-Acid) Cert	-	-	-	-	-	29.5	549	371	0.096	21.5	490	2.5	231	21.8	45.7
CaCO3 Meas	-	-	-	-	-	-	-	-	-	-	-	-	-	-	-
CaCO3 Cert	-	-	-	-	-	-	-	-	-	-	-	-	-	-	-
SdAR-M2 (U.S.G.S.) Meas	-	-	-	-	5.3	12.3	31	235	-	17	-	13	48	735	704
SdAR-M2 (U.S.G.S.) Cert	-	-	-	-	5.1	12.4	49.6	236	-	17.9	-	13.3	48.8	808	760
SdAR-M2 (U.S.G.S.) Meas	-	-	-	-	-	-	-	-	-	-	-	-	-	-	-
SdAR-M2 (U.S.G.S.) Cert	-	-	-	-	-	-	-	-	-	-	-	-	-	-	-
GXR-1 Meas	-	-	-	34	2.8	7.4	13	1190	0.8	8	900	18	38	794	843
GXR-1 Cert	-	-	-	31	3.3	8.2	12	1110	0.77	8.2	852	18	41	730	760
GXR-1 Meas	-	-	-	29	2.5	7	14	1160	0.7	7	826	18	37	775	852
GXR-1 Cert	-	-	-	31	3.3	8.2	12	1110	0.77	8.2	852	18	41	730	760
NIST 694 Meas	-	-	-	-	-	-	-	-	-	-	-	-	-	-	-
NIST 694 Cert	-	-	-	-	-	-	-	-	-	-	-	-	-	-	-
DNC-1 Meas	16	1.8	70	-	-	-	-	-	-	-	-	-	-	-	-
DNC-1 Cert	18	2	70	-	-	-	-	-	-	-	-	-	-	-	-
GBW 07113 Meas	-	-	-	-	-	-	-	-	-	-	-	-	-	-	-
GBW 07113 Cert	-	-	-	-	-	-	-	-	-	-	-	-	-	-	-
GXR-4 Meas	-	-	-	4	<0.2	13.1	49	6790	0.2	11	150	320	43	50	71
GXR-4 Cert	-	-	-	4	0.86	14.6	64	6520	0.27	11.1	155	310	42	52	73
GXR-4 Meas	-	-	-	3	<0.2	12.9	63	6440	<0.2	11	162	321	38	50	62.9
GXR-4 Cert	-	-	-	4	0.86	14.6	64	6520	0.27	11.1	155	310	42	52	73

Analyte	Y	Yb	Zn	Ag	Cd	Co	Cr	Cu	In	Li	Mn	Mo	Ni	Pb	Zn
Units	ppm	ppm	ppm	ppm	ppm	ppm	ppm	ppm	ppm	ppm	ppm	ppm	ppm	ppm	ppm
Detection Limit	0.5	0.01	30	1	0.2	0.5	1	0.5	0.2	1	2	1	1	2	0.5
Method	FUS-MS	FUS-MS	FUS-MS	TD-MS	TD-MS	TD-MS	TD-MS	TD-MS	TD-MS	TD-MS	TD-MS	TD-MS	TD-MS	TD-MS	TD-MS
SDC-1 Meas	-	-	-	-	-	16.8	64	27.4	-	36	879	-	32	25	98.9
SDC-1 Cert	-	-	-	-	-	18	64	30	-	34	880	-	38	25	103
SDC-1 Meas	-	-	-	-	-	16.9	60	29.1	-	36	837	-	32	24	108
SDC-1 Cert	-	-	-	-	-	18	64	30	-	34	880	-	38	25	103
GXR-6 Meas	-	-	-	<1	<0.2	13.6	47	72.2	<0.2	37	1070	<1	26	106	133
GXR-6 Cert	-	-	-	1.3	1	13.8	96	66	0.26	32	1010	2.4	27	101	118
GXR-6 Meas	-	-	-	<1	<0.2	13.3	91	70.2	<0.2	35	1070	<1	24	102	120
GXR-6 Cert	-	-	-	1.3	1	13.8	96	66	0.26	32	1010	2.4	27	101	118
LKSD-3 Meas	29	2.7	150	-	-	-	-	-	-	-	-	-	-	-	-
LKSD-3 Cert	30	2.7	152	-	-	-	-	-	-	-	-	-	-	-	-
TDB-1 Meas	36.6	3.3	160	-	-	-	-	-	-	-	-	-	-	-	-
TDB-1 Cert	36	3.4	155	-	-	-	-	-	-	-	-	-	-	-	-
SY-2 Meas	-	-	-	-	-	-	-	-	-	-	-	-	-	-	-
SY-2 Cert	-	-	-	-	-	-	-	-	-	-	-	-	-	-	-
SY-3 Meas	-	-	-	-	-	-	-	-	-	-	-	-	-	-	-
SY-3 Cert	-	-	-	-	-	-	-	-	-	-	-	-	-	-	-
BaSO4 Meas	-	-	-	-	-	-	-	-	-	-	-	-	-	-	-
BaSO4 Cert	-	-	-	-	-	-	-	-	-	-	-	-	-	-	-
BaSO4 Meas	-	-	-	-	-	-	-	-	-	-	-	-	-	-	-
BaSO4 Cert	-	-	-	-	-	-	-	-	-	-	-	-	-	-	-
W-2a Meas	22.5	2.1	80	-	-	-	-	-	-	-	-	-	-	-	-
W-2a Cert	24	2.1	80	-	-	-	-	-	-	-	-	-	-	-	-
SY-4 Meas	-	-	-	-	-	-	-	-	-	-	-	-	-	-	-
SY-4 Cert	-	-	-	-	-	-	-	-	-	-	-	-	-	-	-
CTA-AC-1 Meas	275	10.5	40	-	-	-	-	-	-	-	-	-	-	-	-
CTA-AC-1 Cert	272	11.4	38	-	-	-	-	-	-	-	-	-	-	-	-
BIR-1a Meas	15	1.7	70	-	-	-	-	-	-	-	-	-	-	-	-
BIR-1a Cert	16	1.7	70	-	-	-	-	-	-	-	-	-	-	-	-
BIR-1a Meas	-	-	-	-	-	-	-	-	-	-	-	-	-	-	-
BIR-1a Cert	-	-	-	-	-	-	-	-	-	-	-	-	-	-	-
NCS DC86312 Meas	1040	82.7	-	-	-	-	-	-	-	-	-	-	-	-	-
NCS DC86312 Cert	976	87.79	-	-	-	-	-	-	-	-	-	-	-	-	-
JGb-2 Meas	-	-	-	-	-	-	-	-	-	-	-	-	-	-	-
JGb-2 Cert	-	-	-	-	-	-	-	-	-	-	-	-	-	-	-
JGb-2 Meas	-	-	-	-	-	-	-	-	-	-	-	-	-	-	-
JGb-2 Cert	-	-	-	-	-	-	-	-	-	-	-	-	-	-	-
JGb-2 Meas	-	-	-	-	-	-	-	-	-	-	-	-	-	-	-

Analyte	Y	Yb	Zn	Ag	Cd	Co	Cr	Cu	In	Li	Mn	Mo	Ni	Pb	Zn
Units	ppm	ppm	ppm	ppm	ppm	ppm	ppm	ppm	ppm	ppm	ppm	ppm	ppm	ppm	ppm
Detection Limit	0.5	0.01	30	1	0.2	0.5	1	0.5	0.2	1	2	1	1	2	0.5
Method	FUS-MS	FUS-MS	FUS-MS	TD-MS	TD-MS	TD-MS	TD-MS	TD-MS	TD-MS	TD-MS	TD-MS	TD-MS	TD-MS	TD-MS	TD-MS
JGb-2 Cert	-	-	-	-	-	-	-	-	-	-	-	-	-	-	-
JGb-2 Meas	-	-	-	-	-	-	-	-	-	-	-	-	-	-	-
JGb-2 Cert	-	-	-	-	-	-	-	-	-	-	-	-	-	-	-
NCS DC70009 (GBW07241) Meas	127	16	100	-	-	-	-	-	-	-	-	-	-	-	-
NCS DC70009 (GBW07241) Cert	128	14.9	100	-	-	-	-	-	-	-	-	-	-	-	-
SGR-1b Meas	-	-	-	-	-	-	-	-	-	-	-	-	-	-	-
SGR-1b Cert	-	-	-	-	-	-	-	-	-	-	-	-	-	-	-
SGR-1b Meas	-	-	-	-	-	-	-	-	-	-	-	-	-	-	-
SGR-1b Cert	-	-	-	-	-	-	-	-	-	-	-	-	-	-	-
OREAS 100a (Fusion) Meas	148	15.2	-	-	-	-	-	-	-	-	-	-	-	-	-
OREAS 100a (Fusion) Cert	142	14.9	-	-	-	-	-	-	-	-	-	-	-	-	-
OREAS 101a (Fusion) Meas	169	17.2	-	-	-	-	-	-	-	-	-	-	-	-	-
OREAS 101a (Fusion) Cert	183	17.5	-	-	-	-	-	-	-	-	-	-	-	-	-
OREAS 101b (Fusion) Meas	188	18.2	-	-	-	-	-	-	-	-	-	-	-	-	-
OREAS 101b (Fusion) Cert	178	17.6	-	-	-	-	-	-	-	-	-	-	-	-	-
JR-1 Meas	44	4.59	30	-	-	-	-	-	-	-	-	-	-	-	-
JR-1 Cert	45.1	4.55	30.6	-	-	-	-	-	-	-	-	-	-	-	-
NCS DC86318 Meas	>10000	>1000	-	-	-	-	-	-	-	-	-	-	-	-	-
NCS DC86318 Cert	17008	1840	-	-	-	-	-	-	-	-	-	-	-	-	-
USZ 25-2006 Meas	-	-	-	-	-	-	-	-	-	-	-	-	-	-	-
USZ 25-2006 Cert	-	-	-	-	-	-	-	-	-	-	-	-	-	-	-
USZ 25-2006 Meas	-	-	-	-	-	-	-	-	-	-	-	-	-	-	-
USZ 25-2006 Cert	-	-	-	-	-	-	-	-	-	-	-	-	-	-	-
DNC-1a Meas	-	-	-	-	-	52.5	247	97	-	5	-	-	252	6	64.2
DNC-1a Cert	-	-	-	-	-	57	270	100	-	5.2	-	-	247	6.3	70
DNC-1a Meas	-	-	-	-	-	54.2	208	99.1	-	5	-	-	249	5	62.3
DNC-1a Cert	-	-	-	-	-	57	270	100	-	5.2	-	-	247	6.3	70
PK2 Meas	-	-	-	-	-	-	-	-	-	-	-	-	-	-	-
PK2 Cert	-	-	-	-	-	-	-	-	-	-	-	-	-	-	-
GS311-4 Meas	-	-	-	-	-	-	-	-	-	-	-	-	-	-	-
GS311-4 Cert	-	-	-	-	-	-	-	-	-	-	-	-	-	-	-
GS311-4 Meas	-	-	-	-	-	-	-	-	-	-	-	-	-	-	-
GS311-4 Cert	-	-	-	-	-	-	-	-	-	-	-	-	-	-	-
GS900-5 Meas	-	-	-	-	-	-	-	-	-	-	-	-	-	-	-
GS900-5 Cert	-	-	-	-	-	-	-	-	-	-	-	-	-	-	-
GS900-5 Meas	-	-	-	-	-	-	-	-	-	-	-	-	-	-	-
GS900-5 Cert	-	-	-	-	-	-	-	-	-	-	-	-	-	-	-



Analyte	Y	Yb	Zn	Ag	Cd	Co	Cr	Cu	In	Li	Mn	Mo	Ni	Pb	Zn
Units	ppm	ppm	ppm	ppm	ppm	ppm	ppm	ppm	ppm	ppm	ppm	ppm	ppm	ppm	ppm
Detection Limit	0.5	0.01	30	1	0.2	0.5	1	0.5	0.2	1	2	1	1	2	0.5
Method	FUS-MS	FUS-MS	FUS-MS	TD-MS	TD-MS	TD-MS	TD-MS	TD-MS	TD-MS	TD-MS	TD-MS	TD-MS	TD-MS	TD-MS	TD-MS
OREAS 45d (Aqua Regia) Meas	-	-	-	-	-	-	-	-	-	-	-	-	-	-	-
OREAS 45d (Aqua Regia) Cert	-	-	-	-	-	-	-	-	-	-	-	-	-	-	-
SBC-1 Meas	-	-	-	-	0.3	21.8	78	27.6	-	175	-	2	85	38	217
SBC-1 Cert	-	-	-	-	0.4	22.7	109	31	-	163	-	2	83	35	186
SBC-1 Meas	-	-	-	-	0.3	21.5	115	27.9	-	165	-	2	80	36	198
SBC-1 Cert	-	-	-	-	0.4	22.7	109	31	-	163	-	2	83	35	186
OREAS 45d (4-Acid) Meas	-	-	-	-	-	28.3	636	366	<0.2	21	483	1	218	21	26.6
OREAS 45d (4-Acid) Cert	-	-	-	-	-	29.5	549	371	0.096	21.5	490	2.5	231	21.8	45.7
OxK110 Meas	-	-	-	-	-	-	-	-	-	-	-	-	-	-	-
OxK110 Cert	-	-	-	-	-	-	-	-	-	-	-	-	-	-	-
OXN117 Meas	-	-	-	-	-	-	-	-	-	-	-	-	-	-	-
OXN117 Cert	-	-	-	-	-	-	-	-	-	-	-	-	-	-	-
CaCO3 Meas	-	-	-	-	-	-	-	-	-	-	-	-	-	-	-
CaCO3 Cert	-	-	-	-	-	-	-	-	-	-	-	-	-	-	-
CaCO3 Meas	-	-	-	-	-	-	-	-	-	-	-	-	-	-	-
CaCO3 Cert	-	-	-	-	-	-	-	-	-	-	-	-	-	-	-
SdAR-M2 (U.S.G.S.) Meas	-	-	-	-	5.5	12.8	48	258	-	18	-	13	48	772	883
SdAR-M2 (U.S.G.S.) Cert	-	-	-	-	5.1	12.4	49.6	236	-	18	-	13	49	808	760
GXR-1 Meas	-	-	-	-	-	-	-	-	-	-	-	-	-	-	-
GXR-1 Cert	-	-	-	-	-	-	-	-	-	-	-	-	-	-	-
GXR-1 Meas	-	-	-	-	-	-	-	-	-	-	-	-	-	-	-
GXR-1 Cert	-	-	-	-	-	-	-	-	-	-	-	-	-	-	-
NIST 694 Meas	-	-	-	-	-	-	-	-	-	-	-	-	-	-	-
NIST 694 Cert	-	-	-	-	-	-	-	-	-	-	-	-	-	-	-
DNC-1 Meas	18	1.9	70	-	-	-	-	-	-	-	-	-	-	-	-
DNC-1 Cert	18	2	70	-	-	-	-	-	-	-	-	-	-	-	-
GBW 07113 Meas	-	-	-	-	-	-	-	-	-	-	-	-	-	-	-
GBW 07113 Cert	-	-	-	-	-	-	-	-	-	-	-	-	-	-	-
GXR-4 Meas	-	-	-	4	0.4	13.6	43	6250	0.2	11	142	301	40	51	71.9
GXR-4 Cert	-	-	-	4	0.86	14.6	64	6520	0.27	11.1	155	310	42	52	73
GXR-4 Meas	-	-	-	4	0.4	14	45	6510	0.2	12	145	310	42	51	77.7
GXR-4 Cert	-	-	-	4	0.86	14.6	64	6520	0.27	11.1	155	310	42	52	73
GXR-4 Meas	-	-	-	-	-	-	-	-	-	-	-	-	-	-	-
GXR-4 Cert	-	-	-	-	-	-	-	-	-	-	-	-	-	-	-
SDC-1 Meas	-	-	-	-	-	17.6	42	33.1	-	36	823	-	34	25	104
SDC-1 Cert	-	-	-	-	-	18	64	30	-	34	880	-	38	25	103
SDC-1 Meas	-	-	-	-	-	17.2	57	37.4	-	36	853	-	35	25	109

Analyte	Y	Yb	Zn	Ag	Cd	Co	Cr	Cu	In	Li	Mn	Mo	Ni	Pb	Zn
Units	ppm	ppm	ppm	ppm	ppm	ppm	ppm	ppm	ppm	ppm	ppm	ppm	ppm	ppm	ppm
Detection Limit	0.5	0.01	30	1	0.2	0.5	1	0.5	0.2	1	2	1	1	2	0.5
Method	FUS-MS	FUS-MS	FUS-MS	TD-MS	TD-MS	TD-MS	TD-MS	TD-MS	TD-MS	TD-MS	TD-MS	TD-MS	TD-MS	TD-MS	TD-MS
SDC-1 Cert	-	-	-	-	-	18	64	30	-	34	880	-	38	25	103
GXR-6 Meas	-	-	-	<1	<0.2	12.7	82	65.3	<0.2	36	918	2	24	99	115
GXR-6 Cert	-	-	-	1.3	1	13.8	96	66	0.26	32	1010	2.4	27	101	118
GXR-6 Meas	-	-	-	<1	<0.2	13.2	70	69.2	<0.2	40	1010	1	25	105	132
GXR-6 Cert	-	-	-	1.3	1	13.8	96	66	0.26	32	1010	2.4	27	101	118
GXR-6 Meas	-	-	-	-	-	-	-	-	-	-	-	-	-	-	-
GXR-6 Cert	-	-	-	-	-	-	-	-	-	-	-	-	-	-	-
LKSD-3 Meas	32.2	2.8	150	-	-	-	-	-	-	-	-	-	-	-	-
LKSD-3 Cert	30	2.7	152	-	-	-	-	-	-	-	-	-	-	-	-
TDB-1 Meas	35.7	3.3	140	-	-	-	-	-	-	-	-	-	-	-	-
TDB-1 Cert	36	3.4	155	-	-	-	-	-	-	-	-	-	-	-	-
SY-2 Meas	-	-	-	-	-	-	-	-	-	-	-	-	-	-	-
SY-2 Cert	-	-	-	-	-	-	-	-	-	-	-	-	-	-	-
SY-3 Meas	-	-	-	-	-	-	-	-	-	-	-	-	-	-	-
SY-3 Cert	-	-	-	-	-	-	-	-	-	-	-	-	-	-	-
BaSO4 Meas	-	-	-	-	-	-	-	-	-	-	-	-	-	-	-
BaSO4 Cert	-	-	-	-	-	-	-	-	-	-	-	-	-	-	-
W-2a Meas	21.9	2.1	80	-	-	-	-	-	-	-	-	-	-	-	-
W-2a Cert	24	2.1	80	-	-	-	-	-	-	-	-	-	-	-	-
SY-4 Meas	-	-	-	-	-	-	-	-	-	-	-	-	-	-	-
SY-4 Cert	-	-	-	-	-	-	-	-	-	-	-	-	-	-	-
CTA-AC-1 Meas	280	11.2	40	-	-	-	-	-	-	-	-	-	-	-	-
CTA-AC-1 Cert	272	11.4	38	-	-	-	-	-	-	-	-	-	-	-	-
BIR-1a Meas	15.5	1.7	70	-	-	-	-	-	-	-	-	-	-	-	-
BIR-1a Cert	16	1.7	70	-	-	-	-	-	-	-	-	-	-	-	-
NCS DC86312 Meas	931	83.5	-	-	-	-	-	-	-	-	-	-	-	-	-
NCS DC86312 Cert	976	87.79	-	-	-	-	-	-	-	-	-	-	-	-	-
JGb-2 Meas	-	-	-	-	-	-	-	-	-	-	-	-	-	-	-
JGb-2 Cert	-	-	-	-	-	-	-	-	-	-	-	-	-	-	-
JGb-2 Meas	-	-	-	-	-	-	-	-	-	-	-	-	-	-	-
JGb-2 Cert	-	-	-	-	-	-	-	-	-	-	-	-	-	-	-
JGb-2 Meas	-	-	-	-	-	-	-	-	-	-	-	-	-	-	-
JGb-2 Cert	-	-	-	-	-	-	-	-	-	-	-	-	-	-	-
NCS DC70009 (GBW07241) Meas	128	15.6	100	-	-	-	-	-	-	-	-	-	-	-	-
NCS DC70009 (GBW07241) Cert	128	14.9	100	-	-	-	-	-	-	-	-	-	-	-	-
SGR-1b Meas	-	-	-	-	-	-	-	-	-	-	-	-	-	-	-
SGR-1b Cert	-	-	-	-	-	-	-	-	-	-	-	-	-	-	-

Analyte	Y	Yb	Zn	Ag	Cd	Co	Cr	Cu	In	Li	Mn	Mo	Ni	Pb	Zn
Units	ppm	ppm	ppm	ppm	ppm	ppm	ppm	ppm	ppm	ppm	ppm	ppm	ppm	ppm	ppm
Detection Limit	0.5	0.01	30	1	0.2	0.5	1	0.5	0.2	1	2	1	1	2	0.5
Method	FUS-MS	FUS-MS	FUS-MS	TD-MS	TD-MS	TD-MS	TD-MS	TD-MS	TD-MS	TD-MS	TD-MS	TD-MS	TD-MS	TD-MS	TD-MS
OREAS 100a (Fusion) Meas	143	15	-	-	-	-	-	-	-	-	-	-	-	-	-
OREAS 100a (Fusion) Cert	142	14.9	-	-	-	-	-	-	-	-	-	-	-	-	-
OREAS 101a (Fusion) Meas	179	17.8	-	-	-	-	-	-	-	-	-	-	-	-	-
OREAS 101a (Fusion) Cert	183	17.5	-	-	-	-	-	-	-	-	-	-	-	-	-
OREAS 101b (Fusion) Meas	176	18.1	-	-	-	-	-	-	-	-	-	-	-	-	-
OREAS 101b (Fusion) Cert	178	17.6	-	-	-	-	-	-	-	-	-	-	-	-	-
JR-1 Meas	46.4	4.72	30	-	-	-	-	-	-	-	-	-	-	-	-
JR-1 Cert	45.1	4.55	30.6	-	-	-	-	-	-	-	-	-	-	-	-
NCS DC86318 Meas	>10000	>1000	-	-	-	-	-	-	-	-	-	-	-	-	-
NCS DC86318 Cert	17008	1840	-	-	-	-	-	-	-	-	-	-	-	-	-
USZ 25-2006 Meas	-	-	-	-	-	-	-	-	-	-	-	-	-	-	-
USZ 25-2006 Cert	-	-	-	-	-	-	-	-	-	-	-	-	-	-	-
USZ 25-2006 Meas	-	-	-	-	-	-	-	-	-	-	-	-	-	-	-
USZ 25-2006 Cert	-	-	-	-	-	-	-	-	-	-	-	-	-	-	-
DNC-1a Meas	-	-	-	-	-	54.9	153	98.4	-	5	-	-	256	6	59.1
DNC-1a Cert	-	-	-	-	-	57	270	100	-	5.2	-	-	247	6.3	70
DNC-1a Meas	-	-	-	-	-	56.8	183	104	-	5	-	-	279	7	65.4
DNC-1a Cert	-	-	-	-	-	57	270	100	-	5.2	-	-	247	6.3	70
GS311-4 Meas	-	-	-	-	-	-	-	-	-	-	-	-	-	-	-
GS311-4 Cert	-	-	-	-	-	-	-	-	-	-	-	-	-	-	-
GS900-5 Meas	-	-	-	-	-	-	-	-	-	-	-	-	-	-	-
GS900-5 Cert	-	-	-	-	-	-	-	-	-	-	-	-	-	-	-
OREAS 45d (Aqua Regia) Meas	-	-	-	-	-	-	-	-	-	-	-	-	-	-	-
OREAS 45d (Aqua Regia) Cert	-	-	-	-	-	-	-	-	-	-	-	-	-	-	-
SBC-1 Meas	-	-	-	-	0.4	21.5	71	29.7	-	178	-	2	84	38	193
SBC-1 Cert	-	-	-	-	0.4	22.7	109	31	-	163	-	2	83	35	186
SBC-1 Meas	-	-	-	-	0.4	22.1	96	34.3	-	185	-	3	87	38	206
SBC-1 Cert	-	-	-	-	0.4	22.7	109	31	-	163	-	2	83	35	186
OREAS 45d (4-Acid) Meas	-	-	-	-	-	29	454	366	<0.2	22	461	<1	233	22	42.6
OREAS 45d (4-Acid) Cert	-	-	-	-	-	29.5	549	371	0.096	21.5	490	2.5	231	21.8	45.7
OREAS 45d (4-Acid) Meas	-	-	-	-	-	29.3	523	375	<0.2	23	482	<1	242	22	42.2
OREAS 45d (4-Acid) Cert	-	-	-	-	-	29.5	549	371	0.096	21.5	490	2.5	231	21.8	45.7
CaCO3 Meas	-	-	-	-	-	-	-	-	-	-	-	-	-	-	-
CaCO3 Cert	-	-	-	-	-	-	-	-	-	-	-	-	-	-	-
CaCO3 Meas	-	-	-	-	-	-	-	-	-	-	-	-	-	-	-
CaCO3 Cert	-	-	-	-	-	-	-	-	-	-	-	-	-	-	-
SdAR-M2 (U.S.G.S.) Meas	-	-	-	-	-	-	-	-	-	-	-	-	-	-	-

Analyte	Y	Yb	Zn	Ag	Cd	Co	Cr	Cu	In	Li	Mn	Mo	Ni	Pb	Zn
Units	ppm	ppm	ppm	ppm	ppm	ppm	ppm	ppm	ppm	ppm	ppm	ppm	ppm	ppm	ppm
Detection Limit	0.5	0.01	30	1	0.2	0.5	1	0.5	0.2	1	2	1	1	2	0.5
Method	FUS-MS	FUS-MS	FUS-MS	TD-MS	TD-MS	TD-MS	TD-MS	TD-MS	TD-MS	TD-MS	TD-MS	TD-MS	TD-MS	TD-MS	TD-MS
SdAR-M2 (U.S.G.S.) Cert	-	-	-	-	-	-	-	-	-	-	-	-	-	-	-
SdAR-M2 (U.S.G.S.) Meas	-	-	-	-	-	-	-	-	-	-	-	-	-	-	-
SdAR-M2 (U.S.G.S.) Cert	-	-	-	-	-	-	-	-	-	-	-	-	-	-	-
SdAR-M2 (U.S.G.S.) Meas	-	-	-	-	-	-	-	-	-	-	-	-	-	-	-
SdAR-M2 (U.S.G.S.) Cert	-	-	-	-	-	-	-	-	-	-	-	-	-	-	-
OREAS 214 Meas	-	-	-	-	-	-	-	-	-	-	-	-	-	-	-
OREAS 214 Cert	-	-	-	-	-	-	-	-	-	-	-	-	-	-	-
OREAS 218 Meas	-	-	-	-	-	-	-	-	-	-	-	-	-	-	-
OREAS 218 Cert	-	-	-	-	-	-	-	-	-	-	-	-	-	-	-
OREAS 218 Meas	-	-	-	-	-	-	-	-	-	-	-	-	-	-	-
OREAS 218 Cert	-	-	-	-	-	-	-	-	-	-	-	-	-	-	-
T9 Geochem Orig	-	-	-	-	-	-	-	-	-	-	-	-	-	-	-
T9 Geochem Dup	-	-	-	-	-	-	-	-	-	-	-	-	-	-	-
T14 Geochem Orig	-	-	-	-	-	-	-	-	-	-	-	-	-	-	-
T14 Geochem Dup	-	-	-	-	-	-	-	-	-	-	-	-	-	-	-
T17 Geochem Orig	-	-	-	-	-	-	-	-	-	-	-	-	-	-	-
T17 Geochem Dup	-	-	-	-	-	-	-	-	-	-	-	-	-	-	-
STPL-BAS-025 Orig	-	-	-	-	-	-	-	-	-	-	-	-	-	-	-
STPL-BAS-025 Dup	-	-	-	-	-	-	-	-	-	-	-	-	-	-	-
T24 Geochem Orig	6.5	0.48	-	-	-	-	-	-	-	-	-	-	-	-	-
T24 Geochem Dup	6.1	0.45	-	-	-	-	-	-	-	-	-	-	-	-	-
T27 Geochem Orig	-	-	-	-	-	-	-	-	-	-	-	-	-	-	-
T27 Geochem Dup	-	-	-	-	-	-	-	-	-	-	-	-	-	-	-
T31 Geochem Orig	-	-	-	-	-	-	-	-	-	-	-	-	-	-	-
T31 Geochem Dup	-	-	-	-	-	-	-	-	-	-	-	-	-	-	-
T37 Geochem Orig	-	-	-	-	-	-	-	-	-	-	-	-	-	-	-
T37 Geochem Dup	-	-	-	-	-	-	-	-	-	-	-	-	-	-	-
T42 Geochem Orig	-	-	-	-	-	-	-	-	-	-	-	-	-	-	-
T42 Geochem Dup	-	-	-	-	-	-	-	-	-	-	-	-	-	-	-
T45 Geochem Orig	-	-	-	-	-	-	-	-	-	-	-	-	-	-	-
T45 Geochem Dup	-	-	-	-	-	-	-	-	-	-	-	-	-	-	-
STPL-53-PML-036 Orig	-	-	-	-	-	-	-	-	-	-	-	-	-	-	-
STPL-53-PML-036 Dup	-	-	-	-	-	-	-	-	-	-	-	-	-	-	-
STPL-BAS-025 Orig	-	-	-	<1	<0.2	53.5	155	126	<0.2	14	1250	<1	183	<2	67.8
STPL-BAS-025 Dup	-	-	-	<1	<0.2	53.8	150	126	<0.2	14	1200	<1	184	<2	68.5
T42 Geochem Orig	-	-	-	<1	<0.2	27.9	142	25.5	<0.2	52	729	<1	227	2	85.9
T42 Geochem Dup	-	-	-	<1	<0.2	26.8	145	24.4	<0.2	51	714	<1	218	2	82.3

Analyte	Y	Yb	Zn	Ag	Cd	Co	Cr	Cu	In	Li	Mn	Mo	Ni	Pb	Zn
Units	ppm	ppm	ppm	ppm	ppm	ppm	ppm	ppm	ppm	ppm	ppm	ppm	ppm	ppm	ppm
Detection Limit	0.5	0.01	30	1	0.2	0.5	1	0.5	0.2	1	2	1	1	2	0.5
Method	FUS-MS	FUS-MS	FUS-MS	TD-MS	TD-MS	TD-MS	TD-MS	TD-MS	TD-MS	TD-MS	TD-MS	TD-MS	TD-MS	TD-MS	TD-MS
T45 Geochem Orig	-	-	-	<1	<0.2	1.6	19	14.5	<0.2	11	813	<1	3	3	9.3
T45 Geochem Dup	-	-	-	<1	<0.2	1.3	10	14.2	<0.2	11	745	<1	2	3	8
T59 Orig	-	-	-	-	-	-	-	-	-	-	-	-	-	-	-
T59 Dup	-	-	-	-	-	-	-	-	-	-	-	-	-	-	-
T72 Orig	-	-	-	-	-	-	-	-	-	-	-	-	-	-	-
T72 Dup	-	-	-	-	-	-	-	-	-	-	-	-	-	-	-
T73 Orig	-	-	-	-	-	-	-	-	-	-	-	-	-	-	-
T73 Dup	-	-	-	-	-	-	-	-	-	-	-	-	-	-	-
STPL-BAS-029 Orig	-	-	-	-	-	-	-	-	-	-	-	-	-	-	-
STPL-BAS-029 Dup	-	-	-	-	-	-	-	-	-	-	-	-	-	-	-
T81 Orig	-	-	-	-	-	-	-	-	-	-	-	-	-	-	-
T81 Dup	-	-	-	-	-	-	-	-	-	-	-	-	-	-	-
T86 Orig	-	-	-	-	-	-	-	-	-	-	-	-	-	-	-
T86 Dup	-	-	-	-	-	-	-	-	-	-	-	-	-	-	-
T88 Orig	8.9	0.92	-	-	-	-	-	-	-	-	-	-	-	-	-
T88 Dup	8.9	1.01	-	-	-	-	-	-	-	-	-	-	-	-	-
T89 Orig	-	-	-	-	-	-	-	-	-	-	-	-	-	-	-
T89 Dup	-	-	-	-	-	-	-	-	-	-	-	-	-	-	-
T94 Orig	-	-	-	-	-	-	-	-	-	-	-	-	-	-	-
T94 Dup	-	-	-	-	-	-	-	-	-	-	-	-	-	-	-
T98 Orig	-	-	-	-	-	-	-	-	-	-	-	-	-	-	-
T98 Dup	-	-	-	-	-	-	-	-	-	-	-	-	-	-	-
T99 Orig	-	-	-	-	-	-	-	-	-	-	-	-	-	-	-
T99 Dup	-	-	-	-	-	-	-	-	-	-	-	-	-	-	-
T101 Orig	-	-	-	<1	<0.2	45.4	45	77.9	<0.2	58	1460	<1	44	2	112
T101 Dup	-	-	-	<1	<0.2	46.3	42	75.5	<0.2	61	1470	<1	44	2	111
T102 Orig	-	-	-	-	-	-	-	-	-	-	-	-	-	-	-
T102 Dup	-	-	-	-	-	-	-	-	-	-	-	-	-	-	-
T114 Orig	-	-	-	-	-	-	-	-	-	-	-	-	-	-	-
T114 Dup	-	-	-	-	-	-	-	-	-	-	-	-	-	-	-
T116 Orig	-	-	-	-	-	-	-	-	-	-	-	-	-	-	-
T116 Dup	-	-	-	-	-	-	-	-	-	-	-	-	-	-	-
T117 Orig	7.7	0.78	-	<1	<0.2	11.1	20	54.9	<0.2	22	366	2	11	3	37.2
T117 Split PREP DUP	7.4	0.81	-	<1	<0.2	11.5	18	55.3	<0.2	21	380	2	11	3	39.3
STPL-53-PML-025 Orig	14.7	1.92	-	-	-	-	-	-	-	-	-	-	-	-	-
STPL-53-PML-025 Dup	14.1	1.84	-	-	-	-	-	-	-	-	-	-	-	-	-
T65 Orig	-	-	-	-	-	-	-	-	-	-	-	-	-	-	-

Analyte	Y	Yb	Zn	Ag	Cd	Co	Cr	Cu	In	Li	Mn	Mo	Ni	Pb	Zn
Units	ppm	ppm	ppm	ppm	ppm	ppm	ppm	ppm	ppm	ppm	ppm	ppm	ppm	ppm	ppm
Detection Limit	0.5	0.01	30	1	0.2	0.5	1	0.5	0.2	1	2	1	1	2	0.5
Method	FUS-MS	FUS-MS	FUS-MS	TD-MS	TD-MS	TD-MS	TD-MS	TD-MS	TD-MS	TD-MS	TD-MS	TD-MS	TD-MS	TD-MS	TD-MS
T65 Dup	-	-	-	-	-	-	-	-	-	-	-	-	-	-	-
T106 Orig	-	-	-	-	-	-	-	-	-	-	-	-	-	-	-
T106 Dup	-	-	-	-	-	-	-	-	-	-	-	-	-	-	-
T118 Orig	11.6	1.03	60	-	-	-	-	-	-	-	-	-	-	-	-
T118 Dup	12.2	1.12	70	-	-	-	-	-	-	-	-	-	-	-	-
T141 Orig	-	-	-	-	-	-	-	-	-	-	-	-	-	-	-
T141 Dup	-	-	-	-	-	-	-	-	-	-	-	-	-	-	-
STPL-BAS-023 Orig	-	-	-	-	-	-	-	-	-	-	-	-	-	-	-
STPL-BAS-023 Dup	-	-	-	-	-	-	-	-	-	-	-	-	-	-	-
T154 Orig	-	-	-	-	-	-	-	-	-	-	-	-	-	-	-
T154 Dup	-	-	-	-	-	-	-	-	-	-	-	-	-	-	-
T157 Orig	-	-	-	-	-	-	-	-	-	-	-	-	-	-	-
T157 Dup	-	-	-	-	-	-	-	-	-	-	-	-	-	-	-
T158 Orig	-	-	-	-	-	-	-	-	-	-	-	-	-	-	-
T158 Dup	-	-	-	-	-	-	-	-	-	-	-	-	-	-	-
STPL-PML-53-027 Orig	16.1	2	40	-	-	-	-	-	-	-	-	-	-	-	-
STPL-PML-53-027 Dup	15.9	2.05	30	-	-	-	-	-	-	-	-	-	-	-	-
T182 Orig	-	-	-	-	-	-	-	-	-	-	-	-	-	-	-
T182 Dup	-	-	-	-	-	-	-	-	-	-	-	-	-	-	-
T183 Orig	-	-	-	<1	1.9	10	52	18.8	<0.2	17	2350	1	32	5	698
T183 Dup	-	-	-	<1	1.8	9.5	57	18.3	<0.2	15	2330	2	32	4	687
T187 Orig	-	-	-	-	-	-	-	-	-	-	-	-	-	-	-
T187 Dup	-	-	-	-	-	-	-	-	-	-	-	-	-	-	-
T188 Orig	-	-	-	-	-	-	-	-	-	-	-	-	-	-	-
T188 Dup	-	-	-	-	-	-	-	-	-	-	-	-	-	-	-
T189 Orig	-	-	-	-	-	-	-	-	-	-	-	-	-	-	-
T189 Dup	-	-	-	-	-	-	-	-	-	-	-	-	-	-	-
T200 Orig	12.8	1.5	100	-	-	-	-	-	-	-	-	-	-	-	-
T200 Dup	12.2	1.42	110	-	-	-	-	-	-	-	-	-	-	-	-
T218 Orig	-	-	-	-	-	-	-	-	-	-	-	-	-	-	-
T218 Dup	-	-	-	-	-	-	-	-	-	-	-	-	-	-	-
T239 Orig	-	-	-	-	-	-	-	-	-	-	-	-	-	-	-
T239 Dup	-	-	-	-	-	-	-	-	-	-	-	-	-	-	-
T240 Orig	-	-	-	-	-	-	-	-	-	-	-	-	-	-	-
T240 Dup	-	-	-	-	-	-	-	-	-	-	-	-	-	-	-
T242 Orig	-	-	-	-	-	-	-	-	-	-	-	-	-	-	-
T242 Dup	-	-	-	-	-	-	-	-	-	-	-	-	-	-	-



Analyte	Y	Yb	Zn	Ag	Cd	Co	Cr	Cu	In	Li	Mn	Mo	Ni	Pb	Zn
Units	ppm	ppm	ppm	ppm	ppm	ppm	ppm	ppm	ppm	ppm	ppm	ppm	ppm	ppm	ppm
Detection Limit	0.5	0.01	30	1	0.2	0.5	1	0.5	0.2	1	2	1	1	2	0.5
Method	FUS-MS	FUS-MS	FUS-MS	TD-MS	TD-MS	TD-MS	TD-MS	TD-MS	TD-MS	TD-MS	TD-MS	TD-MS	TD-MS	TD-MS	TD-MS
Method Blank	-	-	-	-	-	-	-	-	-	-	-	-	-	-	-
Method Blank	-	-	-	-	-	-	-	-	-	-	-	-	-	-	-
Method Blank	-	-	-	-	-	-	-	-	-	-	-	-	-	-	-
Method Blank	-	-	-	<1	<0.2	<0.5	1	<0.5	<0.2	<1	4	<1	<1	<2	<0.5
Method Blank	-	-	-	<1	<0.2	<0.5	<1	<0.5	<0.2	<1	6	<1	<1	<2	0.6
Method Blank	-	-	-	<1	<0.2	<0.5	8	<0.5	<0.2	<1	9	<1	<1	<2	<0.5
Method Blank	-	-	-	-	-	-	-	-	-	-	-	-	-	-	-
Method Blank	-	-	-	-	-	-	-	-	-	-	-	-	-	-	-
Method Blank	-	-	-	-	-	-	-	-	-	-	-	-	-	-	-
Method Blank	-	-	-	<1	<0.2	<0.5	12	<0.5	<0.2	<1	12	<1	<1	<2	0.6
Method Blank	-	-	-	-	-	-	-	-	-	-	-	-	-	-	-
Method Blank	<0.5	<0.01	<30	-	-	-	-	-	-	-	-	-	-	-	-
Method Blank	-	-	-	-	-	-	-	-	-	-	-	-	-	-	-
Method Blank	-	-	-	-	-	-	-	-	-	-	-	-	-	-	-
Method Blank	-	-	-	-	-	-	-	-	-	-	-	-	-	-	-
Method Blank	-	-	-	<1	<0.2	<0.5	7	<0.5	<0.2	<1	21	<1	<1	<2	<0.5
Method Blank	-	-	-	<1	<0.2	<0.5	6	<0.5	<0.2	<1	32	<1	<1	<2	0.5
Method Blank	-	-	-	<1	<0.2	<0.5	7	<0.5	<0.2	<1	9	<1	<1	<2	<0.5
Method Blank	-	-	-	<1	<0.2	<0.5	3	<0.5	<0.2	<1	25	<1	<1	<2	<0.5
Method Blank	-	-	-	<1	<0.2	<0.5	6	<0.5	<0.2	<1	21	<1	<1	<2	0.8
Method Blank	-	-	-	<1	<0.2	<0.5	4	<0.5	<0.2	<1	27	<1	<1	<2	1.2
Method Blank	-	-	-	-	-	-	-	-	-	-	-	-	-	-	-
Method Blank	-	-	-	-	-	-	-	-	-	-	-	-	-	-	-
Method Blank	-	-	-	-	-	-	-	-	-	-	-	-	-	-	-
Method Blank	-	-	-	-	-	-	-	-	-	-	-	-	-	-	-
Method Blank	-	-	-	-	-	-	-	-	-	-	-	-	-	-	-
Method Blank	-	-	-	-	-	-	-	-	-	-	-	-	-	-	-
Method Blank	-	-	-	-	-	-	-	-	-	-	-	-	-	-	-
Method Blank	<0.5	<0.01	<30	-	-	-	-	-	-	-	-	-	-	-	-
Method Blank	-	-	-	-	-	-	-	-	-	-	-	-	-	-	-
Method Blank	-	-	-	-	-	-	-	-	-	-	-	-	-	-	-
Method Blank	-	-	-	-	-	-	-	-	-	-	-	-	-	-	-
Method Blank	-	-	-	<1	<0.2	<0.5	10	<0.5	<0.2	<1	21	<1	<1	<2	<0.5
Method Blank	-	-	-	-	-	-	-	-	-	-	-	-	-	-	-
Method Blank	-	-	-	-	-	-	-	-	-	-	-	-	-	-	-
Method Blank	-	-	-	<1	<0.2	<0.5	8	1	<0.2	<1	7	<1	<1	<2	3.9



Analyte	Y	Yb	Zn	Ag	Cd	Co	Cr	Cu	In	Li	Mn	Mo	Ni	Pb	Zn
Units	ppm	ppm	ppm	ppm	ppm	ppm	ppm	ppm	ppm	ppm	ppm	ppm	ppm	ppm	ppm
Detection Limit	0.5	0.01	30	1	0.2	0.5	1	0.5	0.2	1	2	1	1	2	0.5
Method	FUS-MS	FUS-MS	FUS-MS	TD-MS	TD-MS	TD-MS	TD-MS	TD-MS	TD-MS	TD-MS	TD-MS	TD-MS	TD-MS	TD-MS	TD-MS
Method Blank	-	-	-	<1	<0.2	<0.5	11	0.7	<0.2	<1	10	<1	<1	<2	<0.5
Method Blank	-	-	-	<1	<0.2	<0.5	7	<0.5	<0.2	<1	10	<1	<1	<2	<0.5
Method Blank	-	-	-	<1	<0.2	<0.5	11	<0.5	<0.2	<1	24	<1	<1	<2	<0.5
Method Blank	-	-	-	<1	<0.2	<0.5	8	1.2	<0.2	<1	19	<1	<1	<2	<0.5
Method Blank	<0.5	<0.01	<30	-	-	-	-	-	-	-	-	-	-	-	-
Method Blank	-	-	-	<1	<0.2	<0.5	6	<0.5	<0.2	<1	31	<1	<1	<2	0.5
Method Blank	-	-	-	-	-	-	-	-	-	-	-	-	-	-	-
Method Blank	-	-	-	-	-	-	-	-	-	-	-	-	-	-	-
Method Blank	-	-	-	-	-	-	-	-	-	-	-	-	-	-	-
Method Blank	-	-	-	-	-	-	-	-	-	-	-	-	-	-	-
Method Blank	-	-	-	-	-	-	-	-	-	-	-	-	-	-	-
Method Blank	-	-	-	-	-	-	-	-	-	-	-	-	-	-	-
Method Blank	-	-	-	-	-	-	-	-	-	-	-	-	-	-	-
Method Blank	-	-	-	-	-	-	-	-	-	-	-	-	-	-	-
Method Blank	-	-	-	-	-	-	-	-	-	-	-	-	-	-	-
Method Blank	-	-	-	-	-	-	-	-	-	-	-	-	-	-	-
Method Blank	-	-	-	-	-	-	-	-	-	-	-	-	-	-	-
Method Blank	-	-	-	-	-	-	-	-	-	-	-	-	-	-	-
Method Blank	-	-	-	-	-	-	-	-	-	-	-	-	-	-	-
Method Blank	-	-	-	-	-	-	-	-	-	-	-	-	-	-	-
Method Blank	-	-	-	-	-	-	-	-	-	-	-	-	-	-	-
Method Blank	-	-	-	-	-	-	-	-	-	-	-	-	-	-	-
Method Blank	-	-	-	-	-	-	-	-	-	-	-	-	-	-	-
Method Blank	-	-	-	-	-	-	-	-	-	-	-	-	-	-	-
Method Blank	-	-	-	<1	<0.2	<0.5	11	<0.5	<0.2	<1	20	<1	<1	<2	0.8
Method Blank	-	-	-	-	-	-	-	-	-	-	-	-	-	-	-

## **Appendix P**

### **Whole-rock geochemistry QA/QC analysis of duplicates and lab-provided reference materials**

The units for values in the “DL” (detection limit) and “LOQ” (limit of quantification; 3 times DL) columns are indicated in the “Reported Units” column for each row. Std=Standard, RD=Relative difference, CV=Coefficient of variation. Methods are discussed in Section 3.2 and 3.2.1.2.

Analyte	Reported Units	DL	Method	LOQ	Lab-provided Standards			Duplicates			Results Not used
					# of Lab Std Analyses	Average RD (%)	# of Stds < 10x DL	# of Duplicate pair Analyses	Average CV (%)	# of duplicates < 10x DL	
SiO <sub>2</sub>	%	0.01	FUS-ICP	0.03	32	0.3	0	6	1.2	0	
Al <sub>2</sub> O <sub>3</sub>	%	0.01	FUS-ICP	0.03	32	1.4	0	6	2.6	0	
Fe <sub>2</sub> O <sub>3</sub>	%	0.01	FUS-ICP	0.03	0	N/A	0	6	6.5	0	
MnO	%	0	FUS-ICP	0	32	-1.3	0	6	1.2	0	
MgO	%	0.01	FUS-ICP	0.03	32	-2.1	1	6	1.5	0	
CaO	%	0.01	FUS-ICP	0.03	31	0.5	0	6	0.8	0	
Na <sub>2</sub> O	%	0.01	FUS-ICP	0.03	32	0.5	1	6	0.4	1	
K <sub>2</sub> O	%	0.01	FUS-ICP	0.03	32	-6.4	6	6	8.3	2	
TiO <sub>2</sub>	%	0	FUS-ICP	0	32	-0.3	0	6	2.1	0	
P <sub>2</sub> O <sub>5</sub>	%	0.01	FUS-ICP	0.03	32	1.5	16	6	11.9	4	
LOI	%		FUS-ICP		0	N/A	N/A	6	0.7	N/A	
LOI2	%		FUS-ICP		0	N/A	N/A	6	0.6	N/A	Yes
Total	%	0.01	FUS-ICP	0.03	0	N/A	0	6	0.8	0	Yes
Total2	%	0.01	FUS-ICP	0.03	0	N/A	0	6	0.8	0	Yes
Fe <sub>2</sub> O <sub>3</sub> T	%	0.01	FUS-ICP	0.03	32	-1.4	0	6	1.3	0	
Ba	ppm	2	FUS-ICP	6	26	2.3	5	6	2.3	2	
Be	ppm	1	FUS-ICP	3	21	-14.3	21	6	0.0	6	
Sc	ppm	1	FUS-ICP	3	26	-6.7	11	6	19.2	5	
Sr	ppm	2	FUS-ICP	6	26	-1.2	0	6	1.0	0	
V	ppm	5	FUS-ICP	15	31	1.9	11	6	6.9	2	
Zr	ppm	1	FUS-ICP	3	26	-5.0	0	6	5.5	0	
FeO	%	0.1	TITR	0.3	30	-1.7	0	13	4.6	0	
B	ppm	0.5-1	PGNAA	1.5-3	10	0.9	0	2	13.8	0	
Mass	g		PGNAA		0	N/A	N/A	2	2.9	N/A	Yes
C-Total	%	0.01	CS	0.03	35	-2.9	0	9	3.7	1	
S-Total	%	0.01	CS	0.03	50	1.4	0	9	2.4	3	
CO <sub>2</sub>	%	0.01	CO2	0.03	18	0.8	0	9	2.9	0	

Analyte	Reported Units	DL	Method	LOQ	Lab-provided standards			Duplicates			Results Not used
					# of Lab Std Analyses	Average RD (%)	# of Stds < 10x DL	# of Duplicate pair Analyses	Average CV (%)	# of duplicates < 10x DL	
Hg	ppb	5	1G	15	20	-0.7	0	7	0.0	7	
As	ppm	0.1	AR-MS	0.3	32	-20.5	0	6	4.5	2	
Bi	ppm	0.02	AR-MS	0.06	41	-9.8	0	6	21.7	5	
Sb	ppm	0.02	AR-MS	0.06	25	-48.4	0	6	21.9	5	
Se	ppm	0.1	AR-MS	0.3	25	-42.9	9	6	39.8	7	
Te	ppm	0.02	AR-MS	0.06	25	77.7	9	6	33.7	7	
Au	ppb	5	FA-AA	15	3	2.3	0	1	0.0	1	
Au	g/tonne	0.03	FA-GRA	0.09	4	-1.9	0	0	N/A	0	
Au	ppb	1	FA-MS	3	8	0.2	0	11	25.7	4	
Pd	ppb	0.5	FA-MS	1.5	8	0.1	0	11	0.5	11	
Pt	ppb	0.5	FA-MS	1.5	8	1.8	0	11	0.3	10	
Ag	ppm	0.5	FUS-MS	1.5	6	-1.9	6	7	4.1	7	
As	ppm	5	FUS-MS	15	18	19.4	13	7	6.6	7	Yes
Bi	ppm	0.1	FUS-MS	0.3	10	29.8	10	7	0.0	7	Yes
Ce	ppm	0.05	FUS-MS	0.15	60	3.0	0	7	2.4	0	
Co	ppm	1	FUS-MS	3	40	-2.1	4	7	3.7	3	Yes
Cr	ppm	20	FUS-MS	60	30	19.3	14	7	18.8	6	Yes
Cs	ppm	0.1	FUS-MS	0.3	21	0.5	1	7	3.3	2	
Cu	ppm	10	FUS-MS	30	52	5.0	12	7	17.8	7	Yes
Dy	ppm	0.01	FUS-MS	0.03	44	-5.7	0	7	4.7	0	
Er	ppm	0.01	FUS-MS	0.03	34	-2.1	0	7	3.5	0	
Eu	ppm	0.01	FUS-MS	0.02	51	-0.6	0	7	4.8	0	
Ga	ppm	1	FUS-MS	3	22	-0.1	0	7	3.3	1	
Gd	ppm	0.01	FUS-MS	0.03	37	-4.8	0	7	4.3	0	
Ge	ppm	0.5	FUS-MS	1.5	13	23.4	8	7	3.5	7	
Hf	ppm	0.1	FUS-MS	0.3	21	0.5	5	7	19.5	2	
Ho	ppm	0.01	FUS-MS	0.03	36	1.0	0	7	4.7	0	

Analyte	Reported Units	DL	Method	LOQ	Lab-provided Standards			Duplicates			Results Not used
					# of Lab Std Analyses	Average RD (%)	# of Stds < 10x DL	# of Duplicate pair Analyses	Average CV (%)	# of duplicates < 10x DL	
In	ppm	0.1	FUS-MS	0.3	10	35.4	5	7	0.0	7	Yes
La	ppm	0.05	FUS-MS	0.15	64	6.5	0	7	3.0	0	
Lu	ppm	0	FUS-MS	0.01	49	-0.9	0	7	5.8	0	
Mo	ppm	2	FUS-MS	6	30	-0.3	15	7	0.0	7	Yes
Nb	ppm	0.2	FUS-MS	0.6	10	-1.0	1	7	18.1	2	
Nd	ppm	0.05	FUS-MS	0.15	63	-1.0	0	7	5.5	0	
Ni	ppm	20	FUS-MS	60	32	88.3	26	7	1.0	6	Yes
Pb	ppm	5	FUS-MS	15	11	-5.0	11	7	25.6	7	Yes
Pr	ppm	0.01	FUS-MS	0.03	29	-0.6	0	7	4.3	0	
Rb	ppm	1	FUS-MS	3	29	-2.6	1	7	3.1	2	
Sb	ppm	0.2	FUS-MS	0.6	14	-1.2	10	7	32.1	7	Yes
Sm	ppm	0.01	FUS-MS	0.03	50	-2.1	0	7	3.5	0	
Sn	ppm	1	FUS-MS	3	15	-13.5	10	7	0.0	7	
Ta	ppm	0.01	FUS-MS	0.03	18	1.7	0	7	8.4	2	
Tb	ppm	0.01	FUS-MS	0.03	45	-0.3	0	7	2.9	1	
Th	ppm	0.05	FUS-MS	0.15	50	-0.7	0	7	3.9	2	
Tl	ppm	0.05	FUS-MS	0.15	12	-35.4	5	7	21.3	7	
Tm	ppm	0.01	FUS-MS	0.02	36	-2.2	0	7	4.4	0	
U	ppm	0.01	FUS-MS	0.03	34	-0.4	0	7	3.1	0	
W	ppm	0.5	FUS-MS	1.5	15	25.0	10	7	59.6	5	
Y	ppm	0.5	FUS-MS	1.5	62	-2.6	0	7	3.0	0	
Yb	ppm	0.01	FUS-MS	0.03	64	-1.2	0	7	4.4	0	
Zn	ppm	30	FUS-MS	90	24	-0.9	24	3	13.8	3	Yes
Ag	ppm	1	TD-MS	3	24	-26.4	17	6	0.0	6	Yes
Cd	ppm	0.2	TD-MS	0.6	39	-45.4	26	6	1.6	6	
Co	ppm	0.5	TD-MS	1.5	65	-2.1	0	6	6.4	1	
Cr	ppm	1	TD-MS	3	65	-13.6	0	6	18.5	0	

Analyte	Reported Units	DL	Method	LOQ	Lab-provided Standards			Duplicates			Results Not used
					# of Lab Std Analyses	Average RD (%)	# of Stds < 10x DL	# of Duplicate pair Analyses	Average CV (%)	# of duplicates < 10x DL	
<b>Cu</b>	ppm	0.5	TD-MS	1.5	65	0.6	0	6	1.9	0	
<b>In</b>	ppm	0.2	TD-MS	0.6	32	-21.9	32	6	0.0	6	
<b>Li</b>	ppm	1	TD-MS	3	65	2.4	16	6	4.2	0	
<b>Mn</b>	ppm	2	TD-MS	6	41	-4.3	0	6	3.1	0	
<b>Mo</b>	ppm	1	TD-MS	3	47	-17.9	25	6	19.2	6	
<b>Ni</b>	ppm	1	TD-MS	3	65	-2.9	0	6	11.6	1	
<b>Pb</b>	ppm	2	TD-MS	6	65	-0.2	9	6	6.4	6	
<b>Zn</b>	ppm	0.5	TD-MS	1.5	65	1.3	0	6	4.8	0	

## **Appendix Q**

### **Whole-rock geochemistry QA/QC analysis of lab-provided method blanks**

The units for values in the DL (detection limit) column are indicated in the “Reported Units” column for each row. Values in the “< DL”, “DL to 3x DL (inclusive)”, and “> 3x DL” columns are the number of method blanks that fall within the ranges specified. Methods are outlined in Section 3.2 and 3.2.1.2.

Analyte	Reported Units	DL	Method	# of Method Blanks	< DL	DL to 3x DL (inclusive)	> 3x DL	Comments
SiO <sub>2</sub>	%	0.01	FUS-ICP	3	2	1	0	
Al <sub>2</sub> O <sub>3</sub>	%	0.01	FUS-ICP	3	2	1	0	
Fe <sub>2</sub> O <sub>3</sub>	%	0.01	FUS-ICP	0	N/A	N/A	N/A	
MnO	%	0	FUS-ICP	3	1	2	0	
MgO	%	0.01	FUS-ICP	3	2	1	0	
CaO	%	0.01	FUS-ICP	3	2	1	0	
Na <sub>2</sub> O	%	0.01	FUS-ICP	3	3	0	0	
K <sub>2</sub> O	%	0.01	FUS-ICP	3	3	0	0	
TiO <sub>2</sub>	%	0	FUS-ICP	3	0	3	0	
P <sub>2</sub> O <sub>5</sub>	%	0.01	FUS-ICP	3	2	1	0	
LOI	%		FUS-ICP	0	N/A	N/A	N/A	
LOI2	%		FUS-ICP	0	N/A	N/A	N/A	
Total	%	0.01	FUS-ICP	0	N/A	N/A	N/A	
Total2	%	0.01	FUS-ICP	2	2	0	0	
Fe <sub>2</sub> O <sub>3</sub> T	%	0.01	FUS-ICP	3	2	1	0	
Ba	ppm	2	FUS-ICP	3	3	0	0	
Be	ppm	1	FUS-ICP	3	3	0	0	
Sc	ppm	1	FUS-ICP	3	3	0	0	
Sr	ppm	2	FUS-ICP	3	3	0	0	
V	ppm	5	FUS-ICP	3	3	0	0	
Zr	ppm	1	FUS-ICP	3	1	2	0	
FeO	%	0.1	TITR	22	21	1	0	
B	ppm	0.5-1	PGNAA	4	3	1	0	
Mass	g		PGNAA	0	N/A	N/A	N/A	
C-Total	%	0.01	CS	0	N/A	N/A	N/A	
S-Total	%	0.01	CS	0	N/A	N/A	N/A	
CO <sub>2</sub>	%	0.01	CO2	9	8	1	0	
Hg	ppb	5	1G	7	7	0	0	
As	ppm	0.1	AR-MS	11	9	1	1	One blank = 3.4 ppm.



Analyte	Reported Units	DL	Method	# of Method Blanks	< DL	DL to 3x DL (inclusive)	> 3x DL	Comments
Bi	ppm	0.02	AR-MS	11	8	1	2	All blanks within 5 x DL.
Sb	ppm	0.02	AR-MS	11	8	3	0	
Se	ppm	0.1	AR-MS	11	9	2	0	
Te	ppm	0.02	AR-MS	11	10	1	0	
Au	ppb	5	FA-AA	4	4	0	0	
Au	g/tonne	0.03	FA-GRA	2	2	0	0	
Au	ppb	1	FA-MS	14	5	3	6	All blanks within 10 x DL.
Pd	ppb	0.5	FA-MS	14	14	0	0	
Pt	ppb	0.5	FA-MS	14	14	0	0	
Ag	ppm	0.5	FUS-MS	5	5	0	0	
As	ppm	5	FUS-MS	5	5	0	0	
Bi	ppm	0.1	FUS-MS	5	5	0	0	
Ce	ppm	0.05	FUS-MS	5	5	0	0	
Co	ppm	1	FUS-MS	5	5	0	0	
Cr	ppm	20	FUS-MS	5	5	0	0	
Cs	ppm	0.1	FUS-MS	5	5	0	0	
Cu	ppm	10	FUS-MS	5	5	0	0	
Dy	ppm	0.01	FUS-MS	5	5	0	0	
Er	ppm	0.01	FUS-MS	5	5	0	0	
Eu	ppm	0.01	FUS-MS	5	5	0	0	
Ga	ppm	1	FUS-MS	5	5	0	0	
Gd	ppm	0.01	FUS-MS	5	5	0	0	
Ge	ppm	0.5	FUS-MS	5	5	0	0	
Hf	ppm	0.1	FUS-MS	5	5	0	0	
Ho	ppm	0.01	FUS-MS	5	5	0	0	
In	ppm	0.1	FUS-MS	5	5	0	0	
La	ppm	0.05	FUS-MS	5	5	0	0	
Lu	ppm	0	FUS-MS	4	4	0	0	
Mo	ppm	2	FUS-MS	5	5	0	0	

Analyte	Reported Units	DL	Method	# of Method Blanks	< DL	DL to 3x DL (inclusive)	> 3x DL	Comments
Nb	ppm	0.2	FUS-MS	5	5	0	0	
Nd	ppm	0.05	FUS-MS	5	5	0	0	
Ni	ppm	20	FUS-MS	5	5	0	0	
Pb	ppm	5	FUS-MS	5	5	0	0	
Pr	ppm	0.01	FUS-MS	5	5	0	0	
Rb	ppm	1	FUS-MS	5	5	0	0	
Sb	ppm	0.2	FUS-MS	5	5	0	0	
Sm	ppm	0.01	FUS-MS	5	5	0	0	
Sn	ppm	1	FUS-MS	5	5	0	0	
Ta	ppm	0.01	FUS-MS	5	5	0	0	
Tb	ppm	0.01	FUS-MS	5	5	0	0	
Th	ppm	0.05	FUS-MS	5	5	0	0	
Tl	ppm	0.05	FUS-MS	5	5	0	0	
Tm	ppm	0.01	FUS-MS	5	5	0	0	
U	ppm	0.01	FUS-MS	5	5	0	0	
W	ppm	0.5	FUS-MS	5	5	0	0	
Y	ppm	0.5	FUS-MS	5	5	0	0	
Yb	ppm	0.01	FUS-MS	5	5	0	0	
Zn	ppm	30	FUS-MS	3	3	0	0	
Ag	ppm	1	TD-MS	18	18	0	0	
Cd	ppm	0.2	TD-MS	18	18	0	0	
Co	ppm	0.5	TD-MS	18	18	0	0	
Cr	ppm	1	TD-MS	18	1	2	15	All blanks within 12 x DL.
Cu	ppm	0.5	TD-MS	18	15	3	0	
In	ppm	0.2	TD-MS	18	18	0	0	
Li	ppm	1	TD-MS	18	18	0	0	
Mn	ppm	2	TD-MS	18	0	2	16	All blanks within 16 x DL. Results not used.
Mo	ppm	1	TD-MS	18	18	0	0	

Analyte	Reported Units	DL	Method	# of Method Blanks	< DL	DL to 3x DL (inclusive)	> 3x DL	Comments
Ni	ppm	1	TD-MS	18	18	0	0	
Pb	ppm	2	TD-MS	18	18	0	0	
Zn	ppm	0.5	TD-MS	18	10	7	1	All blanks within 4 x DL.

## **Appendix R**

### **Whole-rock geochemistry QA/QC analysis of NRCan-provided reference materials**

Historical standard data was provided by Natural Resources Canada (NRCan, personal communication, 2018). The units for values in “DL”, “Avg”, and “Std Dev” columns are specified in the “Reported Units” column for each row. DL=detection limit, Avg=Average, Std Dev=Standard deviation, RD=Relative difference, RSD=Relative standard deviation. Methods are discussed in Section 3.2 and 3.2.1.1.

STPL-BAS				Historical		This Dataset							
Analyte	Reported Units	DL (this dataset)	DL (historical)	Method	Avg (n=50)	Std Dev (n=50)	# of Stds Analyzed	Avg	Std Dev	Avg RD (%)	RSD (%)	Avg (this dataset) < 10x DL (this dataset)	Results Not Used
SiO <sub>2</sub>	%	0.01	0.01	FUS-ICP	46.67	0.54	7	46.34	0.57	-0.7	1.2		
Al <sub>2</sub> O <sub>3</sub>	%	0.01	0.01	FUS-ICP	16.10	0.35	7	16.18	0.44	0.5	2.7		
Fe <sub>2</sub> O <sub>3</sub>	%	0.01	0.01	FUS-ICP	2.38	0.72	7	2.45	0.69	2.6	28.1		
MnO	%	0.001	0.001	FUS-ICP	0.17	0.00	7	0.17	0.00	-1.2	1.7		
MgO	%	0.01	0.01	FUS-ICP	8.78	0.17	7	8.68	0.09	-1.1	1.1		
CaO	%	0.01	0.01	FUS-ICP	11.14	0.15	7	11.13	0.15	-0.1	1.4		
Na <sub>2</sub> O	%	0.01	0.01	FUS-ICP	1.82	0.04	7	1.81	0.03	-0.9	1.8		
K <sub>2</sub> O	%	0.01	0.01	FUS-ICP	0.04	0.01	7	0.05	0.01	7.4	16.0	Yes	
TiO <sub>2</sub>	%	0.001	0.001	FUS-ICP	0.84	0.02	7	0.84	0.04	-0.5	4.3		
P <sub>2</sub> O <sub>5</sub>	%	0.01	0.01	FUS-ICP	0.06	0.01	7	0.06	0.01	-4.3	13.6	Yes	
LOI	%			FUS-ICP	3.29	0.23	7	3.62	0.22	10.2	6.2	N/A	
LOI2	%			FUS-ICP	2.64	0.69	7	3.23	0.98	22.1	30.4	N/A	Yes
Total	%	0.01	0.01	FUS-ICP	99.86	0.75	7	99.53	0.37	-0.3	0.4		Yes
Total2	%	0.01	0.01	FUS-ICP	99.28	0.80	7	99.13	1.02	-0.1	1.0		Yes
Fe <sub>2</sub> O <sub>3</sub> T	%	0.01	0.01	FUS-ICP	10.91	0.33	7	10.66	0.22	-2.3	2.1		
Ba	ppm	2	2-3	FUS-ICP	15.24	1.76	7	14.00	2.58	-8.1	18.4	Yes	
Be	ppm	1	1	FUS-ICP	1.50	0.50	7	0.50	0.00	-66.7	0.0	Yes	
Sc	ppm	1	1	FUS-ICP	38.48	0.70	7	38.00	1.00	-1.2	2.6		
Sr	ppm	2	2	FUS-ICP	113.46	2.86	7	114.29	2.87	0.7	2.5		
V	ppm	5	5	FUS-ICP	262.55	6.19	7	253.57	7.37	-3.4	2.9		
Zr	ppm	1	1	FUS-ICP	30.46	3.93	7	29.43	5.13	-3.4	17.4		
FeO	%	0.1	0.01-0.1	TITR	7.68	0.60	7	7.39	0.58	-3.8	7.8		
B	ppm	0.5-1	0.5-1	PGNAA	7.16	4.18	5	6.50	4.83	-9.3	74.3	Yes	
Mass	g			PGNAA			5	1.06	0.03	N/A	2.4	N/A	Yes
C-Total	%	0.01	0.01	CS	0.05	0.01	7	0.05	0.02	3.4	34.6	Yes	
S-Total	%	0.01	0.01	CS	0.08	0.01	7	0.08	0.01	-6.3	10.4	Yes	

Analyte	STPL-BAS				Historical		This Dataset						
	Reported Units	DL (this dataset)	DL (historical)	Method	Avg (n=50)	Std Dev (n=50)	# of Stds Analyzed	Avg	Std Dev	Avg RD (%)	RSD (%)	Avg (this dataset) < 10x DL (this dataset)	Results Not Used
CO <sub>2</sub>	%	0.01	0.01	CO2	0.16	0.04	7	0.18	0.03	10.6	14.4		
Hg	ppb	5		1G			2	2.50	0.00	N/A	0.0	Yes	
As	ppm	0.1	0.1	AR-MS	11.38	29.30	7	14.17	29.95	24.5	211.3		
Bi	ppm	0.02	0.02	AR-MS	0.50	0.62	7	0.15	0.37	-70.3	246.8	Yes	
Sb	ppm	0.02	0.02	AR-MS	0.33	0.26	7	0.43	0.39	30.7	92.2		
Se	ppm	0.1	0.1	AR-MS	0.39	0.31	7	0.23	0.31	-40.7	136.5	Yes	
Te	ppm	0.02	0.02	AR-MS	0.14	0.14	7	0.05	0.04	-63.3	70.5	Yes	
Au	ppb	5	5	FA-AA	9.20	3.94	1	9.00	N/A	-2.2	N/A	Yes	
Au	g/tonne	0.03		FA-GRA			0			N/A	N/A	N/A	
Au	ppb	1	1	FA-MS	6.09	2.07	6	6.50	2.07	6.7	31.9	Yes	
Pd	ppb	0.5	0.5	FA-MS	11.08	1.69	6	11.58	1.73	4.5	14.9		
Pt	ppb	0.5	0.5	FA-MS	8.17	0.99	6	8.60	0.97	5.2	11.2		
Ag	ppm	0.5	0.5	FUS-MS			7	0.30	0.13	N/A	44.1	Yes	
As	ppm	5	5	FUS-MS	24.13	27.68	7	11.79	23.06	-51.1	195.7	Yes	Yes
Bi	ppm	0.1	<u>0.05-0.1</u>	FUS-MS	0.50	0.32	7	0.11	0.17	-77.1	148.8	Yes	Yes
Ce	ppm	0.05	0.05	FUS-MS	5.31	0.48	7	5.65	0.27	6.4	4.7		
Co	ppm	1	1	FUS-MS	47.32	3.17	7	48.43	1.40	2.3	2.9		Yes
Cr	ppm	20	20	FUS-MS	294.52	62.85	7	318.57	12.15	8.2	3.8		Yes
Cs	ppm	0.1	0.1	FUS-MS	0.21	0.04	7	0.21	0.04	2.9	17.6	Yes	
Cu	ppm	10	10	FUS-MS	116.80	8.11	7	121.43	6.90	4.0	5.7		Yes
Dy	ppm	0.01	0.01	FUS-MS	2.21	0.14	7	2.33	0.05	5.6	2.3		
Er	ppm	0.01	0.01	FUS-MS	1.37	0.12	7	1.44	0.04	4.8	2.9		
Eu	ppm	0.005	0.005	FUS-MS	0.60	0.04	7	0.64	0.02	6.6	3.2		
Ga	ppm	1	1	FUS-MS	15.40	1.04	7	16.00	0.82	3.9	5.1		
Gd	ppm	0.01	0.01	FUS-MS	1.86	0.13	7	1.96	0.10	5.2	4.9		
Ge	ppm	0.5	0.5	FUS-MS	1.79	0.41	7	1.51	0.13	-15.4	8.9	Yes	
Hf	ppm	0.1	0.1	FUS-MS	0.83	0.10	7	0.87	0.10	5.5	10.9	Yes	

Analyte	STPL-BAS				Historical		This Dataset						
	Reported Units	DL (this dataset)	DL (historical)	Method	Avg (n=50)	Std Dev (n=50)	# of Stds Analyzed	Avg	Std Dev	Avg RD (%)	RSD (%)	Avg (this dataset) < 10x DL (this dataset)	Results Not Used
Ho	ppm	0.01	0.01	FUS-MS	0.46	0.03	7	0.49	0.02	5.5	3.3		
In	ppm	0.1	0.1	FUS-MS			7	0.05	0.00	N/A	0.0	Yes	Yes
La	ppm	0.05	0.05	FUS-MS	2.01	0.30	7	2.00	0.24	-0.2	12.2		
Lu	ppm	0.002	0.002	FUS-MS	0.21	0.02	7	0.22	0.01	4.1	3.3		
Mo	ppm	2	2	FUS-MS			7	1.00	0.00	N/A	0.0	Yes	Yes
Nb	ppm	0.2	0.2	FUS-MS	1.26	0.44	7	1.43	0.08	13.8	5.3	Yes	
Nd	ppm	0.05	0.05	FUS-MS	4.33	0.30	7	4.57	0.14	5.5	3.2		
Ni	ppm	20	20	FUS-MS	173.60	16.22	7	185.71	7.87	7.0	4.2	Yes	Yes
Pb	ppm	5	5	FUS-MS			7	2.50	0.00	N/A	0.0	Yes	Yes
Pr	ppm	0.01	0.01	FUS-MS	0.83	0.06	7	0.87	0.05	4.4	6.2		
Rb	ppm	1	1	FUS-MS	2.00	0.76	7	0.93	0.73	-53.6	78.8	Yes	
Sb	ppm	0.2	0.2	FUS-MS	0.97	0.72	7	0.80	0.37	-17.9	46.2	Yes	Yes
Sm	ppm	0.01	0.01	FUS-MS	1.40	0.09	7	1.47	0.09	4.6	6.4		
Sn	ppm	1	1	FUS-MS			7	0.50	0.00	N/A	0.0	Yes	
Ta	ppm	0.01	0.01	FUS-MS	0.12	0.13	7	0.10	0.02	-21.2	18.5	Yes	
Tb	ppm	0.01	0.01	FUS-MS	0.34	0.02	7	0.36	0.01	5.6	3.4		
Th	ppm	0.05	0.05	FUS-MS	0.14	0.14	7	0.11	0.01	-17.4	6.9	Yes	
Tl	ppm	0.05	0.05	FUS-MS	0.29	0.24	7	0.03	0.02	-88.7	63.3	Yes	
Tm	ppm	0.005	0.005	FUS-MS	0.21	0.02	7	0.21	0.00	2.7	2.0		
U	ppm	0.01	0.01	FUS-MS	0.05	0.08	7	0.06	0.08	22.4	140.0	Yes	
W	ppm	0.5	0.5	FUS-MS	4.36	5.11	7	2.76	4.01	-36.8	145.4	Yes	
Y	ppm	0.5	0.5	FUS-MS	12.51	1.08	7	13.07	0.29	4.5	2.2		
Yb	ppm	0.01	0.01	FUS-MS	1.38	0.10	7	1.44	0.06	4.3	3.9		
Zn	ppm	30		FUS-MS	68.94	24.61	3	96.67	20.82	40.2	21.5	Yes	Yes
Ag	ppm	1	1	TD-MS			7	0.50	0.00	N/A	0.0	Yes	Yes
Cd	ppm	0.2	0.2	TD-MS	0.27	0.05	7	0.10	0.00	-62.5	0.0	Yes	
Co	ppm	0.5	0.5	TD-MS	50.63	3.07	7	50.31	2.29	-0.6	4.6		

<b>Cr</b>	ppm	1	1	TD-MS	200.00	44.86	7	189.86	35.24	-5.1	18.6		
<b>Cu</b>	ppm	0.5	0.5	TD-MS	123.67	8.66	7	124.43	4.86	0.6	3.9		
<b>In</b>	ppm	0.2	<u>0.1</u>	TD-MS			7	0.10	0.00	N/A	0.0	Yes	
<b>Li</b>	ppm	1	1	TD-MS	14.45	1.83	7	13.71	0.49	-5.1	3.6		
<b>Mn</b>	ppm	2	2	TD-MS	1250.31	95.59	7	1277.14	80.36	2.1	6.3		
<b>Mo</b>	ppm	1	1	TD-MS	1.27	0.55	7	0.50	0.00	-60.5	0.0	Yes	
<b>Ni</b>	ppm	1	1	TD-MS	185.49	12.41	7	175.57	5.26	-5.3	3.0		
<b>Pb</b>	ppm	2	2	TD-MS	6.86	6.39	7	1.57	1.51	-77.1	96.2	Yes	
<b>Zn</b>	ppm	0.5	0.5	TD-MS	71.06	16.83	7	64.49	6.73	-9.3	10.4		



STPL-PML-53				Historical		This Dataset							
Analyte	Reported Units	DL (this dataset)	DL (historical)	Method	Avg (n=48)	Std Dev (n=48)	# of Stds Analyzed	Avg	Std Dev	Avg RD (%)	RSD (%)	Avg (this dataset) < 10x DL (this dataset)	Results Not Used
SiO <sub>2</sub>	%	0.01	0.01	FUS-ICP	75.89	0.72	3	75.64	0.47	-0.3	0.6		
Al <sub>2</sub> O <sub>3</sub>	%	0.01	0.01	FUS-ICP	12.58	0.28	3	12.64	0.41	0.4	3.2		
Fe <sub>2</sub> O <sub>3</sub>	%	0.01	0.01	FUS-ICP	0.40	0.23	3	0.39	0.30	-1.9	76.9		
MnO	%	0.001	0.001	FUS-ICP	0.03	0.00	3	0.03	0.00	1.4	3.5		
MgO	%	0.01	0.01	FUS-ICP	0.54	0.01	3	0.55	0.02	1.5	2.8		
CaO	%	0.01	0.01	FUS-ICP	1.39	0.04	3	1.40	0.02	0.4	1.1		
Na <sub>2</sub> O	%	0.01	0.01	FUS-ICP	3.43	0.06	3	3.44	0.05	0.2	1.3		
K <sub>2</sub> O	%	0.01	0.01	FUS-ICP	2.13	0.05	3	2.10	0.02	-1.4	1.0		
TiO <sub>2</sub>	%	0.001	0.001	FUS-ICP	0.19	0.00	3	0.19	0.00	-0.3	1.1		
P <sub>2</sub> O <sub>5</sub>	%	0.01	0.01	FUS-ICP	0.04	0.01	3	0.04	0.00	-3.7	0.0	Yes	
LOI	%			FUS-ICP	2.06	0.19	3	2.23	0.29	8.2	13.1	N/A	
LOI2	%			FUS-ICP	1.98	0.22	3	2.19	0.32	10.5	14.6	N/A	Yes
Total	%	0.01	0.01	FUS-ICP	99.63	0.82	3	99.58	0.03	-0.1	0.0		Yes
Total2	%	0.01	0.01	FUS-ICP	99.69	0.69	3	99.54	0.14	-0.1	0.1		Yes
Fe <sub>2</sub> O <sub>3</sub> T	%	0.01	0.01	FUS-ICP	1.36	0.15	3	1.32	0.10	-2.6	7.3		
Ba	ppm	2	<u>2-3</u>	FUS-ICP	523.98	9.61	3	522.67	7.51	-0.3	1.4		
Be	ppm	1	1	FUS-ICP	1.87	5.28	3	1.00	0.00	-46.5	0.0	Yes	
Sc	ppm	1	1	FUS-ICP	2.98	0.14	3	3.00	0.00	0.7	0.0	Yes	
Sr	ppm	2	2	FUS-ICP	144.40	4.89	3	143.67	0.58	-0.5	0.4		
V	ppm	5	5	FUS-ICP	13.32	1.96	3	13.33	2.52	0.1	18.9	Yes	
Zr	ppm	1	1	FUS-ICP	110.21	7.09	3	106.67	4.16	-3.2	3.9		
FeO	%	0.1	<u>0.01-0.1</u>	TITR	0.93	0.38	3	0.83	0.35	-10.0	42.1	Yes	
B	ppm	0.5-1	0.5-1	PGNAA	29.33	14.78	2	41.35	6.15	41.0	14.9		
Mass	g			PGNAA			2	1.05	0.04	N/A	4.0	N/A	Yes
C-Total	%	0.01	0.01	CS	0.29	0.01	3	0.30	0.01	2.9	3.3		
S-Total	%	0.01	0.01	CS	0.07	0.01	3	0.07	0.01	-6.4	8.7	Yes	
CO <sub>2</sub>	%	0.01	0.01	CO2	0.99	0.07	3	0.97	0.02	-1.5	2.1		

STPL-PML-53				Historical		This Dataset							
Analyte	Reported Units	DL (this dataset)	DL (historical)	Method	Avg (n=48)	Std Dev (n=48)	# of Stds Analyzed	Avg	Std Dev	Avg RD (%)	RSD (%)	Avg (this dataset) < 10x DL (this dataset)	Results Not Used
Hg	ppb	5		1G			1	2.50	N/A	N/A	N/A	Yes	
As	ppm	0.1	0.1	AR-MS	45.74	13.34	3	40.13	0.42	-12.3	1.0		
Bi	ppm	0.02	0.02	AR-MS	0.22	0.26	3	0.11	0.02	-50.6	14.3	Yes	
Sb	ppm	0.02	0.02	AR-MS	0.17	0.06	3	0.16	0.09	-5.0	53.4	Yes	
Se	ppm	0.1	0.1	AR-MS	0.52	0.34	3	0.05	0.00	-90.4	0.0	Yes	
Te	ppm	0.02	0.02	AR-MS	0.18	0.18	3	0.02	0.02	-87.1	65.5	Yes	
Au	ppb	5	5	FA-AA	9.53	8.34	0			N/A	N/A	N/A	
Au	g/tonne	0.03		FA-GRA			0			N/A	N/A	N/A	
Au	ppb	1	1	FA-MS	7.57	2.44	3	7.67	3.79	1.3	49.4	Yes	
Pd	ppb	0.5	0.5	FA-MS			3	0.25	0.00	N/A	0.0	Yes	
Pt	ppb	0.5	0.5	FA-MS			3	0.25	0.00	N/A	0.0	Yes	
Ag	ppm	0.5	0.5	FUS-MS			3	0.25	0.00	N/A	0.0	Yes	
As	ppm	5	5	FUS-MS	40.81	11.05	3	35.00	2.00	-14.2	5.7	Yes	Yes
Bi	ppm	0.1	<u>0.05-0.1</u>	FUS-MS	0.29	0.59	3	0.05	0.00	-82.6	0.0	Yes	Yes
Ce	ppm	0.05	0.05	FUS-MS	72.53	3.61	3	75.10	2.10	3.6	2.8		
Co	ppm	1	1	FUS-MS	1.04	0.19	3	0.67	0.29	-35.6	43.3	Yes	Yes
Cr	ppm	20	20	FUS-MS	49.93	15.60	3	46.67	5.77	-6.5	12.4	Yes	Yes
Cs	ppm	0.1	0.1	FUS-MS	2.10	0.14	3	2.00	0.20	-5.0	10.0		
Cu	ppm	10	10	FUS-MS	17.14	10.97	3	13.33	5.77	-22.2	43.3	Yes	Yes
Dy	ppm	0.01	0.01	FUS-MS	2.38	0.13	3	2.45	0.13	3.2	5.3		
Er	ppm	0.01	0.01	FUS-MS	1.59	0.12	3	1.63	0.06	2.5	3.4		
Eu	ppm	0.005	0.005	FUS-MS	0.67	0.04	3	0.70	0.03	4.9	4.3		
Ga	ppm	1	1	FUS-MS	12.00	0.58	3	11.67	0.58	-2.8	4.9		
Gd	ppm	0.01	0.01	FUS-MS	2.53	0.18	3	2.55	0.11	0.8	4.4		
Ge	ppm	0.5	0.5	FUS-MS	1.80	0.63	3	1.40	0.10	-22.2	7.1	Yes	
Hf	ppm	0.1	0.1	FUS-MS	2.70	0.26	3	2.53	0.21	-6.2	8.2		
Ho	ppm	0.01	0.01	FUS-MS	0.50	0.03	3	0.52	0.03	3.2	5.6		

STPL-PML-53				Historical		This Dataset							
Analyte	Reported Units	DL (this dataset)	DL (historical)	Method	Avg (n=48)	Std Dev (n=48)	# of Stds Analyzed	Avg	Std Dev	Avg RD (%)	RSD (%)	Avg (this dataset) < 10x DL (this dataset)	Results Not Used
In	ppm	0.1	0.1	FUS-MS	0.50	0.40	3	0.05	0.00	-90.0	0.0	Yes	Yes
La	ppm	0.05	0.05	FUS-MS	41.55	1.89	3	42.23	1.15	1.6	2.7		
Lu	ppm	0.002	0.002	FUS-MS	0.34	0.03	3	0.34	0.01	-0.4	4.2		
Mo	ppm	2	2	FUS-MS			3	1.00	0.00	N/A	0.0	Yes	Yes
Nb	ppm	0.2	0.2	FUS-MS	9.64	1.22	3	8.30	0.82	-13.9	9.9		
Nd	ppm	0.05	0.05	FUS-MS	23.04	1.30	3	23.90	0.44	3.7	1.8		
Ni	ppm	20	20	FUS-MS			3	10.00	0.00	N/A	0.0	Yes	Yes
Pb	ppm	5	5	FUS-MS	8.07	2.14	3	8.00	0.00	-0.8	0.0	Yes	Yes
Pr	ppm	0.01	0.01	FUS-MS	7.25	0.32	3	7.37	0.20	1.7	2.7		
Rb	ppm	1	1	FUS-MS	69.00	3.35	3	66.00	4.36	-4.3	6.6		
Sb	ppm	0.2	0.2	FUS-MS	0.62	0.73	3	0.10	0.00	-83.8	0.0	Yes	Yes
Sm	ppm	0.01	0.01	FUS-MS	3.43	0.19	3	3.63	0.10	5.7	2.8		
Sn	ppm	1	1	FUS-MS			3	0.50	0.00	N/A	0.0	Yes	
Ta	ppm	0.01	0.01	FUS-MS	0.97	0.19	3	0.85	0.08	-12.8	9.2		
Tb	ppm	0.01	0.01	FUS-MS	0.40	0.02	3	0.40	0.01	2.1	2.9		
Th	ppm	0.05	0.05	FUS-MS	10.56	0.40	3	10.30	0.20	-2.5	1.9		
Tl	ppm	0.05	0.05	FUS-MS	0.24	0.21	3	0.11	0.01	-55.6	5.4	Yes	
Tm	ppm	0.005	0.005	FUS-MS	0.27	0.02	3	0.28	0.02	2.0	7.1		
U	ppm	0.01	0.01	FUS-MS	2.60	0.51	3	2.41	0.08	-7.3	3.4		
W	ppm	0.5	0.5	FUS-MS	3.91	4.44	3	1.50	0.61	-61.6	40.6	Yes	
Y	ppm	0.5	0.5	FUS-MS	15.47	1.06	3	15.40	0.87	-0.5	5.7		
Yb	ppm	0.01	0.01	FUS-MS	1.99	0.16	3	2.02	0.14	1.4	6.7		
Zn	ppm	30		FUS-MS	82.60	61.41	1	40.00	N/A	-51.6	N/A	Yes	Yes
Ag	ppm	1	1	TD-MS			3	0.50	0.00	N/A	0.0	Yes	Yes
Cd	ppm	0.2	0.2	TD-MS	0.15	0.05	3	0.10	0.00	-33.3	0.0	Yes	
Co	ppm	0.5	0.5	TD-MS	1.19	0.14	3	1.17	0.12	-1.9	9.9	Yes	
Cr	ppm	1	1	TD-MS	30.18	10.06	3	30.67	8.39	1.6	27.3		

STPL-PML-53				Historical		This Dataset							
Analyte	Reported Units	DL (this dataset)	DL (historical)	Method	Avg (n=48)	Std Dev (n=48)	# of Stds Analyzed	Avg	Std Dev	Avg RD (%)	RSD (%)	Avg (this dataset) < 10x DL (this dataset)	Results Not Used
Cu	ppm	0.5	0.5	TD-MS	10.94	4.54	3	14.67	6.53	34.1	44.5		
In	ppm	0.2	0.1	TD-MS			3	0.10	0.00	N/A	0.0	Yes	
Li	ppm	1	1	TD-MS	11.59	1.62	3	11.00	1.00	-5.1	9.1		
Mn	ppm	2	2	TD-MS	231.24	20.75	3	248.00	8.89	7.2	3.6		
Mo	ppm	1	1	TD-MS	1.27	0.54	3	0.50	0.00	-60.5	0.0	Yes	
Ni	ppm	1	1	TD-MS	2.28	0.49	3	2.00	0.00	-12.2	0.0	Yes	
Pb	ppm	2	2	TD-MS	7.65	1.43	3	8.67	1.15	13.2	13.3	Yes	
Zn	ppm	0.5	0.5	TD-MS	33.29	17.47	3	44.03	29.77	32.3	67.6		

## **Appendix S**

### **Isocon results summary**

Results of mass balance calculations based off of the analysis of Isocon diagrams for altered/less-altered pairs are displayed in this appendix. Methods are discussed in Sections 3.2.2 and 3.2.4. Elements selected as immobile are used to determine the slope of the Isocon and are deemed neither enriched nor depleted (referred to as “Immobile” in the tables below). The cause of the alteration (e.g.  $V_{GD}$  veins) and lithology (e.g. dacite) is indicated for each altered/less-altered pair. Descriptive terms for the approximate location within the deposit where dacitic altered/less-altered pairs affected by auriferous quartz veining were taken from are included. The locations of each of the alteration envelopes described using these terms are shown in Figure 19. LOI=Loss on ignition,  $Fe_2O_3T$ =Total Iron.

	Dacite, V <sub>1</sub> -V <sub>2</sub> , Shallow			Dacite, V <sub>1</sub> -V <sub>2</sub> , East			Dacite, V <sub>1</sub> -V <sub>2</sub> , West		
	184vs188	184vs186	186vs188	154vs157	154vs156	156vs157	73vs72	65vs73	65vs72
<b>Ag</b>	535.1%	DL	552.3%	DL	DL	DL	-70.9%	48.7%	-56.8%
<b>Al<sub>2</sub>O<sub>3</sub></b>	Immobile	Immobile	3.8%	-19.6%	-3.1%	Immobile	7.7%	17.1%	26.1%
<b>As</b>	4015.7%	270.9%	1100.2%	207698.8%	20434.6%	1065.8%	1056.7%	21242.6%	246794.3%
<b>Au</b>	10532.1%	199.2%	3743.4%	40641.6%	11138.1%	317.7%	297.2%	2014.7%	8301.3%
<b>B</b>	202.9%	135.9%	38.9%	-7.3%	-96.9%	3333.1%	-92.5%	4837.0%	272.7%
<b>Ba</b>	31.2%	-12.9%	62.9%	-32.0%	-33.7%	18.1%	67.7%	-48.3%	-13.3%
<b>Bi</b>	174.8%	689.9%	-62.4%	799.9%	273.4%	177.7%	380.4%	680.8%	3651.8%
<b>C</b>	81.1%	40.4%	39.5%	33.2%	70.7%	-10.1%	-2.7%	392.3%	378.8%
<b>CaO</b>	5.4%	13.4%	0.5%	-17.2%	4.5%	-8.7%	-28.3%	76.2%	26.4%
<b>Ce</b>	14.7%	25.9%	-1.4%	-13.8%	-14.9%	16.7%	40.7%	-27.4%	2.2%
<b>Co</b>	3.5%	-0.7%	12.7%	29.8%	27.9%	16.9%	21.7%	67.9%	104.4%
<b>CO<sub>2</sub></b>	78.2%	33.6%	44.3%	32.9%	73.4%	-11.7%	-2.6%	415.3%	401.9%
<b>Cr</b>	6.4%	0.2%	14.8%	-18.2%	65.6%	-43.1%	37.5%	-6.5%	28.6%
<b>Cs</b>	266.4%	75.5%	125.8%	30.9%	-0.4%	51.5%	47.2%	-42.2%	-14.8%
<b>Cu</b>	-18.8%	-7.4%	-5.1%	190.6%	560.7%	-49.3%	90.7%	-1.0%	88.9%
<b>Dy</b>	Immobile	8.8%	Immobile	12.9%	-2.3%	33.1%	13.3%	Immobile	14.9%
<b>Er</b>	Immobile	Immobile	Immobile	6.9%	Immobile	15.4%	5.1%	-1.1%	4.0%
<b>Eu</b>	0.3%	19.5%	-9.3%	9.7%	-11.0%	42.1%	30.9%	-15.3%	10.8%
<b>Fe<sub>2</sub>O<sub>3</sub></b>	76.4%	-86.2%	1279.8%	182.8%	89.3%	72.1%	-19.9%	186.9%	129.7%
<b>Fe<sub>2</sub>O<sub>3</sub>T</b>	2.3%	3.8%	6.6%	12.0%	20.0%	7.5%	-29.3%	85.2%	31.0%
<b>FeO</b>	-13.6%	23.3%	-24.2%	-14.2%	9.3%	-9.5%	-35.1%	51.2%	-1.9%
<b>Ga</b>	15.4%	5.3%	18.5%	-18.2%	-11.3%	6.3%	-15.9%	43.8%	21.0%
<b>Gd</b>	5.4%	23.7%	-7.9%	3.0%	-5.6%	25.6%	10.0%	-8.8%	Immobile
<b>Ge</b>	77.7%	-4.2%	100.7%	-30.8%	-28.2%	11.1%	8.5%	73.5%	88.3%
<b>Hf</b>	-7.5%	Immobile	Immobile	-27.8%	-23.1%	8.2%	6.8%	Immobile	13.7%
<b>Ho</b>	Immobile	13.2%	-3.7%	9.9%	Immobile	21.7%	4.3%	Immobile	11.9%
<b>K<sub>2</sub>O</b>	365.2%	78.9%	181.2%	97.6%	47.0%	54.9%	71.9%	124.9%	286.6%
<b>La</b>	15.5%	24.9%	0.0%	-16.7%	-18.0%	17.1%	44.0%	-25.0%	8.0%

	Dacite, V <sub>1</sub> -V <sub>2</sub> , Shallow			Dacite, V <sub>1</sub> -V <sub>2</sub> , East			Dacite, V <sub>1</sub> -V <sub>2</sub> , West		
	184vs188	184vs186	186vs188	154vs157	154vs156	156vs157	73vs72	65vs73	65vs72
<b>Li</b>	-51.8%	-14.1%	-39.3%	-75.8%	-72.3%	1.0%	-21.3%	9.1%	-14.1%
<b>LOI</b>	87.4%	25.1%	62.0%	48.9%	31.8%	30.1%	56.5%	212.2%	388.6%
<b>Lu</b>	5.5%	-7.2%	23.0%	Immobile	Immobile	10.4%	-19.3%	16.3%	-6.2%
<b>MgO</b>	-6.7%	0.2%	0.7%	-27.6%	36.3%	-38.8%	-41.2%	5.0%	-38.3%
<b>MnO</b>	39.8%	4.1%	45.3%	-23.5%	9.0%	-19.2%	-21.5%	199.1%	134.8%
<b>Mo</b>	DL	DL	DL	390.9%	DL	505.8%	-7.0%	-34.9%	-39.5%
<b>Na<sub>2</sub>O</b>	-76.8%	-11.3%	-71.7%	-7.9%	49.1%	-28.8%	-30.0%	-29.1%	-50.3%
<b>Nb</b>	-13.1%	Immobile	-12.7%	-38.6%	-30.0%	Immobile	-7.0%	Immobile	Immobile
<b>Nd</b>	18.0%	19.5%	6.8%	-6.4%	-7.6%	16.8%	50.3%	-35.2%	-2.6%
<b>Ni</b>	4.4%	3.4%	9.2%	32.9%	40.0%	9.4%	73.3%	-1.3%	71.1%
<b>P<sub>2</sub>O<sub>5</sub></b>	8.6%	5.3%	11.5%	-33.5%	-12.5%	-12.5%	-15.5%	-24.7%	-36.3%
<b>Pb</b>	83.2%	268.6%	-46.2%	9.1%	24.5%	1.0%	-7.0%	30.1%	21.0%
<b>Pr</b>	15.7%	25.8%	-0.5%	-10.2%	-12.0%	17.6%	48.5%	-32.2%	0.8%
<b>Rb</b>	315.3%	75.5%	155.9%	84.1%	40.0%	51.5%	59.8%	81.3%	189.6%
<b>S</b>	1352.2%	52.1%	932.4%	18225.6%	3586.9%	472.6%	74.2%	20461.8%	35723.9%
<b>Sb</b>	449.6%	321.3%	41.1%	-18.2%	-27.4%	29.8%	117.0%	-91.1%	-80.7%
<b>Sc</b>	Immobile	-4.2%	12.9%	Immobile	24.5%	-7.4%	16.2%	15.7%	34.5%
<b>Se</b>	877.2%	DL	903.5%	881.7%	DL	1111.7%	DL	DL	DL
<b>SiO<sub>2</sub></b>	25.2%	2.0%	32.8%	-28.3%	-16.4%	-1.2%	-9.0%	24.5%	13.3%
<b>Sm</b>	18.4%	23.9%	3.4%	2.5%	-2.5%	21.1%	33.8%	-24.4%	1.2%
<b>Sr</b>	-45.7%	-8.7%	-35.6%	-38.3%	-25.1%	-5.1%	-21.6%	-15.6%	-33.8%
<b>Ta</b>	Immobile	19.6%	-7.4%	-43.9%	-33.3%	Immobile	5.8%	17.9%	24.8%
<b>Tb</b>	Immobile	13.6%	Immobile	11.4%	-1.5%	30.2%	11.6%	-4.8%	6.3%
<b>Te</b>	9427.2%	5.3%	9684.0%	2681.6%	273.4%	758.3%	17.8%	1852.1%	2199.5%
<b>Th</b>	Immobile	16.9%	-7.4%	-37.0%	-24.6%	Immobile	13.4%	Immobile	16.4%
<b>TiO<sub>2</sub></b>	Immobile	Immobile	Immobile	-9.7%	Immobile	Immobile	Immobile	20.3%	24.9%
<b>Tl</b>	437.4%	279.2%	53.3%	26.4%	18.8%	22.6%	532.3%	-70.4%	87.0%
<b>Tm</b>	Immobile	Immobile	8.4%	Immobile	Immobile	9.2%	Immobile	Immobile	Immobile

	Dacite, V <sub>1</sub> -V <sub>2</sub> , Shallow			Dacite, V <sub>1</sub> -V <sub>2</sub> , East			Dacite, V <sub>1</sub> -V <sub>2</sub> , West		
	<b>184vs188</b>	<b>184vs186</b>	<b>186vs188</b>	<b>154vs157</b>	<b>154vs156</b>	<b>156vs157</b>	<b>73vs72</b>	<b>65vs73</b>	<b>65vs72</b>
<b>U</b>	4.7%	5.3%	7.5%	-37.0%	-15.8%	-13.7%	9.0%	-19.9%	-12.7%
<b>V</b>	1.8%	-2.2%	12.6%	-2.9%	22.0%	-8.3%	11.6%	17.6%	31.2%
<b>W</b>	9741.3%	104.6%	5101.9%	653.8%	780.1%	-1.3%	100.5%	3231.5%	6580.7%
<b>Y</b>	Immobile	Immobile	Immobile	12.9%	Immobile	30.2%	Immobile	Immobile	Immobile
<b>Yb</b>	Immobile	-2.1%	10.1%	Immobile	Immobile	9.9%	-15.6%	Immobile	-8.2%
<b>Zn</b>	-55.9%	30.6%	-63.4%	-59.6%	10.5%	-57.9%	-75.2%	167.8%	-33.5%
<b>Zr</b>	Immobile	Immobile	7.0%	-33.5%	-23.4%	Immobile	Immobile	Immobile	Immobile



	Dacite, V <sub>1</sub> -V <sub>2</sub> , Centre		Dacite, V <sub>1</sub> -V <sub>2</sub> , Deep		Dacite, V <sub>GD</sub> , Goudreau			Dacite, Cb-Sr alt	
	59vs56	59vs58	164vs162	241vs162	115vs113	115vs114	116vs113	11vs218	241vs218
<b>Ag</b>	-25.2%	15.1%	69.4%	341.4%	23.7%	17.3%	12.2%	-51.2%	DL
<b>Al<sub>2</sub>O<sub>3</sub></b>	Immobile	19.9%	Immobile	26.4%	4.5%	Immobile	Immobile	62.4%	4.8%
<b>As</b>	1016.6%	98.7%	28596.2%	149428.9%	978.7%	341.2%	31304.2%	-97.9%	DL
<b>Au</b>	62036.9%	243.6%	5733.6%	33337.1%	10252.1%	290.9%	123834.3%	186.0%	366.0%
<b>B</b>	234.2%	118.2%	-75.6%	-31.0%	57.7%	-15.1%	134.4%	440.1%	694.3%
<b>Ba</b>	101.1%	175.2%	37.9%	91.4%	-11.6%	9.0%	79.7%	141.9%	14.3%
<b>Bi</b>	797.5%	195.8%	1170.7%	-21.2%	1548.8%	193.2%	797.3%	3644.5%	21.0%
<b>C</b>	-76.8%	-99.2%	16.5%	175.9%	0.2%	-24.2%	49.5%	531.3%	1575.3%
<b>CaO</b>	-60.5%	-88.2%	-37.0%	73.8%	0.2%	-20.9%	19.3%	73.8%	127.0%
<b>Ce</b>	-16.9%	13.2%	-6.3%	38.9%	-6.9%	1.8%	-13.6%	-33.6%	-18.7%
<b>Co</b>	82.6%	-40.0%	-72.3%	-44.0%	-3.9%	-18.2%	25.0%	26.1%	41.6%
<b>CO<sub>2</sub></b>	-66.8%	-95.3%	13.8%	204.2%	3.9%	-21.0%	53.1%	575.7%	1499.5%
<b>Cr</b>	21.6%	27.2%	-61.3%	67.0%	39.7%	11.0%	32.0%	-11.4%	17.1%
<b>Cs</b>	279.0%	327.3%	-27.5%	63.0%	7.0%	35.3%	152.4%	243.2%	5.9%
<b>Cu</b>	-6.3%	181.3%	8.4%	573.9%	79.6%	257.1%	6545.3%	-43.6%	865.3%
<b>Dy</b>	18.1%	Immobile	-25.4%	6.9%	-13.6%	-2.7%	-4.8%	-5.2%	Immobile
<b>Er</b>	46.3%	-6.0%	-27.5%	Immobile	-2.1%	Immobile	11.2%	Immobile	Immobile
<b>Eu</b>	-1.1%	-4.1%	-26.5%	31.8%	-11.0%	2.4%	-10.9%	-9.3%	4.3%
<b>Fe<sub>2</sub>O<sub>3</sub></b>	141.4%	-85.3%	-56.8%	44.8%	98.7%	53.6%	626.8%	97.5%	114.5%
<b>Fe<sub>2</sub>O<sub>3</sub>T</b>	160.8%	-38.2%	-46.7%	-12.4%	9.6%	6.8%	31.5%	28.4%	15.3%
<b>FeO</b>	169.3%	-17.8%	-44.5%	-18.0%	-7.5%	-2.3%	-1.9%	20.3%	5.9%
<b>Ga</b>	Immobile	17.4%	Immobile	37.9%	-7.3%	Immobile	-3.9%	40.4%	Immobile
<b>Gd</b>	-5.1%	6.5%	-25.6%	9.5%	-11.5%	-1.3%	-12.6%	-12.9%	-8.5%
<b>Ge</b>	199.2%	23.3%	37.7%	124.2%	20.2%	5.9%	42.7%	56.0%	45.6%
<b>Hf</b>	Immobile	12.7%	20.0%	51.3%	Immobile	-2.3%	-4.8%	31.6%	-7.8%
<b>Ho</b>	31.3%	Immobile	-26.2%	Immobile	-8.9%	-4.5%	Immobile	Immobile	Immobile
<b>K<sub>2</sub>O</b>	243.5%	353.3%	82.6%	364.8%	10.2%	26.7%	201.3%	252.7%	69.5%
<b>La</b>	-13.6%	16.0%	0.2%	41.5%	-7.9%	0.2%	-14.8%	-36.8%	-25.0%

	Dacite, V <sub>1</sub> -V <sub>2</sub> , Centre		Dacite, V <sub>1</sub> -V <sub>2</sub> , Deep		Dacite, V <sub>GD</sub> , Goudreau			Dacite, Cb-Sr alt	
	59vs56	59vs58	164vs162	241vs162	115vs113	115vs114	116vs113	11vs218	241vs218
Li	105.2%	40.9%	-26.3%	76.6%	6.5%	14.0%	-8.5%	122.9%	-15.3%
LOI	37.3%	-17.7%	38.8%	284.4%	-3.6%	-10.1%	45.2%	369.2%	731.9%
Lu	89.2%	10.8%	-28.2%	Immobil	-2.7%	-6.5%	7.9%	-8.5%	Immobil
MgO	259.0%	-23.0%	-74.3%	-31.0%	-5.3%	10.5%	36.2%	30.5%	60.7%
MnO	18.0%	-85.1%	-38.1%	-9.6%	-1.2%	-11.4%	8.6%	29.3%	58.9%
Mo	618.0%	DL	323.6%	451.8%	106.1%	DL	124.3%	DL	DL
Na <sub>2</sub> O	-60.0%	-66.0%	-0.7%	-20.9%	-1.7%	-36.2%	-21.9%	8.5%	-37.4%
Nb	-16.2%	Immobil	Immobil	23.7%	Immobil	14.0%	-16.4%	13.9%	Immobil
Nd	-9.8%	16.0%	-15.0%	35.6%	-6.0%	5.3%	-12.9%	-34.0%	-11.8%
Ni	-50.6%	-45.8%	-96.5%	-83.8%	6.5%	2.6%	33.7%	70.6%	118.1%
P <sub>2</sub> O <sub>5</sub>	-42.6%	2.6%	-4.7%	77.4%	-6.8%	-2.3%	-3.1%	-50.7%	-9.2%
Pb	19.7%	-50.7%	85.3%	865.6%	-22.7%	-75.6%	68.2%	56.0%	323.6%
Pr	-11.8%	15.2%	-12.5%	35.8%	-9.2%	-1.3%	-11.8%	-35.6%	-15.7%
Rb	234.5%	334.8%	29.1%	258.6%	5.3%	28.1%	145.7%	180.8%	90.6%
S	2163.8%	234.2%	5988.7%	15763.3%	1342.7%	366.9%	28163.8%	212.0%	111.8%
Sb	156.4%	-57.7%	32.4%	37.9%	724.4%	584.1%	348.6%	56.0%	27.1%
Sc	39.6%	20.5%	-68.2%	-54.0%	3.1%	6.6%	12.2%	41.8%	17.7%
Se	DL	DL	DL	DL	DL	DL	DL	DL	DL
SiO <sub>2</sub>	117.1%	2.4%	18.0%	43.2%	6.2%	-0.2%	9.6%	48.5%	-6.8%
Sm	-20.0%	10.6%	-20.3%	34.3%	-6.5%	2.7%	-9.9%	-18.9%	-3.4%
Sr	-32.6%	-64.1%	-14.9%	109.9%	-7.3%	-32.4%	-57.8%	-2.5%	85.2%
Ta	Immobil	6.0%	Immobil	20.7%	-13.7%	8.3%	-19.1%	35.9%	-10.6%
Tb	Immobil	3.2%	-21.4%	13.3%	-14.1%	Immobil	Immobil	-7.1%	-5.4%
Te	5404.9%	163.0%	958.9%	2658.8%	1136.6%	486.4%	1245.9%	DL	DL
Th	-15.7%	17.9%	Immobil	Immobil	Immobil	Immobil	-6.7%	Immobil	-25.3%
TiO <sub>2</sub>	46.5%	21.8%	-37.0%	-6.8%	3.4%	Immobil	Immobil	24.9%	9.3%
Tl	1479.7%	846.7%	14.7%	617.3%	DL	DL	DL	-61.0%	DL
Tm	50.4%	Immobil	-24.1%	-6.3%	-5.9%	-9.7%	19.2%	Immobil	Immobil

	Dacite, V <sub>1</sub> -V <sub>2</sub> , Centre		Dacite, V <sub>1</sub> -V <sub>2</sub> , Deep		Dacite, V <sub>GD</sub> , Goudreau			Dacite, Cb-Sr alt	
	<b>59vs56</b>	<b>59vs58</b>	<b>164vs162</b>	<b>241vs162</b>	<b>115vs113</b>	<b>115vs114</b>	<b>116vs113</b>	<b>11vs218</b>	<b>241vs218</b>
<b>U</b>	-8.6%	0.5%	21.7%	9.5%	-7.8%	4.6%	68.2%	-11.2%	-36.1%
<b>V</b>	51.3%	23.0%	-76.9%	-62.6%	0.7%	3.3%	10.9%	32.8%	21.0%
<b>W</b>	1418.1%	3083.9%	178.7%	3427.4%	100.0%	95.5%	224.0%	-44.3%	-62.2%
<b>Y</b>	21.6%	-16.1%	-26.3%	Immobile	-16.9%	-8.3%	Immobile	Immobile	Immobile
<b>Yb</b>	71.2%	10.1%	-27.9%	Immobile	-3.3%	-7.5%	10.1%	Immobile	Immobile
<b>Zn</b>	127.2%	-48.7%	91.8%	299.1%	10.8%	17.3%	51.6%	-27.2%	-20.7%
<b>Zr</b>	Immobile	Immobile	28.5%	79.1%	Immobile	Immobile	Immobile	24.3%	Immobile

	Gabbro, V <sub>1</sub> -V <sub>2</sub>			Webb Lake stock, V <sub>1</sub> -V <sub>2</sub>			Gabbro/Lamp, V <sub>3</sub>		SPDM, V <sub>3</sub>	
	139vs140	139vs141	140vs141	192vs194	192vs195	194vs195	81vs213	239vs213	66vs245	216vs245
<b>Ag</b>	DL	DL	DL	95.5%	223.5%	58.8%	-54.3%	DL	-0.4%	5.0%
<b>Al<sub>2</sub>O<sub>3</sub></b>	2.9%	Immobile	Immobile	Immobile	4.4%	Immobile	Immobile	Immobile	Immobile	Immobile
<b>As</b>	3866.6%	3382.5%	-12.1%	DL	148500.5%	145780.9%	20926.5%	539.2%	303.5%	40.2%
<b>Au</b>	896.1%	1236.7%	34.3%	393.1%	6404.8%	1166.1%	1202.7%	1927.6%	520.8%	562.9%
<b>B</b>	180.6%	519.1%	120.8%	291.1%	1416.3%	272.1%	44.3%	18.6%	-17.0%	-10.0%
<b>Ba</b>	127.2%	201.5%	32.8%	-4.5%	28.7%	29.2%	2436.9%	1246.1%	-86.8%	-87.7%
<b>Bi</b>	-3.3%	-27.4%	-24.9%	12.8%	646.5%	535.1%	2459.7%	13.2%	431.4%	-28.0%
<b>C</b>	-26.7%	-24.1%	3.6%	24.4%	80.7%	39.4%	-13.4%	-27.4%	-30.5%	-45.7%
<b>CaO</b>	-10.9%	-10.3%	0.7%	-4.0%	-21.6%	-21.6%	-24.7%	-35.2%	8.5%	3.1%
<b>Ce</b>	-4.8%	2.1%	7.3%	-13.4%	-6.5%	3.6%	1.2%	1.5%	-0.4%	46.5%
<b>Co</b>	-2.2%	6.0%	8.5%	-11.5%	-11.3%	-3.9%	-50.6%	-39.3%	-5.0%	17.5%
<b>CO<sub>2</sub></b>	-25.3%	-25.3%	0.1%	31.3%	82.0%	33.0%	-20.6%	-28.6%	-27.6%	-45.2%
<b>Cr</b>	-7.6%	2.2%	10.7%	284.1%	37.2%	-65.7%	15.5%	35.3%	-29.3%	-10.0%
<b>Cs</b>	35.4%	122.5%	64.4%	56.4%	41.5%	-13.2%	220.0%	55.6%	-85.5%	-91.5%
<b>Cu</b>	-8.1%	11.5%	21.3%	303.6%	499.5%	42.6%	-8.6%	12.6%	-39.7%	-10.2%
<b>Dy</b>	-3.3%	3.3%	6.9%	-9.8%	-7.3%	Immobile	-13.7%	-12.5%	-4.6%	67.0%
<b>Er</b>	Immobile	Immobile	2.0%	-10.1%	Immobile	5.7%	-9.3%	-11.1%	Immobile	31.3%
<b>Eu</b>	-5.7%	-1.6%	4.4%	-11.6%	-5.1%	3.0%	-18.7%	19.2%	-11.9%	72.3%
<b>Fe<sub>2</sub>O<sub>3</sub></b>	60.7%	-2.7%	-39.4%	235.2%	571.5%	92.3%	-43.5%	62.4%	-55.3%	-59.1%
<b>Fe<sub>2</sub>O<sub>3</sub>T</b>	2.5%	-2.4%	-4.7%	-2.0%	-1.0%	-3.0%	-20.4%	4.9%	-1.9%	6.9%
<b>FeO</b>	-5.9%	-2.4%	3.9%	-10.0%	-20.2%	-14.9%	-18.1%	2.6%	9.0%	23.6%
<b>Ga</b>	-8.3%	-8.4%	Immobile	-2.2%	6.4%	4.5%	5.5%	2.6%	-17.9%	-3.0%
<b>Gd</b>	Immobile	-0.8%	0.8%	-9.5%	-5.5%	Immobile	-7.3%	Immobile	-4.4%	104.3%
<b>Ge</b>	-3.3%	-10.7%	-7.6%	17.3%	51.6%	24.0%	16.4%	24.5%	-31.5%	10.0%
<b>Hf</b>	0.8%	Immobile	Immobile	Immobile	15.5%	13.4%	10.3%	Immobile	10.7%	32.4%
<b>Ho</b>	-4.9%	Immobile	5.3%	-5.2%	Immobile	Immobile	Immobile	-13.0%	Immobile	47.9%
<b>K<sub>2</sub>O</b>	185.1%	314.9%	45.6%	90.9%	230.6%	66.2%	597.1%	146.6%	-67.3%	-56.0%
<b>La</b>	-6.8%	1.7%	9.3%	-14.6%	-8.2%	3.2%	2.3%	0.1%	-1.9%	43.5%

	Gabbro, V <sub>1</sub> -V <sub>2</sub>			Webb Lake stock, V <sub>1</sub> -V <sub>2</sub>			Gabbro/Lamp, V <sub>3</sub>		SPDM, V <sub>3</sub>	
	139vs140	139vs141	140vs141	192vs194	192vs195	194vs195	81vs213	239vs213	66vs245	216vs245
Li	13.3%	32.1%	16.7%	3.5%	1.1%	-6.3%	63.4%	91.5%	16.2%	68.0%
LOI	-14.2%	-11.6%	3.2%	7.7%	99.2%	77.6%	-15.7%	-22.2%	-9.8%	-25.4%
Lu	-5.2%	Immobile	5.2%	-11.7%	5.0%	14.1%	-13.4%	-5.8%	-5.9%	Immobile
MgO	-6.5%	-0.5%	6.5%	6.6%	2.5%	-7.7%	-5.3%	-3.7%	7.3%	-5.1%
MnO	0.4%	0.4%	0.1%	-0.6%	-10.5%	-13.6%	-50.3%	-31.0%	8.4%	-2.7%
Mo	DL	DL	DL	2832.9%	3539.2%	19.1%	82.8%	77.9%	DL	-55.0%
Na <sub>2</sub> O	-20.7%	-38.2%	-22.0%	-17.8%	-53.6%	-45.8%	-9.2%	-7.8%	-36.1%	-56.5%
Nb	Immobile	-6.8%	Immobile	Immobile	50.0%	47.3%	17.3%	Immobile	Immobile	-71.7%
Nd	-1.3%	1.5%	3.0%	-11.8%	-7.5%	0.7%	-5.2%	3.0%	-4.3%	59.2%
Ni	-14.2%	4.9%	22.3%	5.3%	-6.7%	-14.9%	-37.7%	-43.9%	-2.5%	-56.0%
P <sub>2</sub> O <sub>5</sub>	-16.2%	-22.6%	-7.6%	14.1%	1.1%	-14.9%	-14.3%	2.6%	-10.0%	77.7%
Pb	45.1%	45.1%	0.1%	-2.2%	34.8%	32.3%	-8.6%	-11.1%	-50.2%	-55.0%
Pr	-5.7%	1.6%	7.8%	-11.3%	-4.0%	3.9%	-3.0%	3.3%	-1.2%	51.8%
Rb	104.2%	243.9%	68.5%	117.3%	169.6%	19.1%	387.6%	137.1%	-63.8%	-60.0%
S	65.5%	210.6%	87.8%	1366.5%	8391.5%	455.7%	DL	DL	114.6%	26.0%
Sb	-35.5%	-51.6%	-24.9%	-34.8%	102.2%	197.7%	52.4%	11.2%	-50.2%	-61.4%
Sc	2.1%	-3.3%	-5.2%	-13.1%	-10.1%	-0.8%	3.6%	Immobile	10.3%	86.1%
Se	DL	DL	DL	DL	102.2%	98.5%	DL	-55.5%	DL	-77.5%
SiO <sub>2</sub>	-1.3%	-1.2%	0.2%	-2.7%	-0.5%	-1.8%	-4.3%	-8.2%	5.9%	-8.9%
Sm	0.1%	2.4%	2.3%	-8.8%	-6.8%	-1.9%	-7.4%	10.3%	-0.4%	92.6%
Sr	9.3%	13.5%	3.9%	-47.7%	-29.1%	30.0%	70.9%	172.9%	-41.6%	-54.3%
Ta	-9.3%	-3.3%	6.7%	5.0%	34.8%	23.2%	Immobile	Immobile	24.5%	-69.7%
Tb	Immobile	Immobile	2.5%	-8.3%	-5.2%	Immobile	-13.7%	-7.4%	-6.8%	84.7%
Te	33.0%	117.7%	63.7%	584.4%	6167.5%	779.0%	DL	DL	996.0%	890.3%
Th	-8.6%	Immobile	11.8%	-8.2%	3.7%	8.5%	5.0%	-7.8%	Immobile	-22.5%
TiO <sub>2</sub>	3.2%	-5.9%	-8.7%	Immobile	6.6%	Immobile	Immobile	Immobile	-8.2%	Immobile
Tl	-19.9%	-30.0%	-12.4%	6.7%	-8.1%	-17.3%	DL	DL	DL	DL
Tm	Immobile	Immobile	1.5%	-13.3%	Immobile	8.2%	-13.7%	-13.7%	Immobile	24.5%

	Gabbro, V <sub>1</sub> -V <sub>2</sub>			Webb Lake stock, V <sub>1</sub> -V <sub>2</sub>			Gabbro/Lamp, V <sub>3</sub>		SPDM, V <sub>3</sub>	
	<b>139vs140</b>	<b>139vs141</b>	<b>140vs141</b>	<b>192vs194</b>	<b>192vs195</b>	<b>194vs195</b>	<b>81vs213</b>	<b>239vs213</b>	<b>66vs245</b>	<b>216vs245</b>
<b>U</b>	-3.3%	7.5%	11.2%	15.0%	42.7%	19.1%	2.8%	-5.4%	-5.0%	-10.0%
<b>V</b>	2.6%	-3.6%	-5.9%	-0.9%	2.5%	-0.8%	22.9%	6.5%	-10.4%	43.8%
<b>W</b>	47.3%	33.5%	-9.2%	227.0%	1409.4%	343.0%	20.2%	271.4%	510.2%	2946.7%
<b>Y</b>	-3.6%	Immobile	3.8%	-7.4%	Immobile	3.7%	-7.9%	-14.4%	Immobile	44.7%
<b>Yb</b>	-5.4%	Immobile	5.8%	-11.4%	2.1%	10.6%	-8.6%	-4.0%	Immobile	9.6%
<b>Zn</b>	-7.3%	-2.6%	5.2%	-2.5%	2.9%	1.3%	54.7%	144.1%	-15.8%	28.6%
<b>Zr</b>	Immobile	Immobile	Immobile	-45.5%	-37.0%	10.9%	7.2%	Immobile	Immobile	24.0%